National Research
Council Canada

Conseil national
de recherches Canada

NRC · CNRC

Canadian Journal of Fisheries and Aquatic Sciences

Journal canadien des sciences halieutiques et aquatiques

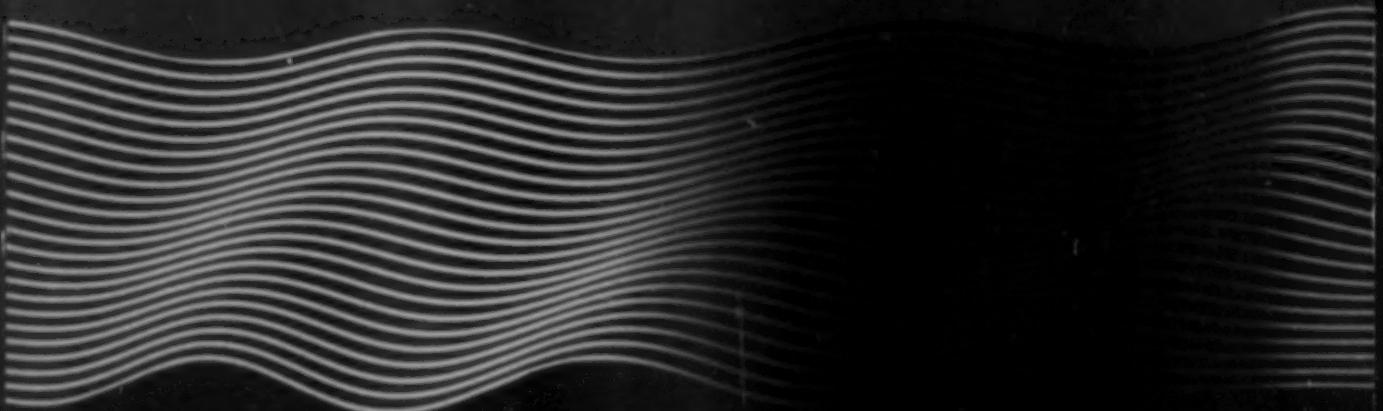

http://cjfas.nrc.ca

http://jcsha.cnrc.ca

ISSN 0706-652X / CJFSDX 63(12) 2603–2836 (2006)

The *Canadian Journal of Fisheries and Aquatic Sciences*, previously published as *Contributions to Canadian Biology* 1901–1925, *Contributions to Canadian Biology and Fisheries* 1926–1934, *Journal of the Biological Board of Canada* 1934–1937, and *Journal of the Fisheries Research Board of Canada* 1938–1979, is issued monthly to form annual volumes of 12 numbers plus supplements.

Editorial policy. The Journal publishes original research articles, perspectives (syntheses, critiques, re-evaluations), discussions (comment and reply), and rapid communications. Manuscripts may concern cells, organisms, populations, communities, ecosystems, or processes that affect aquatic systems. They may cover a range of disciplines including biology and ecology of marine and freshwater organisms, limnology, oceanography, physiology, toxicology, genetics, economics, disease, and management. Preference will be given to manuscripts that emphasize understanding of observed phenomena and interpretation of experimental results. The Journal encourages papers that lead from clearly stated purpose or rationale and from testable hypotheses, concepts, or questions to identifiable conclusions or syntheses. Such papers may amplify, modify, question, or redirect accumulated knowledge embodied in contemporary perceptions of a particular state of aquatic sciences. The Journal discourages papers that are essentially descriptive, except in emerging disciplines; have only site-specific or local applications (a certain year, place, taxon, chemical compound, etc.); only confirm previously established principles; or apply standard techniques without breaking new methodological ground.

Manuscripts for publication should be submitted to the Editorial Office via NRC Research Press' online submission and peer review system (**OSPR**EY) at http://pubs.nrc-cnrc.gc.ca/cjfas/osprey. Alternatively, manuscripts may be submitted to the Senior Editor, *Canadian Journal of Fisheries and Aquatic Sciences*, Department of Integrative Biology, Building #006, Room 118, University of Guelph, Guelph, ON N1G 2W1, Canada (519-824-4120 ext. 52646; fax: 519-767-9798; e-mail: cjfas@uoguelph.ca).

Submissions in either English or French are acceptable. The information must be original, that is, not copyrighted, published, or submitted elsewhere except in abstract form or unless by written consent of the Editor.

Correspondence concerning accepted manuscripts and corrected proofs should be sent to NRC Research Press, National Research Council of Canada, Ottawa, ON K1A 0R6, Canada (fax: 613-952-7656; e-mail: pubs@nrc-cnrc.gc.ca).

Instructions to Authors are published once a year in the first issue of each volume. Copies are available from NRC Research Press or at http://cjfas.nrc.ca. The **Publication Policy** of NRC Research Press is available at http://pubs.nrc-cnrc.gc.ca.

Microfilm. Issues from 1934 through the current volume can be purchased on 16- or 35-mm microfilm. Photocopies of individual articles or issues can be purchased from University Microfilms International, 330 North Zeeb Road, Ann Arbor, MI 48106, USA.

The *Canadian Journal of Fisheries and Aquatic Sciences*, ISSN 0706-652X, is published monthly, 12 times per year, by NRC Research Press, c/o USACAN Media Dist. Srv. Corp. at 26 Power Dam Way, Suite S1-S3, Plattsburgh, NY 12901, USA. Periodicals postage paid at Plattsburgh, NY. POSTMASTER: Send address changes to *Canadian Journal of Fisheries and Aquatic Sciences*, c/o NRC, P.O. Box 2888, Plattsburgh, NY 12901, USA.

Publié sans interruption depuis 1901, le *Journal canadien des sciences halieutiques et aquatiques* a paru sous plusieurs titres : *Contributions to Canadian Biology* 1901–1925, *Contributions to Canadian Biology and Fisheries* 1926–1934, *Journal of the Biological Board of Canada* 1934–1937, et *Journal of the Fisheries Research Board of Canada* 1938–1979. Le Journal paraît tous les mois, formant ainsi un volume de 12 numéros, et offre en plus jusqu'à deux suppléments par année.

Politique éditoriale. On publie, dans le Journal, des articles rendant compte de recherche originale, des perspectives (synthèses, critiques et réévaluations), des discussions (commentaires et réponses) et des communications rapides. Les documents peuvent porter sur les cellules, organismes, populations, communautés, écosystèmes ou processus qui affectent les systèmes aquatiques. Ils peuvent relever de divers domaines y compris la biologie et l'écologie des organismes marins et d'eau douce, la limnologie, l'océanographie, la physiologie, la toxicologie, la génétique, l'économie, la pathologie et la gestion. On accorde la préséance aux articles qui contribuent à la compréhension de phénomènes observés et à l'interprétation de résultats expérimentaux. On invite les auteurs à soumettre des articles ayant des objectifs précis ou relevant d'hypothèses, de concepts ou de questions vérifiables et se terminant par de solides conclusions ou d'utiles synthèses. Ces articles enrichissent, changent, mettent en question ou réorientent les connaissances acquises sur divers aspects des sciences aquatiques. On décourage toutefois la soumission d'articles simplement descriptifs (à moins qu'il ne s'agisse de nouvelles disciplines), d'application très limitée (applicables à une seule année, une seule région ou un seul taxon, portant sur un unique composé chimique, etc.); d'articles qui ne font que reprendre les principes énoncés dans des articles précédents; et d'articles rendant compte de l'application de normes sans gain de méthodologie.

Les auteurs sont invités à soumettre leur **manuscrit** au Bureau de la rédaction par le truchement du Système de soumission et d'examen en direct des articles (**OSPR**EY) des Presses scientifique du CNRC à http://pubs.nrc-cnrc.gc.ca/jcsha/osprey. Sinon, ils peuvent transmettre leur manuscrit par la poste à la directrice scientifique principale, *Journal canadien des sciences halieutiques et aquatiques*, Département de biologie intégrative, édifice 006, bureau 118, University of Guelph, Guelph, ON N1G 2W1, Canada (519-824-4120 poste 52646; télécopieur : 519-767-9798; courriel : cjfas@uoguelph.ca).

Les contributions peuvent être en anglais ou en français. Elles doivent être originales, c.-à.-d. qu'elles ne doivent pas avoir fait l'objet d'un copyright, avoir été publiées ou soumises ailleurs, sauf sous forme abrégée ou avec le consentement du rédacteur. Le CNRC ne se tient en aucune façon responsable des opinions exprimées par un collaborateur ou des déclarations qui pourrait faire ce dernier.

La correspondance ayant trait aux manuscrits acceptés et les **épreuves corrigés** doivent être envoyées aux Presses scientifiques du CNRC, Conseil national de recherches du Canada, Ottawa, ON K1A 0R6, Canada (télécopieur : 613-952-7656; courriel : pubs@nrc-cnrc.gc.ca).

Les Recommandations aux auteurs sont publiées une fois par année dans le premier numéro de chaque volume. Des copies sont disponibles auprès du Bureau de la rédaction aux Presses scientifiques du CNRC ou au http://jcsha.cnrc.ca. **La Politique de publication** est disponible auprès des Presses scientifiques du CNRC ou au http://pubs.nrc-cnrc.gc.ca.

Microfilms. On peut acheter sur microfilms de 16 ou 35 mm tous les numéros depuis 1934. Des photocopies d'articles ou de numéros individuels sont aussi en vente auprès de University Microfilms International, 330 North Zeeb Road, Ann Arbor, MI 48106, É.-U.

This Journal is indexed or abstracted in / Cette revue est signalée ou résumée dans
ABSEARCH; Applied Science and Technology Index and Abstracts; Aquatic Sciences and Fisheries Abstracts; Biological Abstracts; Biological and Agricultural Abstracts; CAB Abstracts; Chemical Abstracts; Current Contents; Elsevier BIOBASE; Environmental Abstracts; ETDE Energy Database; General Science Index and Abstracts; GEOBASE; GeoRef; Life Sciences Collection; Meteorological and Geoastrophysical Abstracts; Oceanic Abstracts; PASCAL Database; Science Citation Index.

Volume 63, Number 12, December 2006

Canadian Journal of Fisheries and Aquatic Sciences

Published by the National Research Council of Canada

Volume 63, numéro 12, décembre 2006

Journal canadien des sciences halieutiques et aquatiques

Publié par le Conseil national de recherches du Canada

Senior Editor / Directrice scientifique principale Moira M. Ferguson

Editors / Directeurs

Jeffrey A. Hutchings, *Dalhousie University, Halifax*
Pierre Pepin, *Northwest Atlantic Fisheries Centre, DFO/MPO, St. John's, Newfoundland*
W. Gary Sprules, *University of Toronto at Mississauga*
Assistant to the Editors / Adjointe aux directeurs scientifiques **Holly Foster**

Associate Editors / Directeurs scientifiques associés

D. Boisclair, *Université de Montréal*
U. Borgmann, *Environment Canada, Burlington*
M.J. Bradford, *DFO/MPO and Simon Fraser University*
S.E. Campana, *DFO/MPO, Dartmouth*
R. Carignan, *Université de Montréal*
K.T. Frank, *DFO/MPO, Dartmouth*
J.W.A. Grant, *Concordia University*
M.M. Hansen, *Danish Institute for Fisheries Research, Silkeborg, Denmark*
R. Hilborn, *University of Washington*
D.F. Houlihan, *University of Aberdeen*
F.A. Huntingford, *University of Glasgow*
J.M. Jech, *NFSC/NOAA, Woods Hole, Mass.*
B. Jonsson, *Norwegian Institute for Nature Research, Oslo, Norway*
K.A. Kidd, *University of New Brunswick*
D.L. MacLatchy, *University of New Brunswick, Saint John*
P. Magnan, *Université du Québec à Trois Rivières*
C.T. Marshall, *University of Aberdeen*
R.B. Millar, *University of Auckland, New Zealand*
W.P. Patterson, *University of Saskatchewan*
Y.T. Prairie, *Université du Québec à Montréal*
T.J. Quinn II, *University of Alaska–Fairbanks, Juneau, Alaska*
T.P. Quinn, *University of Washington*
C.W. Ramcharan, *Laurentian University*
J.S. Richardson, *The University of British Columbia*
B. Sainte-Marie, *DFO/MPO, Mont-Joli*
R.E.H. Smith, *University of Waterloo*
S.J. Smith, *DFO/MPO, Dartmouth*
E.B. Taylor, *The University of British Columbia*
W.F. Vincent, *Université Laval*
R.D. Vinebrooke, *University of Alberta*
C.J. Walters, *The University of British Columbia*
B. de Young, *Memorial University of Newfoundland*

NRC Research Press / Presses scientifiques du CNRC

Editor-in-Chief / Directeur scientifique en chef **Bruce P. Dancik**
Assistant Editor-in-Chief / Adjoint au directeur scientifique en chef **Iain E.P. Taylor**

Journals Program / Programme des revues

Fax / Télécopieur : 613-952-7656; e-mail / courriel : pubs@nrc-cnrc.gc.ca; URL / URL : pubs.nrc-cnrc.gc.ca
Director / Directeur **Cameron D. Macdonald**
Business Manager / Gestionnaire des affaires **Jason Charron**
Manager, Journals Program / Gestionnaire, Programme des revues **Carolyn Brown**
Managing Editor / Rédactrice administrative **Cecily M. Pearson** (613-993-9099)
Publication Officers / Agents de publication **Jennifer McColl, Thad Costigan**
Advertising and reprints / Annonces publicitaires et tirés à part **Roxanne Landriault** (613-990-2254)
Subscriptions / Abonnements **Eileen Evans-Nantais** (613-990-7873)

The National Research Council of Canada accepts no responsibility for statements or opinions expressed by a contributor. Acceptance of an advertisement, announcement, or other material does not imply endorsement by either the Journal's Senior Editor or the National Research Council.

© National Research Council of Canada 2006. All rights reserved.

No part of this publication may be reproduced, stored, or transmitted in any form or by any means, without the written permission of the publisher, except as stated below.

The National Research Council of Canada grants **permission*** to individuals to make single copies of articles for personal use. Any person may reproduce short excerpts from articles in the journal for any purpose that respects the moral rights of authors, provided that the source is fully acknowledged. As a courtesy, the consent of authors of such material should be obtained directly from the author.

Authorization to reproduce items for other than personal use, as stated above, is granted by the National Research Council of Canada provided that the copyright fee of $7.00 per copy is paid directly to Access Copyright, The Canadian Copyright Licensing Agency, One Yonge Street, Suite 800, Toronto, ON M5E 1E5, Canada.

*The above permission does not extend to other kinds of copying, such as copying for general distribution, for advertising, or promotional purposes, for creating new collective works, or for resale. For such copying, arrangements must be made with the publisher, National Research Council of Canada, Ottawa, ON K1A 0R6, Canada.

Subscription information

The *Canadian Journal of Fisheries and Aquatic Sciences* (ISSN 0706-652X) is published monthly by the National Research Council of Canada. The 2007 annual subscription rates (second class postage) for Canada are $1051CAN institutional and $325CAN personal, for US & foreign $1051US institutional and $325US personal. For air mail add $150US to foreign rate. Canadian customers please include 6% GST (business no. 12149 1807 RT 0275). Subscriptions are entered for the calendar year. Remittances should be made payable to the Receiver General for Canada, credit NRC. Price for regular single issues: institutional, $110.00; personal, $35.00. Supplements will be priced separately. Special rates apply to members of Canadian scientific and engineering societies if they subscribe through their respective societies.

There are no refunds on cancelled subscriptions once delivery has begun. Claims for missing issues should be made within four months (N. America) or six months (outside N. America) following the date of publication. The publisher expects to supply missing issues only when losses have occurred in transit and when the reserve stock will permit. For change of address and subscription enquiries: Subscription Office, NRC Research Press, National Research Council of Canada, Ottawa, ON K1A 0R6, Canada; tel.: 613-993-9084; fax: 613-952-7656; e-mail: pubs@nrc-cnrc.gc.ca.

Microform backfiles are available from UMI, P.O. Box 1346, Ann Arbor, MI 48106-1346, USA, and Micromedia Ltd., 20 Victoria St., Toronto, ON M5C 2N8, Canada.

All issues of the *Canadian Journal of Fisheries and Aquatic Sciences* since 1996 are available on the Web. Pricing information can be found at http://pubs.nrc-cnrc.gc.ca.

Le Conseil national de recherches du Canada ne se tient en aucune façon responsable des opinions exprimées par un collaborateur ou des déclarations que pourrait faire ce dernier. La publication d'annonces publicitaires, d'avis et autres n'implique pas l'endossement de leur contenu par la directrice principale de la Revue ou le CNRC.

© Conseil national de recherches du Canada 2006. Tous droits réservés.

Il est interdit de reproduire, de sauvegarder ou de transmettre quelque partie de la présente publication dans quelque format ou de quelque façon sans le consentement écrit de l'éditeur, à l'exception des conditions suivantes.

Le Conseil national de recherches du Canada accorde aux particuliers le droit de faire des copies individuelles pour leur usage personnel. Toute personne peut reproduire de courts extraits des articles de la Revue pour autant que les droits moraux de l'auteur soient respectés et que la mention de provenance soit clairement indiquée. Il est de convenance de demander le consentement de l'auteur avant de faire mention de son travail.

On obtiendra l'autorisation de reproduire des articles à d'autres fins que l'usage personnel (tel qu'on l'a décrit ci-dessus) auprès du Conseil national de recherches du Canada pour autant que des redevances de droits d'auteurs de 7,00 $/copie soient versées au Access Copyright, The Canadian Copyright Licensing Agency, 1, rue Yonge, bureau 800, Toronto, ON M5E 1E5, Canada.

*La permission ci-dessus ne s'applique pas à la reproduction à grande échelle, telle que la reproduction aux fins de distribution générale, publicitaire ou promotionnelle, de compilation de nouveaux ouvrages collectifs ou de revente. Dans de tels cas, il faudra ratifier une entente particulière avec l'éditeur, le Conseil national de recherches du Canada, Ottawa, ON K1A 0R6, Canada.

Renseignements sur l'abonnement

Journal canadien des sciences halieutiques et aquatiques (ISSN 0706-652X) est une publication mensuelle du Conseil national de recherches du Canada. Le prix de l'abonnement annuel en 2007 au Canada (courrier de deuxième classe) est de 1051 $CAN pour les organismes et de 325 $CAN pour les particuliers. À l'étranger (y compris les É.-U.), le prix de l'abonnement est de 1051 $US pour les organismes et de 325 $US pour les particuliers. L'expédition par avion exige des frais de 150 $US en sus du prix d'abonnement à l'étranger. Les clients du Canada doivent ajouter la TPS de 6 % (numéro d'entreprise 12149 1807 RT 0275). Les abonnements sont pour l'année civile. Tout paiement doit être adressé au Receveur général du Canada, crédit du CNRC. Le prix par numéro est de 110 $ pour les organismes et de 35 $ pour les particuliers. Le prix des hors-série varie. Les membres des sociétés canadiennes de sciences et de génie bénéficient de taux préférentiels en s'abonnant via leurs sociétés respectives.

Aucun remboursement ne sera accordé ni aucune annulation acceptée une fois que les livraisons auront commencé. Les réclamations de numéros manquants devront être soumises dans les quatre mois (Amérique du Nord) ou dans les six mois (à l'extérieur de l'Amérique du Nord) suivant la date de publication. L'éditeur ne fournira de numéros manquants que si le document a été perdu pendant l'expédition et que si le stock le permet. Adressez tout changement d'adresse ou toute question quant à l'abonnement au : Bureau des abonnements, Presses scientifiques du CNRC, Conseil national de recherches Canada, Ottawa, ON K1A 0R6, Canada; téléphone : 613-993-9084; télécopieur : 613-952-7656; courriel : pubs@nrc-cnrc.gc.ca.

On peut obtenir les fichiers rétrospectifs sur **microforme** auprès de UMI, P.O. Box 1346, Ann Arbor, MI 48106-1346, É.-U., et auprès de Micromedia Ltée, 20, rue Victoria, Toronto, ON M5C 2N8, Canada.

À partir de 1996, tous les numéros de *Journal canadien des sciences halieutiques et aquatiques* sont accessibles sur le Web. On trouvera des renseignements sur les tarifs à http://pubs.nrc-cnrc.gc.ca.

ANNOUNCEMENT / COMMUNIQUÉ

Call for nominations for the Timothy R. Parsons Medal in ocean sciences

Nominations are being solicited for the Timothy R. Parsons Medal for distinguished contributions to multidisciplinary research in ocean sciences and are due 28 February 2007. In 2006, two awards were made to Dr. Ken Denman and Dr. Trevor Platt. Researchers working for Canadian institutions to benefit Canada are eligible for nomination. Awards will be considered for either lifetime achievement or a recent outstanding accomplishment. Fisheries and Oceans Canada will present the 2007 Parsons Medal at the Canadian Meteorological and Oceanographic Society Congress in May 2007 in St. John’s, Newfoundland and Labrador.

Please use the online form at http://www.dfo-mpo.gc.ca/science/Awards/Parsons_e.htm or send via a fax to 613-990-0313, or mail to

Timothy R. Parsons Medal Committee,
c/o Strategic Science Outreach Branch,
Stn. 8W135, 200 Kent Street,
Ottawa, ON K1A 0E6

Appel de candidatures pour la médaille Timothy R. Parsons (sciences de la mer)

Nous sollicitons des mises en candidature pour la médaille Timothy R. Parsons, remise à des scientifiques qui se sont distingués dans un domaine de recherche multidisciplinaire lié aux sciences de la mer. Veuillez nous les faire parvenir d’ici le 28 février 2007. En 2006, Ken Denman et Trevor Platt ont tous deux reçu une médaille. Les chercheurs qui œuvrent au sein d’une institution canadienne et dont les travaux profitent au Canada sont admissibles. Une médaille sera décernée pour souligner une carrière extraordinaire ou une réalisation exceptionnelle récente. Pêches et Océans Canada remettra la médaille Timothy R. Parsons 2007 dans le cadre du Congrès de la Société canadienne de météorologie et d’océanographie, qui se tiendra en mai 2007, à St. John’s (Terre-Neuve-et-Labrador).

Vous pouvez remplir le formulaire en ligne à http://www.dfo-mpo.gc.ca/science/Awards/Parsons_f.htm, nous le faire parvenir par télécopieur, au 613-990-0313, ou par la poste, aux coordonnées suivantes :

Comité de la médaille Timothy R. Parsons
Bureau de la promotion stratégique des sciences
200, rue Kent, bureau 8W135
Ottawa, ON K1A 0E6

RAPID COMMUNICATION / COMMUNICATION RAPIDE

“Big” concerns with high latitude marine protected areas (MPAs): trends in connectivity and MPA size

Benjamin J. Laurel and Ian R. Bradbury

Abstract: The success of marine protected areas (MPAs) as fisheries management tools in tropical latitudes has generated interest in their applicability and potential elsewhere. Here we suggest that dispersal and gene flow in marine fish populations (a primary biological consideration for marine reserve design) increases with latitude. For example, north temperate fish species at latitudes between 40° and 45° had about three times greater dispersal potential (planktonic larval duration (PLD), $n = 96$ species) and genetic homogeneity (F_{ST}, $n = 100$ species) than fish species near equatorial regions. Using the PLD and F_{ST} relationships, dispersal increases at a rate of ~8% per degree of latitude north or south of the equator. Therefore tropical MPAs should not serve as direct scalar templates in other regions, but rather should be used as a basis against which higher-latitude MPAs should be scaled. However, a review of 429 existing MPAs indicates that no such changes in reserve size have been implemented with respect to latitude. Fisheries managers must be prepared and willing to implement MPAs at large scales in high latitudes, either as single reserves or in a network, or else we lose the legitimacy of a new and promising management tool for conserving marine biodiversity in cold ocean regions.

Résumé : Le succès des zones de protection marine (MPAs) comme outils de gestion des pêches dans les latitudes tropicales a généré un intérêt pour leur potentiel et leur utilisation possible ailleurs dans le monde. Nous croyons que la dispersion et le flux génétique (des éléments biologiques importants dans la planification des réserves marines) augmentent en fonction de la latitude. Par exemple, les espèces de poissons des latitudes tempérées nordiques entre 40° et 45° ont environ trois fois plus de potentiel de dispersion (durée de la vie larvaire planctonique (PLD), $n = 96$ espèces) et d'homogénéité génétique (F_{ST}, $n = 100$ espèces) que les espèces de poissons habitant près des régions équatoriales. D'après les relations de PLD et de F_{ST}, la dispersion augmente à un taux de ~8 % par degré de latitude au nord ou au sud de l'équateur. Les MPAs tropicales ne doivent donc pas devenir des modèles scalaires directs pour les autres régions, mais devraient plutôt servir de base sur laquelle on met à l'échelle les MPAs des latitudes plus élevées. Cependant, une revue de 429 MPAs existantes montre qu'il n'existe pas de variation de la taille des réserves en fonction de la latitude. Les gestionnaires de la pêches doivent vouloir être prêts à mettre en place des MPAs à grande échelle dans les latitudes élevées, soit en réserves uniques, soit en réseaux; sinon, nous perdons la légitimité d'un outil de gestion neuf et prometteur pour la conservation de la biodiversité marine dans les régions océaniques froides.

[Traduit par la Rédaction]

Introduction

The implementation of spatial management tools such as marine reserves, marine protected areas, and fishery closed areas (hereafter collectively referred to as MPAs) has been suggested as one means of remedying the mismanagement of marine populations (NRC 2000). Appropriately designed MPAs excel over traditional single-species management in their protection of the entire ecosystem (i.e., spawning areas, nursery habitat, prey species, etc.) rather than simply con-

Received 2 August 2006. Accepted 17 October 2006. Published on the NRC Research Press Web site at http://cjfas.nrc.ca on 10 November 2006.
J19459

B.J. Laurel.[1,2] Fisheries and Oceans Canada, Environmental and Ecosystems Sciences Section, P.O. Box 5667, St. John's, NL A1C 5X1, Canada.
I.R. Bradbury. Marine Gene Probe Lab, Biology Department, Dalhousie University, Halifax, NS B3H 4R2, Canada.

[1] Corresponding author (e-mail: ben.laurel@noaa.gov).
[2] Present address: National Marine Fisheries Service – NOAA, Alaska Fisheries Science Center, Hatfield Marine Science Center, Newport, OR 97365, USA.

Can. J. Fish. Aquat. Sci. 63: 2603–2607 (2006) doi:10.1139/F06-151

trolling harvest rates on the adult population. Empirical examinations of worldwide MPA success indicate that exploited species often increase in size and number within MPA boundaries (Halpern 2003), although the effect may be species-specific (Roberts 2002). Such data are encouraging but may not reflect equally trends throughout oceanic regions. MPAs are found with greater frequency at lower latitudes (Fig. 1*a*), and consequently, most research on their design, implementation, and evaluation is based on tropical examples. The potential efficacy of MPAs for managing fisheries beyond low-latitude regions remains uncertain, yet such information is fundamentally important for fisheries in the United States (US), Canada, Europe, Australia, and New Zealand, where ecosystem-based management has recently been mandated.

An MPA's ability to successfully manage a fish population is driven largely by the dispersal rates of individuals across reserve boundaries (Botsford et al. 2003; Hilborn et al. 2004). From a conservation perspective, excessive export from within the MPA can result in overfishing, yet no export can limit its success in restocking depleted areas and fisheries (Sale et al. 2005). Accordingly, several attempts to quantify the scale of population persistence under area-based management schemes have been made (Palumbi 2003). Dispersal potential changes with ontogeny in marine species, but the larval stage of most marine organisms gauges the minimum dimensions for marine reserve functioning (Botsford et al. 2003; Palumbi 2003; Sale et al. 2005). Direct estimates of dispersal at these early life stages are rare, but indirect measures can be obtained by estimating the planktonic duration of the egg–larval period (Bradbury and Snelgrove 2001). Realized average dispersal over the entire life history (e.g., plankton larval period and adult migratory stage) of the organism can further be estimated from spatial structure in multilocus genotypic data (Neigel 2002). Both measures of dispersal provide a relative means by which we can examine the scale at which marine populations persist and, similarly, at what scale a successful MPA should function. Here we examine whether dispersal rates of marine fish species change across latitude to evaluate large-scale changes in connectivity and relate to the design of currently established MPAs worldwide.

We hypothesized that two patterns in dispersal would emerge from environmentally associated changes with latitude. First, cooler water masses at higher latitudes would lead to an extended planktonic larval duration (PLD) resulting from decreased growth and development rates. Second, we predicted that increases in planktonic duration would result in greater genetic homogeneity as reflected by various genetic markers, e.g., allozymes, microsatellites, mitochondrial DNA. Admittedly, spatial genetic structure results from a complex interaction of contemporary and historical processes, and the inference of present-day gene flow may be problematic; nonetheless, given the range of species, types of markers, and broad geographic area, it seems unlikely that a systematic bias correlated with latitude may be present. The observed trends in dispersal (potential and realized) were compared with the scale at which MPAs are designed and implemented worldwide in an attempt to evaluate the degree to which dispersal has been a focal point of their design and ability to conserve regional marine fish populations.

Materials and methods

Genetic database

Estimates of F_{ST} were compiled from the literature (1973 to present) with efforts taken to minimize confounding factors influencing population genetic structure. Pelagic species were included in the database with the exception of elasmobranches, which lack a larval dispersal phase. Included studies had two or more subpopulations and utilized one of three types of genetic marker (i.e., mitochondrial DNA (mtDNA), microsatellites, or allozymes). Allozyme studies also had to survey randomly selected loci from 15 or more individuals per subpopulation to be included in the database. In addition, the studies had to provide information on F_{ST} either directly (e.g., global or pairwise F_{ST}) or indirectly (e.g., allele frequency table, expected and observed heterozygosities). For the latter, F_{ST} measures were calculated using Biosys-2 software (version 1.7; available from W.C. Black, Department of Microbiology, Colorado State University, Fort Collins, CO 50823, USA). Studies using mtDNA to calculate F_{ST} were adjusted to assume an island model with diploid gene flow to make mtDNA- and nuclear-derived F_{ST} values comparable (e.g., Kinlan and Gaines 2003). A genetic database of 100 marine fish species from naturally occurring populations was assembled using such methods and criteria (see http://myweb.dal.ca/ibradbur/ for F_{ST} database and references). Maximum latitude of occurrence for each species was gathered using either the FAO Fisheries Global Information System (FIGIS; http://www.fao.org) or the online database FishBase (www.fishbase.org).

Distance between subpopulations from each study was seldom reported in the methods, but geographic information was available from a map of sampling locations and (or) a list of latitude–longitude positions. These data were plotted using mapping software to estimate the maximum distance separating sampled subpopulations for each study. If a landmass separated populations, distance measurements were made around the barrier within 5–10 km of the coastline.

Larval dispersal potential database

The majority of fish species assembled for the dispersal potential database were low- and mid-latitude species, i.e., ranging between 15° and 45° latitude north or south. Our examination of dispersal potential based on published data necessitates several generalizations and assumptions. Factors such as temperature, salinity, and prey density on larval duration were not included owing to lack of information. Moreover, data given on larval duration often represent a single estimate of a range of possible values. Whenever possible, median duration values have been estimated for a given taxon. Most published data are from studies of otolith microstructure in juveniles or adults and therefore represent the time since hatch rather than from fertilization.

Global MPA database

Data on MPA size and central location were gathered using the online MPA Global Database (http://www.mpaglobal.org). Currently, the database contains management areas comprised of both marine and terrestrial components, e.g., nature reserves, national parks, wildlife refuges, etc. Therefore, MPAs were only selected if they had some

Fig. 1. Descriptive statistics on proposed and designated marine protected areas (MPAs) with latitude (north or south). (*a*) Frequency of MPAs by bin sizes 0°–9°, 10°–19°, 20°–29°, etc. (data compiled from multiple sources; see Materials and methods). (*b*) Changes in reserve size with latitude (north or south). Global data set: $\log(y) = 1.68 - 0.0154x$, $R^2 = 0.03$, $N = 439$, $P < 0.05$. Data are from the West Indian Ocean (●), East Indian Ocean (○), West Pacific Ocean (▼), South Pacific Ocean (▽), Australia and New Zealand (■), North America (□), Central America (◆), South America (◇), Caribbean (▲), Europe (△), and West Africa (●).

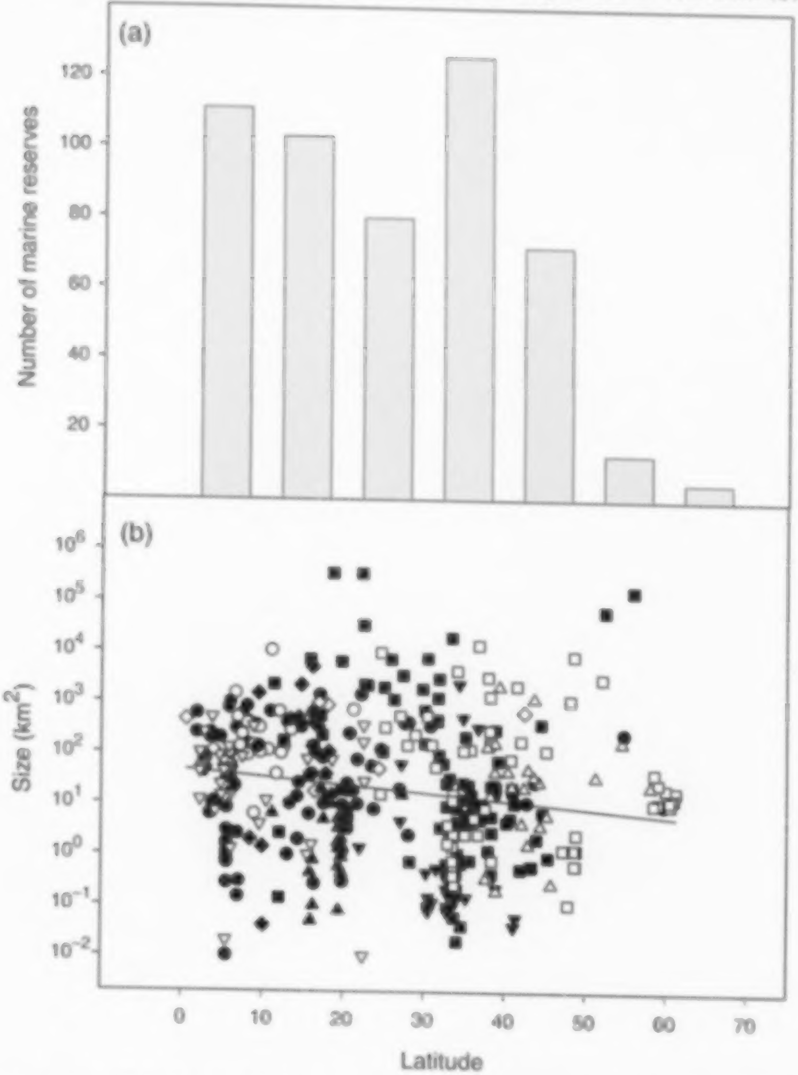

sort of marine designation or explicit description, e.g., marine park, fish nursery reserve, marine conservation area, etc. Ambiguous sites were verified using additional regional online databases where available (West Indian Ocean, http://www.wiomsa.org; North America, http://www2.mpa.gov; Australia, http:// www.deh.gov.au) or otherwise were not included.

Results and discussion

Data on the duration of the planktonic larval period were complied from the literature on 96 species of marine fish (see Bradbury and Snelgrove (2001) for data). Inclusion was limited to species with a clear transition between larval and adult stages and (or) measured using microstructure of the otolith or ear bone. The length of the planktonic larval period was significantly correlated with the maximum latitude of occurrence, supporting our prediction of increases in dispersal potential with latitude (Fig. 2*a*; $R^2 = 42\%$, $N = 96$, $P < 0.001$). As estimates of PLD measure only the larval stage, the inherent assumption is that dispersal potential during the egg stage is consistent between regions or at least not larger at low latitudes. In a separate analysis, we observed a significant increase in the occurrence of species with pelagic eggs at high latitudes, suggesting that increases in dispersal potential observed at high latitudes may indeed

Fig. 2. General characteristics of gene flow (F_{ST}) and dispersal relationships of marine fish populations. (*a*) Planktonic larval durations (PLD) of 96 marine fish species versus maximum latitude (north or south) occupied by marine fish species: $y = 1.108 + 0.097x$, $R^2 = 0.42$, $N = 96$, $P < 0.001$. (*b*) Residuals of F_{ST}–scale (km) relationship versus maximum latitude (north or south) occupied by each marine fish species: $y = 0.858 - 0.0166x$, $R^2 = 0.21$, $N = 100$, $P < 0.001$.

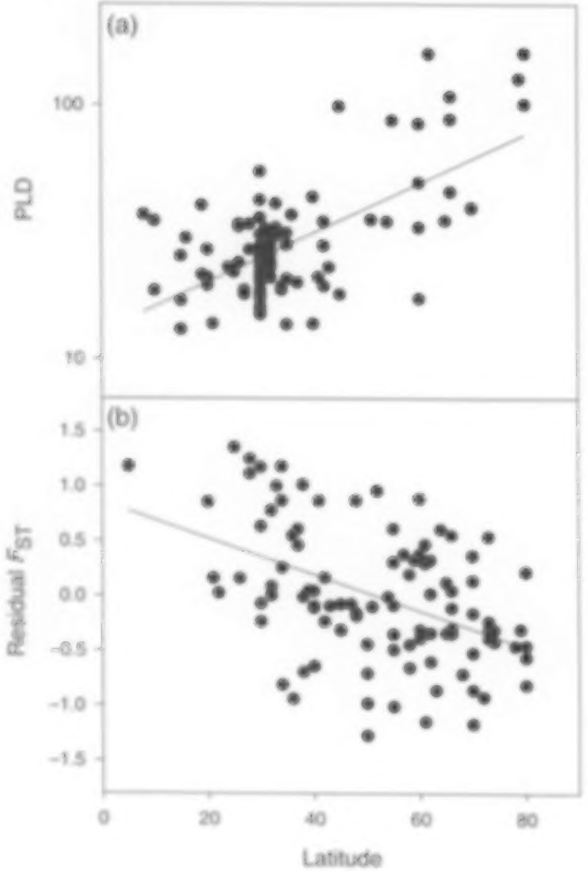

be higher than observed here (I.R. Bradbury, unpublished data).

However, the key question remains: does dispersal potential confer realized dispersal? We examined realized dispersal through a genetic database of 100 marine fish species from naturally occurring populations described in the literature (1973–2004). From these studies, we were able to collect and standardize measures of population subdivision for each species (i.e., F_{ST}; see Materials and methods). F_{ST} measures by themselves are often imprecise, but they provide an indication of average effects of gene flow for comparative purposes (Neigel 2002). The difficulty in F_{ST} meta-analysis is the necessity to account for differences in sampling scale between studies. Sampling scale was decoupled from gene flow using the residuals of the least squares regression of sampling distance and F_{ST}. Regression analysis of those residuals with maximum latitude at which each species occurs indicated a significant relationship (Fig. 2*b*; $R^2 = 21\%$, $N = 100$, $P < 0.001$). Although the F_{ST} relationship is weaker than the PLD trend with latitude, we suspect that much of the variance stems from unaccounted differences in sampling, genetic marker bias, local oceanography, and species-specific phylogeographic patterns.

Marine fish populations seem to be less isolated and experiencing greater levels of gene flow at higher latitudes, very likely the result of an increased PLD. Effective management of marine species requires an understanding of the scales at which such populations are regulated, and our data suggest that spatial management strategies such as implementation of marine reserves will be less effective at high latitudes if they are constructed at scales similar to reserves in tropical regions. Based on the statistical models for both PLD and F_{ST}, there is an ~8% increase in dispersal potential and weakening in population substructure (i.e., F_{ST} using the anti-log) per degree latitude (north or south) from the equator. It is uncertain how to most precisely translate these rates into effective MPA size as neither F_{ST} nor PLD measures are directly linked to spatial scale. Still, we contend that the rate changes of gene flow and PLD with latitude could serve as a benchmark for helping policymakers gauge MPA size – network spacing, especially in situations where more detailed local information on dispersal and fish movements are unknown.

Currently, it is estimated that there are over 4100 protected areas distributed worldwide with at least some marine component, with many of these areas having been constructed with the intent of conserving or increasing local fish populations for the purpose of tourism or regional fisheries. Contrary to expectation, however, we observed only a weak relationship in MPA size with latitude where such data were available (*n* = 439), and furthermore, the relationship was negative and in contradiction to the patterns observed in PLD and gene flow (Fig. 1*b*). This is particularly alarming considering that marine reserves at lower latitudes are often smaller than the dispersal distances of their local fish populations (Nystrom and Folke 2001).

It is possible that the species examined for genetic differentiation and PLD are not a random sample of marine communities. A further analysis by phylogenetic groups was not possible given the limited data. However, comprehensiveness of the data was maximized through large sample sizes and comparison of independent databases. Moreover, an analysis of large-scale trends in dispersal, controlling for body size, and habitat (i.e., depth) suggests latitude as a determining factor (I.R. Bradbury, unpublished data), supporting patterns observed here. Although it is impossible to refute the role of phylogeographic factors in contributing to spatial genetic structure, given the range of species and markers, a systematic bias associated with latitude seems unlikely.

We recognize that designing and implementing MPAs requires consideration of a host of factors other than just dispersal dynamics, of which some are ecologically based (e.g., local biodiversity, habitat availability, etc.) and others are logistical in nature (e.g., sociopolitical, economic, enforceability, etc.; NRC 2000). The degree to which these other variables factor into MPA design depends on goals of that particular MPA. Nonetheless, the scale of dispersal in marine species continues to be singled out as a critical component in successful MPA design (Sale et al. 2005). Given the scarcity of dispersal data for marine species, it is not surprising that empirical demonstrations linking dispersal and MPA function are lacking in the literature. Nonetheless, in light of the substantial theoretical basis for such an association (Botsford et al. 2001; Hilborn et al. 2004), it seems likely that dispersal plays a critical role and should not be ignored.

Marine reserves are probably the best-understood management strategy for marine ecosystems: they reduce fish catch, reduce damage to demersal habitats, and protect diversity. However, as a fisheries management tool, acting either independently or together with other management strategies (e.g., quotas, gear restrictions, etc.), effective MPA design will depend largely on the dispersal dynamics of the marine species that they aim to protect. For this reason, MPAs will only achieve their potential as fisheries management tools if they are based and evaluated on scientific criteria (Sale et al. 2005). We must proceed cautiously as we begin to apply them in higher-latitude regions where the scale of dispersal will undoubtedly pose new challenges in reserve – reserve network design.

Acknowledgements

We thank P. Bentzen, R.S. Gregory, P.V.R. Snelgrove, A.W. Stoner, and M.W. Davis for their comments on early drafts of this manuscript. B. Laurel was supported by funding from the Oceans Branch of Fisheries and Oceans Canada. I. Bradbury was supported by fellowships from the Natural Sciences and Engineering Research Council of Canada (NSERC) and the Killam Trusts.

References

Botsford, L.W., Hastings, A., and Gaines, S.D. 2001. Dependence of sustainability on the configuration of marine reserves and larval dispersal distance. Ecol. Lett. **4**: 144–150.

Botsford, L.W., Micheli, F., and Hastings, A. 2003. Principles for the design of marine reserves. Ecol. Appl. **13**(1): S25–S31.

Bradbury, I.R., and Snelgrove, P.V.R. 2001. Contrasting larval transport in demersal fish and benthic invertebrates: the role of behavior and advective processes in determining spatial pattern. Can. J. Fish. Aquat. Sci. **58**: 811–823.

Hilborn, R., Stokes, K., Maguire, J.J., Smith, A.D.M., Botsford, L.W., Mangel, M., Orensanz, J., Parma, A., Rice, J., Bell, J., Cochrane, K.L., Garcia, S., Hall, S.J., Kirkwood, G.P., Sainsbury, K., Stefansson, G., and Walters, C.J. 2004. When can marine reserves improve fisheries management? Ocean Coast. Manag. **47**: 197–205.

Halpern, B.S. 2003. The impact of marine reserves: do reserves work and does reserve size matter? Ecol. Appl. **13**: S117–S137.

Kinlan, B., and Gaines, S. D. 2003. Propagule dispersal in marine and terrestrial environments: a community perspective. Ecology, **84**: 2007–2020.

National Research Council. 2000. Marine protected areas: tools for sustaining ocean ecosystems. National Academy Press, Washington, D.C.

Neigel, J.E. 2002. Is F_{ST} obsolete? Conserv. Genet. **3**: 167–173.

Nystrom, M., and Folke, C. 2001. Spatial resilience of coral reefs. Ecosystems, **4**: 406–417.

Palumbi, S.R. 2003. Population genetics, demographic connectivity, and the design of marine reserves. Ecol. Appl. **13**: S146–S158.

Roberts, C.M. 2002. Deep impact: the rising toll of fishing in the deep sea. Trend. Ecol. Evol. **17**: 242–245.

Sale, P.F., Cowen, R.K., Danilowicz, B.S., Jones, G.P., Kritzer, J.P., Lindeman, K.C., Planes, S., Polunin, N.V.C., Russ, G.R., Sadovy, Y.J., and Steneck, R.S. 2005. Critical science gaps impede use of no-take fishery reserves. Trends Ecol. Evol. **20**: 74–80.

Efficiencies of benthic and pelagic trophic pathways in a subalpine lake

M. Jake Vander Zanden, Sudeep Chandra, Sang-Kyu Park,
Yvonne Vadeboncoeur, and Charles R. Goldman

Abstract: Although the study of lakes has traditionally focused on pelagic production pathways, recent stable isotope and diet evidence indicates that benthic algal production is an important contributor to fish production. This has led to the suggestion that energy may be more efficiently passed along benthic food chains relative to their pelagic counterparts. To test this idea, we combined stable isotope based assessments of energy flow pathways with estimates of pelagic- and benthic-based primary and secondary production in Castle Lake, California. Approximately 50% of whole-lake primary production and 30% of whole-lake secondary production occurred in benthic habitats. Stable carbon isotopes and dietary data indicated that fish were predominantly supported by benthic (63%) and terrestrial (24%) secondary production. Ecological efficiencies (algal production / invertebrate production) were low in Castle Lake (<3%), though zoobenthic production was more efficiently passed to fish than was zooplankton production. The larger size of benthic prey relative to pelagic prey may affect fish prey selection and foraging efficiency, resulting in differences in ecological efficiency between pelagic and benthic trophic pathways.

Résumé : Alors que l'étude des lacs s'est traditionnellement concentrée sur les voies de production pélagiques, des données récentes provenant d'études des isotopes stables et des régimes alimentaires indiquent que la production des algues benthiques contribue de façon substantielle à la production de poissons. En conséquence, on a suggéré que l'énergie peut être transmise plus efficacement par les chaînes trophiques benthiques que par les chaînes pélagiques correspondantes. Afin de vérifier cette proposition, nous combinons des évaluations des voies du flux énergétique faites à l'aide d'isotopes stables avec des estimations des productions primaire et secondaire, tant pélagique que benthique, au lac Castle, Californie. Environ 50 % de la production primaire du lac entier et 30 % de la production secondaire du lac entier se réalisent dans les habitats benthiques. Les données d'isotopes stables de carbone et les analyses des régimes alimentaires indiquent que les poissons sont surtout alimentés par la production secondaire du benthos (63 %) et du milieu terrestre (24 %). Les efficacités écologiques (production des algues / production des invertébrés) sont faibles au lac Castle (<3 %), bien que la production du zoobenthos soit transmise plus efficacement aux poissons que celle du zooplancton. La taille plus grande des proies benthiques par rapport aux proies pélagiques peut affecter la sélection des proies et l'efficacité de l'alimentation chez les poissons, ce qui entraine des différences d'efficacité écologique entre les voies trophiques pélagique et benthique.

[Traduit par la Rédaction]

Introduction

Several recent studies using stable carbon isotopes ($\delta^{13}C$) have reported that benthic algal production appears to be an important contributor to the production of higher trophic levels in lakes (Hecky and Hesslein 1995; Schindler and Scheuerell 2002; Vander Zanden and Vadeboncoeur 2002). In parallel, it has been recognized that benthic primary production can comprise a substantial portion of whole-lake primary production, with the actual contribution depending on factors such as substrate, lake area, morphometry, and trophic state (Vadeboncoeur et al. 2002, 2003). It is notable that benthic pathways appear to be important even in large lakes in which benthic primary production is expected to be a minor contributor at the whole-lake level (Bootsma et al. 1996). Based in part on this observation, Hecky and

Received 20 October 2005. Accepted 19 May 2006. Published on the NRC Research Press Web site at http://cjfas.nrc.ca on
11 November 2006.
J18952

M.J. Vander Zanden[1] **and S. Chandra.**[2] Center for Limnology, 680 N. Park Street, University of Wisconsin – Madison, Madison, WI 53706, USA.
S.-K. Park. Division of Natural Sciences, Ajou University, San 5 Woncheong-dong, Yeongtong-gu, Suwon, 443-749, South Korea.
Y. Vadeboncoeur. Department of Biological Sciences, 235A BH, Wright State University, Dayton, OH 45435, USA.
C.R. Goldman. Department of Environmental Science and Policy, One Shields Avenue, University of California – Davis, Davis, CA 95616, USA.

[1] Corresponding author (e-mail: mjvanderzand@wisc.edu).
[2] Present address: Department of Natural Resources and Environmental Science, University of Nevada, Reno, 1000 Valley Road, Reno, NV 89512, USA.

doi:10.1139/F06-148

Hesslein (1995) suggested that benthic primary production is more efficiently transferred up the food chain and incorporated into consumer biomass relative to pelagic production. This would suggest that benthic trophic pathways are even more important than one would expect given their relative contributions to whole-lake primary production.

Though some limnological studies have recognized the potential for these dual trophic pathways in lakes (Lindeman 1942; Likens 1985; Jónasson et al. 1990), a pelagic-based paradigm has clearly dominated studies of lakes, particularly during recent decades. Viewing lakes as potentially composed of dual trophic pathways leads to consideration of how benthic and pelagic production and processes are linked (Schindler and Scheuerell 2002; Vadeboncoeur et al. 2002; Vanni 2002). If benthic pathways are as energetically important as indicated by stable isotope surveys, then it is imperative that their role in whole-lake production dynamics is understood. For example, studies that consider only pelagic production would tend to underestimate the productive capacity of ecosystems. Also, the assumption that phytoplankton production represents whole-lake production leads to an overestimate of the efficiency of energy transfer from primary producers to higher consumers if they exploit alternative (benthic and terrestrial) resources. Finally, a number of anthropogenic stresses on aquatic systems directly affect energy flow pathways. Exotic species such as zebra mussels (*Dreseina polymorpha*) and rusty crayfish (*Orconectes rusticus*) can reshuffle production pathways and affect energy flow and trophic efficiencies (Lodge et al. 1994; Karatayev et al. 2002). Lake eutrophication directly affects the distribution of primary and secondary production between habitats in lakes (Vadeboncoeur and Lodge 2000), and the removal of coarse woody habitat from lakes is correlated with reduced growth rates of recreationally important fish species (Schindler et al. 2000). Understanding the linkages between these dual trophic pathways is imperative in light of these management challenges.

Stable isotopes ($\delta^{13}C$ and $\delta^{15}N$) are useful tracers of energy flow pathways and niche partitioning in aquatic food webs (Peterson and Fry 1987; Fry 1988; Kelly et al. 2004). For non-herbivores, there is a 3.4‰ (±0.4‰) increase in $\delta^{15}N$ from prey to predator, such that $\delta^{15}N$ reflects a consumer's trophic position (Minagawa and Wada 1984; Hesslein et al. 1991; Vander Zanden and Rasmussen 2001). Stable carbon isotope values ($\delta^{13}C$) tend to be conserved between prey and predator. The $\delta^{13}C$ of phytoplankton is isotopically depleted relative to benthic algae (Hecky and Hesslein 1995; Vander Zanden and Rasmussen 1999) and can be used to estimate the contributions of littoral and pelagic production to higher trophic levels (Hecky and Hesslein 1995; Vander Zanden and Rasmussen 2001). Thus, concurrent examination of $\delta^{13}C$ and $\delta^{15}N$ allows for descriptions of lake food webs in terms of energy sources and trophic position (Hecky and Hesslein 1995).

In this study, we quantify energy flow and ecological efficiencies for both benthic and pelagic food chains in a well-studied subalpine lake, Castle Lake, California. Our analysis is based on estimates of benthic and pelagic components of primary and secondary production, combined with gut content and stable isotope ($\delta^{13}C$ and $\delta^{15}N$) analysis of food web pathways (Grey et al. 2002). The simple food web structure of Castle Lake provides an opportunity to track energy flow through benthic and pelagic pathways to higher trophic levels and to test the hypothesis that trophic energy transfer is more efficient along benthic pathways (Hecky and Hesslein 1995).

Materials and methods

Study site

Castle Lake (Fig. 1) is located in a protected cirque basin in the Siskiyou Mountains of Northern California (41°13′N, 122°22′W, elevation = 1657 m). It has a maximum depth of 35 m, a mean depth of 11.4 m, summer epilimnion depth averaging 6 m, and a surface area of 20.1 ha. Castle Lake is typically ice-covered for >200 days per year (typically November to June), and mean summer Secchi depth ranges from 9 to 13 m (Elser et al. 1995). Water chemistry, Secchi depth, and phytoplankton production have been monitored annually since 1959 by researchers at University of California – Davis, and there have been no directional changes in water quality variables over this period (Jassby et al. 1990; Elser et al. 1995). Approximately 50% of the surface area of the lake overlies littoral habitat <6 m deep (Axler and Reuter 1996). This habitat is dominated by highly organic sediment (~90%) and rocks (~10%). Macrophytes are sparse and benthic primary production is dominated by periphyton. Castle Lake lacks zooplankton predators such as *Mysis* and *Chaoborus* but supports three fish species: annually stocked rainbow trout (*Oncorhynchus mykiss*) and self-sustaining populations of brook trout (*Salvelinus fontinalis*) and golden shiner (*Notemigonus crysoleucas*).

Pelagic primary production

We measured pelagic and benthic primary productivity along depth profiles and calculated whole-lake productivity using lake bathymetry (Fig. 1), incident solar radiation, and light attenuation rates. Phytoplankton primary productivity (PPR_P) and chlorophyll were measured weekly at the deepest part of the lake between late June and mid-August 2000. Water was collected at 13 depths between the surface and 30 m, and duplicate samples were incubated in situ at each depth using a standard ^{14}C pelagic primary production method, which is described elsewhere (Goldman et al. 1963; Goldman 1968). Total daily incident solar radiation was measured throughout the summer with a LI-COR Li-200 pyranometer. We took weekly light profiles on the days that photosynthesis was measured using a LI-COR Li-193 quantum spherical sensor. Daily phytoplankton productivity rates ($mg\ C \cdot m^{-3} \cdot day^{-1}$) were calculated by dividing productivity measured during the incubation period by the fraction of total daily photosynthetically active radiation received during the incubation.

For each sample depth, we averaged daily phytoplankton productivity from all sample dates ($n = 7$) to produce a single average summer depth profile of PPR_P (Fig. 2*a*). Total areal phytoplankton production was estimated using the following equation:

Fig. 1. Bathymetric map of Castle Lake, California, USA. Zoobenthos sampling locations are indicated with an "X".

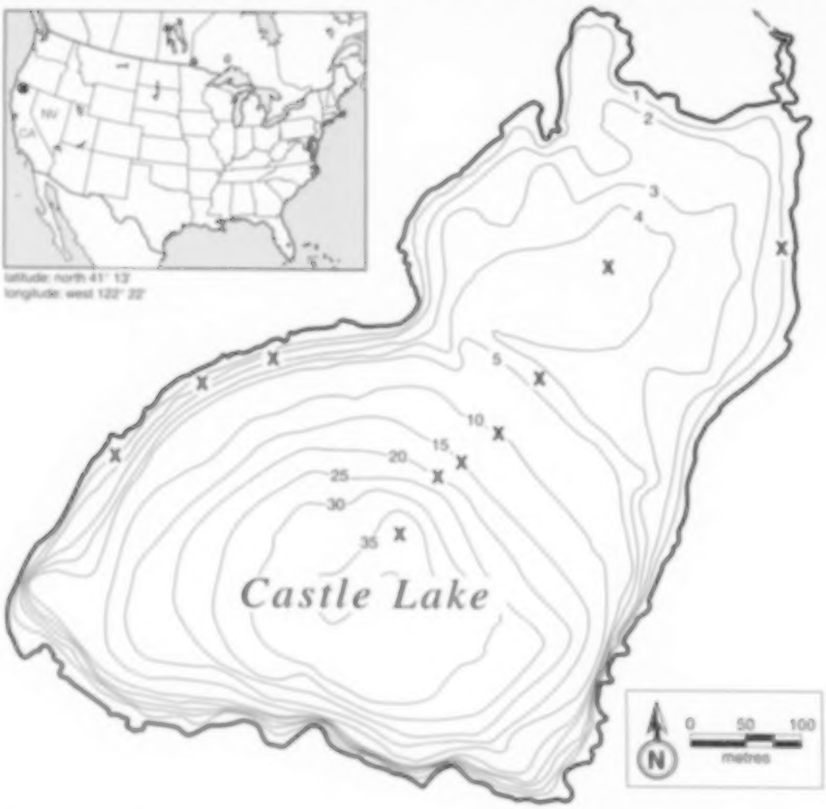

$$\text{(1)} \qquad \mathrm{TPPR_P} = \frac{\left(\sum_{z=0}^{30} V_z \mathrm{PPR}_{\mathrm{P}_{z+0.5}}\right)}{A_0}$$

where $\mathrm{TPPR_P}$ is total pelagic production per square metre of lake (g C·m^{-2}·day^{-1}), z is depth, V_z is the volume of water between depth z and $z + 1$ (calculated as a frustum; Wetzel 2001), A_0 is lake surface area, and $\mathrm{PPR}_{\mathrm{P}_{z+0.5}}$ is the average summer phytoplankton productivity in the middle of each 1 m depth stratum calculated from the linear interpolation between depths of $\mathrm{PPR_P}$ (Fig. 2*a*).

Benthic primary production

Bulk oxygen exchange methods were used to estimate benthic primary productivity on sediment (epipelic) and rock (epilithic) from three depths on one occasion during mid-August 2004. To measure epilithic primary productivity, we placed three light and two dark chambers over large boulders at each of three depths. Each chamber (inner dimensions 10 cm × 10 cm × 8 cm high) was sealed to the rock by placing a 2 kg ring of lead shot over a 10 cm neoprene skirt that extended from the bottom edge of the chamber. Water samples were withdrawn through a port sealed with a serum stopper, and a manually operated paddle was used to disrupt oxygen gradients immediately before withdrawing water samples. Water samples were removed with a 60 cm^3 syringe at the beginning of incubations and upon termination 2 h later. Water samples were fixed for Winkler titration immediately after divers returned to the surface. For epipelic primary productivity, we collected intact sediment cores (5 cm diameter × 8 cm deep, three light, two dark) in acrylic tubes at three depths and incubated them for 2 h at depth. Upon retrieving the cores, overlying water was removed and fixed for Winkler titrations. We calculated gross primary production per square metre of substratum as the net hourly oxygen increase in the light chambers plus the hourly community respiration rate in the dark chambers.

Our approach for extrapolating benthic productivity to the whole lake was slightly different than that for phytoplankton. Benthic productivity is strongly dependent on light (Vadeboncoeur et al. 2001), and our light data were more comprehensive than our benthic productivity data. Therefore, we used daily solar radiation data for the month of August to calculate whole-lake productivity based on our more limited (compared with phytoplankton) in situ production measurements. Benthic primary productivity ($\mathrm{PPR_B}$) was measured during midday in full sun and thus represents $P_{\mathrm{B}_{\max}}$ at the three depths for both sediment and rock (sediment, $P_{\mathrm{B}_{\max}} = -6.55 \times \text{depth} + 76.4$, $r^2 = 0.98$; rock, $P_{\mathrm{B}_{\max}} = -4.5 \times \text{depth} + 46$, $r^2 = 0.70$). $P_{\mathrm{B}_{\max}}$ declined linearly with depth and reached zero at 11.7 m. Periphyton productivity was estimated daily at 0.1 m depth intervals from sunrise to sunset using the following equation:

Fig. 2. Depth-specific production values and carbon isotope values for Castle Lake, California: (*a*) mean summer phytoplankton primary production (PPR_P), (*b*) benthic primary production (PPR_B), (*c*) benthic secondary production (by month), and (*d*) $\delta^{13}C$ of benthic chironomids and oligochaetes by depth.

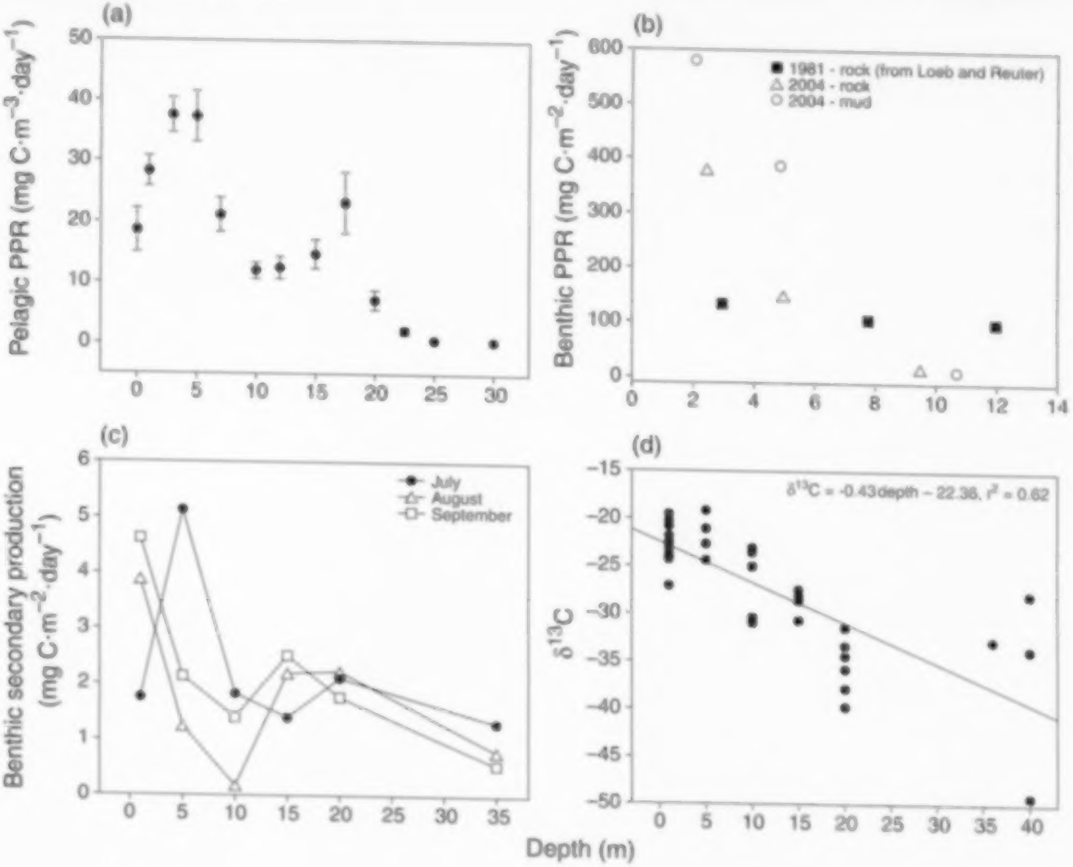

$$(2a)\qquad PPR_{B_z} = \Delta t \sum_{\text{sunrise}}^{\text{sunset}} P_{B_{\max,z}} \tanh(I_{zt}/I_k)$$

where $P_{B_{\max,z}}$ at depth was estimated from the above regression equations. Surface irradiance was estimated at 0.5 h (Δt) time intervals using a sine function, and maximum light measured midday light intensities (McBride 1992). Light intensity at depth for each 0.5 h interval (I_{zt}) was calculated from surface irradiance and K_d (0.24). The light intensity of onset of saturation (I_k) was set to 400 µmol·m^{-2}·s^{-1}. Whole-lake benthic primary production (g C·day^{-1}) was estimated at 0.1 m depth increments for depths between 1.5 and 12 m:

$$(2b)\qquad TPPR_B = \frac{\left(\sum_{z=1.5}^{12} a_z PPR_{B_z}\right)}{A_0}$$

Periphyton mats were much less well developed between 0 and 1.5 m. To be conservative, we did not estimate primary production for these shallow depths. a_z is the surface area of sediments that occurs at a given water column depth and is calculated using the planar surface area of the lake at the top and bottom of each depth interval ($a_z = A_z - A_{z+i}$, where i is the vertical depth increment (e.g., 0.1)). We made no correction for the increase in sediment surface area attributable to basin slope. Based on habitat surveys, we assumed that 10% and 90% of littoral surface area consisted of large rocks and soft sediments, respectively.

Macrophyte biomass and production are negligible in Castle Lake (Hagley 1989) and were thus ignored in our whole-ecosystem production calculations. Excluding macrophytes provided a more conservative measure of the contribution of benthic production to the lake.

Secondary production

Secondary productivity (mg C·m^{-3}·day^{-1}) of the dominant zooplankton, *Daphnia rosea*, was estimated using the egg ratio method and data collected in 2000. This approach calculates the product of biomass and estimated growth rate for the summer growth season (Saunders and Lewis 1988). Numerical growth rate (*b*) is used as a proxy for biomass growth rate (Paterson et al. 1997). A Schindler trap (12 L volume, 80 µm mesh) was used to collect zooplankton four times (June, July, August, September) from depths of 1, 3, and 5 m (epilimnetic) during day (1300) and night (2200).

Using the equation of Paloheimo (1974), *Daphnia* production (volumetric) was estimated as the mean of the four nighttime epilimnetic samples. Biomass was converted to carbon by assuming 40% carbon content (dry weight). Whole-lake *Daphnia* production was estimated as the product of epilimnetic volume (depth of 6 m) and the volumetric estimate of *Daphnia* production from nighttime epilimnetic samples. The *Daphnia* production estimate was converted to whole-lake zooplankton production by multiplying by 1.24, which is the average weekly ratio of zooplankton production to *Daphnia* production estimated from 1996 data (S.-K. Park, unpublished data).

Benthic secondary production was estimated as the product of individual mass, population density, and estimated production to biomass (*P*/*B*) ratios (Strayer and Likens 1986). Zoobenthos samples were collected along a single depth transect at 1, 5, 10, 15, 20, and 35 m (Fig. 1) on 18–19 July, 22–25 August, and 12–13 September 2000. On soft substrates (>2 m depths), each sample was a composite of four Ekman grab samples (0.0225 m^2). Four additional littoral zone samples were collected from hard or heterogeneous substrates (<2 m depths) on each date. A snorkeler used a battery-powered underwater suction sampling device similar to that described by Taylor et al. (1995) to collect organic material to a maximum depth of 10 cm within a randomly placed 0.25 m quadrat. The benthic samples were sieved (500 μm), sorted, and preserved in 70% ethanol. Invertebrates were identified to family (Chironomidae and Oligochaeta only) or most often genus, enumerated, dried at 70 °C for 24 h, and weighed. Taxon-specific annual *P*/*B* was estimated from the invertebrate allometric equation (Banse and Mosher 1980). *P*/*B* was multiplied by biomass ($mg \cdot m^{-2}$) at each site for each taxon (genus or family), giving the taxon-specific annual production ($mg \cdot m^{-2} \cdot year^{-1}$). Summing these across taxa at a sampling site gave an estimate of total annual production ($mg \cdot m^{-2} \cdot year^{-1}$) for a site. Annual production estimates were converted into daily carbon units ($mg\ C \cdot m^{-2} \cdot day^{-1}$) by assuming that dry biomass was 45% carbon by weight (Strayer and Likens 1986; Wetzel 2001) and dividing annual production by 150, which is the number of ice-free days. By dividing by the number of ice-free days (rather than by 365 (the total number of days in the year)), we maintain consistency with our other production estimates, which are based on the summer ice-free season only. Furthermore, the growth rate of benthic invertebrates (and thus secondary production) is low at the cold temperatures associated with the winter ice-cover period (Wetzel 2001; O'Sullivan and Reynolds 2004).

Summer averages for benthic secondary production were calculated for 1, 5, 10, 15, 20, and 35 m. Linear interpolation was used to estimate production at 1 m intervals at depths <5 m and 5 m intervals at depths > 5 m. Whole-lake benthic secondary production was estimated as $\Sigma a_z\ \mathrm{BSP}_z$, where a_z is the surface area of sediments at depth z, as described for periphyton, and BSP_z is secondary production rate ($mg\ C \cdot m^{-2} \cdot day^{-1}$) at depth z.

Fish

For each of the three fish species in Castle Lake, reliance on benthic, pelagic, and terrestrial sources was estimated using diet data and stable isotopes (below). We did not attempt to estimate ecological efficiencies for fish in this study, though to generalize fish species-specific trophic reliance to the whole-lake level, we needed some way to weight the contribution of the three fish species to whole-lake fish production. One approach would be to weight the three fish species equally, though they likely differ in their contribution to whole-lake fish production. We used previous quantitative fish survey data to estimate production for the three species and weighted the contribution of the fish species according to estimated production. Elser et al. (1995) estimated fish density and biomass during the period 1989–1991 in Castle Lake. We used only data from 1989, the first year of three in which rainbow trout were not stocked in Castle Lake. The fish community in 1989 was still dominated by rainbow trout and would be most similar to the present-day rainbow trout stocking regime (S. Baumgartner, California Fish and Game, 601 Locust Street, Redding, CA 96001, USA, personal communication). Annual production of rainbow trout, brook trout, and golden shiner were approximated as the product of biomass from 1989 hydroacoustic surveys (gill netting and purse seining used to partition according to species) and the annual *P*/*B* for each species reported by Randall and Minns (2000). Contributions of the three fish species to total fish production were estimate to be 42% brook trout, 45% rainbow trout, and 13% golden shiner. Isotope-based estimates of resource use for each fish species (mean from the two methods) were weighted according to the above estimates of fish species contribution to total fish production.

Stable isotopes

Benthic macroinvertebrates were collected for stable isotope analysis during the summer of 2000 at the same sites (Fig. 1) and dates as the estimates of benthic secondary production and were sorted to genus or family. Samples collected at 1 m depths were considered shallow water sites. Terrestrial invertebrates were collected from vegetation within 1 m of shore using a sweep net or were recovered from fish stomachs. Terrestrial invertebrate taxa were identified to family. Stable isotope analysis was performed on samples identified to genus or family, but values were later aggregated to family or order for reporting (Table 1; Fig. 3).

Zooplankton was collected for stable isotope analysis on eight dates between 28 June and 15 September during 1999 and 2000. Samples were collected by 30 m vertical tows using an 80 μm mesh zooplankton net near the deepwater sampling station. *Daphnia rosea*, *Diaptomus novamexicanus*, and *Holopedium gibberum* were sorted and analyzed separately. On five dates, profundal *Daphnia middendorffiana* (profundal-dwelling *Daphnia*) were collected from 30 to 34 m using a Schindler trap (80 μm mesh).

Rainbow trout, brook trout, and golden shiner were collected using gill nets, minnow traps, and angling for stable isotope analysis and gut content enumeration from 27 June to 10 September 2000 (Table 2). Additionally, six large (>30 cm; mean length = 39 cm) rainbow trout were angled through the ice on 5 May 2001. Stomach contents were removed within 1 h of capture and immediately frozen. Contents were later identified to the lowest taxonomic level possible (typically family) and weighed. Contents were categorized as detritus, fish, zooplankton, terrestrial insects,

Table 1. Stable carbon and nitrogen isotope data (mean values and 1 standard error, SE) from Castle Lake biota collected in 2000.

Taxa	*n*	δ^{15}N	SE	δ^{13}C	SE	Depth or habitat
Daphnia rosea	11	2.7	0.2	–31.3	0.4	Epilimnion and metalimnion
Diaptomus novamexicanus	8	3.9	0.6	–31.4	0.7	Epilimnion and metalimnion
Holopedium gibberum	3	—	—	–33.5	1.3	Epilimnion and metalimnion
Oligochaeta–Chironomidae	19	1.5	0.3	–22.4	0.4	Littoral benthic
Ephemeroptera	15	1.0	0.2	–21.5	0.8	Littoral benthic
Odonata	18	3.4	0.2	–22.0	0.3	Littoral benthic
Megaloptera	8	3.5	0.2	–21.3	0.6	Littoral benthic
Trichoptera	15	2.0	0.5	–24.6	0.8	Littoral benthic
Bivalvia	4	2.1	0.4	–26.2	0.4	Littoral benthic
Terrestrial (predatory)	4	3.9	1.6	–27.0	0.5	Riparian
Terrestrial (herbivorous)	8	1.3	1.2	–24.4	0.6	Riparian
Oligochaete–Chironomidae	10	2.9	0.3	–27.6	0.9	Benthic (10–15 m)
Oligochaete–Chironomidae	12	2.3	0.6	–33.6	2.0	Benthic (20–40 m)
Daphnia middendorffiana	13	1.4	0.3	–43.5	0.5	Benthic–profundal (34 m)
California newt	2	6.4	0.5	–24.0	0.2	Littoral benthic
Brook trout	37	8.4	0.2	–25.2	0.4	—
Golden shiner	14	7.7	0.2	–22.9	0.4	—
Rainbow trout (<30 cm)	16	8.6	0.5	–23.2	0.7	—
Rainbow trout (>30 cm)	7	12.0	0.1	–19.9	0.2	—

Fig. 3. Stable isotope (δ^{15}N and δ^{13}C) food web diagram for the major taxa of Castle Lake, California. Symbols are as follows: D-P, profundal *Daphnia middendorffiana*; D-M, metalimnetic *Daphnia rosea*; COP, copepods; CHOL-D, deepwater chironomids and oligochates; CHOL-I, intermediate depth chironomids and oligochates; CHOL-S, shallow-water chironomids and oligochates; BIV, bivalves; TRI, trichoptera; EPH, ephemeroptera; ODO, odonates; SIA, sialids; TER-P, predatory terrestrial insects; TER-H, herbivorous terrestrial insects; GS, golden shiner (*Notemigonus crysoleucas*); BT, brook trout (*Salvelinus fontinalis*); RBT-S, small (<30 cm) rainbow trout (*Oncorhynchus mykiss*); RBT-L, large (>30 cm) rainbow trout.

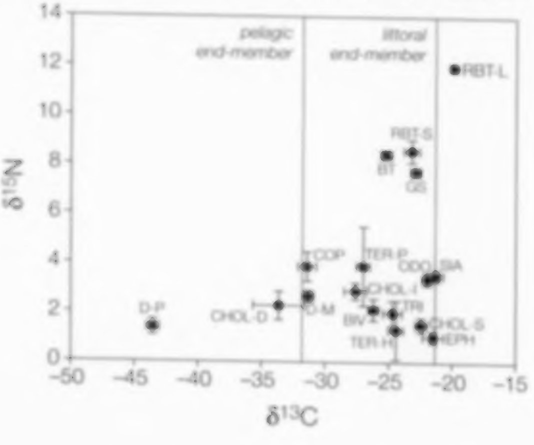

aquatic insects, and unidentified insects. Not enough golden shiners were collected in 2000 for an adequate diet assessment. Detritus comprised <0.2% of gut content for both salmonids and was thus not included further in the analysis. Twenty-five percent of the total gut content (dry weight) for rainbow trout and 15% for brook trout could be classified no further than unidentified insects. This prey category was omitted so that diets are expressed as percentage of identifiable prey items to total gut content weight (dry weight). The effect of this assumption is conservative in that it would tend to overestimate the importance of zooplankton to fish diets.

Dorsal muscle tissue was removed from each fish and frozen for stable isotope analysis. Fish and invertebrate samples were dried at 60 °C for at least 24 h and ground into a fine powder using mortar and pestle. Samples were packed into 8 mm × 5 mm tin capsules and analyzed for nitrogen and carbon isotope signatures using continuous flow isotope ratio mass spectrometry (20–20 mass spectrometer; Europa Scientific, Sandbach, UK). Isotopic ratios were expressed as a per mil (‰) deviation defined by the following equations: $\delta^{13}C = [(^{13}C/^{12}C)_{sample}/[(^{13}C/^{12}C)_{standard} - 1]] \times 1000$ and $\delta^{15}N = [(^{15}N/^{14}N)_{sample}/[(^{15}N/^{14}N)_{standard} - 1]] \times 1000$. More positive values are isotopically enriched, meaning that they contain proportionally higher concentrations of the heavier ^{13}C or ^{15}N isotope. Replicate samples and a standard material were analyzed approximately every 20 samples for quality control. Replicate variation was less than 3% and machine analytical error was within 0.2‰ for both δ^{15}N and δ^{13}C.

Isotope models

Zoobenthos, zooplankton, and terrestrial insects are all known prey of Castle Lake fishes. Each of these prey items have a unique δ^{13}C value, though they can not be differentiated using δ^{15}N. Finding a unique solution for the contribution of these three sources would require two tracers. Here, we use two approaches to approximate contributions of these three sources to fish production. First, we apply the probabilistic mixing model (IsoSource, version 1.2) of Phillips and Gregg (2003), which calculates the range of possible solution values for the three potential sources. End-members for the mixing model were as follows: pelagic (mean δ^{13}C values of individual, nonprofundal zooplankton; n = 22, –31.6‰); terrestrial (mean of all terrestrial insects; n = 12, –25.3‰);

Table 2. Diet data, expressed as percentage of total gut volume or weight, from brook trout (*Salvelinus fontinalis*), rainbow trout (*Oncorhynchus mykiss*), and golden shiner (*Notemigonus crysoleucas*) from Castle Lake from multiple time periods.

Year	*n*	Planktonic	Benthic	Terrestrial	Fish	Reference
Brook trout						
1941–1944	180	22	28	48	3	Wales 1946
1963–1965	175	14	76	10	0	Swift 1970
1989	—[a]	18	74	8	0	Elser et al. 1995
1990	—[a]	18	53	29	0	Elser et al. 1995
1991	—[a]	0	26	74	0	Elser et al. 1995
2000	43	<0.5	91	6	2	This study
Mean		12	58	29	1	
SD		9.5	26.9	27.3	1.3	
Rainbow trout						
1941–1944	134	13	19	62	7	Wales 1946
1963–1965	275	33	22	45	0	Swift 1970
1989	—[a]	24	44	33	0	Elser et al. 1995
1990	—[a]	20	66	15	0	Elser et al. 1995
1991	—[a]	0	36	64	0	Elser et al. 1995
2000	24	0	59	41	0	This study
Mean		11	51	38	0	
SD		12.6	13.4	20.4	—	
Golden shiner						
1989	—[a]	40	20	40	0	Elser et al. 1995
1990	—[a]	50	4	46	0	Elser et al. 1995
1991	—[a]	47	25	28	0	Elser et al. 1995
Mean		46	16	38	0	
SD		5.1	11.0	9.2	—	

[a] Elser et al. (1995) reported that diets were analyzed for "up to 50 individuals of each species" in each year.

and littoral (mean of Ephemeroptera, Oligochaeta, and Chironomidae from <5 m depth; $n = 34$, −22.0‰). These particular primary consumer taxa were chosen as the littoral end-member because they are ^{13}C-enriched and are thus most indicative of a pure periphyton signal.

To provide an independent estimate of benthic reliance and to validate results from the Phillips and Gregg (2003) approach, we use gut content data on percent consumption of terrestrial prey to constrain the mixing model so as to provide a unique solution for zoobenthos and zooplankton sources. Assuming no fractionation, the δ^{13}C of a consumer (fish) is the diet-weighted average of its various prey:

$$(3)\qquad \delta^{13}\mathrm{C}_{\mathrm{cons}} = (\delta^{13}\mathrm{C}_{\mathrm{terr}}\, t) + (\delta^{13}\mathrm{C}_{\mathrm{ben}}\, b) + (\delta^{13}\mathrm{C}_{\mathrm{pel}}\, p)$$

where t, b, and p are the proportional contributions of terrestrial, benthic, and pelagic prey, respectively. By approximating the percent contribution of terrestrial insects from gut content data from Castle Lake (Wales 1946; Swift 1970; Elser et al. 1995), there exists a unique solution for the mixing model. From eq. 3, setting $p = 1 - (b + t)$ and solving for b yields

$$(4)\qquad b = -\frac{(\delta^{13}\mathrm{C}_{\mathrm{terr}}\, t) + \delta^{13}\mathrm{C}_{\mathrm{pel}} - (\delta^{13}\mathrm{C}_{\mathrm{pel}}\, t) - \delta^{13}\mathrm{C}_{\mathrm{cons}}}{\delta^{13}\mathrm{C}_{\mathrm{ben}} - \delta^{13}\mathrm{C}_{\mathrm{pel}}}$$

Contributions of pelagic and benthic prey to fish diets were estimated using eq. 4 and the mean terrestrial consumption values from Table 2. We increased and decreased (relative to the mean value) the values for percent terrestrial diet by 30% (relative to the original value) to assess sensitivity to this assumption.

Ecological efficiencies and benthic–pelagic coupling

Ecological efficiencies (EE_i) were calculated separately for benthic and pelagic pathways:

$$(5)\qquad \mathrm{EE}_i = \left(\frac{P_{n,i}}{P_{n-1,i}}\right) \times 100$$

where EE_i is the ecological efficiency for pathway i, $P_{n,i}$ is the production at trophic level n supported by pathway i, and $P_{n-1,i}$ is the production at trophic level $n - 1$ from pathway i.

Benthic secondary production is supported by a mix of pelagic (phytoplankton fallout) and benthic–littoral primary production sources. To estimate the relative contribution of these two primary production sources to zoobenthos, we estimated zoobenthos δ^{13}C at each of 12 depth intervals from the regression equation in Fig. 2*d*. For each depth, we used a two-source mixing model (pelagic end-member = −31.6‰, littoral end-member = −22‰) to estimate the contribution of pelagic (phytoplankton) primary production. The contribution (%) of pelagic sources to benthic secondary production at the whole-lake level was estimated as follows:

$$(6)\qquad \mathrm{ZP}_{\mathrm{pel}} = \sum a_z\, \mathrm{BSP}_z\, \mathrm{pel}_z$$

where a_z is lake area (m^2) at depth z, BSP$_z$ is benthic secondary production rate (mg C·m^{-2}·day^{-1}) at depth z, and pel$_z$ is percent pelagic reliance (from mixing model above) at depth z. Dividing this value by total benthic secondary production yields the (proportional) contribution of pelagic primary production to benthic secondary production.

Results

Primary and secondary production

The daily summer average phytoplankton primary production (PPR$_P$; mg C·m^{-3}·day^{-1}) varied as a function of lake depth, with peak values of 37 mg C·m^{-3}·day^{-1} at 3–5 m and a secondary peak of 23 mg C·m^{-3}·day^{-1} at 17.5 m (Fig. 2*a*). Benthic primary production declined with depth and was effectively 0 at 12 m for both epilithic and epipelic primary production (Fig. 2*b*). The mean coefficient of variation for benthic primary production measurements at a site was 31%. Benthic primary production values from 2004 were higher than those reported by Loeb and Reuter (1981). Whole-lake primary production (benthic + pelagic) was estimated to be 464 mg C·m^{-2}·day^{-1} (total production = 93 300 g C·day^{-1}). Of this, 47% was benthic (220 mg C·m^{-2}·day^{-1}) and 53% was pelagic (244 mg C·m^{-2}·day^{-1}).

Benthic secondary production for Castle Lake was estimated to be 2.4 mg C·m^{-2}·day^{-1}. Benthic secondary production tended to decrease with depth (BSP = –0.061 × depth + 2.94, r^2 = 0.28; Fig. 2*c*). Benthic secondary production estimates show a secondary peak at intermediate depths (15–20 m). Chironomid and oligochaete carbon isotope values become isotopically depleted with depth (Fig. 2*d*), indicating a shift from benthic algae to phytoplankton-derived detritus with depth. Zooplankton production was estimated to be 5.5 mg C·m^{-2}·day^{-1}. Whole-lake secondary production was thus estimated to be 7.9 mg C·m^{-2}·day^{-1} (1583 g C·day^{-1}), with approximately 30% being benthic (475 g C·day^{-1}) and the remaining 70% (1108 g C·day^{-1}) being pelagic.

Stable isotopes and diets

Mean δ^{13}C and δ^{15}N values (±1 standard error, SE) for major taxonomic groups of the Castle Lake food web were calculated (Table 1), and values were plotted in a δ^{13}C–δ^{15}N biplot (Fig. 3). Zooplankton δ^{13}C values averaged –31‰, whereas littoral benthic invertebrates were in the –21‰ to –25‰ range. Terrestrial insects averaged –25‰. Profundal zoobenthos (chironomids and oligochaetes) and profundal-dwelling *Daphnia middendorffiana* exhibited δ^{13}C values that were highly depleted (Table 1).

Rainbow trout (<30 cm), brook trout, and golden shiner all had δ^{15}N values ~4‰ above that of invertebrates and δ^{13}C values indicative of benthic- and (or) terrestrial-dominated diets. Rainbow trout δ^{15}N and δ^{13}C increased with size, with large (>30 cm) rainbow trout exhibiting elevated nitrogen and carbon signatures, indicating a diet of small benthivorous fishes.

In 2000, brook trout gut contents were dominated by zoobenthos (90%), with minor contributions of terrestrial insects (Table 2). Rainbow trout smaller than 30 cm consumed a mix of zoobenthos and terrestrial insects. Large (>30 cm) rainbow trout (n = 7) all had empty stomachs. Neither rainbow trout nor brook trout consumed substantial amounts of zooplankton in 2000. Historical data also showed that brook trout and rainbow trout preyed primarily on zoobenthos (averaging 50%–60%) and terrestrial insects (averaging 30%–40%) (Wales 1946; Swift 1970; Elser et al. 1995). Elser et al. (1995) reported that zooplankton were also a component (10%) of trout diets. We did not conduct gut content analysis for golden shiners, but historical data (1989–1991) indicate that golden shiners consumed a mix of zooplankton (46%), terrestrial insects (38%), and zoobenthos (16%). Fish diets varied widely from year to year and among studies (Table 2).

Stable isotopes also indicated high reliance of Castle Lake fishes on benthic prey. Mean (±1 SD) zoobenthivory estimates using IsoSource 1.2 (Phillips and Gregg 2003) were 38% (±18%) for brook trout, 74% (±11%) for golden shiner, and 69% (±12%) for small rainbow trout (Table 3). Estimates based on eq. 4 (using gut content based estimates of terrestrial insect contributions to diet) were similar to those using IsoSource (Table 3). Increasing and decreasing estimates of terrestrial consumption by 30% produced a range of benthic reliance estimates (shown in parentheses in Table 3). Overall, isotope-based estimates of benthic reliance corresponded with dietary estimates, although stable isotopes indicated lower pelagic reliance than diet data for golden shiner.

Ecological efficiencies

Ecological efficiencies (primary production / secondary production) for benthic and pelagic pathways were estimated to be 1% and 3%, respectively (Fig. 4). Approximately 35% of whole-lake zoobenthic production in Castle Lake was supported by phytoplankton detritus. Adjusting for this reduced the ecological efficiency for the benthic primary–secondary production link from 1% to ~0.6%.

The contributions of benthic, pelagic, and terrestrial prey in supporting Castle Lake fish were estimated to be 63%, 13%, and 24%, respectively. We did not estimate absolute ecological efficiencies at the invertebrate–fish link for benthic and pelagic pathways, because the available fish production data were from a different year than that of our study. We can estimate relative differences in benthic and pelagic ecological efficiencies and find that benthic ecological efficiency at the invertebrate–fish level is nearly 20 times higher than that for pelagic pathways (Fig. 4).

Discussion

Energy efficiencies

Benthic and, secondarily, terrestrial production pathways appear to be most important in supporting fish populations in Castle Lake, California. Although the pelagic zone supported the majority (~70%) of whole-lake secondary production, zooplankton production did not contribute substantially to the adult fish population. Rather, the primary energy source supporting fish was benthic, based on independent stable isotope and dietary evidence. This general result supports the hypothesis of Hecky and Hesslein (1995) that benthic production is efficiently passed up the food chain to higher consumers relative to pelagic primary production, though we also found that at the primary–secondary produc-

Table 3. Estimates (%) of the contributions of zooplankton, zoobenthos, and terrestrial prey to rainbow trout (*Oncorhynchus mykiss*), brook trout (*Salvelinus fontinalis*), and golden shiner (*Notemigonus crysoleucas*) in Castle Lake, California.

	δ^{13}C (‰)	Zooplankton (–31.6‰)[a]	Zoobenthos (–22‰)[a]	Terrestrial (–25.3‰)[a]
IsoSource (version 1.2)				
Rainbow trout (<30 cm)	–23.18	7.5 (5.5)	69.9 (13.9)	22.7 (16.1)
Brook trout	–25.2	18.4 (10.3)	37.0 (18.9)	44.6 (26.5)
Golden shiner	–22.86	6.3 (4.8)	74.4 (12.3)	19.3 (14.0)
Equation 4				
Rainbow trout (<30 cm)	–23.18	0	62 (56–70)	38
Brook trout	–25.2	23	47 (42–54)	29
Golden shiner	–22.86	0	62 (51–73)	38

Note: IsoSource (version 1.2) is from the method of Phillips and Gregg (2003). Values are mean (±1 standard deviation). Equation 4 uses gut content data to approximate consumption of terrestrial prey. Values in parentheses are zoobenthivory estimates resulting from a 30% increase and 30% decrease, respectively, in terrestrial prey consumption.

[a] Values in parentheses (after zooplankton, zoobethos, and terresirial) are end-member values used in mixing models.

Fig. 4. Contributions of benthic, pelagic, and terrestrial production to total production for primary producers, primary consumers, and fish in Castle Lake, California. Ecological efficiency = (predator production / prey production) × 100.

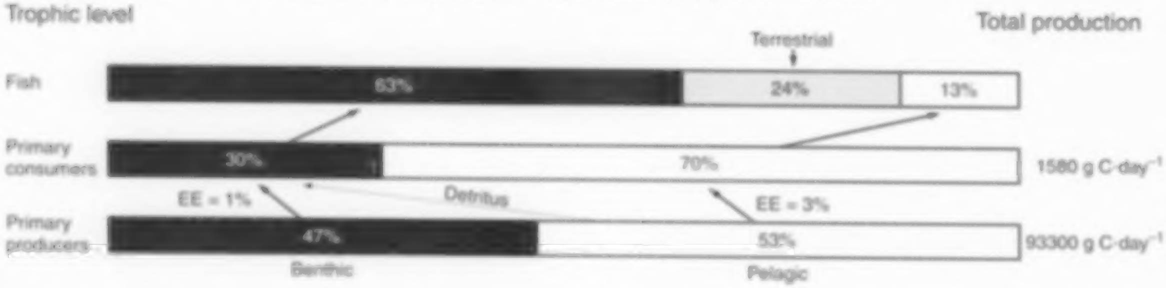

tion link, pelagic trophic transfer appeared to be more efficient than the benthic pathway.

The stable isotope approach traces the ultimate source of primary production, such that profundal zoobenthos supported by phytoplankton detritus are considered to be pelagic in origin. We estimated that roughly 35% of whole-lake zoobenthos production in Castle Lake was supported by pelagic phytoplankton detritus. This has the effect of reducing the benthic primary–secondary ecological efficiency estimate, as profundal zoobenthos production is partially supported by pelagic resources. Fish stable carbon isotope values tend to be enriched, indicating little reliance on profundal resources. The approach of lumping littoral and profundal benthic prey as zoobenthos may not be appropriate, as fish seem to exploit the littoral component of the zoobenthos pool. The above discussion highlights the importance of considering benthic–pelagic coupling in its many forms, including the role of phytoplankton detritus in supporting profundal zoobenthos, and also highlights how zoobenthos from different habitats are used by higher trophic levels.

Our whole-lake estimates of benthic primary production in Castle Lake are higher than previous estimates of epilithic primary production for this lake (Loeb and Reuter 1981). This may be partly due to the differences in methods. In both Lake Tahoe and Castle Lake, our estimates of primary production on rocks using oxygen methods in 2004 were two to three times those using ^{14}C in the late 1970s (Loeb and Reuter 1981). However, given that we do not correct for increased surface area due to littoral slope, the average hourly estimates of littoral primary production on rocks used here may not be substantially different than earlier measurements (Loeb et al. 1983). Additionally, we measured primary production on organic sediments, the dominant substratum in Castle Lake. Sediments consistently have five to 10 times higher rates of production than periphyton on rocks (Vadeboncoeur et al. 2001). The high metabolic activity of sediments relative to rocks in Castle Lake was also seen in a whole-lake epilimnetic nitrogen addition in which algae on sediments took up over 50% of added nitrogen (Axler and Reuter 1996). Indeed, previous estimates of whole-lake epipelic production using ^{14}C indicated that whole-lake epipelic primary production equaled or exceeded whole-lake phytoplankton production (Sanders 1976; Axler and Reuter 1996). Our measurements over 30 years later yielded the same result. Thus, we conclude that the difference in substratum, not the difference in methods, is primarily responsible for the higher rates of benthic primary productivity measured in this study.

Ecological efficiencies at the primary producer – primary consumer link differed between benthic and pelagic habitats. The ecological efficiency of the benthic primary producer – zoobenthos (0.5%–1%) link is lower than that for phytoplankton–zooplankton (3%). A part of this disparity could be attributed to using O_2 exchange methods for benthic algae and ^{14}C methods for phytoplankton. However, similar differences at the primary producer – primary consumer link have been observed in other lakes. In Lake Thingvallavatn, Iceland, the ecological efficiency between phytoplankton and zooplankton is 5.2%, whereas it is 2.1% between periphyton and zoobenthos (Jónasson 1992). The differences in ecological efficiency may be indicative of real, but as yet unexplored, ecological contrasts between habitats. Zooplankton can be efficient at depleting their food supply (Cyr and Pace 1993), but similar analyses are not available for epipelon and benthic grazers. Furthermore, we included benthic predators (megalopterans and odonates) in our estimates of zoobenthic production, which has the effect of depressing estimates of ecological efficiency.

Our estimates of ecological efficiency (consumer production / prey production) are the result of two separate efficiencies: growth conversion efficiency (growth / consumption rate) and consumption efficiency (consumption rate / available production) (see Strayer 1991). The low ecological efficiencies reported here suggest that consumers are not efficiently consuming the available production at the preceding trophic level. Zooplankton appear to be an underexploited prey item of fish in this lake, though consumption by juvenile and young-of-the-year fishes was not quantified in this study. Previous studies indicate that this can be an important source of zooplanktivory in lakes (Post et al. 1997).

Why might ecological efficiencies be higher at the zoobenthos–fish link compared with the zooplankton–fish link? Clearly the specific feeding adaptations of the fish species being studied will influence relative prey profitability (Werner and Gilliam 1984). All three fish species in Castle Lake are known to have diverse diets, feeding on a mix of zoobenthos, zooplankton, surface insects, and fish as available (Wales 1946; Swift 1970; Elser et al. 1995), and none of these species is considered strict zooplanktivore or zoobenthivore.

One potential explanation for the efficient use of zoobenthic resources involves the differences in body size between zoobenthos and zooplankton. In Castle Lake, zoobenthos prey weights were, on average, more than two orders of magnitude larger than zooplankton weights. Furthermore, the zoobenthos size-frequency distribution has an extended tail of large-sized individuals. Even if our sampling protocol missed the small end of the zoobenthos size distribution, the existence of large-sized zoobenthic prey (relative to zooplankton) translates into greater foraging profitability for fish feeding on zoobenthos relative to zooplankton, though prey abundance and (or) availability undoubtedly also plays a role in determining relative prey profitability. The energetic benefits of feeding on benthic prey have been quantified in studies of optimal foraging theory in littoral fishes (Werner and Hall 1974), but the ecosystem-level implications for patterns of energy flow through linked food webs remain poorly appreciated.

In addition to these differences in prey body size, physical differences between pelagic and benthic habitats may influence the efficiency with which fish predators are able to exploit invertebrate prey. In the benthic environment, prey inhabit an environment that more closely resembles a two-dimensional surface. The result is that benthic secondary production is more spatially concentrated and potentially more easily detected and exploited by fish. In lakes with abundant macrophyte cover, the two-dimensional comparison may be less applicable, though prey resources are still likely to be spatially concentrated. The three-dimensional nature of the pelagic environment has the effect of diluting the zooplankton production base, particularly in deep lakes such as Castle Lake. This may challenge the food-gathering capacity of fishes, particularly those lacking specific adaptations for zooplanktivory. In addition to these physical habitat differences, both zoobenthos and zooplankton have evolved refuges from predation. Zooplankton may undertake daily vertical migrations to minimize predation risks from fish. Although zoobenthos are more concentrated in their two-dimensional habitat, the benthic substrate may offer zoobenthos a refuge from fish predation. It is likely that differences in both habitat structure and prey body size are responsible for the differences between benthic and pelagic ecological efficiencies.

Finally, differences in food quality between zoobenthos and zooplankton could also explain these efficiency patterns, though caloric content of zoobenthos was not notably higher than that of zooplankton (Cummins and Wuycheck 1971). Fatty acid biomarkers may be useful indicators of food quality for comparing benthic and pelagic trophic pathways (Muller-Navarra et al. 2000; Park et al. 2002).

Trophic dynamics

An earlier study in Castle Lake found that cessation of rainbow trout stocking resulted in a compensatory increase in golden shiner and brook trout recruitment and population size (Elser et al. 1995). The consequence was that total zooplanktivory actually increased as rainbow trout populations declined over the study period, and a corresponding, predation-driven shift in the zooplankton community was observed. In that earlier study, zooplankton constituted a portion of the diet of all three fish species. In the present study, zooplankton was found to be a minor prey item, which is consistent with our stable isotope results. Why the importance of zooplankton in fish diets differs between these time periods is not known, although fish diets can show a high degree of interannual variability.

Although consumption of benthic prey by fish is thought to subsidize top-down control in the pelagic zone in some systems (Schindler et al. 1996; Schindler and Scheuerell 2002; Vander Zanden and Vadeboncoeur 2002), this was not apparent in Castle Lake. Both stable isotopes and diet data indicate that zooplankton were a minor energy source for adult fish in 2000, and fish do not show a preference for foraging on zooplankton in this system. The low estimates of ecological efficiency for the pelagic trophic chain indicates that a small proportion of zooplankton production is consumed by adult fish, though as noted above, consumption by young-of-the-year fishes was not included in the analysis. The apparent low level of zooplanktivory has obvious implications for patterns of top-down control in the pelagic zone of Castle Lake. Strong (1992) defined trophic cascades as "runaway consumption", that is, top-down control requires that predators efficiently exploit their prey (i.e., consume the available production). Our results strongly suggest that the zooplankton community was not regulated by top-down factors in 2000, though it should be noted that zooplankton averaged 12% of salmonid diets across all years for which data were available, and golden shiner diets were nearly half zooplankton in the 1989–1991 period (Elser et al. 1995).

Rainbow trout are stocked into Castle Lake on an annual basis. In the years before our data collection (1997–1999), both catchable size fish (200–400 g) and fingerlings (2–4 g) were stocked at an average rate of 790 (range 500–1125) and 16 800 (15 000 – 20 000) fish per year, respectively. This species was supported primarily by terrestrial and benthic invertebrate prey, although $\delta^{15}N$ signatures indicate that large (>30 cm) rainbow trout are piscivorous, presumably feeding on juvenile brook trout and golden shiner, which appear to be supported by littoral production (based on high rainbow trout $\delta^{13}C$ values). Continued stocking of rainbow trout maintains the population, with a portion becoming large enough to become piscivorous. The consequence may be maintenance of intense predation on juvenile brook trout and golden shiners. Consistent with this suggestion, Elser et al. (1995) reported that stocking of rainbow trout suppressed natural recruitment of brook trout and golden shiner and that relaxing stocking during the period 1998–1991 allowed a recruitment boom for these two species.

Isotopic interpretations

As mentioned above, a mix of catchable size and juvenile rainbow trout are annually stocked into Castle Lake. Interpretation of isotopic signatures of this species could be confounded by the residual isotopic signature of their hatchery food, though this prospect seems unlikely. The hatchery-derived isotopic signature of stocked fingerlings would be rapidly diluted by fish growth in the Castle Lake environment (Fry and Arnold 1982; Hesslein et al. 1993). The hatchery isotopic signal of catchable size rainbow trout could be retained in the population for a period of many months. The small rainbow trout sampled were less than 200 g in weight, indicating they were stocked as fingerlings. The large rainbow trout captured in May 2001 ranged from 400 to 1190 g (mean = 760 g). If these fish had been stocked as catchable size fish, they would have spent at least a year in the lake, which would have allowed time for growth and tissue turnover to dilute the hatchery isotopic signal (Hesslein et al. 1991).

For Castle Lake fish, there were three main prey types, though they differed only in $\delta^{13}C$ values. IsoSource (version 1.2; Phillips and Gregg 2003) was used to estimate the mean and range of values for reliance on these three prey. As an alternative approach, we used an equation that provides a unique solution for a one-isotope mixing model with three sources, provided that the contribution of one source is known. Assumptions of this approach are that the contribution for the one source is correct and that prey contribution to diet is equivalent to assimilation. A benefit of using stable isotopes over direct diet data is that it offers a time-integrated measure of energy pathways and prey assimilation, whereas diet studies offer just a snapshot of which prey were consumed. This benefit is lost when we assume these two to be equivalent. Furthermore, error in the contribution of the known prey item to the consumer diet produces error in the two sources being estimated. Here, we note a high degree of diet variation among years, such that a major source of error could be introduced in this term. Nevertheless, we found that the mean prey reliance (percentage of diet) given by IsoSource (version 1.2) and estimates from eq. 4 corresponded quite well (eq. 4 estimate = 0.791 × IsoSource + 6.86, $n = 9$, $r^2 = 0.75$).

The extreme negative $\delta^{13}C$ signatures of profundal primary consumers in Castle Lake (–44‰) are some of the more negative isotopic values published. One explanation is the uptake of isotopically light, respired carbon by phytoplankton (Rau 1978, 1980; Peterson and Fry 1987), although if this were the case, this depleted carbon signature would also be detected in metalimnetic zooplankton. Another explanation is the effect of methanogenic bacteria (Fry and Sherr 1984). Methanogenesis occurs in anoxic hypolimnetic sediments, producing ^{13}C-depleted CH_4 (–50‰) and bacteria (–64‰) (Whiticar et al. 1986; Jones and Grey 2004). It is evident from fish $\delta^{13}C$ values in Castle Lake that these ^{13}C-depleted profundal primary consumers are not an energy source to higher consumers.

Sources of error

There are a number of potential sources of error associated with our assessment of benthic and pelagic productivity and ecological efficiencies for Castle Lake. Central to our approach is the assumption that a relatively small number of productivity estimates can be extrapolated to make broad generalizations about whole-lake productivity and trophic pathways in Castle Lake. Benthic primary productivity was estimated on a single date at three depths and two habitats, and light data were used to generalize these measurements to the ice-free season. Similarly, pelagic primary production was based on seven primary production vertical profiles from 2000 and was taken as representative of Castle Lake. *P*/*B* ratios were used for estimating benthic secondary production from biomass data, an approach that can be subject to error because *P*/*B* is not likely a constant for a taxa or species of a given body size. For zooplankton, we used the egg ratio method to estimate production for the dominant zooplankton, *Daphnia rosea*. We extrapolated this estimate to the zooplankton community using data on the contribution of *Daphnia* to community zooplankton production. Though *Daphnia* are the dominant zooplankter in Castle Lake, interannual differences in zooplankton communities would be another source of error in our production estimates. Clearly there are numerous sources of error involved in assessing benthic and pelagic trophic pathways, and our production estimates are undoubtedly important potential sources of error in this study. An additional limitation of this study was that we were not able to estimate fish production for Castle Lake, and we felt it was not justified to use fish data collected a decade earlier (Elser et al. 1995), as fish populations are likely to change over time. Fish production estimates using data from Elser et al. (1995) were only used to estimate relative contributions of the three fish species to fish production in Castle Lake.

Despite the above sources of error in our study, this analysis provides a broad-scale picture of energy flow and ecological efficiencies in a subalpine lake and highlights the importance of benthic trophic pathways at the whole-ecosystem level. It is critical to be aware of the potential sources of error and variability in the present analysis. We believe that it is equally important to expand this type of analysis to a broader range of lakes using more refined methods and a more explicit assessment of fish production.

Recent stable isotope studies have revealed an important role for benthic energy flow pathways to higher trophic levels in lakes (Hecky and Hesslein 1995; Schindler and Scheuerell 2002; Vander Zanden and Vadeboncoeur 2002). These analyses have not been extended to combine stable isotope analysis of food web pathways with estimations of production at different trophic levels for benthic and pelagic food chains. The present paper presents such an analysis for Castle Lake, California, thus allowing simultaneous estimation of ecological efficiency along benthic and pelagic trophic pathways. Although primary production was nearly evenly split between the two habitats, invertebrate secondary production was dominated by pelagic production (70% of whole-lake secondary production). Despite this, fish were predominantly supported by benthic pathways, though an important limitation of our study was that we did not have a reliable estimate of fish production for Castle Lake. Still, our findings indicate an important role for benthic production in supporting higher trophic levels in this subalpine lake (Hecky and Hesslein 1995). Such patterns need to be examined in other systems, though this work indicates an important role of benthic pathways to higher trophic levels, likely as a result of the efficient exploitation of zoobenthos by fishes. This work builds on a long history of the study of energy flow pathways in lakes that dates back to Lindeman (1942) and highlights the value of integrated studies of benthic and pelagic processes in lakes (Vadeboncoeur et al. 2002). The view that benthic and pelagic food chains can be treated as separate entities is not supported by a growing body of literature revealing the importance of habitat coupling in lakes (Vanni 1996; Schindler and Scheuerell 2002; Vander Zanden and Vadeboncoeur 2002).

Acknowledgements

Helen Sarakinos, Isaac Kaplan, Katrina Butkas, Lucas Joppa, and Tony Ives provided valuable comments and discussion on the manuscript. Bill Feeny produced the Castle Lake map and assisted with figures. Steve Baumgartner provided fish stocking information. Assistance in the lab and field was provided by Elliott Matchett, Erin Gibson, Bonnie Luke, and Helen DeGuero. JVZ and YV were supported by the US National Science Foundation grant DEB-0449076.

References

Axler, R.P., and Reuter, J.E. 1996. Nitrate uptake by phytoplankton and periphyton: whole-lake enrichments and mesocosm-^{15}N experiments in an oligotrophic lake. Limnol. Oceanogr. **41**: 659–671.

Banse, K., and Mosher, S. 1980. Adult body mass and annual production/biomass relationships of field populations. Ecol. Monogr. **50**: 355–379.

Bootsma, H.A., Hecky, R.E., Hesslein, R.H., and Turner, G.F. 1996. Food partitioning among Lake Malawi nearshore fishes as revealed by stable isotope analyses. Ecology, **77**: 1286–1290.

Cummins, K.W., and Wuycheck, J.C. 1971. Caloric equivalents for investigations in ecological energetics. Int. Assoc. Theor. Appl. Limnol. **18**: 1–158.

Cyr, H., and Pace, M.L. 1993. Magnitude and pattern of herbivory in aquatic and terrestrial ecosystems. Nature (London), **361**: 148–150.

Elser, J.J., Luecke, C., Brett, M.T., and Goldman, C.R. 1995. Effects of food web compensation after manipulation of rainbow trout in an oligotrophic lake. Ecology, **76**: 52–69.

Fry, B. 1988. Food web structure on Georges Bank from stable C, N, and S isotopic compositions. Limnol. Oceanogr. **33**: 1182–1190.

Fry, B., and Arnold, C. 1982. Rapid ^{13}C/^{12}C turnover during growth of brown shrimp (*Penaeus aztecus*). Oecologia, **54**: 200–204.

Fry, B., and Sherr, E.B. 1984. δ^{13}C measurements as indicators of carbon flow in marine and freshwater ecosystems. Contrib. Mar. Sci. **27**: 13–47.

Goldman, C.R. 1968. The use of absolute activity for eliminating serious errors in the measurement of primary productivity with 14-C. Extrait J. Cons. Int. Explor. Mer, **32**: 172–179.

Goldman, C.R., Mason, D.T., and Woode, B.J.B. 1963. Light injury and inhibition in Antarctic freshwater phytoplankton. Limnol. Oceanogr. **8**: 313–322.

Grey, J., Thackeray, S.J., Jones, R.I., and Shine, A. 2002. Ferox trout (*Salmo trutta*) as 'Russian dolls': complementary gut content and stable isotope analyses of the Loch Ness foodweb. Freshw. Biol. **47**: 1235–1243.

Hagley, C.A. 1989. The ecology of the aquatic macrophyte *Isoetes occidentalis* in Castle Lake, California. M.S. thesis, University of California – Davis, Davis, Calif.

Hecky, R.E., and Hesslein, R.H. 1995. Contributions of benthic algae to lake food webs as revealed by stable isotope analysis. J. North Am. Benthol. Soc. **14**: 631–653.

Hesslein, R.H., Capel, M.J., Fox, D.E., and Hallard, K.A. 1991. Stable isotopes of sulfur, carbon, and nitrogen as indicators of trophic level and fish migration in the lower Mackenzie River basin, Canada. Can. J. Fish. Aquat. Sci. **48**: 2259–2265.

Hesslein, R.H., Hallard, K.A., and Ramlal, P. 1993. Replacement of sulfur, carbon, and nitrogen in tissue of growing broad whitefish (*Coregonus nasus*) in response to a change in diet traced by δ^{34}S, δ^{13}C, and δ^{15}N. Can. J. Fish. Aquat. Sci. **50**: 2071–2076.

Jassby, A.D., Powell, T.M., and Goldman, C.R. 1990. Interannual fluctuations in primary production: direct physical effects and the trophic cascade at Castle Lake, California. Limnol. Oceanogr. **35**: 1021–1038.

Jónasson, P.M. 1992. The ecosystem of Thingvallavatn: a synthesis. Oikos, **64**: 405–434.

Jónasson, P.M., Lindegaard, C., Dall, P.C., Hamburger, K., and Adalsteinsson, H. 1990. Ecosystem studies on temperate Lake Esrom and the subarctic Lakes Mývatn and Thingvallavatn. Limnologica, **20**: 259–266.

Jones, R.I., and Grey, J. 2004. Stable isotope analysis of chironomid larvae from some Finnish forest lakes indicates dietary contribution from biogenic methane. Boreal Environ. Res. **9**: 17–23.

Karatayev, A.Y., Burlakova, L.E., and Padilla, D.K. 2002. Impacts of zebra mussels on aquatic communities and their role as ecosystem engineers. *In* Invasive aquatic species of Europe — distribution, impacts, and management. *Edited by* E. Leppakoski, S. Gollasch, and S. Olenin. Kluwer Academic Publishers, Dordrecht, the Netherlands. pp. 433–446.

Kelly, A., Jones, R.I., and Grey, J. 2004. Stable isotope analysis provides fresh insights into dietary separation between *Chironomus anthracinus* and *C. plumosus*. J. North Am. Benthol. Soc. **23**: 287–296.

Likens, G.E. 1985. An ecosystem approach to aquatic ecology: Mirror Lake and its environment. Springer-Verlag, New York.

Lindeman, R.L. 1942. The trophic-dynamic aspect of ecology. Ecology, **23**: 399–418.

Lodge, D.M., Kershner, M.W., Aloi, J.E., and Covich, A.P. 1994. Effects of an omnivorous crayfish (*Orconectes rusticus*) on a freshwater littoral food web. Ecology, **55**: 1265–1281.

Loeb, S.L., and Reuter, J.E. 1981. The epilithic periphyton community: a five lake comparative study of community productivity, nitrogen metabolism and depth-distribution of standing crop. Verh. Int. Verein. Limnol. **21**: 346–352.

Loeb, S.L., Reuter, J.E., and Goldman, C.R. 1983. Littoral zone production of oligotrophic lakes. *In* Periphyton of freshwater ecosystems. *Edited by* R.G. Wetzel. Dr. W. Junk Publishers, The Hague. pp. 161–167.

McBride, G.B. 1992. Simple calculation of daily photosynthesis by means of five photosynthesis-light equations. Limnol. Oceanogr. **37**: 1796–1808.

Minagawa, M., and Wada, E. 1984. Stepwise enrichment of ^{15}N along food chains: further evidence and the relation between δ^{15}N and animal age. Geochim. Cosmochim. Acta, **48**: 1135–1140.

Muller-Navarra, D.C., Brett, M.T., Liston, A.M., and Goldman, C.R. 2000. A highly unsaturated fatty acid predicts carbon transfer between primary producers and consumers. Nature (London), **403**: 74–77.

O'Sullivan, P.E., and Reynolds, C.S. 2004. The lakes handbook. Vol. 1. Blackwell Publishing, Oxford, UK.

Paloheimo, J.E. 1974. Calculation of instantaneous birth rate. Limnol. Oceanogr. **19**: 692–694.

Park, S., Brett, M.T., Muller-Navarra, D.C., and Goldman, C.R. 2002. Essential fatty acid content and the phosphorus to carbon ratio in cultured algae as indicators of food quality for *Daphnia*. Freshw. Biol. **47**: 1377–1390.

Paterson, M.J., Findlay, D., Beaty, K., Findlay, W., Schindler, E.U., Stainton, M., and McCullough, G. 1997. Changes in the planktonic food web of a new experimental reservoir. Can. J. Fish. Aquat. Sci. **54**: 1088–1102.

Peterson, B.J., and Fry, B. 1987. Stable isotopes in ecosystem studies. Annu. Rev. Ecol. Syst. **18**: 293–320.

Phillips, D.L., and Gregg, J.W. 2003. Source partitioning using stable isotopes: coping with too many sources. Oecologia, **136**: 261–269.

Post, D.M., Carpenter, S.R., Christensen, D.L., Cottingham, K.L., Kitchell, J.F., Schindler, D.E., and Hodgson, J.R. 1997. Seasonal effects of variable recruitment of a dominant piscivore on pelagic food web structure. Limnol. Oceanogr. **42**: 722–729.

Randall, R.G., and Minns, C.K. 2000. Use of fish production per unit biomass ratios for measuring the productive capacity of fish habitats. Can. J. Fish. Aquat. Sci. **57**: 1657–1667.

Rau, G.H. 1978. Carbon-13 depletion in a subalpine lake: carbon flow implications. Science (Washington, D.C.), **201**: 901–902.

Rau, G.H. 1980. Carbon-13/carbon-12 variation in subalpine lake aquatic insects: food source implications. Can. J. Fish. Aquat. Sci. **37**: 742–746.

Sanders, F.S. 1976. An investigation of carbon flux in the sediments of Castle Lake Calif. Ph.D. thesis, University of California – Davis, Davis, Calif.

Saunders, J.F., and Lewis, W.M. 1988. Dynamics and control mechanisms in a tropical zooplankton community (Lake Valencia, Venezuela). Ecol. Monogr. **58**: 337–353.

Schindler, D.E., and Scheuerell, M.D. 2002. Habitat coupling in lake ecosystems. Oikos, **98**: 177–189.

Schindler, D.E., Carpenter, S.R., Cottingham, K.L., He, X., Hodgson, J.R., Kitchell, J.F., and Soranno, P.A. 1996. Food web structure and littoral zone coupling to pelagic trophic cascades. *In* Food webs: integration of patterns and dynamics. *Edited by* G.A. Polis and K.O. Winemiller. Chapman and Hall, New York. pp. 95–105.

Schindler, D.E., Geib, S.I., and Williams, M.R. 2000. Patterns of fish growth along a residential development gradient in north temperate lakes. Ecosystems, **3**: 229–237.

Strayer, D. 1991. Notes on Lindeman's progressive efficiency. Ecology, **72**: 348–350.

Strayer, D., and Likens, G.E. 1986. An energy budget for the zoobenthos of Mirror Lake, New Hampshire. Ecology, **67**: 303–313.

Strong, D.R. 1992. Are trophic cascades all wet? Differentiation and donor-control in speciose ecosystems. Ecology, **73**: 747–754.

Swift, M.C. 1970. A qualitative and quantitative study of trout food in Castle Lake, California. Calif. Fish Game, **56**: 109–120.

Taylor, R.B., Blackburn, R.I., and Evans, J.H. 1995. A portable battery-powered suction device for the quantitative sampling of small benthic invertebrates. J. Exp. Mar. Biol. Ecol. **194**: 1–7.

Vadeboncoeur, Y., and Lodge, D.M. 2000. Periphyton production on wood and sediment: substratum-specific response to laboratory and whole-lake nutrient manipulations. J. North Am. Benthol. Soc. **19**: 68–81.

Vadeboncoeur, Y., Lodge, D.M., and Carpenter, S.R. 2001. Whole-lake fertilization effects on distribution of primary production between benthic and pelagic habitats. Ecology, **82**: 1065–1077.

Vadeboncoeur, Y., Vander Zanden, M.J., and Lodge, D.M. 2002. Putting the lake back together: reintegrating benthic pathways into lake food web models. Bioscience, **52**: 44–54.

Vadeboncoeur, Y., Jeppesen, E., Vander Zanden, M.J., Schierup, H.H., Christoffersen, K., and Lodge, D.M. 2003. From Greenland to green lakes: cultural eutrophication and the loss of benthic energy pathways in lakes. Limnol. Oceanogr. **48**: 1408–1418.

Vander Zanden, M.J., and Rasmussen, J.B. 1999. Primary consumer δ^{15}N and δ^{13}C and the trophic position of aquatic consumers. Ecology, **80**: 1395–1404.

Vander Zanden, M.J., and Rasmussen, J.B. 2001. Variation in δ^{15}N and δ^{13}C trophic fractionation: implications for aquatic food web studies. Limnol. Oceanogr. **46**: 2061–2066.

Vander Zanden, M.J., and Vadeboncoeur, Y. 2002. Fishes as integrators of benthic and pelagic food webs in lakes. Ecology, **83**: 2152–2161.

Vanni, M.J. 1996. Nutrient transport and recycling by consumers in lake food webs: implications for algal communities. *In* Food webs: integration of patterns and dynamics. *Edited by* G.A. Polis and K.O. Winemiller. Chapman and Hall, New York. pp. 81–95.

Vanni, M.J. 2002. Nutrient cycling by animals in freshwater ecosystems. Annu. Rev. Ecol. Syst. **33**: 341–370.

Wales, J.H. 1946. Castle Lake trout investigation. Calif. Fish Game, **32**: 109–143.

Werner, E.E., and Gilliam, J.F. 1984. The ontogenic niche and species interactions in size-structured populations. Annu. Rev. Ecol. Syst. **15**: 393–426.

Werner, E.E., and Hall, D.J. 1974. Optimal foraging and the size selection of prey by bluegill sunfish (*Lepomis macrochirus*). Ecology, **55**: 1042–1052.

Wetzel, R.G. 2001. Limnology: lake and river ecosystems. Saunders College Publishing, Fort Worth, Texas.

Whiticar, M.J., Faber, E., and Schoell, M. 1986. Biogenic methane formation in marine and freshwater environments: CO_2 reduction vs. acetate fermentation — isotopic evidence. Geochim. Cosmochim. Acta, **50**: 693–709.

Relationships among nutrients, algae, and land use in urbanized southern California streams

Lilian B. Busse, Juliet C. Simpson, and Scott D. Cooper

Abstract: We surveyed algal cover, algal biomass, and physical and chemical factors at 14 sites representing a range of land use types in the Malibu Creek watershed in southern California, USA. We also conducted nutrient diffuser substrate experiments to identify the nutrient limiting algal growth. Algal biomass increased with urbanization, reaching very high levels in the most urbanized streams (up to 322.4 mg chlorophyll $a \cdot m^{-2}$). Total nitrogen, total phosphorus, and benthic and total chlorophyll concentrations were positively correlated with the proportion of upstream land covered by impervious surfaces. Relationships between land use and algal biomass or nutrient concentrations were evaluated at 100 m, 500 m, and whole subwatershed scales. The closest relationships were found at the 500 m scale, where 56% of the variation in total chlorophyll could be explained by the proportion of land within a 500 m radius upstream covered by impervious surfaces. Floating macroalgae were observed in the summer in pools with high nutrient and light levels, whereas benthic algal biomass was positively related to total phosphorus concentrations and current speed. Other methods of determining nutrient limitation (nutrient diffuser substrate experiment, molar N/P ratios in stream water) produced conflicting results, possibly because algal growth was saturated by high nutrient levels at some of the study sites.

Résumé : Nous avons inventorié la couverture d'algues, la biomasse des algues et les facteurs physiques et chimiques à 14 sites qui représentent une gamme d'utilisation des terres dans le bassin versant de Malibu Creek dans le sud de la Californie, É.-U. Nous avons aussi mené des expériences de substrats diffuseurs de nutriments afin d'identifier les nutriments qui limitent la croissance des algues. La biomasse des algues croît en fonction de l'urbanisation, atteignant de très hautes valeurs dans les cours d'eau les plus urbanisés (jusqu'à 322,4 mg chlorophyll $a \cdot m^{-2}$). Il y a une corrélation positive entre l'azote total, le phosphore total et les concentrations benthiques et totales de chlorophylle, d'une part, et la proportion des terres en aval recouvertes de surfaces imperméables, d'autre part. Nous avons évalué les relations entre l'utilisation des terres et la biomasse des algues ou la concentration des nutriments aux échelles de 100 m, de 500 m et des sous-bassins versants entiers. Les relations les plus fortes s'observent à l'échelle de 500 m où 56 % de la variation de la chlorophylle totale peut s'expliquer par la proportion des terres en aval dans un rayon de 500 m couvertes de surfaces imperméables. Des macro-algues flottantes se retrouvent l'été dans les fosses à fortes concentrations de nutriments et à éclairement élevé, alors que la biomasse des algues benthiques est reliée directement aux concentrations de le phosphore total et à la vitesse du courant. D'autres méthodes de rechange pour déterminer les limitations dues au nutriments (expérience NDS, rapports molaires N/P dans les cours d'eau) génèrent des résultats contradictoires, probablement parce que la croissance des algues est saturée par les fortes concentrations de nutriments à certains des sites d'étude.

[Traduit par la Rédaction]

Introduction

Stream ecosystems have been affected greatly by rapidly increasing human populations (Meybeck 2003; Feminella and Walsh 2005). Human activities can strongly influence light and nutrient availability, sedimentation, and disturbance frequency in freshwater systems (Walsh et al. 2005), with consequent effects on the structure and function of primary producer communities (Paul and Meyer 2001; Malmqvist and Rundle 2002). Because nitrogen (N), phosphorus (P), or light commonly limit the growth of stream algae, elevated levels of these resources often result in nuisance algal blooms (Grimm and Fisher 1986; Winterbourn 1990; Borchardt 1996).

Primary producer communities in temperate streams have been well studied (see review in Stevenson et al. 1996), and recent work has focused on describing quantitative relationships among stream algae, physical–chemical conditions,

Received 14 December 2005. Accepted 4 September 2006. Published on the NRC Research Press Web site at http://cjfas.nrc.ca on 15 November 2006.
J19046

L.B. Busse,[1,2] J.C. Simpson, and S.D. Cooper. Marine Science Institute and Department of Ecology, Evolution and Marine Biology, University of California – Santa Barbara, Santa Barbara, CA 93106, USA.

[1] Corresponding author (e-mail: busse@coast.ucsd.edu).

[2] Present address: Integrative Oceanography Division, Scripps Institution of Oceanography, University of California – San Diego, La Jolla, CA 92093-0227, USA.

Can. J. Fish. Aquat. Sci. 63: 2621–2638 (2006) doi:10.1139/F06-146

and land use in the surrounding catchment (e.g., Dodds and Oakes 2004; Taylor et al. 2004; Carr et al. 2005). Streams in regions with Mediterranean climates (i.e., southern California, Chile, southwestern South Africa, western and southern Australia, and the Mediterranean Sea basin) differ from streams in other temperate climates and are much less studied (Sabater et al. 1995; Gasith and Resh 1999). Mediterranean climates are characterized by long, dry summers, with 80%–90% of annual precipitation falling during isolated winter storm events (DeCastri and Mooney 1973). This climate regime produces brief, severe flood disturbances in streams, which occur during the few wet months, and greatly reduced surface flows during summer months. Benthic algal communities undergo succession after scouring flood events and are greatly affected by light levels, nutrient availability, and grazing (Cooper et al. 1986; Dudley 1992; Sabater et al. 2005). Increased nutrient loading, in particular, may have strong effects on streams in Mediterranean climates affected by urban development because these systems have high light levels, owing to the removal of riparian vegetation, and low dry season flows, which minimize the dilution of nutrient inputs (Sabater et al. 1998; Gasith and Resh 1999; Sabater et al. 2000*a*).

Rates of urban development in southern California are among the highest in the United States. (Beighley et al. 2003). Human population growth and associated urban development will likely have large impacts on stream ecosystems in southern California. Only a few studies have assessed the effects of urbanization on algal communities (Sabater et al. 2000*b*; Walsh et al. 2005), and none of these studies were conducted in streams in Mediterranean climates.

Because little is known about relationships among land use patterns, chemical and physical parameters, and algal communities in streams in Mediterranean climates, we conducted a study in the Malibu Creek watershed in southern California, USA, in 2001 and 2002. The Malibu Creek watershed has areas that have been subjected to rapid development in recent decades, but other areas have remained relatively undisturbed. At multiple sites within the watershed and across several seasons, we measured algal cover and biomass, nutrient concentrations, and light availability. In 2002, we also performed nutrient diffusing substrate (NDS) experiments at six sites to examine the nature of nutrient limitation and its relationships to land use. We compared our results with data from other temperate streams to assess the interacting effects of climate, land use, and physical–chemical conditions on algal biomass.

Materials and methods

Watershed description and sites

The Malibu Creek watershed is located on the coast of southern California, ~55 km west of Los Angeles (34°02′N, 118°40 W; Fig. 1). The Malibu Creek basin encompasses ~280 km^2, ranging in elevation from ~1000 m down to sea level at Malibu Lagoon, where the creek flows into the Pacific Ocean. The watershed contains many undeveloped areas, but there is intense urban development along portions of Malibu Creek's major tributaries. The vegetation within the watershed mainly consists of chaparral, scrub communities, grasslands (native and nonnative), and woodlands.

In 2001, we chose 11 sites for our survey, ranging from first- to fourth-order streams. These included two reference sites (surrounded by protected, undeveloped land), two rural sites with low housing densities, two suburban sites with high housing densities (residential sites), one commercial site (commercial land use consisting of industrial land use (shopping centers, retail–office–service use, small commercial use), institutional land use (schools and civic centers), and transportation networks (roads and freeways)), one site downstream from an area with several large horse stables and riding areas adjacent to the creek, one site just downstream of a golf course, and two sites in the lower catchment surrounded by undeveloped land, but with developed areas upstream (State Park 1 and 2) (Fig. 1). In addition, the State Park 2 site was located downstream from the outflow of a wastewater treatment plant; however, the treatment plant was not discharging effluent into the creek during the summer and fall months when our study was conducted. All sites were sampled on 22–24 August and 22–24 October 2001 to capture peak summer and fall algal biomass, respectively. In 2002, we selected seven sites representing a gradient of human activity within the Malibu Creek watershed for stream surveys and NDS experiments. Four of these sites had been surveyed in 2001 (Reference 1, Residential 1, Commercial 1, and State Park 2), and three sites were sampled only in 2002, including one additional commercial site (same land use as other commercial site, see above) and two multiple land use sites (Fig. 1). The two multiple land use sites on Las Virgenes Creek were influenced by both surrounding residential development and nearby historical sludge injection fields that continue to leach nutrients into the creek (R. Orton, Las Virgenes Municipal Water District, Calabasas, CA 91302-1994, USA, personal communication). Sites were sampled on 24–25 June 2002, 27–28 August 2002, and 22–24 October 2002 during steady flow when algal biomass reached maximum values. NDS experiments were conducted in pools or slow runs at the Reference 1, Residential 1, Commercial 2, Multiple 1 and 2, and State Park 2 sites between 27 August and 28 September 2002 (Reference, Residential, and State Park 2 sites: pools, current speed 0–0.02 m·s^{-1}; Commercial 2 and Multiple 1 and 2 sites: slow runs, current speed 0.02–0.18 m·s^{-1}).

Land use

As a first step in examining correlations between land use patterns and the values of physical, chemical, and biological variables at our stream sites, we compared our visual assessments of land use with published land use data. Other studies have found correlations between land use and stream nutrient concentrations at small (91 m; Sonoda et al. 2001) and large scales (whole drainage basin; Carr et al. 2005), as well as between land use and biological conditions at intermediate scales (300 m; Strayer et al. 2003). We analyzed land use patterns over a similar range of multiple spatial scales (subwatershed, 500 m buffer, and 100 m buffer) to investigate relationships between land use and measured physical, chemical, and biological variables.

Fig. 1. Map of the Malibu Creek watershed and location of study sites (inset shows location in California, USA). Broken lines denote streams and solid lines delineate subwatershed boundaries. 1, Reference 1; 2, Reference 2; 3, State Park 1; 4, Rural 2; 5, Horse; 6, State Park 2; 7, Rural 1; 8, Multiple 2; 9, Commercial 2; 10, Residential 2; 11, Residential 1; 12, Golf; 13, Multiple 1; 14, Commercial 1.

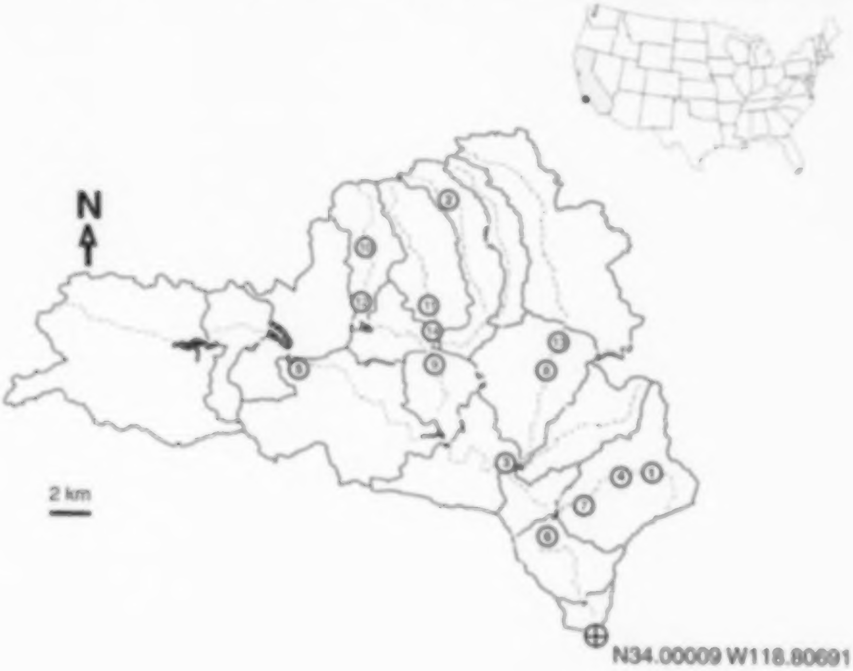

Data from the USDA Natural Resources Conservation Service Lancaster provided land use characteristics for each subwatershed. The subwatershed information contained data on land use parameters for each subwatershed, regardless of where the site was located within the subwatershed.

Land use data for the smaller scales were obtained from the Southern California Association of Governments (SCAG, Los Angeles, California). For the analyses, SCAG's land use designations in 2000 were placed into the following four categories: urban (including multiple-family apartment buildings, commercial, industrial, institutional, and transportation land uses), residential (high-, medium-, and low-density single-family houses, typically with lawns and (or) gardens), open (improved land without major buildings, including golf courses, public parks, and cemeteries), or vacant (undeveloped land). The western portion of the Malibu Creek watershed contains some agricultural land, but there was no surface water in any of the streams in that region during our sampling periods; therefore, agricultural land uses were omitted from this study. Land use patterns were delineated at the two smaller scales (100 m and 500 m) using ArcGIS v.9 (ESRI, Redlands, California). To define areas of influence upstream of each site, we delineated cone-shaped areas on the land use map with the point of the cone set on the field sampling site and the cone extending upstream, centered on the stream (as described in Sonoda et al. 2001). Each cone had an angle of 120° and a radius of either 100 or 500 m. Each land use type contained a defined percentage of imperviousness. Percent impervious surface (e.g., concrete, asphalt) and percent cover of different land use types was then calculated for each cone area.

Sampling design

In 2001, we established three cross-stream transects at each site (10 m apart). To more precisely characterize each site, in 2002 we established three equally spaced cross-stream transects in each of six subhabitat types, including shaded pools, shaded riffles, shaded runs, sunny pools, sunny riffles, and sunny runs (pools: average 0.01 $m \cdot s^{-1}$; run: average 0.07 $m \cdot s^{-1}$; riffle: average 0.21 $m \cdot s^{-1}$; sunny habitat: average 62.6% open canopy cover; shady habitat: average 9.0% open canopy cover). Not all sites had the full range of subhabitat types, but we sampled all subhabitats that were available.

Physical measurements

In 2001 and 2002, water temperature and current speed were measured at the center of each transect using a YSI dissolved oxygen meter (model 59, YSI Incorporated, Yellow Springs, Ohio) and a Marsh-McBirney portable water current meter (Model 201D, Marsh-McBirney Inc., Frederick, Maryland), respectively. To avoid the bias in light measurement created by diurnal variations in solar angle, light availability at each site was estimated by measuring canopy cover with a Model-A spherical densiometer (Forest Densiometers, Bartlesville, Oklahoma) at the center of each transect in all four directions. In 2001, we compared canopy cover data with percent light reduction data calculated from photosynthetically active radiation (400–700 nm) levels measured above the water's surface at each site and at an adjacent, unshaded area (usually a street or parking lot) using a LI-COR line quantum sensor 191 (LI-COR Biosciences, Lincoln, Nebraska) (R. Ambrose and S. Lee, School of Public Health, University of California, Los Angeles, CA 90095-1772, USA, unpublished data). Because canopy cover at most sites was relatively evenly distributed with respect to ordinal direction, this method should be minimally biased by time of day. The percent reduction of light over the stream channel relative to full sunlight was correlated tightly with canopy cover estimated from our densiometer data (linear regression, $R^2 = 0.95$); consequently, we used densiometer readings in both years to represent proportionate light reduction.

Water chemistry sampling and analysis

Water samples for ammonia (NH_4), nitrate (NO_3), soluble reactive phosphorus (SRP), total phosphorus (TP), and total nitrogen (TN) concentrations were taken from the downstream transect at each site just before algae were sampled. Samples for dissolved inorganic nutrients were filtered immediately through a 0.45 µm polycarbonate membrane filter (Poretics Corp., Livermore, California) (2001) or a Whatman GF/C glass fiber filter (Whatman Inc., Florham Park, New Jersey) (2002). In 2001, all samples were held on ice for 3–60 h, then frozen in the laboratory until analysis up to 1 month later. In 2002, all samples were taken within 1 h on the last day of sampling and placed on ice, and dissolved inorganic nutrient concentrations were measured within 24 h. Samples for TN and TP were oxidized with persulfate using the Valderrama method (Valderrama 1981). Dissolved nutrients and oxidized samples for TN and TP were measured spectrophotometrically on a Lachat QuikChem 8000 flow injection analyzer (Lachat Instruments, Milwaukee, Wisconsin) using standard methods (SRP, TP: reaction with ammonium molybdate and ascorbic acid; NO_2–NO_3, TN: reduction of nitrate to nitrite, nitrite was diazotized with sulfanilamide and coupled with ethylenediamine dihydrochloride; NH_4: phenolate method). Conductivity was measured at the center of each transect using an Orion 128 conductivity meter (Orion Research Inc., Cambridge, Massachusetts).

Algal sampling and analysis

The percent cover of different algae types and bare space at each site were assessed visually using the Environmental Protection Agency's (EPA) rapid bioassessment protocol (Barbour et al. 1999), which entails using an underwater viewing bucket with a grid (28 cm × 28 cm) of 50 evenly spaced dots on the clear bottom surface. Under each dot, macroalgae were identified to genus, and diatom films were classified as thin (<0.5 mm in height), medium (0.5–2.0 mm), or thick (>2.0 mm). Percent cover of each algal type was determined at three evenly spaced points along each transect. Benthic algae were sampled at five evenly spaced locations along each transect with a 26 mm diameter periphyton sampler, consisting of an open-ended syringe cylinder with removable scouring pad affixed to the bottom of the central plunger (described by Davies and Gee 1993). Davies and Gee (1993) showed that this periphyton sampler removed algae more effectively than other standard periphyton sampling techniques. After algae had been scraped from the tops of rocks or other hard substrata (e.g., logs or concrete where no rocks were available) using this scouring pad sampler, pads containing algal samples were removed and stored for subsequent laboratory extraction and analysis. If floating macroalgae were present at a sampling location, the outer cylinder of the sampler was used to bore a 26 mm diameter hole through the floating mat, and these algae also were retained for analysis. All benthic and floating algae samples from each transect were combined to make one composite benthic and one composite floating algae sample for each transect. Where floating macroalgal mats were present in 2002, we sampled both the mats and the benthic algae underneath the mats using the syringe sampler. Chlorophyll *a* (Chl *a*) concentrations in floating, benthic, and total (benthic + floating) algae samples were averaged across the three transects per site (2001) or subhabitat type (2002) to provide an estimate of Chl *a* concentration for each site or subhabitat. In 2002, chlorophyll values for the subhabitats at each site were averaged to provide an estimate of chlorophyll concentration for each site.

In the laboratory, benthic periphyton samples were rinsed from the scouring pads with deionized water. Floating macroalgae and benthic algae samples from each transect were homogenized in 850 mL of deionized water using a Waring commercial blender (model 31BL91, Waring Products, Torrington, Connecticut) and stirred thoroughly, then subsamples (usually 100 mL) were removed and filtered through Whatman GF/C glass fiber filters. Chl *a* in subsamples was measured using the EPA rapid bioassessment protocol for streams and wadeable rivers (USEPA 1992) with a Turner 10-AU field flourometer (Turner Designs, Inc., Sunnyvale, California) (extraction in 90% acetone for 24 h, correction for phaeophytin). Ash-free dry mass (AFDM) was measured by drying separate subsamples in Whatman GF/C glass fiber filters at 60 °C for 24 h, then ashing for 2 h at 500 °C.

Nutrient limitation experiment

We used NDS to determine the nature and degree of nutrient limitation for periphyton biomass (modification of the Biggs et al. (1998*a*) method). Each NDS consisted of a 4 oz. (120 mL) Mason jar filled with 4% agar. We added N and (or) P to the agar to create four experimental treatments: +N, +P, +N+P, and controls with no nutrient additions. N addition treatments contained 0.5 $mol \cdot L^{-1}$ $NaNO_3$; P addition treatments contained 0.5 $mol \cdot L^{-1}$ KH_2PO_4, and +N+P treatments contained 0.5 $mol \cdot L^{-1}$ concentrations of both $NaNO_3$ and KH_2PO_4. A 10 cm square of 20 µm Nitex polyester mesh covered the mouth of each jar and was held in place by a plastic lid with a 5.6 cm diameter hole cut in the center. To protect the NDS from abrasion and animal interference, each unit was placed in a cubic cage, 15 cm on a side, constructed of stainless steel hardware cloth with 6 mm × 6 mm mesh. The cages were affixed to 20 cm × 20 cm concrete cinder blocks using ultraviolet-resistant plastic cable ties and deployed in pools or slow runs (current velocity always less than 20 $cm \cdot s^{-1}$) at each site.

Twelve diffusers (four treatments × three replicates per treatment) were deployed in representative areas at each of six sites on 27–28 August 2002 (Reference 1, Residential 1, Commercial 2, Multiple 1 and 2, and State Park 2 sites). At each site, they were deployed at depths of <50 cm to minimize light attenuation through the water column. Algae growing on enclosing cage walls were scrubbed three times during the experiment to minimize shading. NDS were deployed for 1 month to allow adequate time for the accrual of algal biomass. On 28 September, the NDS units were retrieved and Nitex surfaces were removed, transported immediately to the laboratory on ice, and frozen at −20 °C until analysis. Because algae sometimes grew directly on agar surfaces underneath the Nitex, we also removed the top 1 cm of agar from each NDS and retained these samples for analysis. The diffuser arrays at the State Park 2 site were discovered to have been removed from the water on 9 September; however, they were placed immediately back in the stream where they remained undisturbed until the end of the experiment (19 days). Visual examination of the NDS at this site 1 week after NDS replacement suggested that algae quickly recolonized the substrata; consequently, we are confident that the results from this site reflect responses of algae to the intended treatments. In addition, 19 days is well within the range of deployment times used in several other NDS experiments (e.g., Grimm and Fisher 1986; Francoeur et al. 1999); however, we caution that results from this site are not directly comparable with results from our other sites because of the different durations of deployment.

In the laboratory, we cut the Nitex surfaces into quarters. One Nitex quarter from each jar was immersed in 50 mL of 90% acetone and placed in a −20 °C freezer, and then Chl *a* concentration was measured according to USEPA (1992). To extract Chl *a* from the agar surface scrapes, each scrape was diluted with deionized water to a volume of 60 mL and homogenized by high-speed mixing for 5 s. We then took a 10 mL subsample of the homogenate, added 40 mL of pure acetone, and extracted the chlorophyll in the freezer as for the Nitex samples. Although the acetone concentration for the scrape extractions was 80%, we assume that this had very little effect on overall chlorophyll concentrations because chlorophyll levels on the scrapes were very low. Chl *a* concentrations on the Nitex surface and agar scrape from each NDS were summed to obtain a total chlorophyll value per unit area of growth substratum.

Data analysis

In all analyses, we used Chl *a* concentration as an index of algal biomass. Because biomass-specific Chl *a* concentrations can vary across different types of algae (e.g., green vs. brown) and with environmental conditions (particularly light availability), we compared Chl *a* and AFDM results for all of our samples to estimate the reliability of chlorophyll as an index of algal biomass. There was a tight relationship between Chl *a* and AFDM concentrations for both floating and benthic algae (linear regression, R^2 values ranged from 0.69 to 0.72; slopes varied only slightly with algal type). We also found tight relationships between Chl *a* concentrations for floating algae and percent cover by macroalgae and between benthic algal Chl *a* concentrations and percent cover by thick and medium diatom films (R^2 from 0.71 to 0.88). As a consequence, we assumed that Chl *a* was a reasonable index of algal biomass.

Multiple regressions were conducted on survey data to determine relationships between algal biomass (floating, benthic, and total biomass) or cover and physical–chemical variables (TN, TP, NO_3, NH_4, SRP, light, current speed). Because conductivity, TN, and TP were intercorrelated, conductivity was not entered and only TN or TP, but not both, were included in initial regression models. Nonsignificant ($P > 0.1$) variables were eliminated through a process of backward elimination to create the model that best fit the data. Simple regression analyses were conducted to examine relationships between algal parameters or physical–chemical variables and land use characteristics (percent urbanized, percent impervious surface) and between stream order and biological, chemical, and physical variables. All data were transformed to meet parametric assumptions, including ln transformations (or $\ln(n + 0.1)$ where zero values were present) for chlorophyll, nutrient, and current speed data and arcsine square root transformations for proportion canopy cover or land use data. Residuals and skewness of transformed data were examined for conformance to parametric assumptions (e.g., normality, homogeneity of variances).

Using the method described by Tank and Dodds (2003) to determine whether N or P had significant effects on the accumulation of algal biomass, chlorophyll data from the NDS experiments were analyzed using two-way analyses of variance (ANOVAs), followed by a least-squares means test when the ANOVA was significant ($P < 0.05$). Statistical analyses were performed using S-Plus (S-Plus Professional Release 3, MathSoft Inc., Cambridge, Massachusetts) and JMP (Version 5.1.1, SAS Institute Inc., Cary, North Carolina).

Results

Physical–chemical parameters

Average current speeds ranged from 0 to 0.50 $m \cdot s^{-1}$ across sites and were nearly zero at the Reference 2 and Horse sites (Table 1). Current speed varied minimally through time at all sites. pH ranged from 7.6 to 8.1 and did not differ among sites or sampling dates (Table 1). Light levels >60% of full sunlight were measured at the Rural 1, Residential 1, Golf, and Commercial sites, whereas all other sites had light levels <35% full sun (Table 1). Conductivity values ranged from 0.67 to 3.61 $mS \cdot cm^{-1}$ across sites and were higher at sites with greater human influence (Pearson's $R = 0.78$, $P < 0.01$ for the correlation between conductivity and percent impervious surfaces, 500 m scale of analysis).

Nutrient concentrations

Sites with no or low anthropogenic influence generally had lower TP and TN concentrations than sites with more development, although there were some exceptions (Table 1). The Reference, Rural, Residential 2, and Horse sites consistently had TP concentrations <100 $\mu g \cdot L^{-1}$, whereas all other sites had higher concentrations, and three sites showed TP levels >240 $\mu g \cdot L^{-1}$ (Multiple 1 and 2; State Park 2). TP concentrations were consistently higher in 2002 than in 2001 (paired *t* test for sites sampled in both years, $P < 0.02$). On average, SRP contributed 20%–70% to TP concentrations across all sites, except the Multiple sites where SRP accounted for over 80% of TP concentrations. The Reference, Rural, Horse, and State Park 1 sites showed low

Table 1. Site names; % of subcatchment area that is impervious (% imp.); sampling dates; and selected physical, chemical, and biological data for study sites in the Malibu Creek watershed.

		Sampling dates													
Site ID	% imp.	Aug. 2001	Oct. 2001	June 2002	Aug. 2002	Oct. 2002	Current speed ($m \cdot s^{-1}$)	Conductivity ($mS \cdot cm^{-1}$)	% full sun	DIN ($\mu g \cdot L^{-1}$)	SRP ($\mu g \cdot L^{-1}$)	TN ($\mu g \cdot L^{-1}$)	TP ($\mu g \cdot L^{-1}$)	Molar TN/TP ratio	Total Chl *a* ($mg \cdot m^{-2}$)
Reference 1*	2	×	×	×	×	×	0.05	0.67	11.5	29.9	43.2	424.2	64.9	14.5	6.5
Reference 2	2	×	×				0.00	1.73	ND	9.8	7.8	615.0	45.1	30.2	1.8
State Park 1	2	×	×				0.13	2.35	18.0	43.2	56.4	394.5	101.9	8.6	52.0
Rural 2	5	×	×				0.05	1.34	8.9	72.6	18.6	545.8	37.4	32.3	4.9
Horse	7	×	×				0.00	1.34	22.5	21.5	27.2	394.3	97.9	8.9	27.7
State Park 2*	9	×	×		×	×	0.12	2.75	26.4	599.9	176.8	1278.0	247.7	11.4	188.2
Rural 1	12	×	×				0.03	1.24	61.8	266.2	27.2	440.6	75.9	12.8	26.1
Multiple 2*	26			×	×	×	0.10	3.61	0.6	4090.6	308.0	4489.5	371.8	26.7	217.5
Commercial 2*	39			×	×	×	0.18	3.04	84.2	508.1	94.1	1824.3	118.0	34.2	322.4
Residential 2	41	×	×				0.08	2.34	5.2	222.4	25.5	1254.3	72.9	38.1	26.1
Residential 1*	45	×	×	×	×	×	0.08	3.49	62.8	208.0	107.3	790.2	136.6	12.8	96.3
Golf	46	×	×				0.50	2.90	99.5	421.7	82.6	1524.6	144.1	23.4	88.6
Multiple 1*	47				×	×	0.11	3.58	34.0	3270.3	319.7	3536.6	398.0	19.7	275.9
Commercial 1	55	×	×	×	×	×	0.17	3.06	95.2	520.7	75.4	1220.2	142.1	19.0	220.1

Note: Data represent averages over all sampling days at each site. Asterisks (*) indicate sites where nutrient diffusing substrata (NDS) experiments were performed. DIN, dissolved inorganic nitrogen; SRP, soluble reactive phosphorus; TN, total nitrogen; TP, total phosphorus; Chl *a*, chlorophyll *a*; ND, no data.

average TN concentrations ($<750\ \mu g \cdot L^{-1}$), whereas all other sites had TN concentrations $>750\ \mu g \cdot L^{-1}$, with the Multiple sites showing extremely high TN concentrations ($>3500\ \mu g \cdot L^{-1}$). The highest TN concentrations were recorded in October 2002. The main inorganic contributor to TN concentrations across sites was nitrate–nitrite (on average between 0%–40% of TN was NO_2–NO_3-N at the Rural 2, Residential 2, and the Multiple sites; 60%–100% of TN concentrations consisted of NO_2–NO_3-N at all other sites). NH_4-N only contributed 0–10% to TN concentrations. Molar TN/TP ratios ranged from 38 to <1 and were generally lower in 2002 than in 2001, although the decrease was not statistically significant. TN/TP averaged <10 at 2 of our 14 sites (Horse, State Park 1) and were >20 at six sites (Reference 2, Rural 2, Multiple 2, Commercial 2, Residential 2, and Golf), with all other sites having TN/TP ratios between 10 and 20 (Table 1).

Algal cover and composition

Benthic algae were found at all sites in all seasons and years and consisted primarily of thin, medium, or thick diatom films (Figs. 2*a*–2*e*). Thin diatom films were composed largely of *Cymbella*, *Navicula*, *Achnanthes*, and *Nitzschia* spp., whereas medium and thick diatom films were composed mainly of *Melosira* sp. Reference and rural sites were dominated by thin diatom films in 2001 and by thin and medium diatom films in 2002. Sites with substantial human activity (e.g., residential, multiple, commercial, and State Park sites) had a higher coverage by medium and thick diatom mats in both years compared with reference and rural sites (*t* test, $P < 0.01$). From August to October 2001, thin diatom films became thicker at more developed sites, whereas the reference and rural sites were consistently dominated by thin diatom films in 2001 and by thin–medium diatom films in 2002.

Macroalgae occurred at stream sites surrounded by a variety of land use types (e.g., rural, residential, multiple, commercial, and State Park 2), but tended to have the highest cover at the commercial and State Park 2 sites (Figs. 2*a*–2*e*). In 2001, macroalgal species composition differed among sites, with *Rhizoclonium* and (or) *Enteromorpha* dominating at the Rural 1, Residential 1, State Park 2, and Commercial sites; *Spirogyra* dominating at the Horse site; and *Cladophora* occupying substantial amounts of space at the State Park 2 site. In June and August 2002, macroalgal assemblages were dominated by *Rhizoclonium*, *Enteromorpha*, *Cladophora*, and *Spirogyra* at the developed sites (Residential, Commercial, and Multiple), whereas the State Park 2 site contained only *Spirogyra*. In October 2002, macroalgal assemblages were composed almost entirely of *Rhizoclonium* and (or) *Enteromorpha*. The percent cover of macroalgae decreased at all sites where macroalgae were present from August to October 2001 and from June to October 2002, except the Reference 1 and Commercial 1 sites in 2002 (paired *t* test between dates within each year, $P < 0.02$). *Cladophora* was present at the Reference 1 site in both August and October 2002, but not in June 2002, and macroalgae at the Commercial sites were removed via dredging and scraping by Flood Control personnel on multiple occasions during the summer and fall of 2002.

Fig. 2. The percent cover of different algal types at stream sites in the Malibu Creek watershed in (*a*) August 2001, (*b*) October 2001, (*c*) June 2002, (*d*) August 2002, and (*e*) October 2002. Graphs show algal cover averaged over all transects from each site.

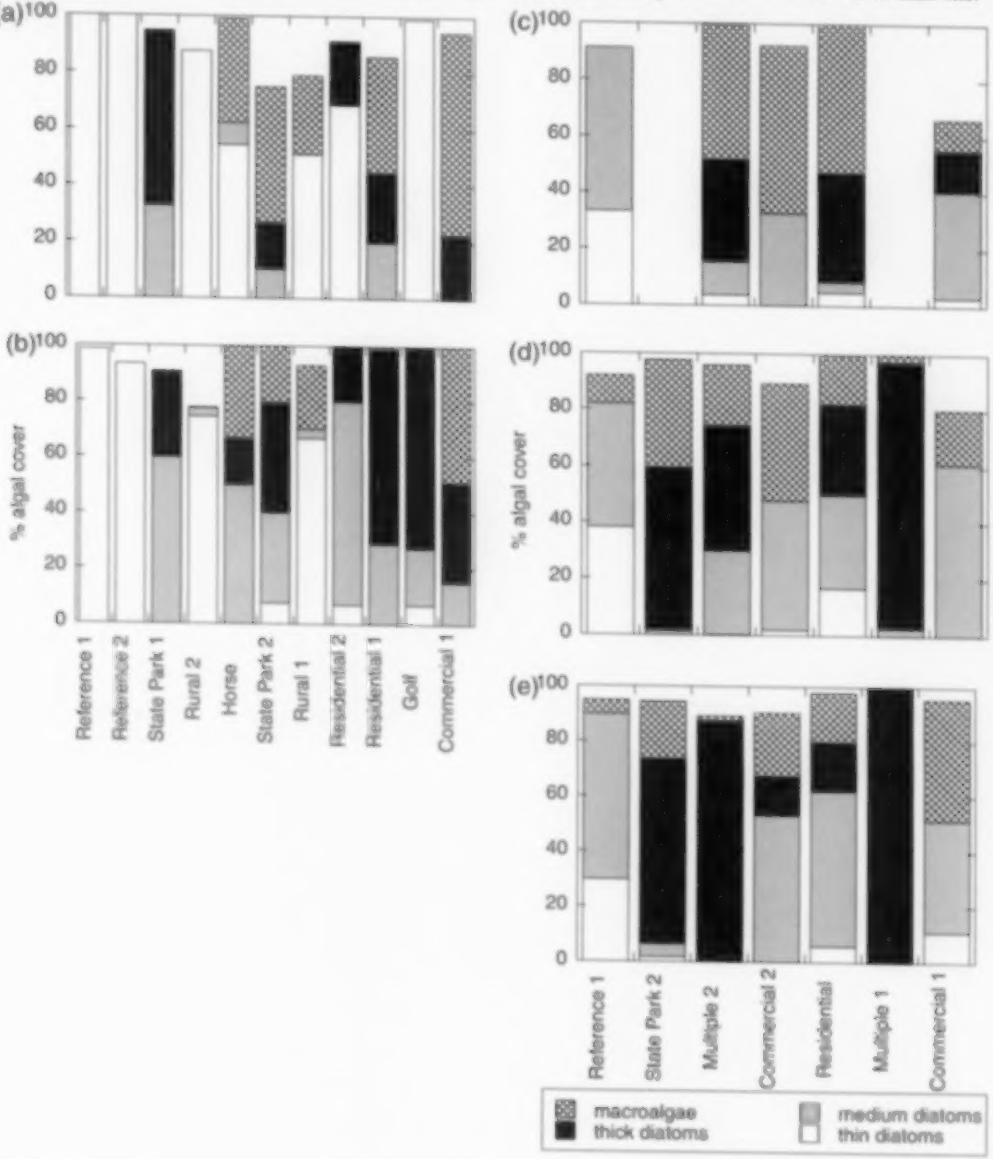

Chlorophyll *a* concentrations

Total and benthic Chl *a* concentrations were low ($<30\ \mathrm{mg\cdot m^{-2}}$) at reference and rural sites and tended to increase with increasing urban development (residential to multiple to commercial sites) in both years (Table 2; Figs. 3*a*, 3*b*). The reference, rural, horse stable, golf course, Residential 2, Multiple 1, and State Park 1 sites showed no or low concentrations of floating algae (Fig. 3*c*). The highest total chlorophyll concentrations were recorded at the Commercial, Multiple, and State Park 2 sites ($185–325\ \mathrm{mg\cdot m^{-2}}$), and all of these sites, except Multiple 1, were characterized by high biomasses of both floating and benthic algae (Fig. 3*a*). Benthic chlorophyll concentrations were higher in October than August in 2001 at all sites (paired *t* test, $P < 0.04$), whereas benthic chlorophyll concentrations were higher in August than in June or October at most undredged sites in 2002 (paired *t* test, $P < 0.02$; Fig. 3*b*). At undredged sites where floating algae were present, floating algal biomass decreased between August and October in both years (Fig. 3*c*).

Nutrient diffuser experiment

Nitrogen addition had a significant, positive effect on Chl *a* levels at the Reference 1 and State Park 2 sites (least squares means (LSM) test, $P < 0.001$ for each); however, P

Table 2. Pearson's correlation coefficients for relationships among land use and measured physical, chemical, and biological variables

		100 m			500 m			Catchment
		Urban	Urban + residential	Impervious	Urban	Urban + residential	Impervious	Urban
100 m	Urban	1	0.52	0.73	0.51	0.43	0.50	0.51
	Urban + residential		1	**0.95**	0.54	**0.80**	0.75	0.72
	Impervious			1	0.63	**0.80**	**0.80**	0.75
500 m	Urban				1	0.73	**0.80**	0.48
	Urban + residential					1	**0.97**	0.64
	Impervious						1	0.69
Catchment	Urban							1
Chl *a*	Benthic							
	Floating							
	Total							
	TP							
	TN							
	Current							
	% full sun							

Note: All variables were ln, ln $(x + 1)$, or arcsine square-root-transformed. $n = 14$ for all correlations except those involving light, where $n = 13$. Bold for statistical significance were determined through Bonferroni adjustments, treating each scale of analysis separately (Rice 1989). Chl *a*, chlorophyll *a*;

addition at those sites had a significant, negative effect (LSM test, $P < 0.002$ and $P < 0.001$, respectively; Figs. 4*a*, 4*f*). P addition also had a negative effect on Chl *a* concentration at the Residential 1 site, and both P and N additions had negative effects on Chl *a* concentrations at the Multiple 1 site ($P < 0.002$ to 0.007; Figs. 4*b* and 4*d*). Although Chl *a* concentrations declined with nutrient additions at the Commercial 2 and Multiple 2 sites (Figs. 4*c*, 4*e*), these declines were not statistically significant. Chl *a* values on diffusers at the Commercial 2 site were roughly an order of magnitude higher than at all other sites (Fig. 4*c*).

Relationships among land use and physical–chemical and algal variables

In regression models, we focused on using TP as an index of nutrient availability because the ln-transformed concentrations of dissolved inorganic nutrients, SRP, TN, and TP were highly intercorrelated (R values = 0.78 to 0.94), correlation coefficients between chlorophyll and P variables were greater than those between chlorophyll and N variables, and TP and SRP were very highly interrelated ($R = 0.94$, $P < 0.001$). Furthermore, when both ln(TN) and ln(TP) were entered into a regression model with Chl *a* concentration as the dependent variable, the TN slope became negligible (0.11) and nonsignificant ($P = 0.83$), whereas the TP slope was steep (1.90) and highly significantly different from 0 ($P = 0.007$).

Using data averaged across all sampling dates for each site, total chlorophyll concentrations were related positively to TP and light levels (Table 3; Fig. 5*a*). The relationship between ln(chlorophyll) and ln(TP) appeared to reach an asymptote (Fig. 5*a*), so a variety of curve forms were fit to these data (LOWESS for visualization; piecewise, quadratic, and linear equations for statistical fits). Iterative piecewise regression produced a ln(TP) threshold that was near the maximum TP values measured and produced a coefficient of determination that was not different from that produced by linear regression, probably because there were too few data points in the putative asymptotic part of the relationship. The best-fit model over the range of TP values measured was a quadratic equation with linear and quadratic terms that were significantly different from 0 ($P < 0.01$, $P < 0.02$, respectively). The quadratic model accounted for substantially greater amounts of the variation in the data set than did the linear model (linear $R^2 = 0.74$, $P = 0.001$; R^2 for quadratic model = 0.85, $P < 0.001$). These analyses indicate that the slope between ln(chlorophyll) and ln(TP) declined over the range of TP values measured, leveling off at the high end of the measured TP range.

Benthic chlorophyll concentrations were positively related to TP concentrations and current speed, whereas floating algae chlorophyll levels were not related to any physical or chemical variables (Table 3; Fig. 5*b*).

Because of consistently observed differences in the abundance of floating algae between August and October of both years, we also performed regressions using only August or only October data (average of 2001 and 2002 measurements) (see Table 3). Total and benthic chlorophyll concentrations were strongly, positively related to TP concentrations in both August and October; however, benthic and total chlorophyll concentrations also were positively related to light availability in October (Table 3). In August, floating algae Chl *a* concentrations increased with increasing light and TP levels and decreased with increasing current speeds (Table 3; Fig. 5*c*). Floating algae were not correlated with any physical or chemical parameters in October.

Relationships between the degree of urban development (measured as percent land in the urban and residential categories) and biological, physical, or chemical parameters were generally strongest when examining land use within the 500 m upstream cone and generally weak or nonexistent at both the 100 m and entire subwatershed scales (Table 2). The percentage of the land area that was covered by impervious surfaces and the percentage of land area classified as urban plus residential were significantly related to benthic and total chlorophyll concentrations at the 500 m scale (Table 2; Fig. 5*d*).

at three different spatial scales.

Chl *a*						
Benthic	Floating	Total	TP	TN	Current	% full sun
0.29	0.32	0.34	0.08	0.22	0.47	0.63
0.50	−0.07	0.47	0.32	0.33	0.29	0.10
0.56	0.04	0.54	0.38	0.46	0.44	0.27
0.67	0.52	0.69	0.46	0.63	0.42	0.29
0.75	0.29	**0.75**	0.57	0.61	0.50	0.32
0.77	0.29	**0.75**	0.57	0.65	0.58	0.43
0.25	−0.17	0.17	0.16	0.35	0.18	0.22
1	0.41	**0.98**	**0.88**	**0.75**	0.73	0.22
	1	0.57	0.36	0.29	0.15	0.42
		1	**0.86**	0.71	0.67	0.30
			1	**0.82**	0.50	−0.05
				1	0.55	0.04
					1	0.52
						1

type indicates correlations that are significant at $P < 0.05$. Threshold levels TP, total phosphorus; TN, total nitrogen.

Although floating algal Chl *a* was not correlated with the percentage of land area covered by impervious surfaces at this scale, floating algal chlorophyll was related to the magnitude of urban land use. No physical, chemical, or biological variables were correlated significantly with stream order.

Percent cover of macroalgae was closely correlated with Chl *a* of floating algae ($R = 0.94$, $P < 0.001$), as most of the macroalgae we observed were floating on the surface. Benthic Chl *a* was positively correlated with both percent cover of thick diatom films ($R = 0.87$, $P < 0.001$) and thick plus medium diatom films ($R = 0.84$, $P < 0.001$). Total Chl *a* was positively correlated with percent cover of nuisance algae, where nuisance algae is defined as the sum of floating macroalgae plus thick and medium diatom films ($R = 0.87$, $P < 0.001$).

Discussion

Land use patterns

Human activity and land use changes have long been known to influence the physical, chemical, and biological characteristics of streams (e.g., Omernik 1976; Peierls et al. 1991; Carpenter et al. 1998). In many developed watersheds, agriculture occupies the largest fraction of land area, whereas urban land use typically covers a much smaller fraction (Allan 2004). Urban land use, however, may have a disproportionately large influence on the chemistry and biology of streams (Paul and Meyer 2001), particularly in small catchments, such as those in southern California, where a large percentage of the drainage basin may be covered by urban uses (Beighley et al. 2003; Allan 2004). Urbanization of a catchment affects the ecology of streams in a number of predictable ways, including increased nutrient concentrations, altered hydrology, increased light levels and water temperature owing to the loss of riparian vegetation, stream channelization, and increased basin erosion (Paul and Meyer 2001; Meyer et al. 2005; Walsh et al. 2005). In our study streams, TN, TP, and benthic and total Chl *a* concentrations all increased with increases in urbanization.

The lack of correlations between measured variables and stream order suggests that land use was a much stronger determinant of water quality than stream order at this scale. Urbanization and stream order were not correlated in our system, because most of the urbanization was concentrated at intermediate elevations (i.e., around second- and third-order streams), whereas the upper and lower portions of this basin were largely undeveloped. Stream order is also difficult to define in this watershed, because surface flows are often intermittent or completely absent during the dry summer period.

The percentage of basin area that was covered by impervious surfaces and the percentage of land use classified as residential plus urban were correlated positively with benthic and total chlorophyll concentrations in our study, primarily at the 500 m scale of analysis. Although many factors can influence algal biomass, about 59% of the variation in benthic algal biomass and 56% of the variation in total chlorophyll concentrations could be explained by the percentage of land surface that was covered by impervious surfaces within a 500 m radius upstream. Increases in resource availability (primarily nutrients, but also light) appear to be the most important mechanisms by which urbanization influences algal biomass in our streams. Because measures of urbanization correlated more closely with algal biomass than with nutrient concentrations in this study, we suggest that there may be secondary mechanisms by which urbanization influences algal growth and accumulation. These mechanisms could include increased current speed (and hence increased nutrient delivery), environmental suppression of grazer populations by habitat simplification or toxic runoff (e.g., commercial pesticides), and increased micronutrient availability. Urbanization can incorporate all of these mechanisms. However, our analysis showing that nutrient concentrations explained much of the variability in chlorophyll suggests that increased nutrient loading is likely the dominant mode of influence.

Other studies comparing relationships among land use, nutrient concentrations, and algal biomass in streams have found closer relationships between land use and chlorophyll concentrations than between nutrients and chlorophyll (Taylor et al. 2004; Carr et al. 2005). In this study, we report tighter relationships between TN–TP concentrations and algal biomass in streams than reported in other studies, perhaps because such relationships become more manifest when algal succession and accumulation are not interrupted by floods and nutrient concentrations have stabilized, a situation that occurs over the long California dry season.

Our results also indicate that chemical and biological variables are responding primarily to human impacts on the landscape at the scale of the site and at an intermediate distance upstream (500 m). These results suggest that the 100 m scale may be too local to adequately capture upstream impacts on the sampled site. The subwatershed scale may be too large to detect land use – stream variable relationships because the subwatershed data do not reflect the spatial arrangement of land uses within the landscape and do not capture the effects of local land use patterns on the sampled site. The impacts of a particular land use on a given site will depend, to some de-

Fig. 3. Chlorophyll *a* concentrations (mg·m^{-2}) at stream sites in the Malibu Creek watershed, including (*a*) total chlorophyll concentrations (benthic + floating), (*b*) benthic chlorophyll concentrations, and (*c*) floating algae chlorophyll concentrations for all sampling dates. The heights of histograms indicate the average value for each site on each date (averaged over all transects at each site) and the error bar represents ±1 standard error.

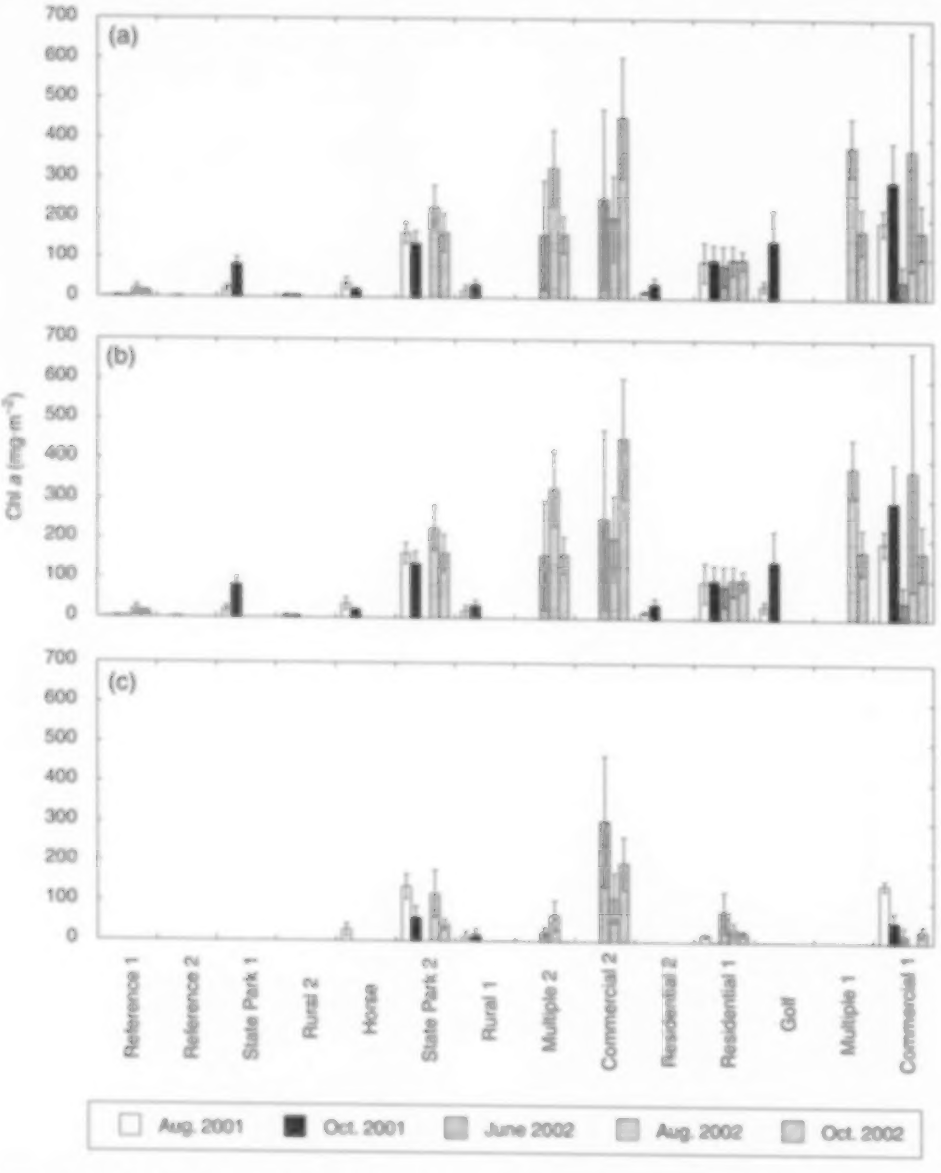

gree, on the proximity of that land use to that site (see also Strayer et al. 2003). In this study, land use was related to light availability at the smallest scale (100 m), probably because of local human impacts on riparian vegetation.

In predicting the impacts of land use patterns on stream ecosystems, the choice of the scale of analysis and prediction may depend on the nature of the predominant land use (e.g., agriculture vs. urban). Caraco and Cole (1999) found that nitrate export was strongly correlated with human population density at the scale of large watersheds (e.g., the Mississippi drainage). Strayer et al. (2003) compared nitrate export to land use metrics at watershed, stream corridor, and local (300 m radius) scales within the Chesapeake Bay watershed and found that land use at the largest scale was the best predictor of nitrate. Carr et al. (2005) also found correlations between agricultural land use metrics and nutrient concentrations at the watershed scale. All of these studies encompassed large areas of agricultural land use, whereas agricultural activity did not occur near our sites, and the predominant human influences were related to urbanization.

Fig. 4. Chlorophyll *a* (mean + 1 standard error) levels on nutrient diffusing substrata (NDS) arrays at selected stream sites within the Malibu Creek watershed for the period 28 August – 28 September 2002: (*a*) Reference 1, (*b*) Residential 1, (*c*) Commercial 2, (*d*) Multiple 1, (*e*) Multiple 2, (*f*) State Park 2. Asterisks over bars indicate significant N effects or P effects as determined by two-way analysis of variance (ANOVA) ($P < 0.01$). No interaction effects were detected. Note different scale of *y* axis in panel (*c*). Also, in panel (*f*) for the State Park 2 site, chlorophyll *a* levels on NDSs can be compared with levels from the other sites only with caution, because NDSs from this site were deployed for a shorter time period. C, control; N, +nitrogen; P, +phosphorus; NP, +nitrogen +phosphorus.

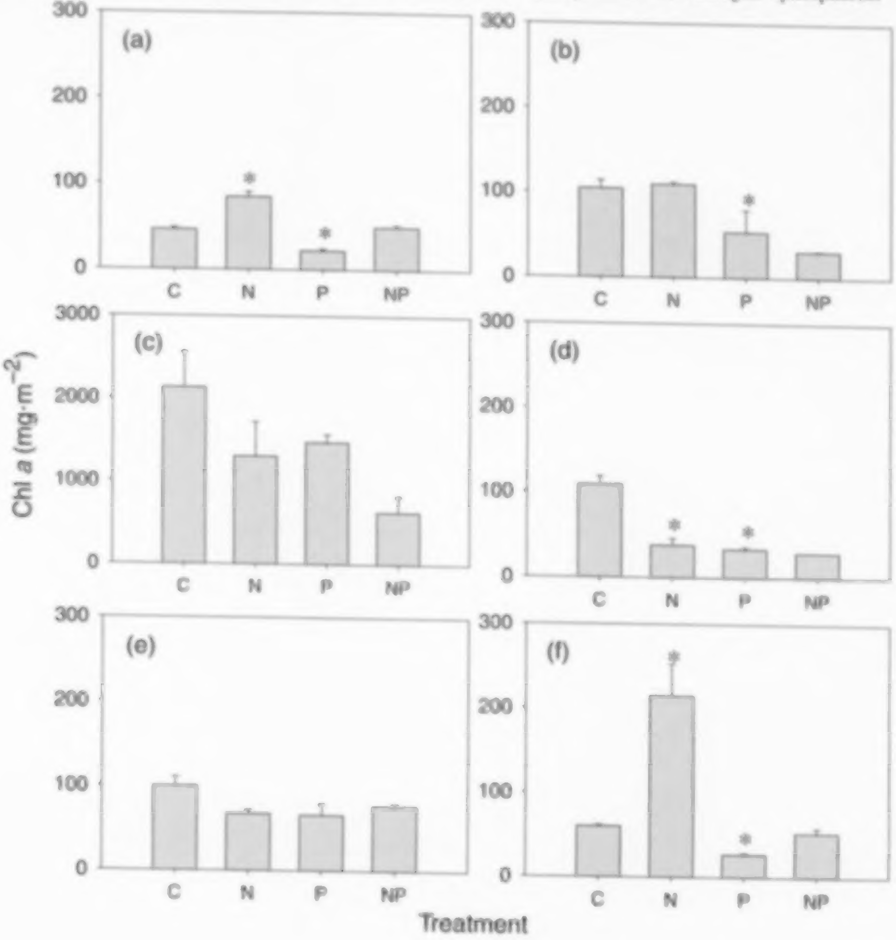

Nutrients

Nutrient concentrations at our developed sites were high compared with concentrations reported in the literature, even for those reported from urban streams. Studies in temperate urban streams have reported a wide range of nutrient concentrations (37–398 μg·L^{-1} TP, 394–4489 μg·L^{-1} TN (this study); 4–79 μg·L^{-1} SRP, 16–199 μg·L^{-1} NH_4-N (Meyer et al. 2005); 5–60 μg·L^{-1} TP (Bourassa and Cattaneo 1998); 42.9 μg·L^{-1} TP, 535 μg·L^{-1} TN (Cattaneo et al. 1997)). Two Mediterranean streams in Spain had mean nutrient values ranging from 181.3 to 470.8 μg·L^{-1} NO_3-N and from 7.9 to 19.2 μg·L^{-1} SRP (Marti and Sabater 1996). The highest TP concentrations we observed were similar to those reported from urban streams in southern Australia; however, our highest TN concentrations were nearly two times higher than those measured in those streams (350 μg·L^{-1} TP, 2100 μg·L^{-1} TN; Taylor et al. 2004). In contrast, our dissolved inorganic nitrogen (DIN) concentrations were similar to NO_3 concentrations found in urban streams in southwestern North America, but our SRP concentrations were approximately twice as high as SRP measured in the same streams (23–128 μg·L^{-1} SRP, 5–4024 μg·L^{-1} NO_3-N; Grimm et al. 2005). Finally, nutrient concentrations in an urbanized Atlantic stream system in Spain (with intense agricultural, urban, and industrial use) showed higher nutrient values than we measured (twice as high for nitrate, four times as high for TP; Sabater et al. 2000*b*). Background TP concentrations were high at our reference sites, probably owing to the weathering of volcanic soils and recent marine sediments that underlie much of the Malibu drainage basin (Brinck 1978; USGS 1997).

Dodds et al. (1998), surveying data from over 1000 temperate streams, designated streams with TP concentrations <25 μg·L^{-1} or TN concentrations <700 μg·L^{-1} as oligotrophic

Fig. 5. Scatter plots for various biological, physical, and chemical variables. (*a*) ln of total chlorophyll concentration vs. ln total phosphorus (TP) concentration across all sites (data averaged across all sampling dates). ln(chlorophyll) = −28.4 + 11.6(ln TP) − 0.99(ln TP)^2; $R^2 = 0.85$, $P < 0.0001$. Both the linear and quadratic coefficients were significantly different from 0 ($P < 0.01$ and $P < 0.02$, respectively). (*b*) ln benthic chlorophyll concentration vs. ln current speed across all sites (data averaged across all sampling dates). ln(chlorophyll) = 1.06(ln current speed) + 6.4; $R^2 = 0.53$, $P < 0.01$. (*c*) ln floating algae chlorophyll concentration vs. arcsine square root proportion of light availability for August (2001 and 2002 average for each site; one data point was excluded from this graph because the algae at this site had been scraped clean by county Flood Control just before sampling). ln(chlorophyll *a*) = 1.93 arcsine sqrt(light) + 0.70; $R^2 = 0.18$, $P < 0.15$. (*d*) ln total chlorophyll vs. arcsine square root proportion of land covered by impervious surfaces at the 500 m scale. ln(chlorophyll) = 4.56[arcsine sqrt (proportion impervious)] + 1.83; $R^2 = 0.56$, $P < 0.01$.

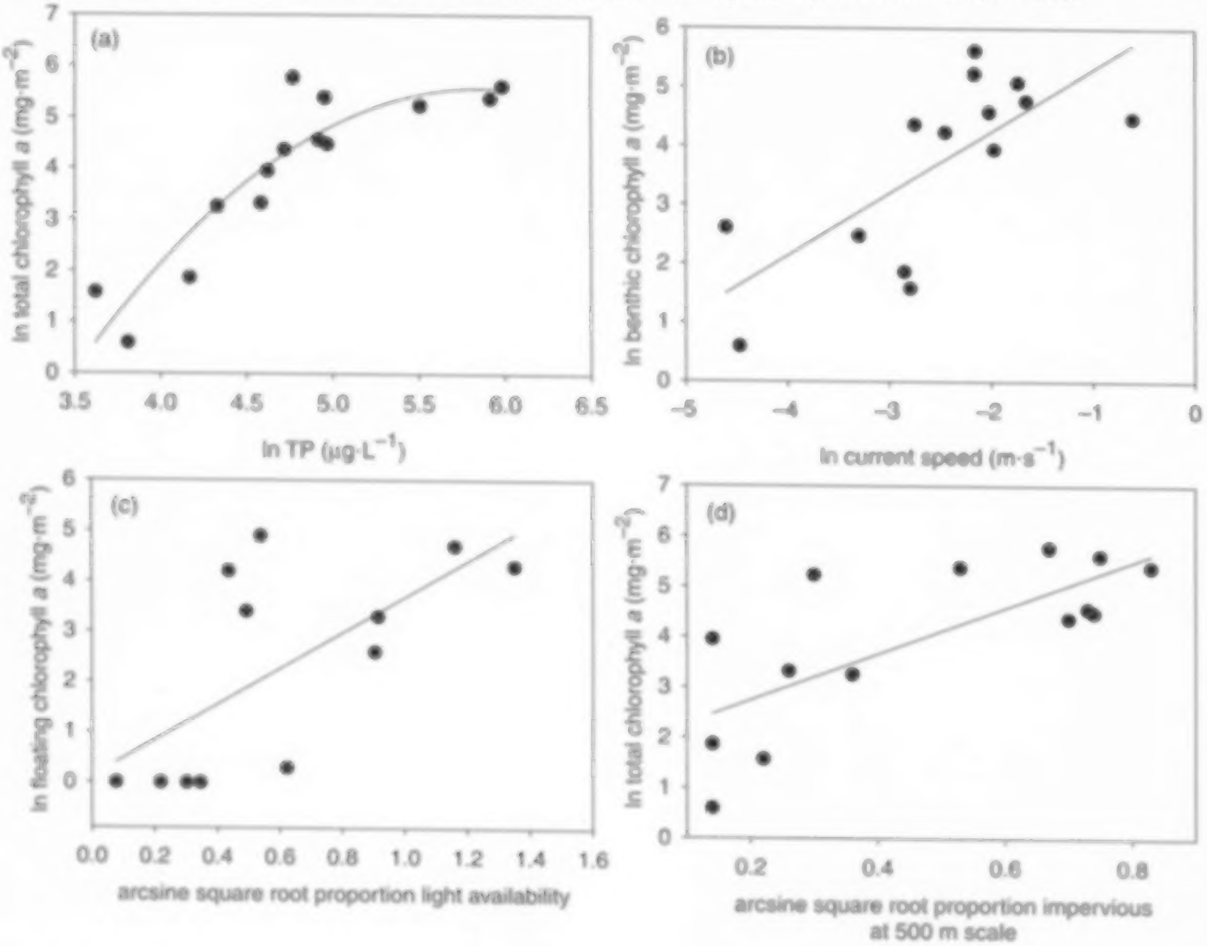

and streams with TP concentrations >75 µg·L^{-1} or TN concentrations >1500 µg·L^{-1} as eutrophic. Using these TP thresholds, all of our sites would be considered eutrophic, except the Reference and Rural 2 sites. In contrast, six sites would be classified as oligotrophic and only four sites would be classified as eutrophic using TN thresholds of Dodds et al. (1998). The classification scheme based on TN concentrations is not a good predictor of stream trophic state in the Malibu Creek watershed, because several of the streams classified as oligotrophic using this scheme had high biomasses of benthic algae. The TN concentrations in our streams were low compared with concentrations reported in Dodds et al. (1998), possibly because many North American basins are subjected to agricultural use (Allan 2004), and N additions through fertilizer applications may elevate N levels much more in agricultural than in urbanized watersheds.

Algal data

Biggs (2000*a*) recommended a maximum percent cover by filamentous algae of 30% in streams to protect stream aesthetics, benthic biodiversity, trout habitat, and sports fisheries. In August 2001, four of our study sites exceeded 30% cover by filamentous algae (Horse, State Park 2, Residential 1, and Commercial 1), whereas in October 2001, only Horse and Commercial 1 contained >30% cover by filamentous algae. In 2002, three sites (Multiple 2, Commercial 2, and

Table 3. Significant multiple regression models for relationships between chlorophyll *a* (Chl *a*) concentration and selected physical and chemical variables.

Chl *a*	Physical–chemical variable	Partial coefficient	P	Model overall P	RSE	Error df	Multiple R^2
Mean of all sampling dates							
Total	TP	1.78	<0.001	0.008	0.63	10	0.83
	% full sun	1.07	0.024				
Benthic only	TP	1.55	<0.001	0.006	0.56	11	0.89
	Current speed	0.55	0.007				
Floating only	No significant models						
August 2001–2002							
Total	TP	2.21	0.001	0.012	1.29	12	0.59
Benthic only	TP	2.27	0.001	0.01	1.18	12	0.65
Floating only	% full sun	3.61	0.014	0.042	1.56	9	0.58
	TP	1.81	0.041				
	Current speed	−1.83	0.021				
October 2001–2002							
Total	TP	1.43	<0.001	0.006	0.60	10	0.84
	% full sun	1.76	0.001				
Benthic only	TP	1.43	<0.001	0.007	0.57	10	0.84
	% full sun	1.54	0.002				
Floating only	No significant models						

Note: All dependent and independent variables were ln, ln(n + 1), ln(n + 0.1), or arcsine square-root-transformed. Independent variables included in initial regression models were current speed, light availability, and TP. The most parsimonious models for explaining variation in Chl *a* concentrations were determined through backward stepwise elimination, with all final model terms accounting for a significant amount of the variation in Chl *a* concentrations. Because the August and October data were averaged across years to produce a data set of mean levels of chlorophyll concentrations and physical and chemical variables across the entire study, the August and October data were not independent of the data of means across all sampling dates. A simple Bonferroni adjustment for determining statistical significance for all nine regression analyses produced the same results as the unadjusted analyses, with the exception of the regression analysis for factors determining floating algae Chl *a* concentrations in August. We have retained the unadjusted results for this variable and month here, because the P value for the relationship between floating algae and light levels is low, the coefficient of determination for the overall regression is relatively high, and these results accord with our broader scale observations of floating algae distributions, with the cautionary note that these results are of uncertain statistical validity. All regression analyses that were not significant with either the unadjusted or Bonferroni-adjusted probability levels are listed as "No significant models" here. P, probability value for t test examining the difference of the slope from 0; RSE, residual standard error; df, degrees of freedom; multiple R^2 and model overall P, overall regression model coefficient of determination and associated probability value, respectively; TP, total phosphorus.

Residential 1) in June, two sites (State Park 2, Commercial 2) in August, and just one site (Commercial 1) in October exceeded this recommended level of algal cover.

Suren et al. (2003) reported high coverage by filamentous green algae (up to 50% algal cover) and thick brown mats (up to 20% algal cover) in enriched stream sites at low flow, at a time when there were only thin algal films in an unenriched stream. Biggs and Price (1987) also reported benthic coverage by filamentous algae exceeding 40% along the banks of most New Zealand rivers under low-flow conditions, similar to filamentous algal coverage observed in this study. Butturini and Sabater (1998) found up to 41.4% algal cover by filamentous algae in a Mediterranean stream in summer, comparable with what we found.

Most of our sites in developed areas had extremely high algal biomass, with floating algae contributing a substantial proportion of the algal biomass at some of these sites. Although a high biomass of floating algae in streams has rarely been reported, Biggs and Price (1987) found high abundances of filamentous green algae (both floating and attached) in New Zealand rivers during an extensive drought, when physical and chemical conditions in their streams were similar to those found during the extended summer in southern California streams. Typically, studies of temperate urban streams have reported lower periphyton biomass (e.g., 1–146 mg Chl $a{\cdot}m^{-2}$ (Cattaneo et al. 1997; Bourassa and Cattaneo 1998; Taylor et al. 2004) than observed in our study (1.8–322.4 $mg{\cdot}m^{-2}$), but chlorophyll concentrations comparable with ours have been occasionally reported (281 $mg{\cdot}m^{-2}$, Biggs 2000*b*; 188.8 ± 34 $mg{\cdot}m^{-2}$, Suren et al. 2003), and a few studies have observed higher maximum chlorophyll levels (1396 $mg{\cdot}m^{-2}$, Biggs 2000*b*; 1232 $mg{\cdot}m^{-2}$, Taylor et al. 2004).

Differences in algal biomass observed in urban streams across different studies can be attributed, perhaps, to climatic differences among study locations. The lack of spates and low current speeds in southern California streams in the dry season probably promote the accumulation of algal biomass and create stagnant, high resource conditions favorable to mats of floating algae. Sabater and Sabater (1992), working in a Mediterranean river with a similar flow pattern, observed similar average spring chlorophyll concentrations (38.6 mg Chl $a{\cdot}m^{-2}$) to those in our study (38.5 mg Chl $a{\cdot}m^{-2}$), but average summer chlorophyll concentrations were much higher in our stream system (127.3 mg Chl $a{\cdot}m^{-2}$) than at their sites (58.3 mg Chl $a{\cdot}m^{-2}$). Extremely high mean chlorophyll concentrations have been found in highly disturbed Mediterranean streams in Spain (311 mg Chl $a{\cdot}m^{-2}$), with maximum chlorophyll levels (834 mg Chl $a{\cdot}m^{-2}$) comparable with those at our unshaded study sites (Sabater et al.

Table 4. Suggested thresholds for benthic biomass levels (as chlorophyll *a* (Chl *a*) concentrations) that create problems for the recreational use and aesthetic enjoyment of streams.

Upper limit of acceptable mean Chl *a* concentration (mg·m^{-2})	Comment	Reference
150–200	Based on perceived impairment	Welch et al. 1989
100–150	Based on 19 enrichment cases and surveys	Welch et al. 1989; Horner et al. 1983
50–100	British Columbia Ministry of Environment guideline	Nordin 1985
150	Based on survey of 286 cases	Dodds et al. 1998
120	Based on New Zealand stream surveys	Biggs 2000*a*

Note: Adapted from Dodds et al. (1998).

1998; Romani and Sabater 2000). An Atlantic stream system in Spain with high levels of human impact showed nutrient concentrations and average chlorophyll concentrations (spring: 214 mg Chl *a*·m^{-2}; summer: 389 mg Chl *a*·m^{-2}) much higher than those we measured in our study (spring: 38.5 mg Chl *a*·m^{-2}; summer: 127.3 mg Chl *a*·m^{-2}) (Sabater et al. 2000*b*).

It is possible that nutrient inputs into our system are high enough to drive the accumulation of algae, overriding any top-down control by grazers. Suren et al. (2003) also found filamentous algae dominating a low-flow, enriched stream in New Zealand and suggested that periphyton production rates were far greater than potential invertebrate grazing rates. Chlorophyll concentrations similar to those we found are observed primarily in experimental studies where nutrient inputs are highly elevated. Kjeldsen (1996) reported that algal biomass peaked at 844 mg Chl *a*·m^{-2} in open, unshaded stream reaches when grazers were absent.

Recently, researchers have set thresholds indicating algal biomass levels that create problems for water quality and the recreational use of streams (Table 4). Dodds et al. (1998), surveying data from 286 temperate streams, designated streams with <20 mg Chl *a*·m^{-2} as oligotrophic, those with 20–70 mg Chl *a*·m^{-2} as mesotrophic, and those with >70 mg Chl *a*·m^{-2} as eutrophic. Using this scheme, the majority of our stream reaches would be classified as eutrophic, and only the Reference and Rural 2 sites would be considered oligotrophic. Other researchers have set impairment limits for maximum chlorophyll levels in streams ranging from 50 to 200 mg Chl *a*·m^{-2} (see Table 4; e.g., Welch et al. 1988; Biggs 2000*a*; Dodds and Welch 2000). Using the higher threshold for stream impairment of 200 mg Chl *a*·m^{-2}, four out of twelve of our study reaches in 2001 and six out of seven reaches in 2002 exceeded acceptable thresholds, including all sites with considerable urban development (residential, commercial, multiple sites). Other researchers, such as Biggs (2000*a*), have suggested that average chlorophyll levels ≤15 mg·m^{-2} are needed to maintain a high diversity of benthic invertebrates, values that we only observed at the reference sites (both years) and at one of the rural sites (Rural 2 in 2001). Although high chlorophyll concentrations are likely in many urban streams, literature data on urban streams are scarce.

Some studies have suggested that the percent cover of different types of filamentous algae could be used as a measure of habitat quality and the success of restoration efforts (Suren et al. 2003; Pan et al. 2004). We found tight correlations between chlorophyll concentrations and the percent cover of easily definable categories of algae (floating macroalgae; thin, medium, or thick diatom films), indicating that nuisance algal cover values may suffice in monitoring stream systems when it is difficult to measure chlorophyll levels.

Factors promoting high levels of algal biomass

In the summer, floating algal chlorophyll concentrations were positively related to light and nutrient levels and negatively related to current speeds, reaching their highest levels in slow, sunny, enriched sites. We found floating macroalgae, primarily *Enteromorpha* and *Rhizoclonium*, in sunny pools and slow runs (current speed <0.2 m·s^{-1}) where riparian vegetation had been reduced or completely removed by human activity. It has been found that the growth and biomass of floating macroalgae are greatest under high nutrient and light conditions (Dell'Uomo 1991; J. Simpson and G. Creeely, unpublished data), and these algae flourish in stagnant or low-flow environments because they would be washed away by substantial currents. Floating algae biomass was not related to physical–chemical variables in October, probably because of the overall low abundances of floating macroalgae in the autumn.

Benthic algal biomass was positively related to current speed, consistent with the results of other studies that have shown that increased current speeds increase the delivery rates of nutrients to algae, particularly when benthic periphyton grow in thick, multilayered communities (Stevenson and Glover 1993; Stevenson et al. 1996). Within algal mats, nutrient depletion can occur rapidly because of reduced nutrient transport through the biofilm matrix, nutrient uptake by overlying periphyton layers, and an increased thickness of the boundary layer. Increasing the current speed decreases the thickness of the boundary layer and increases nutrient flux rates. Many sites in our study had thick benthic algal mats, so it was unclear if algal growth was limited more by the delivery rate of nutrients than by absolute nutrient concentrations. As current speeds increase above a threshold, algal biomass accumulation may decrease or level off as biomass is lost to shear stress. Our data suggest that this threshold occurs around 0.4 m·s^{-1}.

Although benthic chlorophyll concentrations were strongly related to TP concentrations, they were only related to light levels in October. It is possible that light is not limiting during summer months, but becomes more so in the autumn months when day length grows shorter and overall light inputs decrease. Elevated nutrient availability might be able to compensate for low light availability; benthic diatoms maintained very high biomass levels (measured both as chlorophyll and as the percent cover and thickness of diatom mats) at our Multiple 1 and 2 sites, which both had very high TP and very low light availability because of a dense riparian canopy. Diatoms in previous studies have demonstrated broad shade tolerance (Sundback et al. 1996), probably owing to their ability to adjust their photosynthetic efficiency (Hill et al. 1995) or switch to heterotrophic metabolism (Tuchman et al. 2006). Even so, low light availability probably engenders nutrient saturation at lower nutrient concentrations.

In this study, we found that total and benthic algal biomass was tightly related to TP concentrations, suggesting that nutrients limited algal biomass accrual in streams of the Malibu Creek watershed and corroborating literature results emphasizing the importance of nutrient limitation to algae (see review by Borchardt 1996). Chlorophyll also was positively related to TN concentrations, although the relationship was not as strong or as tight as the chlorophyll–TP relationship. Comparisons of these correlative results with data on molar TN/TP ratios and results from the NDS experiments, however, produced conflicting conclusions.

Molar TN/TP ratios in stream water have been used to predict the nutrient-limiting algal growth and biomass, with $N/P > 20$ suggesting P limitation, $N/P < 10$ suggesting N limitation, and $10 < N/P < 20$ suggesting colimitation by both N and P or limitation by neither (Schanz and Juon 1983; Grimm and Fisher 1986; Hill and Knight 1988). By these criteria, two of our sites appeared to be N-limited, six sites appeared to be P-limited, and six of our sites fell between 10 and 20, suggesting colimitation by both N and P or limitation by neither. Based on molar TN/TP ratios, Francoeur et al. (1999) reported that different streams in New Zealand appeared to be limited by N, P, or both. A study of urban Australian streams suggested that P was the nutrient likely limiting algal growth based on TN/TP ratios (Taylor et al. 2004); however, Dodds et al. (2002) have suggested that nutrients may no longer limit algal growth at very high nutrient levels regardless of N/P ratios.

N/P ratios in stream water may be of limited use for determining the nature and degree of nutrient limitation for several reasons. Complex algal communities may have nonlinear, distinctive responses to the addition of different nutrients, algae may engage in luxury uptake and storage of either N or P, and the physical structure of algal communities or the form of N and P available may influence algal uptake (see Francoeur et al. 1999). Also, when algal biomass is high and flows are low, rapid rates of nutrient uptake can reduce concentrations of N and P in the water column, obscuring the actual rate of nutrient delivery or amounts of N or P available to the algae.

In the NDS experiments, we found increases in chlorophyll concentrations with N addition at the Reference and State Park 2 sites, although molar TN/TP ratios for these sites (14.5, 11.4) would suggest no limitation or colimitation of algal growth by N and P. Nitrogen limitation at the reference site was likely due to high background phosphate concentrations at a site where N concentrations were relatively low. Algal biomass at the State Park 2 site also increased with N inputs, although nutrient levels were high; however, this site had the lowest TN/TP ratio (11.4) among the sites tested with NDS assays. Both N and P levels were at very high, perhaps saturating, levels at the remaining four sites where NDS arrays were deployed, and molar TN/TP ratios were highly variable among these sites (12.8, 19.7, 26.7, 34.2).

At these sites, algal biomass either did not change with nutrient additions (Commercial and Multiple 2 sites) or actually declined with N and (or) P additions compared with the controls (Residential 1 and Multiple 1 sites). Reductions in chlorophyll concentrations with increased P inputs have been observed in a number of other NDS studies (see review by Francoeur 2001), suggesting that NDS methods may produce anomalous results particularly when nutrient levels are high (this study). A brief survey of published NDS studies in which this apparent inhibitory P effect occurred showed no obvious connection with type, pH, or concentration of phosphate or with environmental conditions (e.g., light availability, current speed, ambient chlorophyll concentrations). Although common, this phenomenon is rarely discussed in the literature (but see Hill and Knight 1988; Tank and Dodds 2003), and to our knowledge no mechanisms for explaining this result have been proposed. Also, NDS assays only measure the biomass of benthic algae, disregarding the floating algae, which were a major component of our system.

Seasonal changes in nutrient limitation may also occur. We performed our NDS experiment in late summer, during the period of highest ambient algal biomass. Using a similar technique across four seasons in an urban stream in southwestern North America, Grimm et al. (2005) found N limitation of algal growth in spring, when algal biomass was low, but not in summer, when algal biomass was approximately an order of magnitude higher. In a similar NDS study in New Zealand, however, Francoeur et al. (1999) found the strongest nutrient limitation in summer, when the accrual of algal biomass was greatest.

The different methods we used to determine the nature and degree of nutrient limitation of algal biomass (regression analysis of survey results, streamwater TN/TP ratios, the NDS experiment) suggested different conclusions regarding nutrient limitation of algal biomass in streams in the Malibu Creek catchment. Regression analysis revealed a clear relationship between algal biomass and TP concentrations, although the form of this relationship indicated that P might have reached saturating levels for algal growth, particularly at sites where light availability was low. TN/TP ratios, on the other hand, indicated N limitation of algal biomass at two sites, P limitation at six sites, and colimitation or no limitation at six sites. The NDS results indicated N limitation at two sites with relatively low to intermediate TN/TP ratios; however, algal biomass either did not respond or actually decreased with nutrient additions at the other four sites, all sites with very high nutrient levels and highly variable TN/TP ratios (12.8 to 34.2).

The NDS and TN/TP methods of determining nutrient limitation may become less applicable when ambient nutrient concentrations are sufficiently high that nutrient limitation is minimal and algal growth becomes limited by other factors, such as light or substrate availability. N and P concentrations at a number of our sites (e.g., Multiple 1 and 2, Commercial 1 and 2, Residential 1 and 2, State Park 2, Golf) were higher than levels reported to saturate algal growth in other studies (8–50 $\mu g \cdot L^{-1}$ for P and 500–700 $\mu g \cdot L^{-1}$ for N; Wuhrmann and Eichenberger 1975; Bothwell 1989; Horner et al. 1990). Dodds et al. (2002) also found evidence for nutrient saturation of algal growth in many temperate climate streams. If both N and P reach or exceed nutrient saturation thresholds, then both the results of NDS assays and N/P ratios have little relevance to algal growth or biomass. Within this context, it should be noted that 8 of the 14 surveyed sites, and five of the six sites where NDS arrays were deployed, had nutrient levels that exceeded saturation thresholds reported in the literature.

In their analysis of data from over 100 streams, Dodds et al. (2002) found significant relationships between nutrient concentrations and maximum chlorophyll concentrations. We found such relationships in our data, although the correlations were not as strong as with average chlorophyll (maximum chlorophyll vs. TP, $R^2 = 0.67$). This suggests that nutrient conditions can be useful predictors of both mean and maximum chlorophyll.

Biggs (2000*a*) suggested that nutrients will primarily influence the accrual of algal biomass in streams with relatively benign hydrological conditions or during extended periods of low flow, which exactly describes dry season conditions in streams in Mediterranean climates. In the absence of disturbance, algal biomass will increase with increasing nutrient levels to an asymptote where algae become limited by other factors (e.g., light at the stream bottom or within the algal mat, space for attachment and growth). Because the Mediterranean climate in southern California provides a long, undisturbed growing season for algae, and urban streams often have high nutrient levels, some of these other factors may have ultimately limited algal growth and biomass more than nutrient supply, particularly given the very high algal biomasses recorded in this study.

Our results clearly show that urban development and human activities strongly affect stream algal communities in the Malibu Creek basin, probably via land use effects on nutrient and light availability. Our results also indicate that benthic and floating algae respond differently to changes in physical and chemical variables (light, current speed, nutrient concentrations). Because blooms of benthic and floating algae can reduce stream water quality and affect ecosystem function and recreational use, regulatory agencies need to consider both types of algae when formulating management plans. For example, management actions that reduce light availability in streams (e.g., by replanting riparian vegetation) may reduce the biomass of floating macroalgae, but may have little effect on benthic diatoms. Increased stream flows could reduce the biomass of floating algae by washing these algae downstream, but could increase the biomass of benthic algae. Finally, reducing nutrient loading to streams by controlling point and nonpoint nutrient sources would probably reduce the biomass of both types of algae, but large reductions in nutrient loading may be necessary before a decrease in algal biomass is observed. Thus, the control of algal growth may require site-specific management practices focused on the particular types of algae causing nuisance blooms.

Although high densities and floating mats of *Enteromorpha* or *Rhizoclonium* have not been commonly reported in the literature, our observations of the coastal streams of southern California, ranging from San Diego north to Point Conception, indicate that floating mats are common in streams draining catchments modified by agricultural or urban development in this region (L. Busse and J. Simpson, personal observation). If these types of algae are becoming more abundant in streams draining catchments subjected to urbanization in other parts of the world, it is clear that more research on the factors controlling the distribution, abundance, and composition of floating algae, and their effects on stream ecosystems, is warranted.

The standard model of algal growth and biomass controlled by resource supply, disturbance, and grazing (Biggs et al. 1998*a*, 1998*b*) requires adjustment to accurately represent streams in Mediterranean climates, where spates occur almost exclusively during the winter months and where there are long periods of stable low flows during the dry season. The work described here has contributed to our understanding of the effects of urbanization on stream communities, particularly those in Mediterranean climates, and provides a foundation for future research on these little-studied systems.

Acknowledgements

This work was supported by funds from the Los Angeles Regional Water Quality Control Board and the Southern California Coastal Water Research Project. This study also was partially supported by postdoctoral fellowships from the German Academic Exchange Service (DAAD) and the Santa Barbara Coastal LTER (grant No. OCE99-82105), both to L. Busse. J. Simpson was supported by a National Science Foundation Graduate Research Fellowship. The authors thank the following agencies, organizations, and individuals for permission to visit sampling sites: Mountains Restoration Trust, Rancho Simi Parks and Recreation District, Los Angeles County Department of Public Works, National Parks Service, the City of Calabasas, the Lindero Country Club, R. Stewart, and Malibu Creek State Park. The authors also thank M. Abramson and S. Luce of Heal the Bay and R. Ambrose from UCLA for their assistance in site selection and access; M. Abramson and W. McClintock for assistance with the acquisition and analysis of land use data; and R. Orton of the Las Virgenes Municipal Water District for assistance with data interpretation. G.M. Carr and two anonymous reviewers provided very thoughtful comments, which improved the manuscript.

References

Allan, J.D. 2004. Landscapes and riverscapes: the influence of land use on stream ecosystems. Annu. Rev. Ecol. Evol. Syst. **35**: 257–284.

Barbour, M.T., Gerritsen, J., Snyder, B.D., and Stribling, J.B. 1999. Rapid bioassessment protocols for use in streams and wadeable rivers: periphyton, benthic macroinvertebrates and fish. 2nd ed. US Environmental Protection Agency, Office of Water, Washington, D.C. EPA 841-B-99-002.

Beighley, R.E., Melack, J.M., and Dunne, T. 2003. Impacts of California's climatic regimes and coastal land use change on streamflow characteristics. J. Am. Water Res. Assoc. **39**(6): 1419–1433.

Biggs, B.J.F. 2000*a*. New Zealand periphyton guidelines: detecting, monitoring and managing the enrichment of rivers. Background and guidelines. Ministry for the Environment, Wellington, New Zealand.

Biggs, B.J.F. 2000*b*. Eutrophication of streams and rivers: dissolved nutrient–chlorophyll relationships for benthic algae. J. North Am. Benthol. Soc. **19**(1): 17–31.

Biggs, B.J.F., and Price, G.M. 1987. A survey of filamentous algal proliferations in New Zealand rivers. N.Z. J. Mar. Freshw. Res. **21**(2): 175–191.

Biggs, B.J.F., Kilroy, C., and Lowe, R.L. 1998*a*. Periphyton development in three valley segments of a New Zealand grassland river: test of a habitat matrix conceptual model within a catchment. Arch. Hydrobiol. **143**(2): 147–177.

Biggs, B.J.F., Stevenson, R.J., and Lowe, R.L. 1998*b*. A habitat matrix conceptual model for stream periphyton. Arch. Hydrobiol. **143**(1): 21–56.

Borchardt, M.A. 1996. Factors affecting benthic algae: nutrients. *In* Algal ecology: freshwater benthic ecosystems. *Edited by* R.J. Stevenson, M.L. Bothwell, and R.L. Lowe. Academic Press, San Diego. pp. 184–217.

Bothwell, M.L. 1989. Phosphorus-limited growth dynamics of lotic periphytic diatom communities: areal biomass and cellular growth rate responses. Can. J. Fish. Aquat. Sci. **46**(8): 1293–1301.

Bourassa, N., and Cattaneo, A. 1998. Control of periphyton biomass in Laurentian streams (Quebec). J. North Am. Benthol. Soc. **17**(4): 420–429.

Brinck, J.W. 1978. World resources of phosphorus. *In* Phosphorus in the environment. *Edited by* R. Porter and D.W. Fitzsimons. Elsevier, Amsterdam. pp. 23–44.

Butturini, A., and Sabater, F. 1998. Ammonium and phosphate retention in a Mediterranean stream: hydrological versus temperate control. Can. J. Fish. Aquat. Sci. **55**: 1938–1945.

Caraco, N.F., and Cole, J.J. 1999. Human impact on nitrate export: an analysis using major world rivers. Ambio, **28**: 167–70.

Carpenter, S.R., Caraco, N.F., Correll, D.L., Howarth, R.W., Sharpley, A.N, and Smith, V.H. 1998. Nonpoint pollution of surface waters with phosphorus and nitrogen. Ecol. Appl. **8**(3): 559–568.

Carr, G.M., Chambers, P.A., and Morin, A. 2005. Periphyton, water quality, and land use at multiple spatial scales in Alberta rivers. Can. J. Fish. Aquat. Sci. **62**: 1309–1319.

Cattaneo, A., Kerimian, T., Roberge, M., and Marty, J. 1997. Periphyton distribution and abundance on substrata of different size along a gradient of stream trophy. Hydrobiologia, **354**: 101–110.

Cooper, S.D., Dudley, T.L., and Hemphill, N. 1986. The biology of chaparral streams in southern California. *In* Proceedings of the Chaparral Ecosystems Research Conference, Santa Barbara, California, 16–17 May 1985. *Edited by* J.J. DeVries. Universitry of California – Davis. Water Resources Center Rep. No. 62. pp. 139–151.

Davies, A.L., and Gee, J.H.R. 1993. A simple periphyton sampler for algal biomass estimates in streams. Freshw. Biol. **30**: 47–51.

DeCastri, F., and Mooney, H.A. (*Editors*). 1973. Mediterranean type ecosystems, origin and structure. Springer-Verlag, New York.

Dell'Uomo, A. 1991. Use of benthic macroalgae for monitoring rivers in Italy. *In* Use of algae for monitoring rivers. III. *Edited by* B.A. Whitton, E. Rott, and G. Friedrich. E. Rott, Innsbruck, Austria. pp. 129–138.

Dodds, W.K., and Oakes, R.M. 2004. A technique for establishing reference nutrient concentrations across watersheds affected by humans. Limnology and Oceanography: Methods, **2**: 333–341.

Dodds, W.K., and Welch, E.B. 2000. Establishing nutrient criteria in streams. J. North Am. Benth. Soc. **19**(1): 186–196.

Dodds, W.K., Jones, J.R., and Welch, E.B. 1998. Suggested classification of stream trophic state: distributions of temperate stream types by chlorophyll, total nitrogen, and phosphorus. Water Res. **32**(5): 1455–1462.

Dodds, W.K., Smith, V.H., and Lohman, K. 2002. Nitrogen and phosphorus relationships to benthic algal biomass in temperate streams. Can. J. Fish. Aquat. Sci. **59**: 865–874.

Dudley, T.L. 1992. Beneficial effects of herbivores on stream macroalgae via epiphyte removal. Oikos, **65**(1): 121–127.

Feminella, J.W., and Walsh, C.J. 2005. Urbanization and stream ecology: an introduction to the series. J. North Am. Benthol. Soc. **24**(3): 585–587.

Francoeur, S.N. 2001. Meta-analysis of lotic nutrient amendment experiments: detecting and quantifying subtle responses. J. North Am. Benthol. Soc. **20**(3): 358–368.

Francoeur, S.N., Biggs, B.J.F., Smith, R.A., and Lowe, R.L. 1999. Nutrient limitation of algal biomass accrual in streams: seasonal patterns and a comparison of methods. J. North Am. Benthol. Soc. **18**(2): 242–260.

Gasith, A., and Resh, V.H. 1999. Streams in Mediterranean climate regions: abiotic influences and biotic responses to predictable seasonal events. Annu. Rev. Ecol. Syst. **30**: 51–81.

Grimm, N.B., and Fisher, S.G. 1986. Nitrogen limitation in a Sonoran Desert stream. J. North Am. Benthol. Soc. **5**(1): 2–15.

Grimm, N.B., Sheibley, R.W., Crenshaw, C.L., Dahm, C.N., Roach, W.J., and Zeglin, L.H. 2005. N retention and transformation in urban streams. J. North Am. Benthol. Soc. **24**(3): 626–642.

Hill, W.R., and Knight, A.W. 1988. Nutrient and light limitation of algae in two northern Californian streams. J. Phycol. **24**: 125–132.

Hill, W.R., Ryon, M.G., and Schilling, E.M. 1995. Light limitation in a stream ecosystem: responses by primary producers and consumers. Ecology, **76**: 1297–1309.

Horner, R.R., Welch, E.B., and Veenstra, R.B. 1983. Development of nuisance periphytic algae in laboratory streams in relation to enrichment and velocity. *In* Periphyton of freshwater ecosystems. *Edited by* R.G. Wetzel. Dr. W. Junk Publishers, The Hague. pp. 121–134.

Horner, R.R., Welch, E.B., Seeley, M.R., and Jacoby, J.M. 1990. Responses of periphyton to changes in current velocity, suspended sediment, and phosphorus concentration. Freshw. Biol. **24**: 215–232.

Kjeldsen, K. 1996. Regulation of algal biomass in a small lowland stream: field experiments on the role of invertebrate grazing, phosphorus and irradiance. Freshw. Biol. **36**: 535–546.

Malmqvist, B., and Rundle, S. 2002. Threats to the running water ecosystems of the world. Environ. Conserv. **29**(2): 134–153.

Marti, E., and Sabater, F. 1996. High variability in temporal and spatial nutrient retention in Mediterranean streams. Ecology, **77**(3): 854–869.

Meybeck, M. 2003. Global analysis of river systems: from Earth system controls to Anthropocene syndromes. Philos. Trans. R. Soc. B Lond. B. Biol. Sci. **358**(1440): 1935–1955.

Meyer, J.L., Paul, M.J., and Taulbee, W.K. 2005. Stream ecosystem function in urbanizing landscapes. J. North Am. Benthol. Soc. **24**(3): 602–612.

Nordin, R.H. 1985. Water quality criteria for nutrients and algae (technical appendix). Water Quality Unit, Resource Quality Section, Water Management Branch, B.C. Ministry of Environment, Victoria, B.C.

Omernik, J.M. 1976. The influence of land use on stream nutrient levels. US Environmental Protection Agency, Office of Research and Development, Corvallis Environmental Research Laboratory, Eutrophication Survey Branch, Springfield, Va. EPA-600/3-76-014.

Pan, Y.D., Herlihy, A., Kaufmann, P., Wigington, J., van Sickle, J., and Moser, T. 2004. Linkages among land-use, water quality, physical habitat conditions and lotic diatom assemblages: a multi-spatial scale assessment. Hydrobiologia, **515**(1–3): 59–73.

Paul, M.J., and Meyer, J.L. 2001. Streams in the urban landscape. Annu. Rev. Ecol. Syst. **32**: 333–65.

Peierls, B.L., Caraco, N.F., Pace, M.L., and Colem, J.J. 1991. Human influence on river nitrogen. Nature (London), **350**(6317): 386–387.

Rice, W.R. 1989. Analyzing tables of statistical tests. Evolution, **43**(1):223–225.

Romani, A.M., and Sabater, S. 2000. Variability of heterotrophic activity in Mediterranean stream biofilms: a multivariate analysis of physical–chemical and biological factors. Aquat. Sci. **62**: 205–215.

Sabater, F., Guasch, H., Marti, E., Armengol, J., and Sabater, S. 1995. The Ter: a Mediterranean river case-study in Spain. *In* Ecosystems of the world. River and stream ecosystems. *Edited by* C.E. Cushing, K.W. Cummins, and G.W. Minshall. Elsevier Science Publishing, New York. pp. 419–438.

Sabater, F., Buttrini, A., Marti, E., Munoz, I., Romani, A., Wray, J., and Sabater, S. 2000*a*. Effects of riparian vegetation removal on nutrient retention in a Mediterranean stream. J. North Am. Benthol. Soc. **19**(4): 609–620.

Sabater, S., and Sabater, F. 1992. Longitudinal changes of benthic algal biomass in a Mediterranean river during two high production periods. Arch. Hydrobiol. **124**(4): 475–487.

Sabater, S., Buttrini, A., Munoz, I., Romani, A., Wray, J., and Sabater, F. 1998. Effects of removal of riparian vegetation on algae and heterotrophs in a Mediterranean stream. J. Aquat. Ecosyst. Stress Recovery, **6**: 129–140.

Sabater, S., Armengol, J., Comas, E., Sabater, F., Urrizalqui, I., and Urrutia, I. 2000*b*. Algal biomass in a disturbed Atlantic river: water quality relationships and environmental implications. Sci. Total Environ. **263**: 185–195.

Sabater, S., Acuna, V., Giorgi, A., Guerra, E., Munoz, I., and Romani, A.M. 2005. Effects of nutrient inputs in a forested Mediterranean stream under moderate light availability. Arch. Hydrobiol. **163**(4): 479–496.

Schanz, F., and Juon, H. 1983. Two different methods of evaluating nutrient limitations of periphyton bioassays, using water from the River Rhine and eight of its tributaries. Hydrobiologia, **102**(3): 187–195.

Sonoda, K., Yeakley, J.A., and Walker, C.E. 2001. Near-stream land use effects on streamwater nutrient distribution in an urbanizing watershed. J. Am. Water Res. Assoc. **37**(6): 1517–1532.

Stevenson, R.J., and Glover, R. 1993. Effects of algal density and current on ion transport through periphyton communities. Limnol. Oceanogr. **38**: 1276–1281.

Stevenson, R.J., Bothwell, M.L., and Lowe, R.L. 1996. Algal ecology: freshwater benthic ecosystems. Academic Press, San Diego, Calif.

Strayer, D.L., Beighley, R.E., Thompson, L.C., Brooks, S., Nilsson, C., Pinay, G., and Naiman, R.J. 2003. Effects of land cover on stream ecosystems: roles of empirical models and scaling issues. Ecosystems, **6**(5): 407–423.

Sundback, K., Carlson, L., Nilsson, C., Jonsson, B., Wulff, A., and Odmark, S. 1996. Response of benthic microbial mats to drifting green algal mats. Aquat. Microb. Ecol. **10**(2): 195–208.

Suren, A.M., Biggs, B.J.F., Kilroy, C., and Bergey, L. 2003. Benthic community dynamics during summer low-flows in two rivers of contrasting enrichment 1. Periphyton. N.Z. J. Mar. Freshw. Res. **37**(1): 53–70.

Tank, J.L., and Dodds, W.K. 2003. Nutrient limitation of epilithic and epixylic biofilms in ten North American streams. Freshw. Biol. **48**: 1031–1049.

Taylor, S.L., Roberts, S.C., Walsh, C.J., and Hatt, B.E. 2004. Catchment urbanisation and increased benthic algal biomass in streams: linking mechanisms to management. Freshw. Biol. **49**: 835–851.

Tuchman, N.C., Schollett, M.A., Rier, S.T., and Geddes, P. 2006. Differential heterotrophic utilization of organic compounds by diatoms and bacteria under light and dark conditions. Hydrobiologia, **561**: 167–177.

USEPA. 1992. Framework for ecological risk assessment. US Environmental Protection Agency, Washington, D.C. EPA/630/R-92/001.

USGS. 1997. Preliminary geologic map of the Malibu Beach 7.5′ quadrangle, southern California: a digital database. File Rep. 97-257.

Valderrama, J.C. 1981. The simultaneous analysis of total nitrogen and total phosphorus in natural waters. Mar. Chem. **1**: 109–122.

Walsh, C.J., Roy, A.L., Feminella, J.W., Cottingham, P.D., Groffman, P.M., and Morgan, R.P., II. 2005. The urban stream syndrome: current knowledge and the search for a cure. J. North Am. Benthol. Soc. **24**(3): 706–723.

Welch, E.B., Jacoby, J.M., Horner, R.R., and Seeley, M.R. 1988. Nuisance biomass levels of periphytic algae in streams. Hydrobiologia, **157**: 161–168.

Welch, E.B., Horner, R.R., and Patmont, C.R. 1989. Prediction of nuisance periphytic biomass — a management approach. Water Res. **23**(4): 401–405.

Winterbourn, M.J. 1990. Interactions among nutrients, algae, and invertebrates in a New Zealand mountain stream. Freshw. Biol. **23**: 463–474.

Wuhrmann, K., and Eichenberger, E. 1975. Experiments on the effects of inorganic enrichment of rivers on periphyton primary production. Verh. Int. Verh. Theor. Angew. Limnol. **19**: 2028–2030.

Field validation of an instantaneous estimate of in situ development and growth for marine copepod communities

Akash R. Sastri and John F. Dower

Abstract: To date, efforts to develop a method for rapidly measuring the development and growth rates of marine zooplankton have met with little success. In recent years, however, a simple assay based on a crustacean moulting enzyme, chitobiase, has shown considerable promise. Previous laboratory studies have demonstrated that chitobiase activity is proportional to individual body size across three species of freshwater daphnids. Here, we show that a significant positive relationship exists between chitobiase activity and body length (and weight) across four species of marine copepods collected from natural populations in coastal British Columbia, Canada. We measured the decay rate of chitobiase in the water column and estimated in situ moulting and growth rates of the entire copepod community, which are in good agreement (5%–15%) with conventional moulting rates and literature-based estimates. This method can be applied at a relatively high spatial and temporal resolution and its utility is potentially analogous to conventional community-wide productivity estimates for phytoplankton and bacterioplankton in marine and freshwater systems.

Résumé : À ce jour, les tentatives pour trouver une méthode pour mesurer rapidement le développement et les taux de croissance du zooplancton marin ont connu peu de succès. Néanmoins, ces dernières années, un dosage simple basé sur la chitobiase, un enzyme de la mue chez les crustacés, offre un grand potentiel dans ce domaine. Des études antérieures de laboratoire ont montré que l'activité de la chitobiase est proportionnelle à la taille individuelle chez trois espèces de daphniidés d'eau douce. Nous démontrons ici qu'il existe une relation positive significative entre l'activité de la chitobiase et la longueur (et la masse) du corps chez quatre espèces de copépodes marins prélevés dans des populations naturelles de la côte de la Colombie-Britannique, Canada. Nous avons mesuré le taux de décomposition de la chitobiase dans la colonne d'eau et estimé les taux de mue et de croissance in situ de la communauté de copépodes dans son entier; ces taux s'accordent bien (5 – 15 %) avec les taux de mue conventionnels et les estimations calculées d'après la littérature. La méthode peut être utilisée à des résolutions spatiale et temporelle relativement fines et son utilité est potentiellement analogue à celles des estimations conventionnelles de productivité à l'échelle de la communauté faites sur le phytoplancton et le bactérioplancton dans les systèmes marins et les systèmes d'eau douce.

[Traduit par la Rédaction]

Introduction

Although many studies have measured copepod egg production, estimates of in situ development and growth rates of nauplii and copepodites remain rare (see Hirst et al. 2003). This disparity is primarily due to various logistical problems associated with conventional methodologies (reviewed by Runge and Roff 2000). Moulting rates can be estimated through serial sampling in situations where the development of crustacean zooplankton populations is seasonal and synchronous. However, these estimates are (*i*) often poorly resolved in space and time, (*ii*) restricted to individual species, and (*iii*) highly labour intensive. To estimate development and growth of juvenile copepods at meaningful spatiotemporal scales requires instantaneous estimates of these rates that avoid biases associated with handling and incubations and can be applied routinely at sea. Although several radiochemical and biochemical indices have been explored to date (Runge and Roff 2000), none has demonstrated a routine applicability across species.

Recently, a new approach has been proposed based on the crustacean moulting enzyme chitobiase (Sastri and Roff 2000). This method is attractive because it is based on a simple enzyme assay of ambient seawater surrounding the moulting community. Chitobiase is one of two chitinolytic enzymes employed by crustaceans during the premoult phase and is secreted into the apolytic space by the epidermis where it catalyses the partial recycling of chitin (Buchholz 1989; Roff et al. 1994).

Vrba and Machacek (1994) first demonstrated that chitobiase activity (CBA) in the medium surrounding an individual following ecdysis is significantly higher than that measured during intermoult and that the liberated CBA increases with body size. Sastri and Roff (2000) applied Vrba

Received 13 April 2006. Accepted 3 September 2006. Published on the NRC Research Press Web site at http://cjfas.nrc.ca on 16 November 2006.
J19272

A.R. Sastri.[1] Department of Biology, University of Victoria, Victoria, BC V8W 3N5, Canada.
J.F. Dower. School of Earth and Ocean Sciences, University of Victoria, Victoria, BC V8W 3P6, Canada.

[1] Corresponding author (e-mail: asastri@uvic.ca).

doi:10.1139/F06-149

and Machacek's (1994) approach to three species of laboratory-reared freshwater Cladocera and found that the species-specific relationships could all be described by a single body-size relationship. Using this common relationship and the rate of decay of CBA in the medium, they were able to estimate mean size weighted stage durations of asynchronous, monospecific, and mixed cultures of freshwater Cladocera. Here we extend this approach to marine copepods, the taxonomic group that dominates virtually all marine mesozooplankton communities. The objectives of this study were (*i*) to determine whether the relationship between liberated chitobiase activity and body size is conserved across marine copepod species and (*ii*) to compare chitobiase-based estimates of copepod community development and growth with conventional estimates for natural communities in coastal British Columbia, Canada.

Materials and methods

Chitobiase assays and homogenates

Chitobiase activity (CBA) in the water column was assayed following Sastri and Roff (2000) with modifications for seawater. Reactions were initiated by the addition of 0.2 mmol methylumbelliferyl *N*-acetyl-β-D-glucosaminide (MBF–NAG; stock dissolved in cellosolve and diluted in citrate–phosphate buffer (CPB)) to 2.0 mL of seawater. Reactions were buffered to pH 6.0 by adding 1.0 mL of 0.15 $mol \cdot L^{-1}$ CPB. The product of this reaction, methylumbelliferone (MBF), fluoresces optimally at pH 10 or higher; however, carbonate precipitation reduces assay sensitivity. Thus, reactions were terminated after 30–60 min by adding 500 µL of a solution of 2 $mol \cdot L^{-1}$ NaOH and 0.4 $mol \cdot L^{-1}$ EDTA. The final reaction solution was always clear, with a pH between 10.5 and 10.7. Background fluorescence of the substrate was assessed in parallel reactions that were terminated at the initiation of the assay. Background and sample fluorescence were measured with a fluorometer (TD-700; Turner Designs, Inc., Sunnyvale, California) equipped a long-wavelength bulb and 300–400 nm excitation and 410–600 nm emission lenses. Raw fluorescence was converted to nanomoles MBF using 4-methylumbelliferone (stock dissolved in cellosolve). CBA is expressed as nanomoles MBF liberated per litre per hour. Reaction temperature was maintained at 25 °C.

CBA in the water column frequently is close to the level of detection of the assay conditions described above, and it is necessary to spike seawater samples with a concentrated source of enzyme to reliably estimate decay rates. A homogenate was prepared by homogenizing 30–50 copepods in seawater using a handheld glass tissue grinder. The homogenate was passed through a 0.2 µm filter and diluted (1:1000 (*v*/*v*)) in seawater samples collected for CBA decay rate estimates. To validate this approach, we compared the CBA decay rates in samples of seawater collected from the same site, time, and depth (west coast of Vancouver Island, June 2005) amended with 100%, 50%, and 25% of homogenate. For pH dependence and all CBA decay rate experiments, substrate saturation was always tested by confirming a linear increase in MBF fluorescence (i.e., fluorescence regressed against time) using parallel reactions that were terminated at 0, 15, 30, 45, and 60 min. CBA assays on native CBA samples were terminated after 60 min, whereas CBA assays on filtered aliquots with homogenate were terminated after 30 min as the concentration of chitobiase was greater.

Chitobiase – body size relationship

Copepods used for individual incubations were collected from the Strait of Georgia and Saanich Inlet, British Columbia (Canada), between March and June 2004 using a Scientific Committee on Oceanic Research (SCOR) net (55 cm diameter, 236 µm mesh) with a nonfiltering cod end to minimize damage to the animals. All moulting incubations were conducted within 48 h of collection. *Tigriopus californicus* were collected from a splash pool at Ten Mile Point in Victoria, British Columbia. Copepodite stages of *Calanus pacificus*, *Metridia pacifica*, and *Pseudocalanus* spp. were identified and then carefully rinsed in sterilized seawater (previously heated to 75 °C and 0.2 µm filtered). Individuals were then placed in well plates containing 2.5 mL of sterilized seawater (for up to 12 h) at the temperature of collection (8–22 °C). At the conclusion of the incubation period, wells were inspected for the presence of exuviae using a dissecting microscope (25× magnification). When exuviae were observed, 2 mL of incubation medium was removed for the chitobiase assay (as above), and the prosome length and width of the moulted animal was measured to the nearest 0.05 mm with an ocular micrometer. All enzyme reactions lasted 60 min, with the exception of those of the largest individuals (CV–CVI *C. pacificus*), which lasted 30 min. Chitobiase activity was regressed against prosome length and dry weight. All individual dry weights presented in this study were estimated using species-specific length–weight relationships obtained from the marine zooplankton database maintained by the Institute of Ocean Sciences, Sidney, British Columbia, Canada.

pH dependence

To determine the extent to which a single chitobiase assay is applicable across species, we compared the pH dependence of a single species (*Neocalanus plumchrus*) with that of mixed copepod homogenates (*C. pacificus*, *M. pacifica*, *Corycaeus anglicus*, and *Pseudocalanus* spp.). Animals (*N. plumchrus*, n = 30–35; mixed species, n = ~100) were homogenized in 4 mL of sterilized, filtered seawater using a handheld tissue grinder. Aliquots of sterilized, filtered seawater were spiked with homogenates of either *N. plumchrus* or the mixed species. Chitobiase reactions proceeded as above, with substrate diluted and reactions buffered using citrate phosphate buffers across a pH range of 4–7 and without buffer (corresponding to a reaction pH of 7.91). Variation of CBA with pH is expressed as percent CBA standard error.

Chitobiase decay rates under field conditions

Seawater samples were collected from a single deepwater (~400 m) station in the Strait of Georgia (49°15′N, 123°45′N) from 5, 10, 30, and 50 m during four cruises bracketing the development and decline of the 2004 spring phytoplankton bloom (29 February, 6 April, 26 April, and 29 May). All samples were screened through 54 µm mesh to exclude crustaceans. At time 0, 15.0 mL of the screened seawater was 0.2 µm filtered and maintained at 4 °C. The CBA in this subsample is hereafter referred to as native CBA (CBA_{nat}). The screened seawater sample was then amended with 0.2 µm filtered copepod homogenate and serially subsampled and 0.2 µm filtered every 1.5 to 3 h for 12 h. All subsamples were maintained at 4 °C until the conclusion of the 12 h incubation period. $\mathrm{CBA}_{\mathrm{nat}}$ was typically assayed within 1 h of collection, whereas CBA in subsamples of amended seawater was assayed concurrently within 4 h of the conclusion of the incubation period. CBA in 0.2 µm filtered seawater remains stable for up to 60 h at room temperature (22 °C) and longer at 5 °C (Vrba and Machacek 1994; Oosterhuis et al. 2000; Sastri 2001). During the incubation period, each amended seawater sample was maintained at ambient sea surface temperature. The in situ ΔCBA (i.e., change in activity per hour) was estimated by applying the slope of the time versus ln(CBA) relationship to the native CBA ($\mathrm{CBA}_{\mathrm{nat}}$) for each depth.

To describe the size-frequency distribution of the copepod community, we collected a series of net casts to correspond to CBA decay rate estimates on each sampling date. Copepods were collected using both a ring net (70 µm mesh) and a SCOR net (236 µm) towed vertically from 50 to 0 m. All individuals in the largest size fractions (>2.5 mm prosome length) were counted in each sample. For animals <2.5 mm in length, the samples were split up to three times (i.e., 1/8 of original sample) using a Folsom splitter.

CBA-based estimates of stage duration

Sastri and Roff (2000) estimated the mean stage duration as follows (with some modification of terms):

$$(1)\qquad D_{\mathrm{sample}} = (\Sigma n_i \cdot \mathrm{CBA}_i)/\Delta\mathrm{CBA}$$

We term this estimate the "sample-based average", where D_{sample} represents the stage duration of the mean-sized individual in the community (as represented by the size-frequency distribution determined from a depth-integrated net sample). The terms n_i and CBA_i represent the number of animals and the CBA per individual (derived from the CBA – prosome length relationship) in size-class i, respectively. We do not include the correction term for deviation from equilibrium between production and decay of CBA in the water column, as stable equilibrium is assumed over the course of the seawater incubation period (i.e., 12 h).

An alternative estimate of the mean community stage duration (D_{CBA}) can be written as

$$(2)\qquad D_{\mathrm{CBA}} = \mathrm{CBA}_{\mathrm{nat}}/\Delta\mathrm{CBA}$$

Equivalently, the slope (k) of the regression of ln(CBA) versus time represents the proportion of the initial CBA lost per hour. Assuming equilibrium, the percent decay represents the percentage of mean-sized individuals (or fraction of total biomass derived from CBA – dry weight relationship) in the community that moult per hour, which is equivalent to the community moulting rate (MR). All water column CBA-based estimates are predicated on the assumptions that copepods dominate the biomass of moulting crustaceans and that there is a balance between CBA production by moulting copepods and CBA decay in the water column. Estimates based on this relationship are therefore not dependent on the contents of a representative net cast. This approach is attractive because developmental rates can be estimated at the conclusion of 12 h of seawater incubation, thus allowing repeated estimates over short time intervals. Using the CBA – body weight relationship, we can also scale the D_{CBA} estimate with body size by modifying eq. 2 such that we assume that an entire community is composed of a single weight class of interest. It is important to note that this estimate maintains the ΔCBA estimated from the field using the following relationship:

$$(3)\qquad D_{\mathrm{CBA}_i} = [(\mathrm{CBA}_i - \mathrm{CBA}_{\mathrm{avg}}) + \mathrm{CBA}_{\mathrm{nat}}]/\Delta\mathrm{CBA}$$

where D_{CBA_i} represents the mean stage duration of the size class of interest and CBA_i represents the CBA predicted for that size class from either the CBA – body weight or the CBA – prosome length relationships. The average CBA ($\mathrm{CBA}_{\mathrm{avg}}$) is defined as the CBA of the average-sized individual (or fraction of total biomass) molting per hour. Although it is not a rate per se (i.e., $\Delta\mathrm{CBA}\cdot\mathrm{h}^{-1}$), this value is equivalent to that of ΔCBA. Applying eq. 3 to all size classes present in a community generates a relationship in which stage duration increases with body size. As this approach is dependent on body size and the measured ΔCBA, estimates will not necessarily reproduce species-specific patterns of development (see Peterson 2001), but rather serves as a generalized estimate for all individuals in a given size class.

D_{CBA_i} was estimated for stage II – stage V *Calanus pacificus* copepodites using the CBA turnover rates measured on each of the four sampling dates (see Table 1). CBA_i for each stage was estimated using standard dry weight values (see above) and the CBA – dry weight relationship (Fig. 1*b*). These stage durations are presented against the depth-integrated (0–50 m) temperature for each sampling date. For comparison, we also include Vidal's (1980) stage-specific estimates of optimal intermoult period (IMP) for copepodite stages CII–CV at 8, 12, and 15.5 °C.

Conventional moulting rate estimates

On each cruise, we also estimated moulting rates using the sieve fractionating method (Peterson et al. 1991). Animals were collected by slowly (~0.5 m^{-1}) towing a SCOR net (fitted with a 1 L nonfiltering cod end) from a depth of 30 m to the surface. The contents of the net cast were passed carefully through a submerged cylinder with a 500 µm mesh bottom and diluted in seawater. This 233–500 µm size fraction was then split gently into six aliquots. The first three aliquots were preserved immediately in 10% buffered formalin seawater and the remaining aliquots were incubated at ambient sea surface temperature (see Table 2.) in 20 L carboys for 48 h. Carboys were filled with 70 µm screened seawater that was pumped from ~2 m below the surface.

Species-specific stage distributions were estimated by examining the entire contents of each preserved aliquot using a dissecting microscope (25× magnification). Moulting rates were estimated using the relationship presented by Peterson et al. (1991):

$$(4)\qquad \mathrm{MR}_i = (P_{t,i+1} - P_{s,i+1})/P_{s,i}$$

where MR_i represents the molting rate of stage i, $P_{s,i}$ and $P_{s,i+1}$ represent the proportion of individuals at stage i and stage i + 1 at the start of the incubation, respectively, and $P_{t,i+1}$ represents the proportion of individuals at stage i + 1 at the end of the incubation period. Stage duration was estimated as the reciprocal of MR_i. These rates were calculated

Table 1. Measured values of native CBA (CBA_{nat}), hourly CBA decay rates ($\Delta CBA \cdot h^{-1}$), D_{sample}, D_{CBA}, D_{CBA_i}, and conventional estimates of stage duration (D_{conv}, h) measured in the Strait of Georgia, British Columbia, Canada, on four dates in the spring of 2004.

Date	CBA_{nat}	$\Delta CBA \cdot h^{-1}$	D_{sample} (h)	D_{CBA} (h)	D_{CBA_i} (h)	D_{conv}* (h)
29 February	1.16	0.00722	71.8	161.1	189.2	152.8 (*i*)
6 April	3.23	0.0354	42.79	91.2	90.7, 94.3	107.2 (*ii*)
25 April	4.27	0.059	54.24	72.4	72.5	—
29 May	3.87	0.068	21.42	56.9	58.1, 59.5	67.4 (*iv*)

*Stage and species at time 0: (*i*) CIV *Pseudocalanus* spp. ; (*ii*) CII *C. pacificus*, CII *Pseudocalanus* spp.; and (*iv*) CV *Acartia longiremis*, CIII *Centropages abdominalis*.

for the species-specific stage dominating the incubations at T_0.

Growth rate estimates

Weight-specific growth rate (g) was estimated as

$$g = \ln(W_2/W_1)/D \tag{5}$$

where W_2/W_1 represents a stage- or size-specific change in body weight. Days (D) represents the time over which the weight change occurred and was estimated from our D_{CBA_i} estimates. Stage-specific growth increments for *Pseudocalanus* spp., *Metridia pacifica*, and *Calanus pacificus* were estimated from successive stage weights using length–weight relationships employed in the CBA – body size relationships. These growth increments were pooled and regressed against CBA predicted for each species and stage-specific postmoult weight. This relationship was described as

$$\log(g_{inc}) = 0.864 \log(CBA_i) - 1.78 \qquad r^2 = 0.73, n = 19, p < 0.0001 \tag{6}$$

where g_{inc} represents the difference in mass between the premoult size class and the stage present in the water column. Thus, W_1 from eq. 5 is equivalent to $W_2 - g_{inc}$. We chose this estimate of growth increment because our CBA-based estimates of D represent the time taken to moult to the stage present in the water column at the time that the CBA decay rate estimates were made.

Growth rates were estimated on a size-class basis and the numerically weighted average was taken as the average community growth rate. These rates were then compared with the relationship describing juvenile copepod (sac and broadcast spawners) growth rates presented by Hirst and Lampitt (1998). We applied our estimates of W_1 (corrected to carbon using a conversion factor of 0.45) as the body weight values for the Hirst and Lampitt (1998) global in situ model.

Statistical analyses

The natural logarithm of CBA was employed for all decay rate experiments in order to normalize distribution of the data. Homogeneity of the slopes in the decay experiments was tested using ANCOVA as outlined by Zar (1984).

Results

When observations from the four marine copepod species were pooled, CBA (nmol MBF·$L^{-1} \cdot h^{-1}$) was found to be positively related to prosome length (mm) as log(CBA) = 2.939 log(PL) – 0.3325 (r^2 = 0.889, n = 44, p < 0.0001; Fig. 1*a*). Chitobiase activity also showed a significant positive relationship with individual dry weight (DW, µg) across the four copepod species. This relationship is described as log(CBA) = 1.149 log(DW) + 1.566 (r^2 = 0.90, n = 44, p < 0.0001; Fig. 1*b*). Homogenates of *Neocalanus plumchrus* and the mixed zooplankton both displayed a pH optimum (expressed as percent CBA) of ~6.0 (Fig. 2).

The time versus ln(CBA) (nmol·$L^{-1} \cdot h^{-1}$) relationships for three samples (500 mL) of seawater, each amended with 500 µL of 100%, 50%, and 25% filtered homogenate are presented (Fig. 3). The slopes of the different samples were not significantly different ($F_{[2,9]}$ = 0.0041, p > 0.05).

Comparisons of CBA-based estimates of the stage duration of the mean-sized individual in the community suggest that estimates based on the D_{sample} method underestimate conventional estimates of stage duration by 53%–68% (Table 1). The D_{CBA} estimates, however, were generally within 5%–15% of conventional stage-duration estimates (Table 2).

Scaling the D_{CBA} estimates, we estimate the size class specific stage duration (D_{CBA_i}) of *Calanus pacificus* copepodites stages II–V (Fig. 4). Our D_{CBA_i} estimates represent stage durations that vary with both developmental stage and temperature in a fashion similar to those of the optimal rates presented by Vidal (1980). Our D_{CBA_i} estimates are in good agreement with the temperature-dependent rates estimated from Vidal (1980). It should be noted that the D_{CBA_i} estimates represent the average stage duration for all individuals in the community occupying a defined size class. During our four sampling trips, the size classes represented by *C. pacificus* CIII–CVI were largely dominated by *C. pacificus* and can thus be considered representative of this species.

Numerically weighted growth rate averages for each date are compared against the body size and temperature-dependent estimates using the Hirst and Lampitt (1998) equation (Table 2). Our growth rate estimates suggest that before the spring phytoplankton bloom (29 February), weight-specific growth rates were comparable to weight- and temperature-specific rates predicted by the Hirst and Lampitt global model for juvenile sac and broadcast spawners. During the peak of the bloom (6 April) and the transition toward a summer copepod community (25 April and 29 May), however, growth rates of the mean-sized individual in the copepod community meet the expectations of a productive coastal system (i.e., the Strait of Georgia; Harrison et al. 1983) when estimated with the CBA method, but are underestimated by rates predicted by the Hirst and Lampitt global in situ model.

Fig. 1. (*a*) Generalized relationship between liberated chitobiase activity (CBA) by individual copepods after moulting and prosome length (PL, mm): log(CBA) = 2.939log(PL) – 0.3325, $r^2 = 0.889$, $n = 44$, $p < 0.0001$. (*b*) Generalized relationship between CBA liberated by individual copepods after moulting and individual dry weight (DW, mg): log(CBA) = 1.149log(DW) + 1.566, $r^2 = 0.90$, $n = 44$, $p < 0.0001$. *Calanus pacificus* (◇), *Metridia pacifica* (○), *Pseudocalanus* spp. (△), and *Tigriopus californicus* (□).

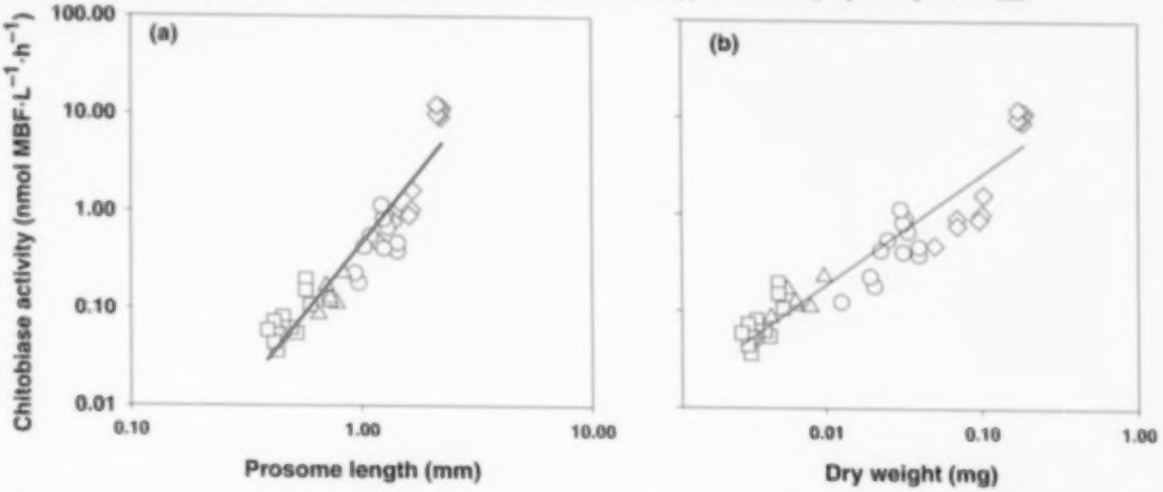

Table 2. Mean community estimates of weight-specific growth rate (day^{-1}) measured in the Strait of Georgia, British Columbia, Canada, on four dates in the spring of 2004.

Date	Temperature (°C)	Individual dry weight (mg)	CBA *g* (day^{-1})	*g* (day^{-1})
29 February	7.82	0.001489	0.0724	0.090
6 April	8.38	0.004406	0.130	0.087
25 April	9.06	0.019404	0.167	0.082
29 May	10.62	0.003063	0.210	0.108

Note: CBA-based estimates (CBA *g*) represent the numerically weighted average (from net casts) of growth rates estimated by using size-scaled D_{CBA} values (Table 1). For comparison, we also include estimates using the temperature and body weight model for in situ juvenile copepod growth rates (*g*) presented by Hirst and Lampitt (1998).

Fig. 2. Comparison of pH dependence of chitobiase activity (%) between homogenates of *Neocalanus plumchrus* (solid symbols; $n = 3$, mean standard error) and mixed copepods (open symbols; *Calanus pacificus*, *Metridia pacifica*, *Corycaeus anglicus*, and *Pseudocalanus* spp.; $n = 3$, mean ± standard error).

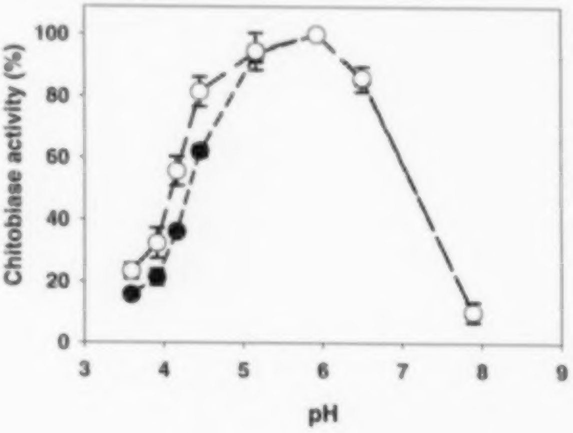

Discussion

Chitobiase – body size relationships

Our results show that CBA can be reliably estimated from prosome length for marine copepods. A simple length-based relationship seems reasonable for the calanoid species examined, given their shared body morphology. We included the splash pool harpacticoid *Tigriopus californicus* in our analysis in order to compare a relatively disparate group with pelagic marine calanoids. However, our results suggest that these groups share similar body size dependence with liberated CBA, despite taxonomic and life history differences.

Although estimates of development rates based on prosome length are appealing (i.e., prosome length is easy to measure), weight-based estimates are more relevant to growth and production studies. Furthermore, estimates using body weight will more accurately represent CBA in situations where the species composition includes groups whose length–weight relationships are not consistent with those of the majority of marine copepods. For instance, *Eucalanus* spp. copepodites weigh less than most other calanoids of a similar length. When these groups dominate the biomass of a size class or the mesozooplankton community, individual biomass measures will be a more appropriate descriptor of liberated CBA. Additional considerations such as lipid accumulation may have to be addressed when attempting to predict both liberated CBA and stage-specific growth increment.

pH dependence and homogenates

It is important to note that CBA in the water column is not due exclusively to aquatic arthropods, as the enzyme is also

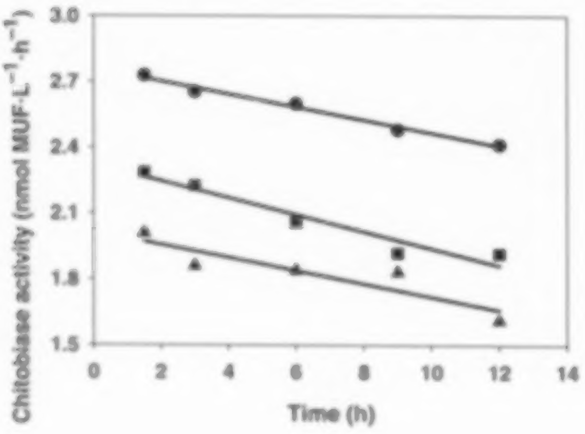

Fig. 3. Time versus ln(chitobiase activity) (nmol·L^{-1}·h^{-1}) relationships for three samples (500 mL) of seawater, each amended with 500 μL of 100% (●), 50% (■), and 25% (▲) filtered homogenate. The slopes of each sample are not significantly different ($F_{[2,9]}$ = 0.0041, $p < 0.01$).

produced by protozoans and bacteria. Vrba et al. (2004) found that pH optima represent a useful means of distinguishing between sources. Our results suggest that a pH of ~6.0 is optimal for single and mixed species of marine copepods, a value that agrees well with Vrba et al. (2004) and Espie and Roff (1995; pH optima = 5.5 for *Daphnia magna*). In addition to a copepod-specific pH optimum, it is also understood that the other sources of chitobiase activity in the medium are particle-bound (>0.2 μm). Thus, in the absence of significant unicellular lysis, dissolved CBA (<0.2 μm) should reflect copepod CBA at pH ~ 6.

Our estimates of CBA decay rates in the water column are based on the rate of decay of a homogenate applied against the native CBA. The slope of time versus ln(CBA) was not significantly different among the three dilutions compared. Estimates of CBA per hour, derived for 100%, 50%, and 25% homogenates were 0.257, 0.332, and 0.259 nmol MBF·L^{-1}·h^{-1}, respectively. These decay rates are similar and suggest that the decay rates estimated from seawater samples amended with homogenate are representative of the in situ decay rate of the enzyme. Furthermore, amending samples with homogenates also reduces the time required for the assay to only 30 min.

CBA-based estimates versus conventional estimates of stage duration

We were not able to estimate moulting rates on 25 April 2004 as there were no significant changes in the stage-frequency distribution for any of the species incubated. Furthermore, we did not note the presence of exuviae in any of our 48-h samples. However, our D_{CBA} estimates were still in good agreement with the conventional estimates for the remaining three sampling dates (i.e., usually within 5%–15%). In contrast, our D_{sample} estimates did not agree well with any of the conventional moulting rate estimates. Where discrepancies were found, we postulate that either the contents of the net casts were not representative of the copepod community biomass and (or) size-frequency distribution or that the animals were not distributed evenly throughout our 0–50 m sampling profile. Thus, our depth-weighted estimates of CBA turnover may not have been appropriately attributed to the contents of the net casts. We assume that most of the developing copepod community was residing in the upper 50 m of the water column during the spring (Mackas 1992). However, all of our experiments were conducted during daylight, and diel vertical migrators (i.e., *Metridia pacifica*) were therefore likely undersampled. Nevertheless, our D_{CBA} estimates were in good agreement with conventional estimates and do not suffer from the potential error associated with a dependence on a quantitative net cast.

Another potential source of error associated with our D_{sample} estimates results from attributing the total CBA estimate strictly to the copepod community. We did not estimate the potential CBA contribution of other groups of planktonic Crustacea (i.e., amphipods, euphausids, decapod larvae, etc.), nor do we have a relationship describing the CBA – body size dependence of these groups. Although copepods typically dominate the crustacean mesozooplankton community, other groups may at times make significant contributions, especially in productive coastal systems such as the Strait of Georgia (Harrison et al. 1983).

Applying a copepod-specific CBA – body size relationship for D_{CBA} estimates is the most appropriate approach, as these estimates are not necessarily dependent on the contents of the plankton nets and are simply measures of the CBA (biomass) turnover rate in the water column. When we scaled and applied our D_{CBA} estimates to the size-frequency distribution of the contents of our nets, our estimates of mean community stage durations were in good agreement with our conventional estimates. This suggests that our net casts did capture a representative sample of the size-frequency distribution of the community.

Laboratory and field studies have demonstrated that stage durations for most copepod species are neither isochronal nor strictly equiproportional (see Hart (1990) and Peterson (2001) for reviews), although the general tendency is for moulting and growth rates to decrease with increasing body size and (or) developmental stage. The dependence of these rates on body size suggests that the potential for variation (or even limitation) in growth associated with food concentration may also increase with body size. If this is generally the case, estimates of the stage duration for the average-sized individual in a population (<0.5 mm locally) may only occasionally indicate those slower rates indicative of the effects of body size and food availability. Thus, it is useful to be able to scale CBA-based rates against size class for a given copepod community. Our size class scaled D_{CBA} estimates (D_{CBA_i}) from eq. 3 are premised on the assumption that D_{CBA} represents not only the proportion of animals moulting per hour, but also the hourly turnover rate of total copepod biomass. Thus, in relative terms, it does not matter whether the hourly production of biomass represents *x*% of the community or that of a single individual.

We explored the validity of this approach by estimating D_{CBA_i} for the copepodite stages CII–CV for *Calanus pacificus*, which were present during our four sampling trips.

Fig. 4. Chitobiase-based stage-specific stage durations (D_{CBA_i}) of *Calanus pacificus* copepodites stages II–V (solid bars). CBA_i for each stage was estimated using the standard dry weight values and the dry weight versus liberated chitobiase (CBA) relationship presented herein. These stage durations are presented against the depth-integrated (0–50 m) temperature for each sampling date. Vidal's (1980) stage-specific estimates (open bars) of optimal intermoult period (IMP) for copepodite stages CII–CV at 8, 12, and 15.5 °C are included for comparison.

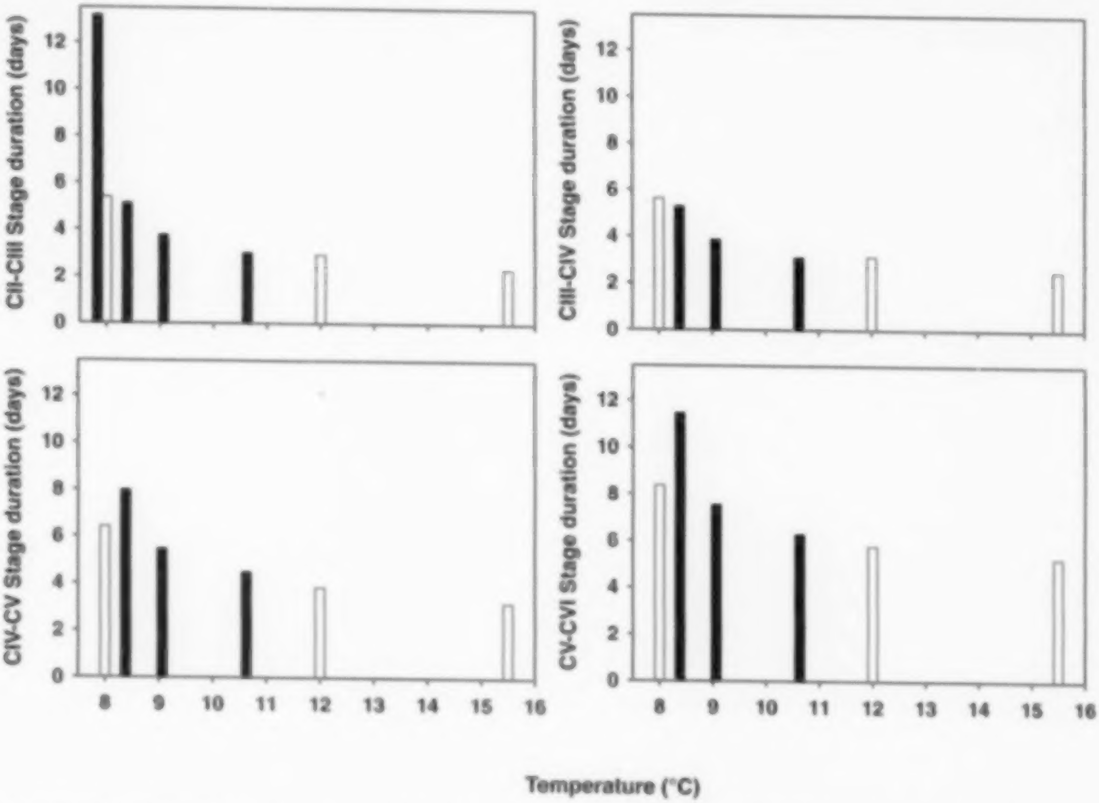

Stage durations for CIII–CV are not presented for the first trip (28 February 2004) because the population consisted of CI–CIIIs with only very few CVIs. Our estimate of D_{CBA_i} for the CV stage duration during this period was ~35 days. However, we did not consider these animals further, as they most likely had just emerged from diapause and were not likely to be moulting from CIV in the upper water column during February 2004 (Fulton 1973).

Although these particular estimates agree well with our expectations of a productive (potentially food-saturated) environment for late-stage *C. pacificus* developmental rates, they are ultimately representative of the mean-sized individual in that size class. Where a diversity of species (each with its own developmental pattern) occupy the same size class, CBA-based moulting rate estimates will represent the community average rather than the species-specific rates. This will almost always be the case for the smaller size classes (<1.5 mm prosome length). However, when a single species dominates the biomass of a larger size class (e.g., *N. plumchrus* CVs in the Strait of Georgia), the D_{CBA_i} estimates, while still influenced by the ΔCBA, will be most representative of that group. Ultimately, however, our objective was to validate a method that can be applied to the entire copepod community. In this respect, our D_{CBA} (eq. 2) estimates best satisfy this objective.

CBA-based estimates of growth rate

The true test of any enzymatic growth index is whether enzyme activity at a particular body size varies with growth rate (Berges et al. 1990). Yebra and Hernandez-Leon (2004) have demonstrated that in vivo activity of aminoacyl-tRNA synthetase provides an index of growth for *Daphnia magna* growing at different rates. Although it has not been tested explicitly, variation of optimized CBA liberated into the water appears to be a function of body size rather than growth rate. Our data set represents animals growing at different temperatures (8–22 °C), and thus it appears that liberated CBA is best described by measures of body size alone. The chitobiase method assumes that liberated CBA is a function of ecdysis and is proportional to body size across species. Liberated CBA surrounding individuals has previously been demonstrated to be significantly greater following ecdysis than during intermoult (Vrba and Machacek 1994; Oosterhuis et al. 2000; Sastri and Roff 2000).

Oosterhuis et al. (2000) found that CBA liberated by *Temora longicornis* copepodites was positively related to the growth increment and were thus able to estimate daily biomass production of a synchronous laboratory culture. Here, we adopt a similar approach using mean dry weights derived from species-specific relationships to estimate a generalized growth increment. Both approaches assume that the weight-specific increment of growth is proportional to the body weight of the preceding stage. The estimates of growth presented here do suffer from recent criticisms of the moult rate method addressed by Hirst et al. (2005). One potential error is a mismatch between the estimated stage duration (from moult to moult) and the time over which a growth increment (derived from mean weights at stage) occurs. We acknowledge this potential source of error with our present growth estimates; however, our purpose was to compare those rates with those of the Hirst and Lampitt (1998) model (a synthesis of "moult rate" method results). For the purpose of this comparison, the mean community growth rates in the Strait of Georgia were comparable to those predicted by the in situ model (Hirst and Lampitt 1998) when growth was <0.10 day^{-1} and greater than those predicted by the model when growth was >0.10 day^{-1}. The results of this comparison are consistent with those of Peterson et al. (2002) in which animals observed to be growing at maximal rates may not be adequately represented by a synthesis of in situ rates. We are presently investigating the potential to use the CBA method to estimate growth without violating the assumptions of the moult rate method.

The CBA – prosome length relationship presented here is based on measurements immediately following ecdysis. Therefore, an appropriate relationship between CBA and the growth increment for which we estimate stage duration can be established. However, (*i*) we did not collect and weigh the cast exuviae and (*ii*) prosome length does not increase (or decrease) appreciably during the intermoult period, whereas body weight does. Establishing an appropriate relationship between liberated CBA and growth increment will require construction of similar relationships to those presented here, with an emphasis on individual body and exoskeleton weights. This would be ideal, as variation in the CBA liberated by an individual appears to be described by body size alone. Thus, a relationship between growth increment and CBA that can be generalized across species would (when combined with the present stage-duration estimates) represent a truly instantaneous estimate of copepod community growth rate. Alternatively, weight-specific growth rates can be estimated directly where mean weights at stage are measured. D_{CBA_i} estimated for two successive stages (weight classes) would represent the time between successive mean weight estimates and, thus, a true measure of growth rate.

In conclusion, the key advantage of the chitobiase method is that it can be applied in situ, at potentially high temporal and spatial resolution, and without the attendant difficulties and errors associated with traditional moult rate techniques (see Miller et al. 1984). Assumptions of asynchronous development and stable age distributions of moulting copepods are also more likely to be met on a community-wide basis (i.e., as opposed to single populations or developmental stages). Furthermore, a general relationship between body size and CBA suggests that mean moulting rate estimates can be easily derived for mixed copepod communities.

We note that this technique can be also extended to produce generalized mortality estimates (i.e., using size or stage duration and size- or stage-frequency estimates), which may prove of equal importance to estimates of growth and production. Although species- and (or) stage-specific differences will almost certainly be obscured in estimates of mean community development and growth, we contend that chitobiase-based estimates are valuable when applied to community level studies in much the same way that phytoplankton ecologists have long relied on the ^{14}C technique to estimate primary production in mixed phytoplankton communities.

Acknowledgements

We thank the captain and crew of the R/V *John Strickland*, J. Rose, undergraduate and graduate volunteers, and our colleagues in the STRATOGEM project for field assistance. We also thank R.W. Campbell, D.L. Mackas, and two anonymous reviewers for helpful comments and suggestions that improved this manuscript. This study is a contribution from the Natural Sciences and Engineering Research Council of Canada (NSERC) funded Strait of Georgia Ecosystem Modeling Study (STRATOGEM).

References

Berges, J.A., Roff, J.C., and Ballantyne, J.S. 1990. Relationships between body size, growth rate and maximal enzyme activities in the brine shrimp *Artemia franciscana*. Biol. Bull. **179**: 287–296.

Buchholz, F. 1989. Molt cycle and seasonal activities of chitinolytic enzymes in the integument and digestive tract of the Antarctic krill, *Euphausia superba*. Polar Biol. **9**: 311–317.

Espie, P.J., and Roff, J.C. 1995. Characterization of chitobiase from *Daphnia magna* and its relation to chitin flux. Physiol. Zool. **68**: 727–748.

Fulton, J. 1973. Some aspects of the life-history of *Calanus plumchrus* in the Strait of Georgia. J. Fish. Res. Board Can. **30**: 811–815.

Harrison, P.J., Fulton, J.D., Taylor, F.J.R., and Parsons, T.R. 1983. Review of the biological oceanography of the Strait of Georgia pelagic environment. Can. J. Fish. Aquat. Sci. **40**: 1064–1094.

Hart, R.C. 1990. Copepod post-embryonic durations: pattern, conformity, and predictability. The realities of isochronal and equiproportional development, and trends in the copepodid–naupliar duration ratio. Hydrobiologia, **206**: 175–206.

Hirst, A.G., and Lampitt, R.S. 1998. Towards a global model of in situ weight-specific growth in marine planktonic copepods. Mar. Biol. **132**: 247–257.

Hirst, A.G., Roff, J.C., and Lampitt, R.S. 2003. A synthesis of growth rates in marine epipelagic invertebrate zooplankton. Adv. Mar. Biol. **44**: 1–142.

Hirst, A.G., Peterson, W.T., and Rothery, P. 2005. Errors in juvenile copepod growth rate estimates are widespread: problems with the moult rate method. Mar. Ecol. Prog. Ser. **296**: 263–279.

Mackas, D.L. 1992. The seasonal cycle of zooplankton off southwestern British Columbia: 1979–89. Can. J. Fish. Aquat. Sci. **49**: 903–921.

Miller, C.B., Huntley, M.E., and Brooks, E.R. 1984. Post-collection molting rates of planktonic, marine copepods: measurement, applications, problems. Limnol. Oceanogr. **29**: 1274–1289.

Oosterhuis, S.S., Baars, M.A., and Klein Breteler, W.C.M. 2000. Release of the enzyme chitobiase by the copepod *Temora* *longicornis*: characteristics and potential tool for estimating crustacean biomass production in the sea. Mar. Ecol. Prog. Ser. **196**: 195–206.

Peterson, W.T. 2001. Patterns in stage duration and development among marine and freshwater calanoid and cyclopoid copepods: a review of rules, physiological constraints, and evolutionary significance. Hydrobiologia, **453**: 91–105.

Peterson, W.T., Tiselius, P., and Kiorboe, T. 1991. Copepod egg production, moulting and growth rates, and secondary production in the Skagerrak in August 1988. J. Plankton Res. **13**: 131–154.

Peterson, W.T., Gomez-Gutierrez, J., and Morgan, C.A. 2002. Cross-shelf variation in calanoid copepod production during summer 1996 off the Oregon coast, USA. Mar. Biol. **141**: 353–365.

Roff, J.C., Kroetsch, J.T., and Clarke, A.J. 1994. A radiochemical method for secondary production in planktonic Crustacea based on the rate of chitin synthesis. J. Plankton Res. **16**: 961–976.

Runge, J.A., and Roff, J.C. 2000. The measurement of growth and reproductive rates. *In* ICES zooplankton methodology manual. Chap. 9. *Edited by* R.P. Harris, P.H. Weibe, J. Lenz, H.R. Skjoldal, and M. Huntley. Academic Press, San Diego, Calif. pp. 401–454.

Sastri, A.R. 2001. The activity of chitobiase in the medium: a biochemical estimate of development rate in planktonic Crustacea. M.Sc. thesis, Zoology Department, University of Guelph, Guelph, Ontario, Canada.

Sastri, A.R., and Roff, J.C. 2000. Rate of chitobiase degradation as a measure of development rate in planktonic Crustacea. Can. J. Fish. Aquat. Sci. **57**: 1965–1968.

Vidal, J. 1980. Physioecology of zooplankton. II. Effects of phytoplankton concentration, temperature, and body size on the development and molting rates of *Calanus pacificus* and *Pseudocalanus* sp. Mar. Biol. **56**: 135–146.

Vrba, J., and Machacek, J. 1994. Release of dissolved extracellular β-*N*-acetylglucosaminidase during crustacean molting. Limnol. Oceanogr. **39**: 712–716.

Vrba, J., Callier, C.T, Simek, K., Bertoni, R., Filandr, P., Hartman, P., Hejzlar, J., Macek, M., and Nedoma, J. 2004. Are bacteria the major producers of gylcolytic enzymes in aquatic environments? Int. Rev. Hydrobiol. **89**: 102–117.

Yebra, L. and Hernandez-Leon, S. 2004. Aminoacyl-tRNA synthetase as a growth index in zooplankton. J. Plankton Res. **26**: 351–356.

Zar, J.H. 1984. Biostatistical analysis. Prentice-Hall, Inc., Englewood Cliffs, N.J.

The relationship between Pacific hake (*Merluccius productus*) distribution and poleward subsurface flow in the California Current System

Vera N. Agostini, Robert C. Francis, Anne B. Hollowed, Stephen D. Pierce, Chris Wilson, and Albert N. Hendrix

Abstract: In a search for ocean conditions potentially affecting the extent of Pacific hake (*Merluccius productus*) feeding migrations, we analyzed data collected in 1995 and 1998 by the National Marine Fisheries Service on abundance and distribution of hake (by echo integration), intensity and distribution of alongshore flow (from acoustic Doppler current profiler), and temperature (conductivity–temperature–depth profiles). Our results show that Pacific hake are associated with subsurface poleward flow and not a specific temperature range. Temporal and spatial patterns characterize both hake distribution and undercurrent characteristics during the two years of this study. We suggest that poleward flow in this area defines adult hake habitat, with flow properties aiding or impeding the poleward migration of the population. We conclude that although physical processes may not directly affect fish production, they may be the link between large-scale ocean–atmosphere variability and pelagic fish distribution.

Résumé : Dans notre recherche des conditions qui affectent potentiellement l'amplitude des migrations alimentaires du merlu du Pacifique (*Merluccius productus*), nous avons analysé des données récoltées en 1995 et 1998 par le National Marine Fisheries Service sur l'abondance et la répartition des merlus (par écho-intégration), l'intensité et la répartition de l'écoulement le long de la côte (à l'aide d'un enregistreur acoustique Doppler des profils de courant) et de la température (profils de conductivité–température–profondeur). Nos résultats montrent que le merlu du Pacifique est associé à l'écoulement vers le pôle qui se produit sous la surface, mais non à une gamme spécifique de températures. Durant les deux années de notre étude, tant la répartition des merlus que les caractéristiques des courants sous la surface suivent des patrons temporels et spatiaux. Nous pensons que l'écoulement vers le pôle dans cette région détermine l'habitat des merlus et que les caractéristiques de l'écoulement facilitent ou entravent la migration de la population vers le pôle. Nous concluons que, bien que les processus physiques peuvent ne pas affecter directement la production des poissons, ils peuvent servir de lien entre la variabilité à grande échelle de l'océan–atmosphère et la répartition des poissons pélagiques.

[Traduit par la Rédaction]

Introduction

The California Current (CC) ecosystem is one of the major eastern boundary current systems of the world, extending from Baja California to the northern tip of Vancouver Island (Fig. 1). The CC originates where the West Wind Drift divides, resulting from a divergence in wind patterns, into two branches near the coast of North America: a northern branch, the Alaska Current, and a southern branch, the CC (Ware and McFarlane 1989) (Fig. 1). The equatorward-flowing surface CC and the poleward-flowing subsurface California Undercurrent (CU) dominate large-scale circulation in this region (Fig. 1). The CU flows poleward from Baja California to Vancouver Island throughout most of the year; it is a relatively narrow current (ca. 10–40 km) and strongest at depths of 100–300 m (Neshyba et al. 1989).

Ocean circulation in this area varies on seasonal, interannual, and interdecadal bases. Two dominant atmospheric pressure regimes drive most of the seasonal, as well as the interdecadal, variability: the Aleutian low pressure system (ALP) during winter and the North Pacific high pressure system during summer (Emery and Hamilton 1985; Mantua et al. 1997). Winds associated with these regimes drive the large-scale surface flow, as well as the local coastal surface

Received 17 January 2006. Accepted 7 July 2006. Published on the NRC Research Press Web site at http://cjfas.nrc.ca on 16 November 2006.
J19110

V.N. Agostini,[1,2] R.C. Francis, and A.N. Hendrix. School of Aquatic and Fishery Science, University of Washington, P.O. Box 355020, Seattle WA 98149, USA.
A.B. Hollowed and C. Wilson. National Marine Fisheries Service, Alaska Fisheries Science Center, 7600 Sand Point Way NE, Seattle, WA 98112, USA.
S.D. Pierce. Oregon State University – COAS, 104 COAS Admin. Building, Corvallis, OR 97331, USA.

[1] Corresponding author (e-mail: vagostini@rsmas.miami.edu).
[2] Present address: Pew Institute for Ocean Science, Rosenstiel School of Marine and Atmospheric Science, University of Miami, 4600 Rickenbacker Way, Miami, FL 33133, USA.

Can. J. Fish. Aquat. Sci. **63**: 2648–2659 (2006) doi:10.1139/F06-139

Fig. 1. Schematic representation of general circulation along the west coast of North America. Box indicates area of study.

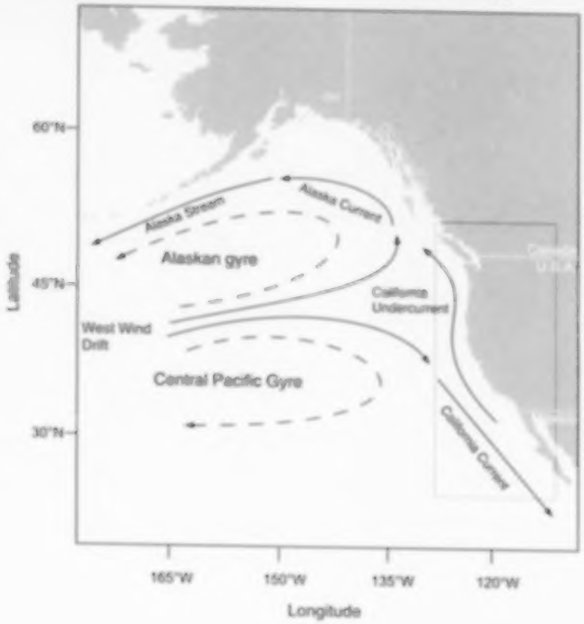

currents and onshore and offshore Ekman transport (Tabata 1975; Hickey 1979). Superimposed on this is the equatorially generated El Niño Southern Oscillation (ENSO), which leads to changes on an interannual scale. All of the above sources of variability affect a suite of local ocean conditions (Chelton 1981; Lynn and Simpson 1987; Strub et al. 1990). For example, El Niño can cause warming of the upper waters off the California coast, a depression of the nearshore thermocline, weakening of the CC, weakening in upwelling intensity, and an intensification of poleward flow (Chelton and Davis 1982; Hollowed 1992; Hickey 1998).

Variability in ocean conditions impacts production of a number of CC species (Francis and Hare 1994; Hare and Mantua 2000; Hollowed et al. 2001). There are four dominant coastal pelagic species in this system: northern anchovy (*Engraulis mordax*), Pacific sardine (*Sardinops sagax*), Pacific hake (*Merluccius productus*), and chub mackerel (*Scomber japonicus*). All of the adults of these species, with the exception of anchovy, conduct extensive migrations poleward in the summer to feed off the Pacific Northwest coast and equatorward in the winter to spawn off southern California (Benson et al. 2002). The northern limit of their feeding migrations appears to be related to oceanic seasons and to the northern boundary of the CC system (Ware and McFarlane 1989), the location of which varies according to climate conditions. Pacific hake (also referred to as Pacific whiting) account for 61% of the pelagic biomass in this system (Ware and McFarlane 1995) and belong mostly to the offshore population (Saunders and McFarlane 1997). There are also distinct populations of Pacific hake in the Strait of Georgia (McFarlane and Beamish 1985), Puget Sound (Pedersen 1985), and inlets of the west coast of Vancouver Island (Beamish and McFarlane 1985). The offshore population is of greatest importance, as it contributes a large biomass for fisheries in both Canadian and United States (US) waters (Francis et al. 1989; Smith et al. 1990). A good deal of controversy and interest revolves around this fishery, as the largest and most valuable fish migrate further north (Beamish and McFarlane 1985) and dramatic variability in year-class strength (Bailey and Francis 1985) affects the interannual distribution of biomass and therefore yield of hake between Canada and the US (Swartzman et al. 1987).

Fig. 2. Schematic representations of Pacific hake (*Merluccius productus*) migrations.

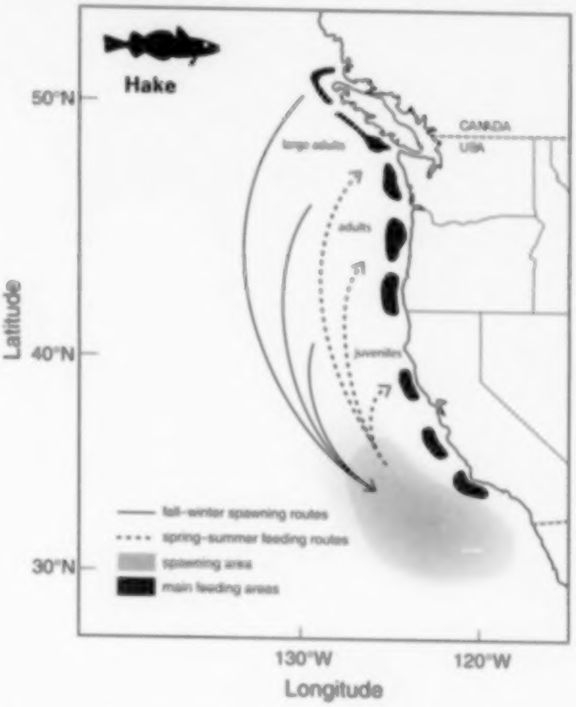

Offshore hake are believed to spawn between January and March each year at depths of 100–200 m (Fig. 2) off the coast of southern California or northern Mexico (Bailey et al. 1982; Bailey and Francis 1985). Offshore hake begin their seasonal northward feeding migration inshore (depths < 100 m) during late spring – early summer; in late fall, they move offshore and then return south to spawn (Bailey et al. 1982) (Fig. 2). Females have been reported to leave the spawning grounds and begin their migration north earlier than males (Saunders and McFarlane 1997). In summer, feeding hake are concentrated in large midwater aggregations centered on the shelf break from central Oregon to northern Vancouver Island (Saunders and McFarlane 1997). Their diet relies primarily on euphausiid in spring and summer and increases in piscivory with size (Bailey et al. 1982; Buckley and Livingston 1997). Cannibalism has been observed on the hake feeding grounds, with older larger hake eating smaller younger hake (Dorn 1995; Buckley and Livingston 1997).

The abundance of hake in Canadian waters has been related to temperature (Dorn 1995; Ware and McFarlane 1995;

Fig. 3. Acoustic backscatter signal representative of hake (*Merluccius productus*) abundance during (*a*) 1998 (warm year) and (*b*) 2001 (cold year). Data are from the National Marine Fisheries Service, Alaska Fisheries Science Center (NMFS–AFSC), Seattle, Washington.

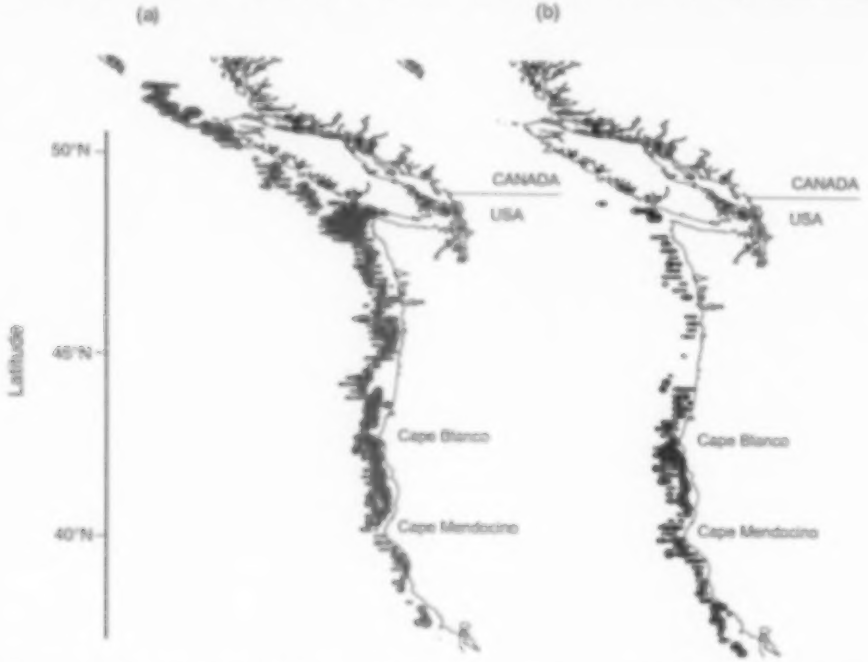

Benson et al. 2002). Hake have been located further north during warm years (Fig. 3) (Dorn 1991, 1995; Wilson and Guttormsen 1998); however, evidence for a relationship between hake distribution and temperature has been weak (Benson et al. 2002). A few authors have suggested that hake distribution may be related instead to poleward flow, with stronger flow aiding the migration of hake and weaker flow impeding it (Smith et al. 1990; Dorn 1995; Benson et al. 2002).

In this study, we use acoustic data to examine the distribution of hake in the CC system in relation to poleward flow and temperature. We test the hypothesis that hake distribution is related to poleward flow. We argue that although physical processes may not directly affect hake production, they may be the link between large-scale ocean–atmosphere variability and hake distribution along the west coast.

Materials and methods

Study area

In 1977, the National Marine Fishery Services (NMFS) began collecting data describing hake abundance and distribution along the west coast of North America; in 1992, the Canadian Department of Fisheries and Oceans (DFO) began collaboration with NMFS in this collection. Echo-integration summer acoustic trawl surveys have been conducted on a triennial basis along the continental shelf from California to the northern limit of hake aggregations in British Columbia (Fig. 3). Recently, survey efforts have extended into Alaskan waters. Details of the triennial surveys are available in Wilson and Guttormsen (1997) and Wilson et al. (2000). Surveys generally occurred from July to September off the west coast of North America. Data were collected along parallel transects, uniformly spaced 18 km apart and 52 km long on average. Transects generally ran midshelf to midslope between the 50 m and 1500 m isobaths. To capture conditions from different climate regimes, survey data were analyzed from 1995 (a neutral year) and 1998 (an El Niño year).

Biological data

Abundance and distribution of adult hake were derived from acoustic data collected using a quantitative echo-sounding system with split-beam transducers (38 kHz and 120 kHz; Simrad EK500; Simrad, Lynnwood, WA 98036, USA) mounted on the bottom of the vessel centerboard, 9 m below the surface. Data collected with the 38 kHz transducer were used in this study. Echo-integration data were sampled with a vertical resolution of about 9 m and a horizontal resolution of 1–2 m. Standard target strength–length relationships were used to convert acoustic backscatter into fish density. The target strength relationship used was $TS = 20\log L - 68$, where L represents fish length measured in centimetres. For detailed methods on data processing, see Wilson and Guttormsen (1997) and Wilson et al. (2000).

Physical data

Distribution and intensity of alongshore (north–south (N–S)) flow were derived from an RD instrument, a 153.6 kHz narrow-band, hull-mounted shipboard acoustic Doppler current profiler (ADCP). A vertical bin width of 8 m, a pulse length of 8 m, and an ensemble averaging time of 2.5 min were used. The depth range of good data (good pings > 30%) was typically 22–362 m. The ADCP was slaved to the Simrad EK500 to avoid interference. Presurvey tests con-

Fig. 4. Frequency distribution of temperature values in hake waters at survey stations during 1995 (solid bars) and 1998 (open bars).

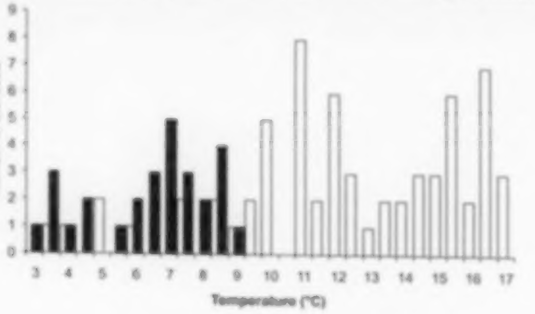

firmed no interference between the two instruments when the ADCP was in water-pulse mode. When the ADCP bottom-track feature was enabled, however, an artificial signal was detected on the EK500. For this reason, bottom tracking was never enabled during the survey. GPS P-code navigation was used for position and gyrocompass was used for heading to determine absolute velocities. Tidal currents remain in the processed ADCP velocities. These are expected to be small (<0.05 m·s^{-1}) offshore of the shelfbreak (Erofeeva et al. 2003). For detailed ADCP processing methods, see Pierce et al. (2000).

Temperature information was derived from conductivity–temperature–depth (CTD) casts (1995, n = 200; 1998, n = 179) made at two or three locations where large aggregations of hake were observed, along every second or third transect, from the surface down to water depths of about 500 m.

Analysis

To describe the relationship between temperature, hake, and alongshore flow distribution the following values were computed for J transects (j = 1, 2, 3, …, J), I_j stations in transect j (i = 1, 2, 3, …, I_j), and $K_{i,j}$ depths at station i_j ($k_{i,j}$ = 1, 2, 3, …, $K_{i,j}$).

Depth (in metres) of center of mass of poleward flow at station i and transect j (as in Pierce et al. 2000), hereafter referred to as core current, was determined by

$$(1)\qquad Z_{c_{i,j}} = \frac{\sum_{k=1}^{k_{i,j}} v_{i,j,k}\, z_{i,j,k}}{\sum_{k=1}^{k_{i,j}} v_{i,j,k}}$$

where $v_{i,j,k}$ represents raw poleward velocity at station i, transect j, and depth k; and $z_{i,j,k}$ is the depth of current measurement at station i, transect j, and depth k.

Weighted mean depth (in metres) of hake at each station i and transect j is determined as follows:

$$(2)\qquad Z_{f_{i,j}} = \frac{\sum_{k=1}^{k_{i,j}} f_{i,j,k}\, z_{i,j,k}}{\sum_{k=1}^{k_{i,j}} f_{i,j,k}}$$

Fig. 5. Frequency distribution of alongshore flow values (m·s^{-1}) in hake waters at survey transects during 1995 (solid bars) and 1998 (open bars). Positive values indicate poleward flow; negative values indicate equatorward flow.

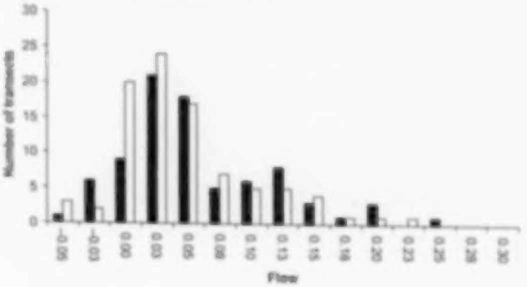

where $f_{i,j,k}$ is the number of fish at station i, transect j, and depth k; and $z_{i,j,k}$ is the depth of fish measurement at station i, transect j, and depth k.

The fish index at each station i and transect j is calculated by

$$(3)\qquad \mathrm{FI}_{i,j} = \frac{\sum_{k=1}^{k_{i,j}} f_{i,j,k}}{f_{\max}}$$

where $f_{i,j,k}$ is as defined for eq. 1, and $f_{\max}$ is the maximum number of fish over the entire survey range.

Weighted alongshore flow velocity (cm·s^{-1}) at each station i and transect j (referred to hereafter as flow velocity of hake waters) is determined as follows:

$$(4)\qquad v_{f_{i,j}} = \frac{\sum_{k=1}^{k_{i,j}} f_{i,j,k}\, v_{i,j,k}}{\sum_{k=1}^{k_{i,j}} f_{i,j,k}}$$

where $f_{i,j,k}$ is as defined earlier, and $v_{i,j,k}$ is the raw N–S flow velocity for bins where number of fish > 0 at station i, transect j, and depth k.

Mean alongshore flow velocity (cm·s^{-1}) at each station i and transect j is calculated by

$$(5)\qquad v_{c_{i,j}} = \frac{\sum_{k=1}^{k_{i,j}} v_{i,j,k}}{n}$$

where $v_{i,j,k}$ is the raw N–S velocity at station i, transect j, and depth k, and n is the number of depth bins.

Weighted temperature (°C) at station i and transect j (referred to hereafter as temperature of hake waters) is determined as follows:

$$(6)\qquad T_{f_{i,j}} = \frac{\sum_{k=1}^{k_{i,j}} T_{i,j,k}\, f_{i,j,k}}{\sum f_{i,j,k}}$$

Fig. 6. Distribution of alongshore flow (in color) and hake (*Merluccius productus*) aggregations (in black contours representing numbers of fish ≥16 × 10^{-3} m^3) for (*a*) a transect located at 41°N sampled in 1995; (*b*) a transect located at 50°N sampled in 1995; (*c*) a transect located at 38°N sampled in 1998; and (*d*) a transect located at 51°N sampled in 1998. The bottom contour is also shown (solid area). Flow velocities greater than 0 indicate poleward flow; flow velocities less than 0 indicate equatorward flow.

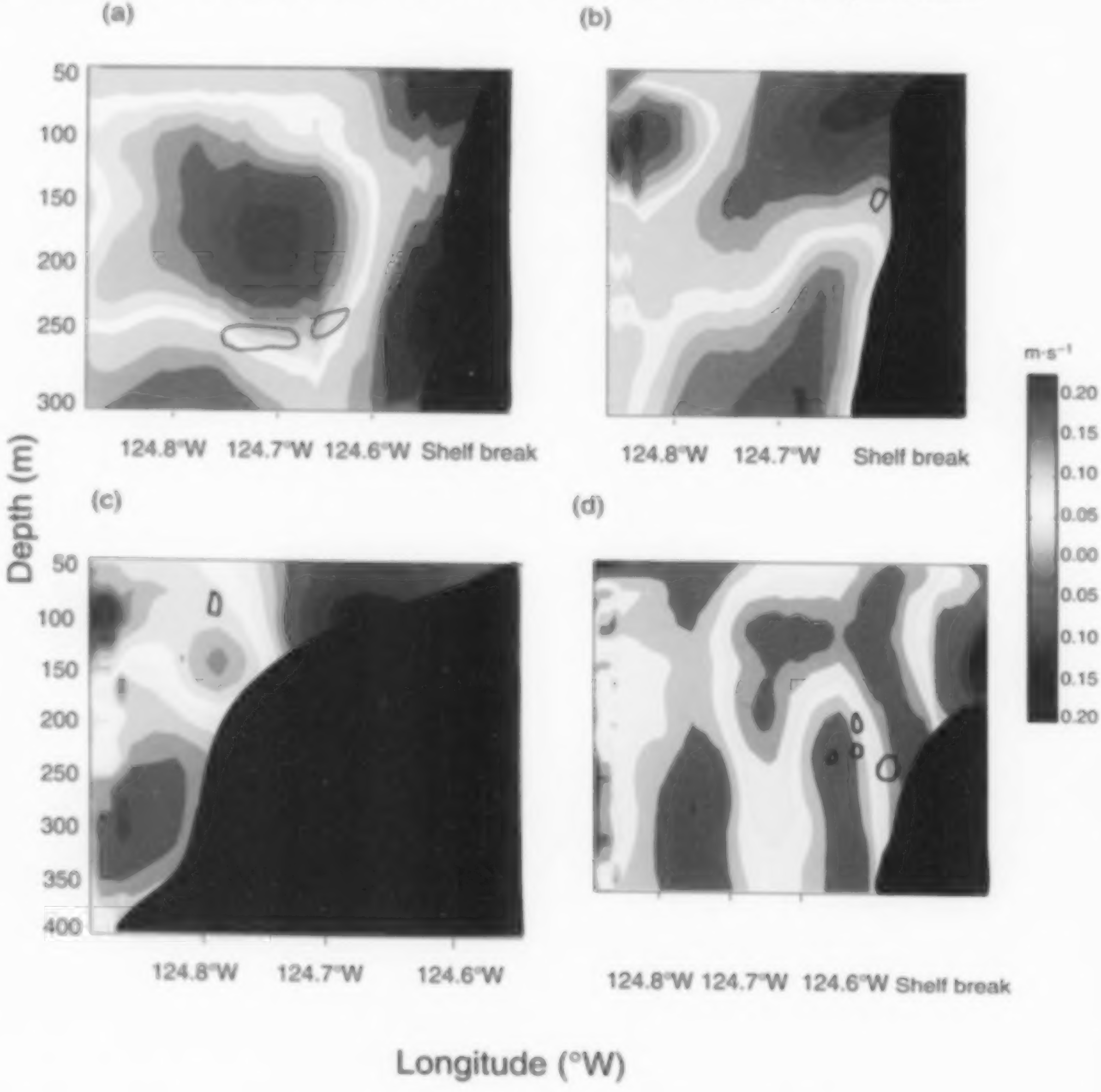

where $T_{i,j,k}$ is the temperature at station *i*, transect *j*, and depth *k* for bins where number of fish > 0, and $f_{i,j,k}$ is as defined earlier.

To aid in spatial analysis, values were averaged over each transect, as well as over four latitudinal blocks (32.5°N–37.5°N, 37.5°N–42.5°N, 42.5°N–47.5°N, 47.5°N–52.5°N). The latitudinal blocks were chosen to coincide with important topographic features, such as capes and promontories, known to influence the oceanography of the region (Hickey 1979). Differences between 1995 and 1998 mean average temperature, flow, and distance of fish from shelf were tested using two-sample *t* tests. Also, to effectively isolate waters where subsurface poleward flow usually occurs, the values above were computed in two ways: (*i*) including measurements from all depths bins, and (*ii*) including only measurements from 120–330 m depth bins (hereafter referred to as subsurface). Any values at depths shallower than 120 m probably do not represent CU flow (Pierce et al. 2000). Also,

Fig. 7. Depth of (*a*) fish and (*b*) core current averaged over four latitudinal blocks (32.5°N–37.5°N, 37.5°N–42.5°N, 42.5°N–47.5°N, 47.5°N–52.5°N). Values for 1995, ◆; values for 1998, ■.

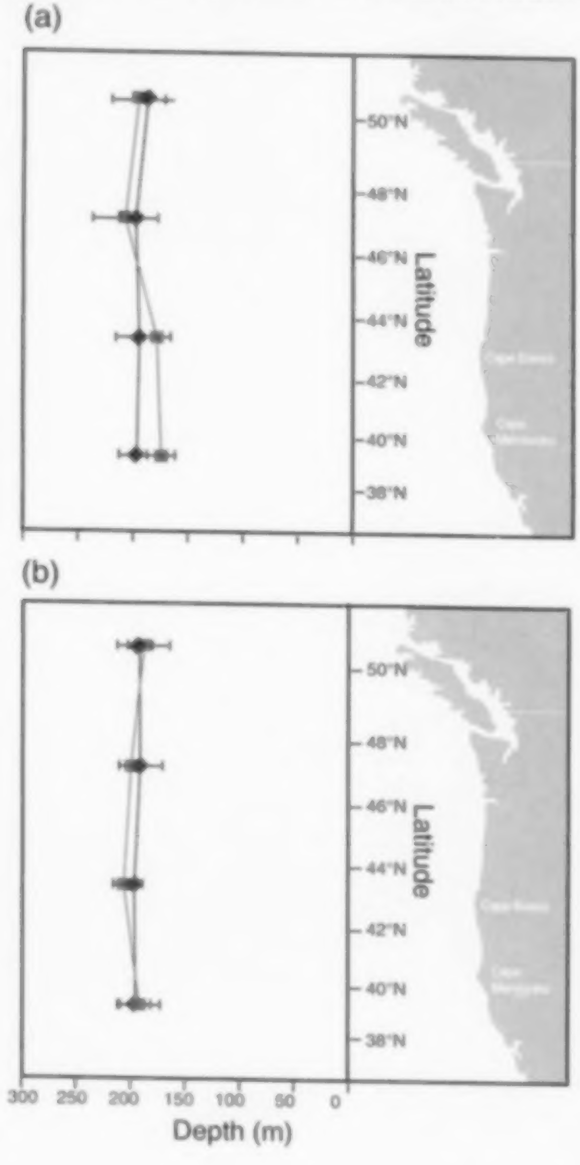

hake were usually not detected at depths shallower than 120 m. Alongshore flow (N–S) will be referred to as "flow" throughout this paper.

Results

To explore the relationship between hake distribution and temperature, we computed average temperature ($\overline{T}$) of hake waters for each CTD station. A frequency histogram of these values reveals that hake occur in waters of a wide range of temperatures (from a minimum of 3.5 °C to a maximum of 17.5 °C) (Fig. 4). As expected, temperatures of hake waters were significantly higher during 1998, an El Niño year ($\overline{T}$ = 12.2 °C, s^2 = 12.1), compared with during 1995, a neutral year ($\overline{T}$ = 5.3 °C, s^2 = 7.0) ($p << 0.01$, df = 81, *t* test for difference between means).

Fig. 8. Average speed of subsurface alongshore flow (m·s^{-1}; negative values indicate equatorward flow; positive values indicate poleward flow) at each transect. Values are averaged over the 120 m to 330 m depth bins. (*a*) 1998, (*b*) 1995.

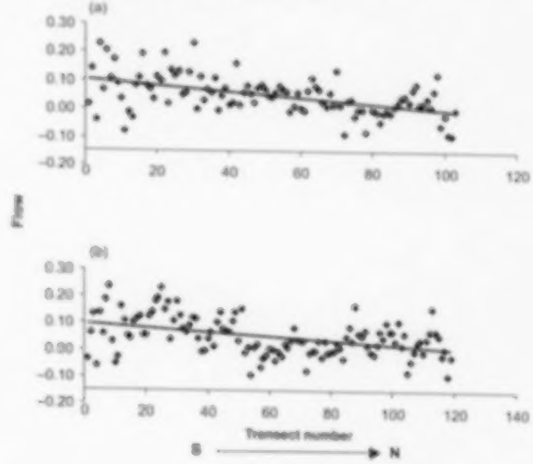

In contrast, average subsurface flow speed in hake waters (Fig. 5) indicates that fish were in waters with a much narrower range of values (between −0.05 and 0.25 m·s^{-1}, where negative values indicate equatorward flow and positive values indicate poleward flow) compared with the temperature values reported above, with most of the flow between 0.025 and 0.075 m·s^{-1}, speeds reported to be typical of the poleward-flowing undercurrent (Pierce et al. 2000). Average subsurface flow speed of hake waters was higher during 1995 ($\bar{x}$ = 0.05 m·s^{-1}, s^2 = 0.004) compared with during 1998 ($\bar{x}$ = 0.03 m·s^{-1}, s^2 = 0.003) (p = 0.04, df = 160, *t* test for difference between means). Similar results were found when considering flow at all depths.

Sections of flow overlaid with hake distribution and abundance data were plotted for each transect, revealing a picture of a ubiquitous core of poleward flow at depth, with its strength and location varying both inshore and offshore and at depth for the two years sampled. Complex flow patterns were evident in each section. The view of geostrophic flow in any one section is confused by the presence of barotropic tidal currents, baroclinic tidal currents, and inertial oscillations (Pierce et al. 2000). For sections where fish were present, concentrations were almost always observed on the edge of the core poleward flow (Figs. 6*a*–6*d*). Depth of fish and core current averaged over latitudinal blocks were similar (Fig. 7) during both 1995 and 1998, with average depths ranging mostly between 170 and 220 m. Depth of core current values are consistent with results from Pierce et al. (2000), as well as with historical estimates of undercurrent depth (Neshyba et al. 1989).

The alongshore subsurface layer flow speeds show significant scatter during both years (Fig. 8), probably because of

Fig. 9. Observed acoustic Doppler current profiler velocity vectors (depth averaged 120–330 m) from a subsection of the National Marine Fisheries Service – Department of Fisheries and Oceans survey for (*a*) 1995 and (*b*) 1998. Black lines parallel to the coast represent the 50 m, 100 m, and 200 m isobaths.

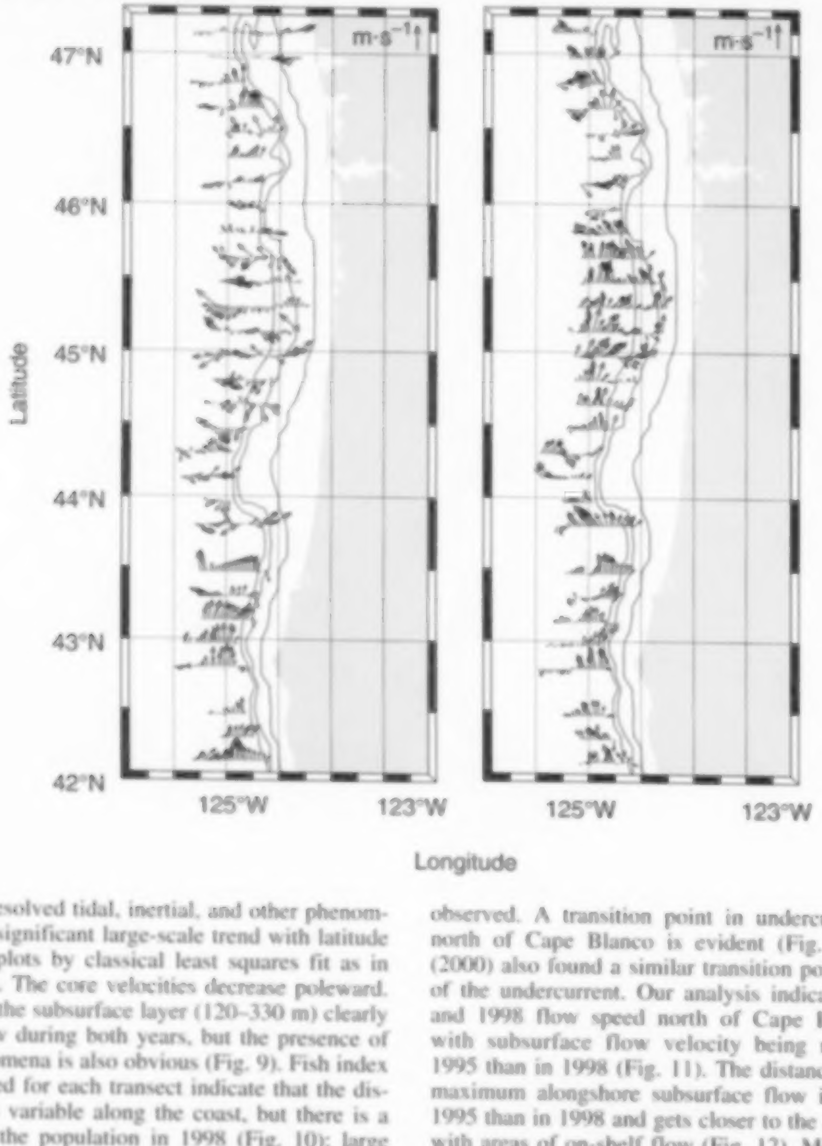

the presence of unresolved tidal, inertial, and other phenomena. A statistically significant large-scale trend with latitude is evident in both plots by classical least squares fit as in Pierce et al. (2000). The core velocities decrease poleward. Current vectors for the subsurface layer (120–330 m) clearly show poleward flow during both years, but the presence of other oceanic phenomena is also obvious (Fig. 9). Fish index (FI) values computed for each transect indicate that the distribution of hake is variable along the coast, but there is a northward shift of the population in 1998 (Fig. 10); large amounts of hake were found north of 50°N (FI between 0.4 and 1) during 1998 in comparison with small (FI < 0.1) to no amounts of hake found in this area during 1995.

A plot of alongshore subsurface flow in hake waters averaged over each transect (Fig. 11) also clearly portrays mostly poleward flow during both years of this study, although variable equatorward flow characterizes some regions (e.g., 44°N–46°N in 1995 and 48°N–50°N in 1998). During 1995, northward flow was measured at 81% of the transects and southward flow at 19% of the transects; during 1998, northerly flow was measured at 85% of the transects and southerly flow at 15%. Interesting latitudinal patterns can also be observed. A transition point in undercurrent strength just north of Cape Blanco is evident (Fig. 11). Pierce et al. (2000) also found a similar transition point in their analysis of the undercurrent. Our analysis indicates that both 1995 and 1998 flow speed north of Cape Blanco diminishes, with subsurface flow velocity being more southward in 1995 than in 1998 (Fig. 11). The distance from the shelf of maximum alongshore subsurface flow is more variable in 1995 than in 1998 and gets closer to the shelf north of 45°N with areas of on-shelf flow (Fig. 12). Maximum alongshore subsurface flow in the southern portion of the survey area (south of 44°N) is significantly closer to the shelf in 1998 ($\bar{X} = 15$, $s^2 = 146$) than in 1995 ($\bar{X} = 19$, $s^2 = 77$, $p < 0.05$) but gets farther away and never migrates onto the shelf north of 44°N in 1998 ($\bar{X} = 28$, $s^2 = 428$) compared with in 1995 ($\bar{X} = 11$, $s^2 = 511$, $p << 0.05$). Distances of maximum fish densities follow this pattern, with maximum fish densities south of 44°N observed slightly (although not significantly) closer to the shelf break in 1998 ($\bar{X} = 10$, $s^2 = 108$) compared with 1995 ($\bar{X} = 12$, $s^2 = 113$). Overall maximum fish distances from the shelf break in 1998 are highly variable and increase northward along the coast.

Fig. 10. Fish index (number of fish per transect/maximum number of fish over survey area) by survey transect in (*a*) 1995 and (*b*) 1998.

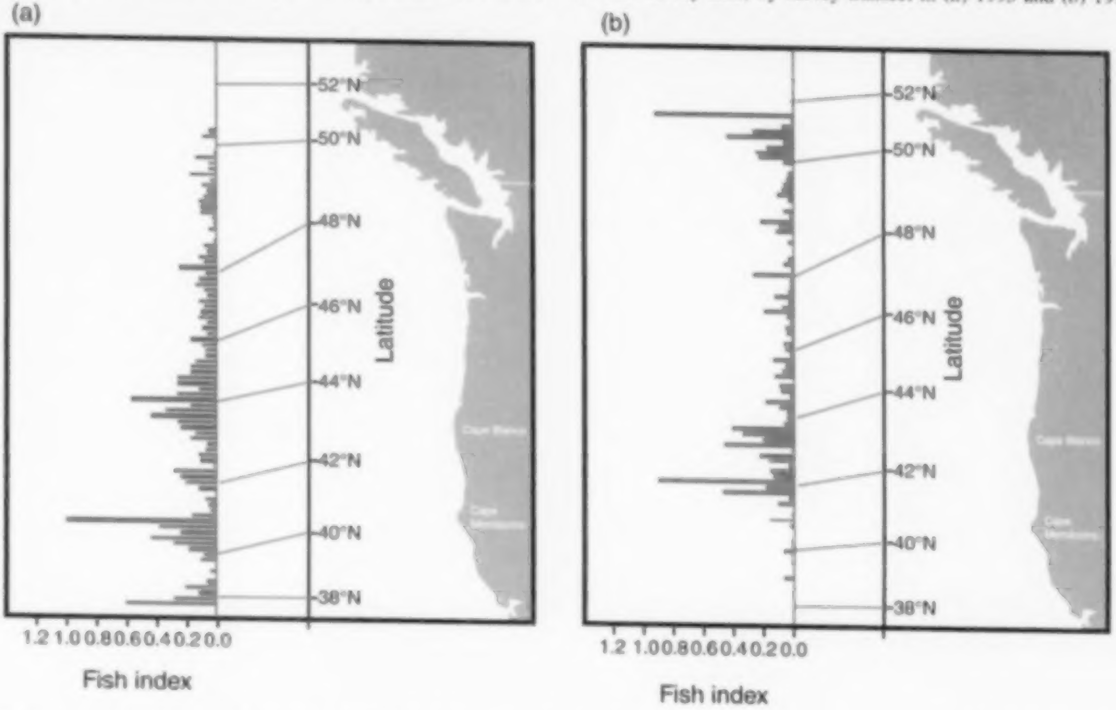

Fig. 11. Subsurface alongshore flow speed (m·s^{-1}) in hake waters for (*a*) 1995 and (*b*) 1998. Positive values indicate poleward flow; negative values indicate equatorward flow.

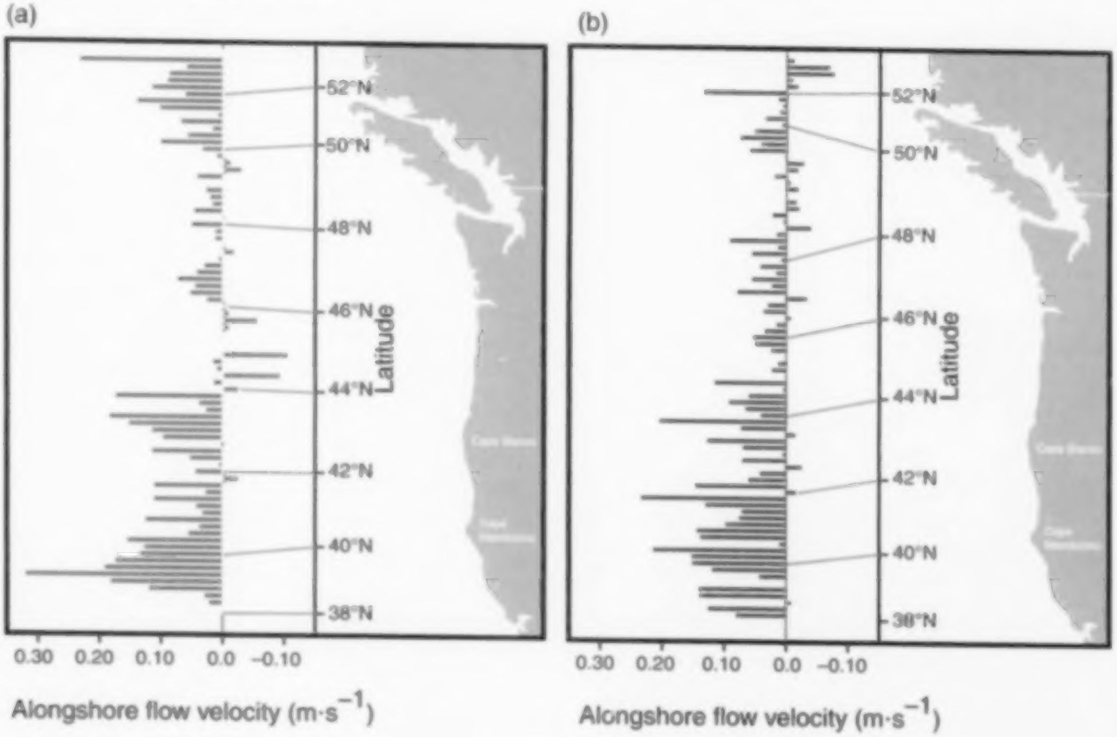

Fig. 12. Distance from shelf (bottom depth = 150 m) of maximum subsurface alongshore flow (m·s^{-1}) in (*a*) 1995 and (*b*) 1998. Negative values indicated on-shelf location; positive values indicate off-shelf location.

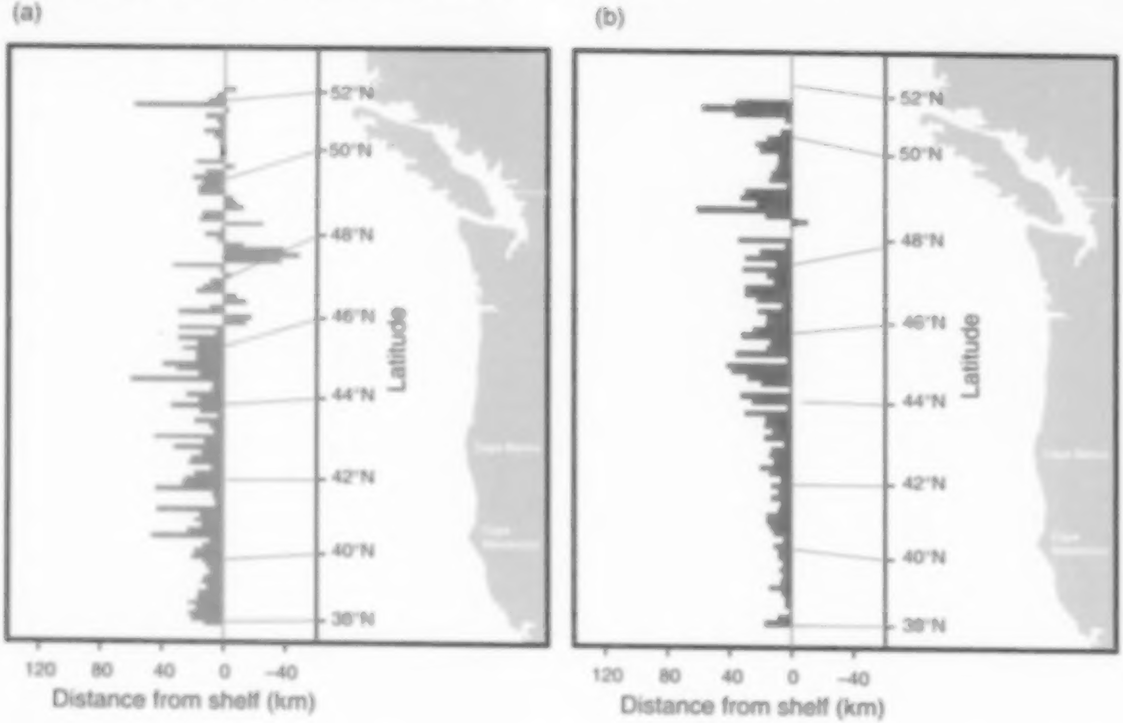

Discussion

The results of our analysis suggest that Pacific hake habitat is associated with subsurface poleward flow and not a specific temperature range. Temperature has been one of the most widespread indices used to relate environmental conditions to abundance and distribution of fish populations. Temperature is known to influence the physiology of some species (Durant et al. 2003) and can be useful as an index of oceanic conditions impacting fish abundance and (or) distribution. However, if a specific process associated with the index has not been identified, the relationship is not likely to hold during different climate regimes and will therefore not be useful to researchers and managers. For example, Benson et al. (2002) looked at how sea surface temperature (SST) and upwelling relate to the presence of hake in Canadian waters. The relationship with SST only existed until a shift to a new climate regime occurred. Upwelling was found to be a better predictor of hake abundance in Canadian waters. The authors note that this type of index includes transport and winds more explicitly and may thus be a better predictor. The influence of transport processes on poleward hake migration was also observed by Smith et al. (1990), who looked at the relationship between a number of oceanographic parameters and the observed length-at-age pattern for Pacific hake sampled off Vancouver Island. Sea-level height, commonly used as an index of transport, had the strongest relationship to interannual variability in hake mean lengths-at-age in Canadian waters. The authors find that years of stronger than normal surface poleward flow (or weaker than normal equatorward flow) result in more, smaller hake arriving off southern Vancouver Island. This suggests that northward migration of hake is assisted in years of strong poleward flow. Dorn's (1995) analysis also suggests that poleward flow influences northward migration of hake.

Temporal and spatial patterns characterize both hake distribution and undercurrent characteristics during the two years of this study. The distribution of Pacific hake shifted north in 1998, with higher densities of fish observed north of 50°N. This shift north can not be explained by a higher number of older fish in the population, because the estimated population's age distribution in 1995 and 1998 are similar, as shown by Helser and Dorn (2001). Instead, favorable flow characteristics could have facilitated the migration of hake north in 1998. The flow was more ubiquitous and coherent in 1998 than in 1995. The literature suggests stronger undercurrent during warm years (Bograd et al. 2001; Lynn and Bograd 2002; Bograd and Lynn 2003). S.D. Pierce and P.M. Kosro (unpublished data cited in Swartzman and Hickey (2003)) report higher average undercurrent volume transport (m^3·s^{-1}) in 1998 than in both 1995 and 2001. Swartzman et al. (2005) also report on higher undercurrent volume transport (m^3·s^{-1}) in specific areas of the CC system.

Flow geometry, such as distance from the shelf and area covered, also differs between the two years of this study. In 1998, subsurface poleward flow was significantly closer to the shelf in the southern part of the survey area (south of 44°N). Swartzman et al. (2005) also found poleward transport to be closer to the shelf in 1998 than in 1995. Along specific sections of the coastline (e.g., from 44.5°N to 46°N and from 48°N to 50°N), alongshore flow was mostly poleward in 1998 and mostly equatorward in 1995. Flow geometry, as well as flow velocity, are likely to affect hake distribution. There is evidence of a higher concentration of prey at shelf-edge environments (Mackas et al. 1980, 1997; Simard and Mackas 1989). Being at the edge of a current closer to the shelf break (as was the case in 1998 in the southern portion of the survey) probably gives hake better access to prey usually found in higher concentrations along the shelf. This is particularly important for younger, thus smaller, hake typically found in the southern portion of the survey area. Thus, the proximity to the shelf break of the flow in the southern area of the survey during 1998 could have facilitated access that year to richer feeding grounds for the smaller, younger fish in the population.

Based on the results of this analysis, we hypothesize that one of the ways that climate influences the population dynamics of hake is by affecting the physical structure of adult hake habitat, expanding and contracting the amount available. We suggest that subsurface poleward flow in this area defines adult hake habitat, with flow properties aiding or impeding the poleward migration of the population. This may be especially true for the southern half of the hake distribution where smaller fish are closer to shore in the juvenile nursery grounds and thus flow closer to the coast is probably easier for them to detect. Favorable current characteristics during warm years (e.g., coherent ubiquitous flow along the coast located close to the shelf break) may facilitate the hake feeding migration north to richer feeding grounds and access to prey along the way. These conditions may also facilitate migration of smaller younger fish that would otherwise have a hard time covering long distances. For example, Smith et al. (1990), as well as Benson et al. (2002), found evidence of a greater number of smaller hake present in Canadian waters during 1998. Wilson and Guttormsen (1997, 1998) found 95% of hake caught off the coast of Washington in 1995 to be above 42 cm in fork length, whereas only 50% in 1998 were in this size category. The presence of smaller younger hake further north could also lead to an increased spatial overlap of age classes and potentially a higher rate of cannibalism during warm years. Field (2004) reports on differences in the amount of hake present in hake diets during warm and cold years, with up to 70% of hake prey being smaller hake during warmer years compared with less than 1% during cooler years.

Our hypothesis that poleward flow defines the amount and location of adult hake habitat might lead the reader to believe that we do not consider food availability to be important. This is not the case. Pacific hake migrations are first and foremost motivated by a search for food and are therefore primarily governed by factors related to food availability. The physical structure of the water column is one of these factors, as it probably influences the distribution of hake prey (i.e., euphausiids) that for the most part are not as able to retain position in the water column in regions of strong flow (Swartzman and Hickey 2003; Ressler, et al. 2005; Swartzman et al. 2005). Swartzman (2001) and Swartzman and Hickey (2003) investigated the relationship between the distribution of euphausiids and hake along the west coast of North America. They found a consistent overlap of large plankton patches and fish shoals near the shelf break, although the degree of clustering between years differed depending on latitude. However, Mackas et al. (1997) pointed out that despite the apparent relationship between euphausiids, hake, and bathymetry evident at a coarser scale (tens of kilometres), this relationship did not hold at a finer scale. Their analysis highlighed the importance of cues provided by flow fields. They did not find an overlap in space between plankton and hake at a finer scale; hake patches were located either above or below euphausiid patches and both organisms seemed to be associated with specific bathymetric contours. Sensory spheres of both zooplankton and fish are quite small (Mackas et al. 1997). Mackas et al. (1997) suggested that hake are cued by their immediate surrounding flow field, rather than by the surrounding bathymetry or prey density (both at ranges ≥10 m).

We also note that hake spawning ground are not fixed but rather variable in location (Sakuma and Ralston 1997; Horne and Smith 1997). It is conceivable that adults could migrate further north in some years when the spawning migration does not extend as far south as other years. However, the degree of variation observed for spawning ground location in consecutive years (Horne and Smith 1997) is too small to justify the observed degree of variation in adult hake distribution. The most appreciable latitudinal changes in spawning grounds location are observed when integrating data over long periods (Horne and Smith 1997). Thus, although spawning ground location may affect the distribution of adult hake, we don't believe it to be potentially a dominant factor in this study.

We propose that Pacific hake gain evolutionary benefits by positioning themselves relative to poleward flow. One advantage is that being at the edge of this current puts them in or close to a location where the food supply is likely to be high (the shelf break). Another advantage is that they expend less energy during their northward migration. What determines competitive advantage of a certain life history strategy over another is ultimately related to energy gain and expenditure. Food allows individuals to gain that energy, but migrating long distances contributes to expending it. Close examination of hake life history traits reveals that hake time their migration in relation to the seasonality of the current. Females, for example, leave the spawning grounds earlier, beginning their migration when the poleward current intensity peaks (Saunders and McFarlane 1997). This suggests that Pacific hake have evolved to take advantage of poleward flow during their feeding migrations. Hake are active swimmers and do not need the current to migrate north. Poleward flow simply allows them to complete their migrations expending less energy and to gain access to new energy by accessing richer northern feeding grounds. There is evidence of poleward flow facilitating hake migration in other areas of the world (Sanchez and Gil 2000). The fact that distant populations are affected by similar environmental processes leads us to believe that an association with poleward flow must provide competitive advantages to this species.

The factors influencing hake year-class strength are multiple and complex; hence, a linear relationship between subsurface poleward flow and the hake production time series will likely not be found. For example, conditions on the larval and juvenile nursery grounds are of primary importance, as is the impact that the fishery has on the population. Here we have formulated hypotheses to explain the variability in hake migration and adult hake habitat that are a part of this puzzle. All of these factors come together to produce the observed production variability. Similar changes in migration patterns have been observed for other CC pelagic species, e.g., sardine and mackerel (Beamish et al. 2000). One thing seems clear: pelagic fish are good indicators of shifts in ocean conditions as their life histories are so tightly related to atmosphere and ocean conditions. This leads us to believe that in the future, pelagic fish distribution might be used as an indicator of climate change. We will, however, only be able to do so if we understand the processes that link climate and pelagic fish production and distribution. This study is a step in that direction.

Acknowledgments

We thank Mike Guttormsen for help with acoustic data processing, Jodie Little and Warren Wooster for helpful discussion and review of this manuscript, John Mickett for help with programming, and Amity Femia for help with graphics. This publication was supported by the JISAO/Climate Impacts Group (University of Washington) under NOAA Cooperative Agreement NA17RJ1231 (contribution no. 1327). S.D. Pierce was partially supported by National Oceanic and Atmospheric Administration (Grant AB133F05SE4205).

References

Bailey, K.M., and Francis, R.C. 1985. Recruitment of Pacific whiting, *Merluccius productus*, and the ocean environment. Mar. Fish. Rev. **47**(2): 8–14.

Bailey, K.M., Francis, R.C., and Stevens, P.R. 1982. The life history and fishery of Pacific whiting, *Merluccius productus*. CalCOFI Rep. **23**: 81–98.

Beamish, R.J., and McFarlane, G.A. 1985. Pacific whiting, *Merluccius productus*, stocks off the west coast of Vancouver Island, Canada. Mar. Fish. Rev. **47**(2): 75–81.

Beamish, R.J., McFarlane, G.A., and King, J.R. 2000. Fisheries climatology: understanding decadal scale processes that naturally regulate British Columbia fish populations. *In* Fisheries oceanography: an integrative approach to fisheries ecology and management. *Edited by* P.J. Harrison and T.R. Parsons. Blackwell Science, Oxford. pp. 94–145.

Benson, A.J., McFarlane, G.A., Allen, S.E., and Dower, J.F. 2002. Changes in Pacific hake (*Merluccius productus*) migration patterns and juvenile growth related to the 1989 regime shift. Can. J. Fish. Aquat. Sci. **59**: 1969–1979.

Bograd, S.J., and Lynn, R.J. 2003. Long-term variability in the Southern California Current System. Deep-Sea Res. II, **50**: 2355–2370.

Bograd, S.J., Chereskin, T.K., and Roemmich, D. 2001. Transport of mass, heat, salt and nutrients in the southern California Current System: annual cycle and interannual variability. J. Geophys. Res. **106**: 9255–9276.

Buckley, T.W., and Livingston, P.A. 1997. Geographic variation in the diet of Pacific hake, with a note on cannibalism. CalCOFI Rep. **38**: 53–62.

Chelton, D.B. 1981. Interannual variability of the California Current physical factors. CalCOFI Rep. **22**: 34–48.

Chelton, D.B., and Davis, R.E. 1982. Monthly mean sea-level variability along the west coast of North America. J. Phys. Ocean. **12**: 757–784.

Dorn, M.W. 1991. Spatial and temporal patterns in the catch of Pacific whiting in the US management zone during 1978–88. NOAA Tech. Memo. No. NMFS F/NWC-205.

Dorn, M.W. 1995. The effects of age composition and oceanographic conditions on the annual migration of Pacific whiting, *Merluccius productus*. CalCOFI Rep. **36**: 97–105.

Durant, J.M., Anker-Nilssen, T., and Stenseth, T.C. 2003. Trophic interactions under climate fluctuations: the Atlantic puffin as an example. Proc. R. Soc. Lond. Ser. B Biol. Sci. **270**(1523): 1461–1466.

Emery, W.J., and Hamilton, K. 1985. Atmospheric forcing of interannual variability in the Northeast Pacific Ocean: connections with El Nino. J. Geophys. Res. **90**: 857–868.

Erofeeva, S.Y., Egbert, G.D., and Kosro, P.M. 2003. Tidal currents on the central Oregon shelf: models, data, and assimilation. J. Geophys. Res. 108, 3148 [doi:10.1029/2002JC001615].

Field, J.C. 2004. Application of ecosystem-based fishery management approaches in the Northern California Current. Ph.D. dissertation, University of Washington, Seattle, Washington.

Francis, R.C., and Hare, S.R. 1994. Decadal-scale regime shifts in the large marine ecosystems of the Northeast Pacific: a case for historical science. Fish. Oceanogr. **7**: 1–20.

Francis, R.C., Adlerstein, S.A., and Hollowed, A.B. 1989. Importance of environmental fluctuations in the management of Pacific hake. *In* Effects of ocean variability on recruitment and an evaluation of parameters used in stock assessment models. *Edited by* R.J. Beamish and G.A. McFarlane. Can. Spec. Publ. Fish. Aquat. Sci. No. 108. pp. 51–56.

Hare, S.R., and Mantua, N.J. 2000. Empirical evidence for North Pacific regime shifts in 1977 and in 1989. Prog. Oceanogr. **47**: 103–145.

Helser, T., and Dorn, M. 2001. Stock assessment of Pacific hake (whiting) in U.S. and Canadian waters in 2001. *In* Pacific Fishery Management Council, status of the Pacific coast groundfish fishery through 2001 and recommended acceptable biological catches in 2003. Pacific Fishery Management Council, 2130 SW Fifth Avenue, Suite 224, Portland, OR 97201, USA. NWFSC, Document ID 5916.

Hickey, B.M. 1979. The California Current system — hypotheses and facts. Prog. Oceanogr. **8**: 191–279.

Hickey, B.M. 1998. Coastal oceanography of western North America from the tip of Baja California to Vancouver Island. *In* The sea. 11. *Edited by* A.R. Robinson and K.H. Brink. John Wiley and Sons, New York. pp. 345–393.

Hollowed, A.B. 1992. Spatial and temporal distributions of Pacific hake, *Merluccius productus*, larvae and estimates of survival during early life history stages. CalCOFI Rep. **33**: 100–133.

Hollowed, A.B., Hare, S.R., and Wooster, W.S. 2001. Pacific basin climate variability and patterns of Northeast Pacific marine fish production. Prog. Oceanogr. **49**: 257–282.

Horne, J.K., and Smith, P.E. 1997. Space and time scales in Pacific hake recruitment processes: latitudinal variation over annual cycles. CalCOFI Rep. **38**: 90–102.

Lynn, R.J., and Bograd, S.J. 2002. Dynamic evolution of the 1997–1999 El Niño–La Niña cycle in the Southern California Current System. Prog. Oceanogr. **54**(1–4): 59–75.

Lynn, R.S., and Simpson, J.J. 1987. The California Current System: the seasonal variability of its physical characteristics. J. Geophys. Res. **92**: 12 947 – 12 966.

Mackas, D.L., Louttit, G.C., and Austin, M.J. 1980. Spatial distribution of zooplankton and phytoplankton in British Columbian coastal waters. Can. J. Fish. Aquat. Sci. **37**: 1476–1487.

Mackas, D.L., Kieser, R., Saunders, M., Yelland, D.R., Brown, R.M., and Moore, D.F. 1997. Aggregation of euphausiids and

Pacific hake (*Merluccius productus*) along the outer continental shelf off Vancouver Island. Can. J. Fish. Aquat. Sci. **54**: 2080–2096.

Mantua, N.J., Hare, S.R., Zhang, Y., Wallace, J.M., and Francis, R.C. 1997. A Pacific interdecadal climate oscillation with impacts on salmon production. Bull. Am. Meteorol. Soc. **78**(6): 1069–1079.

McFarlane, G.A., and Beamish, R.J. 1985. Biology and fishery of Pacific whiting, *Merluccius productus*, in the Strait of Georgia. Mar. Prog. Ser. **47**: 23–34.

Neshyba, S.J., Mooers, C.N.K., Smith, R.L., and Barber, R.T. (*Editors*). 1989. Poleward flows along eastern ocean boundaries. Springer, New York.

Pedersen, M. 1985. Puget Sound Pacific whiting, *Merluccius productus*, resource and industry: an overview. Mar. Fish. Rev. **47**: 35–38.

Pierce, S.D., Smith, R.L., Kosro, P.M., Barth, J.A., and Wilson, C.D. 2000. Continuity of the poleward undercurrent along the eastern boundary of the mid-latitude North Pacific. Deep Sea Res. II, **47**: 811–829.

Ressler, P.H., Brodeur, R.D., Peterson, W.T., Pierce, S.D., Vance, P.M., Rostad, A., and Barth, J.A. 2005. The spatial distribution of euphausiid aggregations in the Northern California Current during August 2000. Deep-Sea Res. II, **52**: 89–108.

Sakuma, K.M., and Ralston, S. 1997. Vertical and horizontal distribution of juvenile Pacific whiting (*Merluccius productus*) in relation to hydrography off California. CalCOFI Rep. **38**: 137–146.

Sanchez, F., and Gil, J. 2000. Hydrographic mesoscale structures and poleward current as a determinant of hake (*Merluccius merluccius*) recruitment in southern Bay of Biscay. ICES J. Mar. Sci. **57**: 152–170.

Saunders, M.W., and McFarlane, G.A. 1997. Observations on the spawning distribution and biology of offshore Pacific hake. CalCOFI Rep. **38**: 147–157.

Simard, Y., and Mackas, D.L. 1989. Mesoscale aggregations of euphausiids sound scattering layers on the continental shelf off Vancouver Island. Can. J. Fish. Aquat. Sci. **46**: 1238–1249.

Smith, B.D., McFarlane, G.A., and Saunders, M.W. 1990. Variation in Pacific hake (*Merluccius productus*) summer length-at-age near southern Vancouver Island and its relationship to fishing and oceanography. Can. J. Fish. Aquat. Sci. **47**: 2195–2211.

Strub, P.T., James, C., Thomas, A.C., and Abbott, M.R. 1990. Seasonal and nonseasonal variability of satellite-derived surface pigment concentration in the California Current. J. Geophys. Res. **92**: 1501–1530.

Swartzman, G. 2001. Spatial patterns of Pacific hake (*Merluccius productus*) shoals and euphausiid patches in the California Current ecosystem. *In* Spatial processes and management of marine populations. Alaska Sea Grant College Program, AK-SG-01-02. pp. 495–511.

Swartzman, G., and Hickey, B. 2003. Evidence for a regime shift after the 1997–1998 El Niño, based on 1995, 1998, and 2001 acoustic surveys in the Pacific Eastern Boundary Current. Estuaries, **26**: 1032–1043.

Swartzman, G.L., Getz, W.M., and Francis, R.C. 1987. Binational management of Pacific hake (*Merluccius productus*): a stochastic modeling approach. Can. J. Fish. Aquat. Sci. **44**: 1053–1063.

Swartzman, G., Hickey, B., Kosro, P.M., and Wilson, C. 2005. Poleward and equatorward currents in the Pacific Eastern Boundary Current in summer 1995 and 1998 and their relationship to the distribution of euphausiids. Deep-Sea Res. II, **52**: 73–88.

Tabata, S. 1975. The general circulation of the Pacific Ocean and a brief account of the oceanographic structure of the North Pacific Ocean. Atmosphere, **13**: 133–168.

Ware, D.M., and McFarlane, G.A. 1989. Fisheries production domains in the Northeast Pacific Ocean. *In* Effects of ocean variability on recruitment and an evaluation of parameters used in stock assessment models. *Edited by* R.J. Beamish and G.A. McFarlane. Can. Spec. Publ. Fish. Aquat. Sci. No. 108. pp. 359–379.

Ware, D.M., and McFarlane, G.A. 1995. Climate-induced changes in Pacific hake (*Merluccius productus*) abundance and pelagic community interactions in the Vancouver Island Upwelling System. *In* Climate change and northern fish populations. *Edited by* R.J. Beamish. Can. Spec. Publ. Fish. Aquat. Sci. No. 121. pp. 509–521.

Wilson, C.D., and Guttormsen, M.A. 1997. Echo integration trawl survey of Pacific hake, *Merluccius productus*, off the Pacific coast of the United States and Canada during July–August 1998. NOAA Tech. Memo. NMFS AFSC-74, Seattle Wash.

Wilson, C.D., and Guttormsen, M.A. 1998. Echo integration trawl survey of Pacific hake, *Merluccius productus*, off the Pacific coast of the United States and Canada. Preliminary cruise results. National Marine Fisheries Service, AFSC, Seattle, Wash. F/AKC2:Sd.

Wilson, C.D., Guttormsen, M.A., Cooke, K., Saunders, M.W., and Kieser, R. 2000. Echo integration trawl survey of Pacific hake, *Merluccius productus*, off the Pacific Coast of the United States and Canada during July–August 1998. NOAA Technical Memo. NMFS-AFSC-118.

The genetic structure of Atlantic cod (*Gadus morhua*) around Iceland: insight from microsatellites, the *Pan* I locus, and tagging experiments

Christophe Pampoulie, Daniel E. Ruzzante, Valérie Chosson, Thóra Dögg Jörundsdóttir, Lorna Taylor, Vilhjálmur Thorsteinsson, Anna Kristín Daníelsdóttir, and Guðrún Marteinsdóttir

Abstract: Allelic variation at nine microsatellite loci and the *Pan* I locus provides evidence that Atlantic cod (*Gadus morhua*) around Iceland is genetically structured (F_{ST} = 0.003 and F_{ST} = 0.261, respectively). A total of 2534 cod were sampled at 22 spawning locations. For both types of markers, most of the significant pairwise F_{ST} resulted from northeastern–southwestern comparisons. A multidimensional scaling analysis based on F_{ST}, a spatial hierarchical analysis of molecular variance (SAMOVA) and a hierarchical analysis of molecular variance (AMOVA), conducted on both types of markers confirmed a genetic differentiation between cod from the northeastern and southwestern regions. Genetic discontinuities were revealed across two main current fronts in the southeast and northwest, where the cold and warm water masses meet. The AMOVA also detected genetic differences with depth. Expected and observed heterozygosity of microsatellite loci significantly decreased with depth, whereas the B allele frequency at the *Pan* I locus increased. A tagging experiment of spawning fish conducted during the same years as the genetic work revealed that tagged individuals released in the southwestern region seldom migrated to the northeastern region and vice versa, suggesting that the southwestern and northeastern populations of Atlantic cod around Iceland represent two distinct spawning components.

Résumé : La variation allélique de neuf microsatellites et du locus *Pan* I met en évidence une structure génétique chez la morue Atlantique (*Gadus morhua*) dans les eaux islandaises (F_{ST} respectifs, F_{ST} = 0,003 et F_{ST} = 0,261). Un total de 2534 morues a été échantillonné sur 22 sites de ponte. Pour les deux marqueurs génétiques utilisés, la majorité des valeurs significatives de F_{ST} par paires de populations est due à des comparaisons nord-est et sud-ouest. Une analyse multidimensionnelle basée sur les F_{ST} par paires de populations, une analyse spatiale hiérarchique de variance moléculaire (SAMOVA) et une analyse hiérarchique de variance moléculaire (AMOVA), réalisées sur les deux types de marqueurs génétiques, révèlent une différenciation significative entre les échantillons du nord-est et du sud-ouest. La recherche de discontinuités génétiques indique la présence de deux barrières au flux génique correspondant aux principaux fronts de courants océaniques localisés dans le nord-ouest et le sud-est du pays aux points où les masses d'eaux chaudes et froides entrent en contact. L'analyse AMOVA détecte aussi des différences génétiques en fonction de la profondeur. Une analyse approfondie montre que les hétérozygoties observées et attendues des microsatellites diminuent significativement avec la profondeur, alors que la fréquence de l'allèle B du locus *Pan* I augmente. Une expérience de « capture–recapture » réalisée sur les sites de pontes en même temps que les études génétiques révèle que des individus marqués et relâchés dans la région du sud-ouest migrent rarement vers la région du nord-est et vice versa, ce qui confirme que les populations du sud-ouest et du nord-est de morues Atlantique dans les eaux islandaises représentent probablement deux unités de reproduction distinctes.

Received 12 February 2006. Accepted 9 October 2006. Published on the NRC Research Press Web site at http://cjfas.nrc.ca on 28 November 2006.
J19170

C. Pampoulie,[1] **V. Chosson, T.D. Jörundsdóttir, L. Taylor, V. Thorsteinsson, and A.K. Daníelsdóttir.** Marine Research Institute, Skúlagata 4, 101 Reykjavík, Iceland.
D.E. Ruzzante. Department of Biology, Dalhousie University, Halifax, NS B3H 4J1, Canada.
G. Marteinsdóttir. Department of Biology, University of Iceland, Sturlugata 7, 101 Reykjavík, Iceland.

[1] Corresponding author (e-mail: chrisp@hafro.is).

Can. J. Fish. Aquat. Sci. 63: 2660–2674 (2006)   doi:10.1139/F06-150

Introduction

Marine fisheries are often managed under the assumption of panmixia without consideration of often suspected or known life history or genetic differences among components of a stock or population complex. In this respect, fishery management is primarily area-based and conducted under the assumption that neglecting the existence of life history or genetic differences among population components is not likely to have detrimental effects on population persistence and stock structure. Failure to recognize the link between management and stock structure can, however, have detrimental effects on genetic and, thus, stock diversity by disproportionately affecting the smaller or less productive population components (Begg et al. 1999; Ward 2000; Swain et al. 2001). In turn, proper management of exploited fish requires full knowledge of stock affiliation across the distribution of the targeted species. Information on stock structure of commercially exploited fish stocks is thus of paramount importance and the ability to discriminate among units that differ in life histories and (or) genetic composition, some of which may migrate seasonally and may at times overlap spatially, is a challenge for conservation biologists, population geneticists, and fishery biologists alike (Ruzzante et al. 2006).

Atlantic cod (*Gadus morhua*) has historically been one of the most valuable commercial fish species inhabiting the continental shelves of the western, central, and eastern North Atlantic. During the last century, however, cod stocks declined dramatically in some regions owing to drastic overexploitation (see Christensen et al. (2003) for a review). The depletion and collapse of cod stocks, as well as other commercial marine fishes, has now been widely interpreted as an example of the failure of sustainable fisheries management (Myers et al. 1996; Cook et al. 1997). It has often been suggested that this failure results in part from the fact that management units do not necessarily reflect biological units as such (Stephenson and Kenchington 2000). Indeed, recent genetic studies using different types of markers have demonstrated the existence of often subtle but biologically meaningful genetic differences among population components within management regions (Ruzzante et al. 1996; Knutsen et al. 2003; Sarvas and Fevolden 2005). Oceanic currents, oceanic topology (inshore and offshore), and geographical distances were shown to be the main factors restricting passive or active exchange of migrants among these subunits. These studies indicate that genetic markers combined with ecological and life history information, as well as with environmental data (e.g., topography, current patterns, salinity, and (or) temperature), are likely to lead to improved insight on the stock composition of exploited marine fishes.

Atlantic cod off Iceland (also referred to as Icelandic cod), though historically exposed to high exploitation rates, has remained relatively stable and is one of only two or three stocks not rated outside safe biological limits by ICES (International Council for the Exploration of the Sea) (Christensen et al. 2003; Marteinsdóttir et al. 2005). Although assessed as a unique stock for management expediency, Icelandic cod have recently been suggested to comprise a multitude of spawning units distributed on offshore and inshore locations around the country, with a major spawning component in an area off the southwestern coast (Fig. 1, area 9) (Marteinsdóttir et al. 2000*a*, 2000*b*; Begg and Marteinsdóttir 2002*a*). The spawning season lasts from mid-March to May, with older individuals spawning earlier and over a longer period than the younger and smaller cod (Marteinsdóttir and Björnsson 1999). Pelagic eggs and larvae drift from the main spawning ground off the southwestern coast with the coastal and offshore currents to the main nursery ground off the northern coast (Begg and Marteinsdóttir 2000, 2002*b*; Marteinsdóttir et al. 2000*a*). After the breeding season, individual cod tend to migrate to the main feeding regions located off the northwestern and northeastern coasts of Iceland (Jónsson 1996), but results from a recent tagging study on the main spawning ground suggest that some individuals stay in relatively shallow, warm waters in regions off the southern coast (Pálsson and Thorsteinsson 2003).

Tag recapture data from studies in the Northwest Atlantic (Taggart et al. 1995; Robichaud and Rose 2004) together with direct observations provide evidence that cod can, and probably most do, exhibit spawning site fidelity potentially promoting genetic divergence among different spawning components. Icelandic cod have also been shown to display high fidelity to local spawning regions (Thorsteinsson and Marteinsdóttir 1992, 1993). Furthermore, as juvenile cod appear to be stationary during the first 2–3 years of their life (Sæmundsson 2005), the majority of dispersal is likely to happen before the juvenile years. Thus oceanic currents promoting dispersal of eggs and larvae are probably the main factors influencing dispersal of young cod around Iceland.

Considerable information exists on the oceanography around Iceland. The region is influenced by the southward flow of cold, low-saline Arctic waters from the north (East Greenland and East Iceland currents; <0 to 2 °C) and the northward flow of warm, saline waters of the North Atlantic Current from the south (6 to 8 °C; Valdimarsson and Malmberg 1999). A branch of the North Atlantic Current, the Irminger Current, flows along the southern and western coasts of Iceland. To the west and northwest of the country, in the Denmark Strait, the Irminger Current meets the East Greenland Current; it then bifurcates, with the main branch turning west towards Greenland and a small branch continuing northwards and flowing into the North Icelandic shelf area as the North Icelandic Irminger Current. Closer to shore is the coastal current, which originates along the southeastern coast of the island and flows in a clockwise direction around it. East of the country, oceanographic conditions are shaped by the southward-flowing Arctic waters of the East Iceland Current and the frontal zone in the area southeast of the country, on the Iceland–Faroe ridge, where the East Iceland Current meets the warm Atlantic waters flowing into the areas from the south and west (Valdimarsson and Malmberg 1999). Therefore, the oceanographic conditions around Iceland are shaped by the two frontal zones located west–northwest and east–southeast of the country where the cold and warm water masses meet. The precise location of these frontal zones naturally varies between years, as well as over longer periods, resulting in large variation in hydrographical conditions (Malmberg et al. 1996).

Fig. 1. Geographical regions, main oceanic currents (modified from Gunnarsson et al. 1998), and sampling locations of Atlantic cod (*Gadus morhua*) around Iceland. Samples were collected in 2002 (●), 2003 (▲), and 2004 (■). Shaded arrows, East Greenland Current; broken shaded arrows, East Icelandic Current; black arrows, warm North Atlantic Current. The geographical areas are delimited by lines; the names of the areas are indicated by numbers. The map at the top illustrates the region from a broader geographical perspective.

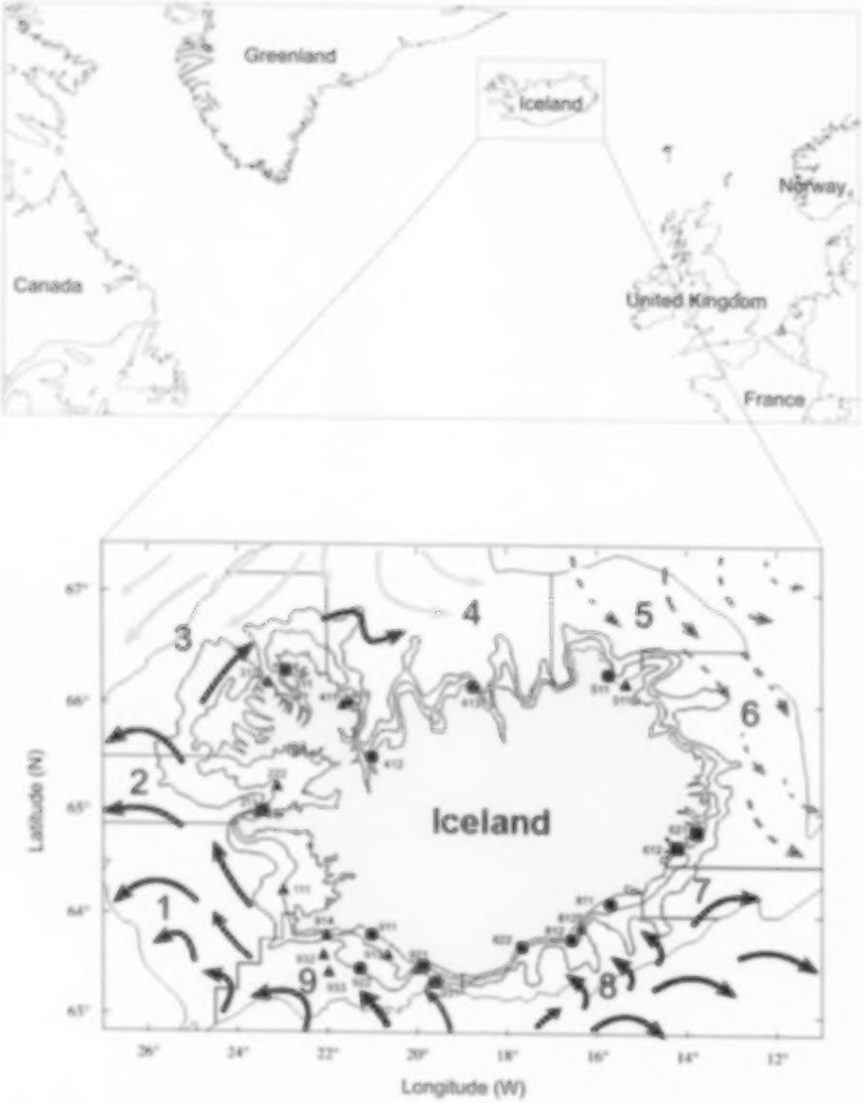

The strength and direction of the Irminger Current, as well as the coastal current, have been shown to influence the transport of cod offspring from the southern spawning grounds onto the northern nursery grounds (Begg and Marteinsdóttir 2002*a*). Little information exists on the potential influence of the oceanographic conditions on dispersal and migration of juvenile and adult cod. Tagging results by Jónsson (1996) have been used to support the general notion that postspawning cod display feeding migrations into the northwestern and northern regions. Re-examination of Jónsson's (1996) results indicate, however, that the majority of tag returns come from the large feeding areas in waters west of the country (located in the vicinity of the frontal zone), whereas few returns come from the more northern regions (Jónsdóttir et al. 2006). Similarly, few cod tagged in the northern region were recaptured in the vicinity of the southern spawning areas (Jónsson 1996; Jónsdóttir et al. 2006).

In this paper, we describe for the first time the genetic structure of Atlantic cod around Iceland. We examine the genetic composition (nine microsatellite DNA loci and the *Pan* I locus) among more than 2500 adult cod collected in spawning condition over a period of two years (2002 and 2003) from 22 spawning locations around the country. Our first objective was to test the null hypothesis that spawning cod around Iceland exhibit no stable genetic differences. This hypothesis was rejected as we describe genetic differences among two major spawning aggregations, one southwest and the other northeast of Iceland. We then examined the influence of geographic, oceanographic, and depth features as potential barriers to gene flow. Lastly, we interpreted our results in light of contemporary tagging experiments conducted on spawning cod.

Materials and methods

Sampling

A total of 2534 individual cod were collected from 22 spawning locations around Iceland during the spring of 2002 and 2003 (Table 1, locations 612 and 621 sampled in 2004). Six of these locations (211, 311, 511, 812, 921, 931; see Fig. 1) were sampled in 2002 and again in 2003 to assess temporal stability; thus in total there were 28 samples. Temporal replicates 311b and 511b (Fig. 1) were collected from different locations in the same fjords within a few kilometres of the corresponding 311 and 511 samples (Fig. 1). Total length (TL, mm) and eviscerated carcass wet weight (*W*, mg) of each individual were recorded, and otoliths (sagittae) were collected for age determination. Temperature data were collected based on a data storage tags (DST) attached to the gillnets that we used to sample spawning cod at each location in 2003 (average temperature during 24 h). Temperature data at the eastern location were based on measurements performed during the sampling.

The nine spawning regions around Iceland were classified (Fig. 1), and our samples were identified with a three-digit number, the first digit indicating spawning region (1–9), the second indicating depth (1, 0–75 m; 2, 75–125 m; 3, ≥125 m), and the third indicating the sampling station (see locations in Fig. 1).

DNA methods

Gill filaments or fin clips were preserved in 1 mL of 96% ethanol, and DNA was extracted using a Chelex (Bio-Rad 10%; Bio-Rad Laboratories, Hercules, California) extraction protocol (Walsh et al. 1991). Samples were genotyped at nine polymorphic microsatellite loci: Gmo2 (Brooker et al. 1994), Gmo8, Gmo19, Gmo34, and Gmo37 (Miller et al. 2000), and Tch5, Tch11, Tch14, and Tch22 (O'Reilly et al. 2000). Polymerase chain reactions (PCR) were performed in a 10 μL volume containing 2 μL of DNA product, 1 μL of 10× buffer (10 $\text{mmol}\cdot\text{L}^{-1}$ Tris–HCl, 50 $\text{mmol}\cdot\text{L}^{-1}$ KCl, 1.5 $\text{mmol}\cdot\text{L}^{-1}$ $MgCl_2$ and 0.1% Triton X-100), 1 μL of 2.5 $\text{mmol}\cdot\text{L}^{-1}$ DNTP, 0.2–0.4 units of DyNAzyme™ DNA polymerase (Finnzymes Oy, Espoo, Finland), and various concentrations of primers. PCR cycles were performed on a multiplex basis in a GeneAmp®2700 thermal block and preceded by an initial denaturation step of 4 min at 94 °C followed by 32 cycles of 40 s at 94 °C, 40 s at annealing temperature (Tch11, Gmo19, Gmo34 at 52 °C; Gmo2 at 50 °C; Tch14 at 56 °C; Gmo8 at 50 °C; Gmo37 at 50 °C; Tch5 at 50 °C; Tch22 at 49 °C), and 40 s at 72 °C. A final elongation step of 4 min at 72 °C was included. PCR products were diluted with sterile distilled water (1:3) and were electrophoresed on 36 cm 6% polyacrylamide gels and detected on an automatic sequencer (ABI 377; Applied Biosystems, Foster City, California) using the software GeneScan (version 3.1.2; Applied Biosystems 2000). Products were scored using the software GeneMapper (version 3.7; Applied Biosystems 2004).

Samples were also genotyped at the pantophysin locus (*Pan* I). PCR were performed in a 15 μL volume containing 2 μL of DNA product, 1.7 μL of 10× buffer (10 $\text{mmol}\cdot\text{L}^{-1}$ Tris–HCl, 50 $\text{mmol}\cdot\text{L}^{-1}$ KCl, 1.5 $\text{mmol}\cdot\text{L}^{-1}$ $MgCl_2$ and 0.1% Triton X-100), 0.5 μL of 50 $\text{mmol}\cdot\text{L}^{-1}$ $MgCl_2$, 1.7 μL of 2.5 $\text{mmol}\cdot\text{L}^{-1}$ DNTP, 1 unit of DyNAzyme™ DNA polymerase (Finnzymes), and 10 $\text{mmol}\cdot\text{L}^{-1}$ of primers (F: TTGGTCCTCTATCTGGGCTTC; R: CGTAGCAGAAGAGTGACACAT). PCR cycles were performed in a GeneAmp®2700 thermal block and preceded by an initial denaturation step of 5 min at 95 °C followed by 30 cycles of 1 min at 94 °C, 1 min at 55 °C, and 1 min at 72 °C. A final elongation step of 7 min at 72 °C was performed. PCR products were then cut with *Dra*I restriction enzyme (Fermentas, Hanover, Maryland) using 15 μL of PCR products and 5 μL of *Dra*I mix containing 18 units of enzyme and 2 μL of B+ buffer per samples. Digested PCR products were visualized in 2% agarose gel stained with ethidium bromide using GELDOC™ 2000 reader (Bio-Rad Laboratories).

Tagging experiments

In April 2002 and 2003, 6536 cod (3624 and 2912 in 2002 and 2003, respectively) were tagged on spawning grounds during peak spawning time at 10 locations around Iceland in 2002 and 12 in 2003 distributed among all nine regions depicted in Fig. 1. Of all individuals tagged in 2002, 159 were recaptured in the spawning seasons (March to May) of 2003 and 2004, and of all individuals tagged in 2003, 81 were recaptured in the 2004 spawning season. For both tagging years, individuals were recaptured from all nine tagging locations in subsequent spawning seasons. These recaptures included only those with sufficient information on position of recapture. Recaptures were assessed by tagging location, with the number of returns by region tabulated. As catch rates differed among locations, the number of recaptures was scaled by the catch in the recapture region using data from fishermen's logbooks and landings to estimate total catch per region, year, and corresponding time period.

Statistical methods

Genetic data

Allele frequencies and observed (H_O) and unbiased expected (H_E) heterozygosity were calculated in GENETIX (version 4.03; Belkhir et al. 1999). Tests of Hardy–Weinberg equilibrium (HWE) were performed using GENEPOP (version 3.1; Raymond and Rousset 1995) using exact tests.

Geographical genetics

Wright's single-locus *F* statistics (Wright 1969) were calculated from allele frequencies at all loci examined for each population according to Weir and Cockerham's (1984) method using GENETIX. Significance of F_{ST} estimates was assessed with exact tests implemented in GENEPOP (multilocus and pairwise estimates). When appropriate, significance levels were adjusted with a sequential Bonferroni test (Rice 1989). To accurately compare the level of genetic di-

Table 1. Sample codes, year of sampling, depth (m), mean total length (TL, cm), mean age (years), percentage of spawning individuals (Spawning), sex ratio (SR, ratio of the number of females to males), number of individuals scored (n), observed heterozygosity (H_O), expected heterozygosity (H_E), and mean number of alleles ($\bar{n}_A$) from 28 samples of cod from the Icelandic waters.

							Microsatellite loci				*Pan* I locus		
Name	Year	Depth (m)	TL (cm)	Age (years)	Spawning (%)	SR	n	H_O	H_E	$\bar{n}_A$	n	H_O	H_E
111	2003	78	86.69	6.64	100.00	0.88	94	**0.8026**	0.8147	19.44	89	0.5169	0.4984
211	2002	64	90.79	7.77	100.00	0.92	94	0.8189	0.8149	18.56	87	0.4368	0.4888
211b	2003	48	78.25	6.25	100.00	1.35	94	0.7931	0.8104	18.44	89	0.4382	0.4270
222	2003	73	79.31	6.38	98.94	0.88	94	0.8381	0.8278	19.33	89	0.5618	0.4820
311	2002	19	70.18	6.84	100.00	0.96	94	0.8227	0.8402	19.56	90	0.4000	0.3310
311b	2003	41	70.76	6.81	95.74	1.35	94	0.8582	0.8455	18.44	91	0.4286	0.4303
411	2003	28	79.42	6.70	98.94	0.74	94	0.8499	0.8403	18.44	87	0.3218	0.3890
412	2002	60	64.64	7.11	92.55	0.54	94	0.8150	0.8358	19.11	93	0.1720	0.1572
413	2002	18	66.43	6.08	82.98	0.54	100	0.8133	0.8356	18.22	97	0.2268	0.2470
414	2003	30	83.47	8.56	100.00	0.88	94	0.8286	0.8251	17.33	94	0.2553	0.2825
511	2002	12	71.05	6.40	90.43	0.92	94	0.8168	0.8323	18.89	90	0.3222	0.3636
511b	2003	16	79.55	8.06	77.00	1.32	94	0.8197	0.8304	18.22	87	0.5172	0.4046
612	2004	50	65.19	—	100.00	1.16	84	0.8343	0.8343	18.00	84	0.0182	0.0180
621	2004	57	70.53	—	100.00	2.34	77	0.8307	0.8526	18.44	77	0.3000	0.2550
811	2002	50	93.89	7.87	98.94	0.47	94	**0.8251**	0.8351	19.11	85	0.5059	0.4200
812	2002	65	101.77	8.52	98.94	1.13	94	0.7754	0.8115	18.78	82	0.4634	0.4997
812b	2003	83	98.27	8.69	96.80	1.09	94	0.7835	0.8455	18.44	92	0.5652	0.4355
822	2002	80	101.14	8.82	97.87	1.09	94	0.7778	0.8135	18.78	88	0.5682	0.4907
911	2002	54	85.88	6.18	98.94	0.77	78	0.8561	0.8450	18.55	76	0.1486	0.1822
912	2003	61	97.31	7.95	81.00	0.57	58	0.8123	0.8044	16.33	59	0.4483	0.4976
914	2003	72	77.23	6.61	97.70	1.02	90	0.8136	0.8196	18.22	88	0.5682	0.3129
921	2002	92	100.46	8.39	100.00	1.02	94	0.8100	0.8076	19.11	77	0.4545	0.4946
921b	2003	88	93.73	8.11	100.00	1.14	94	0.7939	0.8080	17.89	93	0.5054	0.4917
922	2002	92	95.48	7.37	100.00	0.42	94	0.7754	0.8132	18.33	78	0.4744	0.4861
931	2002	200	84.45	7.12	84.00	1.04	94	0.7719	0.7934	19.33	85	0.3412	0.3129
931b	2003	454	78.73	6.73	93.62	0.88	94	0.7352	0.7791	18.56	91	0.2308	0.2041
932	2003	131	77.53	6.32	97.78	0.14	94	0.7766	0.7918	17.44	84	0.3452	0.2856
933	2003	152	77.87	6.24	86.17	0.38	73	0.7884	0.8038	17.68	73	0.3699	0.3015

Note: Bold values: F_{IS} values deviating from Hardy–Weinberg expectation (HWE) after corrections for multiple test (P = 0.000 198).

vergence detected with highly polymorphic microsatellite loci and the bi-allelic *Pan* I locus, a new standardized genetic differentiation measure was used. This new measure is expected to allow comparisons between loci with different level of genetic variation (G'_{ST}; Hedrick 2005). G'_{ST} represents the proportion of the maximum differentiation possible for the level of subpopulation homozygosity observed and is defined as

$$G'_{ST} = \frac{G_{ST}(1 + H_S)}{(1 - H_S)}$$

Pairwise comparisons of temporal samples were carried out using the software Chifish (Ryman 2006), which tests the hypothesis of no difference at any locus by both chi-square and Fisher's method of combining P values obtained by Fisher's exact test (Ryman 2006). This approach has been shown to give better estimation of genetic differentiation than the Fisher's exact test, especially when comparing two populations scored for few loci (Ryman 2006).

We carried out a multidimensional scaling (MDS) approach on the pairwise F_{ST} values for both microsatellite loci and the *Pan* I locus using Statistica 6.0 (StatSoft Inc. 2001). Analysis of genetic linkage disequilibrium between locus pairs was estimated according to Cockerham and Weir (1979) and tested on contingency tables under the null hypothesis of independence.

To estimate the number of genetically distinguishable populations, we used the spatial (geographical) analysis of molecular variance (SAMOVA; Dupanloup et al. 2002) on the microsatellite loci. The SAMOVA method employs a simulated procedure and uses allele frequency data along with geographical coordinates of the sampled populations for identifying groups of populations that exhibit close genetic relationships. The grouping of populations is based on conducting a hierarchical analysis of ρ_{ST} (genetic variation within samples) and maximising the proportion of total genetic variance among groups (ρ_{CT}). We conducted the analysis for two to 15 populations.

We additionally assessed potential barriers to current gene flow events with the software BARRIER (version 2.2; Manni et al. 2004) using the Monmonier's maximum distance algorithm. BARRIER has recently been used to highlight geographical areas with current pronounced genetic discontinuity (Bekkevold et al. 2005; Jørgensen et al. 2005). Basically, geographical coordinates are supplied for each sampling location and connected by Delaunay triangulation associated with genetic distances such as F_{ST}. The algorithm will assess the edge with the largest associated distance in the triangulation network as its starting edge and then extends the barriers across the directly adjacent edge associated with the largest genetic distance. Additional sections are added to the barrier until it reaches the outer edge of the network or meets another barrier (see Manni et al. (2004) for additional information). We conducted the analysis using the F_{ST} values for each of the nine microsatellite loci separately and the overall values based on all microsatellites to ensure that barriers would not be identified by strong differentiation to one or few loci. The number of barriers is set up by the user, and based on the number of loci supporting each barrier, we found that only two barriers were strongly supported by the data (see Results).

Because geographical coordinates between samples might not reflect connection on such a small geographical scale, an analysis of molecular variance (AMOVA) was carried out in ARLEQUIN (version 2.0; Schneider et al. 2000) to assess the hierarchical partitioning of genetic variability among post-hoc defined regions using the observed structure in the MDS analysis for both types of genetic markers (divergence among northeastern and southwestern regions).

Depth pattern

An AMOVA was also used to assess the hierarchical partitioning of genetic variability among post-hoc defined regions using the observed structure in the MDS analysis (divergence among shallow, intermediate, and deep water) for both types of genetic markers.

In addition, we examined whether the effect of depth on genetic diversity as measured by heterozygosity and number and frequency of alleles differed between the genetic markers.

To ensure that the observed genetic divergence between northeastern and southwestern samples was not due to the presence of deep-water samples only available for area 9, we calculated the overall genetic divergence with and without the deep and intermediate depth samples (only shallow water samples). A hierarchical partitioning of genetic variability among post-hoc defined regions (divergence among northeastern and southwestern regions) using only the shallow water samples was also carried out.

Results

Sampled cod

Most of the cod sampled were identified as spawning, i.e., females containing hydrated oocytes in their ovaries and males having running sperm (Table 1).

Genetic variability

All studied microsatellite loci were highly polymorphic. The number of alleles per locus across all samples ranged from 11 (Gmo34) to 52 (Gmo8). Per-sample H_O averaged over all loci ranged from 0.7352 to 0.8582, whereas the per-sample H_E ranged from 0.7791 to 0.8526 (Table 1). Genotypic proportions were out of HWE in only five out of 232 exact tests after Bonferroni correction for multiple tests and were not due to any specific loci or samples. This is less than expected by chance alone. All samples but two (111, 811) exhibited an overall HWE (Table 1). Exact test for linkage disequilibrium did not yield significant values.

H_O per sample at the *Pan* I locus ranged from 0.0182 to 0.5682, whereas H_E ranged from 0.0180 to 0.4997 (Table 1). There was no evidence for departure from HWE for any of the samples (Table 1).

Geographical genetics

The partitioning of genetic variance based on microsatellite loci among and within the 28 samples as estimated by F statistics showed a mean significant F_{ST} value of 0.003 and an F_{IS} of 0.017. After Bonferroni correction (P = 0.000132), pairwise differentiation between populations

Fig. 2. Multidimensional scaling analysis (MDS) on 22 spawning areas of Atlantic cod (*Gadus morhua*) based on F_{ST} values computed for (*a*) nine microsatellite loci and (*b*) the *Pan* I locus. Southwestern samples are encircled.

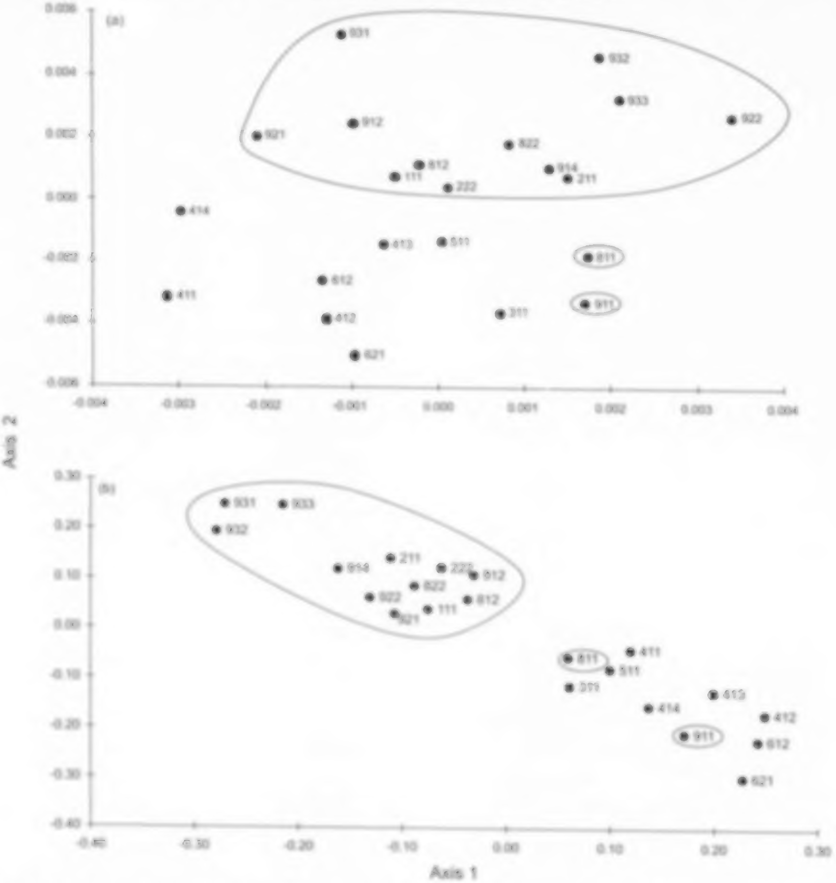

yielded 114 significant comparisons out of 378, among which 36 were due to the samples 931 and 931b (data not shown). Out of those 114 significant pairwise comparisons, 62 were observed between samples from the northeast (regions 3, 4, and 5) and southwest of Iceland (regions 8 and 9). A pairwise comparison of the temporal samples, conducted with Chifish (Ryman 2006), showed that temporal samples (2002 and 2003) from the same spawning location were genetically indistinguishable (211, $F_{ST} = 0.0002$, $P = 0.3973$; 311, $F_{ST} = 0.0038$, $P = 0.0501$; 511, $F_{ST} = 0.0017$, $P = 0.0899$; 812, $F_{ST} = -0.0004$, $P = 0.3664$; 921 $F_{ST} = 0.0070$, $P = 0.0967$; 931 $F_{ST} = 0.0019$, $P = 0.0614$). Additionally, overall within-year spatial genetic divergence was similar in the two years (2002, $F_{ST} = 0.0038$; 2003, $F_{ST} = 0.0029$). Therefore, for further analysis, temporal samples from the same location were clustered into one single group for each location (22 spawning locations).

Based on pairwise F_{ST} values, MDS clearly clustered samples from the northeastern region separate from those from the southwestern region (Fig. 2*a*; stress values on axes 1 and 2, 0.1411). Only two samples from the southwestern region clustered with the northeastern region samples, namely 811 and 911. SAMOVA revealed that genetic differentiation among groups was highest ($\varphi_{CT} = 0.00354$) when samples were pooled into two groups, one comprising the samples from the northeast, and the second, those from the southwest of Iceland (Table 2). Samples 811 and 911, collected from the southwestern region, clustered in the northeastern region, thus confirming the results observed with the MDS analysis. A subsequent AMOVA based on these two sample pools confirmed that among-group differentiation was significant between samples collected from northeastern and southwestern regions (Table 3).

To complement this analysis and detect whether a potential genetic discontinuity (a boundary reflecting relatively low gene flow) could be detected between northeastern and southwestern samples, we carried out an analysis using the software BARRIER. Two relevant genetic discontinuities (barriers to gene flow) were identified and these were located between the northeastern and southwestern samples. The northwestern barrier was supported by four out of nine loci used, whereas the southeastern barrier was supported by five out of nine loci used (Fig. 3). Further genetic discontinuities were detected between samples from different depths collected from area 9 (data not shown). These barriers were supported by four (areas 91 and 92) to six loci (areas 92 and 93). Further barriers identified were supported by only one to three loci and were thus not considered.

Table 2. Results of the spatial analysis of molecular variance (SAMOVA) analyses carried out on microsatellite loci (Dupanloup et al. 2002).

No. of groups	Group composition	ρ_{CT}	ρ_{SC}
2	(111, 211, 222, 812, 822, 912, 914, 921, 922, 931, 932, 933) (311, 411, 412, 413, 414, 511, 612, 621, 811, 911)	0.00354***	0.00132***
3	(931) (912, 932, 933) (other populations)	0.00304***	0.00187***
4	(411) (931) (922, 932, 933) (other populations)	0.00338***	0.00174***
5	(411) (414) (911) (311, 412, 413, 511, 612, 621, 811) (111, 211, 222, 812, 822, 912, 914, 921, 922, 931, 932, 933)	0.00319***	0.00114***
6	(411) (414) (911) (931) (311, 412, 413, 511, 612, 621, 811) (111, 211, 222, 812, 822, 912, 914, 921, 922, 932, 933)	0.00322***	0.00087***
7	(411, 414) (911) (922) (931) (932, 933) (311, 412, 511, 612, 621) (other populations)	0.00300***	0.00083***
10	(311, 411, 511, 612) (412) (413) (414) (621, 811) (911) (912) (111, 211, 222, 413, 812, 822, 914, 921) (922) (931) (932, 933)	0.00300***	0.00063***
15	(111, 211, 222) (311) (411) (413) (414) (511, 612) (811) (931) (921) (922) (911) (411, 914) (812, 822) (932, 933) (912, 914) (412, 621)	0.00328***	0.00013***

Note: The analysis was carried out considering 22 spawning locations. Significance was assessed by 1000 permutation: ***, $P < 0.001$. Groups are presented between parentheses. ρ_{CT} and ρ_{SC} are the genetic variation among groups and among samples within groups, respectively.

Table 3. Hierarchical analysis of molecular variance (AMOVA) among samples of *Gadus morhua* clustered into two groups (depth (shallow, intermediate, and deep waters) and region (northern vs southern components)) for the microsatellite and *Pan* I locus.

Loci	Source of variation	df	Variance components	Variation (%)	Fixation indices	*p* values
Shallow, intermediate, and deep waters						
Pan I	Among groups	2	0.05	17.36	CT = 0.1736	<0.0001
	Among samples within groups	19	0.04	14.66	SC = 0.1774	<0.0001
	Within samples	4766	0.18	67.98	ST = 0.3202	<0.0019
	Total	4787	0.27	100		
Microsatellites	Among groups	2	0.0064	0.17	CT = 0.0017	<0.01
	Among samples within groups	19	0.0086	0.23	SC = 0.0023	<0.0001
	Within samples	5044	3.7158	99.60	ST = 0.0040	<0.0001
	Total	5065	3.7308	100		
Northern vs southern components						
Pan I	Among groups	1	0.08	28.29	CT = 0.2829	<0.0001
	Among samples within groups	20	0.02	8.43	SC = 0.1176	<0.0001
	Within samples	4766	0.18	63.28	ST = 0.3672	<0.0001
	Total	4787	0.28	100		
Microsatellites	Among groups	1	0.010	0.27	CT = 0.0027	<0.0001
	Among samples within groups	20	0.0071	0.19	SC = 0.0019	<0.0001
	Within samples	5044	3.7158	99.54	ST = 0.0046	<0.0001
	Total	5065	3.7331	100		

A comparison of the level of genetic diversity among northeastern and southwestern components using the software FSTAT (Goudet 1995) revealed significant differences at the level of expected and observed heterozygosity (northeastern component, $H_O = 0.825$, $H_E = 0.841$; southwestern component, $H_O = 0.793$, $H_E = 0.813$; $P = 0.009$ and 0.0004, respectively) but not at the level of allelic richness (northeastern component, 16.865; southwestern component, 16.874; $P = 0.965$).

The partitioning of the *Pan* I locus genetic variance among and within the 28 samples as estimated by F statistics showed a mean significant F_{ST} value of 0.261 and an F_{IS} of −0.042. The standardized genetic differentiation measured as G'_{ST} ($G'_{ST} = 0.568$) was tenfold higher than the value observed for microsatellite loci ($G'_{ST} = 0.032$). After Bonferroni correction, pairwise differentiation between populations yielded 261 significant comparisons out of 378, among which 123 were observed between samples from the northeast (areas 3, 4, and 5) and southwest (regions 8 and 9) and 70 of these involved samples from area 9 (sample 931b, 26 comparisons; 931, 23; 911, 21, data not shown). Using χ^2 tests, allele frequencies were significantly different among population samples ($\chi^2_{[23]} = 690.80$, $P = 0.0001$). A pairwise comparison of the temporal samples, conducted with the software Chifish, showed that temporal samples (2002 and 2003) from the same spawning location were genetically indistinguishable (211, $F_{ST} = 0.0104$, $P = 0.0954$; 311, $F_{ST} = 0.0187$, $P = 0.0537$; 511, $F_{ST} = -0.0005$, $P = 0.3596$; 812, $F_{ST} = 0.0033$, $P = 0.2376$; 921, $F_{ST} = -0.0050$, $P = 0.6622$; 931, $F_{ST} = 0.0207$, $P = 0.0524$). Additionally, overall levels of genetic divergence were similar for the years 2002 ($F_{ST} = 0.2289$) and 2003 ($F_{ST} = 0.1970$). Therefore, for further analysis,

Fig. 3. Areas of genetic discontinuity identified by BARRIER using the Monmonier algorithm (Manni et al. 2004): broken lines, Delaunay triangulation; solid lines, barriers to gene flow. Larger numbers at the barriers represent the number of loci supporting the barrier. Samples were collected in 2002 (●), 2003 (▲), and 2004 (■). Circled locations indicate the two pairs of temporal samples that were pooled (they were genetically indistinguishable) despite not being from exactly the same location. Average temperature data of the data storage tags (DST) are given. Temperature of the eastern coast (samples 612 and 621) was recorded during the sampling process.

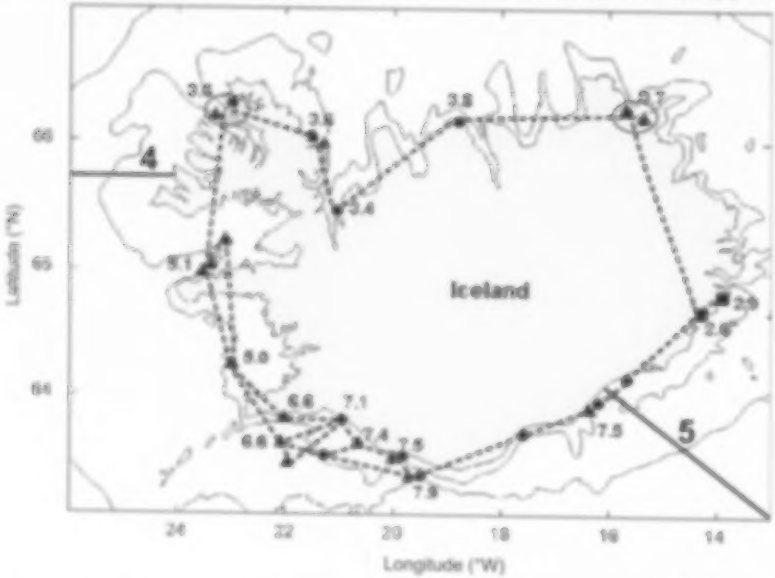

temporal samples from the same location were clustered into one single group for each location (total of 22 spawning locations).

Based on pairwise F_{ST} values, MDS clearly clustered samples of the northeastern region and southwestern region (Fig. 2*b*; stress values on axes 1 and 2, 0.0644). The AMOVA analysis confirmed those results and revealed that among-group differentiation was significant between samples collected in northeastern and southwestern regions (Table 3).

A comparison of the level of genetic diversity among northeastern and southwestern components, using the software Fstat (Goudet 1995), revealed significant differences at the level of expected and observed heterozygosity (northeastern component, $H_O = 0.283$, $H_E = 0.282$; southwestern component, $H_O = 0.445$, $H_E = 0.421$; $P = 0.007$ and 0.014, respectively).

After Bonferroni correction, pairwise genotypic differentiation between populations yielded 298 significant genotype comparisons out of 378 (data not shown). Using χ^2 tests, genotype frequencies were also significantly different among populations ($\chi^2_{(21)} = 1165.92$, $P = 0.0001$; Fig. 4). BB genotypes were present in relatively high proportion in the southwestern but not in the northeastern samples (Fig. 4).

Depth pattern

An AMOVA based on a clustering related to the depth of the collected samples (shallow, intermediate, and deep waters) confirmed that part of the among-group microsatellite differentiation could be explained by depth (Table 3). Depth of sample collection was negatively correlated with microsatellite heterozygosity (see Fig. 5) but not with allelic richness ($r^2 = 0.0293$, $P = 0.4459$, $n = 22$, data not shown). When significant relationships (H_O, H_E) were tested within the two main components separately, they were significant in the southwestern region (H_O, $r^2 = 0.5232$, $P = 0.0035$, $n = 14$; H_E, $r^2 = 0.6006$, $P = 0.0011$, $n = 14$) but not in the northeastern region (H_O, $r^2 = 0.1340$, $P = 0.3721$, $n = 8$; H_E, $r^2 = 0.1146$, $P = 0.4120$, $n = 8$).

Because of this depth pattern and to ensure that the observed genetic divergence at microsatellite loci between northeastern and southwestern samples was not due to the presence of deep-water samples in area 9 and not elsewhere, we calculated the overall genetic divergence without the deep-sea and intermediate water samples (only shallow water samples). The *F*-statistics estimates also showed a mean significant F_{ST} value of 0.002 and an F_{IS} of 0.012, similar to the values obtained when all samples, including those obtained in intermediate and deep waters, were included in the analysis. An AMOVA based on shallow water samples only clearly confirmed that among-group differentiation was significant between samples collected in northeastern and southwestern regions (fixation index: CT = 0.0008, $P = 0.0323$; SC = 0.004, $P = 0.0001$).

An AMOVA based on a clustering related to the depth of the collected samples (shallow, intermediate, and deep waters) confirmed that among-group *Pan* I locus differentiation could be explained by depth (Table 3). Additionally, the frequency of allele B in the *Pan* I locus was found to be positively correlated with depth (Fig. 6), and this correlation persisted in both regions when analysed separately (southwest, $r^2 = 0.6982$, $P = 0.0002$, $n = 14$; northeast, $r^2 = 0.6543$, $P = 0.0150$, $n = 8$). Depth of sample collection was not correlated with *Pan* I locus heterozygosity (data not

Fig. 4. Genotypes distribution of the *Pan* I locus in the different spawning locations: BB genotypes, solid bars; AB genotypes, shaded bars; AA genotypes, open bars.

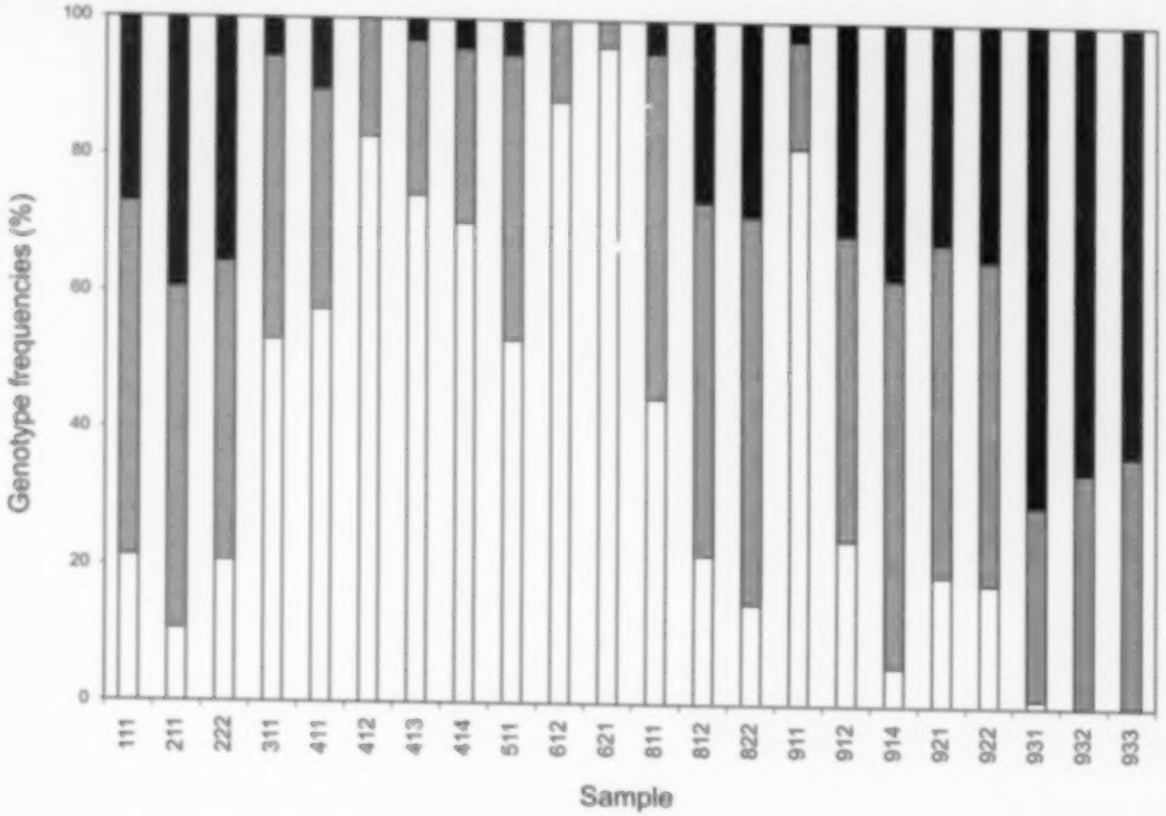

Fig. 5. Microsatellite overall observed heterozygosity (H_O) according to depth (m) ($r^2 = 0.3765$, $P = 0.0030$, $n = 22$). The relationship was also significant for the H_E ($r^2 = 0.3196$, $P = 0.0060$, $n = 22$; data not shown).

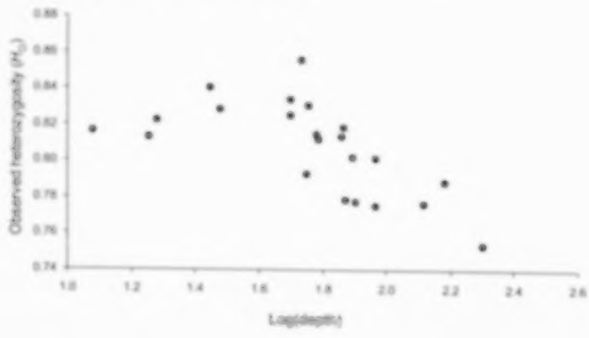

Fig. 6. Frequencies of the B allele of the *Pan* I locus according to depth (m) ($r^2 = 0.5195$, $P = 0.0002$, $n = 22$).

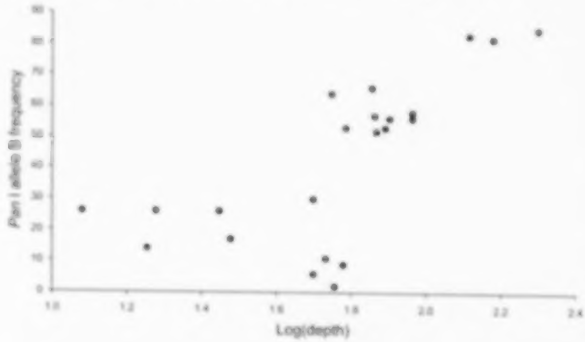

shown) (H_O, $r^2 = 0.0400$, $P = 0.2720$, $n = 22$; H_E, $r^2 = 0.0123$, $P = 0.6332$, $n = 22$).

At the *Pan* I locus, the genetic differentiation between the northeastern and southwestern regions persisted even when only shallow water cod samples were included in the analysis ($F_{ST} = 0.213$, $F_{IS} = -0.016$; AMOVA fixation index: CT = 0.1742, $P = 0.005$; SC = 0.0940, $P = 0.001$).

Tagging

Cod tagged on the different spawning sites demonstrated high fidelity to their tagging sites (Fig. 7). Most of the tagged cod captured the year after tagging were captured during the spawning season within the region in which they were tagged, indicating that they had returned to spawn in the same region in which they had first been captured and tagged. Out of the recaptures for each region of tagging, the

Fig. 7. Icelandic tagging experiment carried out during the spawning peak of 2002 and 2003. The large circle or ellipse represents the area in which spawning Atlantic cod (*Gadus morhua*) were tagged. ○, the position of recapture of each individual (tagged in 2002) during the spawning season of 2003; ×, the position of recapture of each individual (tagged in 2003) during the spawning season of 2004.

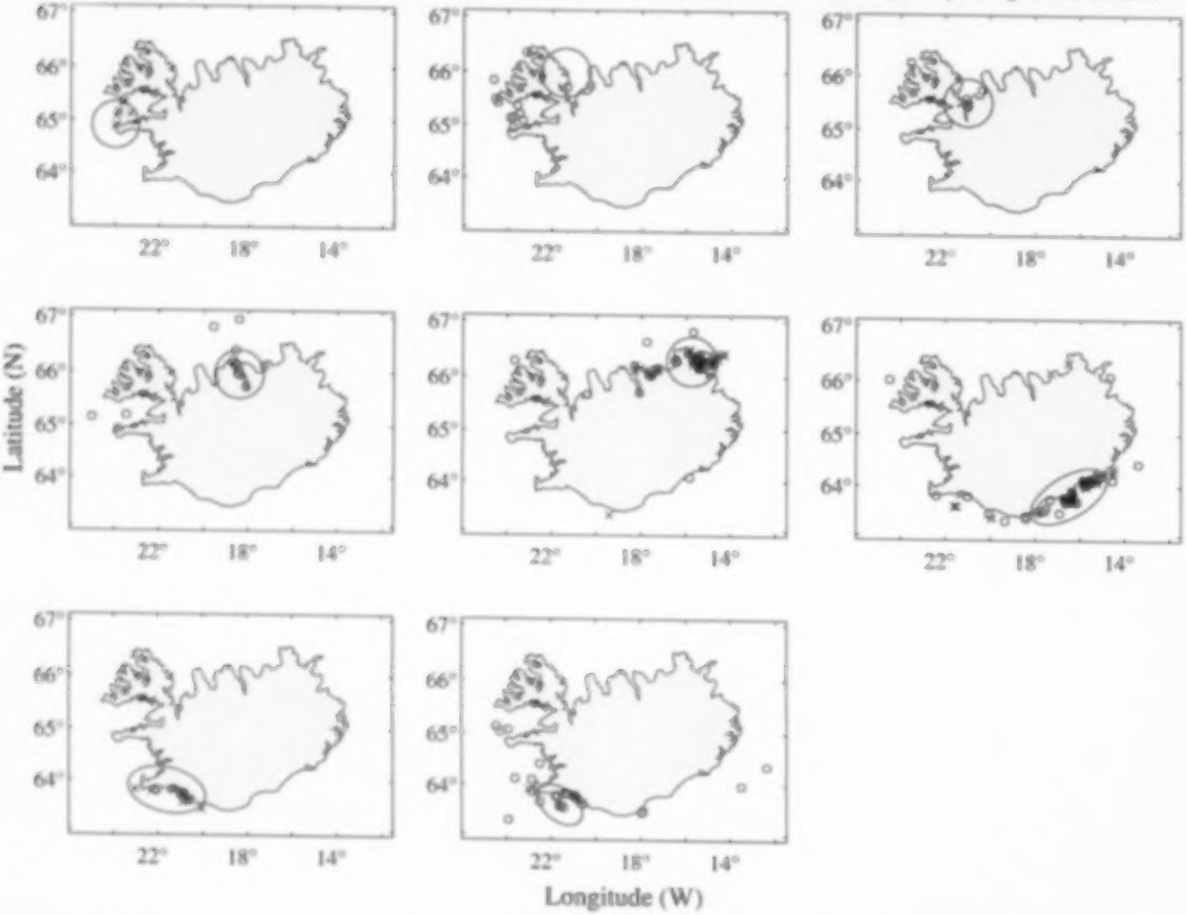

percentage recaptured in the same region was 100% for region 2, 86% for region 4, 72% for region 5, 84% for region 8, and 64% for region 9. The percentage returning to the same or an adjacent region was 100% for region 2, 90% for region 4, 100% for region 5, 91% for region 8, and 87% for region 9.

Discussion

All three of the techniques that we employed to examine spatial structure in Atlantic cod (*Gadus morhua*) around Iceland (microsatellite DNA, the *Pan* I locus, and tagging experiments) clearly reject the hypothesis of panmixia for cod in this region. Although the tagging experiments, which were conducted on adults, provided evidence for homing to the regions where fish had been tagged one or two years before recapture, they naturally do not provide evidence for natal homing. The analysis based on a suite of nine presumed neutral microsatellite DNA loci provided evidence for at least two spatially well defined spawning components of Icelandic cod, one in waters off northeastern Iceland involving regions 3, 4, 5, and 6 and the other in waters off southwestern Iceland involving regions 1, 2, 8, and 9. The spatial structure identified was stable in all the regions for which we had temporal replication. That the evidence for spatial structure identifying two major spawning components was consistent across two types of molecular markers (a suite of neutral markers and a marker known to be under selection) provides strong support for the hypothesis that the structure may be driven by two distinct but nonexclusive processes: (*i*) one of larval–juvenile retention driven by oceanographic mechanisms involving currents, fronts, and eddies, as well as the topography of the ocean floor; and (*ii*) one of adaptive changes driven by natural selection and facilitated perhaps by the differential characteristics of the water masses (e.g., temperature) northeast and southwest of Iceland. Below we discuss each of these issues in detail.

Spatial structure as determined by microsatellites and the *Pan* I locus

The genetic diversity of the nine microsatellite loci assessed as H_E, H_O, and mean number of alleles exhibited a wide range of variation and was generally comparable with what has been observed in marine fishes (DeWoody and Avise 2000). However, with respect to other cod studies, the Icelandic cod samples exhibited a generally higher level of genetic diversity at microsatellite loci, measured either as heterozygosity or allelic richness, than any other European cod populations (Hutchinson et al. 2001; Knutsen et al. 2003; Nielsen et al. 2003) but were, however, comparable with Canadian samples (Ruzzante et al. 1996, 1998; Beacham et al. 2002).

The level of genetic differentiation that we observed with the microsatellite loci is in accordance with earlier findings in cod from coastal regions (Ruzzante et al. 2001, F_{ST} = 0.0039 to 0.0053; Beacham et al. 2002, F_{ST} = 0.0080; Knutsen et al. 2003, F_{ST} = 0.0023). The persistence of the overall genetic signal detected in consecutive years (F_{ST} = 0.0038 for 2002 and F_{ST} = 0.0029 for 2003) suggests that the structure identified is real (Waples 1998). Additionally, temporal stability was observed for all of the repeated samples across years.

Our genetic analyses clearly revealed the presence of two cod spawning components in the Icelandic waters. The MDS analysis clustered the samples in two different groups: the northeastern region (areas 3, 4, 5, and 6 + samples 811 and 911) and the southwestern region (area 1, 2, 8, and 9). The AMOVA conducted on northeastern–southwestern comparisons revealed that the among-group variation (northeast vs southwest) was significant. A recent biological study on fishing mortality and spawning stock biomass for Icelandic cod strongly suggests that the reproductive component is unevenly distributed in waters around the country (Begg and Marteinsdóttir 2003). An important finding of that study was that large fish were caught in the southwestern region where mean cod abundance was lowest and small fish were essentially caught in northeastern region where mean abundance was highest. These results suggest the existence of life history variation among cod from the northern and southern regions (Begg and Marteinsdóttir 2003) and thus support our genetic results. The tagging experiment reported here is also consistent with our genetic results in that we observe strong year-to-year spawning site fidelity, at least to the level of neighbouring areas.

As expected for a genetic marker supposedly under selection, the *Pan* I locus revealed a stronger genetic divergence (F_{ST} = 0.261) than the microsatellite loci among Icelandic populations. Previous studies with this marker revealed similar levels of genetic divergence at broadly comparable geographic scales (Fevolden and Pogson 1997; Pogson and Fevolden 2003; Sarvas and Fevolden 2005) but not at small geographic scales (Jónsdóttir et al. 1999, 2001; Karlsson and Mork 2003). In the present study, the largest difference at the *Pan* I locus occurs between the northeastern and southwestern regions (F_{CT} = 0.283), with B alleles and *Pan* I^{AB}/*Pan* I^{BB} genotypes mainly encountered in the southwestern regions of Iceland (areas 1, 2, 8, and 9). Fevolden and Pogson (1997) investigated the cod structure with *Pan* I locus along the Norwegian coast at a similar geographical scale and found an overall differentiation of 40%, mainly linked to the differentiation of the arctic–coastal cod populations. The Barents Sea exhibited a high *Pan* I^{BB} genotype frequency, which is in contradiction with our findings suggesting that northeastern populations mainly comprise *Pan* I^{AA} genotypes. Recently, the *Pan* I locus has been suggested to experience positive Darwinian selection (Pogson and Fevolden 2003; Pogson and Mesa 2004), and depth, salinity, and temperature have been suggested to be the driving forces (Karlsson and Mork 2003; Case et al. 2005). Thus, the observed discrepancy between our results and those of Fevolden and Pogson (1997) might be due to differences in the selective environment. The northeastern region is affected by the East Greenland and East Icelandic currents originating from the Arctic Ocean and transporting cold water (0–2 °C). In contrast, the southwestern and western regions are affected by the highly saline (35 PSU) and relatively warm (6–8 °C) water originating from the Gulf Stream (Griffiths 1995). It is therefore likely that selection may act differently in the northeastern and southwestern regions, thus leading to the observed genetic divergence (stable over two consecutive years) at the *Pan* I locus.

Oceanography

The very low correlation between genetic differentiation and spatial coordinates detected with microsatellites indicates that gene flow is likely less related to geographic distance per se than it is to oceanic currents and environmental characteristics. Indeed, eggs and (or) larval dispersal can be restricted by physical barriers such as frontal systems (Shaw et al. 2004), oceanic currents (Ruzzante et al. 1998; Knutsen et al. 2003), and estuarine circulation (Pérrin et al. 2004) and to a lesser extent by environmental conditions, which can make habitat unsuitable for settlement (Palumbi 1994). Also, oceanic currents and temperature differences can restrict the dispersal of adults, thus facilitating adaptation to local environmental conditions.

Oceanographic conditions around Iceland are mainly shaped by the two frontal zones located west–northwest and east–southeast of the country, where cold and warm water masses meet, and by temperature differences observed between the northern and southern regions. The pattern of genetic differences observed here for cod around Iceland using neutral, as well as selected, markers suggests that both oceanic currents and environmental conditions such as temperature have a strong structuring effect on this species. The geographical genetics approach conducted with the software BARRIER on the microsatellite loci suggested two main barriers to gene flow located in the two areas that coincide with oceanic fronts, the northwestern and southeastern regions, where warm and cold waters meet.

Previous studies have clearly established the influence of oceanic currents on dispersal of eggs, larvae, and pelagic juveniles, especially those coming from the southern spawning grounds (Begg and Marteinsdóttir 2000, 2003; Marteinsdóttir et al. 2000*a*). In this study, we have added to this knowledge by demonstrating that oceanic currents, temperature, and oceanic fronts may also play an important role in the dispersal of adult cod.

Depth also appears to play a role in the genetic divergence of cod around Iceland as indicated by the differences observed between inshore and offshore samples. Differences between inshore and offshore cod have been shown to exist in the Northwest Atlantic in Newfoundland waters where both types intermingle in inshore areas during the offshore–inshore summer feeding migration (Ruzzante et al. 1996). Similarly, recent tagging experiments suggested that inshore cod are more sedentary than their offshore counterparts (Robichaud and Rose 2004; Storr-Paulsen et al. 2004). Very few data exist on the presence of coastal and offshore cod forms in Iceland and on their migration pattern, but Pálsson and Thorsteinsson (2003) suggested that the deep-water fish migrate to deeper waters after the spawning season, whereas shallow-water fish follow the seasonal trend in temperature for the shelf waters. The tagging experiment conducted during this study was carried out during the breeding season to assess spawning site fidelity. It therefore suggested high spawning site fidelity of cod (64% to 100%) but does not assess the complete migration pattern of cod around Iceland. Additionally, biological data collected in previous studies suggested that a high proportion of postspawning cod migrate to the main feeding grounds located to the northwest and northeast of the country (Begg and Marteinsdóttir 2000, 2002*b*; Marteinsdóttir et al. 2000*a*) and therefore migrate over long distances. Coastal and offshore life forms of cod from other regions of the North Atlantic are known to exhibit different migration patterns, the former being more sedentary than the latter (Knutsen et al. 2004; Robichaud and Rose 2004). The observed high return of Icelandic cod to spawning regions during the breeding season does not mean that coastal cod populations are more sedentary than their offshore counterparts. We therefore interpret that the observed genetic differentiation with depth is not due to the presence of different cod life forms but to the dynamics of cod around Iceland involving spawning site fidelity and postspawning migration to feeding grounds.

Our results therefore indicate that both oceanic fronts and depth have an effect on the genetic composition of cod around Iceland. Additionally, the AMOVA carried out on the shallow water samples suggested that the observed genetic divergence between the northeastern and southwestern regions was not due to the deep-water samples collected in area 9 (931, 932, 933) and therefore that depth was not the primary source of the observed genetic variation.

Gene flow vs local adaptation

The conclusion drawn from genetic data depends crucially on the assumption of selective neutrality of the genetic markers used. The expectation is that all neutral loci would be affected in a similar way by drift and migration (Slatkin 1987), whereas natural selection should affect certain loci differently. One of the recent popular approaches to assessing the potential effect of selection in the genetic structure of a species is to compare genetic patterns obtained from putative selected loci with those of neutral markers such as microsatellite loci. Indeed, the variation of fixation indices among loci and types of marker is one of the most powerful methods for assessing whether natural selection has played a key role in the observed genetic divergence (see Allendorf and Seeb 2000).

In this study, both genetic markers clearly reject the hypothesis of panmixia for cod in Icelandic waters and reveal the presence of two main spawning components. However, the microsatellite loci yielded lower mean fixation indices than the *Pan* I locus, which has been suggested to experience positive Darwinian selection. Although it remains a challenge to compare the amount of differentiation between different loci, the standardized genetic measure (G'_{ST}), which represents the proportion of the maximum differentiation possible for the level of subpopulations homozygosity observed, suggested that the level of genetic divergence is far more pronounced with the *Pan* I locus than with the microsatellite loci. The results might indicate that balancing selection is acting on the microsatellite loci or that divergent selection is acting on the *Pan* I locus. The microsatellite loci are not regarded as being under selection (neutral expectation) unless linked to functional genes under selection, which is unlikely to be a general pattern (Schlötterer and Wiehe 1999). Consequently, divergent selection acting on the *Pan* I locus is probably the most likely explanation for the observed differences in the fixation indices (F_{ST} and G'_{ST}) of both genetic markers.

In conclusion, the present study used three techniques to identify stock components: microsatellite loci, the *Pan* I locus, and a tagging experiment. Both types of genetic markers clearly indicate that Iceland cod is structured genetically into two major components, northeastern and southwestern. The tagging experiment conducted simultaneously with the collection of samples for genetic analysis is consistent with the notion that spawning cod tagged on the southwestern spawning ground of Iceland seldom migrate to the northeastern spawning ground and vice versa. In addition, the interpretation of these results in light of potential effects of geographic, oceanographic, and depth barriers lead us to conclude that environmental conditions such as oceanic fronts and temperature gradient are likely to affect the temporally stable genetic structure we observed and might have lead to local adaptation of spawning cod around Iceland.

Acknowledgments

This research has been carried out under the METACOD EU project (Q5RS-2001-00953). We thank all crews of the vessels for sampling, as well as researchers for their assistance with sampling. We also thank two anonymous referees and an associate editor for their useful comments on the manuscript.

References

Allendorf, F.W., and Seeb, L.W. 2000. Concordance of genetic divergence among sockeye salmon populations at allozyme and mitochondrial DNA markers. Evolution, **54**: 640–651.

Applied Biosystems. 2000. GeneScan. Version 3.1.2. Applied Biosystems, Foster City, California.

Applied Biosystems. 2004. GeneMapper. Version 3.7. Applied Biosystems, Foster City, California.

Beacham, T.D., Brattey, J., Miller, K.M., Le, K.D., and Withler, R.E. 2002. Multiple stock structure of Atlantic cod (*Gadus morhua*) off Newfoundland and Labrador determined from genetic variation. ICES J. Mar. Sci. **59**: 650–665.

Begg, G.A., and Marteinsdóttir, G. 2000. Spawning origins of pelagic juvenile cod *Gadus morhua* inferred from spatially explicit age distribution: potential influence on year-class strength and recruitment. Mar. Ecol. Prog. Ser. **202**: 193–217.

Begg, G.A., and Marteinsdóttir, G. 2002*a*. Environmental and stock effect on spatial distribution and abundance of mature cod *Gadus morhua*. Mar. Ecol. Prog. Ser. **229**: 245–262.

Begg, G.A., and Marteinsdóttir, G. 2002*b*. Environmental and stock effects on spawning origins and recruitment of cod *Gadus morhua*. Mar. Ecol. Prog. Ser. **229**: 263–277.

Begg, G.A., and Marteinsdóttir, G. 2003. Spatial partitioning of relative fish mortality and spawning stock biomass of Icelandic cod. Fish. Res. **59**: 343–362.

Begg, G.A., Friedland, K.D., and Pearce, J.B. 1999. Stock identification and its role in stock assessment and fisheries management: an overview. Fish. Res. **43**: 1–8.

Bekkevold, D., André, C., Dahlgren, T., Mosegaard, H., Clausen, L., Carvalho, G.R., Torstensen, E., Nordinger, E., Andersen, T., and Ruzzante, D.E. 2005. Environmental correlates of population differentiation in Atlantic herring (*Clupea harengus*). Evolution, **59**: 2656–2668.

Belkhir, K., Borsa, P., Goudet, J., and Bonhomme, F. 1999. GENETIX: logiciel sous Windows pour la génétique des populations. Version 4.03. Laboratoire Génome & Population, CNRS–UPR, Université de Montpellier II, Montpellier, France.

Brooker, A.L., Cook, D., Bentzen, P., Wright, J.M., and Doyle, R.W. 1994. Organization of microsatellites differs between mammals and cold-water teleost fishes. Can. J. Fish. Aquat. Sci. **51**: 1959–1966.

Case, R.A.J., Hutchinson, W.F., Hauser, L., Van Oosterhout, C., and Carvalho, G.R. 2005. Macro- and micro-geographic variation in pantophysin (*Pan* I) allele frequencies in NE Atlantic cod *Gadus morhua*. Mar. Ecol. Prog. Ser. **301**: 267–278.

Christensen, V., Guénette, S., Heymans, J.J., Walters, C.J., Watson, R., Zeller, D., and Pauly, D. 2003. Hundred-year decline of North Atlantic predatory fishes. Fish Fish. **4**: 1–24.

Cockerham, C.C., and Weir, B.S. 1979. Digenic descent measures for finite populations. Genet. Res. **30**: 121–147.

Cook, R.M., Sinclair, A., and Stefánsson, G. 1997. Potential collapse of North Sea cod stocks. Nature (London), **385**: 521–522.

DeWoody, J.A., and Avise, J.C. 2000. Microsatellites variation in marine, freshwater and anadromous fishes compared with other animals. J. Fish Biol. **56**: 461–473.

Dupanloup, I., Schneider, S., and Excoffier, L. 2002. A simulated annealing approach to define the genetic structure of populations. Mol. Ecol. **11**: 2571–2581.

Fevolden, S.E., and Pogson, G.H. 1997. Genetic divergence at the synaptophysin (*Syp* I) locus among Norwegian coastal and North-east Arctic populations of Atlantic cod. J. Fish Biol. **51**: 895–908.

Goudet, J. 1995. Fstat. Version 1.2. A computer program to calculate *F*-statistics. J. Hered. **86**: 485–486.

Griffiths, C.A. 1995. A fine resolution numerical model of the Iceland–Faeroe front with open boundary conditions. J. Geophys. Res. **100**: 15915–15931.

Gunnarsson, K., Jónsson, G., and Pálsson, Ó.K. 1998. Sjávarnytjar við Ísland. Mál og menning, Reykjavík.

Hedrick, P.W. 2005. A standardized genetic differentiation measure. Evolution, **59**: 1633–1638.

Hutchinson, W.F., Carvalho, G.R., and Rogers, S.I. 2001. Marked genetic structuring in localised spawning populations of cod *Gadus morhua* in the North Sea and adjoining waters, as revealed by microsatellites. Mar. Ecol. Prog. Ser. **223**: 251–260.

Jónsdóttir, I., Campana, S., and Marteinsdóttir, G. 2006. Otolith shape and temporal stability of spawning groups of Icelandic cod (*Gadus morhua* L.). ICES J. Mar. Sci. **63**: 150–1512.

Jónsdóttir, Ó.D.B., Imsland, A.K., Daníelsdóttir, A.K., Thorsteinsson, V., and Naedval, G. 1999. Genetic differentiation among Atlantic cod in south and south-east Icelandic waters: synaptophysin (*Syp* I) and haemoglobin (*HbI*) variation. J. Fish Biol. **54**: 1259–1274.

Jónsdóttir, Ó.D.B., Daníelsdóttir, A.K., and Naedval, G. 2001. Genetic differentiation among Atlantic cod (*Gadus morhua* L.) in Icelandic waters: temporal stability. ICES J. Mar. Sci. **58**: 114–122.

Jónsson, J. 1996. Tagging of cod (*Gadus morhua*) in Icelandic waters 1948–1986. Rit Fiskid. **14**: 1–82.

Jorgensen, H.B.H., Hansen, M.M., Bekkevold, D., Ruzzante, D.E., and Loeschcke, V. 2005. Marine landscape and population genetic structure of herring (*Clupea harengus* L.) in the Baltic Sea. Mol. Ecol. **14**: 3219–3234.

Karlsson, S., and Mork, J. 2003. Selection-induced variation at the pantophysin locus (*Pan* I) in a Norwegian fjord population of cod (*Gadus morhua*). Mol. Ecol. **12**: 3265–3274.

Knutsen, H., Jorde, P.E., André, C., and Stenseth, N. Chr. 2003. Fine-scaled geographical population structuring in a highly mobile marine species: the Atlantic cod. Mol. Ecol. **12**: 385–394.

Knutsen, H., André, C., Jorde, P.E., Skogen, M.D., Thuróczy, E., and Stenseth, N.Chr. 2004. Transport of North Sea larvae in the Skagerrak coastal populations. Proc. R. Soc. Lond. B, **271**: 1337–1344.

Malmberg, S.A., Valdimarsson, H., and Mortensen, J. 1996. Long-time series in Icelandic waters in relation to physical variability in the northern North Atlantic. NAFO (Northwest Atl. Fish. Organ.) Sci. Counc. Stud. **24**: 6–80.

Manni, F., Guérard, E., and Heyer, E. 2004. Geographic patterns of (genetic, morphologic, linguistic) variation: how barriers can be detected by "Monmonier's algorithm". Hum. Biol. **76**: 173–190.

Marteinsdóttir, G., and Björnsson, H. 1999. Time and duration of spawning of cod in Icelandic waters. ICES CM 1999/Y:34.

Marteinsdóttir, G., Gunnarsson, B., and Suthers, I.M. 2000*a*. Spatial variation in hatch date distributions and origin of pelagic juvenile cod in Icelandic waters. ICES J. Mar. Sci. **57**: 1184–1197.

Marteinsdóttir, G., Guðmundsdóttir, A., Thorsteinsson, V., and Stefánsson, G. 2000*b*. Spatial variation in abundance, size composition and viable egg production of spawning cod (*Gadus morhua* L.) in Icelandic waters. ICES J. Mar. Sci. **57**: 824–83.

Marteinsdóttir, G., Ruzzante, D.E., and Nielsen, E.E. 2005. History of the North Atlantic cod stocks. ICES CM 2005/Q:13.

Miller, K.M., Le, K.D., and Beacham, T.D. 2000. Development of tri- and tetranucleotide repeat microsatellite loci in Atlantic cod (*Gadus morhua*). Mol. Ecol. **9**: 238–239.

Myers, R.A., Hutchings, J.A., and Barrowman, N.J. 1996. Hypotheses for the decline of cod in the North Atlantic. Mar. Ecol. Prog. Ser. **138**: 293–308.

Nielsen, E.E., Hansen, M.M., Ruzzante, D.E., Meldrup, D., and Gronkjaer, P. 2003. Evidence of a hybrid-zone in Atlantic cod (*Gadus morhua*) in the Baltic and the Danish Belt Sea revealed by individual admixture analysis. Mol. Ecol. **12**: 1497–1508.

O'Reilly, P.T., Canino, M.F., Bailey, K.M., and Bentzen, P. 2000. Isolation of twenty low stutter di- and tetranucleotide microsatellites for population analyses of walleye pollock and other gadoids. J. Fish Biol. **56**: 1074–1086.

Pálsson, Ó.K., and Thorsteinsson, V. 2003. Migration patterns, ambient temperature, and growth of Icelandic cod (*Gadus morhua*): evidence from storage tag data. Can. J. Fish. Aquat. Sci. **60**: 1409–1423.

Palumbi, S.R. 1994. Genetic divergence, reproductive isolation, and marine speciation. Annu. Rev. Ecol. Syst. **25**: 547–572.

Pérrin, C., Wing, S.R., and Roy, M.S. 2004. Effect of hydrographic barriers on population genetic structure of the sea star

Coscinasterias muricata (Echinodermata, Asteroida) in the New Zealand fiords. Mol. Ecol. **13**: 2183–2195.

Pogson, G.H., and Fevolden, S.E. 2003. Natural selection and the genetic differentiation of coastal and Arctic population of the Atlantic cod in northern Norway: a test involving nucleotide sequence variation at the pantophysin (*Pan* I) locus. Mol. Ecol. **12**: 63–74.

Pogson, G.H., and Mesa, K.A. 2004. Positive Darwinian selection at the pantophysin (*Pan* I) locus in marine gadid fishes. Mol. Biol. Evol. **21**: 65–75.

Raymond, R., and Rousset, F. 1995. GENEPOP. Version 3.1. Population genetic software for exact tests and ecumenism. J. Hered. **86**: 248–249.

Rice, W.R. 1989. Analyzing table of statistical tests. Evolution, **43**: 223–225.

Robichaud, D., and Rose, G.A. 2004. Migratory behaviour and range in Atlantic cod: inference from a century of tagging. Fish Fish. **5**: 185–214.

Ruzzante, D.E., Taggart, C.T., Cook, D., and Goddard, S.V. 1996. Genetic differentiation between inshore and offshore Atlantic cod (*Gadus morhua* L.) off Newfoundland: microsatellite DNA variation and antifreeze level. Can. J. Fish. Aquat. Sci. **53**: 634–645.

Ruzzante, D.E., Taggart, C.T., and Cook, D. 1998. A nuclear DNA basis for shelf- and bank-scale population structure in Northwest Atlantic cod (*Gadus morhua*): Labrador to Georges Bank. Mol. Ecol. **7**: 1663–1680.

Ruzzante, D.E., Taggart, C.T., Doyle, R.W., and Cook, D. 2001. Stability in the historical pattern of genetic structure of Newfoundland cod (*Gadus morhua*) despite the catastrophic decline in population size from 1964 to 1994. Conserv. Genet. **2**: 257–269.

Ruzzante, D.E., Mariani, S., Bekkevold, D., André, C., Mosegaard, H., Clausen, L.A.W., Dahlgren, T.G., Hutchinson, W.F., Hatfield, E.M.C., Torstensen, E., Brigham, J., Simmonds, E.J., Laikre, L., Larsson, L.C., Stet, R.J.M., Ryman, N., and Carvalho, G.R. 2006. Biocomplexity in a highly migratory pelagic marine fish, Atlantic herring. Proc. R. Soc. Lond. B, **273**: 1459–1464.

Ryman, N. 2006. Chifish: a computer program testing for genetic heterogeneity at multiple loci using chi-square and Fisher's exact test. Mol. Ecol. Notes, **6**: 285–287.

Sæmundsson, K.H. 2005. Geographic distribution and dispersal of juvenile Icelandic cod (*Gadus morhua*). M.Sc. thesis, Department of Biology, University of Iceland, Reykjavík, Iceland.

Sarvas, T.H., and Fevolden, S.E. 2005. Pantophysin (*Pan* I) locus divergence between inshore v. offshore and northern v. southern populations of Atlantic cod in the north-east Atlantic. J. Fish Biol. **67**: 444–469.

Schlötterer, C., and Wiehe, T. 1999. Microsatellites: a neutral marker to infer selective sweeps. *In* Microsatellites: evolution and applications. *Edited by* D.B. Goldstein and C. Schlötterer. Oxford University Press, Oxford, UK. pp. 238–247.

Schneider, S., Roessli, D., and Excoffier, L. 2000. ARLEQUIN. Version 2.0. A software for population genetic analysis. Genetics and Biometry Laboratory, University of Genova, Switzerland.

Shaw, I.W., Arkhipin, A.I., and Al-Khairulla, H. 2004. Genetic structuring of Patagonian toothfish populations in the Southwest Atlantic Ocean: the effect of the Antarctic Polar Front and deep-water troughs as barrier to genetic exchange. Mol. Ecol. **13**: 3293–3303.

Slatkin, M. 1987. Gene flow and the genetic structure of natural population. Science (Washington, D.C.), **236**: 787–792.

StatSoft, Inc. 2001. Statistica (data analysis software system). Version 6.0. Statsoft Inc., Tulsa, Oklahoma (www.statsoft.com).

Stephenson, R., and Kenchington, E. 2000. Conserving fish stock structure is a critical aspect of preserving biodiversity. ICES CM 2000/Mini:07.

Storr-Paulsen, M., Wieland, K., Hovgard, H., and Ratz, H.J. 2004. Stock structure of Atlantic cod (*Gadus morhua*) in West Greenland waters: implications of transport and migration. ICES J. Mar. Sci. **61**: 972–982.

Swain, D.P., Frank, K.T., and Maillet, G. 2001. Delineating stocks of Atlantic cod (*Gadus morhua*) in the Gulf of St. Lawrence and Cabot Strait areas using vertebral number. ICES J. Mar. Sci. **58**: 253–259.

Taggart, C.T., Penney, P., Barrowman, N., and George, C. 1995. The 1954–1993 Newfoundland cod-tagging database: statistical summaries and spatial-temporal distributions. Can. Tech. Rep. Fish. Aquat. Sci. No. 2042.

Thorsteinsson, V., and Marteinsdóttir, G. 1992. Þorskmerkingar við Norðaustur- og Austurland vorið 1991 og endurheimtur sama ár. [Mark–recapture experiments at the northeast and east coasts of Iceland 1991.] Ægir, **85**: 60–64. [In Icelandic.]

Thorsteinsson, V., and Marteinsdóttir, G. 1993. Þorskmerkingar í Stöðvarfirði og Gunnólfsvík 1991 og 1992 og endurheimtur úr þeim til ársloka 1992. Ægir, **2**: 3–10. [In Icelandic.]

Valdimarsson, H., and Malmberg, S.A. 1999. Near-surface circulation in Icelandic waters derived from satellite tracked drifters. Rit Fiskid. **16**: 23–39.

Walsh, P.S., Metzger, D.A., and Higuchi, R. 1991. Chelex 100 as a medium for simple extraction of DNA for PCR-based typing from forensic material. Biotechniques, **10**: 506–513.

Waples, R.S. 1998. Separating the wheat from the chaff: patterns of genetic differentiation in high gene flow species. J. Hered. **89**: 435–450.

Ward, R.D. 2000. Genetic in fisheries management. Hydrobiologia, **420**: 191–201.

Weir, B.S., and Cockerham, C.C. 1984. Estimating *F*-statistics for the analysis of population structure. Evolution, **38**: 1358–1370.

Wright, S. 1969. Evolution and the genetics of populations. Vol. 2. The theory of gene frequencies. University of Chicago Press, Chicago, Illinois.

Temporal and spatial variation in the energy intake of a brook trout (*Salvelinus fontinalis*) population in an Appalachian watershed

Ryan M. Utz and Kyle J. Hartman

Abstract: Stream-dwelling salmonids in eastern North America are often restricted to headwater watersheds, where productivity is low and thus feeding conditions are poor. We sought to quantify how energy intake varies with spatial and temporal variation by monitoring feeding rates in multiple sites over the course of two years. Daily rations were calculated for 939 fish by examining stomach contents. Maintenance rations were compared with daily rations using a bioenergetics model. Consumption peaked in spring, dropped substantially in summer, and remained low until the following spring. A minority of fish fed at very high levels during all seasons, elevating the mean consumption of the population. Fish occupying large sites with low trout densities consistently consumed more energy than fish in smaller streams with high trout densities. A direct relationship between trout density and mean consumption was observed during summer, when feeding conditions were poorest. Our findings suggest that within a headwater watershed, larger reaches of streams where fewer trout are found act as important feeding areas and thus may be important habitat for brook trout (*Salvelinus fontinalis*).

Résumé : Les salmonidés des cours d'eau dans l'est de l'Amérique du nord sont souvent confinés aux bassins versants d'amont où la productivité est faible et conséquemment les conditions alimentaires médiocres. Nous avons cherché à mesurer les variations spatiales et temporelles de l'ingestion d'énergie en suivant les taux d'alimentation à plusieurs sites durant deux années. L'analyse des contenus stomacaux de 939 poissons a permis de calculer les rations journalières. Un modèle bioénergétique a comparé les rations journalières aux rations de maintien. La consommation atteint un maximum au printemps, diminue considérablement en été et reste faible jusqu'au printemps suivant. Un minorité de poissons se nourrit à un taux élevé en toutes saisons, ce qui augmente la consommation moyenne de la population. Les poissons habitant de grands sites à faibles densités d'ombles consomment toujours plus d'énergie que les poissons dans les petits cours d'eau à forte densité d'ombles. On observe une relation directe entre la densité des ombles et la consommation moyenne en été, quand les conditions d'alimentation sont les moins bonnes. Nos observations indiquent que, dans un bassin versant d'amont, les grandes sections habitées par un nombre réduit d'ombles sont des lieux importants d'alimentation et peuvent donc être un habitat vital pour l'omble de fontaine (*Salvelinus fontinalis*).

[Traduit par la Rédaction]

Introduction

Brook trout (*Salvelinus fontinalis*) populations have declined in size and range as the result of a host of historic and persistent anthropogenic impacts, including uncontrolled logging, acidic precipitation, mine runoff, overfishing, and introduced species (Larson and Moore 1985; Marschall and Crowder 1996; Wigington et al. 1996). A number of institutions consider the restoration of brook trout a management goal because of its potential value as a recreational fishery. Recent work has highlighted the importance of small streams with high alkalinity and low levels of fine sediment in maintaining brook trout reproduction and populations (Petty et al. 2005; Hartman and Hakala 2006). However, because of the low productivity of the watersheds that brook trout often occupy in Appalachia and elsewhere, factors other than reproductive success may be important in sustaining and expanding existing populations.

Throughout eastern North America, brook trout are often restricted to headwater watersheds that are naturally infertile. As a result, trout in these watersheds may be subjected to prolonged periods of poor feeding conditions (Cada et al. 1987; Ensign et al. 1990; Forrester et al. 1994), and food abundance may affect trout production (Clarke and Scruton 1999). Such episodes of reduced feeding usually occur during summer when aquatic insect activity is relatively low, although other seasons may present poor foraging opportunities (Sweka and Hartman 2001). Although poor feeding has

Received 22 February 2006. Accepted 2 August 2006. Published on the NRC Research Press Web site at http://cjfas.nrc.ca on 25 November 2006.
J19187

R.M. Utz[1,2] **and K.J. Hartman.** WVU Wildlife and Fisheries Resources Program, Division of Forestry and Natural Resources, Davis College of Agriculture, Forestry, and Consumer Sciences, 320 Percival Hall, Morgantown, WV 26506-6125, USA.

[1] Corresponding author (e-mail: rutz@al.umces.edu).
[2] Present address: University of Maryland Appalachian Laboratory, 301 Braddock Road, Frostburg, MD 21532, USA.

doi:10.1139/F06-152

not been shown to reduce populations under normal conditions, severe summer drought may cause environmental conditions to deteriorate (Hakala and Hartman 2004) along with decreasing foraging rates, potentially resulting in mortality.

A growing body of evidence suggests that lotic salmonids operate under density-dependent processes, which has implications for feeding success. Fish density has been shown to affect growth (Vøllestad et al. 2002; Imre et al. 2004; Lobón-Cerviá 2005) in that fish occupying reaches of streams with less fish per unit area experienced significantly higher growth rates in both natural and simulated settings. The territorial nature of salmonids likely drives this relationship. Density has been found to be positively correlated with emigration and mortality as a result of competitive interactions (Nakano 1995; Imre et al. 2004). Multiple studies have concluded that brook trout may be highly mobile (Gowan and Fausch 1996; Petty et al. 2005). The ability to move coupled with the poor nature of high-density locations suggests that movement into low-density areas should be beneficial. Large adult brook trout have been shown to prefer larger reaches of streams where fish density is typically low (Petty et al. 2005). However, observational data pertaining to energy intake at the watershed scale for stream salmonids remain sparse in the literature.

The concept that feeding intensity may be related to spatial variables has been established for salmonids with the general conclusion that larger bodies of water offer greater feeding potential (Keeley and Grant 2001). However, the extent at which this relationship exists within small watersheds remains to be described with detail. The relationship between density, watershed position, and feeding intensity may be of particular importance in eastern brook trout streams where food resources are often sparse. An understanding of temporal change in feeding intensity at the watershed scale may provide insight into how brook trout use different reaches of habitat to acquire energy. The recent development of a bioenergetics model for brook trout (Hartman and Sweka 2001) facilitates the calculations of a number of feeding variables, including daily ration and maintenance ration. In the current study, we sought to explain how consumption changes temporally and spatially by monitoring the energetic intake of a brook trout population throughout a headwater watershed over the course of two years.

Fig. 1. The upper Middle Fork watershed and all sites described for this study.

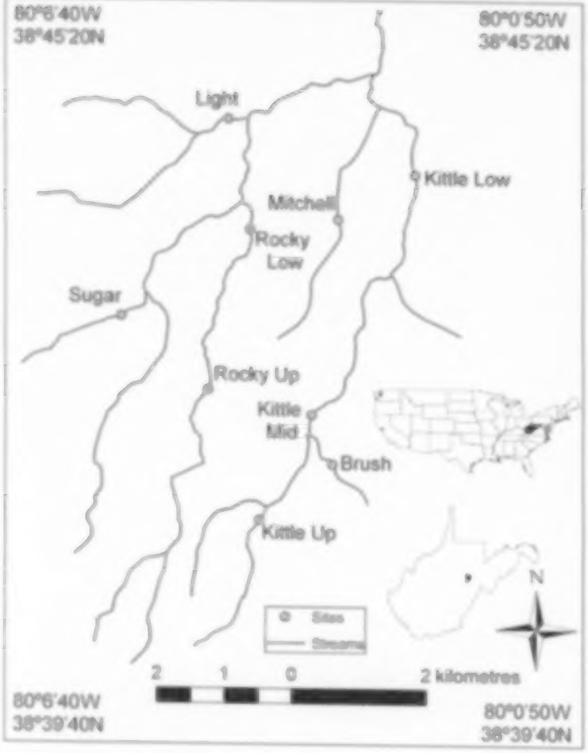

Materials and methods

Study area

This study was conducted within the Middle Fork watershed, a north-flowing tributary of the Tygart River in the central Appalachian Mountains of Randolph County, West Virginia (Fig. 1). Most land cover within the watershed is that of secondary-growth hardwood deciduous forest. All sites in the study are located in the southernmost part of the watershed and are of low order and high gradient. We chose nine 200 m sites encompassing a range of stream sizes (Table 1). All sites met the following criteria: each contained brook trout, consistently held age-0 brook trout (indicating water quality was sufficient for spawning), and was devoid of fish barriers between other sites. Temperature regimens in these reaches are suitable for trout as temperatures rarely exceeded 20 °C through the duration of the study, determined by analysis of temperature logger data conducted for the current and previous studies. The West Virginia Division of Natural Resources (WVDNR) and the West Virginia Department of Environmental Protection have actively added limestone sand to riparian areas of streams within the watershed to remediate the effects of acid precipitation and acid mine drainage in the Middle Fork since the 1990s (WVDNR 2001). This process is commonly used in the region and successfully increases pH, restores fish communities, and increases invertebrate abundance (Clayton et al. 1998), though invertebrate productivity and diversity may not reach preacidification levels following treatment (McClurg 2004). Some sites selected in this study were not actively treated with lime. However, each site without a limestone treatment retained the ability to support brook trout spawning and carry fish populations. To quantify water quality in each site, water samples were taken in February, May, July, and October 2004 and tested for pH and alkalinity in a laboratory at the WVDNR office in Elkins, West Virginia. The means of both measurements were calculated for each site based on the four seasonal measurements; this calculation provided an estimate of average water quality across seasons.

Fish diversity differed across sites but was typical of Appalachian headwater streams. The number of species encountered increased with stream size. In nearly all sites, fish fauna was dominated by brook trout and mottled sculpin (*Cottus bairdii*). Other fish sampled include blacknose dace

Table 1. Physical features and number of fish species encountered for each site in the Middle Fork River watershed.

Site name	Stream	Limed (Y/N)	Stream class	Basin area (km^2)	Mean wetted width (m)	Mean bankful width (m)	Mean pH	Mean alkalinity (mg·L^{-1})	Observed fish species
Brush	Brush Run	N	Upstream	0.83	1.46	3.97	5.17	1.38	1
Kittle Low	Kittle Creek	Y	Downstream	15.38	4.77	9.36	6.27	6.30	8
Kittle Mid	Kittle Creek	Y	Midstream	5.26	2.44	5.89	6.30	5.33	4
Kittle Up	Kittle Creek	Y	Upstream	2.05	2.19	3.98	6.73	15.78	2
Light	Light Run	N	Midstream	5.24	3.13	7.07	6.04	3.60	4
Mitchell	Mitchell Lick Fork	Y	Upstream	1.78	2.08	5.02	6.25	6.25	1
Rocky Low	Rocky Run	Y	Downstream	9.94	4.36	7.98	5.51	2.08	7
Rocky Up	Rocky Run	Y	Midstream	6.44	3.76	9.14	5.42	1.68	1
Sugar	Sugar Drain	N	Upstream	1.64	2.42	5.36	6.47	8.05	2

Note: The column titled "Limed" refers to whether or not (yes (Y) or no (N)) an active limestone treatment site existed above the site reach. If the site was not limed, water quality in the study reach retained the ability to hold young-of-the-year brook trout (*Salvelinus fontinalis*).

(*Rhynichthys obtusus*), longnose dace (*Rhynichthys cataractae*), creek chub (*Semotilus atromaculatus*), white sucker (*Catostomus commersonii*), northern hog sucker (*Hypentelium nigricans*), and fantail darter (*Etheostoma flabellare*).

Fish and stream size sampling

Fish sampling occurred 11 times over the course of two years (Table 2). Sampling was conducted between 0800 and 1600, and the order of sites to sample was randomly chosen during each day. A three-pass depletion electrofishing procedure (Platts and Nelson 1988) was used to estimate fish populations within each 200 m section. Before sampling, block nets were placed at the upstream and downstream ends of each section to restrict fish movement into or out of sections during sampling. Sampling teams used an electrofishing unit (DC, 60 hz, 500–750 V; Smith-Root, Vancouver, Washington) and dip nets to capture fish. Temperatures needed for bioenergetics modeling were recorded during fish sampling using an electronic thermometer.

Following collection, fish were processed at a streamside station. All fish were immobilized with a solution of clove oil and 95% ethanol. Brook trout were weighed to the nearest 0.5 g, and total length was taken to the nearest millimetre. We chose a subset of 10 brook trout per site per month for stomach content removal. Only fish > 110 mm fork length (FL) were considered eligible for gut content removal because of gear restrictions; the gape of fish below this size was usually about the same size of the flushing tube diameter (7 mm). This size class generally represented age-1+ fish, which was apparent in length-frequency histograms (Utz 2005). An attempt was made to collect an equal range of fish sizes to analyze for gut contents at each site; aside from this, fish were chosen randomly. Stomach contents were removed by directing a constant flow of stream water into the foregut (Twomey and Giller 1990). Gut items were filtered through a 250 µm sieve and transferred to 95% ethanol, a process that has proven effective (Light et al. 1983; Sweka 2003). All fish other than trout were counted and weighed. Each fish was allowed to recover from the clove oil treatment and returned to the stream reach within 2 h. A sample of 10 trout, selected for gastric lavage, was randomly collected from sites, frozen, and kept for dry weight analysis during four select sampling periods. This resulted in a removal of 40 fish during the entire course of the study. Brook trout dry weights were needed to estimate fish energy density, a necessary component of bioenergetics modeling.

To determine if fish density was related to consumption at the watershed scale, select habitat variables were calculated at each site. Habitat measurements within each site were recorded during base flow on 17 August 2005. Variables were measured on each 200 m reach of stream. Habitat units within each site were classified as riffle or pool, and the length of each unit was measured. Within each habitat unit, the wetted width and bankful width were taken along a linear transect perpendicular to the stream. The number of transects measured within a habitat unit depended on the length of the unit, with measurements made approximately every 20 m in riffles and every 2 m in pools. Pools were more represented than riffles in mean width estimation because of the tendency for large adults to use this habitat; however, riffles and pools did not differ markedly in widths.

Table 2. Middle Fork River brook trout (*Salvelinus fontinalis*) sampling start and end dates and mean temperatures at all sites for each month.

Sampling period	Start date	End date	Mean temperature (°C)	Designated season
March 2004	13 March	20 March	5.3	Winter
May 2004	5 May	12 May	11.0	Spring
June 2004	13 June	16 June	15.9	Spring
July 2004	16 July	19 July	16.2	Summer–fall
August 2004	16 August	18 August	18.0	Summer–fall
September 2004	24 September	26 September	14.4	Summer–fall
December 2004	2 December	5 December	5.2	Winter
March 2005	12 March	18 March	2.6	Winter
May 2005	9 May	11 May	12.5	Spring
June 2005	9 June	11 June	15.4	Spring
July 2005	12 July	13 July	16.9	Summer–fall

The basin area (km^2) of each site was determined using coordinates derived from a global positioning system at the midpoint of each site and calculated using geographic information systems (GIS).

Laboratory procedures

All prey items were identified to family or the lowest taxonomic classification possible (Merritt and Cummins 1996; Borror et al. 1989) to quantify prey exploitation by frequency and energy. Extremely small (<0.5 mm) organisms or organisms partially destroyed beyond identification to family were classified to order. The lengths of prey items were measured (to estimate dry weight) via an ocular micrometer to the nearest 0.1 mm; when lengths were unavailable, head capsule widths were measured to the nearest 0.1 mm. Crayfish (*Cambarus bartoni*) carapace lengths were measured rather than head capsule width or body length. The dry mass of each organism was estimated using published length or head width to dry mass equations, with the exception of crayfish where a carapace to dry mass equation was used (Sample et al. 1993; Benke et al. 1999; Johnston and Cunjak 1999; Sabo et al. 2002). Vertebrate food items such as frogs, salamanders, and fish were dried at 60 °C for 48 h to calculate dry weight. Frozen brook trout were thawed, weighed to the nearest 0.1 g, and dried at 60 °C for 72 h to calculate percent dry weight used in energy density analysis.

Estimates of consumption and daily ration

Estimates of consumption and maintenance ration were calculated to determine seasonal and spatial variation in energy intake. Comparing estimated consumption with maintenance ration determines if fish are obtaining enough energy to maintain body weight. Estimated maintenance rations (EMR, in joules per gram fish wet weight per day) were calculated based on a bioenergetics model for brook trout (Hartman and Sweka 2001) using fish weight, fish energy density, and observed water temperature (taken with an electronic thermometer streamside during sampling) as variables. Maintenance ration was determined by calculating the energy required to obtain *zero* weight growth over the course of a day. This calculation was conducted for each fish over 110 mm FL (i.e., the size range of fish targeted for diets). Brook trout energy densities were calculated from observed mean energy density in collected fish using a Salmonidae dry weight – energy equation (Hartman and Brandt 1995) and were interpolated from energy densities taken before and after a given collection period. Mean fish energy density was assumed equal across sites during a given month. Consumption estimates were calculated based on a model proposed by Eggers (1977). Each prey item was converted to energy using published dry weight – energy equations based on taxonomy and life stage (Cummins and Wuycheck 1971), and the total energy in the gut was summarized for each fish.

The total energy intake was multiplied by the brook trout gastric evacuation rates (based on temperature; Sweka et al. 2004) and divided by fish weight to calculate an observed consumption value ($J \cdot g^{-1}$ $fish \cdot h^{-1}$) as suggested by Eggers (1977). This estimate was multiplied by 24 to convert it to a daily ration. The mean daily consumption estimates in this study were based on stomach contents obtained during the daylight hours only. Though daily consumption typically requires estimates of feeding activity across a diel cycle (Bowen 1996), multiple studies of indigenous brook trout feeding trends revealed no significant diel pattern (Forrester et al. 1994; Sweka 2003; Mookerji et al. 2004). Further, the evacuation rate of brook trout has proven to be low relative to that of other salmonids (Sweka et al. 2004), meaning that food items remain in the gut long after they have been ingested. Thus the current study made the assumption that a measurement of diet during daylight hours provided sufficient data to calculate daily ration.

Statistical procedures

We calculated population estimates in each site per month and all sites combined per month to determine population change, estimate fish density, and allow comparison of consumption and population variables. Population estimates were calculated for each stream using the depletion process of Zippin in the program CAPTURE (White et al. 1982). If fewer than 30 fish were captured, then the actual number of fish caught was substituted for an estimate (Riley and Fausch 1992). Fish density per site was calculated as the population estimate divided by the wetted area (m^2) at base flow. Although densities were determined via monthly fish populations and one estimate of wetted area per site, we assumed that wetted width estimates among sites would change proportionally to each other over time. This assumption was based on the close proximity of all sites, with a high likelihood that the watersheds are subject to identical climatic conditions. In addition to calculating fish populations and density, we calculated percent habitat saturation (PHS) as an estimate of fish abundance (Grant et al. 1998). We found this variable to be desirable because it incorporates fish size, fish density, and territorial requirements for individual fish, resulting in a single number that considers all variables potentially affecting density-dependent processes. PHS was calculated using the equations derived by Grant and Kramer (1990):

$$\mathrm{PHS} = \sum DT \times 100$$

where D is the density (number·m^{-2}) of fish and T is territory size (m^2), which was calculated using the following equation derived for salmonids similar in size to those encountered in the current study: log(territory size) = 2.61log(FL (cm)) − 2.83. Because we recorded total length in the field, we first converted total length to FL using the equation FL = total length/1.0326 (Carlander 1969).

For analysis of consumption by site, each site was placed into one of three classes (upstream, midstream, or downstream; see Table 1) based on similarities in basin area, trout density, wetted width, and other fish species present. Early analyses showed that each month could be classified into one of three broad seasons (winter, spring, and summer–fall; see Table 2) by means of similarities in temperature and consumption; each season was analyzed separately. Consumption estimates were first square root transformed to approximate normality. Because differences existed in fish size and temperature (at time of sampling) among sites, we tested for the effects of these variables on consumption first (as continuous variables) when testing for differences in consumption rates among sites. If fish size (i.e., weight) or temperature was found to be linearly related to consumption at the $\alpha = 0.05$ level, the variable was retained. Differences in square root transformed consumption estimates across stream classes within each season were tested using analysis of covariance (ANCOVA) if weight or temperature was significant (analysis of variance, ANOVA, if neither weight nor temperature entered the model) and Duncan's repeated-measures test post hoc. Interaction effects were included if weight or temperature entered into the model. For all ANCOVA and ANOVA models, the type III sum of squares was analyzed. If site class did influence consumption, potential relationships between PHS and mean consumption estimates were explored. Nonlinear relationships were considered to test for best fit during these analyses by plotting both original and log-transformed variables. All statistical and analytical procedures were completed using PROC GLM and PROC REG in SAS® 9.1 (SAS Institute Inc. 2003).

Results

Consumption and seasonal change

A total of 939 brook trout was sampled for stomach contents throughout the course of the study, yielding mean estimates of consumption on monthly and seasonal intervals. Brook trout consumption varied significantly throughout the year (Fig. 2). Middle Fork brook trout appeared to exceed metabolic demands only during select seasons. Mean consumption during all spring months was significantly higher than maintenance ration. Only marginal differences were observed between consumption and maintenance ration during the summer or fall. Maintenance ration estimates were higher than mean observed consumptions for both March samples. Despite low consumption estimates during certain months, the number of fish encountered with no food items retrieved was small, with a high of 10 fish in August 2004 and between 0 and 4 fish during all other months. Fish with empty stomach were included in all analyses.

Although comparisons between consumption and maintenance rations suggest that fish were meeting metabolic demands, this mean was elevated by a minority of fish feeding exceptionally well. The distribution of consumption values during each season was skewed to the right, where a minority of individuals consumed a disproportionately large amount of energy relative to the mode (Fig. 3).

Consumption and watershed position

Throughout the year, brook trout density was significantly correlated with watershed position. Trout density was negatively correlated with basin area at the log–log scale ($F = 51.14$, $n = 26$, $p < 0.0001$; Fig. 4).

The location of fish collection seemed to affect feeding conditions. During each of the three seasons, significant differences in consumption were apparent among positions in the watershed, despite differences in fish size or temperature among site classifications (Table 3). Fish size alone was never significantly related to consumption; however, temperature was retained in the model during spring and winter. The interaction of watershed location and temperature, rather than temperature alone, was significantly related to consumption during spring once the full model was explored. In winter, temperature, rather than an interaction effect, was significantly related to consumption estimates. During summer, only watershed location significantly explained variation in consumption estimates. With the exception of winter, site location explained the majority of variation in consumption estimates among sites. Fish in upstream locations consumed significantly less energy than fish occupying downstream and midstream reaches during spring and summer (Table 4). The trend shifted in winter, with upstream consumption significantly greater than mid-order reaches, but not downstream reaches.

Each season was tested separately for an effect of trout PHS on mean consumption. No relationship was found between the two variables during spring or winter (Fig. 5). However, during the summer–fall season, a significant negative nonlinear relationship existed between mean consumption and PHS ($F = 20.41$, $n = 9$, $p = 0.0027$).

Discussion

The relationship detected between watershed position and energy intake highlights the importance of watershed position in successful feeding. With the exception of winter, fish occupying upstream sites fed at significantly lower rates than fish at other sites. During winter, however, temperatures

Fig. 2. Mean (±95% confidence intervals) monthly estimated maintenance ration (open bars) and observed consumption values (shaded bars) across all sites.

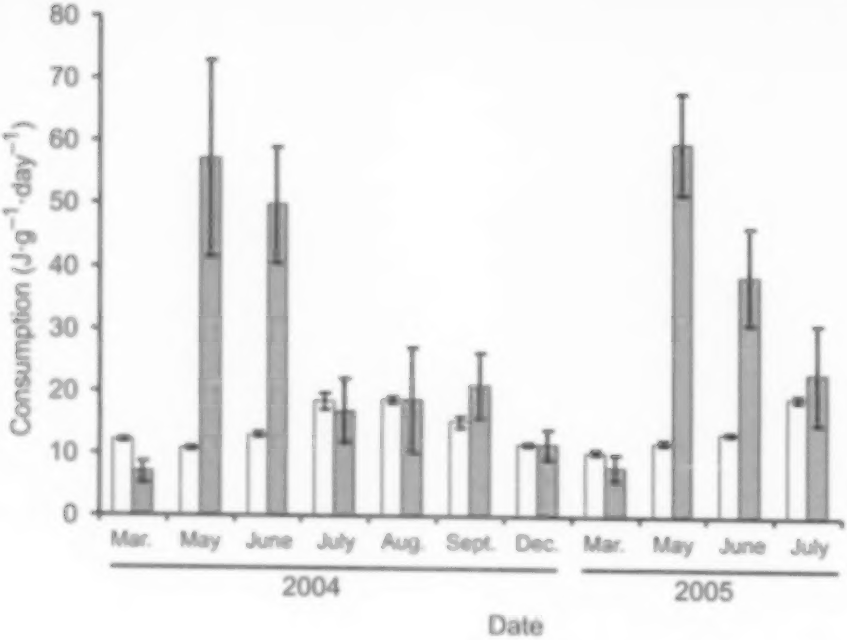

were low and metabolic costs were correspondingly low. Therefore, poor feeding conditions existed in upstream sites during the most critical seasons regarding temperature (spring through fall). An absence of a relationship between PHS and mean consumption during the spring could have been attributed to the abundant food resources available during that season, as territory size may shrink during periods of abundant food resources (Grant et al. 1998). During the summer–fall, however, a direct relationship was detected between PHS and consumption. Therefore, during the season of greatest metabolic costs and lowest food resources (Cada et al. 1987; Ensign et al. 1990; Utz 2005), fish density was particularly important in determining mean energy intake. These findings imply that density-dependent processes or differences in food abundance by site regulate feeding in Appalachian brook trout during certain times of the year.

A number of studies have recently confirmed density-dependent growth in lotic salmonids (Jenkins et al. 1999; Imre et al. 2004; Lobón-Cerviá 2005), a concept that is consistent with findings in the current study. Unfortunately, sufficient data to compare growth rates in our study were not available because of the likelihood that multiple shocking events would have affected growth (Dwyer and White 1995, 1997; Hughes 1998) and the low number of trout encountered in the downstream reaches disallowed sufficient estimates of mean growth. Our findings concur with those examining density-dependent growth, as higher rates of energy intake likely correspond to increased growth rates. Higher values of trout density imply that fish spend more time defending territories and less time foraging, resulting in decreased energy acquisition and (or) increased allocation of energy towards territory defense rather than growth (Elliot 1994; Nakano 1995; Steingrimsson and Grant 1999). Although density-dependent processes have been shown to appear at PHS values of ≥27% (Grant and Kramer 1990), we observed a relationship between mean consumption and PHS at values <27%. If density-dependent processes were occurring at relatively low densities in the Middle Fork watershed, this could have occurred because of lower food resources compared with those in Grant and Kramer (1990).

Alternatively, food abundance may have increased with stream size. Food resource abundance for salmonids typically increases with habitat volume (Keeley and Grant 2001), though few have examined this idea at the scale of a headwater watershed. No measures of food abundance were collected for this study. An attempt at calculating food abundance would be difficult at the large spatial and temporal scales, as well as the ability to quantify both aquatic and terrestrial food abundance. Further, brook trout tend to select for certain items in the drift and also feed on nondrifting prey (Sweka and Hartman 2001). Salmonids in watersheds similar to the Middle Fork have been found to derive most of their energy from terrestrial invertebrates (Forrester et al. 1994; Nakano et al. 1999; Hilderbrand and Kershner 2004*b*), as was the case in our study (Utz 2005). Riparian forest cover and composition in each of the sites were identical; therefore terrestrial insect biomass was likely similar among sites. The finding that temperature was occasionally significantly related to mean consumption among locations was not surprising; temperature is a primary component of the bioenergetics model for brook trout. However, differences in temperature on a larger temporal scale do not likely affect

Fig. 3. Distributions of daily ration estimates by season for (*a*) spring, (*b*) summer and fall, and (*c*) winter. Bars are in increments of five. Solid bars represent estimates above mean maintenance ration for the corresponding season, shaded bars represent estimates below mean maintenance ration, and open bars represent the number of fish either slightly above or slightly below mean maintenance ration.

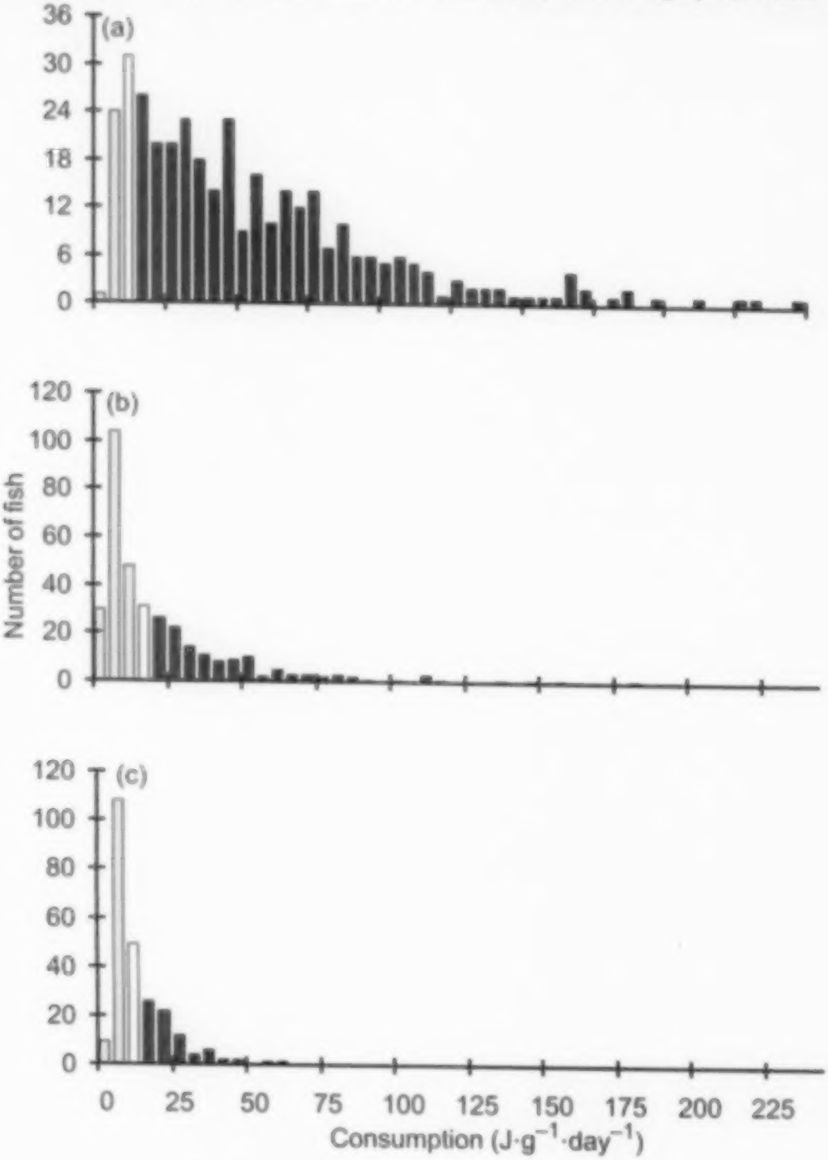

consumption rates at the same scale. Long-term temperature profiles among sites were nearly identical over the course of the study (Utz 2005).

A potential mechanism explaining greater consumption downstream is that of increased piscivory, as fish typically provide more energy than invertebrates (Jonsson et al. 1999; Neveu 1999; Keeley and Grant 2001). Piscivory was rarely encountered in the Middle Fork watershed (n = 19 out of 939 observed fish), though the highest rate was observed at the largest site (Kittle Creek-Low, n = 11). Regardless of whether the trends observed in the Middle Fork were driven by trout density or food abundance, feeding conditions improved with increasing stream size.

The notion that stream-dwelling salmonids, including brook trout in eastern North America (Rodriguez 2002; Logan 2003; Petty et al. 2005), are highly mobile (Gowan et al. 1994; Gowan and Fausch 1996, 2002), as well as the propensity for large adults to seek large reaches of streams, suggests that a proportion of the population may move to seek food resources. Few studies have shown this to be the case

Fig. 4. Fish densities as a function of basin area across all seasons: solid diamonds, summer estimates; shaded triangles, winter estimates; and open squares, spring estimates.

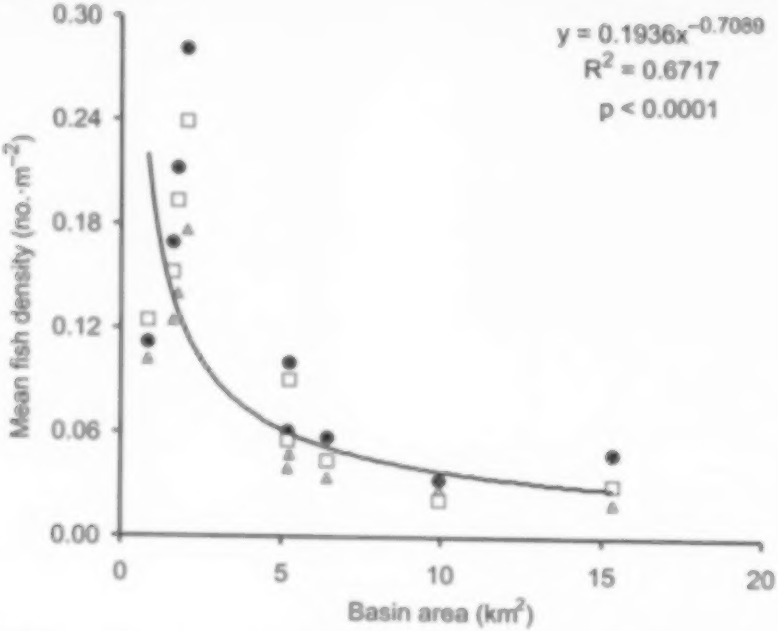

Table 3. Model parameters of the analysis of variance (ANOVA) or analysis of covariance (ANCOVA) models run on square root transformed mean consumption by watershed location (i.e., downstream, midstream, upstream) for each season.

Effect	df	*F* value	*p*
Spring			
Overall model	4	8.68	<0.0001
Watershed location	2	10.37	<0.0001
Temperature	1	3.28	0.0709
Site type × temperature	2	8.44	0.0003
Summer–fall			
Watershed location	2	13.57	<0.0001
Winter			
Overall model	4	6.93	<0.0001
Watershed location	2	3.32	0.0380
Temperature	1	6.40	0.0121
Site type × temperature	2	2.69	0.0699

Table 4. Post-hoc analysis of the analysis of variance (ANOVA) or analysis of covariance (ANCOVA) models on mean consumption by watershed location for each season.

Stream classification	Mean consumption ($J\cdot g^{-1}\cdot day^{-1}$)	Standard error
Spring		
Downstream	58.03a	5.47
Midstream	62.95a	6.01
Upstream	39.42b	3.01
Summer–fall		
Downstream	24.88a	2.60
Midstream	25.74a	3.50
Upstream	13.13b	2.43
Winter		
Downstream	8.89a	1.38
Midstream	5.61b	0.79
Upstream	11.12a	1.03

Note: Means with different letters within a season are significantly different (following a square root transformation) at the $\alpha = 0.05$ level using Duncan's repeated-measures test.

within a headwater watershed. The trends documented in the current study together with the distributional patterns observed in the Shaver's Fork watershed (Petty et al. 2005) suggest that although spawning areas are essential for brook trout abundance, larger reaches of streams with lower trout densities are important in providing improved feeding and growth conditions. However, these concepts must be considered with caution, as other factors may contribute to the tendency for individual fish to move.

Salmonids in lotic environments that undergo movement invoke an energetic cost and other potential risks. As a result, some studies (Naslund et al. 1993; Gowan and Fausch 1996) suggested that mobile trout were in poorer condition than resident trout. However, movement from areas as a result of poor feeding conditions does occur (Wilzbach 1985; Nakano 1995), and in some cases, mobile trout have been shown to be in better condition than the population average (Hilderbrand and Kershner 2004*a*). In addition to the energetic costs of movement, an individual choosing to move downstream may risk higher rates of predation in the form of angling.

Fig. 5. Mean consumption as a function of percent habitat saturation (PHS) by site for (*a*) spring, (*b*) summer and fall, and (*c*) winter. Vertical bars represent 95% confidence intervals. Lines were fitted when the relationship between variables was significant at the α = 0.05 level.

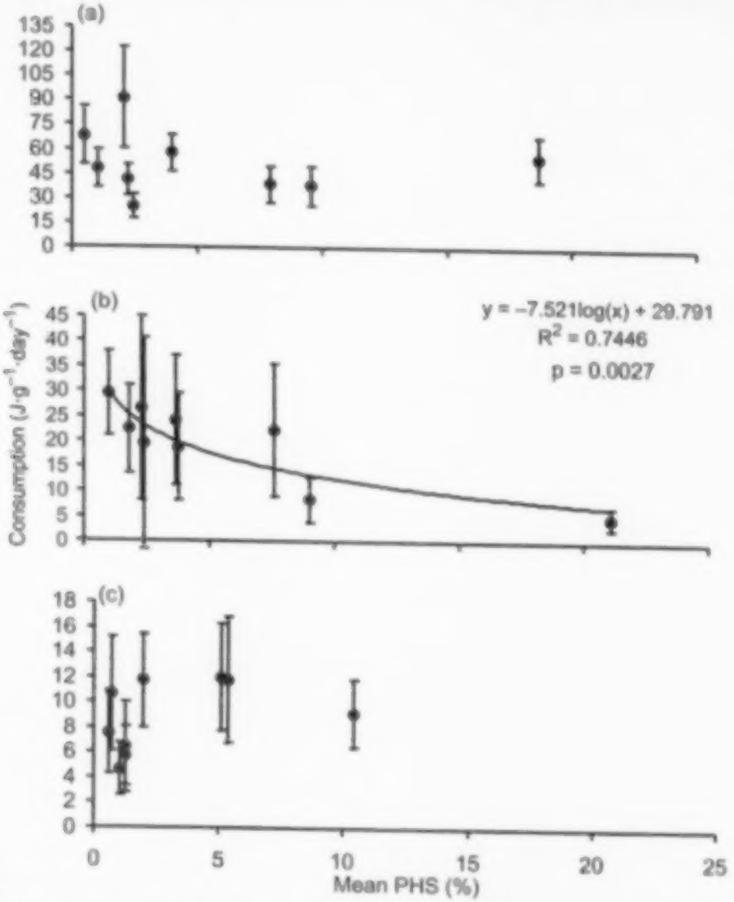

Trends in these data differ somewhat from those of other studies that have observed mean daily ration significantly below maintenance levels during the summer; a lack of such a finding in our study may be attributed to a minority of fish feeding at very high levels when resources were low. Mean estimated daily ration fell below maintenance ration only during winter months. Limitations in summer food intake have previously been inferred or observed in Appalachian salmonids. Cada et al. (1987), Ensign et al. (1990), and Thorne (2004) observed a substantial drop in the number of items and (or) mean stomach content weight found in brook trout stomachs from spring to summer in populations of Appalachian salmonids. Ensign et al. (1990) found that the drop in brook trout consumption was calculated below maintenance ration. Such low food intake was similar to summer rates of the current study, yet our fish consistently attained maintenance ration on average. One potential explanation may be our sampling of a large number of fish per season, which captured the data of a minority of fish that fed exceptionally well.

Environmental conditions for brook trout may be highly variable between years because of drought and flooding (Carline and McCullough 2003; Hakala and Hartman 2004). The summers in the current study were not particularly severe, and it is likely that consumption values during drought years would drop below those observed in this study. Of particular importance is the finding in this study that a minority of fish feeding on large or abundant organisms during the summer elevated the mean consumption estimate of the fish population. Therefore, chance encounters with large prey items may be critical in maintaining brook trout through stressful periods.

Though this study examined the feeding dynamics of brook trout within a single watershed in central Appalachia, the findings of this study are likely applicable to populations of brook trout elsewhere and stream-dwelling salmonids in general. Brook trout populations are often confined to similar-sized, unproductive watersheds throughout their range, including the upper midwestern United States (Zorn et al. 2002), eastern Canada (Clarke and Scruton 1999), and the southern Appalachians, where brook trout populations are critically threatened (Habera and Moore 2005). Further, food resources may limit brook trout production in such watersheds outside of Appalachia (Clarke and Scruton 1999).

Trout populations other than brook trout may be isolated into headwater watersheds by anthropogenic impacts, such as cutthroat trout in western North America (Hilderbrand 2003). If density dependence plays a role in trout feeding capacity as suggested here, applying our results to other trout species may allow insight into the restoration and maintenance of threatened populations.

The intense regimen of electrofishing (monthly in some periods) may have had an effect on individual fish, as growth and short-term behavior are usually affected by the process (Dwyer and White 1995, 1997; Hughes 1998). However, electrofishing effects at the population level have not been observed (Kocovsky et al. 1997). Variables critical to the current study, such as movement or feeding behavior, were not affected by electrofishing when examined in other salmonids (Twomey and Giller 1990; Dunham et al. 2002). An inability of gastric lavage to remove all contents in the gut is another potential source of error. However, previous examinations of gear efficiency for the gear used in this study showed that little to no contents remain after a thorough lavage (Sweka 2003). Further, the items that potentially remain in the gut despite lavage are likely smaller organisms (as larger organisms can be detected outside of the fish) that would not dramatically affect consumption estimates.

Movement downstream by Middle Fork brook trout from areas of high population density to areas of low population density appears to increase foraging success. In systems where food may be potentially limiting, as in the Middle Fork and elsewhere in the brook trout range, migration to downstream reaches may be particularly important. Future management decisions concerning the rehabilitation of brook trout populations will need to consider the spatial heterogeneity of habitats within a watershed. Although small, alkaline streams are crucial for spawning, larger-order reaches of streams provide significantly better feeding conditions than the smaller streams where rearing occurs. Barriers and risks associated with movement into these larger stream reaches, such as acid mine drainage and high angling mortality, may prevent brook trout from exploiting more productive areas in a watershed.

Acknowledgements

The authors thank Brett Moore for his extensive field and laboratory assistance and Ken Sheehan for assistance with illustrations. This study was funded by Mead-Westvaco, the West Virginia Division of Natural Resources, and the United States Department of Agriculture Forest Service's Monongahela National Forest and Northeastern Experiment Station. Care and handling of all fish was completed in accordance with approved protocols filed with the West Virginia University Animal Care and Use Committee.

References

Benke, A.C., Huryn, A.D., Smock, L.A., and Wallace, J.B. 1999. Length–mass relationships for freshwater macroinvertebrates in North America with particular reference to the southeastern United States. J. North Am. Benthol. Soc. **18**: 308–343.

Borror, D.J., Triplehorn, C.A., and Johnson, N.F. 1989. An introduction to the study of insects. 6th ed. Saunders College Publishers, Fort Worth, Texas.

Bowen, S.H. 1996. Quantitative description of the diet. *In* Fisheries techniques. 2nd ed. *Edited by* B.R. Murphy and D.W. Willis. American Fisheries Society, Bethesda, Md. pp. 513–529.

Cada, G.F., Loar, J.M., and Sale, M.J. 1987. Evidence of food limitation of rainbow and brown trout in southern Appalachian soft-water streams. Trans. Am. Fish. Soc. **116**: 692–702.

Carlander, K.D. 1969. Handbook of freshwater fishery biology. Vol. 1. Iowa State University Press, Ames, Iowa.

Carline, R.F., and McCullough, B.J. 2003. Effects of floods on brook trout populations in the Monongahela National Forest, West Virginia. Trans. Am. Fish. Soc. **132**: 1014–1020.

Clarke, K.D., and Scruton, D.A. 1999. Brook trout production dynamics in the streams of a low fertility Newfoundland watershed. Trans. Am. Fish. Soc. **128**: 1222–1229.

Clayton, J.L., Dannaway, E.S., Menendez, R., Rauch, H.W., Renton, J.J., Sherlock, S.M., and Zurbuch, P.E. 1998. Application of limestone to restore fish communities in acidified streams. Am. J. Fish. Manag. **18**: 347–360.

Cummins, K.C., and Wuycheck, J.C. 1971. Caloric equivalents for investigations in ecological energetics. Mitt. Int. Ver. Theor. Angew. Limnol. **18**: 1–158.

Dunham, K.A., Stone, J., and Moring, J.R. 2002. Does electrofishing influence movements of fishes in streams? Experiments with brook trout (*Salvelinus fontinalis*). Fish. Manag. Ecol. **9**: 249–251.

Dwyer, W.P., and White, R.G. 1995. Influence of electroshock on short-term growth of adult rainbow trout and juvenile Arctic grayling and cutthroat trout. N. Am. J. Fish. Manag. **15**: 148–151.

Dwyer, W.P., and White, R.G. 1997. Effect of electroshock on juvenile Arctic grayling and Yellowstone cutthroat trout growth, 100 days after treatment. N. Am. J. Fish. Manag. **17**: 174–177.

Eggers, D.M. 1977. Factors in interpreting data obtained by diel sampling of fish stomachs. J. Fish. Res. Board Can. **34**: 290–294.

Elliot, J.M. 1994. Quantitative ecology and the brown trout. Oxford University Press, Oxford.

Ensign, W.E., Strange, R.J., and Moore, S.E. 1990. Summer food limitation reduces brook and rainbow trout biomass in a southern Appalachian stream. Trans. Am. Fish. Soc. **119**: 894–901.

Forrester, G.E., Chace, J.G., and McCarthy, W. 1994. Diel and density-related changes in food consumption and prey selection by brook charr in a New Hampshire stream. Environ. Biol. Fishes, **39**: 301–311.

Gowan, C., and Fausch, K.D. 1996. Mobile brook trout in two high-elevation Colorado streams: re-evaluating the concept of restricted movement. Can. J. Fish. Aquat. Sci. **53**: 1370–1381.

Gowan, C., and Fausch, K.D. 2002. Why do foraging stream salmonids move during summer? Environ. Biol. Fishes, **64**: 139–153.

Gowan, C., Young, M.K., Fausch, K.D., and Riley, S.C. 1994. Restricted movement in resident stream salmonids: a paradigm lost? Can. J. Fish. Aquat. Sci. **51**: 2626–2637.

Grant, J.W.A., and Kramer, D.L. 1990. Territory size as a predictor of the upper limit to population density of juvenile salmonids in streams. Can. J. Fish. Aquat. Sci. **47**: 1724–1737.

Grant, J.W.A., Steingrimsson, S.O., Keeley, E.R., and Cunjak, R.A. 1998. Implications of territory size for the measurement and prediction of salmonid abundance in streams. Can. J. Fish. Aquat. Sci. **55**(Suppl. 1): 181–190.

Habera, J., and Moore, S. 2005. Managing southern Appalachian brook trout: a position statement. Fisheries, **30**(7): 10–20.

Hakala, J.P., and Hartman, K.J. 2004. Drought effect on stream morphology and brook trout (*Salvelinus fontinalis*) populations in forested headwater streams. Hydrobiologia, **515**: 203–213.

Hartman, K.J., and Brandt, S.B. 1995. Estimating energy density of fish. Trans. Am. Fish. Soc. **124**: 347–355.

Hartman, K.J., and Hakala, J.F. 2006. Relationships between fine sediment and brook trout recruitment in forested headwater streams. J. Freshw. Ecol. **21**: 215–230.

Hartman, K.J., and Sweka, J.A. 2001. Development of a bioenergetics model for Appalachian brook trout. Proc. Annu. Conf. Southeast. Assoc. Fish. Wildl. Agencies, **55**: 38–51.

Hilderbrand, R.H. 2003. The roles of carrying capacity, immigration, and population synchrony on persistence of stream-resident cutthroat trout. Biol. Conserv. **110**: 257–266.

Hilderbrand, R.H., and Kershner, J.L. 2004*a*. Are there differences in growth and condition between mobile and resident cutthroat trout? Trans. Am. Fish. Soc. **133**: 1042–1046.

Hilderbrand, R.H., and Kershner, J.L. 2004*b*. Influence of habitat type on food supply, selectivity, and diet overlap of Bonneville cutthroat trout and nonnative brook trout in Beaver Creek, Idaho. N. Am. J. Fish. Manag. **24**: 33–40.

Hughes, N.F. 1998. Reduction in growth due to electrofishing and tagging may change interannual movement behavior of stream salmonids: evidence from Arctic grayling in an interior Alaskan stream. Trans. Am. Fish. Soc. **127**: 1072–1077.

Imre, I., Grant, W.A., and Keeley, E.R. 2004. The effect of food abundance on territory size and population density of juvenile steelhead trout (*Oncorhynchus mykiss*). Oecologia, **138**: 371–378.

Jenkins, T.M., Diehl, S., Kratz, K.W., and Cooper, S.D. 1999. Effects of population density on individual growth of brown trout in streams. Ecology, **80**: 941–956.

Johnston, T.A., and Cunjak, R.A. 1999. Dry mass–length relationships for benthic insects: a review with new data from Catamaran Brook, New Brunswick, Canada. Freshw. Biol. **41**: 653–674.

Jonsson, N., Næsje, T.F., Jonsson, B., Saksgård, R., and Sandlund, O.T. 1999. The influence of piscivory on life history traits of brown trout. J. Fish Biol. **55**: 1129–1141.

Keeley, E.R., and Grant, J.W.A. 2001. Prey size of salmonid fishes in streams, lakes, and oceans. Can. J. Fish. Aquat. Sci. **58**: 1122–1132.

Kocovsky, P.M., Gowan, C., Fausch, K.D., and Riley, S.C. 1997. Spinal injury rates in three wild trout populations in Colorado after eight years of backpack electrofishing. N. Am. J. Fish. Manag. **17**: 308–313.

Larson, G.L., and Moore, S.E. 1985. Encroachment of exotic rainbow trout into stream populations of native brook trout in the southern Appalachian mountains. Trans. Am. Fish. Soc. **114**: 195–203.

Light, R.W., Adler, P.H., and Arnold, D. 1983. Evaluation of gastric lavage for stomach analyses. N. Am. J. Fish. Manag. **3**: 81–85.

Lobón-Cerviá, J. 2005. Spatial and temporal variation in the influence of density dependence on growth of stream-living brown trout (*Salmo trutta*). Can. J. Fish. Aquat. Sci. **62**: 1231–1242.

Logan, M.N. 2003. Brook trout (*Salvelinus fontinalis*) movement and habitat use in a headwater stream of the central Appalachian mountains of West Virginia. M.Sc. thesis, Division of Forestry, West Virginia University, Morgantown, W.V.

Marschall, E.A., and Crowder, L.B. 1996. Assessing population responses to multiple anthropogenic effects: a case study with brook trout. Ecol. Appl. **6**: 152–167.

McClurg, S.E. 2004. Stream ecosystem response to mitigative limestone treatment in acid impaired, central Appalachian streams. M.Sc. thesis, Division of Forestry, West Virginia University, Morgantown, W.V.

Merritt, R.W., and Cummins, K.W. 1996. An introduction to the aquatic insects of North America. 3rd ed. Kendall and Hunt, Dubuque, Iowa.

Mookerji, N., Weng, Z., and Mazumder, A. 2004. Food partitioning between coexisting Atlantic salmon and brook trout in the Sainte-Marguerite River ecosystem, Quebec. J. Fish Biol. **64**: 680–694.

Nakano, S. 1995. Individual differences in resource use, growth, and emigration under the influence of a dominance hierarchy in fluvial red-spotted masu salmon in a natural habitat. J. Anim. Ecol. **64**: 75–84.

Nakano, S., Miyasaka, H., and Kuhara, N. 1999. Terrestrial–aquatic linkages: riparian arthropod inputs alter trophic cascades in a stream food web. Ecology, **80**: 2435–2441.

Naslund, I., Milbrink, G., Eriksson, O., and Holmgren, S. 1993. Importance of habitat productivity differences, competition, and predation for the migratory behavior of Arctic charr. Oikos, **66**: 538–546.

Neveu, A. 1999. Feeding strategy of the brown trout (*Salmo trutta* L.) in running water. *In* Biology and ecology of the brown and sea trout. *Edited by* J.L. Bagliniere and G. Maisse. Springer, Chichester, UK. pp. 91–113.

Petty, J.T., Lamothe, P.J., and Mazik, P.M. 2005. Spatial and seasonal dynamics of brook trout populations inhabiting a central Appalachian watershed. Trans. Am. Fish. Soc. **134**: 572–587.

Platts, W.S., and Nelson, R.L. 1988. Fluctuations in trout populations and their implications for land-use evaluation. N. Am. J. Fish. Manag. **8**: 333–345.

Riley, S.C., and Fausch, K.D. 1992. Underestimation of trout population size by maximum-likelihood removal estimates in small streams. N. Am. J. Fish. Manag. **12**: 768–776.

Rodriguez, M.A. 2002. Restricted movement of stream fish: the paradigm is incomplete, not lost. Ecology, **83**: 1–13.

Sabo, J.L., Bastow, J.L., and Power, M.E. 2002. Length–mass relationships for adult aquatic and terrestrial invertebrates in a California watershed. J. North Am. Benthol. Soc. **21**: 336–343.

Sample, B.E., Cooper, R.J., Greer, R.D., and Whitmore, R.C. 1993. Estimation of insect bimass by length and weight. Am. Midl. Nat. **129**: 234–240.

SAS Institute Inc. 2003. SAS® 9.1 (computer software). SAS Institute Inc., Cary, North Carolina.

Steingrimsson, S.O., and Grant, J.W.A. 1999. Allometry of territory size and metabolic rate as predictors of self-thinning in young-of-the-year Atlantic salmon. J. Anim. Ecol. **68**: 17–26.

Sweka, J.A. 2003. Aquatic–terrestrial linkages in Appalachian streams: influence of riparian inputs on stream habitat, brook trout populations, and trophic dynamics. Ph.D. dissertation, Division of Forestry, West Virginia University, Morgantown, W.V.

Sweka, J.A., and Hartman, K.J. 2001. Influence of turbidity on brook trout reactive distance and foraging success. Trans. Am. Fish. Soc. **130**: 138–146.

Sweka, J.A., Cox, M.K., and Hartman, K.J. 2004. Gastric evacuation rates of brook trout. Trans. Am. Fish. Soc. **133**: 204–210.

Thorne, D.W. 2004. Spatial and seasonal variation in brook trout diet, growth, and consumption in a complex Appalachian watershed. M.S. thesis, West Virginia University, Morgantown, W.V.

Twomey, H., and Giller, P.S. 1990. Stomach flushing and individual Panjet tattooing of salmonids: an evaluation of the long-term effects on two wild populations. Aquacult. Fish. Manag. **21**: 137–142.

Utz, R.M. 2005. Temporal trends in consumption, growth, and successful feeding traits of a central Appalachian brook trout population at the watershed scale. M.S. thesis, West Virginia University, Morgantown, WV.

Vøllestad, V.A., Olsen, E.M., and Forseth, T. 2002. Growth-rate variation in brown trout in small neighbouring streams: evidence of density dependence? J. Fish Biol. **61**: 1513–1527.

White, G.C., Anderson, D.R., Burnham, K.P., and Otis, D.L. 1982. Capture–recapture and removal methods for sampling closed populations. Los Alamos National Laboratory, Los Alamos, New Mexico. LA-8787-NERP

Wigington, P.J., Jr., Baker, J.P., DeWalle, D.R., Kretser, W.A., Murdoch, P.S., Simonin, H.A., Van Sickle, J., McDowell, M.K., Peck, D.V., and Barchet, W.R. 1996. Episodic acidification of small streams in the northeast United States: episodic response project. Ecol. Appl. **6**: 374–388.

Wilzbach, M.A. 1985. Relative roles of food abundance and cover in determining the habitat distribution of stream-dwelling cutthroat trout (*Salmo clarki*). Can. J. Fish. Aquat. Sci. **42**: 1668–1672.

West Virginia Division of Natural Resources. 2001. Middle Fork River: limestone treatment of acid mine drainage. Wildlife Resources Section, West Virginia Division of Natural Resources, Elkins, West Virginia.

Zorn, T.G., Seelbach, P.W., and Wiley, M.J. 2002. Distribution of stream fishes and their relationship to stream size and hydrology in Michigan's lower peninsula. Trans. Am. Fish. Soc. **131**: 70–85.

Using zooplankton biomass size spectra to assess ecological change in a well-studied freshwater lake ecosystem: Oneida Lake, New York

Allison E. Gamble, Russ Lloyd, John Aiken, Ora E. Johannsson, and Edward L. Mills

Abstract: We explored the sensitivity of three descriptors of zooplankton size spectra (slope, periodic, and Pareto II models) to environmental changes in Oneida Lake, New York, and then used documented environmental changes to model the responses of zooplankton biomass using a general linear model. Using multiple regressions, we identified significant ecological events in Oneida Lake that could affect zooplankton biomass before actual model testing and assessed the three size spectrum models based on their sensitivity to these known variables. The intercept of the slope (linear regression) model was responsive to changes, but the slope was not. The periodic (quadratic) model showed no sensitivity in detecting ecological change. The Pareto II model (probability distribution function) demonstrated the most sensitivity to all ecological variables but was complex to model and there was no direct relationship between its parameters and biological events. The general linear model regression approach proved relatively sensitive to environmental change and had the added benefit of providing a graphical means of biologically assessing differences between years. In general, zooplankton biomass size spectra were responsive to changes in conditions in the Oneida Lake environment, and we believe that size-based approaches have potential as a biotic index in freshwater lake ecosystems.

Résumé : Nous avons examiné la sensibilité de trois descripteurs des spectres de taille du zooplancton (modèle de la pente et les modèles périodique et Pareto II) aux changements environnementaux au lac Oneida, New York; nous avons ensuite utilisé les changements environnementaux connus pour prédire à l'aide d'un modèle linéaire général les réactions de la biomasse du zooplancton. Avant de tester les modèles, nous avons identifié au moyen de régressions multiples les événements écologiques significatifs dans le lac Oneida qui pourraient affecter la biomasse du zooplancton; nous avons alors évalué les trois modèles de structure en taille d'après leur sensibilité à ces variables identifiées. L'ordonnée à l'origine du modèle de la pente (régression linéaire) réagit aux changements, mais non la pente elle-même. La sensibilité du modèle périodique (quadratique) ne permet pas de détecter les changements écologiques. Le modèle Pareto II (fonction de distribution de probabilité) est le plus sensible à toutes les variables écologiques, mais il est complexe à établir et il n'y a pas de relation directe entre ses paramètres et les événements biologiques. La méthode du modèle linéaire général de régression est relativement sensible aux changements du milieu et il permet en plus d'évaluer graphiquement les différences entre les années sur une base biologique. En général, les spectres de taille de la biomasse du zooplancton sont sensibles aux changements de conditions de l'environnement au lac Oneida; nous croyons que les méthodes basées sur les tailles ont le potentiel de servir comme indices biotiques dans les écosystèmes lacustres d'eau douce.

[Traduit par la Rédaction]

Introduction

The search for suitable biotic indicators of ecosystem change in aquatic systems is of paramount importance to scientists because the integrity of these systems is continually compromised by anthropogenic perturbations, invasions by exotics, and environmental degradation (Mills et al. 1994; Vanderploeg et al. 2002; Vinebrooke et al. 2002). Managers also recognize the importance of ecological indicators, especially their use in assessing management and res-

Received 22 April 2006. Accepted 29 August 2006. Published on the NRC Research Press Web site at http://cjfas.nrc.ca on 28 November 2006.
J19287

A.E. Gamble[1,2] and E.L. Mills. Cornell University Biological Field Station, 900 Shackelton Point Road, Bridgeport, NY 13030, USA.
R. Lloyd[3] and J. Aiken. Department of Biological Statistics and Computational Biology, Cornell University, Ithaca, NY 14853, USA.
O.E. Johannsson. Great Lakes Laboratory for Fisheries and Aquatic Sciences, Department of Fisheries and Oceans, Burlington, ON LR7 4A6 Canada.

[1] Corresponding author (e-mail: allisongamble@hotmail.com).

[2] Present address: University of Minnesota Duluth, 252 D Swenson Science Building, 1035 Kirby Drive, Duluth, MN 55812, USA.

[3] Present address: Cornell School of Hotel Administration, 335B Statler Hall, Cornell University, Ithaca, NY 14853, USA.

Can. J. Fish. Aquat. Sci. **63**: 2687–2699 (2006) doi:10.1139/F06-153

toration efforts. For example, total phosphorus has been identified by scientists as a useful ecological indicator as it reflects the degree of eutrophy of an ecosystem and potential food web production (Vollenweider 1968). Managers use total phosphorus not only to assess achievement of water quality restoration goals, but also to evaluate tradeoffs between the goals of water quality management and fish production (Bachmann et al. 1996; Koonce et al. 1996).

Ecological indicators are often used to assess ecosystem response to environmental change and to determine the impact of predation on structure and energy flow (Mazumder 1994; Cyr and Peters 1996; Allen et al. 1999). A common symptom of degraded ecosystems is the distortion of the expected relationship between the biomass of organisms and body size (Sprules et al. 1983; Kerr and Dickie 2001). The virtual absence of large-bodied zooplankton in freshwater lakes in response to intense planktivory by fish, for example, is a deviation from an expected size distribution (Mills and Schiavone 1982; Crowder et al. 1987; Mills et al. 1987). Within a practical framework, scientists and managers can combine information on zooplankton body size and measures of lake productivity (e.g., total phosphorus) to assess population structure, growth, and potential yield of fish (Vollenweider 1968; Mills and Schiavone 1982; Crowder et al. 1987).

Organism body size, particularly zooplankton body size, is a useful indicator of ecosystem status and usually a good indicator of trophic position (Kerr 1974; Mills and Schiavone 1982; Jennings et al. 2002). In aquatic ecosystems, body size is a rough indicator of trophic level because most predators feed on prey species smaller than themselves. Beginning with microscopic primary producers, biomass or energy flow up the food web is equivalent to biomass or energy flow up a spectrum of organism body size. The structure of the ecosystem can, therefore, be described by plotting biomass within various logarithmic size intervals against some function of body size; this is termed the biomass size spectrum (Sheldon et al. 1972; Borgmann 1987). Size spectra have been used to model energy flow of whole communities, in both freshwater and marine ecosystems, and have the advantage of considering the structure and function of the entire ecosystem (Rodriguez and Mullin 1986; Sprules et al. 1991; Gaedke 1993).

Most ecological studies use size spectra as a descriptive and predictive tool and have focused on a limited temporal sequence, e.g., one season or one–two years (Sprules and Munawar 1986; Gaedke 1992; Sprules and Goyke 1994). The predictability of size spectra responses to environmental change has not been established, and its usefulness as a management tool is still open to debate. In this study, we have two primary objectives. The first objective is to test the sensitivity of three size spectrum based models (a slope model, a parabola-based model, and the Pareto II model) to ecological change in aquatic ecosystems. The slope model (Sheldon et al. 1972; Platt and Denman 1978) uses linear regression to describe changes in biomass data. The periodic model is based on work done by Thiebaux and Dickie (1993) and Sprules and Goyke (1994), who fit parabolas to individual trophic levels and fit one overall parabola to all trophic levels. Sprules and Goyke, based on the theoretical work by Thiebaux and Dickie, also described a periodic component seen in the residuals of the modeled biomass data. For this paper, their model has been modified to incorporate the periodic trend and hereafter will be referred to as the periodic model. The final biomass size spectrum model tested is the Pareto II model (Blanco et al. 1994; Vidondo et al. 1997), which is a probability distribution function that determines the relative proportions of different-sized organisms. Specifically, we examine whether the slope, periodic, and Pareto II models capture ecological changes in Oneida Lake, New York (USA), a large freshwater ecosystem with a long-term zooplankton data set and a well-documented history of ecological perturbations. Zooplankton are the focal trophic level for assessing ecological change as these organisms often reflect changes in biotic and abiotic environmental variables (Mills and Forney 1983; Mazumder 1994; Vanderploeg et al. 2002).

Our second objective is to test the responsiveness of zooplankton size spectra to a range of common ecological perturbations in freshwater ecosystems and to assess its usefulness as a potential indicator of environmental state or change. Specifically, we hypothesize that (*i*) years of high nutrients (total phosphorus, soluble reactive phosphorus, nitrate, and nitrite) will increase the biomass across all body sizes of the zooplankton biomass size spectra because of their influence on algal food resources (Smith 1979, 1982; Downing and McCauley 1992); (*ii*) the presence of zebra mussels will decrease the biomass across all body sizes of the zooplankton biomass size spectra because of their potentially competitive influence on zooplankton food resources (Nicholls et al. 1999; Vanderploeg et al. 2002); (*iii*) high age-0 fish predation will decrease only the biomass in the intermediate to larger sizes of the zooplankton biomass size spectra because of selective predation on larger zooplankton (Mills and Forney 1983; Shepherd and Mills 1996); (*iv*) high pH and temperatures will increase the biomass across all body sizes of the zooplankton biomass size spectra because of their connection with plankton growth and turnover rates (Zhang and Prepas 1996; Wolfinbarger 1999); and (*v*) years with high chlorophyll *a* will be associated with a decrease in the biomass only in the intermediate to larger sizes of the zooplankton biomass size spectra because of the increased dominance of inedible algal food resources (Mills et al. 1987; Hansen et al. 1991; Mazumder 1994).

Materials and methods

Study site

Oneida Lake is a 20 700 ha, shallow, productive lake (mean depth 6.8 m, maximum depth 16 m) located on the Lake Ontario Plain of central New York State (Greeson 1971). Because the lake's long axis is oriented west–northwest to east–southeast, its surface waters are fully exposed to the prevailing winds. The lake has a historical zooplankton database (both biomass and body size data) begun in 1975. Since 1975, Oneida Lake has undergone several well-documented ecological changes, including the 1991 invasion of zebra mussels (*Dreissena polymorpha*), mandated reductions in phosphorus, and periodic irruptions of planktivorous fish (Mills et al. 1987; Shepherd and Mills 1996; Idrisi et al. 2001).

The zooplankton community in Oneida Lake is dominated by *Daphnia* species, which are efficient grazers. Shifts to less efficient grazers such as small-bodied copepods and cladocerans occur in some years when larger-bodied *Daphnia* disappear in early summer (Mills et al. 1987). *Daphnia* populations grow in the early spring, when they feed on diatoms, but in the summer, their survival is dependent on fish predation (Mills et al. 1987). The dominant zooplanktivores are age-0 fish; at high densities and biomass, age-0 yellow perch (*Perca flavesens*) and gizzard shad (*Dorosoma cepedianum*) are able to collapse populations of large-bodied *Daphnia pulicaria* (Mills and Forney 1983; Roseman et al. 1996; Shepherd and Mills 1996). *Daphnia pulicaria* shares lake dominance with *Daphnia mendotae*, and in the past 25 years, they have switched dominance several times.

Limnological data

Limnological data were collected weekly at five sites (1975–1997) from April to November (Fig. 1). A tygon tube (2.5 cm inner diameter) was used to collect integrated water samples (surface to 0.5 m above lake bottom) for total phosphorus (TP), soluble reactive phosphorus (SRP), chlorophyll *a* (Chl *a*), dissolved oxygen (DO) (1975–1995), alkalinity (1975–1995), nitrate (NO_3), and nitrite (NO_2). All variables were analyzed following methods in Strickland and Parson (1972), Wetzel and Likens (1979), American Public Health Association, American Water Works Association, and the Water Pollution Control Federation (1976), and Menzel and Corwin (1965). In the field, secchi disc transparency was measured on each sampling date, and temperature was measured at 1 m intervals throughout the water column.

Zooplankton

Zooplankton samples included in these analyses were collected weekly from July to October in 1975 to 1977 and 1979 to 1997 (at the same time and location as limnological collections) with a 153 μm mesh, 0.5 m diameter Nylon net using vertical tows from approximately 0.5 m off the sediment surface to the water surface. Because of the net mesh size, microzooplankton such as rotifers were not included in any sample and represent a gap in the Oneida Lake size spectrum. Data were collected in 1978 but were not stored in a retrievable format and so are not included in this analysis.

All zooplankton were preserved in sugar – 4% formalin or 70% ethyl alcohol. All zooplankton species were enumerated, and body length was recorded with the use of a computer-assisted zooplankton analysis system (Hambright and Fridman 1994). A minimum of 100 individuals were counted and measured per sample. Individual weights were calculated from length – dry weight regressions (E.L. Mills, unpublished data) and converted to wet weight (multiplied by a factor of 10). The biomass (μg·L^{-1}) represented by an individual organism was calculated from density (no.·L^{-1}) multiplied by wet weight (μg). In this paper, all biomass units are presented in grams per square metre.

The final step in formatting the zooplankton data was to bin the data according to biomass size spectrum methodology. Individual zooplankton were placed in size-dependent $\log_2$ bins, based on their wet weight (μg) (Sprules et al. 1991; Blanco et al. 1994). Size bins represented wet weight on a $\log_2$ scale, where the midpoint of an individual bin was double that of the previous bin (Sprules and Munawar 1986; Sprules et al. 1991). The mass associated with each individually measured $\log_2$-binned zooplankton was summed to obtain a total biomass (g·m^{-2}) for each $\log_2$ size bin. Zooplankton data organized in this fashion will be referred to as biomass size spectrum formatted data. The data were divided according to sampling week and site, with year as the main temporal separator. Individual weeks within a year were considered replicates.

Fig. 1. Map of Oneida Lake, New York, showing the five sampling sites for limnological and zooplankton data collection. Shack. Pt., Shackelton Point.

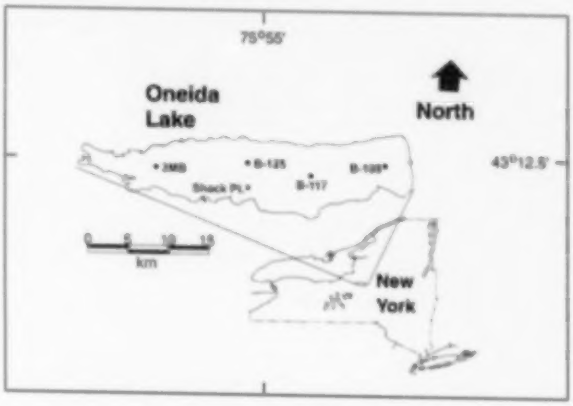

Biomass size spectrum theory assumes that predator–prey interactions produce characteristic size-dependent structuring (Jennings et al. 2002; Thiebaux and Dickie 1992). In Oneida Lake, zooplankton biomass begins to be controlled by predator–prey interactions in early July with the onset of predation by age-0 planktivorous fish (Mills et al. 1987). Consequently, we used zooplankton data for the period from July through October in the size spectrum analyses. Although five sites were usually sampled for zooplankton, previous analyses using principle components analysis have shown that site-specific differences were not significant in Oneida Lake (Gamble 2003). Based on these prior analyses, zooplankton data were averaged across sites. All analyses were run on July–October data, pooled across sites, resulting in at least 16 replicates (a range of $\log_2$-binned zooplankton biomass per week) from each of the 22 years sampled.

Fish

The impact of fish predation was examined through annual changes in age-0 gizzard shad (1984–1997) (count) and yellow perch (1975–1997) (abundance). Age-0 gizzard shad were collected in clear Plexiglas Miller-type fry sampling nets equipped with 530 μm mesh (Noble 1970) from 20 randomly selected sites beginning in June and again at approximately 10-day intervals until the larval fish catch decreased noticeably, which was usually in late August. Age-0 estimates (8–14 mm size range) were used to index annual recruitment (VanDeValk et al. 1999). Age-0 yellow perch abundance was determined from the catch and area swept by an otter trawl with a 5.5 m foot rope and a 6.4 mm mesh cod end. Biomass (kg·hectare^{-1}) was estimated from 10 stations sampled at weekly intervals from August to September.

Data analysis

Environmental variables

To assess the size spectra data, we identified significant events in Oneida Lake that could affect the zooplankton biomass data before actual model testing. The events were based on high levels of abiotic and biotic variables including TP, SRP, NO_3, and NO_2 because of their influence on algal food resources, Chl *a* because it is directly related to total zooplankton food resources, secchi depth because it reflects both density of algal food particles for zooplankton and visibility of zooplankton to fish, age-0 yellow perch and gizzard shad because of their predatory impact on zooplankton, zebra mussels because of their potential competitive influence on zooplankton food resources, and pH and temperature because of their connection with plankton growth and turnover rates.

For each variable, all years were coded either high (1) or not high (0). Data were divided into high and not-high years so that the sensitivity testing could be relatively simple and discrete. High years indicate times when the level of the variable of interest could have noticeably impacted the zooplankton. Years were considered high if the average value of the variable for that year (July to October) was more than 1 standard deviation (SD) above the overall (1975–1997) mean. We believe that 1 SD is a valid metric for identifying times of greater ecological impact, although we would have chosen to use 2 SDs if the time series had been long enough to support that level of sensitivity. Several variables (pH, average temperature, NO_3, and NO_2) were excluded from all analyses immediately after the initial selection process because their values were too constant in Oneida Lake, meaning that no individual yearly average was greater than 1 SD away from the overall mean for all of the data.

We employed multiple regressions (Gamble 2003) in which biomass size spectrum formatted zooplankton biomass (divided by site, on a weekly basis from July to October from 1975 to 1997) was the dependent variable. The environmental factors were the independent variables used to select the final suite of environmental variables to assess the biomass size spectrum models (SRP, TP, secchi depth, Chl *a*, zebra mussels, age-0 yellow perch, and age-0 gizzard shad).

Model testing

To address our first objective, we examined the responses of the slope, periodic, and Pareto II models to changes in Oneida Lake zooplankton biomass, using the high/not-high coding of the seven different variables to define periods of ecological change. For each model, we tested the individual effects of the seven variables on biomass size spectra. The Pareto II provided the highest level of sensitivity to ecological change, whereas the slope and the periodic models were not very sensitive to known ecological changes (Gamble 2003). Details of the slope and periodic model testing are available as supplementary data online or may be purchased from the Depository of Unpublished Data.[4]

Fig. 2. Generalized diagrams and associated formulas for (*a*) slope, (*b*) periodic, and (*c*) Pareto II models. Trophic level A represents the phytoplankton, and trophic level B represents the zooplankton. The *y* values for the slope and periodic models represent the $\log_{10}$((Σbiomass in $\log_2$bin *i*)/width of $\log_2$bin *i*), and the *x* values represent the log(average value of $\log_2$bin *i*). For the Pareto II model, the *y* values represent the probability of being size *x* given the parameters α and σ (estimated from the observed data set), and the *x* values represents size (µg).

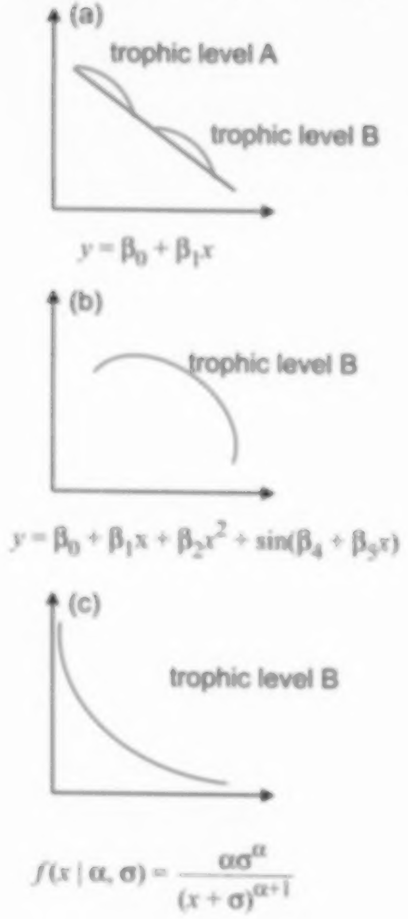
(a)
trophic level A
trophic level B
$y = \beta_0 + \beta_1 x$
(b)
trophic level B
$y = \beta_0 + \beta_1 x + \beta_2 x^2 + \sin(\beta_4 + \beta_5 x)$
(c)
trophic level B
$f(x \mid \alpha, \sigma) = \frac{\alpha\sigma^{\alpha}}{(x + \sigma)^{\alpha+1}}$

Slope model

In the slope model, a linear regression was fit to both phytoplankton and zooplankton size spectra data in the form of $y = B_0 + B_1 x$ (Fig. 2*a*) (supplementary data).[4] When creating the actual biomass size spectrum, the *y* values represented the $\log_{10}$((Σbiomass in $\log_2$ bin *i*)/width of $\log_2$ bin *i*), and the *x* values represented the $\log_{10}$(average value of $\log_2$ bin *i*). Slopes and intercepts were estimated for each week in the data set using least squares regression (because of nonindependence of the model residuals) and coded by month and year (Proc GLM, SAS version 8; SAS Institute Inc. 2001; supplementary data)[4] (Ott 1993; Gamble 2003). Differences in slopes and intercepts between high and not-high years were tested for each environmental variable using two-sample t tests (Proc GLM, $p < 0.1$, Minitab 13.2; Minitab Inc. 2000), with the assumption of unequal variance between the two groups (supplementary data).[4]

---

[4] Supplementary data for this article are available on the journal Web site (http://cjfas.nrc.ca) or may be purchased from the Depository of Unpublished Data, Document Delivery, CISTI, National Research Council Canada, Building M-55, 1200 Montreal Road, Ottawa, ON K1A 0R6, Canada. DUD 5106. For more information on obtaining material refer to http://cisti-icist.nrc-cnrc.gc.ca/irm/unpub_e.shtml.

Periodic model

The periodic model fit a quadratic plus a sine curve to the zooplankton biomass data using the model $y = B_0 + B_1x + B_2x^2 + B_3\sin(B_4 + B_5x)$ (Fig. 2*b*). B_3, B_4, and B_5 (sine curve parameters) attempted to account for the previously observed sinusoidal oscillations around the overall trophic dome (supplementary data[4]; Sprules and Goyke 1994). Proc NLIN in SAS (SAS Institute Inc. 2001) was used to fit the data to the periodic model (supplementary data).[4] We used categorical regression to detect changes in model parameters from high/not-high years ($p < 0.05$) (supplementary data).[4]

Pareto II distribution

The third approach tested, the Pareto distribution, did not bin or logarithmically transform the data (Blanco et al. 1994; Vidondo et al. 1997; Cavender-Bares et al. 2001), but instead used individual organism size (µg) (from the 22 years, with weeks per year as replicates) as input data. The Pareto distribution is a probability distribution function (PDF) with two parameters: *K*, a constant parameter that represents the size of the smallest object, and alpha (α), an empirical constant that describes the decline of probability of being a size as size increases. Work by Vidondo et al. (1997) revealed that the Pareto II distribution actually fit size data better than the Pareto distribution, and therefore the Pareto II was used in this study. The Pareto II has three parameters: K, α, and sigma (σ), an additive constant used to improve the fit of the Pareto in situations where the biomass of particles is lower than predicted by a straight line (Fig. 2*c*) (Vidondo et al. 1997). In this study, the minimum size *K* was assumed to be zero, leaving the two parameters α and σ in the model:

$$f(x \mid \alpha, \sigma) = \frac{\alpha\sigma^{\alpha}}{(x + \sigma)^{\alpha+1}}$$

The distribution required individual organism size in wet weight (µg) as the input data. All Pareto II distribution analyses used Matlab 6.1 (MathWorks, Inc. 1994–2003). The maximum likelihood function:

$$L(\alpha, \sigma \mid x) = \prod_{i=1}^{n} \frac{\alpha\sigma^{\alpha}}{(x_i + \sigma)^{\alpha+1}}$$

was used to estimate α and σ (Mood et al. 1974). The maximization of the likelihood function was a two-dimensional optimization, but partial derivatives were used to reduce that to a one-dimensional optimization for σ, with the estimated α being a function of the σ value. Using basic calculus principles, we evaluated the partial derivative with respect to α, set the result to zero, and solved for α. The partial derivative was then evaluated with respect to σ, where the equation was set to zero and solved for σ, given the substitution in the equation for α in terms of σ. Theoretically, it was possible to get multiple σ values, but in practice this was never observed. If this had occurred, the likelihood function would have been evaluated for all different sets of parameters and the set that maximized the likelihood function would have been used.

Once the σ and α estimation procedures were established, we tested the Pareto II for its sensitivity to changes in biomass using the high/not-high environmental variable based groupings of the data. We used a generalized likelihood ratio test for the equality of the two Pareto II distributions (Mood et al. 1974). Values of α and σ were estimated for each high/not-high grouping. This model used high/not-high environmental variable based divisions of zooplankton size but did not bin the data, using instead wet weight (µg) and the frequency of each wet weight on a yearly basis. Pareto II parameter estimates for α and σ were compared between each high/not-high grouping. The parameter estimates were compared using a generalized likelihood ratio test, which took the following form:

$$\Lambda = \frac{\prod_i f(x_i \mid \hat{\alpha}_{\text{comb}}, \hat{\sigma}_{\text{comb}}) \prod_j f(x_j \mid \hat{\alpha}_{\text{comb}}, \hat{\sigma}_{\text{comb}})}{\prod_i f(x_i \mid \hat{\alpha}_1, \hat{\sigma}_1) \prod_j f(x_j \mid \hat{\alpha}_2, \hat{\sigma}_2)}$$

In this formula, the *i*s were wet weight (*X* values) from time period 1, and the *j*s were wet weight (*X* values) from time period 2. The combined parameter estimates were obtained by combining the data sets for the high and not-high years into one and performing the estimation procedure again. The null hypothesis (H_0) was that there were no differences in the distributions of data from the high and not-high years, with the alternative hypothesis (H_a) that the distributions were not equal. More explicitly,

$$H_0 : \alpha_1 = \alpha_2 \text{ and } \sigma_1 = \sigma_2$$

$$H_a : \alpha_1 \neq \alpha_2 \text{ or } \sigma_1 \neq \sigma_2 \text{ or both}$$

If the parameter estimates for zooplankton biomass from the high and not-high time periods were the same, the ratio of the parameters would be approximately 1. The test statistic was $-2\ln(\Lambda)$ (Λ is as described previously), and H_0 was rejected if the test statistic was greater than the 95th percentile of a chi-square distribution with two degrees of freedom. There were two degrees of freedom associated with the chi-square value because the dimension of the parameter space was reduced by two if the parameters in the two data sets were equal.

Detecting environmental change — a general linear modeling approach

To assess our second objective, we tested the sensitivity of a size spectrum based approach to known ecological changes using a general linear model (GLM) (McCullagh and Nelder 1991) regression. The GLM model was similar to the other size spectrum models, although the binned zooplankton biomass was not normalized (divided by $\log_2$ bin width). The GLM model was similar to a one-way analysis of variance (ANOVA) model, with $\log_2$ bin as the factor (different $\log_2$ bins indicated different "treatments", or categories, where individual means were found for each $\log_2$ bin after accounting for an overall mean) and $\log_2$-binned zooplankton biomass as the response variable. The use of a factor model allowed us not only to examine the overall impact of the environmental variables on zooplankton biomass (as was done for the Pareto II, slope, and periodic models), but also to examine the impact of the environmental variables on biomass in individual $\log_2$ bins and thus identify which size organisms were most impacted.

We first developed a base model that did not include the environmental variables, where the natural log of the sum of the size spectrum formatted zooplankton data in each $\log_2$ bin was the response (y) variable and the predictor variables were the respective $\log_2$ bins:

$$y_{ij} = B_i + \varepsilon_{ij}$$

where y_{ij} = ln(biomass of $\log_2$ bin i ($i = 1, 2, \ldots, 14$) in the jth year (1975–1997)), B_i is the mean ln(biomass of $\log_2$ bin i ($i = 1, 2, \ldots, 14$)), and ε_{ij} is the unexplained error term for ln(biomass of $\log_2$ bin i) in the jth year. The error term indicated how much biomass (y_{ij}) in a particular year deviated from the mean biomass (B_i) in a particular bin. We then included individual environmental variables and determined the significance of their interactions with each $\log_2$ bin using the following model:

$$y_{ij} = B_i + B_{ij} + \varepsilon_{ij}$$

where y_{ij} and ε_{ij} are as previously described, B_i is the mean ln(biomass of bin i) in the years when the environmental variable was not high, and B_{ij} is the change in mean ln(biomass of bin i) from years when the environmental variable was not high to years when it was high. (Note that in years when the environmental variable was not high, $B_{ij} = 0$.) Therefore, B_{ij} indicated whether the high/not-high environmental variable based divisions of the $\log_2$-binned biomass data were significant, both overall and on a bin-by-bin basis. All testing was done in S-PLUS (version 6.0; Insightful Corp. 1988–2002).

GLM output provided an overall F test, which indicated the overall significance of the differences in biomass between high and not-high years of each environmental variable ($p < 0.05$), along with p values giving the significance of the impact of the specific environmental variable on the biomass in each $\log_2$ bin (the factor effect). Bins were considered affected by an environmental variable if a group of at least three consecutive $\log_2$ bin – environmental variable interactions were significant ($p < 0.05$ per bin). We used groups of three $\log_2$ bins as the minimum number for significance to control for type I errors (falsely rejecting the null hypothesis). Because we were testing changes in 14 different $\log_2$ bins, each at the 0.05 level, the probability of at least one type I error could have been as high as 70% ($0.70 = 14 \times 0.05$) (Neter et al. 1996). However, three consecutive $\log_2$ bins had a probability of $0.05 \times 0.05 \times 0.05 = 0.000125$ of occurring if not really significant, and we judged that probability to be sufficiently low that the impact on the bins could be attributed to the environmental variable being tested.

Finally, as an error control measure, we identified whether single environmental variables captured information contained in some of the other selected environmental variables. To assess whether overlap of information was occurring, we used stepwise regression by adding individual variables into the model in a stepwise fashion. An F test determined whether the addition of the environmental variable was significant ($p < 0.05$). Significant values indicated that each particular environmental variable tested identified unique differences in $\log_2$-binned zooplankton biomass and did not have a confounding effect on the other environmental variables.

We graphically examined the effect of each significant environmental variable on the zooplankton biomass data. Plots of mean size spectra for all high years of an environmental variable were compared with mean size spectra from all other years. These plots represented a solely graphical portrayal of the statistical testing done in S-PLUS (Insightful Corp. 1988–2002) and were not intended as a statistical representation. Graphs were not created for any bins or environmental variable groupings that were not significantly different (based on the overall F tests from the GLM model output). We used qualitative analysis of the graphical GLM output to obtain an estimate of the differences in biomass between years with and without the environmental effect. In our analysis, we drew lines from the $\log_2$ bin that was most significantly affected by a variable to obtain the maximum difference in zooplankton biomass between the high and not-high years. This difference was log-transformed and could then be biologically interpreted.

Results

The Oneida Lake zooplankton community and biomass size spectrum

A summary of Oneida Lake zooplankton species $\log_2$-binned according to biomass size spectrum theory is presented in Table 1. *Daphnia* species were dominant in the larger $\log_2$ size bins, whereas copepods and other cladoceran species dominated the smaller-sized $\log_2$ bins. Overall, the larger zooplankton (*Daphnia* spp.) accounted for the highest percentage of the zooplankton community biomass. In some years (e.g., 1975 and 1989), large-bodied *Daphnia* disappeared by August in association with high levels of planktivorous age-0 yellow perch and gizzard shad (Fig. 3). In other years, e.g., 1976 (low levels of age-0 yellow perch) and 1992 (the first year after the zebra mussel invasion and also a year with very low levels of planktivorous fish), the *Daphnia* population did not collapse and remained the dominant component of the zooplankton biomass (May to October) (Fig. 3).

Long-term trends of environmental variables (1975–1997)

Seven biotic and abiotic variables were chosen from the Oneida Lake long-term data set as possible predictors of zooplankton biomass. The environmental variables (gizzard shad, yellow perch, SRP, TP, secchi, Chl *a*, and zebra mussel presence) had both statistical support (Gamble 2003) and biological rationales for the significance of their impact on zooplankton. Long-term trends indicated that no two variables had the same "high" years, although the pattern for secchi depth and dreissenids and for TP and SRP were very similar (Fig. 4). For the planktivorous fish, the highest biomass of age-0 yellow perch was in the late 1970s and early 1980s, whereas the highest numbers of age-0 gizzard shad were in the late 1980s and early 1990s. TP and SRP levels fluctuated greatly but were higher on average in the 1970s

Table 1. Summary of the dominant (by frequency) zooplankton species in each wet weight $\log_2$ bin, based on July–October 1975–1997 data from Oneida Lake.

Bin	Dominant species	Bin upper and lower weight limits (µg)	
		Lower	Upper
16	*Diaptomus minutus*[a]	0.18	0.35
17	*Diaptomus minutus*[a]	0.35	0.71
18	*Chydorus sphaericus*[a]	0.71	1.41
19	*Diaptomus minutus*[a]	1.41	2.82
20	*Diaptomus minutus*,[a] *Chydorus sphaericus*[b]	2.82	5.62
21	*Diaptomus minutus*,[a] *Diaptomus thomasi*[b]	5.62	11.22
22	*Diaptomus thomasi*[a]	11.22	22.39
23	*Diaptomus thomasi*,[a] nauplii[b]	22.39	44.67
24	*Mesocyclops edax*,[a] *Daphnia mendotae*[b]	44.67	89.13
25	*Daphnia mendotae*,[a] *Daphnia pulicaria*[b]	89.13	177.83
26	*Daphnia mendotae*,[a] *Daphnia pulicaria*[b]	177.83	354.81
27	*Daphnia pulicaria*[a]	354.81	707.95
28	*Daphnia pulicaria*[a]	707.95	1412.54
29	Copepod spp.[a]	1412.54	2818.38

[a] The dominant species.

[b] The subdominant species, if present.

Fig. 3. Seasonal trends in the *Daphnia pulicaria* biomass in Oneida Lake for single years with (*a*) high (1995) and (*b*) low (1976) age-0 yellow perch (*Perca flavescens*) predation, (*c*) high (1989) age-0 gizzard shad (*Dorosoma cepedianum*) abundance, and (*d*) high (1992) zebra mussel abundance and low levels of planktivorous fish.

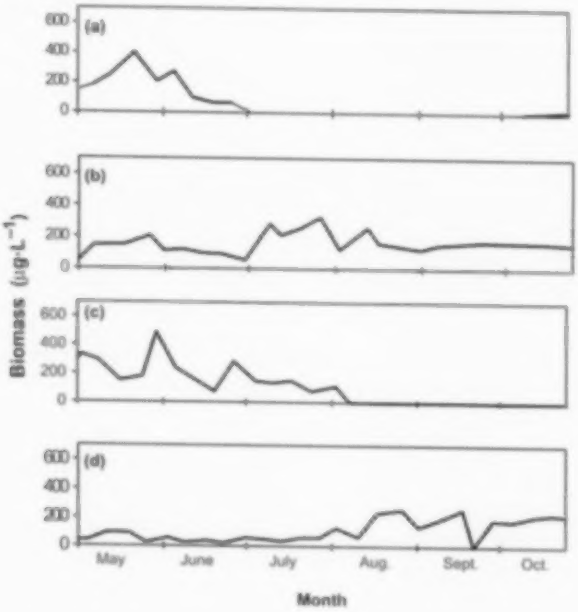

and early 1980s and lower on average since the mid-1980s. Since 1987, mean annual phosphorus levels have generally been less than 30 µg·L⁻¹, and concentrations have remained stable. Secchi depth was highest in years associated with the presence of zebra mussels. High Chl *a* years were mainly in the 1970s, with one additional peak in 1991. Zebra mussels were first identified in Oneida Lake in 1991, and a substantial population appeared in 1992. Years with the highest secchi depths were associated with the presence of zebra mussels.

Model testing

Slope model

The slope model appeared to be more responsive to changes in the intercept than to changes in slopes (supplementary data).[4] Differences in the intercept between high and not-high years were significant ($p < 0.1$) for four of the seven variables (zebra mussels, larval gizzard shad, SRP, and secchi depth), and significant differences in the slope were only seen for age-0 gizzard shad and SRP.

Periodic model

The periodic model was insensitive in detecting the known differences between high and not-high years of Oneida Lake zooplankton biomass for most of the environmental variables (supplementary data).[4] The intercept (B_0) was significantly different for zebra mussel and secchi years ($p < 0.05$) and for yellow perch, Chl *a*, and SRP years ($p < 0.1$). None of the other parameters (B_1–B_5) was significantly different between high and not-high years for any of the variables.

Pareto II

The Pareto II distribution was the most sensitive size spectrum based model we tested and distinguished between all of the high and not-high years of each environmental variable, with the exception of gizzard shad (Table 2). All p values were at least significant to four decimal places, and most of them were significant to over 15 decimal places, indicating that the power of the test was extremely high. Parameter values of σ and α showed slight fluctuations between multiple tests of the same years but gave consistent results in the testing between years.

Fig. 4. Long-term trends (July–October 1975–1997) of mean (±1 standard deviation, SD) annual values of (*a*) secchi depth, (*b*) Chl *a*, (*c*) age-0 yellow perch (*Perca flavescens*), (*d*) soluble reactive phosphorus, (*e*) total phosphorus, and (*f*) age-0 gizzard shad (*Dorosoma cepedianum*). Horizontal lines represent overall means (1975–1997), and asterisks (*) indicate individual years in which the means were at least 1 SD above the overall mean.

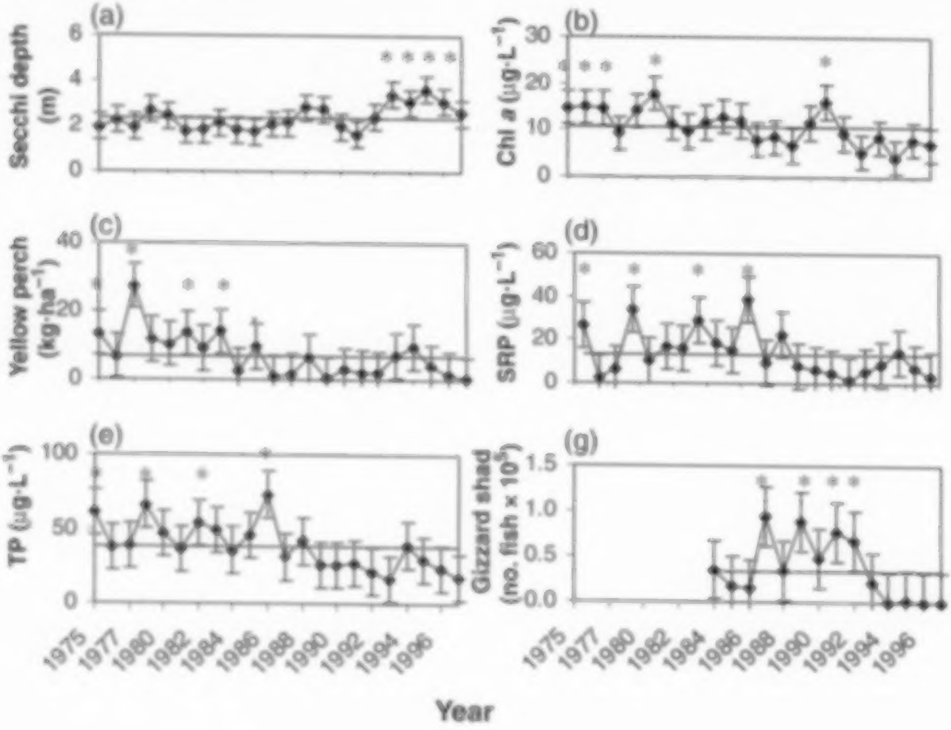

Table 2. Results from the statistical analysis of the Pareto II distribution, giving the significance (**, $p < 0.0001$) of the estimates of the differences between high and not-high years for each environmental variable (σ combined, α combined).

	Significance of difference in parameter estimates	
Variable	σ combined	α combined
Zebra mussel	**	**
Larval gizzard shad	NS	NS
Age-0 yellow perch	**	**
Secchi	**	**
Chlorophyll *a*	**	**
TP	**	**
SRP	**	**

Note: Parameter estimates come from Oneida Lake zooplankton weight and frequency data from July– October 1975–1997. NS, nonsignificant results; TP, total phosphorus; SRP, soluble reactive phosphorus.

Assessing environmental change

We used GLM regressions to determine whether the response of the size spectrum formatted data to the environmental variables supported our original hypotheses. Before the hypothesis testing, we determined that, for each environmental variable (gizzard shad, zebra mussel, yellow perch, SRP, TP, secchi, and Chl *a*), biomass size spectrum formatted zooplankton biomass in years coded as high differed significantly from years coded as not high (*F* test, all *p* values were < 0.005). Zebra mussel years were the most significantly different (Gamble 2003). The stepwise addition of each of the significant environmental variables (significance based on *F* tests, $p < 0.05$) increased the explanatory power of the model, demonstrating that even given the presence of the other variables, all of the environmental variables identified unique divisions of the zooplankton biomass.

We then used the GLM analysis to assess our five hypotheses ($p < 0.05$ per bin). We failed to reject the null hypothesis that years of high nutrients did not increase biomass across all body sizes of the zooplankton. Higher TP and SRP both corresponded to increases in zooplankton biomass in only three of the larger-sized $\log_2$ bins during years that were coded as high. We also failed to reject the null hypothesis that the presence of zebra mussels should not decrease the zooplankton biomass size spectrum. Years with a zebra mussel presence had high biomass in 54% of the $\log_2$ bins, which did not support the initial alternative hypothesis that the biomass across the entire size spectrum should decrease in high zebra mussel years. High secchi depth years (surrogate of zebra mussel effect) showed very similar results.

We rejected the age-0 fish predation null hypothesis, concluding that high age-0 fish predation decreased only the

Fig. 5. Mean biomass size spectrum lines (for $\log_2$ bins 16–29) for all years (*a*) with (1987, 1989, 1991–1992) and (*b*) without (1975–1986, 1988, 1990, 1993–1997) high age-0 gizzard shad (*Dorosoma cepedianum*) biomass compared with size spectrum data points (○) from 1975. The impact of high gizzard shad predation can be seen in the difference, for only the intermediate to larger size $\log_2$ bins in the separation of lines (*a*) and (*b*). Gizzard shad had the most significant impact on $\log_2$ bin 25 (*) (significance based on *t* tests in S-PLUS (Insightful Corp. 1988–2002), $p < 0.05$), so the difference between lines (*c*) and (*d*) represents the greatest impact of gizzard shad on the zooplankton biomass.

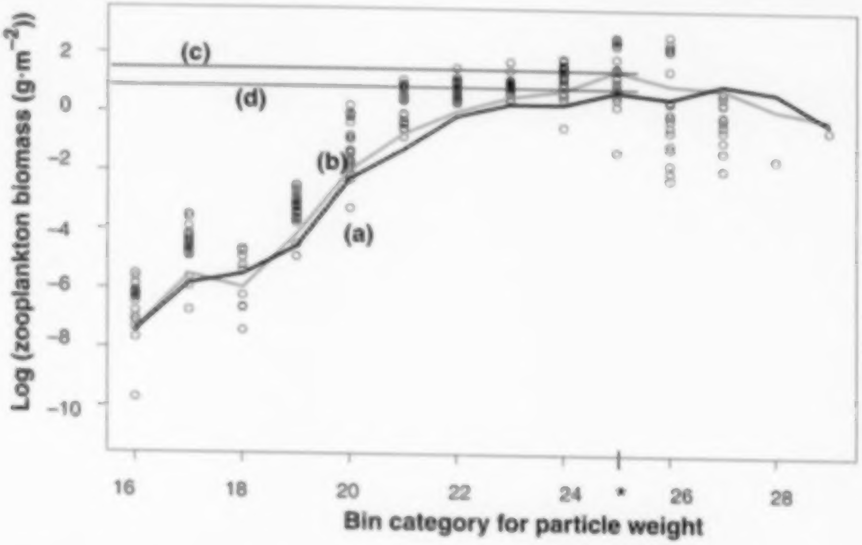

biomass in the intermediate to larger sizes of the zooplankton biomass size spectrum. We used abundance indices of age-0 gizzard shad and yellow perch to test this hypothesis. Both high gizzard shad and yellow perch years affected the biomass size spectrum by negatively impacting the intermediate- to larger-sized $\log_2$ bins. We were unable to test the hypothesis that high pH and temperatures could positively impact the biomass size spectrum because of their relatively constant nature in Oneida Lake. We rejected the Chl *a* null hypothesis, concluding that high Chl *a* years showed a corresponding biomass decrease in the intermediate to larger sizes of the zooplankton biomass size spectrum, because the Chl *a* results showed a decrease in $\log_2$ bins 24 and higher.

We used qualitative analysis of the graphical GLM output to obtain an estimate of the differences in biomass between years with and without the environmental effect for years when that difference had been shown to be statistically significant. For example, the decrease in the intermediate- to larger-sized zooplankton during high gizzard shad years was evident compared with not-high gizzard shad years (Fig. 5). Zooplankton biomass in the $\log_2$ bin with the maximum difference ($\log_2$ bin 25, *Daphnia* dominated, $p < 0.05$) was 1.8 times greater in not-high gizzard shad years than in high years (Fig. 5). The maximum difference between zooplankton biomass (based on the $\log_2$ bin with the maximum observed difference) for high and not-high zebra mussel, total phosphorus, and yellow perch years was 1.5.

Discussion

Model testing

We were interested in assessing the sensitivity of the slope model to changes in phytoplankton and zooplankton biomass, as the preponderance of work to date on the biomass size spectrum has been done using this model (Rodriguez and Mullin 1986; Sprules et al. 1991; Cyr and Peters 1996). However, we encountered problems fitting the slope model to the Oneida Lake plankton biomass, as the sinusoidal pattern observed in the residual plots indicated that the assumption of independence (of error terms) necessary for performing inference from linear regression was violated (see supplementary data).[4] Although we did not investigate residual plots from other lake data sets, we caution that biomass size spectrum formatted data may violate the inferential assumptions of linear regression in those waters as well. To circumvent the violations of linear regression assumptions, we used least squares regression (see supplementary data).[4] The results from the slope analysis showed that the intercept tended to be more responsive to changes in biomass than the slope. The differences in the intercept were significant for four of the seven environmental variables, whereas differences in the slope were only seen for two of the seven variables. Three of the differences in the intercepts were directly related to changes affecting phytoplankton (SRP, secchi, and zebra mussel presence). These findings concur with work done by Cyr and Peters (1996) on biomass size spectra of multiple lakes. They found that the intercept of 24 lakes from many different geographical locations was positively related to primary production, but that the slope showed no relationship.

The lack of sensitivity of the slope model to detecting known changes in zooplankton biomass related to specific perturbations (e.g., age-0 yellow perch predation) indicated that other size spectrum models should also be considered. However, it is possible that the slope of the slope model may reflect the overall pattern of steady state conditions within a system and that the size structure of an ecosystem may fundamentally remain the same. If fluid systems adjust to perturbations relatively quickly by returning to this steady state, this would then be reflected in a relatively unchanging slope (at least on a yearly time scale), depending on the study ecosystem (Sheldon et al. 1972; Quinones et al. 2003; Alvarez-Cobelas et al. 2006). Many studies have demonstrated a generality among size spectra across a broad range of ecosystems and time periods (Rodriguez and Mullin 1986; Sprules and Munawar 1986; Ahrens and Peters 1991), indicating that the size spectrum does reflect some basic underlying ecosystem condition or pattern. Therefore, the slope of the biomass size spectrum, as formulated based on the slope model, could be more indicative of differences between systems (i.e., differences between levels of productivity) than of differences within a system on a relatively short time scale.

We initially had high expectations for the periodic model. The idea that changes in the periodic component of the model could reflect changes in predator–prey interactions seemed like a new and useful application of the biomass size spectrum. Additionally, the insertion of the sine curve into the periodic model did remove what was causing the lack of independence in the slope model residuals by removing the sinusoidal pattern from the periodic residuals. However, the model sensitivity testing showed that the periodic model as formulated was unable to detect known differences in zooplankton biomass. Although it is possible that a different function could capture the periodic variations about the trophic domes, the periodic model in its current formulation did not show promise as a modeling tool. It is also possible that the periodic model, like the slope of the slope model, does not assess ecological change so much as capture steady state conditions.

The Pareto II model was the most sensitive of the three models used to detect known ecological changes. The first practical use of the Pareto model was by Cavender-Bares et al. (2001), who assessed changes in nanoplankton structure in the Atlantic and Pacific oceans. Based on the theoretical work (Blanco et al. 1994; Vidondo et al. 1997) and the practical application of the Pareto model in marine waters, we chose to use the Pareto II distribution to assess the sensitivity of this approach to differences in Oneida Lake zooplankton body size (µg). Graphical analysis by Aiken (2003) previously showed that although the Pareto II parameters changed significantly in the different years, the Pareto II distribution always fit the data. In this paper, we did not assess the Pareto II model graphically, but instead used a likelihood ratio test to determine whether parameter estimates from the high and not-high variable years were significantly different. The Pareto II model was able to detect significant differences in zooplankton size for six of the seven environmental variables, with higher sensitivity than the other models. However, this model was unable to distinguish between the high and not-high gizzard shad years, a finding we attribute to the fact that gizzard shad structure the zooplankton community late in the season (August) and our analyses included July, when the gizzard shad would not yet have impacted the zooplankton (Shepherd and Mills 1996). The p values for the Pareto II tests between time periods were extremely significant, indicating that the Pareto II model would be able to discern differences between time periods or sites given less data than we used.

General linear model (GLM)

The GLM analysis allowed us to statistically test the response of the biomass size spectrum to the hypothesized environmental variable based differences. We hypothesized that higher levels of nutrients (TP and SRP) would positively impact the entire zooplankton biomass size spectrum because the zooplankton would be able to put more energy into growth and maintain a higher biomass (Watson et al. 1992; Paterson et al. 1997). However, the results of the GLM analyses did not support this hypothesis. High years of TP and SRP showed an increase in only three (out of 14) zooplankton size $\log_2$ bins, all of which represented the larger-sized animals. One possible explanation for these results is that because Oneida Lake has moderate to high concentrations of phosphorus, late summer blooms of inedible cyanobacteria are common (Wagner 1983; Mills et al. 1987). When this occurs, both the nonselective and selective zooplankton feeders are forced to expend much more energy filtering food, leading to poor recruitment of small-sized neonates (Burns 1968; Gliwicz 1969; Hansen et al. 1991) and lower zooplankton biomass.

We hypothesized that the presence of zebra mussels should negatively impact the zooplankton biomass size spectrum, as zebra mussel grazing can significantly decrease the edible phytoplankton available to the zooplankton (Vanderploeg et al. 2001), but this was not supported. In Oneida Lake, zooplankton have been able to respond to the intense grazing by zebra mussels by feeding on the increased abundance of small, more edible phytoplankton (Idrisi et al. 2001). In addition, recruitment of age-0 yellow perch during the period before and during the establishment of zebra mussels was poor (L. Rudstam, Cornell Biological Field Station, 900 Shackelton Point Road, Bridgeport, NY 13030, USA, personal communication), leading to lowered planktivory and limiting the predation impact on zooplankton.

We hypothesized that high fish predation should negatively impact only the intermediate- to larger-sized zooplankton. Years with high fish predation resulting from age-0 gizzard shad and yellow perch were years when large-bodied *Daphnia* were depleted, shifting the zooplankton community to smaller-bodied forms (Mills and Forney 1983; Shepherd and Mills 1996). In these years, the biomass size spectrum showed significant decreases in the biomass in the mid- to large-sized $\log_2$ bins, which were dominated by *Daphnia*.

The final hypothesis, that high Chl *a* levels should negatively impact only the intermediate- to larger-sized zooplankton, was also supported. High Chl *a* years were also years with high levels of young-of-the-year planktivorous fish (gizzard shad, yellow perch), all of which tend to selectively target *Daphnia*, which dominated the mid- to large-sized $\log_2$ bins (Mills and Schiavone 1982; Mills and Forney 1983; Shepherd and Mills 1996).

We developed a new graphical approach using the GLM model to visually confirm the results of the hypothesis testing and to qualitatively assess the biological significance of the differences in zooplankton size spectra between high and not-high years. For example, the zooplankton biomass in not-high gizzard shad years was a maximum of 1.8 times greater than in high gizzard shad years. For the Oneida Lake zooplankton, a change in biomass of this magnitude is biologically significant because it represents an approximately 50% decrease in biomass for the affected $\log_2$ bin. The combination of statistical and graphical output in the GLM analysis allows one to provide a biologically based, quantitative assessment of differences in biomass data and also to gauge the magnitude of that impact.

The GLM model is similar to biomass size spectrum models described by Sprules and Munawar (1986) and Sprules et al. (1991) except that the GLM values for the y axis are not normalized (i.e., the sum of the biomass per $\log_2$ bin is not divided by the bin width) and the biomass in each $\log_2$ bin is treated independently of the biomasses in the other $\log_2$ bins. The GLM analysis was run as a factor model, and so the estimate for each $\log_2$ bin was a point estimate. However, these point estimates approximated a continuous model when the output was interpreted by looking for groups of significant $\log_2$ bins. In our analyses, individual $\log_2$ bins that were several bins away from the group of significant $\log_2$ bins were also sometimes significant. For example, the $\log_2$ bins affected by high/not-high gizzard shad years were the larger-sized $\log_2$ bins (24–28), but the small-sized $\log_2$ bin 19 was also significant. This could be due to selective predation, but because other $\log_2$ bins are also dominated by the same species of copepod (*D. minutus*), it is possible that its significance may well be a type I error (falsely rejecting the null hypothesis). We urge caution in the interpretation of individual significant $\log_2$ bins, as those results may or may not be associated with a specific variable. We also urge caution in the use of the parameter estimates for the interaction parameter value as the numerical values are not directly interpretable because of the iterative procedures that S-PLUS (Insightful Corp. 1988–2002) uses to obtain the parameter estimates. The parameter estimates can be interpreted in relation to each other, in terms of their significance, and in a graphical format.

Use of zooplankton biomass size spectra to assess ecological change

In this study, our primary goal was to evaluate the sensitivity of biomass size spectrum based models to changes in community structure by assessing their response (or lack of response) to ecological variables that could influence zooplankton biomass in Oneida Lake. One caveat of all of our size spectra work (with the exception of the Pareto II model) is that the created data structure is artificial. Prior work has indicated that logging and binning of biomass data has the potential to obscure relationships between those data (Gaedke 1992; Blanco et al. 1994; Vidondo et al. 1997). However, although logging may create potentially artificial relationships, our intent in this paper was to identify whether this widely applied technique really did demonstrate sensitivity to ecological change.

The main ecological events we examined were changes in fish communities that structured the zooplankton through predation, the invasion of an exotic species, and fluctuations in nutrient levels, all common ecological events observed in freshwater and marine ecosystems. In general, zooplankton biomass size spectra were responsive to changes in conditions in the Oneida Lake environment, and we believe that size-based approaches have potential as a biotic index in freshwater lake ecosystems. Different aspects of the size spectrum can potentially be used for examining different aspects of an ecosystem. The slope and periodic models could be used to indicate steady state conditions for an ecosystem and to identify the resilience of a system to perturbation or be used to identify differences between systems or between areas with divergent ecosystem characteristics (for example, ecosystems differing in depth, food web composition, or productivity). However, the focus of this paper was to assess sensitivity to within-system differences, and our findings indicate that the Pareto II and GLM models demonstrated many attributes that would be useful for a within-system ecological indicator.

The Pareto II model is computationally sensitive but likely not data-intensive and has the advantage of using original untransformed zooplankton data, and our work demonstrates its utility in freshwater aquatic ecosystems. Furthermore, the Pareto II model fit data well and was extremely sensitive to environmental perturbation and change. However, the Pareto II model needs much more testing before it can be a usable management tool. More work needs to be done to fully understand the relation of its parameters to ecological change, and the programming and analyzing of the data currently requires sophisticated mathematical expertise. We envision that future studies should evolve toward the quantification of the responses of the Pareto II model to environmental perturbations, an assessment of the power of the model and its sensitivity to small ecological changes, and delineation of model data requirements.

The GLM model provided a useful size spectrum based means of quantifying the influence of specific environmental factors on zooplankton biomass and size structure in Oneida Lake. A similar approach could be applied to other lake systems where there is a need to identify the relative importance of a suite of biotic and abiotic factors on environmental change. This is useful as researchers often can list ecologically relevant variables but often cannot easily determine which ones are actually significant and the degree of their importance. The GLM analysis is readily interpretable (both graphically and in the output) and incorporates both temporal and spatial data, and the effect of any environmental variable can easily be tested. The environmental variables either can be categorical or can be run as continuous variables. These attributes mean that the model can be applied to many different lakes and sampling regimes.

Acknowledgements

We acknowledge the generous support of our funding agency, New York Sea Grant (Project No. R/CE-15), to E.L.M. and O.E.J. Pat Sullivan provided significant assistance in formulating and testing the GLM model. Mike Paterson, David Findlay, and Sairah Malkin provided early insight into the scope and shape of this project. We thank Carrie Wafer, Eric Pueschel, Dave Wendell, Jen Chunn, and Kristen Holeck for all their assistance with data entry, data formatting, and conversions. We also thank two anonymous reviewers and Gary Sprules, whose comments and suggestions significantly improved this paper. Finally, we are indebted to the many technicians at the Cornell University Biological Field Station, who collected the long-term Oneida Lake data that made this project possible. This paper represents contribution 239 from the Cornell University Biological Field Station.

References

Ahrens, M.A., and Peters, R.H. 1991. Patterns and limitations in limnoplankton size spectra. Can. J. Fish. Aquat. Sci. **48**: 1967–1978.

Aiken, J. 2003. Biomass size spectra: fit of the Pareto II model and detection of environmental perturbation. B.S. thesis, Department of Biological Statistics and Computational Biology, Cornell University, Ithaca, N.Y.

Allen, A.P., Whittier, T.R., Larsen, D.P., Kaufmann, P.R., O'Connor, R.J., Hughes, R.M., Stemberger, R.S., Dixit, S.S., Brinkhurst, R.O., Herlihy, A.T., and Paulsen, S.G. 1999. Concordance of taxonomic composition patterns across multiple lake assemblages: effects of scale, body size, and land use. Can. J. Fish. Aquat. Sci. **56**: 2029–2040.

Alvarez-Cobelas, M., Rojo, C., Velasco, J.L., and Baltanas, A. 2006. Factors controlling planktonic size spectral responses to autumnal circulation in a Mediterranean lake. Freshw. Biol. **51**: 131–143.

American Public Health Association, American Water Works Association, and the Water Pollution Control Federation. 1976. Standard methods for examination of water and wastewater. 14th ed. American Public Health Association, Washington, D.C.

Bachmann, R.W., Jones, B.L., Fox, D.D., Hoyer, M., Bull, L.A., and Canfield, D.E., Jr. 1996. Relations between trophic state indicators and fish in Florida (U.S.A.) lakes. Can. J. Fish. Aquat. Sci. **53**: 842–855.

Blanco, J.M., Echevarría, F., and García, C.M. 1994. Dealing with size-spectra: some conceptual and mathematical problems. Sci. Mar. **58**(1–2): 17–29.

Borgmann, U. 1987. Models on the slope of, and biomass flow up, the biomass size spectrum. Can. J. Fish. Aquat. Sci. **44**(Suppl. 2): 136–140.

Burns, C.W. 1968. The relationship between body size of filter-feeding Cladocera and the maximum size of particle ingested. Limnol. Oceanogr. **13**: 675–678.

Cavender-Bares, K.K., Rinaldo, A., and Chisholm, S.W. 2001. Microbial size spectra from natural and nutrient enriched ecosystems. Limnol. Oceanogr. **46**(4): 778–789.

Crowder, L.B., McDonald, M.E., and Rice, J.A. 1987. Understanding recruitment of Lake Michigan fishes: the importance of size-based interactions between fish and zooplankton. Can. J. Fish. Aquat. Sci. **44**(Suppl. 2): 141–147.

Cyr, H., and Peters, R.H. 1996. Biomass-size spectra and the prediction of fish biomass in lakes. Can. J. Fish. Aquat. Sci. **53**: 994–1006.

Downing, J.A., and McCauley, E. 1992. The nitrogen:phosphorus relationship in lakes. Limnol. Oceanogr. **37**(5): 936–945.

Gaedke, U. 1992. The size distribution of plankton biomass in a large lake and its seasonal variability. Limnol. Oceanogr. **37**(6): 1202–1220.

Gaedke, U. 1993. Ecosystem analysis based on biomass size distributions: a case study of a plankton community in a large lake. Limnol. Oceanogr. **38**(1): 112–127.

Gamble, A. 2003. The use of zooplankton biomass size spectra as indicators of environmental change in Oneida Lake, New York. M.S. thesis, Department of Natural Resources, Cornell University, Ithaca, N.Y.

Gliwicz, Z.M. 1969. Studies on the feeding of pelagic zooplankton in lakes with varying trophy. Ekol. Pol. **17**: 663–708.

Greeson, P.E. 1971. Limnology of Oneida Lake with emphasis on factors contributing to algal blooms. USGS/New York State Department of Environmental Conservation, Albany, N.Y.

Hambright, K.D., and Fridman, S. 1994. A computer-assisted plankton analysis system for the Macintosh. Fisheries (Bethesda), **19**: 6–8.

Hansen, B., Hansen, P.J., and Nielsen, T.G. 1991. Effects of large nongrazable particles on clearance and swimming behavior of zooplankton. J. Exp. Mar. Biol. Ecol. **153**: 257–269.

Idrisi, N., Mills, E.L., Rudstam, L.G., and Stewart, D.J. 2001. Impact of zebra mussels (*Dreissena polymorpha*) on the pelagic lower trophic levels of Oneida Lake, New York. Can. J. Fish. Aquat. Sci. **58**: 1430–1441.

Insightful Corp. 1988–2002. S-PLUS version 6.0. Insightful Corp., Seattle, Wash.

Jennings, S., Pinnegar, J.K., Polunin, N.V.C., and Warr, K.J. 2002. Linking size-based and trophic analyses of benthic community structure. Mar. Ecol. Prog. Ser. **226**: 77–85.

Kerr, S.R. 1974. Theory of size distribution in ecological communities. J. Fish. Res. Board Can. **31**: 1859–1862.

Kerr, S.R., and Dickie, L.M. 2001. The biomass spectrum: a predator–prey theory of aquatic production. Complexity in ecological systems series. Columbia University Press, New York.

Koonce, J.F., Busch, W.-D.N., and Chapla, T. 1996. Restoration of Lake Erie: contribution of water quality and natural resource management. Can. J. Fish. Aquat. Sci. **53**(Suppl. 1): 105–112.

MathWorks, Inc. 1994–2003. Matlab 6.1. The MathWorks, Inc., Natick, Mass.

Mazumder, A. 1994. Phosphorus–chlorophyll relationships under contrasting zooplankton community structure: potential mechanisms. Can. J. Fish. Aquat. Sci. **51**: 401–407.

McCullagh, P., and Nelder, J.A. 1991. Generalized linear models. 2nd ed. Chapman and Hall, New York.

Menzel, D.W., and Corwin, N. 1965. The measurement of total phosphorus in sea water based on the liberation of organically bound fractions by persulfate oxidation. Limnol. Oceanogr. **10**(2): 280–282.

Mills, E.L., and Forney, J.L. 1983. Impact on *Daphnia pulex* of predation by young yellow perch in Oneida Lake, New York. Trans. Am. Fish. Soc. **112**: 154–161.

Mills, E.L., and Schiavone, A. 1982. Evaluation of fish communities through assessment of zooplankton populations and measures of lake productivity. N. Am. J. Fish. Manag. **2**: 14–27.

Mills, E.L., Forney, J.L., and Wagner, K.J. 1987. Fish predation and its cascading effect in the Oneida Lake food chain. *In* Predation: direct and indirect impacts on aquatic communities. *Edited by* W.C. Kerfoot and A. Sih. University Press of New England, Hanover, N.H. pp. 118–131.

Mills, E.L., Leach, J.H., Carlton, J.T., and Secor, C.L. 1994. Exotic species and the integrity of the Great Lakes: lessons from the past. Bioscience, **44**: 666–676.

Minitab Inc. 2000. Minitab 13.2. Minitab Inc., State College, Pa.

Mood, A.M., Graybill, F.A., and Boes, D.C. 1974. Introduction to the theory of statistics. 3rd ed. McGraw-Hill Inc., New York.

Neter, J.M., Kutner, H., Nachtsheim, C.J., and Wasserman, W. 1996. Applied linear statistical models. 4th ed. WCB/McGraw-Hill Inc., Boston, Mass.

Nicholls, K.H., Hopkins, G.J., and Standke, S.J. 1999. Reduced chlorophyll to phosphorus ratios in nearshore Great Lakes waters coincide with the establishment of dreissenid mussels. Can. J. Fish. Aquat. Sci. **56**: 153–161.

Noble, R.L. 1970. Evaluation of the Miller high-speed sampler for sampling yellow perch and walleye fry. J. Fish. Res. Board Can. **27**(6): 1033–1044.

Ott, R.L. 1993. An introduction to statistical methods and data analysis. 4th ed. Wadsworth, Inc., Belmont, California.

Paterson, M.J., Findlay, D., Beaty, K., Findlay, W., Schindler, E.U., Stainton, M., and McCullough, G. 1997. Changes in the planktonic food web of a new experimental reservoir. Can. J. Fish. Aquat. Sci. **54**: 1088–1102.

Platt, T., and Denman, K.L. 1978. The structure of pelagic ecosystems. Rapp. P.-V. Réun. Cons. Int. Explor. Mer, **176**: 60–65.

Quinones, R.A., Platt, T., and Rodriguez, J. 2003. Patterns of biomass-size spectra from oligotrophic waters of the Northwest Atlantic. Progr. Oceanogr. **57**: 405–427.

Rodriguez, J., and Mullin, M.M. 1986. Relation between biomass and body weight of plankton in a steady state oceanic ecosystem. Limnol. Oceanogr. **31**(2): 361–370.

Roseman, E.F., Mills, E.L., Forney, J.L., and Rudstam, L.G. 1996. Evaluation of competition between age-0 yellow perch (*Perca flavescens*) and gizzard shad (*Dorosoma cepedianum*) in Oneida Lake, New York. Can. J. Fish. Aquat. Sci. **53**: 865–874.

SAS Institute Inc. 2001. SAS version 8. SAS Institute Inc., Cary, N.C.

Sheldon, R.W., Prakash, A., and Sutcliffe, W.H., Jr. 1972. The size distribution of particles in the ocean. Limnol. Oceanogr. **17**(3): 327–340.

Shepherd, W.C., and Mills, E.L. 1996. Diel feeding, daily food intake, and *Daphnia* consumption by age-0 gizzard shad in Oneida Lake, New York. Trans. Am. Fish. Soc. **125**: 411–421.

Smith, V.H. 1979. Nutrient dependence of primary productivity in lakes. Limnol. Oceanogr. **24**(6): 1051–1064.

Smith, V.H. 1982. The nitrogen and phosphorus dependence of algal biomass in lakes: an empirical and theoretical analysis. Limnol. Oceanogr. **27**(6): 1101–1112.

Sprules, W.G., and Goyke, A.P. 1994. Size-based structure and production in the pelagia of Lakes Ontario and Michigan. Can. J. Fish. Aquat. Sci. **51**: 2603–2611.

Sprules, W.G., and Munawar, M. 1986. Plankton size spectra in relation to ecosystem productivity, size, and perturbation. Can. J. Fish. Aquat. Sci. **43**: 1789–1794.

Sprules, W.G., Casselman, J.M., and Shuter, B.J. 1983. Size distribution of pelagic particles in lakes. Can. J. Fish. Aquat. Sci. **40**: 1761–1769.

Sprules, W.G., Brandt, S.B., Stewart, D.J., Munawar, M., Jin, E.H., and Love, J. 1991. Biomass size spectrum of the Lake Michigan pelagic food web. Can. J. Fish. Aquat. Sci. **48**: 105–115.

Strickland, J.D.H., and Parson, T.R. 1972. A practical handbook for the analysis of seawater. Bull. Fish. Res. Board Can. No. 167. 2nd ed.

Thiebaux, M.L., and Dickie, L.M. 1992. Models of aquatic biomass size spectra and the common structure of their solutions. J. Theor. Biol. **159**: 147–161.

Thiebaux, M.L., and Dickie, L.M. 1993. Structure of the body-size spectrum of the biomass in aquatic ecosystems: a consequence of allometry in predator–prey interactions. Can. J. Fish. Aquat. Sci. **50**: 1308–1317.

Vanderploeg, H.A., Liebig, J.R., Carmichael, W.W., Agy, M.A., Johengen, T.H., Fahnenstiel, G.F., and Nalepa, T.F. 2001. Zebra mussel (*Dreissena polymorpha*) selective filtration promoted toxic *Microcystis* blooms in Saginaw Bay (Lake Huron) and Lake Erie. Can. J. Fish. Aquat. Sci. **58**: 1208–1221.

Vanderploeg, H.A., Nalepa, T.F., Jude, D.J., Mills, E.L., Holeck, K.T., Liebig, J.R., Grigorovich, I.A., and Ojaveer, H. 2002. Dispersal and emerging ecological impacts of Ponto-Caspian species in the Larentian Great Lakes. Can. J. Fish. Aquat. Sci. **59**: 1209–1228.

VanDeValk, A.J., Rudstam, L. G., Brooking, T., and Beitler, A. 1999. Walleye stock assessment and population projections for Oneida Lake, 1998–2001. New York State Department of Environmental Convervation, Albany, N.Y.

Vidondo, B., Prairie, Y.T., Blanco, J.M., and Duarte, C.M. 1997. Some aspects of the analysis of size spectra in aquatic ecology. Limnol. Oceanogr. **42**(1): 184–192.

Vinebrooke, R.D., Dixit, S.S., Graham, M.D., Gunn, J.M., Chen, Y.-W., and Belzile, N. 2002. Whole-lake algal responses to a century of acidic industrial deposition on the Canadian Shield. Can. J. Fish. Aquat. Sci. **59**: 483–493.

Vollenweider, R.A. 1968. Scientific fundamentals of the eutrophication of lakes and flowing waters, with particular reference to nitrogen and phosphorus. Organization for Economic Cooperation and Development, Directorate for Scientific Affairs, Paris, France. Publ. No. DAS/SAI/68.27.

Wagner, K. 1983. The impact of natural phytoplankton assemblages on *Daphnia pulex* reproduction in Oneida Lake, New York. M.S. thesis, Cornell University, Ithaca, N.Y.

Watson, S., McCauley, E., and Downing, J.A. 1992. Sigmoid relationships between phosphorus, algal biomass, and algal community structure. Can. J. Fish. Aquat. Sci. **49**: 2605–2610.

Wetzel, R.G., and Likens, G.E. 1979. Limnological analyses. W.B. Saunders Company, Philadephia, Pa.

Wolfinbarger, W.C. 1999. Influences of biotic and abiotic factors on seasonal succession of zooplankton in Hugo Reservoir, Oklahoma, U.S.A. Hydrobiologia, **400**: 13–31.

Zhang, Y., and Prepas, E.E. 1996. Regulation of the dominance of planktonic diatoms and cyanobacteria in four eutrophic hardwater lakes by nutrients, water column stability, and temperature. Can. J. Fish. Aquat. Sci. **53**: 621–633.

Evidence for reduced genetic variation in severely deformed juvenile salmonids

Katriina Tiira, Jorma Piironen, and Craig R. Primmer

Abstract: Inbreeding is one of the factors that can result in high infant mortality. In many species, however, mortality at early life stages is very difficult to observe in the wild and estimates from later life stages may therefore underestimate the effects of reduced genetic variability on fitness. Using microsatellites, we compared the amount of genetic variation in severely deformed fry of Lake Saimaa salmon (Atlantic salmon, *Salmo salar*) and brown trout (*Salmo trutta*) hatchery brood stocks with normal fry from the same brood stocks. We observed significantly lower standardized heterozygosity and higher internal relatedness values for deformed fry of both species compared with normal fry. Our results suggest that (*i*) inbreeding can be an important factor causing severe deformities in juvenile salmonids and (*ii*) high mortality of severely deformed low heterozygosity individuals in early life stages may partly explain why some studies exploring heterozygosity–fitness correlations fail to find any association. An important direction for future research on this topic will be to compare the results of experiments conducted in captivity with those of similar experiments conducted in wild or semi-wild conditions, as such studies would help to better understand the direct relevance of research conducted in captivity with respect to the conservation of wild populations.

Résumé : La consanguinité est un des facteurs qui peuvent causer une forte mortalité des petits. Chez plusieurs espèces, cependant, la mortalité durant les premiers stades en nature est très difficile à observer et les estimations faites à partir des stades plus avancées peuvent sous-estimer les effets de la variabilité génétique réduite sur la fitness. Nous comparons à l'aide de microsatellites l'importance de la variation génétique chez des alevins fortement déformés et des alevins normaux provenant des mêmes stocks reproducteurs de pisciculture de saumons (saumon atlantique, *Salmo salar*) et de truites brunes (*Salmo trutta*) du lac Saimaa. Nous observons une hétérozygotie standardisée plus faible et une parenté interne plus élevée chez les alevins déformés des deux espèces que chez les alevins normaux. Nos résultats indiquent que (*i*) la consanguinité peut être une cause importante de déformations graves chez les jeunes salmonidés et (*ii*) la forte mortalité des individus gravement déformés à faible hétérozygotie durant les premiers stades de vie peut expliquer en partie pourquoi certaines études qui explorent le lien hétérozygotie–fitness ne réussissent pas à trouver de corrélation. Une avenue importante de recherche dans ce domaine serait de comparer les résultats d'expériences faites en captivité avec ceux d'expériences semblables conduites en conditions de liberté ou de semi-liberté; de telles études permettraient de mieux comprendre la pertinence directe des travaux menés en captivité pour la conservation des populations sauvages.

[Traduit par la Rédaction]

Introduction

Rapid genetic deterioration in captive populations compared with wild populations has been observed in several species (bacteria, Lenski and Travisano 1994; fish, Fleming et al. 2000; *Drosophila*, Woodworth et al. 2002). The causes of genetic deterioration in captive populations can include inbreeding depression, loss of genetic diversity, accumulation of new deleterious mutations, and genetic adaptations to the captive environment, which are deleterious in the wild (Frankham 1995). Captive populations often have a small population size (Frankham et al. 2002). Small effective population size, genetic drift, nonrandom mating, and bottlenecks are all factors that increase the chance of inbreeding in a population. Small population size is also an important factor in increasing the loss of genetic variation and accumulation of deleterious mutations (Frankham 1995). Although evidence exists that inbreeding may expose rare recessive deleterious mutations in the homozygous state and, thus, expose them to natural selection (Barret and Charlesworth 1991; Frankham 1995), some studies have suggested that purging may decrease the intensity of inbreeding depression, but not eliminate it (Frankham 1995; Frankham et al. 2002).

Inbreeding in a population is often manifested in high infant and larval mortality (Lacy et al. 1993; Keller and Waller 2002; Wang et al. 2002*b*); however, in many species, mortality at early life stages is very difficult to observe in the wild. This is certainly the case in most fish populations, where the

Received 20 January 2006. Accepted 4 August 2006. Published on the NRC Research Press Web site at http://cjfas.nrc.ca on 6 December 2006.
J19118

K. Tiira.[1] Department of Biological and Environmental Sciences, P.O. Box 65, FIN-00014, University of Helsinki, Finland.
J. Piironen. Joensuu Game and Fisheries Research, Yliopistonkatu 6, FIN-80100 Joensuu, Finland.
C.R. Primmer. Department of Biology, University of Turku, FIN-20014 Turku, Finland.

[1] Corresponding author (e-mail: katriina.tiira@helsinki.fi).

Can. J. Fish. Aquat. Sci. 63: 2700–2707 (2006)
doi:10.1139/F06-154

estimation of egg and larval mortality is very difficult in nature. Severe deformities have been found to be associated with inbreeding in several taxonomic groups (fishes, Agnése et al. 1995; amphibians, Hitchings and Beebee 1998; snakes, Madsen et al. 1996; mammals, Seymour et al. 2001).

Although severely deformed fish are rarely seen in the wild, malformations are often observed in cultured fish populations (Hilomen-Garcia 1997; Ferreri et al. 2000) as the earliest life stages can be monitored. Also, in hatcheries, these severely deformed individuals are observed only at early life stages (before the onset of exogenous feeding), as they rarely survive to later life stages (Andrades et al. 1996; Sadler et al. 2001). Both genetic and environmental factors are suggested to influence the appearance of deformities. Severe skeletal deformities, which are present before first feeding, are rarely observed during later life stages, indicating that the viability of these individuals is critically lowered (genetic factors). On the other hand, less severe deformities can occur after feeding has started, suggesting that environmental factors (such as nutritional factors, inappropriate physical parameters, heavy metals, and pathogenic organisms; reviewed in Chatain (1994) and Cahu et al. (2003)) may play an important role in such cases. Recently, however, evidence was obtained in guppies suggesting that the occurrence of milder vertebral deformities might be associated with overall genomic heterozygosity (Shikano et al. 2005).

Traditionally, the effect of inbreeding on fitness has been studied in laboratory or zoo animals, where the pedigrees of the animals are known (reviewed in Falconer and Mackay (1996) and Ralls and Ballou (1983)). However, as pedigree information is rarely available in most populations, researchers have relied on indirect estimates of inbreeding, e.g., allelic data for molecular markers. Positive associations have been observed between protein heterozygosity as assessed by allozymes and fitness-related traits, including growth (Mitton and Grant 1984; Danzmann et al. 1987), metabolic efficiency (Mitton and Grant 1984), fecundity, and survival (Mitton and Grant 1984; Charlesworth and Charlesworth 1987). Significant heterozygote–fitness correlations (HFC) have also recently been found with noncoding DNA markers such as microsatellites (e.g., Coltman et al. 1998; Hansson et al. 2001; Acevedo-Whitehouse et al. 2003).

Several recent simulations and studies suggest that the likelihood of neutral multilocus heterozygosity estimating the level of individual inbreeding from randomly derived populations is generally low (Balloux et al. 2004; Pemberton 2004; Slate et al. 2004). However, the same study also noted that the likelihood of detecting HFCs could be increased by treating data at the group level, rather than at the individual level (e.g., Acevedo-Whitehouse et al. 2003). The likelihood of finding a positive association between microsatellite markers and fitness may also increase by selecting microsatellites with maximum variability. This also increases the chance of selecting markers that experience balancing selection (Balloux et al. 2004) because microsatellites located in regions under balancing selection are likely to have greater variability because of local heterosis acting to increase the local genetic diversity (Balloux et al. 2004).

How can neutral molecular variation be expected to reflect variation in coding parts of the genome? There are two hypotheses that can explain the correlation between noncoding microsatellites and fitness: (*i*) the local effect and (*ii*) the general effect (David 1998; Hansson and Westerberg 2002). According to the local effect hypothesis, the neutral markers are in linkage disequilibrium with fitness-associated loci, whereas the general effect hypothesis predicts that the homozygosity across all the loci in the genome is correlated, thus signaling inbreeding.

Life stage (along with factors such as genetic background of the population, sample size, number of studied loci, the studied trait, and genetic indices (David 1998; Tsitrone et al. 2001)) is also considered to be an important factor influencing the appearance of HFC. It is assumed that the effects of inbreeding are more visible at early life stages, after which selection acts on individuals with increased homozygosity (David 1998). If increased homozygosity is an important factor influencing the occurrence of severe deformities, then the probability of finding heterozygosity–fitness associations in later life stages will decrease, as the homozygotes with lowered viability (e.g., as the result of deformities) do not survive to later life stages.

In this study, we compare the genetic diversity of deformed and normal hatchery-reared fry of Atlantic salmon (*Salmo salar*) and brown trout (*Salmo trutta*) using polymorphic microsatellite markers. Hatchery fish were used in our study, because severely deformed individuals are very difficult to find in the wild as they rarely survive to swim up from the gravel. We tested the hypothesis that deformed individuals are expected to have lower levels of genetic variation than individuals with no apparent deformities because of increased levels of severe developmental instability caused by increased homozygosity.

Materials and methods

The study fish of both populations originated from first-generation hatchery strains maintained by Saimaa Fisheries Research and Aquaculture, southeastern Finland (62°37′N, 29°50′E). Natural populations of both species are enhanced by releasing hatchery-reared fish into the wild. The Saimaa Atlantic salmon population (hereafter referred to as Saimaa salmon or simply salmon) is the only non-anadromous salmon population in Finand and is considered to be highly endangered (Makkonen et al. 2000). Despite extensive stocking ($>10^5$ individuals per year) for over a decade, the effective number of mature individuals returning to native spawning grounds since 1990 has never exceeded 50 per year and, in some years, has been less than 10 (Pursiainen et al. 1998). The amount of genetic variation in Saimaa salmon is low, less than half that of anadromous Atlantic salmon (Vuorinen 1982; Tonteri et al. 2005); hence, it has the potential to be susceptible to inbreeding. Lake-run brown trout in Lake Saimaa are also threatened (Makkonen et al. 2000); however, the population has a relatively higher level of genetic diversity compared with that of the Saimaa salmon population (Tiira et al. 2006). In the hatchery, 0%–2% of the brown trout fry production is deformed, whereas in salmon, the share of deformed fry is slightly higher (0%–3%) (J. Piironen, personal observation).

Study samples were collected from tanks maintaining standard hatchery fry production in the spring 2001 before the start of exogenous feeding. Saimaa Fisheries Research

Fig. 1. Examples of the observed deformities (from left to right): two-headed Atlantic salmon (*Salmo salar*), spiral-spined Atlantic salmon, and two kinked-spine individuals (Atlantic salmon and brown trout (*Salmo trutta*)).

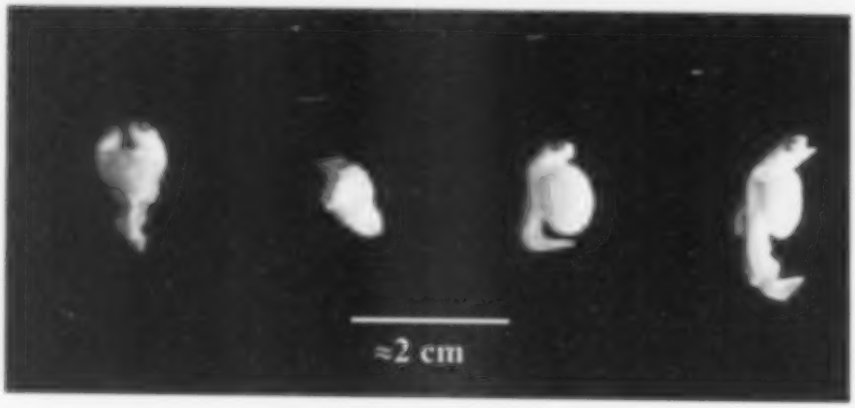

and Aquaculture uses standard hatchery procedures for fish production, where a number of dams and sires are used in fertilizations. The study fish were first hatchery generation fish, where eggs and milt were obtained from fish captured from the wild and the fertilizations were performed in the hatchery. For salmon brood stocks, 42 females and 12 males were used, resulting in 463 families, whereas for brown trout brood stock, nine females and 18 males were used, resulting in 117 families. Eggs of the families were kept in separate family-wise compartments in common garden conditions until the eyed stage, after which an equal number of eggs from each family (5 eggs·family^{-1} in salmon, 12 eggs·family^{-1} in brown trout) were transferred to one large trough for each species. Egg density in each trough was 3000·2.1 m^2, with water flow of 1.2 L·min^{-1}·1000 eggs (water temperature ranged between 1 and 5 °C). This egg density was more than 60 times lower than that recommended for culturing salmonid fish eggs (Bardach et al. 1972) and hence oxygen depletion was highly unlikely. The samples of deformed and normal fry were collected from the large trough about 2 weeks after the eggs had hatched but before the start of exogenous feeding. An individual was considered deformed if it had severe and easily recognizable spinal deformities (spiraled spine, kinked spine) or if it had two heads (Fig. 1). Fry that had no observable abnormalities were classified as normal. The overall proportion of deformed individuals was ~0.7% and ~0.5% for salmon and brown trout, respectively, and included the following deformities: two heads, spiraled spine, and kinked spine (Fig. 1; Table 1).

Table 1. The number of various deformities (Fig. 1) observed in the analyzed individuals.

Deformity	Atlantic salmon, *Salmo salar* (n = 22)	Brown trout, *Salmo trutta* (n = 16)
Spiral spine	12	4
Two heads	3	—
Kinked spine	7	12

Genetic methods

For Saimaa salmon, a total of 13 polymorphic microsatellite loci (Appendix A) were analyzed in 46 salmon from the same broodstock (22 deformed and 24 normal) using polymerase chain reaction (PCR) protocols as described in Tonteri et al. (2005). Similarly, for brown trout, 13 polymorphic microsatellite loci (Appendix A) were analysed in 41 brown trout (16 deformed and 25 normal). Details of the PCR protocols for brown trout loci are found in Tiira et al. (2006), and details of DNA extraction, gel electrophoresis, and data analysis methods are described in Primmer et al. (2000).

Three parameters were used to quantify the intra-individual genetic variation: (*i*) standardized heterozygosity (SH), where heterozygosity in each locus is weighted by the average heterozygosity at that locus (Coltman et al. 1999); (*ii*) standardized mean d^2 (mean d^2_{scaled}), which is the square of the difference in repeat units between two alleles at a locus, standardised with its locus-specific standard deviation (Coltman et al. 1999); and (*iii*) internal relatedness (IR), an estimate of parental similarity that weights the genotype by the frequencies of the alleles involved:

$$\mathrm{IR} = (2H - \sum f_i)/(2N - \sum f_i)$$

where H is the number of the homozygous loci, N is the number of the loci, and f_i is the frequency of the ith allele contained in an individual's genotype (Amos et al. 2001). Standardized measures of heterozygosity and d^2 were chosen to allow direct comparisons of variability levels for the different species, which were analyzed with different sets of microsatellite loci. The genotypes of *Ssa407* and *Ssa408* (tetranucleotide loci) included alleles that differed by only two base pairs in size, i.e., not in accordance with changes solely in repeat unit number. For the calculation of d^2_{scaled}, the allele lengths that differed by only two base pairs were adjusted to the length of the nearest "in-frame" repeat number observed in the population. In cases where there were two equidistant in-frame allele sizes, one was chosen randomly.

The number of sibling groups (i.e., families) in the deformed and normal groups was estimated using Colony 1.1 (Wang 2004) to investigate whether specimens that were sampled from a common trough included individuals from just a small number of families. Nonstandardized heterozy-

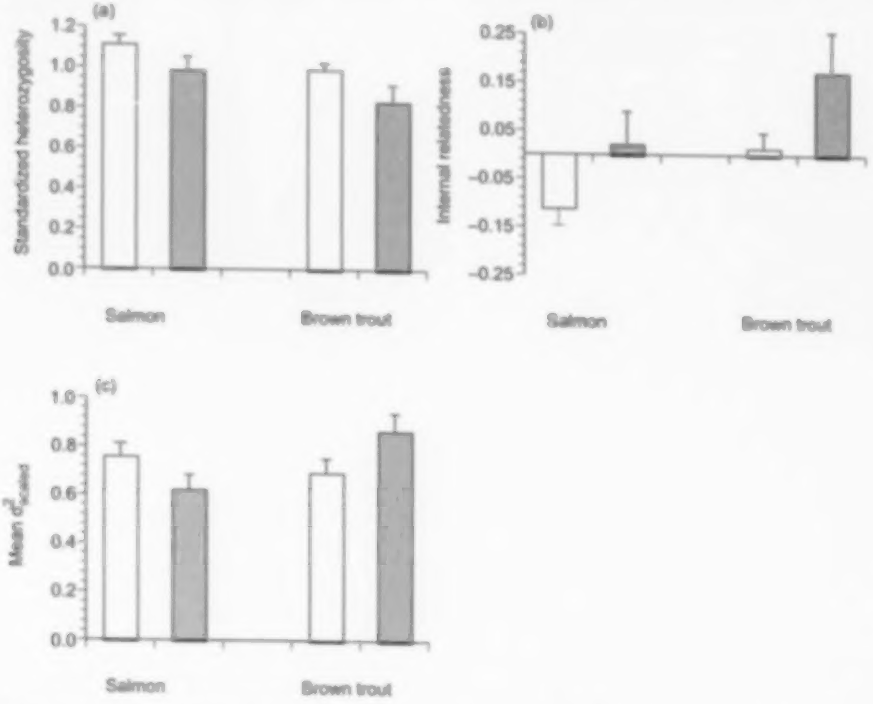

Fig. 2. Mean (± standard error, SE) (*a*) standardized heterozygosity (SH), (*b*) internal relatedness (IR), and (*c*) mean d^2_{scaled} of normal (open bars) and deformed (shaded bars) fry of Saimaa Atlantic salmon (*Salmo salar*, simply referred to as "salmon" in the figure) and brown trout (*Salmo trutta*).

gosity, allele number, and allelic richness values per locus were calculated using FSTAT (version 2.9.3.2; Goudet 1995) and are presented in Appendix A.

Statistical analysis

The data were analyzed with generalized linear mixed models (GLIMMIX in SAS 9.1; SAS Institute Inc. 2003; modeled with binomial error structure), where deformity was the response variable, SH, IR, and mean d^2_{scaled} were used as fixed factors, and species was used as a random factor. We chose to use the model with both fixed and random effects (GLIMMIX), as a model with species as a random effect is more conservative because it takes into account species-related variation when calculating the effects of genetic variability. We also analyzed the data using general linear models (binomial error structure) with only fixed effects (SH, IR, and species) (GENMOD in SAS 9.1; SAS Institute Inc. 2003) and the results were similar (data not shown).

If a positive relationship between neutral microsatellite variation and fitness-associated traits is found, two hypotheses have been proposed. Firstly, if the positive association is due to identity disequilibrium (general effect), the heterozygosity of independent marker loci should be correlated within individuals (Balloux et al. 2004; Pemberton 2004). We investigated this using a method suggested by Balloux et al. (2004), which tested the prediction that the level of variability at one set of loci will correlate with the level of variability calculated from other, independent sets of loci drawn from the same individual only under inbreeding. These correlations (IR–IR and SH–SH) were calculated from our data by repeatedly (1000 times) splitting the loci (16 for salmon, 13 for trout) randomly into two groups. Two IR–SH values were then calculated for each animal in the group, yielding a mean and SD for IR–IR and SH–SH correlations.

Secondly, a positive association between neutral genetic variation and fitness may arise due to linkage between one or few studied loci and fitness loci (local effect). To investigate whether the result would originate from one single locus, we analysed deformity as a binary variable with generalised linear models using locus-specific IR as fixed factors. An *F* test was used to control for overdispersion. If the effect originates from one or few loci, then these are most likely linked with fitness loci in the local chromosomal vicinity of the markers (local effect; Hansson et al. 2004). These statistical analyses were conducted with S-PLUS 6.1 (Crawley 2002).

Results

Severely deformed fry had significantly lower SH and higher IR compared with those of normal fry (Fig. 2; Table 2), indicating that genetic diversity was generally lower in deformed individuals. No significant difference was observed in mean d^2_{scaled} values (Table 2) between the deformed and normal fry (Fig. 2*c*). The different measures of genetic variation correlated with each other as follows: SH–IR, $r = -0.956$, $p < 0.001$; mean d^2_{scaled}–SH, $r = 0.560$, $p < 0.001$; mean d^2_{scaled}–IR, $r = -0.491$, $p < 0.001$ ($N = 87$, Pearson's correlation coefficient). Although we did not directly study the family effects on inbreeding, the fry in the

Table 2. Table presenting the coefficients and *F* statistics for the generalized linear mixed effects models where the response variable deformity was tested for the fixed effects (standardized heterozygosity (SH), internal relatedness (IR), and mean d^2_{scaled}), with species being used as a random factor.

	Coefficient (±SE)	df_{num}	df_{den}	*F*	*p*
SH					
Intercept	5.093(±2.740)				
Deformity	6.078 (±2.58)	1	84	5.55	0.0209
IR					
Intercept	11.205 (±1.025)				
Deformity	–6.812 (±2.70)	1	84	6.37	0.014
Mean d^2_{scaled}					
Intercept	11.091 (±1.831)				
Deformity	0.020 (±2.325)	1	84	0.00	0.993

Note: SE, standard error; df_{num}, degrees of freedom numerator; df_{den}, degrees of freedom denominator.

Table 3. Mean (+ standard deviation, SD) correlation between internal relatedness (IR) and standardised heterozygosity (SH) calculated from one-half of the markers against the IR–SH calculated from the other half of the 13 loci used for brown trout (*Salmo trutta*) and Atlantic salmon (*Salmo salar*).

Status	Mean *r* IR	*P* (IR)	SD (IR)	Mean *r* SH	*P* (SH)	SD (SH)
Brown trout						
Normal	–0.007	0.974	0.148	–0.018	0.933	0.148
Deformed	0.582	**0.018**	0.116	0.558	**0.026**	0.122
Atlantic salmon						
Normal	–0.284	0.179	0.171	–0.265	0.233	0.179
Deformed	0.310	0.160	0.149	0.096	0.670	0.159

Note: Markers were randomly sampled into two groups 1000 times, and mean correlation coefficient and SD were calculated separately for normal and deformed individuals.

deformed and normal groups of both salmon and brown trout were estimated to consist of numerous families (12–16), indicating that the deformed individuals did not originate from just a small number of families.

To find out whether inbreeding (general effect) is an important genetic mechanism behind the observed association between genetic variation and deformity, we calculated correlation between IR and SH values according to the method described in Balloux et al. (2004). In deformed brown trout, the IR–IR and SH–SH correlations were significant, whereas no significant correlation was observed in deformed salmon (Table 3). The IR–IR and SH–SH correlations were not significant in normal individuals of either species (Table 3). To further investigate whether the effect originates from linkage disequilibrium, we performed single-locus analyses. In salmon, four markers were found to be significantly associated with deformity ($0.05 < p > 0.01$), namely *Ssa422*, *Ssa412*, *Ssa202*, and *SLEEN82*, and in *Ssa422*, *Ssa 412*, and *Ssa202*, the deformed individuals had higher IR values. However, none of these markers remained significant after correction for multiple tests. In brown trout, no single locus tests revealed significant associations with deformity.

Discussion

Severely deformed individuals of salmon and brown trout fry, collected from the same brood stock before the start of exogenous feeding, were found to have lower levels of genetic variation compared with that of normal fry. The two main genetic explanations for finding associations between the variability level of selectively neutral microsatellites and fitness traits are identity disequilibrium (general effect) and linkage disequilibrium (local effect) (Bierne et al. 1998; David 1998; Hansson et al. 2004). According to Balloux et al. (2004) and Slate et al. (2004), if heterozygosity is correlated across markers, then the mean heterozygosity of those markers is most likely informative about inbreeding. As the IR values among markers were highly correlated in brown trout, it is safe to assume that the inbreeding has contributed to the observed deformity in brown trout juveniles. This is further supported by the fact that no single locus showed a significant effect with deformity in further analysis. In salmon, the IR–IR correlation among the deformed individuals was not statistically significant, although a correlation coefficient of 0.310 potentially indicates the presence of some inbred individuals. The single-locus analysis revealed three significant markers where the deformed individuals had higher IR values, i.e., in the same direction as the overall result. Although none of these markers remained significant after correction of multiple tests, we cannot exclude the possibility that one or two of these markers may still have a genuine effect. In summary, the general effect is very likely the factor behind this observed association between deformity and genetic variation in brown trout; however, in salmon, neither of the hypotheses could be rejected. Therefore, it is possible that local effect, as well as general effect, is responsible for the HFC in salmon, where neither of the effects is strong alone but together build up a significant correlation with fitness. Such a result may also be explained by the continual low effective size of brood stocks resulting in increased linkage disequilibrium (LD) between loci, which would make distinguishing between the local and general effect hypotheses difficult. In fact, when comparing the number of LDs between the Saimaa salmon population and the Atlantic salmon population in Tornionjoki, northern Finland, there were twice as many significant LDs between the markers in the Saimaa population and those in the Tornionjoki population (Saimaa, 8/66; Tornionjoki, 4/66; comparison made before correction for multiple tests using the 12 microsatellite markers (data not shown)).

An additional alternative hypothesis with the potential to explain the observed result stems from recent reports of the occurrence of aneuploidy, including haplo–diploid individuals, in normal and deformed Pacific salmonids (*Oncorhynchus* spp.) (Tanaka et al. 2003; Masaru et al. 2006). According to this hypothesis, genotypes interpreted as homozygous in the current study could have in fact been hemizygous, i.e., haploid. The assessment of this possibility is beyond the scope of this study, however, as the vast majority of individuals with morphological deformities in the study of Tanaka et al. (2003) had an increase in ploidy level, rather than a decrease. The effect, if any, of this phenomenon on the current study would be a conservative one.

Our study fish originated from a hatchery, and factors such as nonrandom mating, small effective population size, bottlenecks, and founder effects are common in hatchery populations (e.g., Allendorf and Phelps 1980; Ryman and Ståhl 1980; Primmer et al. 1999). These demographic factors can result in increased effects of genetic processes such as genetic drift and partial inbreeding, which in turn increase the chance of identity and linkage disequilibrium (David et al. 1995; Bierne et al. 1998; Hansson and Westerberg 2002). This is particularly so for Saimaa salmon, where the effective number of mature individuals returning to native spawning grounds since 1990 has never exceeded 50 per year and, in some years, has been less than 10 (Pursiainen et al. 1998). Therefore, because of the genetic background of the populations studied, the genetic diversity–fitness association may be more detectable with neutral markers in hatchery fish than in natural populations. More support for this idea comes from a recent study involving nine brown trout populations, where heterozygosity was correlated with social dominance only in populations with longer hatchery backgrounds (Tiira et al. 2006).

Although abnormal fry are common in cultured fish, reduced genetic variation has rarely been noted as a factor causing severe deformities in other studies (Schäperclaus 1992). However, higher frequencies of morphological abnormalities in wild populations or laboratory stocks have been observed to be associated with higher levels of inbreeding in a number of species (rainbow trout, *Oncorhynchus mykiss*, Kincaid 1976; zebra fish, *Danio rerio*, Mrakovcic and Haley 1979; adder, *Vipera berus*, Madsen et al. 1996; koala, *Phascolarctos cinereus*, Seymour et al. 2001; the common toad, *Bufo bufo*, Hitchings and Beebee 1998). Our results suggest that the role of decreased genetic variation as a factor causing severe deformities may be especially important in salmonid fish populations, given their tendency to become isolated and, hence, increasing their chances of inbreeding (Wang et al. 2002*a*).

Severely deformed individuals were found to be more homozygous, and as these fry experience high mortality before and during first feeding, it is logical to expect the population homozygosity level to be lower if assessed in later life stages, assuming that the percentage of deformed individuals is not negligible. In line with this, Liskauskas and Ferguson (1991) found that brook trout (*Salvelinus fontinalis*) fry collected before the start of exogenous feeding had fewer heterozygotes among them than fry collected after feeding had started. Severe deformities will most likely have large detrimental effects on individuals' fitness, and these fry would probably die before or during exogenous feeding. Therefore, intense selection pressure in early life history phases may partly explain why positive associations between genetic variation and fitness-related traits are sometimes not observed in later life history phases (Britten 1996).

Our study was conducted with hatchery stocks of Saimaa Lake salmon and brown trout and suggests that decreased genetic variability can be a factor contributing to the occurrence of severe skeletal deformities in these broodstocks, but do these findings have any relevance for wild populations? Several lines of evidence argue that they do. Firstly, because of their high degree of homing and tendency to evolve local adaptations (Allendorf and Waples 1995), it is reasonable to expect that at least a small proportion of matings may occur between genetically similar individuals (Wang et al. 2002*a*). This creates a possibility for inbreeding and, hence, the negative effects associated with inbreeding depression to also occur in wild salmonid populations. Secondly, that these results are more than simply a statistical association is supported by an independent experiment conducted on one of the two populations investigated in this study (Saimaa salmon). In that study, rather than comparing the genetic diversity in groups of individuals with different levels of fitness, Tiira et al. (2006) compared a fitness-related trait (juvenile aggression) in groups of individuals with different levels of genetic diversity and found significant positive association between genetic diversity and aggression. More generally, given that the probability of breeding with relatives is increased in small populations (Frankham et al. 2002), these findings are potentially of relevance to a broad range of species.

Despite often being logistically difficult, it is nevertheless important to recognize the value of genetic diversity–fitness association studies conducted in the wild as it has been demonstrated that the negative effects of inbreeding depression can be magnified in semi-wild conditions compared with in a benign captive environment (e.g., Meagher et al. 2000). Therefore, an important direction for future research on this topic would be to compare the results of experiments conducted in captivity with those of similar experiments conducted in wild or semi-wild conditions. Such studies would help to better understand the direct relevance of research conducted in captivity with respect to the conservation of wild populations.

Acknowledgements

We thank Saimaa Fisheries Research and Aquaculture for the study samples and Sami Aikio and Bill Amos for the help in IR–IR correlation calculations. Our research was funded by the Finnish Game and Fisheries Research Institute (J.P.) and the Academy of Finland (K.T. (project number 80705) and C.R.P.).

References

Acevedo-Whitehouse, K., Gulland, F., Greig, D., and Amos, W. 2003. Inbreeding: disease susceptibility in California sea lions. Nature (London), **422**: 35.

Agnèse, J-F., Otémé, Z.J., and Gilles, S. 1995. Effects of domestication on genetic variability, fertility and growth rate in a tropical siluriform: *Heterobranchus longifilis* Valenciennes 1840. Aquaculture, **131**: 197–204.

Allendorf, F.W., and Phelps, S.R. 1980. Loss of genetic variation in a hatchery stock of cutthroat trout. Trans. Am. Fish. Soc. **109**: 537–543.

Allendorf, F.W., and Waples, R.S. 1995. Conservation and genetics of salmonid fishes. *In* Conservation genetics: case histories from the nature. *Edited by* J.C. Avise and J.L. Hamrick. Chapman & Hall, New York. pp. 238–280.

Amos, W., Worthington Wilmer, J., Fullard, K., Burg, T.M., Croxall, J.P., Bloch, D., and Coulson, T. 2001. The influence of parental relatedness on reproductive success. Proc. R. Soc. Lond. B, **268**: 2021–2027.

Andrades, J.A., Becerra, J., and Fernández-Llebrez, P. 1996. Skeletal deformities in larval, juvenile and adult stages of cultured gilthead sea bream (*Sparus aurata* L.). Aquaculture, **141**: 1–11.

Balloux, F., Amos, W., and Coulson, T. 2004. Does heterozygosity estimate inbreeding in real populations? Mol. Ecol. **13**: 3021–3031.

Bardach, J.E., Ryther, J.H., and McLarney, W.O. 1972. Aquaculture: the farming and husbandry of freshwater and marine organisms. John Wiley and Sons Ltd., New York. pp. 396–449.

Barret, S.C.H., and Charlesworth, D. 1991. Effect of a change in the level of inbreeding on the genetic load. Nature (London), **352**: 522–524.

Bierne, N., Launey, S., Naciri-Graven, Y., and Bonhomme, F. 1998. Early effects of inbreeding as revealed by microsatellite analysed on *Ostrea edulis* larvae. Genetics, **148**: 1893–1906.

Britten, H.B. 1996. Meta-analysis of the association between multilocus heterozygosity and fitness. Evolution, **50**: 2158–2164.

Cahu, C., Infante, J.Z., and Takeuchi, T. 2003. Nutrional components affecting development in fish larvae. Aquaculture, **227**: 245–258.

Charlesworth, D., and Charlesworth, B. 1987. Inbreeding depression and its evolutionary consequences. Annu. Rev. Ecol. Syst. **18**: 237–268.

Chatain, B. 1994. Abnormal swimbladder development and lordodsis in sea bass (*Dicentrarchus labrax*) and sea bream (*Sparus auratus*). Aquaculture, **119**: 371–379.

Coltman, D.W., Bowen, W.D., and Wright, J.M. 1998. Birth weight and neontal survival of harbour seal pups are positively correlated with genetic variation measured by microsatellites. Proc. R. Soc. Lond. B, **265**: 803–809.

Coltman, D.W., Pilkington, J.G., Smith, J.A., and Pemberton, J.M. 1999. Parasite mediated selection against inbred Soya sheep in a free-living, island population. Evolution, **53**: 191–201.

Crawley, M.J. 2002. Statistical computing. An introduction to data analysis using S-PLUS. John Wiley & Sons Ltd., West Sussex, UK.

Danzmann, R.G., Ferguson, M.M., and Allendorf, F.W. 1987. Heterozygosity and oxygen-consumption rate as predictors of growth and developmental rate in rainbow trout. Physiol. Zool. **60**: 211–220.

David, P. 1998. Heterozygosity–fitness correlations: new perspectives on old problem. Heredity, **80**: 531–537.

David, P., Delay, B., Berthou, P., and Jarne, P. 1995. Alternative models for allozyme-associated heterosis in the marine bivalve *Spisula ovalis*. Genetics, **139**: 1719–1726

Falconer, D.S., and Mackay, T.F.C. 1996. Introduction to quantitative genetics. Longman Group Ltd., Essex, UK.

Ferreri, F., Nicolais, C., Boglione, C., and Bertolini, B. 2000. Skeletal characterization of wild and reared zebrafish: anomalies and meristic characters. J. Fish Biol. **56**: 1115–1128.

Fleming, I.A., Hindar, K., Mjolnerod, I.B., Jonsson, B., Balstad, T., and Lamberg, A. 2000. Lifetime success and interactions of farm salmon invading a native population. Proc. R. Soc. Lond. B, **267**: 1517–1523.

Frankham, R. 1995. Conservation genetics. Annu. Rev. Genetics, **29**: 305–27.

Frankham, R., Ballou, J.D., and Briscoe, D.A. 2002. Introduction to conservation genetics. Cambridge University Press, Cambridge, UK. pp. 254–279.

Goudet, J. 1995. FSTAT. Version 1.2. A computer program to calculate *F*-statistics. J. Hered. **86**: 485–486.

Hansson, B., and Westerberg, L. 2002. On the correlation between heterozygosity and fitness in natural populations. Mol. Ecol. **11**: 2467–2474.

Hansson, B., Bensch, S., Hasselquist, D., and Åkesson, M. 2001. Microsatellite diversity predicts recruitment of sibling great reed warblers. Proc. R. Soc. Lond. B, **268**: 1287–1291.

Hansson, B., Westerdahl, H., Hasselquist, D., Åkesson, M., and Bensch, S. 2004. Does linkage disequilibrium generate heterozygosity–fitness correlations in great reed warblers? Evolution, **58**: 870–879.

Hilomen-Garcia, G.V. 1997. Morphological abnormalities in hatchery bred milkfish (*Chanos chanos* Forsskal) fry and juveniles. Aquaculture, **152**: 155–166.

Hitchings, S.P., and Beebee, T.J.C. 1998. Loss of genetic diversity and fitness in common toad (*Bufo bufo*) populations isolated by inimical habitat. J. Evol. Biol. **11**(3): 269–283.

Keller, L.F., and Waller, D.M. 2002. Inbreeding effects in wild populations. TREE, **17**: 230–241.

Kincaid, H.L. 1976. Inbreeding in rainbow trout (*Salmo gairdneri*). J. Fish. Res. Board Can. **33**: 2420–2426.

Lacy, R.C., Petric, A., and Warneke, M. 1993. Inbreeding and outbreeding in captive populations of wild animal species. *In* Natural history of inbreeding and outbreeding. *Edited by* N.W. Thornhill. University of Chicago Press, Chicago, Ill. pp. 352–374.

Lenski, R.E., and Travisano, M. 1994. Dynamics of adaptation and diversification: a 10 000-generation experiment with bacterial populations. Proc. Natl. Acad. Sci. U.S.A. **91**: 6808–14.

Liskauskas, A.P., and Ferguson, M.M. 1991. Genetic variation and fitness: a test in naturalised population of brook trout (*Salvelinus fontinalis*). Can. J. Fish. Aquat. Sci. **48**: 2152–2162.

Madsen, T., Stille, B., and Shine, R. 1996. Inbreeding depression in as isolated population of adders *Vipera berus*. Biol. Conserv. **75**: 113–118.

Makkonen, J., Westman, K., Pursiainen, M., Heinimaa, P., Eskelinen, U., Pasanen, P., and Kummu, P. 2000. Viljelykantarekisteri. Kala- ja riistaraportteja nro 200. [In Finnish.]

Masaru, Y., Yamaguchi, S., and Arai, K. 2006. Mottled coloration of haploid–diploid and diploid–triploid mosaic amago salmon *Oncorhynchus masou ishikawae*. Fish. Sci. **72**: 157–165.

Meagher, S., Penn, D.J., and Potts, W.K. 2000. Male–male competition magnifies inbreeding depression in wild house mice. Proc. Natl. Acad. Sci. U.S.A. **97**: 3324–3329.

Mitton, J.B., and Grant, M.C. 1984. Associations among protein heterozygosity, growth rate, and developmental homeostasis. Annu. Rev. Ecol. Syst. **15**: 479–499.

Mrakovcic, M., and Haley, L.E. 1979. Inbreeding depression in the Zebra fish *Brachydanio rerio* (Hamilton Buchanan). J. Fish Biol. **15**: 323–327.

Pemberton, J. 2004. Measuring inbreeding depression in the wild: old ways are the best. TREE, **19**: 613–615.

Primmer, C.R., Aho, T., Piironen, J., Estoup, A., Cornuet, J.-M., and Ranta, E. 1999. Microsatellite analysis of hatchery stocks and natural populations of Arctic charr, *Salvelinus alpinus*, from the Nordic region: implications for conservation. Hereditas, **130**: 227–289.

Primmer, C.R., Koskinen, M.T., and Piironen, J. 2000. The one that did not get away: individual assignment using microsatellite data detects a case of fishing competition fraud. Proc. R. Soc. Lond. B, **267**: 1699–1704.

Pursiainen, M., Makkonen, J., and Piironen, J. 1998. Maintenance and exploitation of landlocked salmon, *Salmo salar* m. *sebago*, in the Vuoksi Watercourse. *In* Stocking and introduction of fish. *Edited by* I.G. Cowx. Fishing News Book, Blackwell Science Ltd., London. pp. 946–958.

Ralls, K., and Ballou, J. 1983. Extinction: lessons from zoos. *In* Genetics and conservation: a reference for managing wild animal and plant populations. *Edited by* C.M. Schonewald-Cox, S.M. Chambers, B. MacBryde, and L. Thomas. Benjamin-Cummings, Menlo Park, Calif. pp. 164–184.

Ryman, N., and Ståhl, G. 1980. Genetic changes in hatchery stocks of brown trout (*Salmo trutta*). Can. J. Fish. Aquat. Sci. **37**: 82–87.

Sadler, J., Pankhurst, P.M., and King, H.R. 2001. High prevalence of skeletal deformity and reduced gill surface area in triploid Atlantic salmon (*Salmo salar* L.). Aquaculture, **198**: 369–386.

SAS Institute Inc. 2003. SAS 9.1 [computer program]. SAS Institute Inc., Cary, North Carolina.

Schäperclaus, W. 1992. Fish disease. Vol. 2. Balkema, Rotterdam, the Netherlands.

Seymour, A.M., Montgomery, M.E., Costello, B.H., Ihle, S., Johnsson, G., St. John, B., Taggart, D., and Houlden, B.A. 2001. High effective inbreeding coefficients correlate with morphological abnormalities in populations of South Australian koalas (*Phascolarctos cinereus*). Anim. Conserv. **4**: 211–219.

Shikano, T., Ando, D., and Taniguchi, N. 2005. Relationships of vertebral deformity with genetic variation and heterosis in the guppy (*Poecilia reticulata*). Aquaculture, **246**: 133–138.

Slate, J., David, P., Dodds, K.G., Veenvliet, B.A., Glass, B.C., Broad, T.E., and Ewan, J.C. 2004. Understanding the relationship between the inbreeding coefficient and multilocus heterozygosity: theoretical expectations and empirical data. Heredity, **93**: 255–265.

Tanaka, M., Kimura, S., Fujimoto, T., Sakao, S., Yamaha, S., and Arai, K. 2003. Spontaneous mosaicism occurred in normally fertilized and gynogenetically induced progeny of the kokanee salmon *Oncorhynchus nerka*. Fish. Sci. **69**: 176–180.

Tiira, K., Laurila, A., Enberg, K., Piironen, J., Aikio, S., Ranta, E., and Primmer, C.R. 2006. Heterozygous brown trout (*Salmo trutta*) are more dominant — but it depends on the population history. Behav. Ecol. Sociobiol. **59**: 657–665.

Tonteri, A., Titov, S., Veselov, A., Zubchenko, A., Koskinen, M.T., Lesbarrères, D., Kaluzhin, S., Bakhmet, I., Lumme, J., and Primmer, C.R. 2005. Phylogeography of anadromous and non-anadromous Atlantic salmon (*Salmo salar*) from northern Europe. Ann. Zool. Fenn. **42**: 1–22.

Tsitrone, A., Rousset, F., and David, P. 2001. Heterosis, marker mutational processes and population inbreeding history. Genetics, **159**: 1845–1859.

Vuorinen, J. 1982. Little genetic variation in the Finnish Lake salmon, *Salmo salar sebago* (Girard). Hereditas, **97**: 189–192.

Wang, J. 2004. Sibship reconstruction from genetic data with typing errors. Genetics, **166**: 1963–1979.

Wang, S., Hard, J., and Utter, F. 2002*a*. Genetic variation and fitness in salmonids. Conserv. Genet. **3**: 321–333.

Wang, S., Hard, J., and Utter, F. 2002*b*. Salmonid inbreeding: a review. Rev. Fish Biol. Fish. **11**: 301–319.

Woodworth, L.M., Montgomery, M.E., Briscoe, D.A., and Frankham, R. 2002. Rapid genetic deterioration in captive populations: causes and conservation implications. Conserv. Genet. **3**: 277–288.

Appendix A

Table A1. Heterozygosity (*H*), allele number (*A*), and allelic richness (A_R) values for microsatellite loci analysed in Atlantic salmon (*Salmo salar*) and brown trout (*Salmo trutta*).

	Deformed			Normal		
Locus	*A*	A_R	*H*	*A*	A_R	*H*
Atlantic salmon						
Ssa171	6	4.8	0.66	6	5.1	0.74
Ssa197	6	5.8	0.89	5	5.0	0.71
Ssa202	10	9.3	0.76	7	6.4	1.0
Ssa85	3	2.7	0.10	3	2.5	0.18
SSOSL311	3	3.0	0.61	3	3.0	0.49
SSOSL438	2	2.0	0.26	2	2.0	0.52
SSOSL85	2	2.0	0.32	3	3.0	0.65
SLEEN82	3	2.9	0.69	2	2.0	0.33
Ssa14	2	2.0	0.17	2	1.8	0.08
Ssa412	1	1.0	0	2	2.0	0.19
Ssa422	6	5.8	0.58	4	4.0	0.88
SSOSL25	4	3.5	0.42	2	2.0	0.46
SLEEI84	3	2.6	0.39	2	2.0	0.46
Overall loci	3.9	3.6	0.45	3.3	3.1	0.52
Trout						
MST15	3	3.0	0.58	4	3.4	0.80
MST60	3	2.9	0.31	3	2.7	0.45
MST73	3	3.0	0.83	3	3.0	0.74
One9	4	3.7	0.66	4	3.4	0.58
Ssa197	5	4.8	0.64	6	4.9	0.87
Ssa85	5	4.0	0.13	2	1.5	0.04
SSOSL417	7	6.6	0.65	6	4.6	0.52
BS131	4	3.4	0.53	4	3.7	0.61
MST85	7	5.7	0.45	6	5.5	0.61
Ssa408	9	8.5	0.79	10	8.6	0.87
Strutta7	5	4.9	0.48	5	4.2	0.57
Ssa407	11	11.0	0.94	13	10.1	0.91
Strutta58	5	4.9	0.51	8	7.3	0.67
Overall loci	5.5	5.1	0.58	5.7	4.8	0.63

Note: Original microsatellite locus references for trout and Atlantic salmon can be found in Tiira et al. (2006; Behav. Ecol. Sociobiol. **59**: 657–665) and Tonteri et al. (2005; Ann. Zool. Fenn. **42**: 1–22), respectively.

Patterns of diel vertical migration of zooplankton in acoustic Doppler velocity and backscatter data on the Newfoundland Shelf

Nicholas R. Record and Brad de Young

Abstract: Backscatter data from moored acoustic Doppler current profilers (ADCPs) are analysed to quantify the diel vertical migration patterns of zooplankton on the Newfoundland Shelf, Canada. Data from 11 moorings provide long time series (~100 days each) for in-depth statistical analysis. For one deployment, dry weight measurements of zooplankton are used to calibrate the acoustic backscatter. Quantification methods are developed and applied to the backscatter and vertical velocity time series to determine the characteristics of the observed diel migration. We show that the migration responds to changes in light intensity and water column temperature structure. We have sufficient spatial data to show high correlation of migration characteristics over spatial scales of up to tens of kilometres.

Résumé : Nous analysons les données de rétrodiffusion recueillies par des enregistreurs acoustiques de profils de courants Doppler (ADCP) amarrés sur la plate-forme de Terre-Neuve, Canada, afin de déterminer quantitativement les patrons de migration du zooplancton. Les données provenant de 11 points d'amarrage forment de longues séries (chacune d'environ 100 jours), ce qui rend possible une analyse statistique détaillée. Pour une des séries, des déterminations des masses sèches du zooplancton permettent de calibrer la rétrodiffusion acoustique. Nous mettons au point des méthodes de quantification que nous utilisons pour déterminer les caractéristiques de la migration journalière observée à partir des séries temporelles de rétrodiffusion et de vitesse verticale. Nous démontrons que la migration réagit aux changements d'intensité lumineuse et à la structure thermique de la colonne d'eau. Nous possédons suffisamment de données spatiales pour mettre en évidence une forte corrélation entre les caractéristiques de la migration sur des échelles spatiales pouvant atteindre des dizaines de kilomètres.

[Traduit par la Rédaction]

Introduction

Many species of oceanic zooplankton exhibit patterns of diel vertical migration (DVM). Migration is typically nocturnal; the zooplankton is near the surface at night and at depth during the day. Migration occurs during twilight hours. DVM is of interest for many reasons, including population dynamics, predator–prey interactions (Clark and Levy 1988; Lampert 1989), and contributions to biogeochemical processes, such as transport of dissolved inorganic carbon and nitrogen to deep water (Madin et al. 2001; Hays 2003). Off the northeastern coast of Newfoundland, Canada, zooplankton play a key role in the marine ecosystem as prey for capelin, a major forage and commercial species in the Northwest Atlantic (Carscadden et al. 2001). Recent experimental work (Kunze et al. 2006) supports earlier theoretical calculations (Huntley and Zhou 2004) that zooplankton migration may provide an important source of energy for mixing in coastal waters.

Despite many decades of study, much debate remains regarding both the evolutionary mechanisms behind DVM and the cues influencing it (cf. Lampert 1989; Hays 2003). Predator evasion is currently the most favoured evolutionary hypothesis, i.e., nocturnal zooplankton migration is a result of balancing a need to graze in phytoplankton-rich surface waters with a need to avoid visually orienting predators (Zaret and Suffern 1976). Cues including light, temperature, food availability, predation, and endogenous rhythms (Forward 1988) are believed to influence migration, though the relative importance of each is unresolved. Zooplankton has been observed in the laboratory to respond to changes in light intensity (Clarke 1930). In situ, the synchronisation of migration times to the day–night cycle is further evidence of this relationship (Ashjian et al. 2002), though Lorke et al. (2004) found migration timing in *Chaoborus flavicans* larvae to be unaffected by changes in cloud cover, suggesting an endogenous rhythm. Not surprisingly, water temperature is also important because of its influence on the development and metabolism of zooplankton (McLaren 1963, 1974; Enright 1977). Sea water temperature is highly stratified in the vertical, and this stratification can have a substantial effect on DVM. Isotherms have been observed to define upper

---

Received 6 March 2006. Accepted 8 November 2006. Published on the NRC Research Press Web site at http://cjfas.nrc.ca on 6 December 2006.
J19206

N.R. Record and B. de Young.[1] Department of Physics and Physical Oceanography, Memorial University of Newfoundland, St. John's, NL A1B 3X7, Canada.

[1] Corresponding author (e-mail: bdeyoung@physics.mun.ca).

Can. J. Fish. Aquat. Sci. **63**: 2708–2721 (2006) doi:10.1139/F06-157

and lower migration boundaries (Geller 1986). Many types of zooplankton have also been observed to alter their migration behaviour in response to the presence of predators (Dodson 1988; Neill 1990) and the availability of food (Mauchline 1998).

Bioacoustic techniques provide certain advantages for studying zooplankton DVM in situ. Acoustic instrumentation offers a higher temporal resolution than towed nets, as well as information on the entire water column, without any invasive effects (Brierley et al. 1998). The acoustic Doppler current profiler (ADCP), an instrument designed to measure water velocities, has been shown to have value as a bioacoustic tool, in particular for observing zooplankton DVM (Flagg and Smith 1989; Heywood 1996; Tarling et al. 1998). The ADCP measures three-dimensional velocity vectors of acoustic scatterers in the water column by using the Doppler shift in reflected acoustic signals (at least three beams oriented at different angles to produce a three-dimensional vector). With a high enough concentration of migrating zooplankton in the water column, both the measured velocity and the intensity of the backscattered signal are dominated by zooplankton signal. If enough zooplankton are present, then it should be possible to detect both the presence of zooplankton and its vertical velocity, if large enough (Sindlinger et al. 2005).

There are two facets to the application of acoustic data to zooplankton studies. The first is the need to calibrate the backscatter by correlation of the backscatter with zooplankton abundance, taxonomy, and size. This can be approached as either the "forward problem" of mathematically modelling scattering based on assumptions about the properties of the animal (Stanton and Chu 2000) or the "inverse problem" of determining the properties of the animal based on measured backscatter (Holliday and Pieper 1995). These problems can be very difficult in complex multispecies zooplankton communities requiring multiple frequencies, directed tow studies, and very high-resolution acoustic data, as well as specialised calibration of the instrument (Brierley et al. 1998). The second facet is the common use of backscatter to provide descriptive information regarding spatial and temporal patterns of scattering layers. Use of ADCPs for bioacoustic data in surveys and moorings has become quite common (Thomson and Allen 2000), and calibration and directed tow data are often not available for conversion to zooplankton abundance, taxonomy, and size. This need not limit assessments of these data to the qualitative type. Because of the ease and regularity of collecting such data, it is valuable to develop quantitative techniques for their analysis. These techniques are used here with historical ADCP data to (*i*) examine the vertical swimming velocities of zooplankton measured by the ADCP, (*ii*) assess the influence of light and temperature stratification the observed DVM pattern, and (*iii*) address the issue of horizontal homogeneity at spatial scales from tens of metres to tens of kilometres using data from multiple simultaneous moorings.

Materials and methods

There are several different techniques found in the literature for quantifying the migration of zooplankton, each suited to a different purpose. Ashjian et al. (2002) calculate the biomass median depth from the backscatter field, i.e., the depth that divides the biomass profile in half. Such an approach is valuable provided that there are not multiple simultaneous layers, and it gives a better representation of the layer depth than other quantification techniques, e.g., the depth of maximum backscatter. Rippeth and Simpson (1998) use the velocity field measured by the ADCP to model the path of a hypothetical Lagrangian particle to examine the spatial and temporal dynamics of the zooplankton population.

One advantage of Doppler profilers over other bioacoustic instruments is that information is also provided on the speed of acoustic scatterers. Vertical velocities of water in the ocean are generally on the same order of magnitude as the error in averaged velocity measurements by the ADCP, of the order of several millimetres per second, so that the velocity of migrating zooplankton can be easily discerned, depending on the speed of migration. In addition to resolving swimming velocities, quantification methods allow assessment of how accurately the velocities measured by the ADCP represent actual zooplankton velocities.

Heywood (1996) uses a numerical simulation whereby scatterer distribution in the water column is modelled as a function of time, t, and depth, z, based on the measured vertical velocities, w, according to

$$(1) \qquad \frac{\partial S}{\partial t} = \frac{\partial (wS)}{\partial z}$$

where S is a measure of scatter abundance logarithmically related to relative volume backscatter strength, S_v. This model is used to demonstrate that vertical velocities measured by the ADCP accurately represent migration velocities, though the possibility of a small bias is suggested.

In addition to these techniques, the vertical velocities can also be modelled by applying a velocimetry algorithm to the backscatter array. The technique used here relies on the assumptions that (*i*) the surface (or bottom) provides a closed boundary through which migrators do not pass and (*ii*) the backscatter array represents an essentially one-dimensional phenomenon. The flux of scatterers through any depth z_1 and through time step n is given by

$$(2) \qquad F_S(z_1) = \frac{1}{\Delta t}\sum_{z=z_1}^{\text{surface}}[S(z)_{n+1} - S(z)_n]$$

and the velocity is then given by

$$(3) \qquad w(z_1) = \left(\frac{\Delta z}{\Delta t}\right)\frac{\sum_{z=z_1}^{\text{surface}}[S(z)_{n+1} - S(z)_n]}{S(z_1)}$$

This calculation models the full velocity field based on the backscatter field.

The above quantification techniques, with the exception of the Lagrangian particle path, all rely on an intermediate conversion from S_v to S. Converting backscatter intensity to equivalent zooplankton biomass or some measure of abundance is a tricky process with many parameters to take into account (Stanton et al. 1994; Martin et al. 1996; Fielding et al. 2004). To formulate a reliable conversion, precalibration

Fig. 1. Locations of moorings for 1999, 2001, 2002, and 2004 deployments and automated weather observation system (AWOS) station. Inset map of Canada shows the location of Newfoundland.

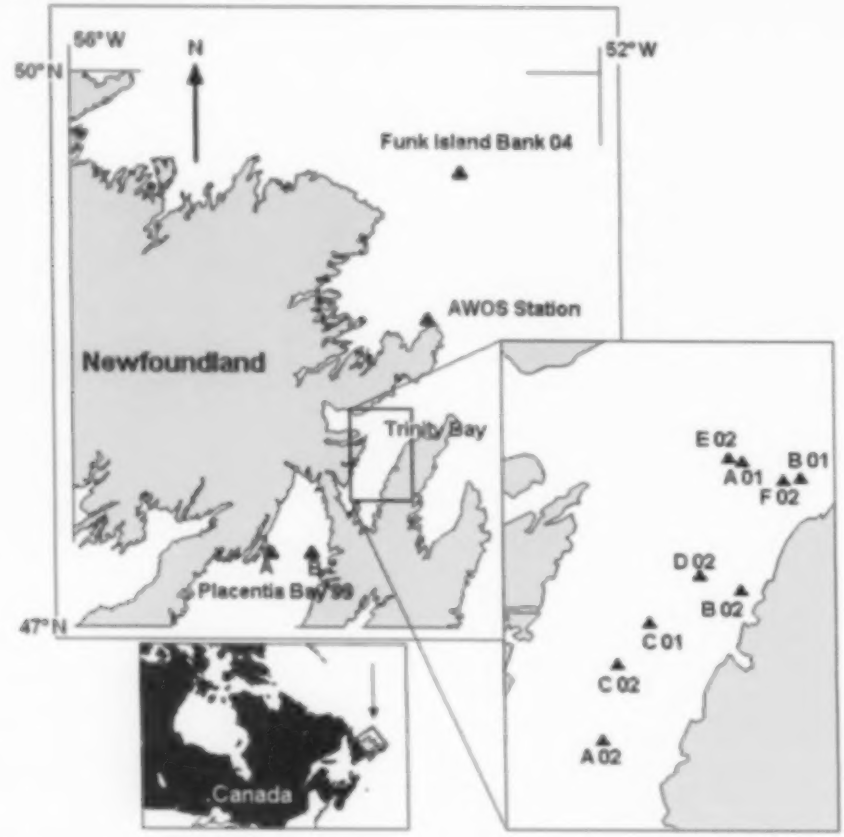

Table 1. Mooring information.

Mooring	Latitude (N)	Longitude (W)	Water depth (m)	Thermistor and ADCP depths (m)	Pings per ensemble	Year days
Placentia Bay 1999						
A	47°24.63′	54°24.17′	428	110 (ADCP)	70	107–180
B	47°24.56′	54°04.27′	304	110 (ADCP)	70	107–180
Trinity Bay 2001						
A	48°04.83′	53°24.53′	240	55, 105 (ADCP), 155, 200, 233	50	140–234
B	48°03.59′	53°17.98′	244	51, 101 (ADCP), 151, 201, 238	50	140–234
C	47°54.68′	53°31.74′	301	50, 100 (ADCP), 150, 200, 294	50	140–234
Trinity Bay 2002						
A	47°47.53′	53°36.17′	340	20, 30, 40, 50, 75 (ADCP), 100, 200	50	126–240
B	47°56.72′	53°23.47′	400	20, 30, 40, 50, 75 (ADCP), 100, 200, 383	50	126–187
C	47°52.16′	53°34.69′	350	20, 30, 40, 50, 75 (ADCP), 100, 200, 338	50	126–240
D	47°57.67′	53°27.19′	449	20, 30, 40, 50, 75 (ADCP), 200, 432	50	126–240
E	48°04.57′	53°23.31′	239	20, 30, 40, 50, 74 (ADCP), 100, 200	50	126–240
F	48°03.47′	53°19.60′	300	20, 30, 40, 50, 75 (ADCP), 100, 200	50	126–240
Funk Island Bank 2004						
	49°27.85′	52°51.30′	327	15, 20, 30, 40, 50, 60, 70, 80, 110 (ADCP), 150, 250, 300	100	219–233

Note: ADCPs operated at 307.2 kHz with bin size 4 m. Time interval of ensemble averaging was 1200 s, with the exception of the Funk Island Bank mooring, which was 600 s.

Fig. 2. Averaged backscatter and vertical velocity data from mooring C, Trinity Bay 2001: (*a*) diel average of measured volume backscatter and (*b*) associated standard deviation; (*c*) diel average of measured vertical velocity and (*d*) associated standard deviation. Averages include year days 141–230. This plot is characteristic of all moorings.

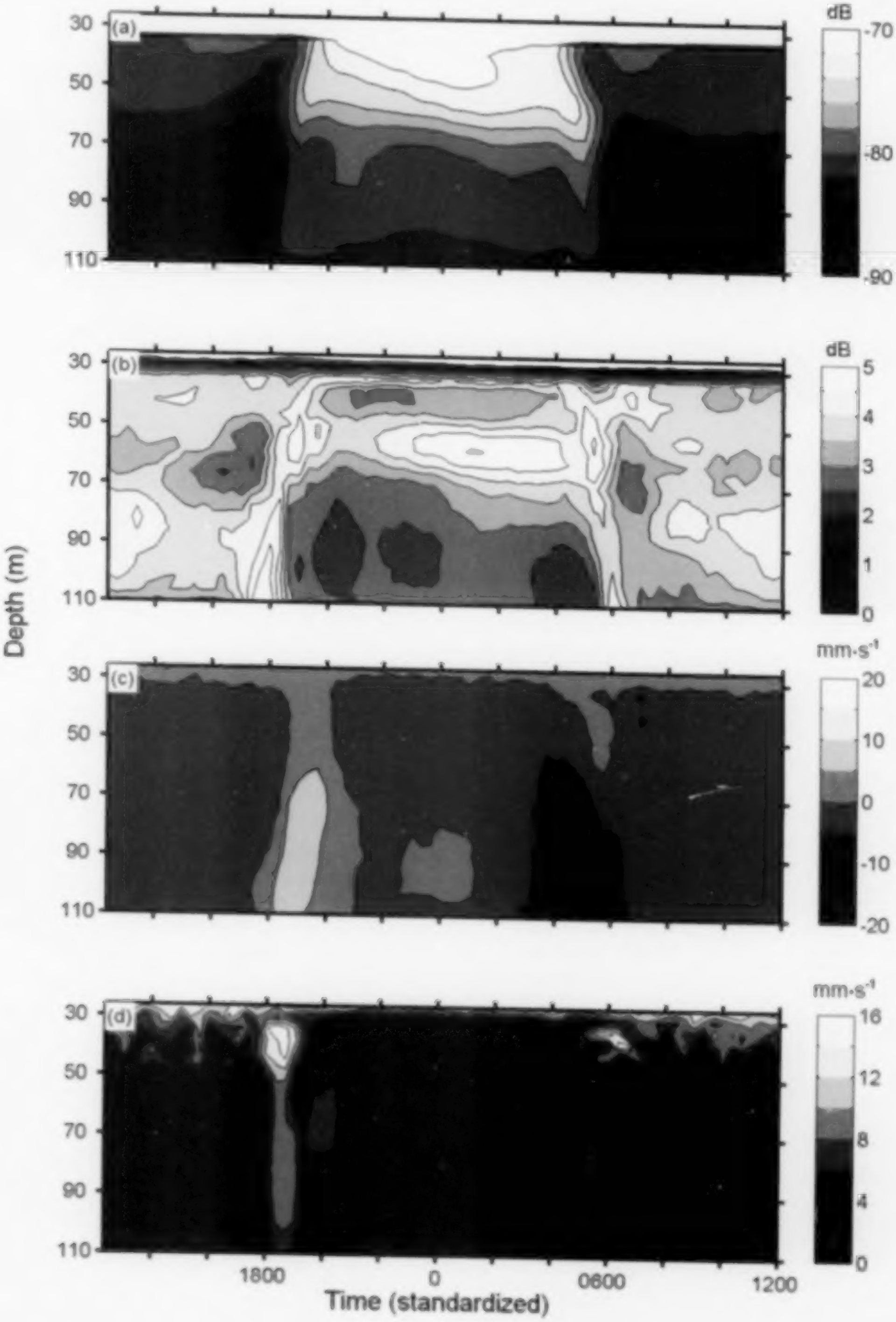

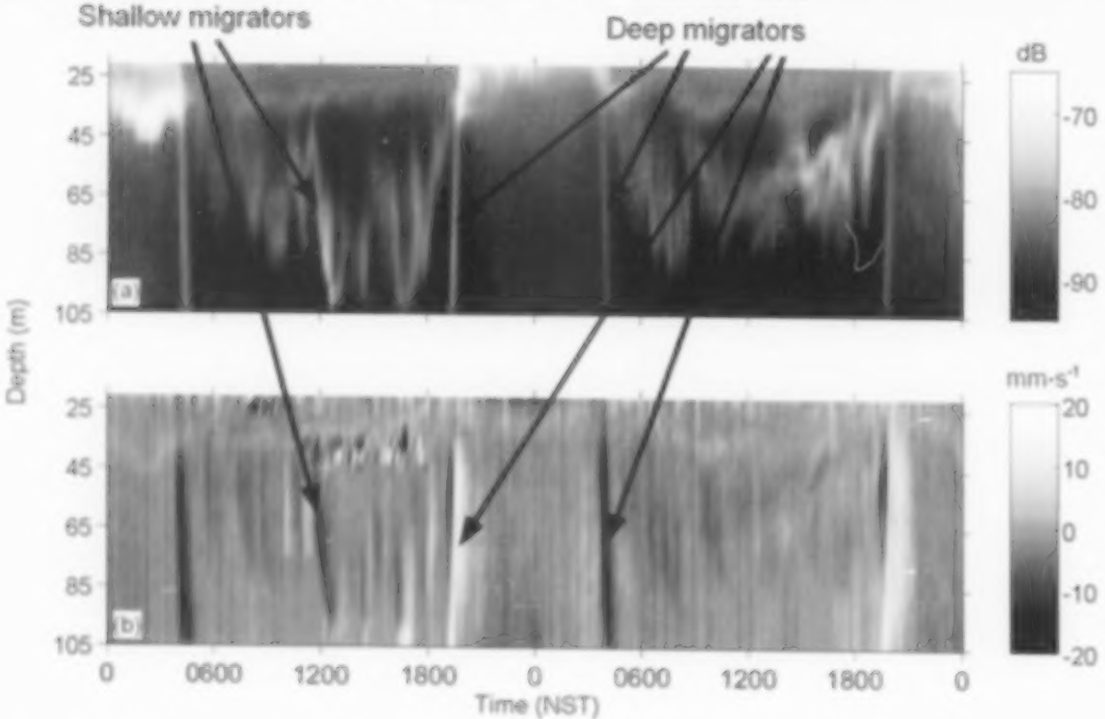

Fig. 3. A 2-day sample of (*a*) backscatter and (*b*) vertical velocity data from the Funk Island Bank 2004 mooring showing the presence of two distinct groups of migrators. Time is shown in Newfoundland Standard Time (NST).

of the ADCP is optimal (Flagg and Smith 1989), and tow data should be directed to this purpose for taxonomic differentiation (Wiebe et al. 1996). Such conversions are typically viewed only as estimates of biomass because many acoustic scatterers in the water column are not captured in zooplankton nets (Ashjian et al. 2002). Because volume backscatter is logarithmically related to measures of abundance, a biomass estimate can be a useful tool for determining relative abundance. Heywood (1996) uses a simple log–antilog relationship, but when tow data are available, better estimates improve the output of the quantification algorithms.

Timing of migration is also of interest. Lorke et al. (2004) determined the timing of migration from the temporal derivative of S_v at a given depth; Ashjian et al. (2002) used peak velocity times.

We applied these techniques to the ADCP data from the Newfoundland Shelf, with a focus on the Northeast Newfoundland Shelf and the coastal embayments (Colbourne et al. 1997; Davidson et al. 2001), and the significant results are presented here. Results of the analysis are used to answer the questions put forth in the introduction of vertical swimming velocity, horizontal homogeneity of the migrating layer over Trinity Bay, and migrator response to light and temperature stratification.

Historical data

We use mooring data primarily from bay circulation studies (e.g., Tittensor et al. 2002). ADCPs that have been moored for studies on physical characteristics of the ocean also collect backscatter data that are in many cases seen to contain valuable information on the DVM patterns of zooplankton. Deployments took place in 1999, 2001, 2002, and 2004; the moorings were located off the eastern coast of Newfoundland (Fig. 1; Table 1).

The Funk Island Bank mooring was deployed as part of a study exploring the relationship between capelin (*Mallotus villosus*), seabirds, and zooplankton. This mooring recorded at a higher temporal resolution and had better thermistor coverage through the water column. It also included a downward-looking ADCP to view the lower portion of the water column, but this ADCP malfunctioned and did not collect data.

ADCP configuration

Each mooring contained an upward-facing 307.2 kHz RDI Workhorse ADCP (Teledyne RD Instruments USA, Poway, California), using a four-beam Janus configuration with a beam angle of 21°. The vertical bin size was 4 m, and ensemble intervals were either 10 or 20 min (Table 1). Relative volume backscatter strength (S_v) was calculated from backscatter (the average of four beams) according to Deines (1999) and is given in decibels (dB) referenced to $(4\pi m)^{-1}$.

Biological sampling

The 2004 data were complimented with oblique bongo net tows (mesh sizes 333 and 232 µm, depths to 100 m) collected as part of a large-scale survey that covered a 100 nautical mile (185 km) grid surrounding the mooring. Mesh

Fig. 4. Distribution of (*a*) upward and (*b*) downward migration velocities (magnitude) for all data. Vertical lines indicate average.

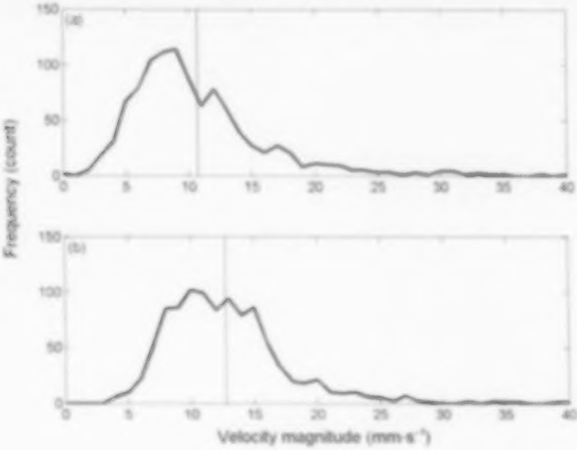

sizes and depths were determined based on zooplankton known to inhabit this area (Dalley et al. 2001). Dry weight was determined after filtering by three sieve sizes (2, 1, and 0.232 mm). The samples were heated at 60 °C for 24 h and weighed. Use of dry weight to calibrate backscatter follows Ashjian et al. (2002).

Additional physical data

Most moorings had thermistors spaced at intervals to collect temperature data over the water column for the duration of the deployment (Table 1). Thermistors were generally arranged to give a higher spatial resolution over the thermocline, and data were linearly interpolated into 4 m bins. Ensemble intervals corresponded to those of the ADCPs.

Cloud opacity data were obtained from Environment Canada, collected at a land-based automated weather observation system (AWOS) at the tip of Bonavista Peninsula (48.68°N, 53.12°W, 27 m elevation) (Fig. 1), to be used as a proxy for light intensity for the 2001 and 2002 deployments. Cloud opacity is calculated from laser ceilometer measurements. The weather station's location at the tip of a peninsula in close proximity to the study area minimises the effect of land on cloud coverage. The 1999 deployment was not considered in light calculations because of the large distance between the moorings and the weather station. The 2004 deployment was not considered because of the short deployment duration.

Results

Migration behaviour is highly persistent at all moorings throughout the deployments. The persistence can be illustrated by taking "diel averages", i.e., averaging each 10 or 20 min time bin over many days to determine the average diel rhythm (Fig. 2). The typical nocturnal migration pattern is easily recognisable in both the volume backscatter and vertical velocity data. The average signal near the surface is 10 dB higher at night than during the day. Because deployments spanned about 3 months, during which twilight times varied a great deal, the data were "time-standardised" following Ashjian et al. (2002) so that sunrise corresponds to 0600 and sunset corresponds to 1800.

Table 2. Mean and extremum ascent and descent velocities of migrating scatterers.

	Ascent velocity (mm·s^{-1})		Descent velocity (mm·s^{-1})	
Mooring	Mean	Maximum	Mean	Minimum
Placentia Bay 1999				
A	10.1	18.6	−10.8	−19.4
B	9.4	21.0	−10.0	−19.7
Trinity Bay 2001				
A	8.4	14.9	−14.1	−22.2
B	12.7	21.1	−15.5	−26.4
C	10.4	18.8	−13.8	−22.6
Trinity Bay 2002				
A	6.7	15.0	−10.2	−19.5
B	5.9	11.1	−10.0	−18.6
C	7.0	14.2	−10.3	−17.5
D	8.9	16.1	−10.7	−18.6
E	9.3	15.3	−8.7	−14.6
F	12.1	22.1	−8.9	−17.0
Funk Island Bank 2004				
	25.2	37.7	−22.5	−13.2

Examination of the time series typically reveals two distinct groups of migrators (Fig. 3). Both occupy the shallow waters at night, yielding a strong scattering layer. In the morning, a group of "deep migrators" travels abruptly to below ADCP depths, out of range, re-emerging as abruptly in the evening. This migration is marked by very large vertical velocities, typically 10–40 mm·s^{-1}. A group of "shallow migrators" descends for the daytime but remains at depths within ADCP range most of the time, visible as a scattering layer at 50–100 m. This latter group is not always detectable in the vertical velocity data, i.e., the migration velocities are often indistinguishable from the background velocities. Shallow migrators are most apparent in the Funk Island Bank and Trinity Bay data sets; they are less apparent in the Placentia Bay data set.

Historical data offer a speculative interpretation of these two groups. Copepods are the most numerous zooplankton in this part of the ocean, and in terms of biomass, *Calanus finmarchicus* is dominant (Dalley et al. 2001). *Calanus finmarchicus* is known to be a shallow migrator relative to other zooplankton (Cushing 1951), suggesting that they are likely to contribute significantly to the shallow migrators seen in the ADCP signal. Indeed, the majority of zooplankton sampled during our net tows was comprised of copepods. The deep migrators are likely composed of other vertical migrators known to be abundant in this region, including amphipods and euphausiids (Dalley et al. 2001), which generally have greater swimming speeds than calanoid zooplankton.

Migration velocity

Migration velocity calculations suggest that descent is more rapid than ascent. The migration velocity was calculated as

Fig. 5. A 4-day sample of (*a*) backscatter data from mooring C, Trinity Bay 2001, and (*b* and *c*) output from quantification algorithms: (*b*) redistribution of scatters based on measured vertical velocities and (*c*) Lagrangian particle path modelled using measured vertical velocities.

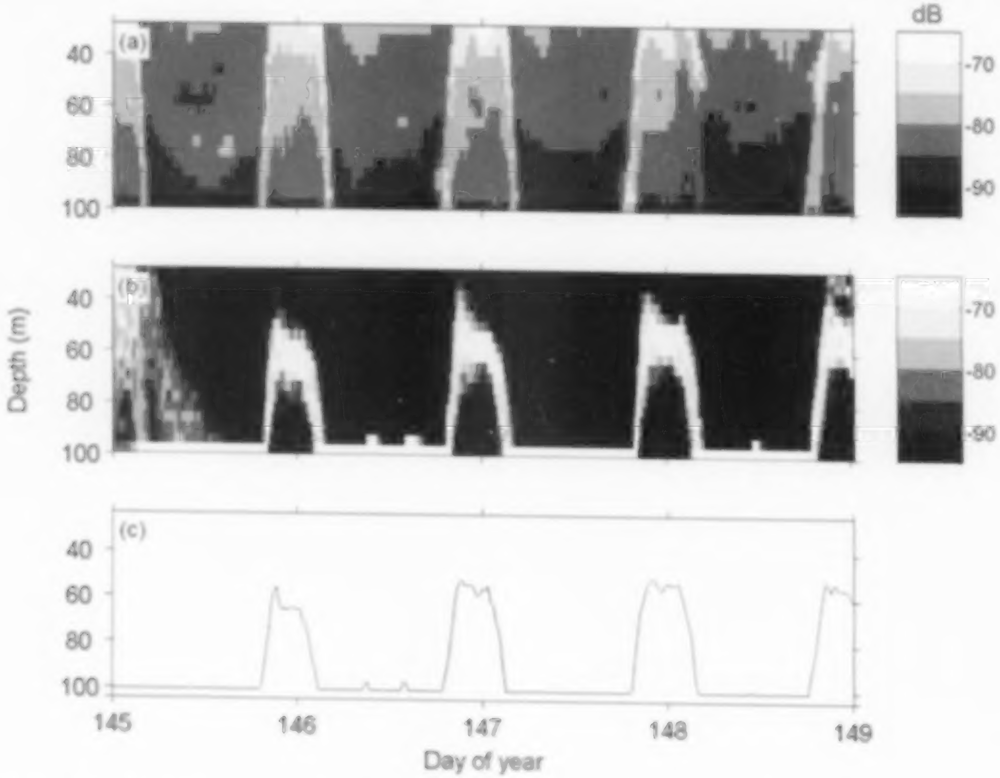

follows. For each day, the maximum velocity was found for each 4 m depth bin within a 20 m interval (the interval from 50 m to 70 m depth was used to maintain consistency between all moorings). These five values were averaged, omitting the two outliers, to give an ascent velocity for that day. Descent velocities were determined analogously using minima. An immediate result of this calculation is that descent velocities are greater in magnitude than ascent velocities (Fig. 4; Table 2).

Each individual velocity measurement represents an ensemble average over many pings. The presence of non-migrating acoustic scatterers throughout the water column is likely to bias the velocity measurement. The measurements themselves suggest a low bias: zooplankton migrating at a mean velocity of only 10 mm·s^{-1} would require almost 3 h to migrate the 100 m viewed by the ADCP. Three aforementioned models were applied to test for this bias: (*i*) Lagrangian particle path (Rippeth and Simpson 1998), (*ii*) redistributing scatterer concentration based on measured velocity according to eq. 1 (Heywood 1996), and (*iii*) velocimetry from backscatter data according to eq. 3. The first two models yield migrating layers that are consistently deeper than the measured scattering layer (Fig. 5), suggesting that measured velocities do not account for the full magnitude of migration. The velocimetry analysis also supports this conclusion, yielding migration velocities that are larger than measured velocities (Fig. 6). The velocimetry algorithm has the added benefit that only migration velocities are modelled, while background velocities are filtered out. That the surface is not a true closed boundary causes some error in velocimetry calculations, which could be reduced by using a downward-looking ADCP, with the bottom as a closed boundary. Patchiness of drifting zooplankton also contributes to the uncertainty of this calculation.

Light

The data from the two Trinity Bay deployments reveal a response by migrators to differences in atmospheric light conditions. The timings of ascent and descent are determined by the maximum and minimum temporal derivatives of backscatter, respectively, for each day. For dusk ascent on a given day, the maximum temporal derivative of backscatter is found for each depth bin (up to 50 m), yielding a time for each depth. These times are averaged, omitting two outliers, to give the timing of ascent. The timing of decent is determined analogously. Some subjectivity exists in choosing the depth interval over which to determine timing. Using a different depth interval alters the resulting values, but the dominant trend, described below, remains.

Cloud opacity data are taken from a land-based weather station at the tip of Bonavista Peninsula (Fig. 1). There is some uncertainty associated with using cloud data as a proxy

Fig. 6. A 4-day sample of (*a*) vertical velocity data from mooring C, Trinity Bay 2001, and (*b*) output from velocimetry algorithm. (*c*) Cross sections of (*a*) and (*b*) at 75 m are shown, indicated by the broken line and the solid line, respectively.

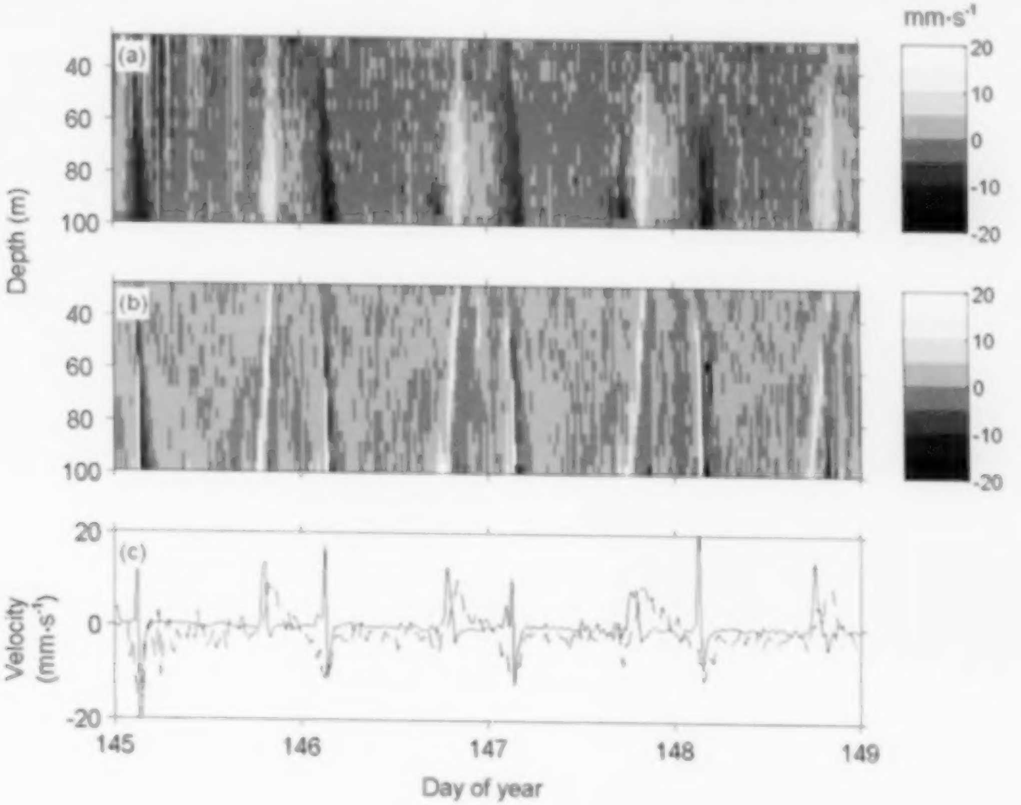

for light, as well as using land-based measurements, and therefore a direct functional relationship between light and migration timing is not apparent, but with large enough data sets, a statistically significant effect becomes clear. Mornings and evenings are classified as "overcast" if cloud opacity is 10/10 during migration (i.e., during 1 h centred at migration timing) and "clear" if cloud opacity is 0/10 during migration. These two cases make up the majority of the data set, and days with intermediate cloud cover are disregarded. Migration timing on clear days is then compared with that on overcast days using *t* tests.

The result is a statistically significant difference in timing between clear days and overcast days, with sample sizes $62 \leq n \leq 85$. For 10 of the 16 tests, $p \leq 0.07$, and for 13 of the 16 of tests, $p \leq 0.2$. Migrators leave the surface 10–20 min later on overcast mornings and arrive at the surface 10–20 min earlier on overcast evenings (Fig. 7; Table 3). This indicates that migrators modify their behaviour to increase their time spent near the surface under darkness. The descent timing shows slightly more statistical significance than that of ascent, suggesting that zooplankton may be more likely to respond to different light conditions while near the surface. Additional tests were performed with artificial cloud data to check for numerical biases, and no statistically significant results were found.

Biomass estimate

Tow data were sufficient for acoustic backscatter calibration, yielding an estimate of relative biomass based on backscatter data (cf. Ashjian et al. 2002). The only mooring for which coincident tow data exist is the Funk Island Bank 2004 mooring, because the other deployments were not explicitly designed for bioacoustic studies. Backscatter data from the 2004 mooring are correlated with tow data from a survey that took place while the ADCP was moored. The biological data collected during this deployment covered a region around the mooring approximately 100 nautical miles (185 km) across. Estimations of biomass based on backscatter intensity at the location of the mooring therefore contain large uncertainties, but a relative index of biomass can be developed as a tool for analysing the diel pattern.

Over a 2-week interval, 50 oblique tows were performed to a depth of 100 m, randomly distributed with respect to time of day. Tow samples consisted almost entirely of copepods, which are historically the most abundant zooplankton on the Newfoundland Shelf, comprising over 80% of sampled zooplankton (Dalley et al. 2001). Other zooplankton included amphipods and euphausiids, comprised less than 20% of the dry weight, and fell entirely within the largest size class, with the exception of one tow. Because of the uncertainty associated with the large spatial scale, we could not

Fig. 7. Frequency of migration times for clear and overcast days — composite of all Trinity Bay 2002 moorings: distributions for (*a* and *b*) overcast days and (*c* and *d*) clear days. Vertical line indicates average time of migration.

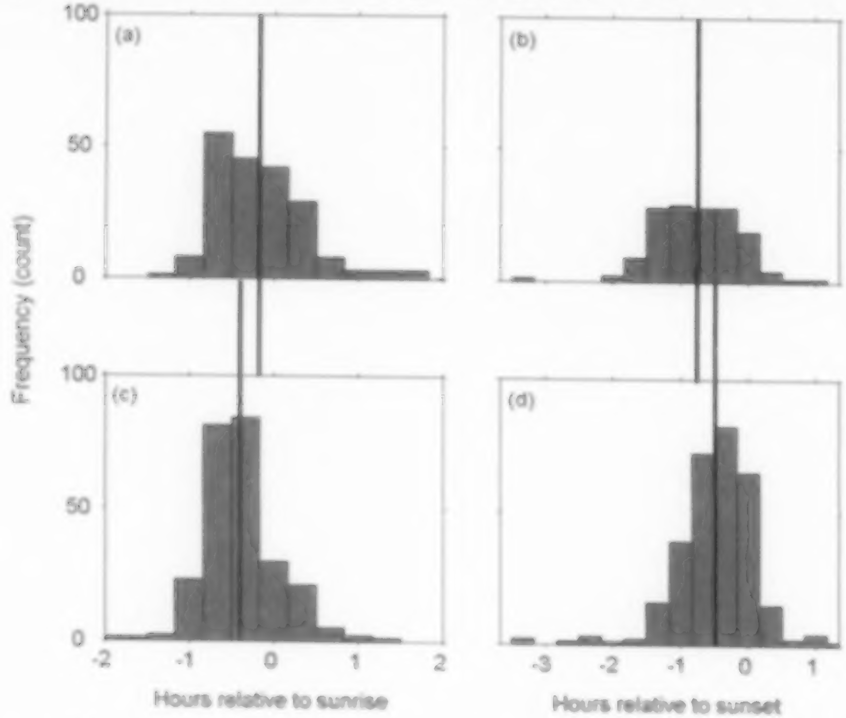

Table 3. Average ascent and descent times of the deep scattering layer on clear days (cloud opacity = 0/10), with the timing difference for overcast days (cloud opacity = 10/10), the *p* value (null hypothesis probability), and the sample size, *n*.

Mooring	Ascent time on clear days	Difference to overcast (min)	*p*	*n*	Descent time on clear days	Difference to overcast (min)	*p*	*n*
Trinity Bay 2001								
A	1829	−14	0.07	73	0553	2	0.80	62
B	1807	−18	0.11	70	0542	16	0.04	70
C	1822	−15	0.07	69	0536	18	0.01	67
Trinity Bay 2002								
A	1811	−13	0.13	83	0523	17	0.03	85
C	1813	−12	0.17	81	0535	13	0.06	85
D	1813	−27	0.00	84	0538	18	0.00	82
E	1810	2	0.70	79	0536	14	0.07	83
F	1818	−22	0.00	81	0541	6	0.46	84

Note: A *p* value of 0.00 indicates that $p < 0.005$. Times are standardised so that 0600 corresponds to sunrise and 1800 corresponds to sunset.

distinguish different types of zooplankton in the acoustic signal. Therefore our analysis is limited to treating the scattering layer as a whole.

The diel average of depth-averaged backscatter is correlated with diel-averaged dry weight from oblique bongo net tows. Depth averaging and oblique tows are both to 100 m. Daily-averaging tow data from an area 100 nautical miles (185 km) across relies on the assumption that variations in the horizontal are small compared with the dominant diel pattern. This question of horizontal homogeneity is addressed in a later section. A log-linear relationship is used because of the logarithmic relationship between backscatter intensity and scatterer abundance ($r^2 = 0.77$):

$$\log(S) = 0.07\,S_v + 5.01 \qquad (4)$$

where S gives a relative index of biomass or scatterer abundance. Because of the assumptions made in the calculation, no absolute biomass estimates are attempted. The relationship is used only in calculations where a relative index of biomass is sufficient, such as in calculating the biomass median depth.

Fig. 8. Horizontal correlations. Diel average of biomass median depth: (*a*) three example time series taken from the Trinity Bay 2001 deployment, and (*b*) correlations of such time series between pairs of moorings taken from the same deployment (all moorings) and pairs of individual beams (Trinity Bay 2001 mooring A), plotted as a function of separation distance between moorings or beams. Seasonal index of migration depth: (*c*) three example time series taken from Trinity Bay 2002 deployment, and (*d*) correlations of such time series between pairs of moorings taken from the same deployment and pairs of individual beams (Trinity Bay 2001 mooring A), plotted as a function of separation distance between moorings or beams. Trinity Bay 2001 mooring A is the only mooring shown for beam-to-beam correlation in (*b*) and (*d*) because all moorings show essentially the same beam-to-beam correlation and separation distance.

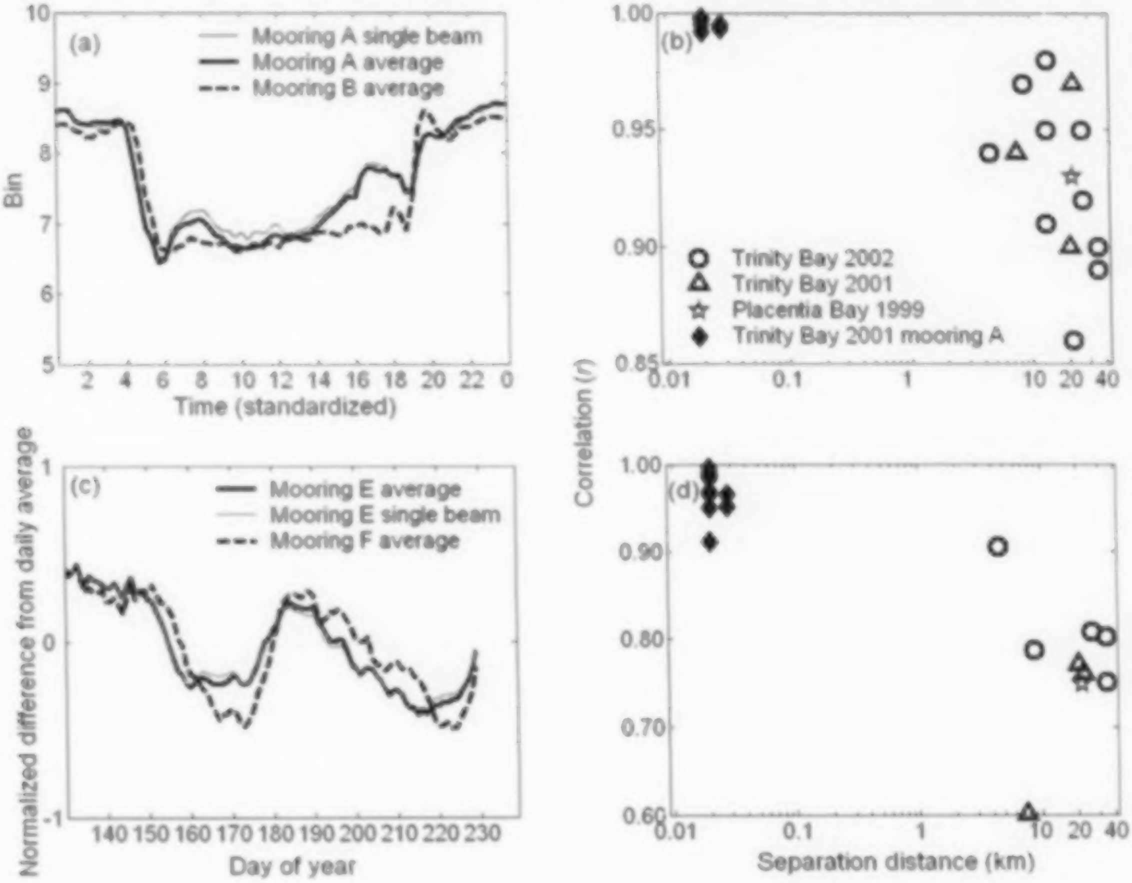

Horizontal homogeneity

High correlations between migration patterns were found across various spatial scales. A general problem in oceanography is that the ocean is large compared with our resources for collecting data. In the case of a single mooring that is to represent a large horizontal area, some assumption of horizontal homogeneity must be made. The Trinity Bay deployments contain multiple moorings separated by tens of kilometres that can be used to assess this assumption. In addition, each ADCP has four beams angled at 21° from the vertical. The beams converge at the ADCP, but for the upper portion of the data, they are separated by distances of tens of metres. The horizontal correlation is found as a function of separation distance, with distances spanning both of these spatial scales. This analysis is performed both for daily-averaged time series and for seasonal time series.

The diel average of biomass median depths for four beams on the same mooring are more highly correlated with each other than with the same series calculated for a nearby mooring (Fig. 8*a*). This calculation excludes the 40 m closest to the ADCP so that the beams reach a separation distance of tens of metres. Correlations are found for this time series between every pair of moorings that were part of the same deployment. There is a trend of decreasing correlation with increasing separation distance (Fig. 8*b*). For time series separated by tens of metres, $r = 0.99$. For time series separated by tens of kilometres, r ranges from approximately 0.9 to 0.95.

The same analysis is performed for seasonal time series. The example shown here is a normalised index of DVM. For each day, the index indicates whether the biomass median depth is shallower or deeper than the diel average for the whole time series. The same trend of decreasing correlation with increasing separation distance is apparent (Figs. 8*c*, 8*d*). Seasonal time series show a lower horizontal correlation than daily-averaged time series. The correlation is still good,

Fig. 9. Biomass median depth and 0 °C isotherm overlaid on volume backscatter for Trinity Bay 2002 mooring A. Each column of data is the average of 6 h centred at midnight for the indicated day. The broken line indicates the biomass median depth, and the solid line indicates the 0 °C isotherm. This plot is characteristic of all moorings.

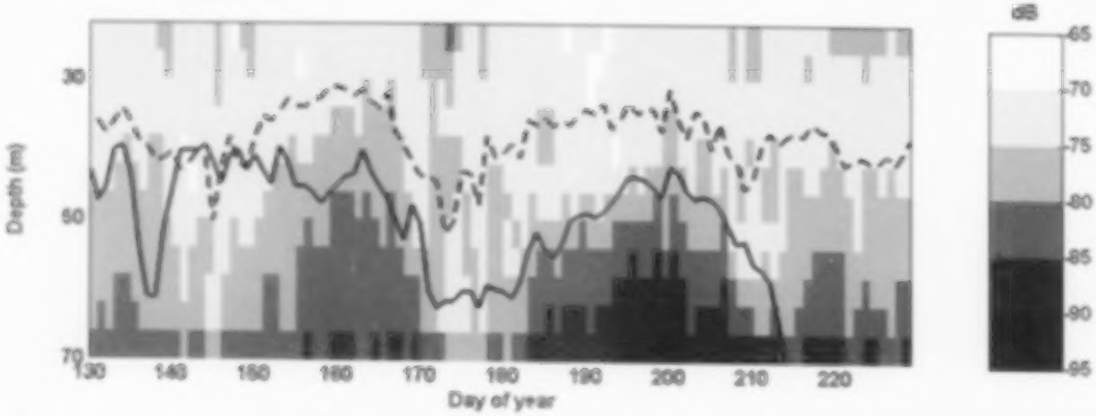

Fig. 10. Isotherms (°C) overlaid on one day of volume backscatter for the Funk Island Bank 2004 mooring showing examples of high-frequency (period << 1 day) response to temperature, as indicated by arrows. Time is shown in Newfoundland Standard Time (NST).

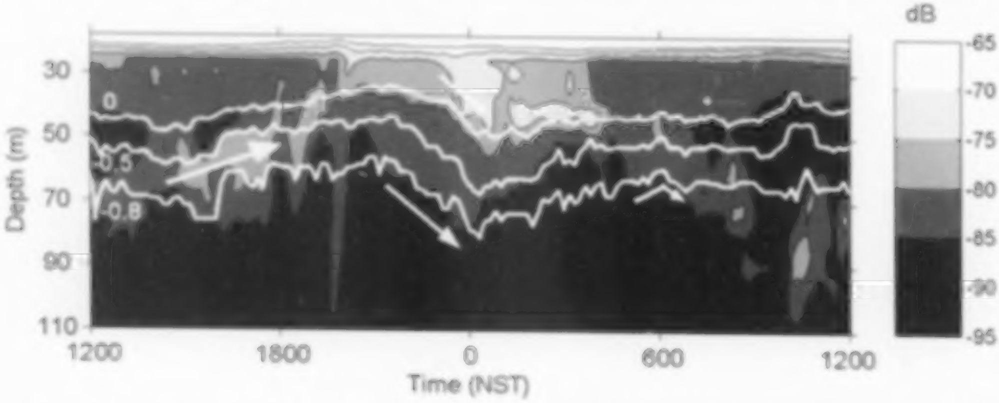

with $r = 0.95$ at scales of tens of metres, and $r = 0.8$ at scales of tens of kilometres.

Temperature

A migratory response to temperature stratification is seen to occur at both large and small time scales. The composition of zooplankton seen during the day is different from that seen at night because of the truncation of data below the ADCP depth, so the following analysis is performed separately for day and night. For day time series, biomass median depth is averaged over 6 h centred at 1200 to give a single depth per day. The same averaging is performed for night at 2400 (Fig. 9). Coherence analysis on the resulting time series shows a high correlation ($r > 0.9$) to isotherm depth (averaged in the same manner) on frequencies less than 0.05 day^{-1} for all moorings. Coherence at higher frequencies varies from mooring to mooring.

There is also a clear response by migrators to abrupt changes in temperature stratification. For most of the moorings, there is substantial surface warming around year day 170, and the 0 °C isotherm deepens abruptly. The biomass median depth deepens in response. A higher-frequency response by migrators to changing temperature stratification can be identified visually in some short stretches in the backscatter data. The response is quite clear for some brief intervals (Fig. 10), but for most of the data, the response is less clear.

Complex migration patterns

Migration patterns other than the typical nocturnal migration are often seen in the ADCP data. In addition to the two aforementioned groups of migrators, other scattering layers often exist, and other migration behaviours are exhibited. Twilight migration (also termed "midnight sinking," where zooplankton ascend to the surface for both dusk and dawn twilight hours, sinking in between (cf. Cushing 1951)) can be identified on occasion, particularly after year day 200. The sinking that occurs following dusk ascent can be seen in the vertical velocity as well (Fig. 11). There are also sometimes multiple distinct scattering layers that ascend at differ-

Fig. 11. One day of (*a*) backscatter and (*b*) vertical velocity data from Trinity Bay 2002 mooring D showing an example of "midnight sinking" and multiple migrating layers. Time is shown in Newfoundland Standard Time (NST).

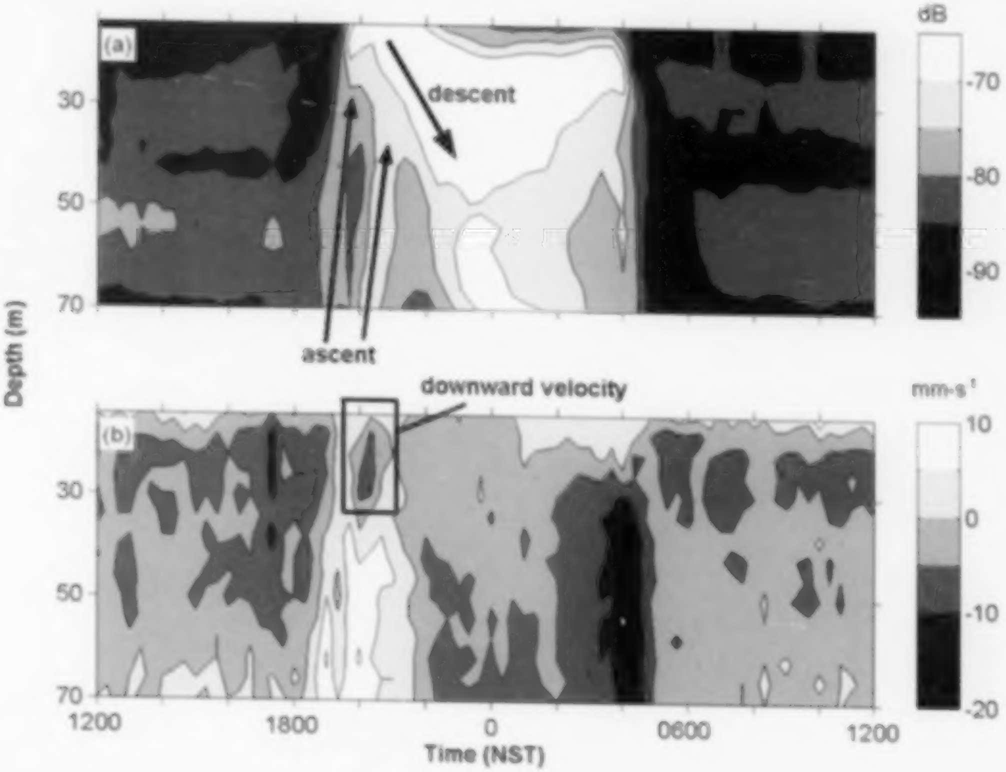

ent times during dusk. These layers can be identified in both the backscatter and velocity data (Fig. 11).

Discussion

ADCPs are powerful bioacoustic tools, particularly when accompanied with detailed taxonomic data. Even in the absence of such data, however, analysis techniques can yield valuable information on the DVM of zooplankton.

In Trinity Bay, zooplankton migrates in a manner that is mostly homogeneous throughout the bay, in terms of both the diel average and the seasonal variation. A single mooring may therefore be appropriate for representing a horizontal area tens of kilometres across. Spatial correlations between seasonal time series were lower than those for diel averages, implying an effect of temporally and spatially local phenomena on migration behaviour.

On the Newfoundland Shelf, a marked difference is seen between upward and downward migration velocities, suggesting that passive sinking plays a role in downward migration. Quantification techniques indicate that velocity measurements are biased low, likely because of ensemble averaging and the presence of nonmigrating acoustic scatterers.

The response by migrators to cloud cover is promising but requires further examination. Reliance on land-based historical cloud cover data as a proxy for light intensity perceived by zooplankton carries a high degree of uncertainty. However, the observed response was persistent and found with high statistical significance. Migrating zooplankton appear to be maximising time spent near the surface under darkness. This supports the predator-avoidance hypothesis of DVM and suggests that a threshold light level, rather than an endogenous rhythm, cues migration. By coordinating ADCP data with light data collected at the mooring location and by obtaining backscatter data from the entire water column, it is possible to examine the response to changes in light intensity in greater detail.

The migration pattern can be viewed with respect to three different time scales. Low-frequency signals within the migration pattern, corresponding to time scales of many days, can be attributed to changes in temperature stratification of the water column. The dominant daily cycle is seen to be driven by light to the extent that cloud cover appears to influence migration timing. In some cases, the higher-frequency variation appears to be driven by changes in temperature stratification, but in many cases, higher-frequency variation remains unexplained. Many possibilities exist. A direct measure of light intensity in close vicinity to a mooring may show that higher-frequency changes in light caused by clouds have a direct effect on the behaviour of shallow migrators. The presence of predators and the local availability of food may also function as important high-frequency cues.

It should also be noted that there are at least two possible explanations for high-frequency responses to changes in temperature stratification: zooplankton may be either actively swimming to remain at a constant temperature or passively transported by some water mass movement such as internal waves. In the former case, one would expect the vertical swimming velocity to be measured by the ADCP. In the latter case, a measured vertical velocity may or may not be associated with change in stratification, depending on the cause of the change in stratification. Because both these cases occur in the data, a more detailed analysis is required to address this question.

The ADCP can record more complex migration patterns when they are present, including reverse migration, twilight migration, and multiple distinct groups of migrators. In complex zooplankton communities, taxonomic identification remains difficult based on acoustic data alone. In conjunction with taxonomic data, the ADCP offers the potential to map multiple simultaneous migration patterns to high temporal and spatial resolution.

Many aspects of zooplankton migration may have implications for higher trophic levels. On the Newfoundland Shelf, capelin preying on zooplankton also undergo a nocturnal diel vertical migration, which likely indicates a dependence on the vertical distribution of their prey (cf. Clark and Levy 1988). Northern gannets (*Morus bassanus*) preying on capelin have been observed to have a distribution of feeding times with peaks during dawn and dusk twilight hours corresponding to the timing of migration (Garthe et al. 2003), suggesting the possibility that capelin are too deep during the day and invisible at night. If this is the case, then the environmental factors that influence timing and depth of zooplankton migration are of importance to ecosystem-scale studies.

Acknowledgements

Jack Foley and Denise Davis helped in data collection and John Anderson provided valuable comments on the manuscript. The support for the 2004 mooring came in part from a Natural Sciences and Engineering Research Council of Canada (NSERC) grant.

References

Ashjian, C.J., Smith, S.L., Flagg, C.N., and Idrisi, N. 2002. Distribution, annual cycle, and vertical migration of acoustically derived biomass in the Arabian Sea during 1994–1995. Deep-Sea Res. II, **49**: 2377–2402.

Brierley, A.S., Brandon, M.A., and Watkins, J.L. 1998. An assessment of the utility of an acoustic Doppler current profiler for biomass estimation. Deep-Sea Res. I, **45**: 1555–1573.

Carscadden, J.E., Frank, K.T., and Leggett, W.C. 2001. Ecosystem changes and the effects on capelin (*Mallotus villosus*), a major forage species. Can. J. Fish. Aquat. Sci. **58**: 73–85.

Clark, C.W., and Levy, D.A. 1988. Diel vertical migrations by juvenile sockeye salmon and the antipredation window. Am. Nat. **131**(2): 271–290.

Clarke, G.L. 1930. Change of phototropic and geotropic signs in *Daphnia* induced by changes of light intensity. J. Exp. Biol. **7**(2): 109–131.

Colbourne, E., deYoung, B., Narayanan, S., and Helbig, J. 1997. Hydrography and circulation on the Newfoundland Shelf. Can. J. Fish. Aquat. Sci. **54**: 149–157.

Cushing, D.H. 1951. The vertical migration of planktonic Crustacea. Biol. Rev. **26**: 158–192.

Dalley, E.L., Anderson, J.T., and Davis, D.J. 2001. Decadal time-series of invertebrate zooplankton on the Newfoundland Shelf and Grand Banks 1991–1999. Can. Sci. Advisory Secretariat Res. Doc. No. 2001/110. pp. 1–29.

Davidson, F.J.M., Greatbatch, R.J., and deYoung, B. 2001. Asymmetry in the response of a stratified coastal embayment to wind forcing. J. Geophys. Res. **106**: 7001–7017.

Deines, K.L. 1999. Backscatter estimation using broadband acoustic Doppler current profilers. *In* Proceeding of the IEEE 6th Working Conference on Current Measurement. *Edited by* S.P. Anderson, E.A. Terray, J. White, and A.J. Williams. IEEE, San Diego, California. pp. 249–253.

Dodson, S. 1988. The ecological role of chemical stimuli for the zooplankton: predator-avoidance behaviour in *Daphnia*. Limnol. Oceanogr. **33**(6, Part 2): 1431–1439.

Enright, J.T. 1977. Diurnal vertical migration: adaptive significance and timing. Part 1. Selective advantage: a metabolic model. Limnol. Oceanogr. **22**(5): 856–872.

Fielding, S., Griffiths, G., and Roe, H.S.J. 2004. The biological validation of ADCP acoustic backscatter through direct comparison with net samples and model predictions based on acoustic-scattering models. ICES J. Mar. Sci. **61**: 184–200.

Flagg, C.N., and Smith, S.L. 1989. On the use of the acoustic Doppler current profiler to measure zooplankton abundance. Deep-Sea Res. **36**(3): 455–474.

Forward, R.B., Jr. 1988. Diel vertical migration: zooplankton photobiology and behaviour. Oceanogr. Mar. Biol. Annu. Rev. **26**: 361–393.

Garthe, S., Benvenuti, S., and Montevecchi, W.A. 2003. Temporal patterns of foraging activities of northern gannets, *Morus bassanus*, in the Northwest Atlantic Ocean. Can. J. Zool. **81**: 453–461.

Geller, W. 1986. Diurnal vertical migration of zooplankton in a temperate great lake (L. Constance): a starvation avoidance mechanism? Arch. Hydrobiol. **74**(Suppl.): 1–60.

Hays, G.C. 2003. A review of the adaptive significance and ecosystem consequences of zooplankton diel vertical migrations. Hydrobiologia, **503**: 163–170.

Heywood, K.J. 1996. Diel vertical migration of zooplankton in the Northeast Atlantic. J. Plankton Res. **18**(2): 163–184.

Holliday, D.V., and Pieper, R.E. 1995. Bioacoustical oceanography at high frequencies. ICES J. Mar. Sci. **52**: 279–296.

Huntley, M.E., and Zhou, M. 2004. Influence of animals on turbulence in the sea. Mar. Ecol. Prog. Ser. **273**: 65–79.

Kunze, E., Dower, J.F., Beveridge, I., Dewey, R., and Bartlett, K.P. 2006. Observations of biologically generated turbulence in a coastal inlet. Science (Washington, D.C.), **313**: 1768–1770.

Lampert, W. 1989. The adaptive significance of diel vertical migration of zooplankton. Funct. Ecol. **3**: 21–27.

Lorke, A., McGinnis, D.R., Spaak, P., and Wüest, A. 2004. Acoustic observations of zooplankton in lakes using a Doppler current profiler. Freshw. Biol. **49**(10): 1280–1292.

Madin, L.P., Horgan, E.F., and Steinberg, D.K. 2001. Zooplankton at the Bermuda Atlantic Time-series Study (BATS) station: diel, seasonal and interannual variation in biomass, 1994–1998. Deep Sea Res. II, **48**(6–9): 2063–2082.

Martin, L.V., Stanton, T.K., Wiebe, P.H., and Lynch, J.F. 1996. Acoustic classification of zooplankton. ICES J. Mar. Sci. **53**: 217–224.

Mauchline, J. 1998. The biology of calanoid copepods. Adv. Mar. Biol. **33**: 1–710.

McLaren, I.A. 1963. Effects of temperature on growth of zooplankton, and the adaptive value of vertical migration. J. Fish. Res. Board Can. **20**(3): 685–727.

McLaren, I.A. 1974. Demographic strategy of vertical migration by a marine copepod. Am. Nat. **108**(959): 91–102.

Neill, E.W. 1990. Induced vertical migration in copepods as a defence against rate predation. Nature (London), **345**: 524–526.

Rippeth, T.P., and Simpson, J.H. 1998. Diurnal signals in vertical motions on the Hebridean Shelf. Limnol. Oceanogr. **43**(7): 1690–1696.

Sindlinger, L.R., Biggs, D.C., and DiMarco, S.R. 2005. Temporal and spatial variability of ADCP backscatter on a continental slope. Cont. Shelf Res. **25**: 259–275.

Stanton, T.K., Wiebe, P.H., Chu, D., Benfield, M.C., Scanlon, L., Martin, L., and Eastwood, R.L. 1994. On acoustic estimates of zooplankton biomass. ICES J. Mar. Sci. **51**: 505–512.

Stanton, T.K., and Chu, D. 2000. Review and recommendations for the modelling of acoustic scattering by fluid-like elongated zooplankton: euphausiids and copepods. ICES J. Mar. Sci. **57**: 793–807.

Tarling, G.A., Matthews, J.B.L., Saborowski, R., and Bochholz, R. 1998. Vertical migratory behaviour of the euphausiid, *Meganyctiphanes norvegica*, and its dispersion in the Kattegat Channel. Hydrobiologia, **375/376**: 331–341.

Thomson, R.E., and Allen, S.E. 2000. Time series acoustic observations of macrozooplankton diel migration and associated pelagic fish abundance. Can. J. Fish. Aquat. Sci. **57**: 1919–1931.

Tittensor, D., Naud, R., de Young, B., and Foley, J.2002. Analysis of physical oceanographic data from Trinity Bay: May–August 2002. Physics and Physical Oceanography Data Rep. No. 2002-2, Memorial University, St. John's, Newfoundland. Available at www.physics.mun.ca/~bdeyoung.

Wiebe, P.H., Mountain, D.G., Stanton, T.K., Greene, C.H., Lough, G., Kaartvedt, S., Dawson, J., and Copley, N. 1996. Acoustical study of the spatial distribution of plankton on Georges Bank and the relationship between volume backscattering strength and the taxonomic composition of the plankton. Deep-Sea Res. II, **43**(7–8): 1971–2001.

Zaret, T.M., and Suffern, J.S. 1976. Vertical migration in zooplankton as a predator avoidance mechanism. Limnol. Oceanogr. **21**(6): 804–813.

Missing the target: uncertainties in achieving management goals in fisheries on Fraser River, British Columbia, sockeye salmon (*Oncorhynchus nerka*)

Carrie A. Holt and Randall M. Peterman

Abstract: In sockeye salmon (*Oncorhynchus nerka*) fisheries, management targets are rarely achieved exactly, thereby creating uncertainties about outcomes from implementing fishing regulations. Although this type of uncertainty may be large, it is seldom incorporated into simulation models that evaluate management options. One objective of this study was to quantify the deviations that occur between realized and target mortality rates (i.e., the target fraction of adult recruits that die each year during return migration, mostly due to harvesting) in fisheries for sockeye salmon from the Fraser River, British Columbia. We found that for some sockeye stocks, realized mortality rates were higher than targets when recruitment was low (resulting in conservation concerns) and lower than targets when recruitment was high (resulting in foregone catch). Scientists and managers can at least partially account for effects of such deviations between realized and target mortality rates (outcome uncertainties) by choosing target harvest rules that reflect typical patterns in those deviations. We derived a method to permit modelers to incorporate those patterns into analyses of management options.

Résumé : Dans les pêches de saumons rouges (*Oncorhynchus nerka*), il est rare d'atteindre exactement les objectifs de gestion, ce qui crée des incertitudes au sujet des résultats de la mise en place des règlements de pêche. Bien que ce type d'incertitude puisse être important, il est rarement inclus dans les modèles de simulation qui évaluent les options de gestion. Un objectif de notre travail est de calculer les déviations qui existent entre les taux de mortalité ciblés et réalisés (c'est-à-dire la fraction de la valeur ciblée représentée par les recrues adultes qui meurent chaque année durant la migration de retour, surtout à cause de la récolte) dans les pêches de saumons rouges dans le Fraser, Colombie-Britannique. Chez certains stocks de saumons rouges, les taux de mortalité réalisés dépassent les valeurs ciblées quand le recrutement est faible (ce qui génère des préoccupations de conservation) et ils sont plus bas que les valeurs ciblées quand le recrutement est important (ce qui cause une perte dans la récolte). Les chercheurs et les gestionnaires peuvent compenser au moins partiellement de telles déviations entre les taux de mortalité réalisés et ciblés (incertitudes de l'issue) en choisissant des règles de récolte ciblée qui tiennent compte de patrons typiques de ces déviations. Nous mettons au point une méthode pour permettre aux modélisateurs d'incorporer ces patrons dans leurs analyses des options de gestion.

[Traduit par la Rédaction]

Introduction

Uncertainties are pervasive in fisheries, and if ignored by managers, they may result in foregone yield or create conservation concerns. One type of uncertainty that has been studied relatively little is the frequently observed difference between a management agency's desired target, such as a harvest rate or abundance of spawners, and the outcome that actually occurs. One source of this difference is the imperfect control that managers have over outcomes after issuing fishing regulations, i.e., "implementation uncertainty" or "implementation error" (Rosenberg and Brault 1993; Kell et al. 1999). That type of uncertainty occurs in part because managers are unable to predict exactly the behaviour of harvesters in response to regulations and therefore usually can not take this behaviour into account when setting regulations. Other factors also affect whether targets are met, e.g., temporal variability in catchability of fish (Cass et al. 2003) and numbers of fishing vessels, as well as errors in estimating fish abundance (Rosenberg and Restrepo 1994). These uncertainties about outcomes from particular fishing regulations can be large and occur in a variety of fisheries. For example, the annual ratio of actual spawner abundance to the target varied between 0.4 and 2.4 for eight sockeye salmon

---

Received 25 January 2006. Accepted 29 September 2006. Published on the NRC Research Press Web site at http://cjfas.nrc.ca on 13 December 2006.
J19132

C.A. Holt[1] and R.M. Peterman. School of Resource and Environmental Management, Simon Fraser University, Burnaby, BC V5A 1S6, Canada.

[1] Corresponding author (e-mail: cholt@sfu.ca).

Can. J. Fish. Aquat. Sci. 63: 2722–2733 (2006)   doi:10.1139/F06-155

(*Oncorhynchus nerka*) stocks in Bristol Bay, Alaska, between 1962 and 1982 (Bocking and Peterman 1988). Such variations are economically important. Rice and Richards (1996) suggested that reductions in implementation uncertainty in British Columbia's (B.C.) rockfish fishery between 1993 and 1994 were partly responsible for the 17% increase in commercial value over that period.

Despite this importance of deviations between targets and outcomes, stock assessments and simulation studies of fisheries on Pacific salmon (*Oncorhynchus* spp.) and other species have usually implicitly assumed that management targets are met and that regulations are implemented as planned (McAllister et al. 1999). In cases where deviations from targets have been accounted for, most have assumed either that those differences are deterministic (Kell et al. 1999) or, if stochastic, that they are unbiased with respect to the target (e.g., Johnston et al. 2000). Furthermore, methods to account for deviations from targets have usually been based more on expert opinion than on data (Peterman et al. 2000; Cass et al. 2003). Some Pacific salmon studies have quantified a few of the many potential sources of deviations between realized mortality rates and targets (e.g., Link and Peterman 1998), which underestimate the total variance in realized mortality rates if only considered on their own. Thus, when these and similar uncertainties are ignored or incorrectly represented, modelers may be providing managers with inappropriate advice about the effectiveness of certain management actions.

To provide more appropriate advice, we need clearer understanding of the properties of the differences between management targets and observed outcomes, as well as the causes of those differences in order to reduce them. In various Pacific salmon fisheries in North America, management goals are typically stated in terms of either target spawner abundances (target escapements) or target fractional mortality rates (i.e., the fraction of total adult returns projected to die during return migration, mostly due to harvesting). Although the differences between these targets and the actual (i.e., realized) spawner abundances or mortality rates have been referred to by most authors as implementation uncertainties, these differences are not just affected by lack of control over harvesting. They are also influenced by, for example, variable mortality during upstream migration (Cooke et al. 2004) and errors in preseason abundance estimates of the potentially fishable stock (Rosenberg and Restrepo 1994). Thus, the term implementation uncertainties or errors may have been used too broadly in the past.

In this study, we empirically estimated the properties of a broader variable, the difference between realized and target mortality rates (outcome uncertainty), and examined several potential sources of those differences, only one of which is implementation uncertainty. We focused on fisheries for sockeye salmon from the Fraser River, B.C., Canada. Recently, managers there have chosen annual target harvest rates based on a combination of forecasts of recruitment (mature adults that return to the coast toward natal spawning areas), estimated productivity (potential rate of change) of sockeye populations, prespecified guidelines regarding harvest rate plus natural mortality rate, and escapement targets (Fraser River Sockeye Spawning Initiative 2005). For the rest of this paper, we use the term "mortality" rates instead of "harvest" rates (i.e., catch/recruitment) because our estimates of realized, or actual, recruitment reflect losses of fish due to factors other than harvesting, such as en route mortality from high water temperatures or parasites (Williams 2005). These losses are particularly relevant for some stocks of Fraser River sockeye salmon.

For Fraser River sockeye, there are at least six potential causes for differences between realized and target mortality rates, the first two of which pertain specifically to implementation uncertainty: (*i*) the degree of compliance with regulations by harvesters; (*ii*) deviations in catchability coefficients from those assumed in assessments (Cass et al. 2003) due to variation in migratory behaviour of fish, environmental conditions, and the efficiency of fishing gear; (*iii*) deviations from initial target mortality rates caused by managers making deliberate trade-offs during the fishing season among management objectives (e.g., among biological escapement, social, and economic objectives) (Wood et al. 1998; Cooke et al. 2004); (*iv*) deviations from the expected natural mortality that occur between the time of harvest and when spawning escapement is estimated (i.e., en route mortality) (Cooke et al. 2004); (*v*) estimation errors in catch and spawner abundances (Pacific Salmon Commission 2002); and (*vi*) incorrect forecasts of abundances that affect calculations of target mortality rates (Bocking and Peterman 1988; Cass et al. 2003).

A closer examination of the latter (forecasting errors) is warranted, given that in the Fraser River sockeye fishery, it is the source of differences in realized mortality rates from targets that scientists can, in theory, reduce through improved forecasting methods. Forecasts of abundance of total adult sockeye recruits are typically made before the fishing season based on various quantitative analyses (Cass 2002), and forecasts are updated during the season using observations from test, commercial, and First Nations fisheries, as well as other sources (Pacific Salmon Commission 2001). As forecasts are updated during the season, management targets are adjusted accordingly.

For sockeye salmon, the direction and magnitude of deviations in realized mortality rates from targets are partly related to both actual recruitment and the direction and magnitude of forecasting errors in recruitment (Bocking and Peterman 1988). For instance, within-season updates of estimated recruitment often occur too late to allow managers to close areas to fishing to correct entirely for forecasts that overestimate abundance, resulting in overexploitation at low recruitment. In contrast, when actual recruitment is higher than the forecast, within-season updates tend to be too late to permit managers to allow enough fishing in various areas to prevent underexploitation. Furthermore, in this latter case, differences between realized and target mortality rates may be further increased at very large recruitment because of limited fishing and processing capacity in remote areas such as Bristol Bay, Alaska (Bocking and Peterman 1988).

If there is a repeatable pattern to the magnitude and direction of deviations in realized mortality rates from targets, then capturing that pattern in simulations that evaluate management options can help managers meet their objectives. Specifically, when simulation models are used to quantitatively evaluate management options, a more accurate representation of those deviations will result in more appropriate estimates of the effects of those options. Ignoring the outcome uncertainties may lead to decisions that do not achieve management objectives.

Research objectives

Our research objectives were therefore to (*i*) quantify the properties (magnitude and nature) of deviations between realized mortality rates and targets in four run-timing groups of Fraser River sockeye salmon, (*ii*) examine the contribution to these deviations by forecasting errors, environmental factors, and specific management situations, and (*iii*) derive a method to permit modelers to incorporate those observed properties into simulations that evaluate management options.

Materials and methods

Instead of comparing annual targets with annual realized outcomes for Fraser River sockeye salmon fisheries, we characterized the differences between target and realized mortality rates by comparing target harvest rules (i.e., state-dependent and time-independent relations that describe changes in target mortality rates or escapement goals) with realized harvest functions that describe the actual mortality rate or escapement that occurred by the end of the fishing season. Specifically, we compared two relations (Fig. 1). The first was desired fractional mortality rate as a function of forecasted recruitment (referred to as the target harvest rule). Such state-dependent harvest rules are now becoming commonplace in fisheries (Butterworth and Punt 1999). They allow for feedback between the estimated fishable stock and target mortality rates. The second relation was realized fractional mortality rate as a function of forecasted recruitment (the realized harvest function) (Fig. 1). By comparing these two relations, we examined patterns of bias in the difference between realized mortality rates and targets that are expected to emerge over the long term, independent of year-to-year variability.

Note that although managers of many sockeye salmon fisheries often use constant escapement goals instead of target harvest rules, these two concepts are closely linked. Below a threshold abundance of adult recruits (the target escapement or the *x* intercept for the target harvest rule in Fig. 1), the target harvest is zero, and above this threshold abundance, all "surplus" recruits are harvested, which produces nonlinearly increasing harvest rates as recruitment increases.

Data

We obtained data from various management-agency sources (Table 1) on abundance of adult sockeye salmon recruits and spawners for 1986 through 2003 for four stock complexes from the Fraser River, B.C., categorized by upstream migration run-timing (Early Stuart, Early Summer, Summer, Late Summer runs). Below we describe how data were generated by management agencies.

Estimates of realized adult recruitment were provided by the Canada Department of Fisheries and Oceans (DFO) and the Pacific Salmon Commission (PSC) (Appendix A). Those estimates included the sum of estimated spawning escapement and catch from marine and in-river commercial and test fisheries, Fraser River First Nations harvests, and catch from recreational fisheries, as well as natural en route mortality, fishing-induced mortality that was not included in catch data, and estimates of unreported catch. Preseason forecasts of recruits from DFO, which were based on abundances of various age groups and environmental indices (e.g., Cass 1998, 2002), were updated during the fishing season. We did not use preseason forecasts but instead used only the final annual within-season forecasts of recruits that could be applied by managers to update target mortality rates during the fishing season. This was because those forecasts tended to be more accurate than preseason forecasts and therefore resulted in realized mortality rates that were closer to targets.

Fig. 1. Hypothetical plot of a target harvest rule for sockeye salmon (*Oncorhynchus nerka*) showing the desired fractional mortality rate (fraction dying) as a function of the forecast of recruitment and the associated realized harvest function showing the fractional mortality rate actually observed as a function of the forecast of recruitment. The parameter *a′* is the maximum mortality rate at high recruitment for the target harvest rule, and *c′* is the "protection level" or abundance of recruits below which target mortality is intended to be zero (i.e., the target escapement). Parameters *a* and *c* without primes are for the actual, or realized, harvest function.

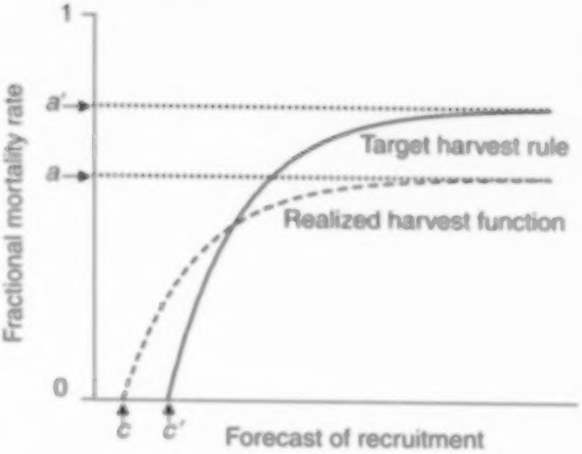

Within-season target mortality rates (and corresponding target escapements) for Fraser River sockeye salmon (Appendix A) were chosen annually by DFO from predetermined decision rules according to a specified percentile (e.g., 50th or 75th) of the probability distribution for forecasts of recruitment. In recent years, additional decision rules were used to keep target mortality rates below a maximum threshold (e.g., no greater than 15% mortality rate in some years to protect certain stocks that were a conservation concern) (Pacific Salmon Commission 2001).

Statistical analysis

Model structure

We used a three-parameter model (eq. 1) to describe the relation between forecasts of adult recruitment in year *t* (R'_t) and either the target fractional mortality rate (D'_t; i.e., the fraction expected to die during return migration) or D_t (the

Table 1. Sources of sockeye salmon (*Oncorhynchus nerka*) data for the Fraser River, British Columbia, that we analyzed for implementation uncertainty.

Type of data	Return years for data	Source
Within-season target spawning escapement	1986–2003	Ian Guthrie[a]
Within-season forecasts of recruitment	1986–2003	Ian Guthrie
Realized spawning escapement	1986–2003	Jeff Grout[b]
Realized recruitment	1986–1995	Pacific Salmon Racial Analyses 1986–1995[c]
Realized recruitment including jacks	1996–2003	Ian Guthrie
Total number of jacks in spawning escapement	1996–2003	Reports of the Fraser River Panel to the Pacific Salmon Commission 1996–2003[d]

Note: "Return years for data" is the duration of the time series. Jacks are males that return to spawn after only 1 year in the ocean (usually as 3-year-olds). Target spawning escapement and forecasts of recruitment are the last within-season values that are used to affect final management decisions. Escapement and recruitment data refer to adults only (i.e., jacks were excluded), unless stated otherwise.

[a] Personal communication, Pacific Salmon Commission, 600–1155 Robson Street, Vancouver, BC V6E 1B5, Canada.

[b] Personal communication, Fisheries and Oceans Canada, 100 Annacis Parkway, Unit 3, Delta, BC V3M 5P8, Canada.

[c] Pacific Salmon Commission 1986–1995.

[d] Pacific Salmon Commission 1996–2003.

fraction that actually died). For the latter, the realized mortality function is

$$(1)\qquad D_t = a(1 - e^{b(c - R'_t)}) \text{ for } R'_t > c$$

and

$$D_t = 0 \text{ for } R'_t \le c$$

where a is the maximum mortality rate at high recruitment, b is a shape parameter, and c is the protection level (minimum escapement target) below which mortality rate is zero (e.g., Fig. 1). We chose this model form because its parameters were directly relevant to managers, and it adequately described the data. The model structure of this realized harvest function was identical to that of the target harvest rule, except the latter calculated D'_t, again as a function of forecasts of R'_t, but using the parameters a', b', and c' instead of a, b, and c, respectively. These models reflect the average target harvest rule or realized harvest function over all years as a function of forecasts of recruitment.

Parameter estimation

The relation among the fraction of fish dying, escapement, and recruitment (for example, for the realized mortality rate, D_t) is

$$(2)\qquad D_t = \left(\frac{R_t - E_t}{R_t}\right)$$

where R_t is realized recruitment and E_t is realized spawning escapement, both based on postseason data provided by management agencies (Appendix A). To estimate the parameters of the target harvest rule and realized harvest function for each sockeye run-timing group, we rearranged eq. 2 to solve for escapement and added an error term:

$$(3)\qquad E_t = [R_t(1 - D_t)]e^{v_t}$$

where v_t has a mean of zero and variance σ_v^2. We added a multiplicative lognormal error term (e^{v_t}) for parameter estimation purposes to reflect the typically observed lognormal distribution for recruitment and escapement of Pacific salmon (Hilborn and Walters 1992). Substituting eq. 1 into eq. 3 allowed us to estimate the parameters of the realized harvest function, a, b, and c, from empirical data (Appendix A) on E_t, R_t, and R'_t, with the latter entering through eq. 1. Although this formulation of the model did not explicitly constrain mortality rates to be between 0 and 1, the best-fit parameters always gave predictions of D_t from eq. 1 that were within that range. To estimate the parameters, we used a maximum likelihood procedure and a robust method, a Cauchy M estimator, because the latter downweights the influence of outliers and, as opposed to other robust methods, has a continuous derivative, thereby producing parameter estimates that are more stable (Huber 1981). We followed an analogous procedure to estimate parameters of the function describing target mortality rates.

Other analyses

We then investigated three potential sources of variability in deviations between realized mortality rates and targets predicted from the harvest rule: forecasting errors, variability in environmentally driven en route mortality, and specific management situations. These sources of outcome uncertainty were not mutually exclusive, e.g., closures to fishing might occur when unfavourable environmental conditions exist.

We examined the extent to which differences between realized mortality rates (eq. 2) and target mortality rates (determined by the target harvest rule (eq. 1) but with D'_t, a', b', and c') were due to variability in forecasting errors for Fraser River sockeye fisheries. We fit a linear relation between those differences and forecasting errors (as defined by the ratio of within-season forecasts of recruitment to actual realized recruitment).

Realized mortality rates of adult recruits may also deviate from targets in part due to interannual variability in environmentally driven en route mortality. Specifically, warm temperatures and high water discharge in the Fraser River increase (*a*) energy expenditure of adult sockeye salmon during upriver migration, (*b*) the duration of this migration, and (*c*) the prevalence and severity of parasites and disease, which can result in dramatically increased mortality (Wagner et al. 2005; Williams 2005). In years when water temperature and discharge exceed critical thresholds for salmon survival, managers typically reduce fishing pressure to attempt to achieve management targets (Pacific Salmon Commission

2005; Ian Guthrie, Pacific Salmon Commission, 600–1155 Robson Street, Vancouver, BC V6E 1B5, personal communication). To reflect this situation, we examined two different thresholds in annual environmental conditions (Ian Guthrie, personal communication; David Patterson and J. Stevenson Macdonald, Fisheries and Oceans Canada, Cooperative Resource Management Institute, Simon Fraser University, 8888 University Drive, Burnaby, BC V5A 1S6, Canada, personal communication). The first threshold for increased sockeye mortality occurred in years when two conditions were met: river temperatures were greater than 18.0 °C at Hell's Gate (B.C.) when averaged over the 31-day period centered around the peak migration period at Hell's Gate, and mean daily temperature exceeded that value for at least 18 days during this period. The second environmental threshold occurred in years when mean water discharge at Hell's Gate was greater than 6400 $m^3 \cdot s^{-1}$ averaged over the same period.

Certain management situations may also cause target and realized mortality rates to differ. Managers of Fraser River sockeye salmon specify targets for the four run-timing groups individually because of their differences in productivity. However, in practice, it is difficult to separately manage these stocks because fishing pressure on one run-timing group affects others because of spatial and temporal overlap of some stocks. To investigate this source of variability, we determined whether deviations between realized and target mortality rates were significantly correlated among run-timing groups.

Conversion factors

If the target harvest rule and realized harvest function for a given stock group differ in a systematic manner (i.e., if differences between realized and target mortality rates have a mean other than zero), then representing that bias in stock assessment models of salmon fisheries may improve predictions of outcomes from applying various harvest strategies. To this end, we estimated stock-specific scalars, or conversion factors (d_0, d_1, and d_2), that transformed the maximum likelihood parameter values for the target harvest rules (a', b', c') into those of the realized harvest functions (a, b, c) (eq. 1). These conversion factors for any one stock group were estimated by first substituting parameters of the target harvest rule (a', b', c') and their unknown respective scalars into the realized harvest function (i.e., substituting $a = d_0 \cdot a'$, $b = d_1 \cdot b'$, and $c = d_2 \cdot c'$ into eq. 1 and then substituting it into eq. 3). To estimate the best-fit values of d_0, d_1, and d_2, we then used the previously estimated values for a', b', and c' along with the same maximum likelihood estimation procedure as noted above that assumed lognormally distributed random errors for eq. 3.

Results

The nature of the deviations between realized and target mortality rates differed among run-timing groups. Specifically, for the Late Summer run, the fitted realized harvest function showed higher fractional mortality rates than the fitted target harvest rule for all historically observed levels of recruitment (Fig. 2*d*). In particular, for that run-timing group, the 95% confidence limits for a' (maximum mortality rate at high recruitment for the target harvest rule) did not include the best estimate for the a parameter from the realized function (Table 2). Because our purpose was to describe patterns in average deviations for use in future modelling and not to test statistical hypotheses about model fits, we state our comparisons of parameters in this way to concisely describe the results. The presence of overlap between 95% confidence intervals of two parameters (or between the interval of one parameter and the best-fit value of the other) was not critical for our analyses. In the year of the largest observed actual recruitment from 1986 through 2003 (12.4 million fish), the realized harvest function predicted a realized catch of 9.4 million fish per year instead of 7.7 million fish predicted from the target harvest rule. These numbers were based on a realized mortality rate of 76% and the target mortality rate of 62%.

For the Early Stuart run, at low recruitment, realized mortality rates also tended to be higher than target mortality rates, but the reverse was true at high recruitment (Fig. 2*a*). For instance, at $R' = 0.25$ million fish, the realized mortality rate predicted from the function was higher than the target predicted from the target harvest rule (0.63 vs 0.41), but at $R' = 1.5$ million fish, the realized mortality rate predicted from the function was lower than the target (0.63 vs 0.70). For this Early Stuart run-timing group, the 95% confidence limits for b', which reflected the rate at which target mortality rates increased with forecasts of recruitment, did not include the best estimate for b from the realized harvest function (Table 2). For the Early Summer and Summer runs, the differences between the target harvest rules and realized harvest functions were small, and the 95% confidence limits for all parameters of the target harvest rules included the best estimates of parameters of the realized harvest functions.

In sensitivity analyses, these observed patterns in deviations between realized and target mortality rates were virtually unaffected by two key uncertainties: the error structure in escapement (normally distributed vs lognormally distributed in eq. 3) and cyclic patterns in recruitment. We considered the latter uncertainty because many Fraser River sockeye salmon populations follow 4-year cycles of abundance in which the "dominant" and "subdominant" cycle lines have higher abundances than the two "off-cycle" lines, and these patterns of abundances may affect the accuracy with which managers achieve target escapements (Cass et al. 2003). However, the direction of bias in deviations between target harvest rules and realized harvest functions did not change when we divided the recruitment and escapement data into dominant–subdominant lines and off-cycle lines.

These results illustrate that outcome uncertainties can be substantial, and for at least one run-timing group (Early Stuart), those differences between realized and target mortality rates show bias that is a nonlinear function of recruitment. In addition, annual data points indicate that there was substantial variability around such underlying functions (Fig. 2). For example, when averaged across run-timing groups, the coefficient of variation in residuals of realized mortality rates from the mortality rates predicted from eq. 1 was 0.35 (ranging from 0.24 to 0.59). Furthermore, the magnitude and direction of deviations in realized mortality rates from targets (identified from the target harvest rule) appear to have changed over time for all four run-timing groups (Fig. 3).

Fig. 2. Data and best-fit curves for target harvest rules (i.e., target fractional mortality rate as a function of the forecast of recruitment, ● and solid lines) and realized harvest functions (i.e., realized fractional mortality rate as a function of that same forecast of recruitment, ○ and broken lines) for four run-timing groups of sockeye salmon (*Oncorhynchus nerka*) from the Fraser River, British Columbia, for return years 1986 through 2003: (*a*) Early Stuart, (*b*) Early Summer, (*c*) Summer, and (*d*) Late Summer.

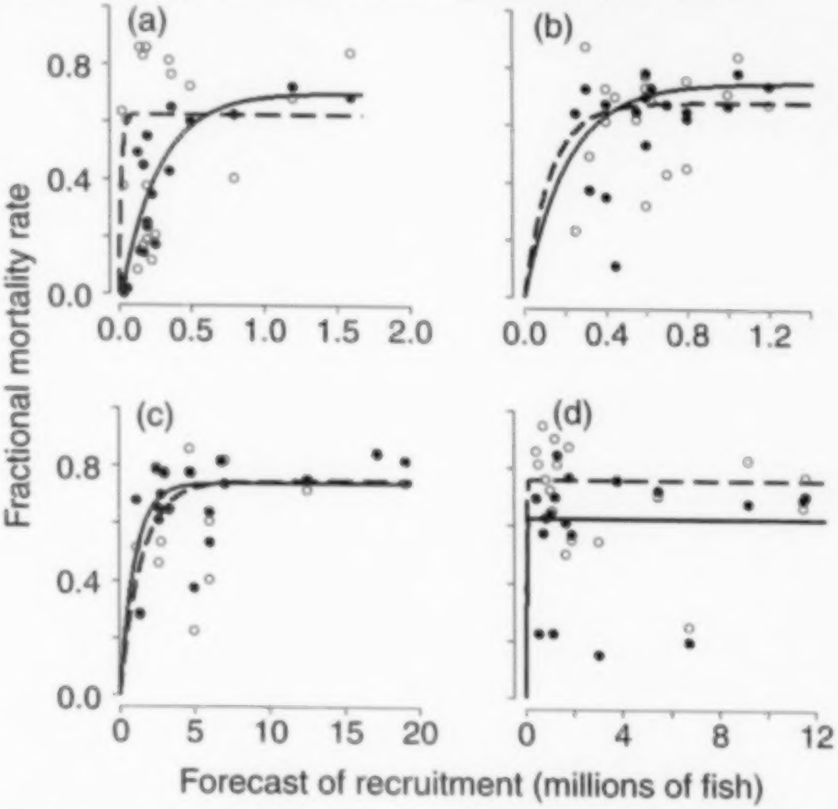

Table 2. Parameter values for target harvest rules (a', b', and c') and realized harvest functions (a, b, and c) for sockeye salmon (*Oncorhynchus nerka*) fisheries in four run-timing groups of the Fraser River, British Columbia.

		Parameter		
Run-timing group		a' (target) or a (realized)	b' (target) or b (realized)	c' (target) or c (realized)
Early Stuart	Target harvest rule	0.70 (0.59, 0.82)	3.75×10^{-6} (1.74×10^{-6}, 7.48×10^{-6})	19 486 (1, 82 370)
	Realized harvest function	0.63 (0.45, 0.94)	5.52×10^{-5} (2.06×10^{-9}, 4.78×10^{-4})	1.83 (6.7×10^{-3}, 294)
Early Summer	Target harvest rule	0.75 (0.68, 1.00)	3.48×10^{-6} (1.24×10^{-6}, 9.50×10^{-6})	1.01 (1.00, 214)
	Realized harvest function	0.68 (0.56, 0.84)	7.69×10^{-6} (5.23×10^{-7}, 3.92×10^{-5})	1
Summer	Target harvest rule	0.74 (0.66, 0.84)	1.01×10^{-6} (3.85×10^{-7}, 3.30×10^{-6})	1.17 (1.00, 252)
	Realized harvest function	0.75 (0.66, 0.82)	6.93×10^{-7} (2.69×10^{-7}, 2.37×10^{-6})	1.44 (1.06, 404)
Late Summer	Target harvest rule	0.62 (0.52, 0.72)	4.54×10^{-5} (6.57×10^{-6}, 8.02×10^{-3})	1808 (259, 368 952)
	Realized harvest function	0.76 (0.67, 0.84)	4.55×10^{-5} (2.06×10^{-9}, 1.21×10^{-2})	1808 (259, 368 952)

Note: Values in parentheses are the lower and upper 95% confidence limits. For the Early Summer run, the c parameter was constrained to equal 1 fish to permit model convergence; therefore, the confidence limits for this parameter were not calculated.

Effects of forecasting errors

Stocks differed in the degree of association between forecasting errors and deviations between realized mortality rates and targets, the latter identified from target harvest rules. We fit a linear relation between these deviations in mortality rates and forecasting errors. For the Early Stuart run, this linear relation was marginally not significant (F = 4.21, P = 0.057, df = 17), and based on adjusted r^2, 16% of the variance in deviations in mortality rates could be explained by forecasting errors. Residuals from this relation were normally distributed. For the Early Summer, Summer, and Late Summer runs, less than 1% of the variance in differences between realized and target mortality rates could be explained by this source of uncertainty, and these relations

Fig. 3. Time series of differences between annual realized fractional mortality rates and the targets that were identified from target harvest rules in those years by run-timing group of sockeye salmon (*Oncorhynchus nerka*) from the Fraser River, British Columbia: Early Stuart (—), Early Summer (—□—), Summer (- - - -), and Late Summer (– –).

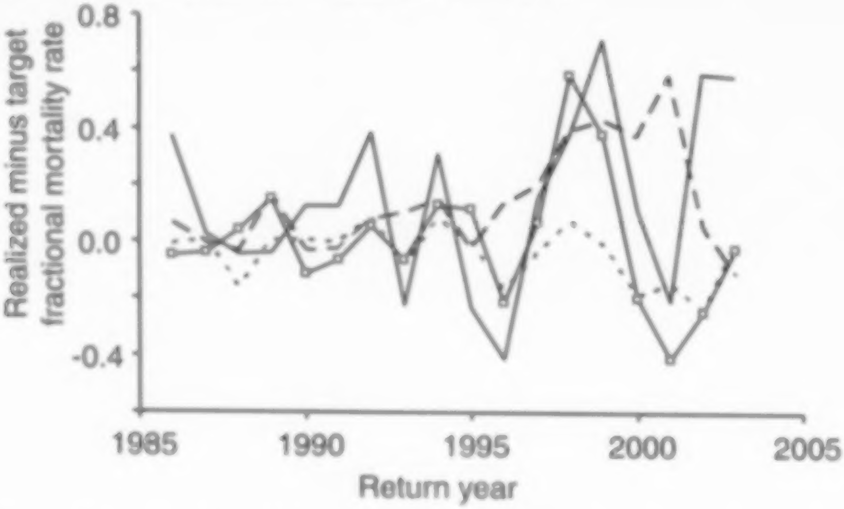

were not statistically significant (P = 0.96, 0.36, and 0.87, respectively). Therefore, factors other than uncertainties in forecasts of recruitment likely accounted for most of the variance in deviations between realized and target mortality rates for these run-timing groups. We explored three possible factors, one related to environmentally driven en route mortality and two related to specific management situations.

Effects of environmentally driven en route mortality

For Early Stuart, Early Summer, and Summer runs, in years when water flows and river temperatures exceeded critical thresholds (Fig. 4, right sides of the six panels), realized mortality rates tended to be greater than those from the target harvest rules (positive residuals). In fact, for those stocks and years for which water flow exceeded the critical threshold, realized mortality rates were always greater than within-season targets. For those stocks and years for which river temperature exceeded the critical threshold, there also tended to be more positive deviations in mortality rates than expected if those deviations were independent of temperature, although the pattern was not statistically significant (binomial test, P = 0.22) (Zar 1999). No such anomalous environmental conditions occurred for the Late Summer run during the period analyzed; hence, this stock is omitted from Fig. 4.

Effects of specific management situations

For the Early Summer run, differences in realized mortality rates from targets were positively correlated with those of the Summer run (r = 0.66, P < 0.01) because timings of upriver migration (when the fish are vulnerable to the main fishery) partially overlapped for these two runs (Pacific Salmon Commission 2001). Fishing pressure on the Early Summer run to some extent affected realized mortality rates on the Summer run, and vice versa.

Furthermore, during the 7 years when Late Summer sockeye migrated earlier than normal, it partly coincided with the Summer run. In those years, realized mortality rates for the Summer run were lower than predicted from the target harvest rule for that stock group (Figs. 4*e* and 4*f*, open circles). This was because mortality rates were affected by deliberate management decisions to reduce fishing pressure on the comigrating Late Summer run, which faced conservation concerns. In contrast, for the Late Summer run, there was no consistent sign of deviations in mortality rates in the years when this run migrated earlier than expected (not shown).

Conversion factors

The factors that convert target harvest rules to realized harvest functions are listed (Table 3). For Early Summer, Summer, and Late Summer runs, the differences between the target harvest rule and realized function were small, so conversion factors for most parameters for those stocks were close to one. The Early Stuart run was the exception.

Discussion

For some sockeye salmon fisheries, actual fractional mortality rates tend to deviate from targets in ways that may hinder achievement of biological conservation and harvesting objectives. For example, for Early Stuart and Late Summer run-timing groups, realized mortality rates generally tended to exceed target mortality rates predicted from target harvest rules at low recruitment (though at all recruitments for the Late Summer run). Where such a bias is not accounted for in preseason stock assessments and evaluations of management options, salmon populations are being put at risk in terms of conservation concerns more often than would be the case if this bias were taken into account. Even though in some cases harvesting occurs at higher rates than initially targeted because of deliberate trade-offs among management objectives in multistock fisheries, this difference between target and realized mortalities should nevertheless be considered when evaluating management options.

Fig. 4. Relation between environmental variables (mean water flow and mean river temperature at Hell's Gate for the 31-day period surrounding peak migration in year *t*) and the difference between the realized fractional mortality rate, D_t, and the target fractional mortality rate, D_t', that was predicted from target harvest rules for three run-timing groups of sockeye salmon (*Oncorhynchus nerka*) in the Fraser River, British Columbia. The horizontal solid lines reflect residuals of zero. The broken vertical lines represent critical thresholds in water flow (6400 $m^3\cdot s^{-1}$) and river temperature (18 °C) for increased natural mortality. In (*e*) and (*f*), the open circles (○) represent years when the timing of the Late Summer run was early (before September 15) and coincided with that of the Summer run.

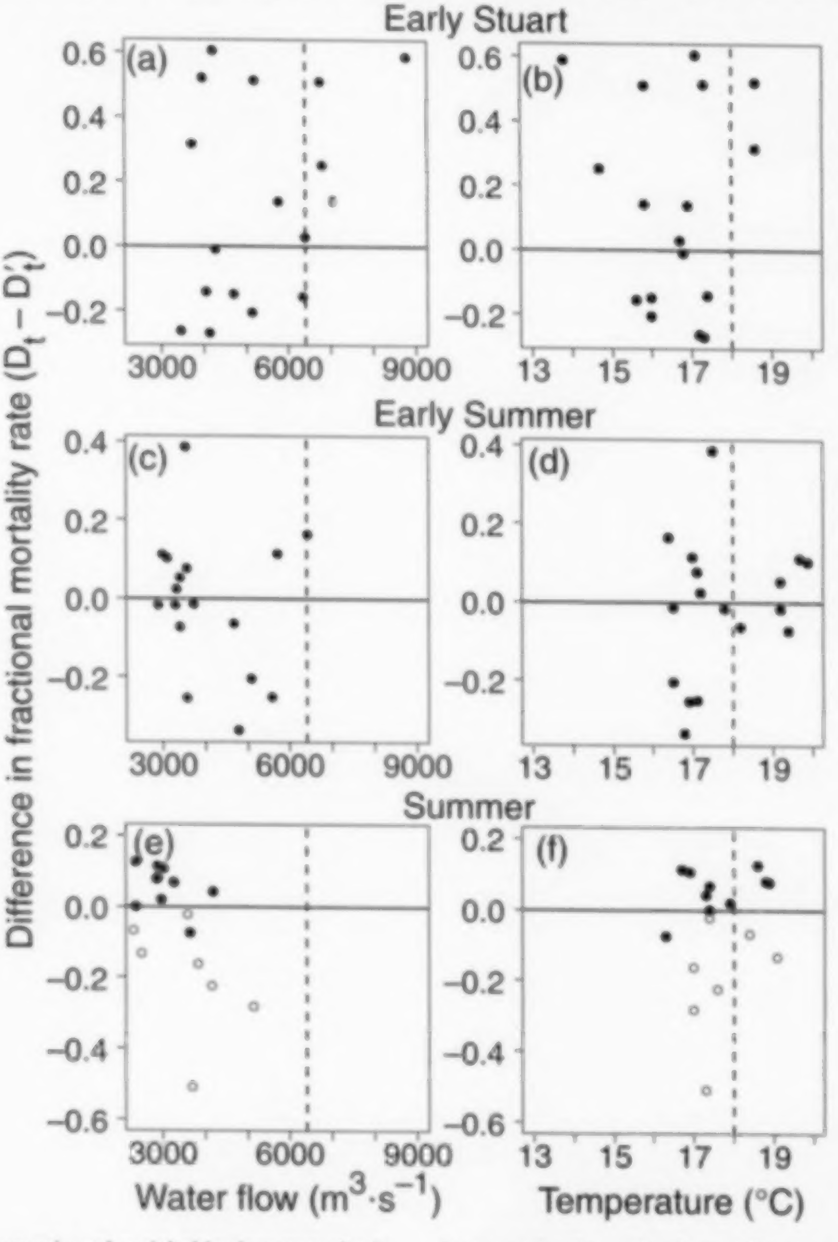

Attainment of economic and social objectives may also be affected by this bias in differences between realized mortality rates and targets. For instance, for the Early Stuart run, the realized mortality rate function tends to fall below the target mortality rate function at high recruitment. In that situation, when recruitment was greater than 1.4 million fish, for example, the realized mortality rate predicted from the realized harvest function was 89% of the target mortality rate. This bias would result in foregone catch when recruitment was high, leading to reduced economic and social benefits associated with harvesting. In future evaluations of management options for Fraser River sockeye salmon

Table 3. Conversion factors (d_0, d_1, d_2) that can be used as multiplicative scalars to transform parameters of the target harvest rules (a', b', and c') into parameters of the realized harvest functions (a, b, and c in eq. 1) for four run-timing groups of sockeye salmon (*Oncorhynchus nerka*) from the Fraser River, British Columbia.

Run-timing group	d_0	d_1	d_2
Early Stuart	0.89	14.73	4.75×10^{-5}
Early Summer	0.91	2.21	1.00
Summer	1.01	0.69	0.082
Late Summer	1.22	1.00	1.33

stocks, scientists and managers can account for both positive and negative biases in realized minus target mortality rates by using models with conversion factors like those identified here.

Another salient feature of our results is the large interannual variation in the magnitude of outcome uncertainties. These large variations mean that the best-fit conversion factors would need to be combined with random error terms to simulate this observed stochasticity in realized mortality rates when evaluating management options. In the short term, such stochastic "noise" may be so large as to mask the differences between forecasted harvest rules and realized harvest functions, but in the long term, the patterns in deviations between realized mortality rates and targets will emerge. For instance, for the Late Summer run, realized mortality rates will be greater on average than target mortality rates, though this will not necessarily be the case in any given year.

Although differences between realized mortality rates and targets could be partially explained by forecasting errors, environmentally driven en route mortality, and specific management situations, these apply only to certain stocks, and much of the total variance remains unexplained. Forecasting errors could explain only a small portion of the variance in deviations between realized and target mortality rates, and environmental conditions could explain only those deviations in years when conditions surpassed critical thresholds. Therefore, other sources of outcome uncertainty are likely important.

For instance, measurement errors in spawner abundances may contribute to variability in estimated in-river mortality rates. The coefficient of variation (CV) in estimates of spawner abundances for nine sockeye salmon stocks in the Fraser River, as derived from mark-recapture studies, ranged from 0.02 to 0.19 from 2001 through 2004 (Chuck Parken, Fisheries and Oceans Canada, Pacific Biological Station, 3190 Hammond Bay Road, Nanaimo, BC V9R 5K6, personal communication). These measurement errors were lower than the coefficient of variation that we calculated for deviations between realized spawning escapements and targets identified from target harvest rules (average CV = 0.65, range 0.47 – 0.82). Therefore, it is likely that estimation error is only a minor contributor to the observed differences between target and realized mortality rates.

Implementation uncertainty is another possibility for those differences. For example, noncompliance with regulations by harvesters may explain part of the observed high realized mortality rates at low recruitment compared with the target. However, we have no data to further analyze this source of implementation uncertainty. Similarly, deviations in catchability coefficients may also explain part of the bias and stochasticity in observed mortality rates because migratory routes of adults vary unpredictably among years (Pacific Salmon Commission 2001).

One limitation to our results is that our conversion factors represent the average deviation over 18 years between realized mortality rates and targets that were identified from harvest rules. However, the magnitude and direction of these differences appear to have changed several times over this period, possibly because of a combination of factors. These include changes in forecasting methods, management objectives, characteristics of the fishing fleet and allocation of harvest among various groups, methods used to estimate abundances of spawners and the catch, environmental factors, en route mortality, and migratory behaviour of recruits. Conversion factors such as ours therefore only reflect long-term average patterns in differences between realized and target mortality rates.

Some previous studies of sockeye salmon examined biases in differences between realized harvest rates (or spawning escapements) and targets. However, they generally have been based more on either expert opinion or qualitative perusal of data than on quantitative analyses of empirical data (e.g., Peterman et al. 2000). Bocking and Peterman (1988) identified differences in annual realized harvest rates from annual target harvest rates (or annual realized escapements from annual target escapements) rather than deviations in actual outcomes from underlying target harvest rules that are time-independent. In contrast to Bocking and Peterman's (1988) approach, Wood et al. (1998), who examined sockeye salmon fisheries on the Skeena River, B.C., attributed the deviations between target harvest rules and actual harvest rates from 1983 through 1997 to trade-offs among objectives by managers in a mixed-stock fishery, although these deviations were not described quantitatively. Furthermore, empirical studies of Pacific salmon fisheries have usually ignored the effect of abundance of recruits on the direction and magnitude of deviations between realized mortality rates and targets (Wood et al. 1998).

Our measure of variability in the difference between realized and target mortality rates was lower than that estimated from another previous study (for sockeye salmon in Bristol Bay, Alaska; Eggers 1992), but higher than others (e.g., for sockeye salmon in Fraser River, B.C.; Cass et al. 2003). The difference in the magnitude of Eggers' (1992) estimates and our values for Fraser River run-timing groups may be due to reduction in forecasting error through managers using within-season updates of recruitment forecasts in the Fraser River cases that were not used in Eggers (1992) for the Bristol Bay fishery. The estimate of variability used by Cass et al. (2003) was based on expert judgment and included only those sources of uncertainty related to variability in catchability of fish, whereas ours was based on empirical data and reflected various sources of uncertainty, including forecasting errors and errors in estimates of spawner abundance.

Management recommendations

Scientists and managers can account for outcome uncertainties, or differences between realized mortality rates and targets, in several ways. First, they can identify appropriate target rules that reflect those differences by building stochastic simulations models. The Fraser River Salmon Spawning Initiative model is being developed with this in mind (Cass et al. 2003). Managers can also reduce those differences by identifying the sources and applying corrective actions. For example, more accurate within-season forecasts of recruitment may bring realized mortality rates closer to targets. For the Fraser River sockeye salmon, managers have attempted this by predicting en route mortality with newly developed management-adjusted (MA) forecasts of spawning escapement. Those MA forecasts account for natural sources of en route mortality, as well as others, such as in-river First Nations fisheries, estimation errors in in-river abundance and at the spawning grounds, and stock identification errors. By doing so, managers aim to reduce deviations between realized mortality rates and targets (Pacific Salmon Commission 2005). For example, the 2004 forecast of spawning escapement for Early Stuart sockeye that included this adjustment was 24% lower than the forecast that ignored it (Ian Guthrie, personal communication). MA forecasts have been implemented in the Fraser River only recently (starting in 2002), and therefore it is too soon to determine their effect on deviations between realized mortality rates and targets. In addition, more effective enforcement of regulations and monitoring of compliance may further reduce implementation uncertainty by deterring harvesters from violating regulations. An example could be to use genetic techniques to identify fish harvested illegally from stocks in areas closed to fishing (Withler et al. 2004). Collectively, these steps should help achieve management objectives more frequently than is currently the case. At the very least, accounting for differences between realized and target mortality rates in simulations of management options should be of value to managers of most fish species.

Acknowledgments

We thank the Pacific Salmon Commission and Fisheries and Oceans Canada for kindly providing the data for sockeye salmon. We thank Ian Guthrie from the Pacific Salmon Commission and Al Cass and Jeff Grout from Fisheries and Oceans Canada for valuable discussions on the Fraser River fishery. Mike Bradford, Chris Wood, Brigitte Dorner, and Ian Guthrie offered helpful critiques of an early version of this manuscript. Two reviewers and an Associate Editor provided extremely valuable suggestions to improve the manuscript. Statistical advice was provided by Bill de la Mare and Sean Cox. Funding for this study was provided by Natural Sciences and Engineering Research Council of Canada grants awarded to R.M. Peterman.

References

Bocking, R.C., and Peterman, R.M. 1988. Preseason forecasts of sockeye salmon (*Oncorhynchus nerka*): comparison of methods and economic considerations. Can. J. Fish. Aquat. Sci. **45**: 1346–1354.

Butterworth, D.S., and Punt, A.E. 1999. Experiences in the evaluation and implementation of management procedures. ICES J. Mar. Sci. **56**: 985–998.

Cass, A.J. 1998. Run size forecasts for Fraser River sockeye salmon in 1998. Canadian Stock Assessment Secretariat Research Document No. 98/44, Fisheries and Oceans Canada, Nanaimo, British Columbia.

Cass, A.J. 2002. Pre-season run size forecasts for Fraser River sockeye and pink salmon in 2003. Canadian Stock Assessment Secretariat Research Document No. 2002/116, Fisheries and Oceans Canada, Nanaimo, British Columbia.

Cass, A., Folkes, M., and Pestal, G. 2003. Methods for assessing harvest rules for Fraser River sockeye salmon. Pacific Scientific Advice Review Committee Working Paper No. S2003-14, Fisheries and Oceans Canada, Nanaimo, British Columbia.

Cooke, S.J., Hinch, S.G., Farrell, A.P., Lapointe, M.F., Jones, S.R.M., Macdonald, J.S., Patterson, D.A., Healey, M.C., and Van Der Kraak, G. 2004. Abnormal migration timing and high en route mortality of sockeye salmon in the Fraser River, British Columbia. Fisheries (Bethesda), **29**: 22–33.

Eggers, D.M. 1992. The benefits and costs of the management program for natural sockeye salmon stocks in Bristol Bay, Alaska. Fish. Res. **14**: 159–177.

Fraser River Sockeye Spawning Initiative. 2005. Report of the Technical Working Group on the Fraser River Sockeye Spawning Initiative. Fisheries and Oceans Canada, Vancouver, British Columbia.

Hilborn, R., and Walters, C.J. 1992. Quantitative fisheries stock assessment. Chapman and Hall, New York.

Huber, P.J. 1981. Robust statistics. John Wiley & Sons, Toronto.

Kell, L.T., O'Brien, C.M., Smith, M.T., Stokes, T.K., and Rackham, B.C. 1999. An evaluation of management procedures for implementing a precautionary approach in the ICES context of North Sea plaice (*Pleuronectes platessa* L.). ICES J. Mar. Sci. **56**: 834–845.

Link, M.R., and Peterman, R.M. 1998. Estimating the value of in-season estimates of abundance of sockeye salmon (*Oncorhynchus nerka*). Can. J. Fish. Aquat. Sci. **55**: 1408–1418.

McAllister, M.K., Starr, P.J., Restrepo, V.R., and Kirkwood, G.P. 1999. Formulating quantitative methods to evaluate fishery-management systems: what fishery processes should be modelled and what trade-offs should be made? ICES J. Mar. Sci. **56**: 900–916.

Pacific Salmon Commission. 1986–1995. Sockeye salmon racial analyses: Fraser River sockeye salmon racial statistics. Pacific Salmon Commission, Vancouver, British Columbia.

Pacific Salmon Commission. 1996–2003. Reports of the Fraser River Panel to the Pacific Salmon Commission on the Fraser River sockeye salmon fishing season. Fisheries Management Division of the Pacific Salmon Commission, Vancouver, British Columbia.

Pacific Salmon Commission. 2001. Report of the Fraser River Panel to the Pacific Salmon Commission on the 2000 Fraser River sockeye salmon fishing season. Pacific Salmon Commission, Vancouver, British Columbia.

Pacific Salmon Commission. 2002. Relating risk of management error to lower bounds of escapement for additional management action. Joint Chinook Technical Committee Report No. TCCHINOOK(2002)-02, Pacific Salmon Commission, Vancouver, British Columbia.

Pacific Salmon Commission. 2005. 19th Annual report 2002/2003. Pacific Salmon Commission, Vancouver, British Columbia.

Peterman, R.M., Pyper, B.J., and Grout, J.A. 2000. Comparison of parameter estimation methods for detecting climate-induced changes in productivity of Pacific salmon (*Oncorhynchus* spp.). Can. J. Fish. Aquat. Sci. **57**: 181–191.

Rice, J.C., and Richards, L.J. 1996. A framework for reducing implementation uncertainty in fisheries management. N. Am. J. Fish. Manag. **16**: 488–494.

Rosenberg, A.A., and Brault, S. 1993. Choosing a management strategy for stock rebuilding when control is uncertain. Can. Spec. Publ. Fish. Aquat. Sci. No. 120. pp. 243–249.

Rosenberg, A.A., and Restrepo, V.R. 1994. Uncertainty and risk evaluation in stock assessment advice for U.S. marine fisheries. Can. J. Fish. Aquat. Sci. **51**: 2715–2720.

Wagner, G.N., Hinch, S.G., Kuchel, L.J., Lotto, A., Jones, S.R.M., Patterson, D.A., Macdonald, J.S., Van Der Kraak, G., Shrimpton, M., English, K.K., Larsson, S., Cooke, S.J., Healey, M.C., and Farrell, A.P. 2005. Metabolic rates and swimming performances of adult Fraser River sockeye salmon (*Oncorhynchus nerka*) after a controlled infection with *Parvicapsula minibicornis*. Can. J. Fish. Aquat. Sci. **62**: 2124–2133.

Williams, B. 2005. 2004 Southern salmon fishery post-season review: part one — Fraser River Sockeye Report [online]. Available from http://www-comm.pac.dfo-mpo.gc.ca/publications/2004psr/default_e.htm [accessed 20 January 2006].

Withler, R.E., Candy, J.R., Beacham, T.D., and Miller, K.M. 2004. Forensic DNA analysis of Pacific salmonid samples for species and stock identification. Environ. Biol. Fishes, **69**: 275–285.

Wood, C.C., Rutherford, D.T., Bailey, D., and Jakubowski, M. 1998. Assessment of sockeye salmon production in Babine Lake, British Columbia, with forecast for 1998. Can. Tech. Rep. Fish. Aquat. Sci. No. 2241.

Zar, J.H. 1999. Biostatistical analysis. Prentice-Hall, Upper Saddle River, New Jersey.

Appendix A

Table A1. Within-season forecasts of recruitment (R') and target escapement (E') and actual (i.e., realized) recruitment (R) and realized escapement (E) for four run-timing groups of the Fraser River (Early Stuart, Early Summer, Summer, and Late Summer) from 1986 through 2003.

	Within-season forecast		Realized	
Return year	R'	E'	R	E
Early Stuart run-timing group				
1986	35 000	35 000	45 600	28 584
1987	175 000	150 000	177 767	148 194
1988	195 000	150 000	221 575	179 807
1989	1 200 000	333 000	1 211 799	384 799
1990	200 000	150 000	154 864	97 035
1991	500 000	200 000	512 453	141 119
1992	350 000	200 000	350 406	65 617
1993	800 000	300 000	1 151 643	688 013
1994	200 000	90 000	204 245	29 126
1995	230 000	150 000	138 503	122 856
1996	130 000	66 000	95 397	87 570
1997	1 600 000	500 000	1 675 061	265 698
1998	175 000	97 000	189 780	32 570
1999	150 000	128 000	171 627	24 532
2000	370 000	130 000	378 193	89 747
2001	260 000	154 000	214 187	170 906
2002	60 000	59 000	62 664	24 637
2003	30 000	28 500	35 800	13 166
Early Summer run-timing group				
1986	600 000	130 000	840 890	225 403
1987	625 000	169 000	641 514	200 037
1988	1 000 000	330 000	749 014	217 763
1989	303 000	83 000	506 786	63 275
1990	1 900 000	398 000	1 361 146	440 958
1991	1 200 000	314 000	826 725	270 073
1992	1 050 000	225 000	650 376	102 336
1993	400 000	130 000	222 874	86 492
1994	800 000	300 000	1 018 707	248 147
1995	320 000	200 000	313 384	159 725
1996	600 000	280 000	534 333	363 090

Table A1 *(concluded).*

Return year	Within-season forecast		Realized	
	R′	*E′*	*R*	*E*
1997	600 000	180 000	389 053	88 949
1998	450 000	400 000	747 974	226 662
1999	400 000	260 000	385 546	104 741
2000	800 000	280 000	1 050 152	574 334
2001	250 000	89 000	392 983	301 788
2002	700 000	227 000	801 634	457 532
2003	550 000	193 000	513 523	193 490
Summer run-timing group				
1986	3 000 000	675 000	2 505 120	581 163
1987	2 500 000	535 000	3 161 545	659 118
1988	1 100 000	355 000	1 530 749	745 040
1989	17 150 000	2 753 000	16 334 300	2 557 032
1990	6 800 000	1 280 000	8 673 094	1 597 295
1991	4 700 000	1 062 000	5 524 474	1 256 770
1992	4 650 000	1 046 000	4 394 084	634 729
1993	19 000 000	3 480 000	19 394 157	5 071 720
1994	7 000 000	1 847 000	7 227 933	1 324 723
1995	2 600 000	1 012 000	2 355 394	917 511
1996	2 800 000	840 000	3 025 711	1 411 690
1997	12 500 000	3 124 000	13 370 101	3 807 463
1998	6 000 000	2 800 000	6 020 294	2 382 300
1999	1 400 000	1 000 000	1 771 844	1 280 669
2000	2 600 000	910 000	3 063 991	1 650 410
2001	5 000 000	3 124 000	6 043 349	4 683 377
2002	6 000 000	2 160 000	6 351 403	3 803 591
2003	3 300 000	1 155 000	2 814 772	1 003 214
Late Summer run-timing group				
1986	11 600 000	3 405 000	12 446 091	2 822 048
1987	3 800 000	906 000	3 663 863	888 558
1988	1 325 000	205 000	1 207 293	227 414
1989	432 000	131 000	414 912	59 100
1990	11 500 000	3 532 000	11 765 353	3 928 427
1991	5 500 000	1 519 000	5 496 107	1 638 210
1992	1 000 000	357 000	956 371	266 124
1993	1 800 000	420 000	2 807 985	356 149
1994	9 200 000	2 960 000	8 820 345	1 498 971
1995	1 900 000	816 000	1 189 479	538 444
1996	800 000	300 000	829 004	199 241
1997	1 200 000	360 000	903 554	89 756
1998	3 000 000	2 550 000	3 907 204	1 780 543
1999	1 100 000	853 000	1 308 454	455 330
2000	700 000	300 000	707 904	38 439
2001	550 000	426 000	541 635	100 631
2002	6 727 000	5 422 000	7 916 492	5 946 184
2003	1 641 000	638 000	1 535 818	767 764

Note: Within-season estimates were the latest ones made during the fishing season, when managers could still adjust fishing regulations to achieve targets. Realized values are those actually observed after the end of the fishing season. Data were obtained from Fisheries and Oceans Canada and the Pacific Salmon Commission (Table 1).

Mysid and fish zooplanktivory in Lake Ontario: quantification of direct and indirect effects

Gideon Gal, Lars G. Rudstam, Edward L. Mills, Jana R. Lantry, Ora E. Johannsson, and Charles H. Greene

Abstract: *Mysis relicta* and planktivorous fish feed on zooplankton in Lake Ontario and form a trophic triangle that includes intraguild predation by fish on mysids. Thus, fish affect zooplankton both directly and indirectly. To evaluate the importance of alewife (*Alosa pseudoharengus*), rainbow smelt (*Osmerus mordax*), and mysids as zooplanktivores in Lake Ontario, we measured abundances and distributions, assessed diets, and computed mysid and fish consumption rates based on bioenergetics models. We further estimated indirect effects by comparing clearance rates given observed and potential mysid distributions. Estimated consumption rates varied widely with season and water depth and ranged between 2.6×10^{-3} and $1.3\ g \cdot m^{-2} \cdot day^{-1}$ for mysids and between 1.4×10^{-3} and $0.5\ g \cdot m^{-2} \cdot day^{-1}$ for fish, representing a daily removal of zooplankton of up to $10.2\% \cdot day^{-1}$ and $2.0\% \cdot day^{-1}$ by mysids and fish, respectively. Mysid planktivory exceeded fish planktivory in May and August, but fish planktivory dominated in October. Estimated mysid planktivory rates were 2- to 90-fold lower than the potential rate if mysids moved to temperatures that maximized their predation rates, suggesting an indirect positive effect of fish on zooplankton.

Résumé : Dans le lac Ontario, *Mysis relica* et les poissons planctonophages se nourrissent de zooplancton et forment ainsi un triangle trophique qui inclut la prédation par des membres de la guilde des poissons sur les mysidacés. Les poissons affectent donc le zooplancton à la fois directement et indirectement. Afin d'évaluer l'importance de la consommation de zooplancton par le gaspareau (*Alosa pseudoharengus*), l'éperlan arc-en-ciel (*Osmerus mordax*) et les mysidacés, nous avons mesuré les abondances et les répartitions, déterminé les régimes alimentaires et calculé les taux de consommation des mysidacés et des poissons d'après des modèles bioénergétiques. Nous avons estimé, de plus, les effets indirects en comparant les taux de clearance, compte tenu des répartitions observées et potentielles des mysidacés. Les taux de consommation estimés varient considérablement en fonction de la saison et de la profondeur de l'eau: ils vont de 2.6×10^{-3} à $1.3\ g \cdot m^{-2} \cdot jour^{-1}$ chez les mysidacés et de 1.4×10^{-3} à $0.5\ g \cdot m^{-2} \cdot jour^{-1}$ chez les poissons, ce qui correspond à des retraits quotidiens du zooplancton respectifs de jusqu'à 10.2 % par jour et de 2.0 % par jour. La consommation de plancton par les mysidacés dépasse celle des poissons en mai et en août, mais celle effectuée par les poissons domine en octobre. Les taux estimés de consommation du plancton par les mysidacés sont 2–90 fois plus faibles que les taux potentiels que l'on obtiendrait si les mysidacés se déplaçaient vers les températures qui maximisent leur taux de prédation; il semble donc y avoir un effet indirect positif des poissons sur le zooplancton.

[Traduit par la Rédaction]

Introduction

Intraguild predation (IGP) is a common feature in ecosystems. IGP occurs when a consumer of a resource (the IG predator) also preys upon on a second consumer of that resource (the IG prey) thereby setting the stage for predator–prey and competitor interactions between the two consumers (Polis and Holt 1992; Mylius et al. 2001). Unexpected results of food web manipulations have often been linked to IGP and complex forms of the food web (Hart 2002). Thus, to fully understand a food web that includes IGP dynamics, separate analysis of its IGP components should be conducted. IGP dynamics is a relatively common occurrence in aquatic systems (Rudstam et al. 1992; Gismervik and Andersen

Received 1 March 2006. Accepted 8 November 2006. Published on the NRC Research Press Web site at http://cjfas.nrc.ca on 8 December 2006.
J19200

G. Gal.[1] Kinneret Limnological Laboratory, IOLR, P.O. Box 447, Migdal, Israel.
L.G. Rudstam and E.L. Mills. Cornell Biological Field Station, Department of Natural Resources, 900 Shackelton Pt. Road, Bridgeport, NY 13030, USA.
J.R. Lantry. New York State Department of Environmental Conservation, Cape Vincent Fisheries Station, 541 East Broadway, Cape Vincent, NY 13618, USA.
O.E. Johannsson. Great Lakes Laboratory for Fisheries and Aquatic Sciences, Department of Fisheries and Oceans, Canada Centre for Inland Waters, 867 Lakeshore Road, Burlington, ON L7R 4A6, Canada.
C.H. Greene. Ocean Resources and Ecosystem Program, Snee Hall, Cornell University, Ithaca, NY 14853, USA.

[1] Corresponding author (e-mail: gal@ocean.org.il).

Can. J. Fish. Aquat. Sci. 63: 2734–2747 (2006) doi:10.1139/F06-156

1997; Hart 2002), often including a planktivorous fish as the IG predator and a planktivorous or omnivorous invertebrate as the IG prey (e.g., Dodson 1974; Mills et al. 2003; Wissel et al. 2003). Hence, IGP dynamics include trophic interactions in which the planktivorous fish affect zooplankton both directly and indirectly. The Lake Ontario food web is an example of a food web containing IGP components. It consists of three major larger planktivores: two fish species, alewife (*Alosa pseudoharengus*) and rainbow smelt (*Osmerus mordax*), and an invertebrate, the mysid shrimp *Mysis relicta*.

The importance of mysids in lake ecosystems is most apparent when they are introduced to lakes as a potential prey for young piscivores, a practice that has now been discontinued (Lasenby et al. 1986). The main reason for ending this program was that the results were not always as intended. For example, *Mysis* have affected zooplankton species composition, decreased growth rates of planktivorous fish, and increased trophic level of, and therefore accumulation of, toxins in lake trout (Cabana and Rasmussen 1994; Spencer et al. 1999). Clearly, mysids are a pivotal group for understanding food web interactions in the Laurentian Great Lakes and elsewhere (Johannsson et al. 2003).

Mysids are omnivorous and perform diel vertical migration, residing in the deep waters during the day and migrating up into the upper hypolimnion and lower metalimnion during the night. The extent of their vertical migration is governed predominately by light and temperature (Beeton and Bowers 1982; Gal et al. 1999*a*). Mysid feeding is determined to a large extent by their vertical migration. They feed on benthic zooplankton, invertebrates, algae, and detritus during the day and on zooplankton and phytoplankton in the water column during the night in the offshore of the Great Lakes (Grossnickle 1982). Zooplankton are mysids' main dietary source in Lake Ontario, contributing 50%–80% of dietary biomass, the remainder being diatoms in the spring and benthic material during the summer and fall (Johannsson et al. 2001). At the same time, mysids are prey for numerous Great Lakes' fish species such as alewife, rainbow smelt, and sculpins, *Cottus* spp. (Owens and Weber 1995; Rand et al. 1995).

Differences in thermal preference have resulted in habitat segregation between alewife and rainbow smelt and, as a result, differences in their diet composition. The alewife diet in Lake Ontario consists mainly of zooplankton, with mysids and amphipods making up about 25% of the alewife diet by weight over the year (Mills et al. 1992), whereas the rainbow smelt diet consists of a larger proportion of mysids and benthic amphipods, *Diporeia* spp. (Rand et al. 1995; Johannsson et al. 2003). Hence, the interactions between the two species of planktivorous fish and mysids include both competition for prey (zooplankton) and intraguild predation.

Previous studies of Lake Ontario trophic interactions between planktivores and zooplankton have typically combined zooplankton and mysid production as a pooled resource available to planktivores in the lake (Borgmann and Whittle 1994; Sprules and Goyke 1994; Rand et al. 1995). These studies have not usually accounted for the impact of mysid predation on zooplankton populations. If mysid and fish consumption of zooplankton are of the same magnitude, then zooplankton and mysid production can not be combined as a single resource for fish when attempting to understand food web dynamics in the lake.

The level of predation on zooplankton by both mysids and planktivorous fish may also be indirectly affected by interactions among predators. In trophic triangles that include intraguild predation, the top predator (fish) or IG predator can decrease the abundance of the IG prey (mysids) and thereby decrease predation on the mutual resource, i.e., zooplankton. However, the top predator can also affect the behavior of the IG prey in ways that decrease its ability to feed. These behavioral effects can be substantial (Turner and Mittelbach 1990; Abrams et al. 1996; Romare and Hansson 2003) but are often overlooked. In our fish–mysid–zooplankton system, the presence of fish may inhibit the vertical migration of mysids into zooplankton-rich waters in the metalimnion, thereby reducing potential food intake by mysids.

In this study, we focus on two issues critical to the understanding of the interactions within the Lake Ontario food web and the transfer of energy within the food web as an example for many aquatic ecosystems with similar trophic dynamics. First, we compare mysid and fish planktivory over temporal and spatial gradients in the lake by applying bioenergetics models to both mysids and fish. Second, we assess the potential importance of indirect impacts. To assess the potential importance of the indirect effects of fish on mysid behavior, we compared the feeding rates of mysids on zooplankton, given the observed distribution of both groups (mysids and zooplankton) in the water column, with the hypothetical feeding rates based on a mysid vertical distribution model predicting that mysids move to water that maximizes their feeding rates (Gal et al. 2004).

Materials and methods

Field sampling and analysis

Three cruises were conducted in the southeastern corner of Lake Ontario, just north of Oswego, New York, during the summer of 1995 (15–16 August), spring of 1996 (5–6 May), and fall of 1996 (1–2 October). During these cruises, we sampled planktivorous fish, mysids, and zooplankton at offshore (bottom depth (BD) > 120 and 90–100 m) and nearshore (BD 60–70 and 30–40 m) stations. During the August cruise, we conducted sampling only at the BD 90 m station. Complimentary data were derived from an earlier cruise carried out during the summer of 1995 (31 July – 1 August) at a midlake station (station 41, BD = 130 m). This station is located some 80 km from the transect stations.

Temperature profiles

Temperature profiles were conducted using a Hydrolab profiler (Hach Company, Loveland, Colorato) to record depth, temperature, and percent oxygen saturation at each station during the day before the start of acoustic sampling. In some cases, profiles were also conducted during the night at individual stations.

Fish sampling

A midwater trawl with a 57 m^2 opening and a cod end with a ½-inch stretch mesh (6 mm bar) was used for fish sampling. Trawls were conducted at night, typically for a duration of 15 min at a tow speed of ~6.5 $km \cdot h^{-1}$. The depth of the net was determined with a headrope transducer acoustically linked to the sampling vessel. Fish sampled were weighed and counted by species (alewife or rainbow smelt), and up to 50 individuals of each species were measured to the nearest millimetre. When possible, up to 30 individuals representing size ranges of each species trawled were preserved with 10% formalin for diet analysis. These fish data were used to determine rainbow smelt growth rates (see below), for diet analysis, and for separating the observed acoustic distribution into the appropriate fish species. Trawling results, however, suffer from a sampling bias: assuming a trawl selectivity similar to that exhibited by gill nets, a 6 mm bar would result in decreased catchability for alewife 50 mm or smaller (Warner et al. 2002). The bias against small rainbow smelt is likely larger. These biases would be especially important in August and most likely October cruises when young-of-the-year (YOY) fish are abundant in the lake but underrepresented in the trawl nets we used. In contrast, the acoustics estimates include fish as small as 20 mm (see below). Therefore, we calculated an average representative weight for each species based on the weight of an age-1 fish and the method described below (see Fish zooplanktivory) and applied the value to the acoustically estimated numerical density, resulting in fish biomass in grams wet weight per unit volume (m^{-3}) for each 1 m depth bin.

When available, we examined the stomach contents of 10 alewife and rainbow smelt from each age class (subadult and adult) for each time period sampled. Fish total length was measured to the nearest millimetre and stomachs were removed. Fish lengths were then converted to fish wet weight as described below. Contents of the dissected stomach (anterior and posterior portions) were suspended in a quartered petri dish and viewed under a dissecting microscope (20× power). All macroinvertebrate prey items were removed from each stomach and counted. Mysid lengths were reconstructed from eye stalk lengths, which were readily identifiable in the fish stomachs. We derived a regression of eye stalk length (EL) to total mysid body lengths (BL) based on measurements of 39 animals caught in May 1995 and 56 animals caught in October 1995. For the May and October 1996 diets, we used regressions based on animals caught in May and October 1995, respectively, and for August, we used a regression based on the combined data ($BL = 16.45EL - 4.61$, $n = 95$, $r^2 = 0.92$, $p < 0.001$). There were no significant differences between this equation and equations specific for the months of May and October (univariate analysis of variance and homogeneity of regressions assumption, $n = 95$, $p > 0.5$). Standard body length was then converted to dry weight (Johannsson 1995).

All microinvertebrate prey items in the stomach were counted when <200 individual zooplankton were present. If 200–800 prey items were present, the sample was homogeneously mixed and prey items in one-quarter of the petri dish were counted. Stomach contents in excess of 800 individual prey items were suspended in 35–45 mL of filtered lake water, a 1 mL subsample was removed, and prey items were counted. Counted prey items were identified to zooplankton species when possible. Counts of subsampled stomachs were expanded to determine the total number of prey items in the stomach. A subsample of about 100 whole zooplankton from each stomach was identified to species and measured to the nearest 0.1 mm, and average dry weight for each species was determined using length–weight regressions (Klumb 2003) in conjunction with a computer-assisted plankton analysis system (CAPAS; Hambright and Fridman 1994). The dry weights for all species were summed to provide an estimate of total stomach content weight for each fish stomach.

Mysid net sampling

Net samples of mysids were collected using a 1 mm mesh, 1 m diameter opening–closing net, with the exception of the early August 1995 cruise in which a 500 μm mesh, 1 m^2 square opening net was used. All net samples were collected during the night. The net samples were used to confirm our acoustic data, and as such, the sampling depths were determined based on the acoustically observed depths of the mysid layer, with samples being collected from above, within, and below the layer. In addition, the data gained from the net samples were used to provide information on the size distribution of mysids in the water column. We applied the size distribution determined from the net samples to the numerical density, as determined acoustically (see below), and employed a length–weight regression (Johannsson 1995) to calculate dry weight (DW) per unit volume. DW was then converted to wet weight (WW) assuming a DW–WW ratio of 0.15 (Johannsson et al. 1994). This resulted in mysid biomass estimates in grams wet weight per unit volume ($g\ WW \cdot m^{-3}$) for 2 m vertical layers over the entire water column.

Acoustic sampling

Fish and mysid sampling was conducted with a dual-frequency (1996 cruises) or single-frequency (August 1995) acoustic system. A 420 kHz single-beam (6° half-power beam width) digital echosounder (Biosonics, Inc., Seattle, Washington) was used for all cruises, and a 70 kHz, split-beam (11.3° half-power beam width) echosounder (Simrad, Inc., Horten, Norway) was used in conjunction with the 420 kHz system during the 1996 cruises. Ping rate was 1 $ping \cdot s^{-1}$, and pulse length was 0.4 ms and 0.6 ms for the 420 kHz and 70 kHz systems, respectively. When both frequencies were used, the 420 kHz system was triggered externally by the 70 kHz system, and both transducers were mounted on the same towed body. The 420 kHz system was calibrated in July 1995 and again in August 1996. No adjustments were required following the latter calibration. The 70 kHz system was calibrated in October 1996 and was within 0.4 dB of the gains used in 1995 and 1996.

Acoustic analysis

We used the 420 kHz data to calculate mysid density and the 70 kHz data to calculate fish density. Volume backscattering at 420 kHz was obtained with Visual Analyzer (version 3.1, BioSonics, Inc.) using a lower threshold of –100 dB. Mysid mean backscattering cross section was estimated based on the distribution of mean mysid lengths in the net samples and the mysid target strength (TS) model evaluated by Gal et al. (1999*b*). The mean TS was applied to the echo-integration values collected with the 420 kHz unit to provide estimates of the vertical distribution of mysid densities (mysids·m^{-3}). For echo integration, 10 to 50 pings were averaged per report, and mean (± standard error, SE) abundances were determined by averaging across nonconsecutive reports to a total of 150–330 pings.

Fish vertical density distribution was estimated using in situ TS values to transform echo-integration data into numerical abundance data. Echo-integration and TS estimates were estimated using EP-500 software for the 70 kHz unit (version 5.2, Simrad, Inc.) and lower thresholds of –61 dB (TS) and –80 dB (echo integration). A minimum TS of –61 dB will include most echoes from alewife and rainbow smelt larger than 20 mm (Warner et al. 2002; Rudstam et al. 2003). For echo integration, 200–220 pings were averaged per report, and mean (±SE) densities were determined by averaging across reports and a total of 600–660 pings. In some cases, during the spring and fall, fish and mysids overlapped spatially in the water column, restricting the ability to determine the density of each group. Therefore, in the spring, we selected regions at several points in time in which there was no obvious overlap to determine the densities of fish and mysids. At the 60 m station, it was not possible to determine mysid density because of relatively high fish density throughout the water column at all times. During the fall, it was clear from visual inspection of the echograms that fish and mysid overlap occurred mainly within a narrow region. Above that region, high densities of fish were obvious, whereas few fish, if any, were observed below. Hence, mysid densities were estimated for the water column ranging between the narrow overlapping region to the bottom. Fish densities were estimated for the entire water column by using individual acoustic targets above a lower threshold (–61 dB), thereby reducing the possibility of including mysids. Although there was a clear spatial segregation between alewife and rainbow smelt in the summer and fall, the vertical differentiation was not clear in the spring. We therefore applied the proportions found in the trawl catches. The alewife represented, on average, 67% of the catch across all the trawls in May 1996, a value which was then used to allocate the fish density acoustically observed in the water column.

The 70 kHz system was not used during the August 1995 cruises. We therefore determined the mean backscattering cross section for fish by analyzing the 420 kHz data using the EMS procedure within Visual Analyzer (Hedgepeth et al. 1999). The mean backscattering cross section was then applied to the volume backscattering values to determine fish abundance. A lower threshold of –70 dB was used for echo integration and –61 dB for target recognition, and at least 200 targets were required for successful completion of the EMS procedure.

Zooplankton sampling

Vertical hauls using a standard, unmetered, opening–closing plankton net (0.5 m diameter net with 64 µm mesh) were conducted at night at each station. During the spring cruise, prior to stratification, zooplankton and mysid sampling was determined based on the depth of the mysid layer that was observed acoustically. At each station, one sample was collected from above the mysid layer to the surface and a second was collected from below the mysid layer to the surface. For the summer and fall cruises, sampling depth was determined based on the positions of the thermocline and mysid layer. During the summer cruises, samples of the epilimnion, of the mysid layer, and from 70 or 80 m to the depth of the mysid layer were collected at each station. During the fall, samples were collected between 30 m and surface, 60 m to 30 m, and 80 m to 60 m. The August 1995 zooplankton samples were analyzed using CAPAS (Hambright and Fridman 1994), resulting in a size distribution, abundance, and mean weight for each species. The 1996 samples were subsampled and enumerated under a dissecting microscope. All subsamples contained a minimum of 300 individuals. The results of all zooplankton sample analyses were grouped into four taxonomic groups: cladocerans, copepods, nauplii, and *Limnocalanus macrurus*. *Limnocalanus macrurus* was separated from the other copepods because of its large size and the lower clearance rate exhibited by mysids for this species (Bowers and Vanderploeg 1982; Nero and Sprules 1986). All analyses of zooplankton were conducted with these four groups.

We estimated mean zooplankton biomass based on mean body weights and mean densities of each of the four groups separately. Mean body weights were determined from the zooplankton size distribution in the net samples (August 1995) or from size distributions from samples obtained a year earlier during the same months and at similar stations (1996 samples). Mean biomass for the four groups was estimated by applying the average weight to the average densities of the 1995 and 1996 zooplankton samples. All body weights were converted from dry weight to wet weight assuming a dry–wet weight ratio of 0.1 (Johannsson 2003).

Fish zooplanktivory

Fish were sampled and preserved for diet composition analysis during all cruises, except at the 130 m station in August 1995 (31 July 31 – 1 August). For this cruise, we used results of the deeper trawls from the second August cruise. The water temperature at the depth at which fish were located was determined by comparing vertical temperature profiles and fish distributions. The depths occupied by each species were obtained from the results of the trawl sampling. As described above, the trawl samples are biased against YOY fish. To minimize this bias, we used average yearling weights for fish bioenergetics calculations rather than the actual trawl data. Alewife yearling weights were based on fish surveys conducted in April of each year (R. O'Gorman, US Geological Survey, Lake Ontario Biological Station, 17 Lake Street, Oswego, NY 13126, USA, unpublished data). Because rainbow smelt yearling data were not available, we used published yearling weights of 1.72 g on 1 May (Lantry and Stewart 1993). Average weight of these fish in August and October was estimated from observed growth rates. We then applied the temperatures occupied by each species to species-specific bioenergetic models

Table 1. Parameter values applied to bioenergetics model computation.

Parameter	Alewife	Rainbow smelt	Mysid
Egestion (F)	0.16C	0.16C	0.15C
Excretion (E)	$0.1(C-F)$	$0.1(C-F)$	$0.18(C-F)$
SDA	$0.175(C-F)$	$0.175(C-F)$	$0.18(C-F)$
Growth rate (% biomass·day^{-1})	0.015 (May) 0.23 (July–Nov.)	0.0 (May) 0.51 (June–Oct.)	0.44–1.17 (immature)[a] 0.14–0.32 (adult) 0.06–0.4 (winter)
Respiration (cal·g^{-1}·day^{-1})	$24(0.9146\,W^{-0.215}e^{0.0548T})$	$24(0.3646\,W^{-0.216}e^{0.036T})$	$24(0.2457\,W^{-0.161}e^{0.0752T})$

Note: Consumption (C) was calculated based on the equation $C = G + R + E + F + \mathrm{SDA}$, where G is growth, E is excretion, F is egestion, and SDA is specific dynamic action or the metabolic cost of digestion and assimilation. Respiration (R) equations assume a routine activity and metabolism adequately representative of average daily activity, and therefore no additional correction for swimming speed is made. W represents body weight and T represents water temperature.

[a] The minimum and maximum growth rates for all sizes of mysids are given based on growth rates of 0.035 and 0.029 mm·day^{-1} for juveniles and adults, respectively, for all months except winter months when growth rate was assumed to be 0.012 mm·day^{-1} for all size groups.

(alewife, Stewart and Binkowski 1986; rainbow smelt, Lantry and Stewart 1993; Table 1). Consumption (C) was calculated based on the equation $C = G + R + E + F + \mathrm{SDA}$, where G is growth, E is excretion, F is egestion, and SDA is specific dynamic action or the metabolic cost of digestion and assimilation. The respiration (R) equation for rainbow smelt assumes a routine metabolism representative of average daily activity, and therefore no additional correction for swimming speed is made. The respiration equation of Stewart and Binkowski (1986) includes a swimming speed component that is a function of fish weight. We modified this equation to include the activity cost in the temperature function. Our modified equation gives values for respiration within 5% of the original equation for age-1 alewife. Calculated consumption rates with our equations are expressed in calories per gram fish per day and converted to grams zooplankton per gram fish per day by dividing by the energy density of zooplankton (475 cal·g WW^{-1}; Lantry and Stewart 1993). Reported growth rates for alewife range between 0.00% and 0.03% of their body weight per day during the period beginning in May and ending 1 July and between 0.16% and 0.3%·day^{-1} for the period 1 July to 1 November (Rand et al. 1995). We used the median values for each period: 0.015% for May and 0.23%·day^{-1} for August and October. Rainbow smelt growth rates were determined from the change in the size distribution between the May and October 1996 cruises. The change in weight distribution was divided by the number of days, resulting in a mean growth rate of 0.51%·day^{-1}. Consumption rates were calculated in units of volume and time (g·m^{-3}·day^{-1}). The consumption due to predation on zooplankton (see below) was summed to provide areal-based estimates (g·m^{-2}·day^{-1}). Consumption rates were calculated separately for alewife and rainbow smelt, based on their distribution and diet composition, and later combined to provide overall fish consumption rates on zooplankton.

Mysid zooplanktivory

Mysid zooplanktivory was estimated using a bioenergetics model (Rudstam 1989). The model was based on *M. relicta* energetics and has been applied to mysid populations in the Baltic Sea (Rudstam et al. 1992) and Lakes Ontario and Michigan (Johannsson et al. 1994). We assumed growth rates of 0.035 and 0.029 mm·day^{-1} for juveniles and adults, respectively, and the winter growth rate was assumed to be 0.012 mm·day^{-1} for both immature and adult mysids (Johannsson 1992; Johannsson et al. 1994). Growth rates were converted to growth as a percent of body length for lengths ranging between 3 and 20 mm (Table 1). Respiration, which is temperature-dependent, was calculated in grams O_2 per gram per day and converted to calories per gram per day assuming an oxycaloric coefficient of 3240 cal·g^{-1} (Elliot and Davidson 1975) and then to gram zooplankton per gram mysid per day assuming a zooplankton caloric content of 475 cal·g^{-1} (Lantry and Stewart 1993). Bioenergetic estimates of an organism's consumption rate will vary depending on the temperature of the environment. By combining the vertical temperature profile, the vertical mysid density distribution, and size distribution, as determined from the net samples, we estimated the average daily mysid consumption rate in units of gram wet weight food per gram wet weight mysid per day. As 50% of the assimilated mysid diet in the spring is comprised of diatoms (Johannsson et al. 2001), we assumed that only 50% of the mysid growth during that period was linked to zooplanktivory. The diet of mysids caught in the summer and fall of 1995 were dominated by zooplankton (Johannsson et al. 2001, 2003).

Indirect effects

In order to consider the effect that the presence of planktivorous fish may have on mysid consumption, we estimated potential mysid consumption rates of zooplankton for hypothetical situations in which mysids vertically migrated to the temperature at which consumption rates are maximized (Rudstam et al. 1999*a*). Gal et al. (2004) used the relationship between consumption rate and temperature as an indication of mysid temperature preference in a diel vertical migration (DVM) model. Previous reports (Beeton 1960; Gal et al. 2004) have suggested that the thermocline is the primary environmental condition limiting mysid upward migration, and this has been hypothesized to be an avoidance reaction to fish (Gal et al. 2004). We assumed that mysids, in the absence of fish, would ascend to their preferred light and thermal conditions as defined in Gal et al. (2004). We then applied the predicted mysid vertical distribution to two mysid clearance models (Bowers and Vanderploeg 1982; Nero and Sprules 1986). The two models were used to calculate potential mysid consumption rates with no fish in the water column. Prey-specific clearance rates for the four zooplankton prey groups (see above) were obtained from the

Fig. 1. Vertical profiles of fish (broken line with dots) and mysid (solid line) biomass and temperature (dotted line) at stations sampled in southeastern Lake Ontario. Four stations were sampled in May ((*a*) 30 m, (*b*) 60 m, (*c*) 90 m, (*d*) 120 m) and October ((*g*) 30 m, (*h*) 60 m, (*i*) 90 m, (*j*) 120 m) of 1996. Only two stations were sampled in August 1995 ((*e*) 90 m, (*f*) 120 m). Temperature (°C) is on the bottom axis, and biomass ($g \cdot m^{-3}$) is on the top axis. Temperature profiles were not conducted at the 90 m station in the spring and fall.

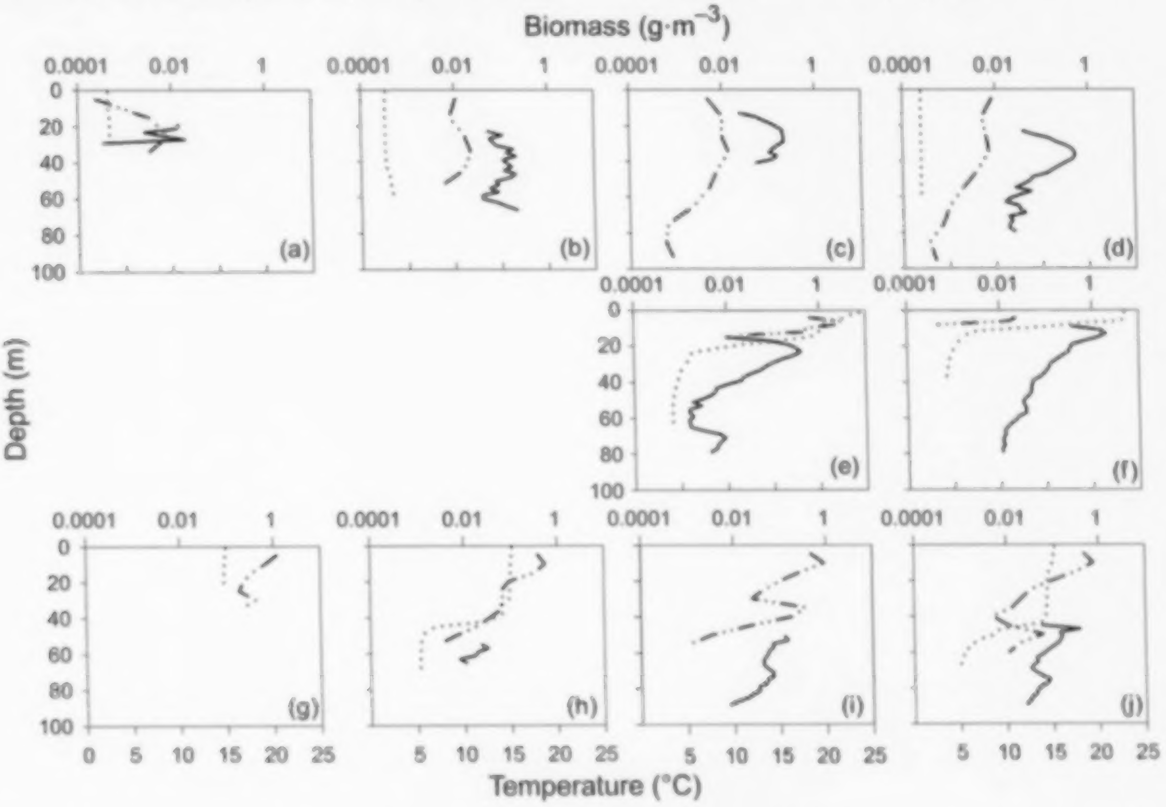

two models. Mysid consumption rates ($Cons_m$; $g\ WW \cdot m^{-2} \cdot day^{-1}$) were therefore determined as follows:

$$(1) \quad Cons_m = D_m\left(D_z\left(\sum P_i CR_i \overline{W}_i\right)\right) t \cdot z$$

where D_m and D_z are mysid and zooplankton density ($individuals \cdot m^{-3}$), respectively; i represents the zooplankton taxonomic group (copepods, cladocerans, *L. macrurus*, and nauplii); P_i is proportion of taxonomic group i of the total zooplankton density as determined from the net samples; CR_i is the taxon-specific mysid clearance rate ($m^3 \cdot h^{-1} \cdot mysid^{-1}$); and $\overline{W}_i$ is the average wet weight (g) for taxonomic group i. Average weights of zooplankton taxa were based on values calculated from the August 1995 cruises. The number of feeding hours per day, t, was assumed to be the period between sunset and sunrise minus 2 h to account for migration time (G. Gal, personal observation), and z is the water column depth (= station depth) in metres over which the consumption rates were calculated. Mysid potential consumption rates, therefore, consisted of the estimated consumption at the mysid's preferred feeding conditions. These were compared with consumption rates calculated using the actual observed mysid vertical distributions.

Statistical analysis

To test for differences in the areal density of mysids between nearshore and offshore stations, we used a Mann–Whitney test. Although it is possible to assume that the nearshore versus the offshore station samples were independent, it is hard to assume that a normal distribution of densities occurs at both sites. A need for a nonparametric equivalence to the t test was therefore required. Significant differences between net and acoustic estimates of mysid density were also tested. In addition to the small sample size, it was also not possible to assume a normal distribution in this case, therefore the nonparametric Mann–Whitney test was used.

Results

Vertical and horizontal distributions

Fish

There was no clear spatial gradient in the distribution of fish biomass, although in general, fish biomass was higher at the shallower stations in the fall and summer (Fig. 1). Mysid biomass was generally higher than fish biomass at the offshore stations by up to more than an order of magnitude in the spring and at the 90 m and 130 m stations in the sum-

Table 2. Mysid and planktivore abundance, biomass, and bioenergetic-based consumption values for the shallowest and deepest station of each season, respectively.

	Season	Alewife	Rainbow smelt	Mysids
Abundance (individuals·m^{-2})	Spring	8.0×10^{-3}–0.38	4.0×10^{-3}–0.02	3.9–334.5
	Summer	0.4–2.0×10^{-3}	2.6×10^{-3}–8.3×10^{-5}	392.3–574.5
	Fall	0.2–0.3	8.0×10^{-3}–0.04	0–81.1
Biomass (g·m^{-2})	Spring	0.03–0.15	7.0×10^{-3}–0.03	0.09–8.0
	Summer	2.40–0.01	7.7×10^{-3}–2.4×10^{-4}	3.7–16.85
	Fall	3.90–1.70	0.15–0.16	0.0–3.1
Daily zooplankton consumption rate (g·m^{-2}·day^{-1})	Spring	1.3×10^{-3}–6.4×10^{-3}	4.3×10^{-4}–2.0×10^{-4}	2.6×10^{-3}–0.2
	Summer	0.3–1.9×10^{-3}	2.1×10^{-5}–6.8×10^{-6}	0.4–1.3
	Fall	0.5–0.22	1.7×10^{-3}–2.5×10^{-3}	0^{a}–0.3

Note: Spring, May 1996; summer, August 1995; fall, October 1996. The summer stations are 90 m and 130 m.

[a] No mysids were found at this station.

Table 3. The relative contributions of alewife (*Alosa pseudoharengus*) and rainbow smelt (*Osmerus mordax*) in trawl samples for spring (May 1996), summer (August 1995), and fall (October 1996).

Season	Bottom depth (m)	Tow depth (m)	Depth (m) of metalimnion	Alewife (%)	Rainbow smelt (%)	No. of fish counted	No. of trawls
Spring	35–45	4–15	None	57	32	137	3
	60–80	35–45	None	64	36	140	1
	105–130	45–50	None	81	19	143	2
Summer	92–125	7–18	16–22	68	32	314	5
	155–189	7.5–17	7–13	79	21	339	5
Fall	30	7.5–15	None	100	0	116	1
	60	13–20	40–60	100	0	85	1
	60	33–40	40–60	62	38	76	1
	120	13–20	43–56	100	0	68	1
	120	33–40	43–56	64	36	69	1

mer. This trend was reversed at the 30 m and 60 m stations in the spring and fall (again, no summer data). During the summer and fall, fish were found above or in the thermocline always above the mysids (Fig. 1). Total fish biomass ranged between 2.4 and 0.01 g·m^{-2} in the summer (90 m and 130 m BD, respectively) and peaked in the fall at 3.9 g·m^{-2} at the shallowest station (Table 2). The mean offshore biomass (BD of 90 m and greater) was 1.2 and 2.1 g·m^{-2} in the summer and fall, respectively. The mean nearshore biomass at the 30 m and 60 m stations was 3.0 g·m^{-2} during the fall. Alewife biomass exceeded rainbow smelt biomass by greater than 20-fold, on average, across all stations during the summer and fall, with the exception of the deep summer station in which rainbow smelt biomass was extremely low and the difference between the specieses was even greater. During the spring, the fish were more evenly distributed in the water column and extended down to greater depths. The mean nearshore and offshore biomasses in the spring were 0.1 and 0.2 g·m^{-2}, respectively. The planktivores occupied a wider range of water temperatures than mysids and were found mainly in temperatures ranging between 15 and 22 °C in August and October (Fig. 1). Alewife was the dominant species in the epilimnetic trawls. Rainbow smelt abundance increased within and below the metalimnion or with depth in the fall when the epilimnetic temperature had dropped to 15 °C (Fig. 1; Table 3).

Mysids

The mysid vertical distribution varied both spatially and temporally. Mysid biomass increased with distance from shore (Fig. 1), and areal mysid densities (individuals·m^{-2}) were significantly lower at nearshore stations (30 m and 60 m) then at offshore stations (90, 120 m) in the spring (nearshore sample size, n = 5; offshore, n = 11), summer (between the 90 m and 130 m stations, n = 20 and 33, respectively), and fall (nearshore, n = 6; offshore, n = 7) (p = 0.008, $p \leq 0.001$, p = 0.003, respectively). The mysid biomasses at the shallowest stations (BD = 30 m) were typically one to two orders of magnitude lower than those observed at the deepest stations. Mysid biomasses at the 30 m stations ranged between 0.0 (fall) and 0.09 (spring) g·m^{-2}, whereas at the deepest stations, they ranged between 3.1 (fall) and 16.8 (summer) g·m^{-2} (Table 2). During both the summer and fall, the depth of the peak mysid distribution was associated with the bottom of the thermocline (Fig. 1). During the spring cruise, before stratification, the depth of the peak distribution varied among stations. During all cruises, most mysids did not reach the temperature of maximum food intake of 11 °C, only 2%–11% and 0.5%–5% of the mysid population were found at 11 °C or above in August and October, respectively.

Acoustic and net estimates of mysid density compared favorably. The mean (±SE) mysid areal density based on all nighttime net samples collected (n = 39) was 398.27 (172.89) and 41.59 (23.78) individuals·m^{-2} at the offshore and nearshore stations, respectively. The mean (±SE) mysid areal density based on the average of the acoustically estimated seasonal densities (n = 10) was 267.32 (97.46) and

Table 4. Nighttime crustacean zooplankton density and biomass for spring (May 1996), summer (August 1995), and fall (October 1996) cruises for each station sampled.

Season	Bottom depths (m)	Depth range (m)	Density (individuals·L^{-1})	Biomass (µg wet weight·L^{-1})
Spring	30	0–30	2.0	0.06
	55	0–25	1.0	0.03
	55	25–55	0.4	0.01
	150	0–40	2.9	0.35
	150	40–60	1.3	0.16
Summer	85	16–0	42.7	2.31
	120	0–100	9.4	0.41
	130	0–10	136.7	2.95
	130	10–30	4.0	0.09
	130	30–70	0.2	0.04
Fall	30	0–30	51.6	1.01
	60	0–50	10.1	0.20
	60	50–60	12.4	0.24
	120	0–30	34.0	0.85
	120	30–60	0.6	0.02
	120	60–80	0.4	0.01

Table 5. Fish diet data: percent contribution of crustacean zooplankton to total weight of fish guts.

				Alewife		Rainbow smelt	
Date	No. of trawls	Bottom depth (m)	Tow depth (m)	*N*	Percent of diet (SE)	*N*	Percent of diet (SE)
Aug. 1995	3	90–130	7–18	40	91.5 (5.0)	39	7.7 (4.3)
	3	165–180	7.5–17	40	70.0 (17.4)	40	0 (0)
May 1996	2	30–38	4–15	0	93.3 (6.7)	11	14.3 (11.3)
	2	60–80	35–45	20	100 (0)	32	3.33 (3.2)
	2	105–150	40–50	14	100 (0)	22	15.8 (8.0)
Oct. 1996	1	30	15	6	100 (0)	3	33.3 (33.3)
	2	60	20–40	12	100 (0)	14	0.01 (10.5)
	2	125	20–40	15	97.0 (3.0)	11	10.0 (12.3)

Note: *N*, number of guts examined.

82.95 (94.42) individuals·m^{-2} at the offshore and nearshore stations, respectively. There was no significant difference between the two methods of sampling ($p > 0.7$).

Zooplankton

Zooplankton distribution at night was highly dependent on the thermal structure of the water column (Table 4). Prior to stratification, zooplankton were well mixed in the water column with densities only two times higher when closer to the surface than at depth. Spring densities ranged between 0.4 and 2.9 individuals·L^{-1}. During the stratified periods, the zooplankton distribution was characterized by high densities in the epilimnion and sharply reduced densities below this layer. Zooplankton density in the epilimnion was often one to two orders of magnitude greater than in the hypolimnion when comparing across all sites. Epilimnion densities ranged between 34.0 and 136.7 individuals·L^{-1} during the summer and fall cruises, respectively, whereas hypolimnion densities ranged between 0.2 and 0.4 individuals·L^{-1} during the summer and fall cruises, respectively.

Estimated zooplankton biomass was lowest during the spring and highest during the summer (Table 4). The mean spring areal biomass (within the top 60 m) was 17.2 g·m^{-2} at the deepest station and decreased towards shore. No consistent pattern in total water column biomass along the gradient from the nearshore to the offshore was evident across seasons. In the summer, most biomass occurred in the epilimnion and was similar at the 90 m site to that found at the 130 m site (32.8–40.6 g·m^{-2}). No shallower stations were sampled during the summer. In the fall, biomass was lowest at intermediate depths and ranged from 30.3 g·m^{-2} at the shallow station to 12.4 and 26.2 g·m^{-2} at the 60 m and 120 m stations, respectively.

Fish zooplanktivory

There were clear differences in alewife and rainbow smelt diets. Zooplankton was the major contributor to alewife diets (Table 5). Zooplankton contribution reached 100% of alewife diet and was typically >90%. In contrast, zooplankton contribution to rainbow smelt diets was not higher than 33% and was in most cases <15%. Most of the remaining portion in the rainbow smelt guts was composed of mysids.

There was no clear spatial trend in fish zooplanktivory estimates (Fig. 2). Fish consumption was estimated to be highest in the fall, with a peak at the 30 m station. In May and August, the consumption was highest at a bottom depth of

Table 6. The estimated percent of zooplankton biomass consumed daily by mysids and planktivores based on the bioenergetic models as calculated from the ratio of consumption rate to zooplankton biomass for spring (May 1996), summer (August 1995), and fall (October 1996).

	Spring			Summer		Fall		
	>120[a]	~60	~30	>120	~90	>120	~60	~30
Mysids	1.19	10.20	0.13	3.95	0.77	0.97	0.07	0[b]
Fish	0.04	0.58	0.07	0.006	0.63	0.82	2.02	1.66
Total	1.23	10.78	0.20	3.96	1.40	1.80	2.09	1.66
Mysid:total	0.96	0.95	0.65	1.0	0.55	0.54	0.03	0[b]

[a] Station bottom depth (m).

[b] No mysids were found at this station.

Fig. 2. A comparison between the bioenergetics based estimates of zooplankton consumption by planktivorous fish (alewife, *Alosa pseudoharengus*, and rainbow smelt, *Osmerus mordax*; open bars) and mysids (solid bars). The consumption rates represent the estimated mean values for all stations: four stations in (*a*) May and (*c*) October and (*b*) two stations in August.

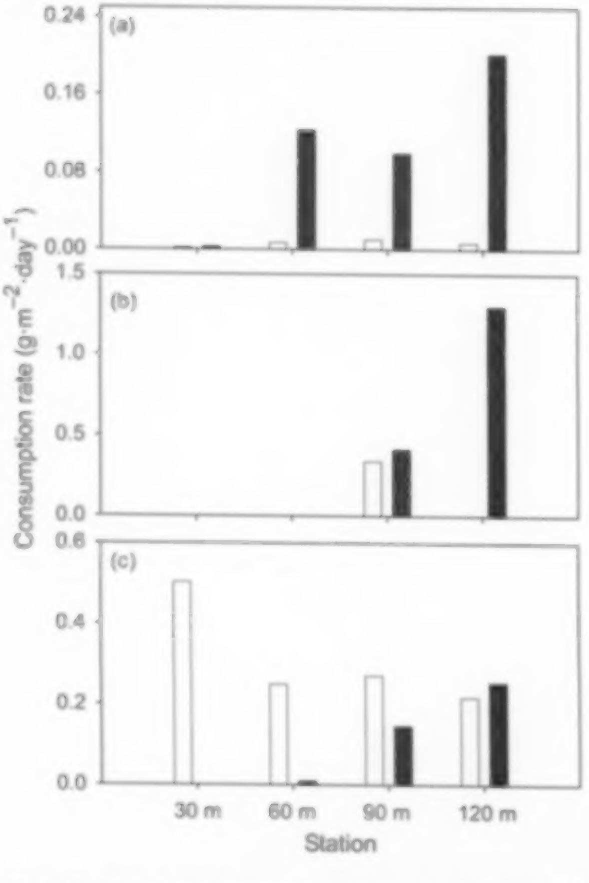

90 m. Estimated zooplankton consumption by fish, over all stations, ranged between 1.4 × 10^{-3} and 0.01 g·m^{-2}·day^{-1} in the spring, 1.9 × 10^{-3} and 0.34 g·m^{-2}·day^{-1} in the summer, and 0.22 and 0.50 g·m^{-2}·day^{-1} in the fall (Table 2). The spatial variability within seasons was driven by the spatial patterns in fish abundance. Zooplanktivory by rainbow smelt was much lower than zooplanktivory by alewife because of lower biomass, lower occupied temperatures, and lower proportion of zooplankton in their diet. As a consequence, across seasons and stations, rainbow smelt zooplanktivory never exceeded 3% of the total estimated fish zooplanktivory. On average, across stations and seasons, fish consumed daily 0.7% of the total available zooplankton biomass, though a maximum value of 2% was achieved at the 60 m station in the fall (Table 6).

Mysid zooplanktivory

The estimated consumption of zooplankton by mysids varied primarily with changes in mysid density across bottom depths and seasons (Fig. 2; Table 2). Consumption at the deepest stations ranged from 0.2 in spring to 1.3 in summer and 0.3 g WW·m^{-2}·day^{-1} in fall and from 0.1 in spring to 0.009 g WW·m^{-2}·day^{-1} in fall at a bottom depth of 60 m. On average, across stations and seasons, daily mysid consumption was 2.5% (Table 6) of the available zooplankton biomass.

Indirect effects

The DVM (diurnal vertical migration) model predicted the mysid distribution to be higher in the water column for all stations in both the summer and fall, with the exception of the summer 90 m station. In the latter case, mysids were predicted to reside at about the same depth. The expected shallowing of the mysid layer in the other cases exposed the mysids to high densities of prey, leading to higher consumption rates based on the clearance rates models. The increased consumption rate ranged between 1.9- and 90-fold greater (average 37) than the estimated consumption rates, given the observed mysid and zooplankton vertical distribution (Fig. 3). The average mysid consumption rates, based on the actual observed distribution and the Nero and Sprules (1986) clearance rates model, ranged between 0.24 and 2.7 g·m^{-2}·day^{-1} in the summer and 0 and 0.02 g·m^{-2}·day^{-1} in the fall. As a consequence of their predicted shallower distribution, potential consumption rates increased in the summer, ranging from 1.04 to15.7 g·m^{-2}·day^{-1}, and in the fall, reaching a value of 1.5 g·m^{-2}·day^{-1} at the deepest station. It should be noted that there were also differences when comparing the estimated consumption rates based on the two clearance rate models. Estimates based on Nero and Sprules (1986) were on average 74% (SD = 2%) of the values estimated by the Bowers and Vanderploeg's (1982) model. With either model, the potential mysid zooplanktivory rates increased ~30-fold compared with calculated zooplanktivory rates (based on ob-

Fig. 3. A comparison between estimated actual (solid bars) and potential (open bars) consumption rates for mysids across stations and seasons. Both actual and potential rates are the estimated average consumption values based on two clearance rate models (Bowers and Vanderploeg 1982; Nero and Sprules 1986). The consumption rates represent the estimated mean values for all stations; four stations in (*a*) May and (*c*) October and (*b*) two stations in August. No consumption rates were calculated for the 30 m station in October as no mysids were found at that station in October.

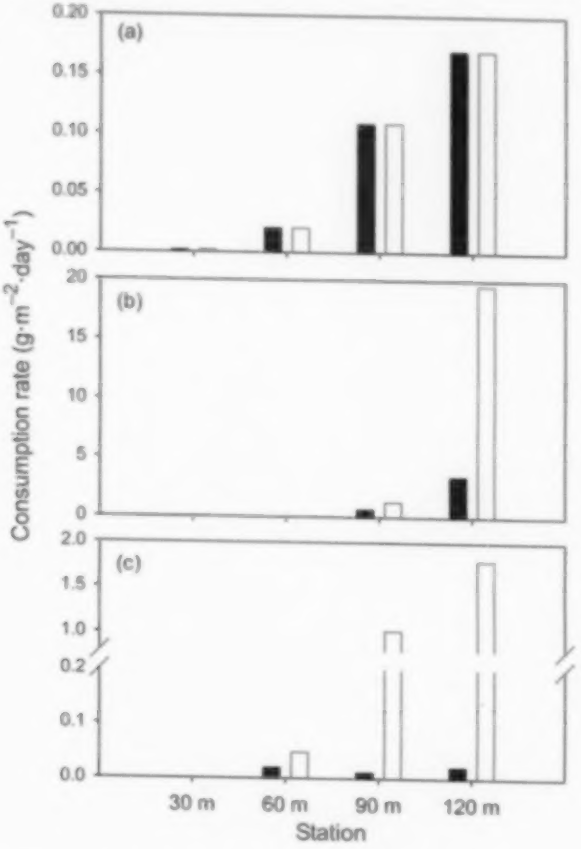

served distributions) mainly because of the large differences at the deep stations in the fall (Fig. 3).

Discussion

The trophic interactions between zooplankton and their predators play an important role in determining the flow of energy in the Lake Ontario food web. Quantifying those interactions is key to understanding changes in the food web dynamics, which in turn is critical to efficient management of the lake's ecosystems. An important example of such interactions is the intraguild interactions between alewife, rainbow smelt, and mysids and their impact, via consumption, on the zooplankton population. Previous studies have typically considered mysid consumption of zooplankton separate and secondary to planktivorous fish consumption of zooplankton (Rand et al. 1995). Accordingly, studies have grouped mysids with zooplankton when discussing trophic interactions of the Lake Ontario food web (Borgmann and Whittle 1994; Sprules and Goyke 1994). In contrast, our results indicate that mysid predation on zooplankton is comparable with and exceeds that exerted by alewife and rainbow smelt during the spring and summer. Mysid consumption at the deep stations (BD ≥ 90 m) was estimated to range between 0.1 and 0.2 g·m^{-2}·day^{-1} in May and 0.4 and 1.3 g·m^{-2}·day^{-1} in August. Mysid zooplanktivory exceeded fish zooplanktivory at all stations in the spring and summer, with fish consumption of zooplankton comparable only at the 90 m station in August. In contrast, fish zooplanktivory was higher than mysid zooplanktivory at the three shallowest stations in the fall but lower than mysid consumption at the deepest station. The increase in fish planktivory in the fall was associated with increased fish abundance during this period. As a consequence, fish planktivory exceeded mysid planktivory by up to more than an order of magnitude at bottom depths of 60 m or shallower. Clearly, there is a strong spatial component to the importance of mysid and fish planktivory in Lake Ontario.

Uncertainty in bioenergetics calculations

These comparisons between fish and mysid planktivory are based on bioenergetics models and their input variables, including animal size, growth rates, acoustic estimates of abundance and distribution, water temperatures, and diet. There is uncertainty in the model parameters, as well as in the input variables, that may affect our conclusions. Of these input variables, the observed temperatures and diets are expected to have the lowest uncertainty, though there is some evidence to suggest that alewives are moving down to the metalimnion to feed during the day (G. Gal and L.G. Rudstam, unpublished data), which would result in lower water temperatures experienced by the alewife and, consequently, lower consumption rates. The three bioenergetics models have similar structure, and sensitivity analyses of those parameters with highest uncertainty have been conducted on these models in the past (Lantry and Stewart 1993; Rand et al. 1995; Chipps and Bennett 2002). The models are sensitive to energy density of the prey, respiration rates, and growth rates. Energy density of zooplankton will not affect the comparison between fish and mysid planktivory as we used the same value for both predators. However, this parameter will affect the comparison of daily planktivory rates and zooplankton standing stock. As rainbow smelt contributed less than 3% of the total fish planktivory because of their lower biomass and the large portion of mysids in their diets, the sensitivity of the rainbow smelt bioenergetics model is of less importance in the current study and is not considered further.

Growth rates for age-1 fish used in the calculations were obtained from the change in weight between age-1 and age-2 alewife caught in April of 1995, 1996, and 1997 obtained from R. O'Gorman (US Geological Survey, Lake Ontario Biological Station, 17 Lake Street, Oswego, NY 13126, USA, 2001) and the assumption of equal growth rates from June through October. This resulted in an instantaneous growth rate of 1.27 (average of 1.2 for age 1 in 1995 and 1.36 for age 1 in 1996). We assumed little growth in May. This is close to the upper values of the range of instantaneous growth rates (0.98–1.4) reported by O'Gorman et al. (1997). We, therefore, assume that the alewife growth rates used in the present study are fair estimates of the growth rate in the lake during the period of our study. Decreasing growth rates to the lower values of this range (0.98) would decrease zooplankton consumption by alewife by approximately 22%. If growth rates in the lake were closer to the highest values reported by O'Gorman et al. (1997), consumption rates by alewife would increase by 10%. In either case, our conclusions about the importance of fish and mysid planktivory would not change. Growth rates of mysids were taken from Johannsson et al. (1994) using data from the 1980s and may have changed. However, there was not a large change in mysid size structure indicative of changes in growth rates through the 1990s (Johannsson et al. 2003).

The techniques used to acoustically estimate abundance were consistent across cruises for mysid and for fish with the exception of fish in the August cruises. Seasonal and spatial patterns within species are therefore dependable. Differences between net and acoustics mysid estimates were not large (see also Gal et al. 1999*b*). The estimates of fish biomass most likely include a larger component of uncertainty because of large variations in fish TS and a bias in the trawl estimates of fish size distribution and density as described above. The method used for the August fish data (Hedgepeth et al. 1999) is not as widely applied, but even large errors associated with the estimated fish biomass in August would not have changed the overall conclusions of this paper. Also, similar fish density estimates have been obtained with single-beam methods similar to the one we used and split-beam methods for rainbow smelt in Lake Erie (Rudstam et al. 1999*b*).

The assumption of an average alewife biomass and consumption rates based on weight of age-1 alewife is likely the largest source of uncertainty in our analysis. If we instead assumed that the fish caught in the trawl were representative of fish present in the lake, the consumption rates would increase three-fold. However, the 1995 year class was relatively strong (Owens et al. 2003) and should have been the most abundant alewife age group present in the summer of 1995 and throughout 1996. Assuming all alewife detected acoustically to be the adults caught in the trawls would therefore most likely lead to a large overestimation of alewife biomass. Recall that the acoustic density estimates include YOY alewife in August (fish larger than 20 mm; Warner et al. 2002). We acknowledge that this is a potentially large uncertainty but believe our assumptions to be reasonable.

The bioenergetic models are also sensitive to uncertainty in the parameters governing respiration (Bartell et al. 1986; Chipps and Bennett 2002). Recently, modifications to the mysid bioenergetics model have been suggested based on refined laboratory experiments (Gorokhova 1998; Chipps and Bennett 2002). In this paper, we used the original model. Incorporating the modifications suggested by Chipps and Bennett (2002) to respiration rates would have resulted in a reduction of up to 20% in the daily mysid consumption of zooplankton. For alewife, Klumb et al. (2003) showed that the different component of the alewife respiration model needs to be modified for YOY alewife and therefore may also be biased for age-1 fish. However, the combined respiration costs calculated from the Stewart and Binkowski model were in good agreement with their experimental results (Klumb et al. 2003).

Other input variables to the bioenergetics model include water temperatures, abundance, and weight. We have discussed these variables for alewife above. Our mysid bioenergetics estimates of consumption varied both spatially and seasonally. Temperature occupied by mysids was lowest during the spring but similar during the summer and fall and in all cases comparable across stations. Although mean body weights varied little between stations and seasons, exceptions were observed, including smaller animals by up to a factor of 5 (based on biomass) at the 90 m summer and 30 m fall stations and larger mysids (by a factor of 2) at the deep station in the fall. Consequently, most of the spatial variability in bioenergetic-based estimates of mysid consumption reflects variability in mysid abundance. Bioenergetic consumption estimates also mirrored the consistent inshore–offshore gradient in mysid abundance of increasing densities as distance from the shore increased. Seasonal variation was therefore the result of the combination of seasonal changes in water temperature (e.g., the spring) and mysid distribution as illustrated by the high summer consumption rates and much lower values in the fall.

As mentioned previously, mysids are known to complement their diet by grazing phytoplankton and exploiting benthic sources (Bowers and Grossnickle 1978; Johannsson et al. 2001). Algal grazing can represent approximately 50% of the mysid diet in the spring and a negligible amount in the fall; the contribution of amphipods to the fall diet is also negligible (Johannsson et al. 2001). We compensated for the algal contribution by assuming only 50% of spring consumption was zooplankton. Alewife and rainbow smelt are also known to utilize additional prey resources (Mills et al. 1992; Lantry and Stewart 1993) and we accounted for this in our consumption estimates by considering the proportion of zooplankton in the fish guts.

Uncertainty in clearance rate calculations

The estimated clearance rates are dependent on the prey density and composition available to the mysids. The clearance rates published by Nero and Sprules (1986) and by Bowers and Vanderploeg (1982) differ mainly in relation to the mysid clearance rates on cladocerans and nauplii. Accordingly, the major differences in the estimated consumption rates between the two models occurred during the summer owing to the relatively large portion of cladocerans and nauplii in the zooplankton samples. Prey density differed greatly both between seasons and over the water column. Stratification of the water column led to stratification of the zooplankton population, thereby reducing the abundance of prey available to mysids during the stratified seasons, resulting in lower consumption rates. Observed zooplankton density was generally lower in the spring and fall, resulting in reduced consumption rates during these seasons in comparison with during the summer. The reversed onshore–offshore gradient in mysid consumption predicted for the fall arose from the prey distribution. In contrast to the deeper stations, zooplankton at the 60 m station were present in the water column down to ~50 m at a constant, albeit low, density. This condition resulted in higher overlap between mysids and zooplankton, thereby increasing the estimated consumption rates at the 60 m station based on clearance rate models.

Clearance rates vs bioenergetics estimates

The estimated mysid consumption rates varied both between and within the two methods employed (bioenergetics and clearance rates models). Bioenergetic estimates generally resulted in higher consumption rates than the clearance rate based estimates. The discrepancies are a result of the differences between the underlying assumptions and information input to the two methods. For example, bioenergetics growth rates include all dietary sources and integrate feeding conducted over long periods of time, whereas clearance rate estimates are based on the observed prey density only in the mysid regions, thus overlooking any possible foraging forays into the richer prey areas of the metalimnion. Furthermore, although daytime feeding by mysids can play an important role in their daily caloric intake (Johannsson et al. 2001), only nighttime feeding is used for the clearance rate values, so they represent underestimates. The largest differences, however, most likely relate to the time scale of comparisons. Bioenergetic estimates are based on growth rates integrated over extended periods of times (weeks to months), thereby reducing the potential variability on daily time scales. The clearance rate values were estimated based on data collected on specific dates, increasing the importance of sampling error. These estimates are based on factors such as mysid and zooplankton density and distribution, taxonomic breakdown of the zooplankton population, and species-specific clearance rates. All of these factors have errors of varying magnitude associated with them. The mysid and zooplankton distributions can be highly patchy, and although errors associated with mysid patchiness are limited by the use of acoustics, this is not the case for our zooplankton estimates, which were based on a limited number of net samples. The patchiness can further affect the species composition in the samples.

Comparison between planktivory and zooplankton biomass

Planktivorous fish removed between 0.005% and 2.0%·day^{-1} of the total zooplankton biomass, but with the exception of the shallowest stations in the fall, mysids removed a greater portion of the zooplankton than did the fish. We did not estimate zooplankton production in our study and therefore can not compare prey production with predator consumption. Rand et al. (1995) estimated mean monthly (August–October) consumption of zooplankton in Lake Ontario by alewife at 2 g·m^{-2}·day^{-1} (calculated from their monthly values), noticeably higher than the upper range of estimates in this study. Their estimated consumption values were also greater than their estimated zooplankton production rates. Other independent estimates of zooplankton production in the lake (Borgmann et al. 1984; Kuns and Sprules 2000) would suggest that our consumption values might be in balance with prey production rates.

The percent consumption rates of zooplankton by fish and mysids are comparable to zooplankton production to biomass (*P*/*B*) ratios. Daily *P*/*B* ratios at 4 °C are 2.1%·day^{-1} and 0.8%·day^{-1} for cyclopoids and calanoids, respectively, whereas epilimnetic values for cladocerans assuming 15 °C is 10%·day^{-1} (Shuter and Ing 1997). Although the results presented here are limited in their spatial extent, they do suggest that zooplankton production in the hypolimnion and metalimnion are less than mysid demand but on par with fish demand.

Our results indicate that indirect effects of fish on zooplankton are significant. Converting the indirect effects into mysid consumption of zooplankton could lead to an increase of up to a factor of 3.8 in the summer and a 90-fold increase in consumption rates in the fall because of mysid migration into regions they currently avoid. As a consequence, consumption rates by mysids during the summer would be much higher then the current estimated consumption rates at the deeper station in both the summer and fall. The upward migration of mysids to shallower, warmer waters would expose them to higher prey concentrations, enhancing growth rates and consumption rates, resulting in shorter generation times not accounted for in the current study. Under such a scenario, the ecosystem would maintain its stability and not be food-limiting only if the additional mysid consumption did not exceed the current fish consumption. Additional indirect pathways exist that we did not include, for example, the effect of planktivorous fish preying on mysids, thereby reducing predation by mysids on zooplankton. As we considered only one possible indirect pathway, the contribution of the indirect effects is most likely larger than we have concluded in this study.

Implications

The recent changes in the planktivore community and decline of the alewife population (Schaner and Lantry 1998; Mills et al. 2003; O'Gorman et al. 2004) may lead to changes in intraguild interactions in Lake Ontario. As indicated in our results and in previous studies (Rand et al. 1995), alewife is an important planktivore in the lake. Reduction in the alewife population may lead to a reduction in competition for zooplankton resources and thereby increase zooplankton availability to mysids. Assuming that mysid DVM is a response to predation pressure as shown for other zooplankton species (Gliwicz 1986), a marked decrease in both alewife and rainbow smelt predation pressure should result in mysids moving higher in the water column, thus increasing their predatory effect on zooplankton. Although the results presented here are limited in their spatial extent, they do suggest that zooplankton production in the hypolimnion and metalimnion are less than mysid demand but on par with fish demand. This leads to a number of possible propositions: (*i*) predation is important in the decrease in copepod biomass over the winter; (*ii*) it supports the results of Johannsson et al. (2001) that other dietary sources are important to mysid survival; and (*iii*) it suggests that mysids may be making forays into the warmer and zooplankton-richer epilimnetic waters. If the last proposition were true, it would impact the clearance rate based consumption estimated in this study. Shallower excursions by mysids under favorable conditions are known to occur (Chipps 1997), thus a change in their behavior is possible. The change in their vertical position, even in the absence of fish, will be limited, however, as mysid survival and feeding rates are greatly reduced at temperatures of 18 °C or higher (Rudstam et al.

1999*a*). Even so, understanding the food web interactions in Lake Ontario and similar ecosystems with migrating invertebrate predators requires consideration of both invertebrate and vertebrate planktivory and the possible indirect interactions mediated by effects on spatial distributions of the predators and prey. The ongoing changes to the Lake Ontario planktivore population and the likely consequences to predation on zooplankton in the lake may lead to significant changes in the Lake Ontario food web in coming years. In a study similar to ours, Rudstam, Hansson, and colleagues studied a trophic triangle of a coastal ecosystem in the Baltic Sea that included a mysid (*Mysis mixta*) (Hansson et al. 1990; Rudstam et al. 1992). There too, the mysid proved to be a key planktivore in the trophic dynamics and on par with the planktivorous fish. In the current study, we extend their approach by examining the potential indirect effects of fish on the zooplankton and demonstrate that indirect affects can potentially exceed the estimated direct affects.

Acknowledgments

We thank two anonymous reviewers for their constructive comments. We also thank T. Owens for critical and valuable comments on earlier drafts of this manuscript, A. Mohammadian for technical assistance, and the captains and crews of the R/V *Seth Green* and R/V *Lauzier* for their assistance. Ship time was provided by NY State Department of Environmental Conservation and by Canada Centre for Inland Waters. This paper is a result of research funded by the National Oceanic and Atmospheric Administration (NOAA) award No. NA86RG0056 to the Research Foundation of State University of New York for New York Sea Grant. The US Government is authorized to produce and distribute reprints for governmental purposes notwithstanding any copyright notation that may appear hereon. The views expressed herein are those of the authors and do not necessarily reflect the views of NOAA or any of its subagencies. This is contribution No. 240 of the Cornell Biological Field Station.

References

Abrams, P.A., Menge, B.A., Mittelbach, G.G., Spiller, D., and Yodiz, P. 1996. The role of indirect effects in food webs. *In* Food webs: intergration of patterns and dynamics. *Edited by* G.A. Polis and K.O. Winemiller. Chapman and Hall, London. pp. 371–395.

Bartell, S.M., Breck, J.E., Gardner, R.H., and Brenkert, A.L. 1986. Individual parameter perturbation and error analysis of fish bioenergetics models. Can. J. Fish. Aquat. Sci. **43**: 160–168.

Beeton, A.M. 1960. The vertical migration of *Mysis relicta* in Lakes Huron and Michigan. J. Fish. Res. Board Can. **14**: 517–539.

Beeton, A.M., and Bowers, J.A. 1982. Vertical migration of *Mysis relicta* Loven. Hydrobiologia, **93**: 53–61.

Borgmann, U., Shear, H., and Moore, J. 1984. Zooplankton and potential fish production in Lake Ontario. Can. J. Fish. Aquat. Sci. **41**: 1303–1309.

Borgmann, U., and Whittle, D.M. 1994. Particle-size-conversion efficiency, invertebrate production, and potential fish production in Lake Ontario. Can. J. Fish. Aquat. Sci. **51**: 693–700.

Bowers, J.A., and Grossnickle, N.E. 1978. The herbivorous habits of *Mysis relicta* in Lake Michigan. Limnol. Oceanogr. **23**: 767–776.

Bowers, J.A., and Vanderploeg, H.A. 1982. In situ predatory behavior of *Mysis relicta* in Lake Michigan. Hydrobiologia, **93**: 121–131.

Cabana, G., and Rasmussen, J.B. 1994. Modelling food chain structure and contaminant bioaccumulation using stable nitrogen isotopes. Nature (London), **372**: 255–257.

Chipps, S.R. 1997. *Mysis relicta* in Lake Pend Oreille: seasonal energy requirements and implications for trophic interactions in Lake Pend Oreille, Idaho. Ph.D. thesis, Department of Fish and Wildlife Resources, University of Idaho, Moscow, Id.

Chipps, S.R., and Bennett, D.H. 2002. Evaluation of a *Mysis* bioenergetics model. J. Plankton Res. **24**: 77–82.

Dodson, S.I. 1974. Zooplankton competition and predation: an experimental test of the size efficiency hypothesis. Ecology, **55**: 605–613.

Elliot, J.M., and Davidson, W. 1975. Energy equivalents of oxygen consumption in animal energetics. Oecologia, **19**: 195–201.

Gal, G., Loew, E.R., Rudstam, L.G., and Mohammadian, A.M. 1999*a*. Light and diel vertical migration: spectral sensitivity and light avoidance by *Mysis relicta*. Can. J. Fish. Aquat. Sci. **56**: 311–322.

Gal, G., Rudstam, L.G., and Greene, C.H. 1999*b*. Acoustic characterization of *Mysis relicta*. Limnol. Oceanogr. **44**: 371–381.

Gal, G., Rudstam, L.G., and Johannsson, O.E. 2004. Predicting *Mysis relicta* vertical distribution in Lake Ontario. Arch. Hydrobiol. **159**: 1–23.

Gismervik, I., and Andersen, T. 1997. Prey switching by *Acartia clusi*: experimental evidence and implications of intraguild predation assessed by a model. Mar. Ecol. Prog. Ser. **157**: 247–259.

Gliwicz, M.Z. 1986. Predation and the evolution of vertical migration in zooplankton. Nature (London), **320**: 746–748.

Gorokhova, E. 1998. Exploring and modelling the growth dynamics of *Mysis mixta*. Ecol. Model. **110**: 45–54.

Grossnickle, N.E. 1982. Feeding habits of *Mysis relicta* — an overview. Hydrobiologia, **93**: 101–107.

Hambright, K.D., and Fridman, S. 1994. A computer-assisted plankton analysis system for the Macintosh. Fisheries (Bethesda), **19**: 6–8.

Hansson, S., Larsson, U., and Johansson, S. 1990. Selective predation by herring and mysids, and zooplankton community structure in a Baltic Sea coastal area. J. Plankton Res. **12**:1099–1116.

Hart, R.D. 2002. Intraguild predation, invertebrate predators, and trophic cascades in lake food webs. J. Theor. Biol. **218**: 111–128.

Hedgepeth, J.B., Gallucci, V.F., O'Sullivan, F., and Thorne, R.E. 1999. An expectation maximization and smoothing approach for indirect acoustic estimation of fish size and density. ICES J. Mar. Sci. **56**: 36–50.

Johannsson, O.E. 1992. Life history and productivity of *Mysis relicta* in Lake Ontario. J. Gt. Lakes Res. **18**: 154–168.

Johannsson, O.E. 1995. Response of *Mysis relicta* population dynamics and productivity to spatial and seasonal gradients in Lake Ontario. Can. J. Fish. Aquat. Sci. **52**: 1509–1522.

Johannsson, O. E. 2003. Zooplankton community structure and function in Lake Ontario. *In* State of Lake Ontario ecosystem: past, present and future. *Edited by* M. Munawar. Backhuys Publishers, Leiden, the Netherlands. pp. 221–256.

Johannsson, O.E., Rudstam, L.G., and Lasenby, D.C. 1994. *Mysis relicta*: assessment of metalimnetic feeding and implications for competition with fish in Lakes Ontario and Michigan. Can. J. Fish. Aquat. Sci. **51**: 2591–2602.

Johannsson, O.E., Leggett, M.F., Rudstam, L.G., Servos, M.R., Mohammadian, M.A., Gal, G., Dermott, R.M., and Hesslein, R.H. 2001. Diet of *Mysis relicta* in Lake Ontario as revealed by stable isotope and gut content analysis. Can. J. Fish. Aquat. Sci. **58**: 1975–1986.

Johannsson, O.E., Rudstam, L.G., Gal, G., and Mills, E.L. 2003. *Mysis relicta* in Lake Ontario — life history and food web linkages. *In* The state of Lake Ontario ecosystem: past, present and future. *Edited by* M. Munawar. Backhuys Publishers, Leiden, the Netherlands. pp. 257–287.

Klumb, R.A. 2003. The role of embayments and nearshore habitats of Lake Ontario as nursery grounds for young-of-the-year alewives *Alosa pseudoharengus* and other species. Ph.D. thesis, Department of Natural Resources, Cornell University, Ithaca, N.Y.

Klumb, R.A., Rudstam, L.G., and Mills, E.L. 2003. Comparison of alewife young-of-the-year and adult respiration and swimming speed bioenergetics model parameters: implications of extrapolation. Trans. Am. Fish. Soc. **132**: 1089–1103.

Kuns, M.M., and Sprules, W.G. 2000. Zooplankton production in Lake Ontario: a multistrata approach. Can. J. Fish. Aquat. Sci. **57**: 2240–2247.

Lantry, B.F., and Stewart, D.J. 1993. Ecological energetics of rainbow smelt in the Laurentian Great Lakes: an interlake comparison. Trans. Am. Fish. Soc. **122**: 951–976.

Lasenby, D.C., Northcote, T.G., and Furst, M. 1986. Theory, practice and effect of *Mysis relicta* introductions to North American and Scandinavian lakes. Can. J. Fish. Aquat. Sci. **43**: 1277–1284.

Mills, E.L., O'Gorman, R., Degisi, J., Heberger, R.F., and House, R.A. 1992. Food of the alewife *Alosa pseudoharengus* in Lake Ontario before and after the establishment of *Bythotrephes cederstroemi*. Can. J. Fish. Aquat. Sci. **49**: 2009–2019.

Mills, E.L., Casselman, J.M., Dermott, R.M., Fitzsimons, J.D., Gal, G., Holeck, K.T., Hoyle, J.A., Johannsson, O.E., Lantry, B.F., Makarewicz, J.C., Millard, E.S., Munawar, I.F., Munawar, M., O'Gorman, R., Owens, R.W., Rudstam, L.G., Schaner, T., and Stewart, T.J. 2003. Lake Ontario: food web dynamics in a changing ecosystem (1970–2000). Can. J. Fish. Aquat. Sci. **60**: 471–490.

Mylius, S.D., Klumpers, K., De Roos, A.M., and Persson, L. 2001. Impact of intraguild predation and stage structure on simple communities along a productivity gradient. Am. Nat. **158**: 259–276.

Nero, R.W., and Sprules, W.G. 1986. Predation by three glacial opportunists on natural zooplankton communities. Can. J. Zool. **64**: 57–64.

O'Gorman, R., Johannsson, O.E., and Schneider, C.P. 1997. Age and growth of alewives in the changing pelagia of Lake Ontario, 1978–1992. Trans. Am. Fish. Soc. **126**: 112–126.

O'Gorman, R., Lantry, B.F., and Schneider, C.P. 2004. Effect of stock size, climate, predation, and trophic status on recruitment of alewives in Lake Ontario, 1978–2000. Trans. Am. Fish. Soc. **133**: 855–867.

Owens, R.W., and Weber, P.G. 1995. Predation on *Mysis relicta* by slimy sculpins (*Cottus cognatus*) in southern Lake Ontario. J. Gt. Lakes Res. **21**: 275–283.

Owens, R.W., O'Gorman, R., Eckert, T.H., and Lantry, B.F. 2003. The offshore fish community in southern Lake Ontario 1972–1998. *In* The state of Lake Ontario ecosystem: past, present and future. *Edited by* M. Munawar. Backhuys Publishers, Leiden, the Netherlands. pp. 407–441.

Polis, G.A., and Holt, R.D. 1992. Intraguild predation: the dynamics of complex trophic interactions. Trend. Ecol. Evol. **7**: 151–155.

Rand, P.S., Stewart, D.J., Lantry, B.F., Rudstam, L.G., Johannsson, O.E., Goyke, A.P., Brandt, S.B., O'Gorman, R., and Eck, G.W. 1995. Effect of lake-wide planktivory by the pelagic prey fish community in Lakes Michigan and Ontario. Can. J. Fish. Aquat. Sci. **52**: 1546–1563.

Romare, P., and Hansson, L.A. 2003. A behavioral cascade: top-predator induced behavioral shifts in planktivorous fish and zooplankton. Limnol. Oceanogr. **48**: 1956–1964.

Rudstam, L.G. 1989. A bioenergetic model for mysis growth and consumption applied to a Baltic population of *Mysis mixta*. J. Plankton Res. **11**: 971–984.

Rudstam, L.G., Hansson, S., Johansson, S., and Larsson, U. 1992. Dynamics of planktivory in a coastal area of the northern Baltic Sea. Mar. Ecol. Prog. Ser. **80**: 159–173.

Rudstam, L.G., Hetherington, A.L., and Mohammadian, A.M. 1999*a*. Effect of temperature on feeding and survival of *Mysis relicta*. J. Gt. Lakes Res. **25**: 363–371.

Rudstam, L.G., Hansson, S., Lindem, T., and Einhouse, D.W. 1999*b*. Comparison of target strength distributions and fish densities obtained with split and single beam echo sounders. Fish. Res. **42**: 207–214.

Rudstam, L.G., Parker, S.L., Einhouse, D.W., Witzel, L.D., Warner, D.M., Stritzel, J.L., Parrish, D.L., and Sullivan, P.J. 2003. Application of in situ target strength estimations in lakes: examples from rainbow-smelt surveys in Lakes Erie and Champlain. ICES J. Mar. Sci. **60**: 500–507.

Schaner, T., and Lantry, B.F. 1998. Pelagic planktivores. *In* Lake Ontario Management Unit 1998 annual report, section 1. New York State Department of Environmental Conservation, Albany, N.Y.

Shuter, B.J., and Ing, K.K. 1997. Factors affecting the production of zooplankton in lakes. Can. J. Fish. Aquat. Sci. **54**: 359–377.

Spencer, C.N., Potter, D.S., Bukantis, R.T., and Stanford, J.A. 1999. Impact of predation by *Mysis relicta* on zooplankton in Flathead Lake, Montana, USA. J. Plankton Res. **21**: 51–64.

Sprules, W.G., and Goyke, A.P. 1994. Size-based structure and production in the pelagia of Lakes Ontario and Michigan. Can. J. Fish. Aquat. Sci. **51**: 2603–2611.

Stewart, D.J., and Binkowski, F.P. 1986. Dynamics of consumption and food conversion by Lake Michigan alewives: an energetics-modeling synthesis. Trans. Am. Fish. Soc. **115**: 643–661.

Turner, A.M., and Mittelbach, G.G. 1990. Predator avoidance and community structure: interactions among piscivores, planktivores, and plankton. Ecology, **71**: 2241–2254.

Warner, D.M., Rudstam, L.G., and Klumb, R.A. 2002. In situ target strength of alewives in freshwater. Trans. Am. Fish. Soc. **131**: 212–223.

Wissel, B., Boeing, W.J., and Ramcharan, C.W. 2003. Effects of water color on predation regimes and zooplankton assemblages in freshwater lakes. Limnol. Oceanogr. **48**: 1965–1976.

Risk assessment model for dispersion of ballast water organisms in shelf seas

David Brickman

Abstract: The recommendation of mid-ocean exchange of ballast water has resulted in significant release of aquatic invasive species in shelf areas. This paper describes a semiquantitative risk assessment model developed for dispersion of ballast water organisms in shelf seas. The model simulates ballast water exchange as the release of tracer into the surface layer of a circulation model of the Scotian Shelf and Gulf of Maine. Three metrics are proposed to describe the risk of invasion: (*i*) the time-integrated concentration at a given location (the cumulative exposure index); (*ii*) the time taken for organisms to reach a given area (the invasion time); and (*iii*) the onshelf average concentration. A risk equation is derived that computes the relative overall risk of invasion for exchange segments along vessel tracks. Model results confirm the choice of offshelf alternate ballast water exchange zone advised by Department of Fisheries and Oceans, Canada. Low risk segments tend to be adjacent to one another. A four- to eight-fold reduction in invasion risk is possible, although this is likely a lower bound because of the use of monthly mean velocity fields. The model can be run in an operational mode to provide real-time risk assessment for vessel ballast water exchange.

Résumé : La recommandation de faire les échanges d'eau de ballastage au milieu de l'océan a eu pour effet de libérer des espèces exotiques envahissantes dans les zones du plateau continental. On trouvera dans cet article un modèle semi-quantitatif d'évaluation des risques mis au point pour décrire la dispersion des organismes de l'eau de ballastage sur les plateaux continentaux. Le modèle simule les échanges d'eau de ballastage comme la libération d'un traceur dans la couche superficielle dans un modèle de circulation de la plate-forme néo-écossaise et du golfe du Maine. Trois métriques proposées servent à décrire le risque d'invasion : (*i*) la concentration intégrée en fonction du temps à un point donné (l'indice d'exposition cumulée), (*ii*) le temps nécessaire à un organisme pour atteindre une région donnée (le temps d'invasion) et (*iii*) la concentration moyenne sur la plate-forme. On peut ainsi obtenir une équation du risque qui calcule le risque relatif global d'invasion pour les différents segments le long des tracés de déplacement des navires. Les résultats du modèle appuient la recommandation de Pêches et océans Canada d'utiliser de préférence une zone d'échange des eaux de ballastage au large du plateau continental. Les segments de risque réduit tendent à être adjacents les uns aux autres. Il est possible de réduire le risque d'invasion par un facteur de quatre à huit; c'est là une limite inférieure, car le modèle emploie des champs de vitesse moyenne mensuels. Le modèle peut être utilisé en mode opérationnel pour fournir une évaluation en temps réel du risque relié à l'échange des eaux de ballastage par les navires.

[Traduit par la Rédaction]

Introduction

Vessel ballast water is used for providing stability, maintaining trim, compensating for weight changes during load transfers, and reducing stress on hulls. The intake of ballast water (BW) at a given location and subsequent release at another location has been identified as a principal mechanism for introducing nonindigenous species (NIS) into aquatic ecosystems worldwide (Ruiz et al. 2000).

The dispersion of nonindigenous species by ships likely began with the onset of transoceanic travel some 500 years ago. These first aquatic invasive species (AIS) would have been attached to the hulls of early wooden vessels. The late 1800s marked a change in the transport mechanism due to the advent of iron ships with ballast water holding tanks, and this likely led to a marked increase in the invasion of NIS (Carlton 1985). Subsequently, with the increase in global oceanic trade during the 20th century, establishment of AIS has become a major environmental and economic problem worldwide.

In a key paper, Carlton (1985) outlined the sequence of events in the dispersal and introduction of species carried by ballast water. The sequence begins with the introduction of species into ballast water tanks in the source (or donor) port, followed by their survival during voyage, release into destination port, and subsequent (potential) establishment. Recognizing the significance of AIS, the International Maritime Organization (IMO), a specialized agency of the United Nations, developed a series of voluntary guidelines for preventing the introduction of unwanted aquatic organisms. In 2004, the International Convention for the Control and Management of Ships Ballast Water and Sediments was adopted by

Received 24 January 2006. Accepted 21 July 2006. Published on the NRC Research Press Web site at http://cjfas.nrc.ca on 6 December 2006.
J19128

D. Brickman. Department of Fisheries and Oceans, P.O. Box 1006, Dartmouth, NS B2Y 4A2, Canada (e-mail: brickmand@dfo-mpo.gc.ca).

Can. J. Fish. Aquat. Sci. 63: 2748–2759 (2006) doi:10.1139/F06-158

consensus at a diplomatic conference at the IMO in London. This convention, which is currently awaiting ratification, includes technical standards and requirements in the Regulations for the control and management of ships' ballast water and sediments. (More information on this regulatory sequence, which started in the early 1990s, can be found at http://www.imo.org.)

Despite the voluntary nature of the guidelines and the fact that even today there is no international law for ballast water management, numerous countries have acted on their own to include requirements for BW exchange and reporting. For example, Canada, in 1989, developed the Great Lakes Ballast Water Control Guidelines (Locke et al. 1993), which were extended to national guidelines in 2001. Starting in 1996, the US required vessels travelling to the Great Lakes and Hudson River to exchange ballast water and recommended that the exchange take place outside of the 200-mile exclusive economic zone (EEZ). Vessels travelling in coastal waters were exempted. In 2001, Australia introduced mandatory BW exchange requirements for vessels entering their coastal waters (AQIS, http://www.affa.gov.au). In 2004, the US Coast Guard began requiring all vessels to complete ballast water reporting forms and those crossing the EEZ to exchange BW.

An essential element of these ballast water guidelines is a recommendation for mid-ocean exchange (MOE) to be performed. (Historically, this meant outside of the EEZ and in waters >2000 m deep. The 2004, IMO convention states "at least 200 nautical miles from the nearest land and in water at least 200 metres in depth".) The rationale for MOE is that most coastal organisms will be flushed out during exchange (being replaced by less abundant, less diverse mid-ocean species) and that the high-salinity ocean water will produce high mortality in those that remain. Similarly, mid-ocean species released into low-salinity port water will be unlikely to survive or establish themselves.

There have been numerous studies on the effectiveness of MOE and the premises upon which it is based, with varying results. For example, Wonham et al. (2001) found that organism densities in unexchanged tanks decreased by greater than 98% during a 16-day overseas trip from Israel, and no original Israeli port organisms survived in Baltimore harbour water. However, mid-ocean exchange actually increased the abundance and diversity of organisms. This is similar to the finding of Carver and Mallet (2002, 2004), who looked at exchange along a route from Chesapeake Bay to two locations in Nova Scotia. Lavoie et al. (1999) found an average abundance decline of about 60% during a 36 h intracoastal voyage, but this number varied from close to zero to greater than 99% and was also taxon-specific. Locke et al. (1993) observed living zooplankton after 32 days in transit. Carlton (1985) cites instances of taxa surviving for as long as 95 days in unexchanged tanks. (This Carlton paper also contains numerous other examples of survival in adverse conditions, including transoceanic voyages of live fish.)

The estimated exchange efficiency from these studies ranged from 40% (Carver and Mallet 2004) to almost 100% (Wonham et al. 2001), although these results depend on definition. For example, in Wonham et al. (2001), exchange efficiency was almost 100% when based on salinity considerations, but 80%–100% when based on species considerations. This points out the complication that organisms can sink to the tank bottom and (or) be retained in tank sediment and released later. This can be a particular concern for encysting organisms such as toxic phytoplankton (McCollin et al. 2000).

The strategy of MOE creates a new dimension in the invasive species problem. Historically, invasions were essentially a port-to-port problem. Now, on the eastern seaboard of North America, as well as other coastal regions with significant vessel traffic, ballast water is often released onshelf, mainly because coastal traffic may be exempt from exchange or is not required to perform MOE if this results in too large a trip diversion. As well, transoceanic voyages may opt to perform exchange in coastal areas if MOE is deemed a safety risk. The invasion of Georges Bank by the sea squirt (*Didemnum*) is thought to be an example of the result of this change in BW practice (see http://woodshole.er.usgs.gov/project-pages/stellwagen/didemnum). Thus the risks of such practice need to be assessed.

Risk assessment models are categorized into three types (Clarke et al. 2003): qualitative, semiquantitative, and quantitative, although as pointed by Hayes (1998), the distinction between the latter two is often blurred. Regardless, in all cases, the risk model contains some subjective or qualitative decisions in its formulation. To date, no risk assessment models have been developed that quantify the risks of open-ocean exchange. The main goal of this paper is to show how such a model can be formulated. The model, really a risk assessment modelling system, has three main components: (*i*) a numerical circulation model of the Scotian Shelf (SS) and Gulf of Maine (GoM), which provides the fields for advecting and diffusing simulated ballast water releases; (*ii*) an analysis module which computes space–time characteristics of dispersion; and (*iii*) a risk model, which computes a relative overall risk (ROR) for the dispersion of ballast water organisms along various exchange routes on the SS and GoM. An important aspect of the modelling system is the development of a series of robust metrics describing potential invasion risk for open-ocean-released ballast water.

In this paper, the Materials and methods section describes the circulation model, how ballast water release was simulated, the analyses of dispersion, and the risk equation. The idea of the cumulative exposure index (CXI: the time-integrated concentration as a function of position (and time)) is introduced as a metric for potential invasion. The next section presents solutions to the risk equation. Five models are used, solved along one grouped and 12 separate tracks. Solution properties are investigated for individual tracks and for all tracks combined ("global properties"). The last section is a discussion.

Materials and methods

Numerical circulation model

The model used in this study was a version of CANDIE (a three-dimensional, nonlinear, prognostic, z-level model with a free surface) (Sheng et al. 1998; Lu et al. 2001). The model uses a Smagorinsky scheme to compute horizontal diffusivity and has a vertical diffusivity that depends on surface forcing and stratification. Vertical resolution ranges from 4 m in the top 20 m, 5 m from 20 to 50 m, and increases thereafter. The bottom layer is a partial cell that matches the bathymetry. Horizontal resolution was 5 km.

The model was configured to run on a SS–GoM domain (Fig. 1) and simulate the climatological seasonal cycle of circulation. Velocity forcing at the open boundaries was determined from a combination of published and unpublished studies (Drinkwater et al. 1979; Saucier et al. 2003; J. Chassé and F. Dupont, Bedford Institute of Oceanography, Department of Fisheries and Oceans, P.O. Box 1006, Dartmouth, NS B2Y 4A2, personal communications, 2003) and thermal wind analysis. The result was constant velocity forcing at all inflow–outflow locations except Cabot Strait (CS), where an analytic seasonal cycle was applied. The surface was forced by restoring boundary conditions on temperature and salinity based on monthly values determined from the BIO database, interpolated in time to provide daily forcing. The above constitute forcing on seasonal time scales. One tidal component (*M*2) was modelled to better simulate mixing and reproduce the known tidal residual field. The wind stress field from the Ocean Model Intercomparison Project (OMIP) data set (Röske 2006) was used as the primary forcing for subtidal variability on the shelf. This daily data set, based on an analysis of a 15-year ECMWF (European Center for Medium Range Weather Forecasting) atmospheric reanalysis run, provides a 360-day cyclical year of forcing representing climatological storminess across the globe.

Daily model output was saved, averaged over the last tidal cycle of the day, providing 360 realizations of the flow. The model was able to reproduce the main climatological features of the circulation on the SS and GoM, e.g., the gyres around Western Bank and Georges Bank, the Nova Scotia (NS) current and GoM coastal current (see Hannah et al. 2001), and prognostically simulate transports through the Cabot Strait, Halifax, and Cape Sable Island sections that are consistent with published data (Smith 1983; Anderson and Smith 1989; Loder at al. 2003). For more details on the circulation modelling system, see Brickman et al. (2004).

Simulating ballast water releases

Ballast water contains a diverse suite of organisms (bacteria, phytoplankton, zooplankton, ichthyoplankton) ranging in size from nanometres to centimetres. These organisms exhibit a range of buoyant behaviours, e.g., neutrally and nonneutrally buoyant, buoyancy adjusting, vertically migrating, etc. Detailed modelling of dispersion for this range of behaviours is an intractable problem. To proceed, the simple approach of modelling the exchange of ballast water as the release of a passive tracer into the surface layer of the model ocean was adopted.

The origin of most ballast water released in Atlantic Canada are ports along the eastern coast of the US (about 80%; Balaban 2001). Much of this traffic does not routinely travel offshelf, and the IMO convention states that vessels required to undertake BW exchange should not incur a significant trip diversion. Therefore, it is relevant to simulate BW exchange along all principal onshelf vessel corridors in this region.

The determination of relevant vessel corridors is based on Kelly (2002) and Kelly (2003). In the former, Kelly analyzed vessel tracks based on the Eastern Canada Traffic System (ECAREG) data set and derived vessel transect density maps for eastern Canada. In the latter, Kelly extracted ballast water exchange endpoints from ballast water reporting forms to create vessel exchange movement tracks. When such maps are combined with great circle routes, a generally consistent picture emerges of vessel traffic converging to destination points along the eastern seaboard then following rhumblines (lines of constant compass angle) to port. Overlays of vessel density and ballast water exchange maps were used to eliminate corridors with high traffic and low exchange (and vice versa) and thus determine the set of corridors along which to simulate dispersion (Fig. 2*a*).

Open-ocean ballast water exchange occurs while the vessel is moving and takes between 18 and 36 h (Carver and Mallet 2004). At typical vessel speeds, this translates into a distance of roughly 300–500 km. This exchange distance will be called a corridor "segment". The goal is to determine the relative risk along segments of the principal vessel corridors.

The ocean model provides 360 realizations of the circulation representing the responses of SS and GoM to periods of stormy and calm conditions. This provides the opportunity for investigation of dispersion under a number of scenarios. As the emphasis here is to introduce the risk assessment model and illustrate its basic properties, circulation model output was averaged to produce monthly mean fields with which to investigate dispersal. Risk model behaviour under other flow scenarios is the subject for future work. Because the typical exchange time is about 24 h, the flow is taken as stationary during the exchange process. Noting that the principal vessel corridors are of finite width, releases are mod-

Fig. 1. The domain for the circulation model (outlined area). The solid arrows denote time-independent boundary velocity forcing. The shaded arrow indicates where an analytic seasonal cycle is applied. Cabot Strait (CS), the Western Bank complex (WB), and Georges Bank (GB) are marked. Bold lines mark the CS, Halifax (HFX), and Cape Sable Island (CSI) sections refered to in the text.

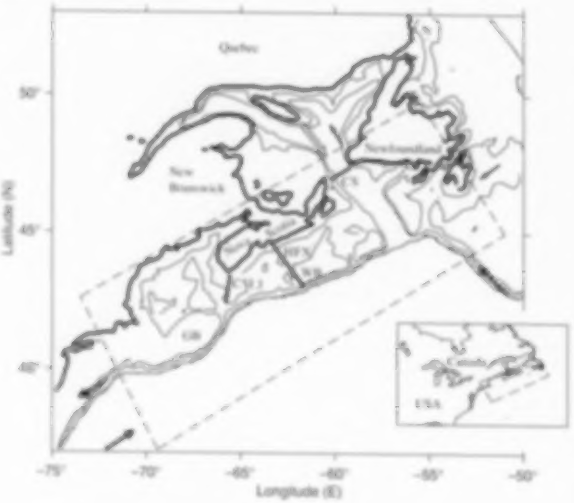

Fig. 2. (*a*) Principal vessel corridors on the Scotian Shelf, as derived from vessel transect density and endpoint exchange maps. The shaded lines denote traffic coming to or from the US. The broken line is an offshelf corridor considered as an alternate ballast water exchange zone. (*b*) Example of conversion of vessel corridors to discretized model tracks. Segment numbers on boxes refer to the last box in the eight-box segment. Tic marks are at 100 km spacing.

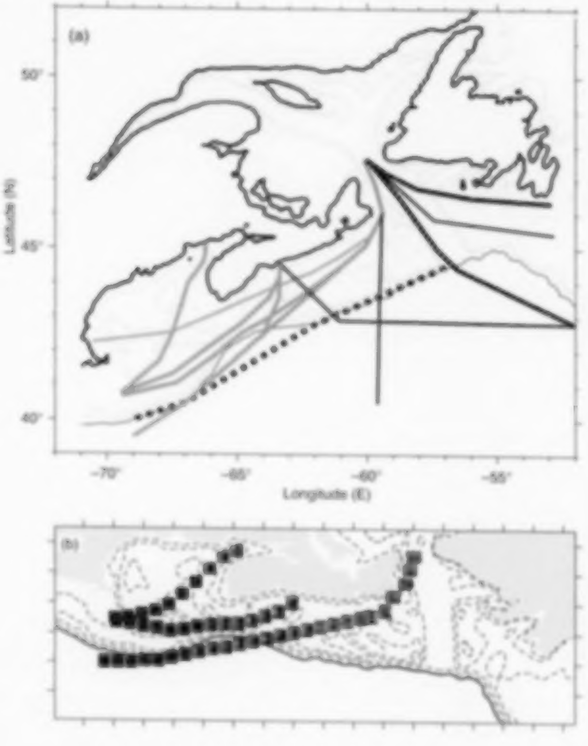

elled to have a footprint of 45 × 45 km, i.e., tracer is released in 9 × 9 model cell "boxes", and the standard segment is defined to be a sequence of eight consecutive boxes equaling (nominally) 360 km in length. (This length, arguably a bit short, is roughly consistent with proposed alternate BW exchange zones in eastern Canada (Brickman et al. 2004).) An example of the rendering of vessel corridors into discrete segments is provided (Fig. 2*b*).

To compute various dispersion metrics along a segment, use is made of the linearity of the advection–diffusion (tracer) equation, which allows one to create a total concentration field by adding the contributions from the various boxes. Therefore, for a given month and track, tracer is released separately from each of the boxes constituting the track, integrated forward in time for 30 days, and the results are stored. A postprocessing program assembles the boxes into segments and computes the various dispersion metrics.

The strategy of reassembling individual releases into segments was designed to allow exibility in the modelling system. Because the goal here is to demonstrate a dispersion risk assessment model and because longer segment choices did not significantly affect the results, only eight box segment results will be presented in this paper.

Dispersion metrics related to invasion risk

An example of the simulated dispersion of ballast water 15 days after release is provided (Fig. 3). Aspects to note are as follows: (*i*) the tracer occupies a finite area or volume of the domain; (*ii*) the concentration field is not uniform in space; (*iii*) there is drift into what are regarded as sensitive areas (in this case, the coastal zone plus the Gully marine protected area (MPA)). The following metrics are proposed as relevant to the potential risk of invasion by BW organisms.

(*a*) The time it takes to reach a sensitive area. It is generally accepted that the abundance of released organisms decreases with time, owing to various mortality mechanisms. Therefore, a given BW exchange segment is potentially riskier if it disperses organisms into a sensitive region faster than a different segment. This is a particular concern for inshore areas, which are often economically important (e.g., aquaculture) and considered susceptible to invasion because of their shallow depth plus potentially enhanced nutrient availability. This is likely less true for non-inshore regions, although this metric can be applied to any subregion if deemed necessary. This risk measure will be called the invasion time and is explicitly tied to a location (or locations) on the SS–GoM.

(*b*) Onshelf average concentration (OAC). The lower the average concentration onshelf, the lower is the probability of organisms establishing themselves (and vice versa). The OAC is a bulk measure, one value for the whole domain, and is a function of time since release. It can be considered to represent a "dilution is the solution" metric.

(*c*) The CXI. Consider the following simple model of invasion probability. Organisms (of one type for simplicity) are released into a region of the ocean, a fraction of which contains suitable habitat. The organisms, because of turbulence and possibly behaviour, essentially perform a random walk through the water column. The probability of encountering suitable habitat is a function of the volume searched by the organisms, which depends on the number of organisms released and the time spent in the region. The latter is true because, in a random walk, the volume searched is an increasing function of time. Therefore, it is proposed that a metric for assessing invasion risk is

$$(1) \qquad \mathrm{CXI}(x, y, t) = \int_0^t c(x, y, t')\,\mathrm{d}t'$$

where $c(x, y, t')$ is the concentration (vertically integrated) at a given (x, y) and t is time since release. The CXI formalizes an equivalence between the encounter probability of a high number of organisms occupying a region for a short period of time and a small number of organisms occupying the same region for a long period of time.

In the above, habitat can be quite general. For example, for floating species (holoplankton), "habitat" could mean food resources, which would also be encountered as a function of the CXI. Also, the probability of successful mating can be related to the CXI.

Fig. 3. Surface concentration fields 15 days after release, for selected corridor segments (month = August): (*a*) shelfbreak GB to Cabot Strait, (*b*) Nantucket Shoals to Halifax, (*c*) Nantucket Shoals to Saint John, (*d*) offshelf to Cabot Strait. Segment boxes are outlined by thin lines, the Gully MPA is outlined by a thick line. GB (solid area) is shown in panel *d*. Concentration scales from black (high) to white (low) in arbitrary units.

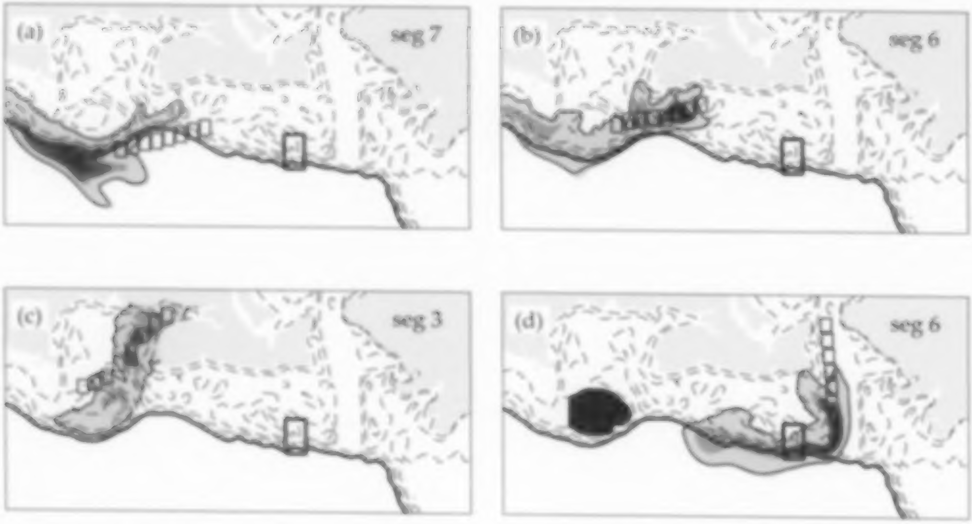

Table 1. Acronyms used in the risk model and elsewhere in the text.

OAC	Onshelf average concentration
CXI	Cumulative exposure index
MOCXI	Maximum onshelf CXI
CIT	Coastal invasion time
ROR	Relative overall risk
ABWEZ	Alternate ballast water exchange zone
AIS	Aquatic invasive species
BW	Ballast water
CS	Cabot Strait
EEZ	Exclusive economic zone
GB	Georges Bank
GoM	Gulf of Maine
IMO	International Maritime Organization
MOE	Mid-ocean exchange
MPA	Marine protected area
NIS	Nonindigenous species
OMIP	Ocean Model Intercomparison Project
SS	Scotian Shelf

Table 2. Coefficient definitions for the risk model.

C1	OAC
C2	MOCXI
C3	CIT
C4	Average CXI, Gully
C5	Average CXI, Georges Bank

Table 3. Table of coefficient weights for the five models.

Model no.	w_1	w_2	w_3	w_4	w_5
0	1	1	1	1	1
1	0	1	1	1	1
2	1	0	1	1	1
3	1	1	1	0	0
4	0	0	0	1	1

Note that one could be interested in the CXI(t) averaged over a given subregion of the shelf or in terms of its maximum value anywhere on the shelf. Both variants will be used in the risk model.

More generally, one might consider a modified version of the above

$$(2)\qquad \text{risk} \sim \text{metric} \times [f_1 \times f_2 \times \ldots]$$

where the f_i represent weighting functions that are, potentially, functions of position and time. A simple example would be to weight the CXI by 1/depth so that the probability of invasion, for a given CXI, is higher in shallow water than in deep water. Other examples include species-specific functions related to habitat suitability, temperature, salinity, predation pressure, etc. In other words, biological information, if it exists, can be simply incorporated into the risk metrics.

Other risk indicators related to spatial inhomogeneities can be formulated (e.g., the maximum concentration found as a function of time); however, it is felt that the CXI is superior to this class of indicators. Therefore the risk metrics used will be the invasion time, the CXI, and the average concentration onshelf. These metrics are proposed as robust general indicators of invasion risk for dispersion of BW organisms in open-ocean waters.

Risk model formulation

The goal of the risk model is to assess the relative risk of a set of possible BW exchange segments along typical vessel

Fig. 4. Risk model 0 solution for the offshelf corridor. (*a*) Segments of the track. The number denotes the last box in the eight-box segment. (*b*) Contour plot of ROR (by month versus segment number). Contour values are indicated.

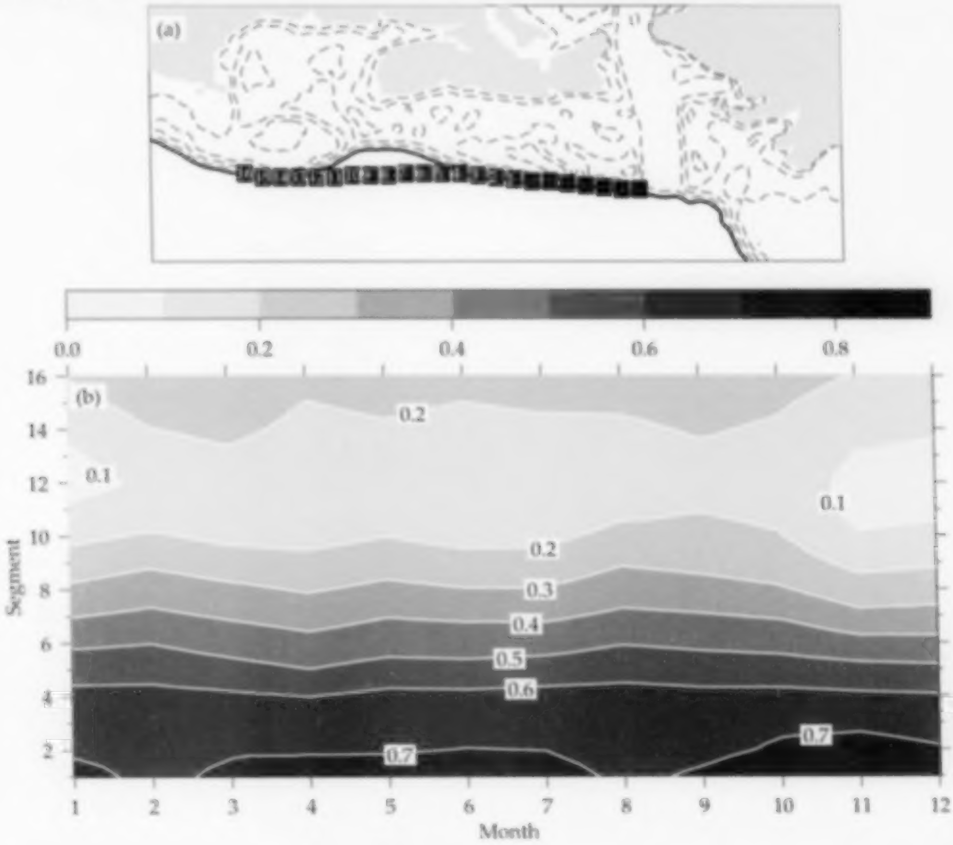

transect routes in Atlantic Canada (Fig. 2). The idea behind the risk equation is that it should be flexible in order to reflect the various opinions that different groups have with respect to potential areas of invasion and relevant metrics. This need became evident at meetings on alternate BW exchange routes in Atlantic Canada (see Department of Fisheries and Oceans (DFO) 2004). Three categories of interest, with specific examples, are considered: (*a*) general interest, the entire shelf; (*b*) specific area(s) of general interest, the coastal zone; and (*c*) areas of special interest, the Gully MPA and Georges Bank (GB).

To assess the risk for these interests the following combinations of metrics will be used. For the Gully and GB, the average CXI within the areas (at release day 30) is computed. The invasion time will be assessed for the coastal region (within 10 km = two grid cells of the coastline). For the entire shelf, the OAC and maximum onshelf CXI (MOCXI) are computed. The OAC and MOCXI are complementary measures, the former giving a sense of overall dispersion and the latter accounting for (the time history of) inhomogeneities in dispersion.

The risk equation is modelled after that used in the GloBallast system (http://globallast.imo.org), which uses a combination of coefficients of relative risk. Consider the OAC for the set of segments for one of the chosen tracks. The relative risk coefficient for segment *i* is defined as

$$C1(i) = \mathrm{OAC}(i)/\max(\mathrm{OAC}) \tag{3}$$

where max(OAC) is the maximum OAC for the set of segments constituting the track. $C1$ is bounded by 0 and 1, with lower values denoting lower relative risk. The coefficients of risk for the other metrics are defined in a similar fashion, i.e., with lower values denoting lower risk. (Note that a coeficient of zero is not meant to denote zero risk but, rather, the lowest relative risk.)

The general risk equation (for segment *i*) is

$$\mathrm{ROR}(i) = \frac{\sum_{j=1}^{5} w_j\, Cj(i)}{\sum w_j} \tag{4}$$

where ROR is the relative overall risk, w is a weighting factor, and $Cj = C1, \ldots, C5$ are risk coefficients for OAC, MOCXI, coastal invasion time (CIT), average Gully CXI, and average GB CXI, respectively. The denominator guarantees that the $\mathrm{ROR} \leq 1$. The weights allow the various factors to assume more or less importance. The acronyms and coefficients used in eq. 4 are summarized in Tables 1 and 2.

Fig. 5. (*a*) Annually averaged ROR (<ROR>) normalized by minimum annual value ($<ROR>_{min}$) versus segment number (■); number of times that a segment was ranked number 1 (●). (*b*) ROR normalized by minimum value on a monthly basis. Model 0 results are shown.

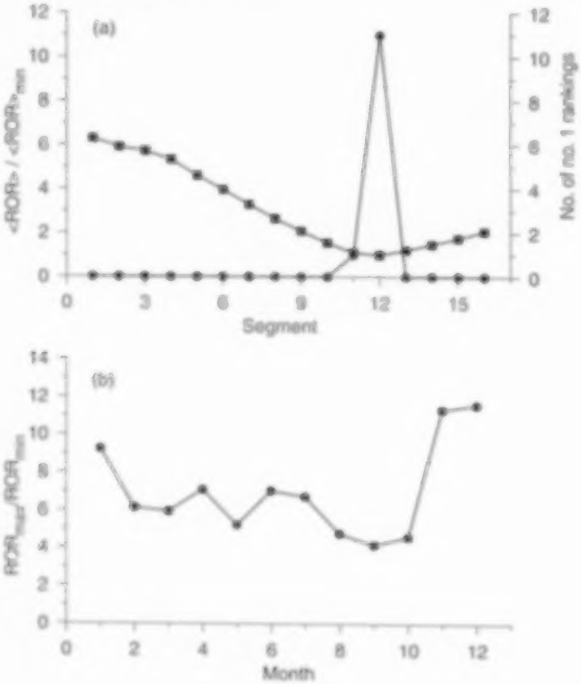

Note that this equation is identical in form to the GloBallast model, although the coefficients have different meanings.

The coefficients of risk are quantitative measures representing the severity of an event relative to the population of outcomes. The form of eq. 4 and the values of its weights are subjective decisions, and thus the system is "semi-quantitative". The sensitivity of eq. 4 under various sets of values for the weights will be evaluated. As well, because monthly averaged flow fields are used, we are able to look at how the ROR changes on a seasonal time scale.

Results

In this section, solutions of the risk equation along selected vessel tracks are presented. Five models are considered (Table 3) that are meant to represent simple "end-member" possibilities. The baseline model (model 0) has equal weighting for all five coefficients in eq. 4. Because the OAC and MOCXI are complementary measures, models 1 and 2 eliminate each of these, in turn, to compare with model 0. Model 3 contains no special interests (i.e., Gully and GB), and model 4 contains only the special interests. For each model, properties of the solution are investigated for all 12 tracks pooled together, and these "global" properties are compared across models.

By way of introducing model results, we start by considering two specific corridors of interest. One is the offshore track, part of which was recommended by DFO as an alternate ballast water exchange zone (ABWEZ) for traffic into Atlantic Canada (DFO 2004). Thus we will quantitatively assess the DFO advice. The other one is the pair of corridors from Nantucket Shoals to CS and offshelf GB to CS, grouped together (see Fig. 2). This allows comparison of an onshelf corridor to an offshelf one that could serve as an alternative route.

Fig. 6. (*a*) Geographic scatter plot of the three lowest risk segments for all five models. The complete track is boldly outlined. The best segments are indicated as solid, and the second and third best are shaded from dark to light, respectively, and are offset for clarity. (*b*) The best (■), second best (◆), and third best (○) segments versus model number.

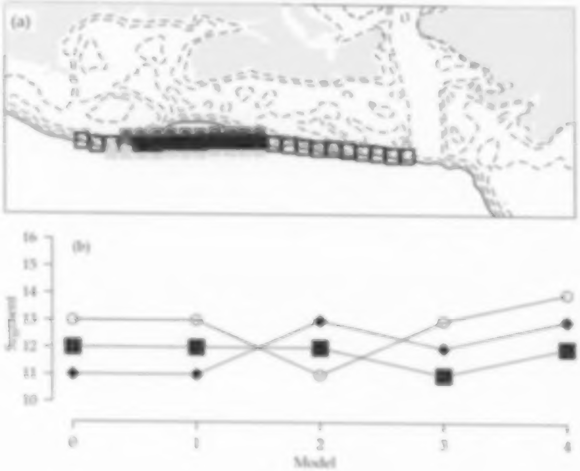

Offshelf ABWEZ

A month-segment contour plot of ROR values for the complete offshelf track (Fig. 4) for the baseline model (Table 3, model 0) illustrates that segment 12 is of lowest risk for most months and that, in general, exchange segments west of the Gully are of lower risk than eastern segments.

Three properties of interest are as follows: (*i*) the "stability" of the best (or lowest risk, rank) segment, the degree to which the best segment changes during the course of a year; (*ii*) the range of ROR values, indicating how preferable the best segments are, and (*iii*) the "adjacency" of the best segments, indicating the tendency for lowest risk segments to be sequential.

With respect to stability, we see that segment 12 is the lowest risk segment in 11 out of 12 months (Fig. 5*a*, ●). In terms of the range of values, segment 12 is about seven times less risky than the most easterly segment on an annual basis (Fig. 5*a*, ■) and that ROR values on a monthly basis vary by about a factor of 5–12 (Fig. 5*b*). The results for models 1–3 are similar to the above. However, model 4, which considers only the special interests (the Gully and GB), has a monthly ROR range factor of 24–250, because segments west of the Gully exhibit virtually no dispersion into that region.

The adjacency of the best segments is illustrated by a geographic scatterplot of the annually averaged three best segments for all five models (Fig. 6). We see that the lowest risk exchange segments describe a continuous region (Fig. 6*a*) and

Fig. 7. Risk model 0 solution for the grouped corridors ending at CS. (*a*) Segments of the track. The number denotes the last box in the eight-box segment. (*b*) Contour plot of ROR (by month versus segment number). Contour values are indicated.

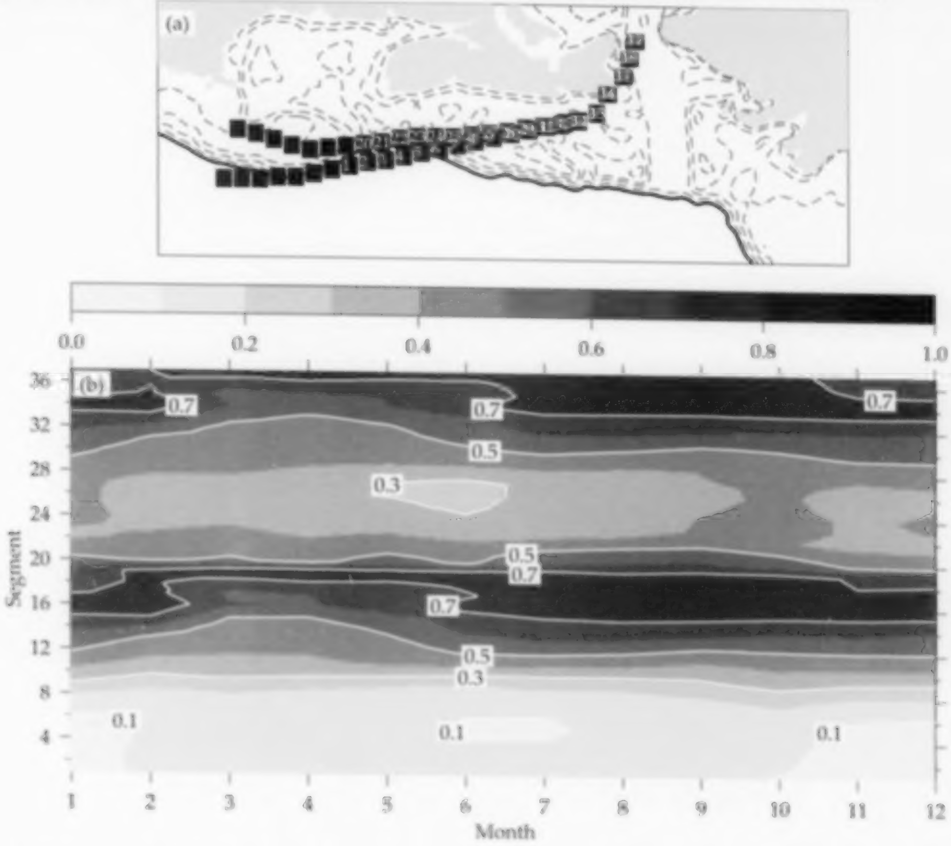

that the best segments are consistent across models (Fig. 6*b*). The geographic region of lowest risk is consistent with that recommended by DFO as an ABWEZ.

Offshelf versus onshelf corridors

The risk model computes the relative overall risk for each segment of a given track, for each month of the year. To compute the RORs for a group of tracks or segments, the data are first pooled and then the model is run. As such, the combined tracks starting from offshelf GB and Nantucket Shoals and ending at CS, comprised of 19 and 18 segments, respectively, become one grouped track of 37 segments. The month–segment contour plot of the ROR values for the baseline model (Table 3, model 0; Fig. 7) illustrates that exchange segments 1–6 from the offshelf track are of lowest risk and that risk progressively increases for more onshelf exchanges.

For this combined track, we find (Fig. 8*a*) that segments 1–6 have essentially equal annually averaged ROR (<ROR>) and segments 5 and 1 are ranked number 1 in 7 and 5 months, respectively. In terms of the range in ROR, on an annual basis (Fig. 8*a*), the total range is ~7 and the best segment(s) from the onshelf track is (are) roughly 3.5 times more risky than segments 1–6. On a monthly basis (Fig. 8*b*), the ROR varies by a factor of 6–13 (mean ~ 8.5) across all segments, whereas the ratio of the best onshelf versus best offshelf track varies from 2.5 to 6.0. From Fig. 7, we can see that the best segments tend to be adjacent to each other for all months.

The variability in best segments among the five models is illustrated using geographic scatterplots (Fig. 9). A consistent pattern emerges showing that the offshelf portion of the tracks are the preferred regions to exchange ballast water for all models.

Global properties

To investigate the general properties of the risk model solutions over the entire SS–GoM region, the five versions of the model were run on 12 separate tracks. Of primary interest are the stability, range, and adjacency of the lowest risk segments.

The number of times that the annually averaged best segment was ranked number 1 was computed for each track (as in Figs. 5*a* and 8*a*). To illustrate global stability, this quantity was averaged over the 12 tracks of each model. We find that the mean number of top rankings varied from ~9 to 11 (Fig. 10) and that model 2 was the least variable. This indicates that the lowest risk segment on an annual basis tends to be a good choice on a monthly basis and that this result is relatively model-insensitive.

Fig. 8. (*a*) Annually averaged ROR normalized by minimum annual value versus segment number (■); number of times a segment was ranked number 1 (●). The vertical broken line separates the offshelf from the onshelf tracks. (*b*) ROR normalized by minimum value on a monthly basis (■); ratio of best onshelf (on) to best offshelf (off) segment versus month (●).

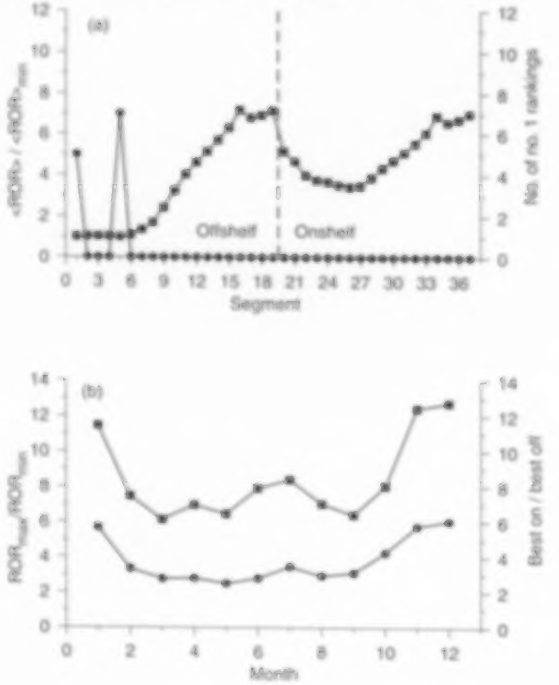

Fig. 9. (*a*) Geographic scatter plot of the three lowest risk segments for all five models. The complete track is boldly outlined. The best segments are indicated as solid, and the second and third best are shaded from dark to light, respectively, and are offset for clarity. (*b*) The best (■), second best (◆), and third best (○) segments versus model number.

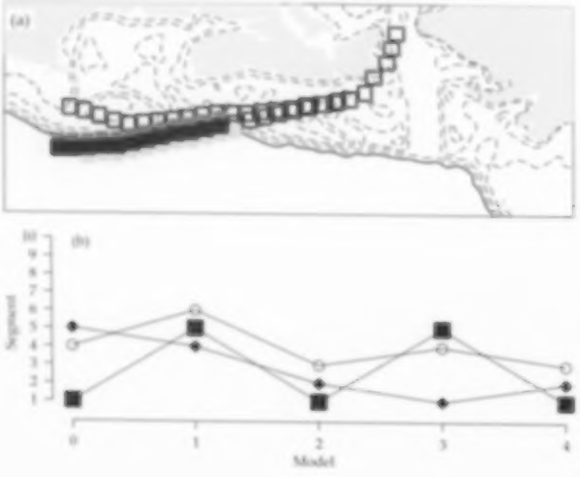

Fig. 10. The number of times that the annually averaged best segment was ranked number 1, averaged over the 12 tracks of each model (ave). The standard deviations (SD), maxima (max), and minima (min) are shown.

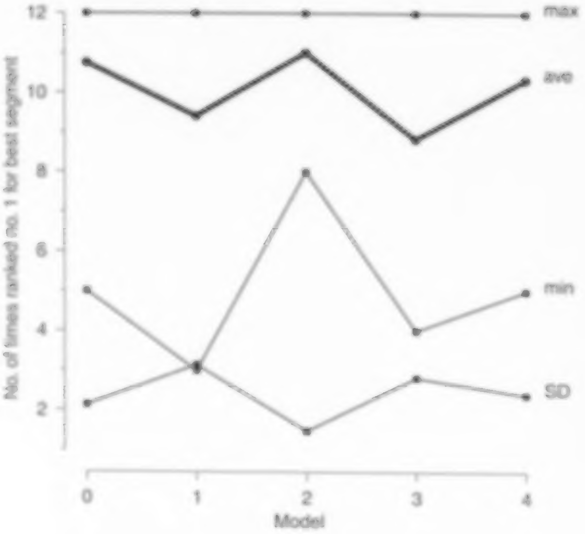

Histograms of the monthly range in ROR values for the 12 tracks of each model were computed. For models 0–3, about 70% of the ROR ranges are ≤4 (i.e., >100 of the 12 months × 12 tracks = 144 outcomes). In other words, the risk for the majority of the worst segments is ≤4 times higher than the risk for the best segments. The total ranges of values, means, and medians for these four models are 11 to 17, 3.1 to 5.0, and 1.7 to 2.1, respectively. Model 4 is characterized by a much greater total range of values (maximum = 250), with 70% of the ROR ranges ≤ 8, because this model considers only the special interests (the Gully and GB), which results in much greater ranges along certain tracks because some segments do not disperse into these areas.

Segment adjacency is computed as the numerical difference between the two best segment numbers for each month of each track. All models showed a high degree of adjacency with over 80% (>120/144) of the best segments within two segment numbers of each other. The histograms (not shown) have slight blips near separations of 11 segments (16 segments for model 4) and four segments. These outliers are due primarily to two tracks (see below), with monthly variability from other tracks being a secondary contributor.

Model solutions for all tracks investigated are illustrated using geographic scatterplots of the annually averaged three best segments (Fig. 11). For 10 of the 12 tracks, there is a high degree of overlap between the best segments for all models, which is the source of the high adjacency noted above. Tracks 7 and 8 are the exceptions, with the former being a track that crosses the GoM with a long nearshore section and the latter having segments releasing along the Laurentian Channel slope. In both cases, no obvious reason was found for this complex behaviour.

Models 0–2 use combinations of OAC and MOCXI (Table 3) to represent risk to the entire shelf region. The results presented above (plus other analyses not included) indicate

Fig. 11. Geographic scatter plot of the three lowest risk segments for all five models for each of the 12 tracks investigated. The complete track is boldly outlined. The best segments are indicated as solid, and the second and third best are shaded from dark to light, respectively, and are offset for clarity.

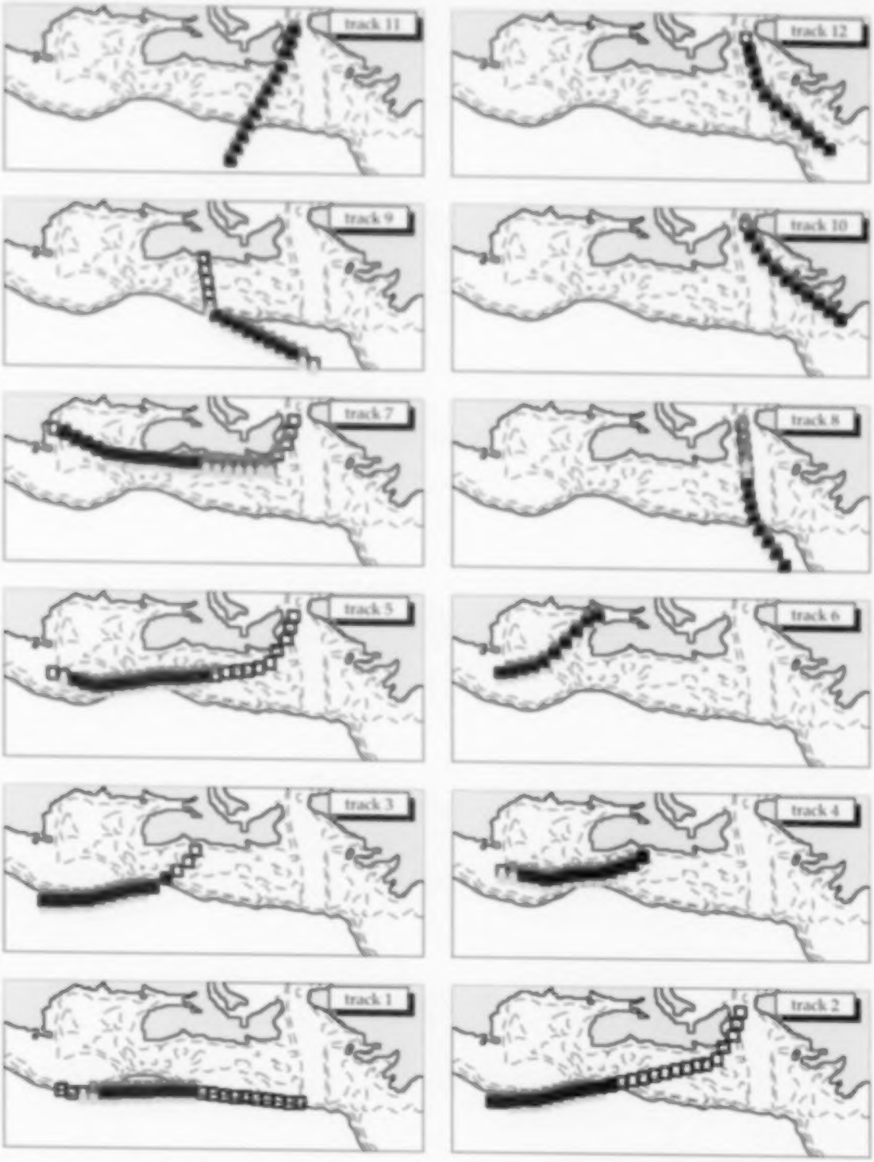

that the choice of OAC + MOCXI, just MOCXI, or just OAC makes little difference to the conclusions.

Discussion

In this paper, a risk assessment model for the dispersion of ballast water organisms in shelf seas has been presented. The model is based on three metrics of invasion risk: the time taken for ballast water to invade the coastal zone, the average concentration of ballast water onshelf at a certain time after release, and the CXI. The latter, equal to the time (and vertically) integrated concentration as a function of space and time, was shown to relate to the probability of finding suitable habitat, where habitat could more generally mean food, a mate, etc. These metrics formed the basis for risk coefficients that express risk relative to the population of possible outcomes. The risk equation, consisting of the weighted sum of five risk coefficients, determines the relative overall risk of invasion at specified areas of interest on the shelf.

The use of a number of invasion risk metrics reflects the fact that any one metric has its weaknesses. For example, objections to an average concentration metric are that it ignores such things as the time to invade a sensitive area and the possibility that an overall dispersed ballast water release could still have local regions of high concentration that could relate to invasion risk.

The model simulated the ballast water exchange process as the dispersion of a passive tracer released at the surface of the ocean. Many organisms do not behave in a passive fashion. If enough information was available about a specific organism, then it would be a simple matter to incorporate this into the dispersion module. Similarly, any knowledge about growth, reproduction, and mortality could also be included, making the dispersion module similar to a planktonic ecosystem model. However, given the rudimentary knowledge available in these instances, such complications should be approached with caution.

Five different versions of the risk model meant to represent possible end-member combinations of the risk coefficients were considered. The model was applied along one combined plus 12 separate vessel corridors on the SS and GoM to determine the lowest risk BW exchange segment(s) for each track. Monthly mean circulation model flow fields were used to simulate BW releases. Results were pooled for the 12 tracks to produce global statistics, which were looked at across the five models.

In general, we found that the monthly range in risk values varied over a factor of about four, indicating that the highest risk exchange segment was on average four times more risky than the lowest risk segment. The exception was the model that considered only the risk associated with invasion of the Gully MPA and Georges Bank. In this case, the range was much higher, with the majority of values lying within a factor of eight.

The best exchange segments tended to be adjacent to one another, indicating that broad regions of lower risk existed for most tracks. Tracks 7 and 8 were the exception, although the reason for their complex behaviour was not obvious.

With respect to month-to-month variability, we found that the best segment on an annual basis was typically the best choice on a monthly basis as well. However, this result should not be interpreted as commenting on potential variability, as individual storms can lead to much greater variability in shelf circulation than is portrayed by monthly averaged flow fields.

The offshelf corridor, part of which was recommended as an alternative ballast water exchange zone by DFO (DFO 2004), was specifically considered. Within that zone, the best exchange region was west of the Gully MPA and east of GB, essentially coincident with the zone recommended by DFO. On a monthly basis, for models 0–3, the highest risk segment, always in the east, was 3.3–12.2 times more risky than the lowest one. For model 4, however, which considered only the invasion risk to the Gully and GB, the monthly ROR range factor was 24–250. This analysis quantifies the advice brought forward by DFO.

We looked at a combined offshelf–onshelf track, with the offshelf option representing a possible alternate route for vessel traffic to and from the eastern coast of the US. We found that exchange segments from the offshelf tracks were consistently of lower risk than their onshelf counterparts, by a factor of about four on an annual basis with a monthly range of 2.5–8.0. This is the first time that such a difference has been quantified.

The main goal of this paper was to show how a risk model assessing the potential of invasion by ballast water organisms released in shelf seas could be formulated and applied. The model treats the open-ocean exchange problem as one in which organism dispersion is considered to be of primary importance. Addition of specific biological effects is straightforward, if such information exists.

The mid-ocean exchange of ballast water and associated risk of invasion is a complicated problem combining ocean physics and biology. The model computes the risk relative to the population of possible outcomes, allowing a decision to be made regarding the safest region in which to exchange ballast water. We are still a long way away from determining the absolute risk associated with this process.

More than 500 vessels per year exchange their ballast water in the SS and GoM regions (Kelly 2003). Application of the risk assessement model presented here indicates that, on average, a four- to eight-fold reduction in invasion risk is possible. However, this is likely a lower bound because the monthly mean flow fields used in this study smooth out the variability produced by the passage of individual storms over the shelf, thus leading to reduced along-track variability. The model could be run in an operational mode whereby advice regarding where to exchange ballast water is given to vessels as they report their intended route. In this case, operational circulation models with some forecast capability would have to be running, and this is becoming more possible as computer power plus data assimilation capabilities increase. The dispersion and risk modules can be run efficiently once the flow fields are determined. Under quasi-real-time conditions, or using simulated flow fields produced from time varying forcing, it would be interesting to see how the variability in the range of ROR values and locations of lowest risk segments changes. This is the subject of future work.

Acknowledgements

The author thanks Drs. Peter Smith and Brian Petrie for suggestions on an earlier version. The comments of two anonymous reviewers greatly improved the manuscript.

References

Anderson, C., and Smith, P.C. 1989. Oceanographic observations on the Scotian Shelf during CASP. Atmos.-Ocean, **29**(1): 130–156.

Balaban, M. 2001. Vessel traffic / vessel shipping patterns on the east coast of Canada 2000 shipping season. Transport Canada Marine Safety Technical Report. Transport Canada, Dartmouth, Nova Scotia.

Brickman, D., Petrie, B.D., and Smith, P.C. 2004. Assessing ballast water exchange zones on the Scotian Shelf and Gulf of Maine. Canadian Science Advisory Secretariat (CSAS) Res. Doc. No. 2004/119.

Carlton, J.T. 1985. Transoceanic and interoceanic dispersal of coastal marine organisms: the biology of ballast water. Oceanogr. Mar. Biol. Annu. Rev. **23**: 313–371.

Carver, C.E., and Mallet, A.L. 2002. An assessment of the risk of ballast water-mediated introduction of non-indigenous phytoplankton and zooplankton into Atlantic Canadian waters. Mallet Research Services Ltd., Dartmouth, Nova Scotia.

Carver, C.E., and Mallet, A.L. 2004. Investigating potential ballast water management strategies for ships travelling from Chesapeake Bay to ports in Nova Scotia. Mallet Research Services Ltd., Dartmouth, Nova Scotia.

Clarke, C., Hayes, T., Hilliard, R., Kayvanrad, N., Taymourtash, H., Parhizi, A., Yavari, V., and Raaymakers, S. 2003. Ballast water risk assessment, Port of Khark Island, Islamic Republic of Iran. GloBallast Monogr. Ser. 8. International Maritime Organization (IMO), London, UK.

Department of Fisheries and Oceans. 2004. Science Proceedings. Alternative ballast water exchange zones, 30 November – 1 December 2004, Montreal, Quebec. http://www.dfo-mpo.gc.ca/csas/Csas/proceedings/2004/PRO2004 042 B.pdf.

Drinkwater, K., Petrie, B.D., and Sutcliffe, W.H., Jr. 1979. Seasonal geostrophic volume transports along the Scotian Shelf. Estuar. Coast. Mar. Sci. **9**: 17–27.

Hannah, C.G., Shore, J.A., Loder, J.W., and Naimie, C.E. 2001. Seasonal circulation on the western and central Scotian Shelf. J. Phys. Ocean. **31**: 591–615.

Hayes, K.R. 1998. Ecological risk assessment for ballast water introductions: a suggested approach. ICES J. Mar. Sci. **55**: 201–212.

Kelly, B. 2002. Marine commercial vessel traffic activity in Canada's Atlantic region. Report to Fisheries and Oceans Canada and Environment Canada. Fisheries and Oceans Canada, Oceans and Coastal Management Division, Dartmouth, Nova Scotia.

Kelly, B. 2003. GIS mapping of marine vessel ballast water exchange endpoint data in Atlantic Canada, for the 2002 shipping season. Report to Marine Safety. Transport Canada, Dartmouth, Nova Scotia.

Lavoie, D.M., Smith, L.D., and Ruiz, G.M. 1999. The potential for intracoastal transfer of non-indigenous species in the ballast water of ships. Estuar. Coast. Shelf Sci. **48**: 551–564.

Locke, A., Reid, D.M., van Leeuwen, H.C., Sprules, W.G., and Carlton, J.T. 1993. Ballast water exchange as a means of controlling dispersal of freshwater organisms by ships. Can. J. Fish. Aquat. Sci. **50**: 2086–2093.

Loder, J.W., Hannah, C.G., Petrie, B.D., and Gonzalez, E.A. 2003. Hydrographic and transport variability on the Halifax section. J. Geophys. Res. **108**(C11), 8003, doi:10.1029/2001JC001267.

Lu, Y., Wright, D.G., and Brickman, D. 2001. Internal tide generation over topography: experiments with a free-surface z-level ocean model. J. Atmos. Oceanic Technol. **18**: 1076–1091.

McCollin, T.A., Hamer, J.P., and Lucas, I.A.N. 2000. Transport of phytoplankton via ship's ballast into ports around England and Wales. *In* Marine Bioinvasions: Proceedings of the First International Conference. *Edited by* J. Pedersen. Massachusetts Institute of Technology Sea Grant, Cambridge, Mass. pp. 282–288.

Röske, F. 2006. A global heat and freshwater forcing dataset for ocean modelling. Oceal Modell. **11**: 235–297.

Ruiz, G.M., Fofonoff, R.W., Wonham, M.J., and Hines, A.H. 2000. Invasion of coastal marine communities in North America: apparent patterns, processes, and biases. Annu. Rev. Ecol. Syst. **31**: 481–531.

Saucier, F.J., Roy, F., Gilbert, D., Pellerin, P., and Ritchie, H. 2003. Modeling the formation and circulation processes of water masses and sea ice in the Gulf of St. Lawrence, Canada. J. Geophys. Res. **108**(C8), 3269, doi:10.1029/2000JC000686.

Sheng, J., Wright, D.G., Greatbatch, R.J., and Dietrich, D.E. 1998. CANDIE: a new version of the DieCast ocean circulation model. J. Atmos. Oceanic Technol. **15**: 1414–1432.

Smith, P.C. 1983. The mean and seasonal circulation off southwest Nova Scotia. J. Phys. Oceanogr. **13**(6): 1034–1054.

Wonham, M.J.,Walton, W.C., Ruiz, G.M., Frese, A.M., and Galil, B.S. 2001. Going to the source: role of the invasion pathway in determining potential invaders. Mar. Ecol. Prog. Ser. **215**: 1–12.

Fatty acid dynamics during the spring bloom in a High Arctic fjord: importance of abiotic factors versus community changes

Eva Leu, Stig Falk-Petersen, Slawomir Kwaśniewski, Angela Wulff, Kåre Edvardsen, and Dag O. Hessen

Abstract: We followed the fatty acid composition of particulate organic matter (POM) in a High Arctic fjord (79°N; Svalbard, Norway) during and after the spring bloom. The content of essential polyunsaturated fatty acids (PUFAs) was highest (45% of total fatty acids) at the beginning of the bloom, well before the biomass maximum, and decreased linearly towards the end (30%). During the postbloom period, the concentrations of PUFAs remained stable, between 25% and 30%. Redundancy analysis was used to identify the environmental factors that explained the observed variability in the fatty acid composition of phytoplankton. A particular emphasis was put on the potential influence of high irradiances. During the spring bloom, nutrient availability (Si and N), as well as shifts in phytoplankton community composition and chlorophyll *a*, were shown to account for much of the pattern in fatty acid composition. During the postbloom period, particularly during periods of stratification, light had a pronounced effect on the fatty acid composition. In general, we found a decrease in the relative amount of PUFAs under high light intensities and nutrient limitation.

Résumé : Nous avons suivi la composition en acides gras de la matière organique particulaire (POM) dans un fjord du haut-arctique (79°N, Svalbard, Norvège) avant et après la prolifération printanière des algues. La concentration d'acides gras polyinsaturés (PUFA) essentiels est maximale (45 % des acides gras totaux) au début de la période de prolifération, bien avant le maximum de biomasse; elle décline ensuite linéairement jusqu'à la fin (30%). Durant la période qui suit la prolifération, les concentrations de PUFA restent stables, à 25–30 %. Une analyse de redondance permet d'identifier les facteurs du milieu qui expliquent la variabilité observée de la composition en acides gras du phytoplancton. Nous nous intéressons en particulier au rôle potentiel des fortes irradiations. Durant la prolifération printanière, la disponibilité des nutriments (Si et N), de même que les changements de composition de la communauté phytoplanctonique et de la chlorophylle *a*, expliquent en grande partie les patrons de composition en acides gras. Après la prolifération, surtout durant les périodes de stratification, la lumière a un effet marqué sur la composition en acides gras. En général, il se produit une diminution de la quantité relative de PUFA dans les conditions de fortes intensité lumineuse et de limitation des nutriments.

[Traduit par la Rédaction]

Introduction

The High Arctic is characterized by a strong seasonality and, in general, a brief spring bloom when the bulk of the autotrophic biomass is produced. Hence, for the entire ecosystem, productivity is acutely susceptible to environmental conditions during this period. Light is supposed to be the key regulator of production in ice-covered areas (Smetacek and Nicol 2005), yet it plays a dual role. Despite being essential for primary production, light, especially ultraviolet radiation (UVR, 280 00 nm), has been proven to inhibit algal photosynthesis and growth (Cullen and Neale 1994; Hanelt 1996; Vernet 2000).

Interestingly, light has also been identified as one of the main factors determining food quality in terms of stoichiometry and fatty acids (Thompson et al. 1993; Urabe and Sterner 1996). The nutritional quality of available food affects the transport of energy and matter through the food web (Gulati and DeMott 1997; Anderson and Pond 2000; Arendt et al. 2005). Polyunsaturated fatty acids (PUFAs) are

---

Received 14 December 2005. Accepted 29 September 2006. Published on the NRC Research Press Web site at http://cjfas.nrc.ca on 15 December 2006.
J19047

E. Leu[1,2] and D.O. Hessen. University of Oslo, Department of Biology, P.O. Box 1066, 0316 Oslo, Norway.
S. Falk-Petersen. Norwegian Polar Institute, 9296 Tromsø, Norway.
S. Kwaśniewski. Institute of Oceanology, Polish Academy of Sciences, Marine Ecology Department, Powstancow Warszawy 55, 81-712 Sopot, Poland.
A. Wulff. Göteborg University, Department of Marine Ecology, Marine Botany, P.O. Box 461, 40530 Göteborg, Sweden.
K. Edvardsen. Norwegian Institute for Air Research (NILU), 9296 Tromsø, Norway.

[1] Corresponding author (e-mail: e.s.leu@bio.uio.no).
[2] Present address: Norwegian Polar Institute, 9296 Tromsø, Norway.

Can. J. Fish. Aquat. Sci. **63**: 2760–2779 (2006) doi:10.1139/F06-159

essential key metabolites, synthesized only by algae (Sargent et al. 1995), and are of particular importance in polar ecosystems. Most organisms at these latitudes use lipid reserves to cope with periods of poor food supply (Falk-Petersen et al. 2000; Hagen and Auel 2001). Hence, lipids and essential PUFAs are transported and enriched effectively in the pelagic food web (Falk-Petersen et al. 1990). PUFAs are necessary for the functioning of vital membrane-bound physiological processes and contribute to the regulation of membrane fluidity, particularly under low temperatures (Nishida and Murata 1996; Hall et al. 2002). Studies of biochemical changes in particulate organic matter (POM) have revealed a strong seasonality of fatty acid composition (Mayzaud et al. 1989; Skerratt et al. 1995; Reuss and Poulsen 2002), with the highest amounts of PUFAs usually found during the early phase of spring bloom (Parrish et al. 2005). The results of these studies point to two main drivers for the dynamics in fatty acid profiles: (*i*) changes in species composition due to natural succession, and (*ii*) the physiological state of the phytoplankton determined mainly by the availability of nutrients. The importance of both has been confirmed further in mesocosm experiments (Mayzaud et al. 1990; Hayakawa et al. 1996).

Adding to these two drivers, light potentially may also affect fatty acid composition in autotrophs. In laboratory studies, photosynthetically active radiation (PAR; 400–700 nm) and UVR have been shown to affect phytoplankton fatty acid composition (Thompson et al. 1993; Goes et al. 1994; Skerratt et al. 1998). Experimental studies by our group revealed that fast changing or high intensities of PAR can lead to major reductions in the relative amount of PUFAs in the Arctic diatom *Thalassiosira antarctica* var. *borealis*, thereby decreasing its nutritional quality for grazers (Leu et al. 2006*b*), whereas UVR had no negative effect on the relative amount of PUFAs in several diatom species (Leu et al. 2007). However, the relevance of these observations for the in situ situation remained to be verified. The spring bloom in the High Arctic starts shortly before or after ice breakup (Wiktor 1999; Engelsen et al. 2002; Sakshaug 2004) and usually follows the retreating ice edge northwards (Sakshaug and Slagstad 1991; Sakshaug 2004), with the bulk of autotrophic biomass concentrated in the nutrient-rich meltwater layer close to the surface, stabilized by a halocline (Engelsen et al. 2004). Ice breakup, as well as rapidly changing albedo, and weather conditions with shifting cloud cover expose phytoplankton to variable and temporarily very high irradiances. In addition, temporal fluctuations and seasonal depletion of stratospheric ozone are frequently observed during the Arctic spring (Dahlback 2002), resulting in a periodic increase of potentially harmful UVB radiation (280–320 nm). Little is known about the extent to which the interplay between these factors may affect the nutritional quality in terms of fatty acid composition of POM in the Arctic pelagic ecosystem.

Thus, we followed the temporal development of POM fatty acid composition in a High Arctic fjord during and after spring bloom, with special focus on the relative amount of PUFAs. In addition to spectral vertical profiles of underwater irradiance, PAR and UVR were measured continuously in air. Phytoplankton species composition, photosynthetic and photoprotective pigments, nutrient availability, and hydrographic conditions were monitored throughout the sampling period. Environmental factors explaining the observed variability in fatty acid composition were identified using redundancy analysis (RDA). In particular, we wanted to clarify the potential impact of irradiance on POM fatty acid composition in situ compared with species composition and nutrient availability.

Materials and methods

Study area and sampling

Waters in Kongsfjorden, Svalbard, Norway (78°57′N, 11°50′E), were sampled about twice a week from 17 April to 23 May 2003 and from 8 May to 8 June 2004 at station K3 (Fig. 1). Two additional stations in the outer part of the fjord (Fig. 1, K1 and K2) were sampled once each year (23 May 2003 and 8 June 2004). Sampling was usually performed during daytime, although the transect samples in 2004 were taken during night (midnight sun). Vertical profiles of temperature, salinity, density, and in situ fluorescence were measured with a CTD (conductivity, temperature, and depth) profiler (SD 204; SAIV A/S, Bergen, Norway), equipped with a Seapoint chlorophyll fluorometer (Seapoint Sensors Inc., Exeter, New Hampshire). Water samples were taken from six different depths (0, 5, 8, 15, 25, and 35 m) with a 10 L Niskin bottle (Ocean Test Equipment Inc., Fort Lauderdale, Florida). Three depths represented the uppermost 10 m (potentially exposed to detrimental irradiances), and three depths represented the layer from 10 to 50 m, where no detrimental impact of high irradiances was expected. If there was a clear fluorescence maximum deeper than the standard sampling depths, additional samples were taken. Subsamples were filtered for analyses of the following variables: fatty acid composition, chlorophyll *a* (Chl *a*), pigment composition, and elemental ratios (C, N, P) of the POM. In addition, 250 mL from each depth were preserved in a 1.6% formalin solution, buffered with borax, for quantitative analysis and identification of phytoplankton species. Unfiltered water samples were taken for nutrient analysis (total N, Si, P) at the outset, middle, and end of each year's sampling series.

Phytoplankton identification and counting were carried out at the Institute of Oceanology of the Polish Academy of Science in Sopot using an inverted microscope (Nikon TM-300 at magnifications of 100× and 400×) and following the method described by Utermöhl (1958). Diatoms and dinoflagellates were identified to the species or genus level, whereas other flagellates were identified to family or noted as unidentified. Biomasses (μg $C \cdot L^{-1}$) of dominating taxa were calculated according to geometrical measurements obtained during the microscopic analyses or simply taken from Biological Atlas of the Arctic Seas 2000, Plankton of the Barents and Kara Seas (http://www.nodc.noaa.gov/OC5/BARPLANK/WWW/HTML/plankton.html).

UV and PAR measurements

In 2003, underwater profiles of UVR were measured down to a depth of 20 m using a custom-made underwater radiometer (NILU-UV; NILU Products AS, Kjeller, Norway) measuring at wavelengths of 305, 312, 320, 340, and 380 nm. In 2004, we used a custom-made RAMSES ACC UV sensor (TriOS GmbH, Oldenburg, Germany) to measure

Fig. 1. Sampling area (Kongsfjorden, Svalbard) indicating the locations of the three sampling stations K1, K2 and K3. Standard sampling was carried out at K3.

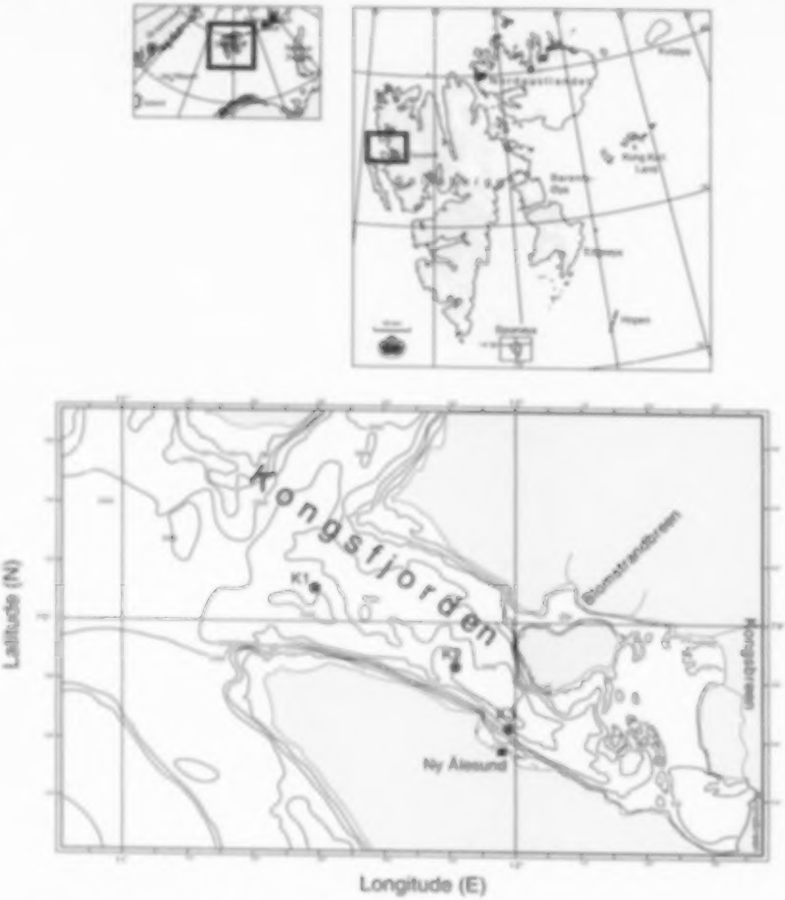

wavelengths over the 290–400 nm range. The depths of the 10% and 1% relative UVR levels were calculated using the following equation (see, e.g., Kirk 1994):

$$I(z) = I_0 \exp(-z K_d)$$

where $I(z)$ is the radiation level at depth z, I_0 is the incidence surface level, and K_d is the diffuse attenuation coefficient as calculated from the measurements. Daily average values of stratospheric ozone, as well as erythemally weighted daily doses of UVR (CIE, Commision International de l'Eclaire) were obtained from the GUV radiometer (Biospherical Instruments Inc., San Diego, California), located on the roof of the Sverdrup Research Station (Norwegian Polar Institute), Ny-Ålesund (78°55′N, 11°56′E).

Underwater profiles (0–40 m) of PAR (400–700 nm) were only measured in 2004, using an underwater spherical quantum sensor (Quantum Li-193 SA; LiCor, Lincoln, Nebraska), and a cosine-corrected flat-head reference sensor (Quantum Li-190SA; LiCor). PAR in the air was recorded continuously with a cosine-corrected Quantum sensor (QS-200; Delta-T Devices Ltd., Cambridge, UK) located on the roof of the Sverdrup Research Station.

Table 1. Fatty acid trophic markers (FATM) for different phytoplankton groups.

Taxonomic group	FATM	Reference
Diatoms	20:5(*n*-3)	Dalsgaard et al. (2003)
	16:4(*n*-1)	Mayzaud et al. (1990)
Flagellates	18:4(*n*-3)	Reuss and Poulsen (2002)
	22:6(*n*-3)	
Phaeocystis pouchetii	18:1(*n*-9)	Reuss and Poulsen (2002)
	18:1(*n*-7)	Dalsgaard et al. (2003)
	14:0	Skerratt et al. (1995)

Fatty acid analysis

Two water samples of 3 L each from six different depths (0, 5, 8, 15, 25, 35 m) were filtered onto GF/C glass fibre filters (Whatman, Maidstone, UK) prewashed with chloroform–methanol (2:1, *v/v*). The filters were transferred to glass vials with Teflon-lined caps, 8 mL chloroform–methanol (2:1, *v/v*) was added, and the vials were stored at –80 °C. Because little material was available in 2004, samples from 0, 5, and 8 m and from 15, 25, and 35 m were

Table 2. Photosynthetic marker pigments for specific taxonomic groups of phytoplankton.

Taxonomic group	Marker pigment	Reference
Diatoms	Fucoxanthin	Stauber and Jeffrey (1988)
Phaeocystis pouchetii	19′-butanoyloxyfucoxanthin	Jeffrey and Wright (1994)
Dinoflagellates	Peridinin	Jeffrey et al. (1975)
Cryptophytes	Alloxanthin	Pennington et al. (1985)
Chlorophytes	Chlorophyll *b* Neoxanthin	Jeffrey and Vesk (1997)
Some prasinophytes	Prasinoxanthin	Foss et al. (1984)

pooled before analysis. Total lipid was extracted according to the procedure described in Folch et al. (1957). A known amount of heneicosanoic acid (21:0) was added as internal standard, and an acid-catalysed transesterification was carried out with 1% sulfuric acid in methanol (Christie 1982). The extract was cleaned on a silica column (Christie 1982). The percent composition of fatty acid methyl esters (FAME) was determined using a N gas chromatograph (Agilent 6890; Agilent Technologies, Santa Clara, California) equipped with a fused silica, wall-coated capillary column (50 m × 0.25 mm inner diameter, Varian Select FAME) and an Agilent 7683 injector and flame ionization detector. Hydrogen was used as carrier gas. Samples were injected at a temperature of 280 °C, and the thermal gradient was raised from 60 to 150 °C at 30 $°C \cdot min^{-1}$ and then to a final temperature of 230 °C at 1.5 $°C \cdot min^{-1}$ (maintained for 2 min). Individual FAME were identified by comparison with two known standards (GLC-96 quantitative standard for identification and quantification of FAME (Nu-Chek Prep Inc., Elysian, Minnesota) and MARINOL qualitative standard obtained from James Henderson (University of Stirling, personal communication)) and were quantified using the HPChemStation software (Hewlett-Packard Co., Palo Alto, California). Certain fatty acids are characteristic for specific taxonomic groups of phytoplankton and can therefore be used as (trophic) markers (see Table 1 and Dalsgaard et al. 2003).

Photosynthetic pigments

Samples from all six depths were taken for a complete analysis of all photosynthetic pigments by high performance liquid chromatography (HPLC). Seawater (500–1000 mL) was filtered onto GF/C filters. The filters were put in liquid nitrogen (–196 °C) and later stored at –80 °C. The pigments were extracted in 1.5 mL 100% MeOH. The extracts were sonicated for 30 s using a Vibra-cell sonicator (Sonics and Materials Inc., Danbury, Connecticut) equipped with a 3 mm diameter probe (cf. Wright and Jeffrey 1997). The extraction and HPLC analyses were carried out according to Wright and Jeffrey (1997), using an absorbance diode-array detector (Spectra-Physics UV6000LP; Newport Corporation, Spectra-Physics Finnigan, Thermo Fisher Scientific, Waltham, Mass.) equipped with a 150 × 3.20 mm C18 column (Ultracarb 3 µm ODS (20); Phenomenex, Torrance, California) and a 4 × 3.0 mm C18 guard column (SecurityGuard; Phenomenex). Chlorophyll breakdown products were integrated and quantified at 668 nm. The breakdown products were pooled and the ratio to Chl *a* (668 nm) was calculated. The HPLC system was calibrated with pigment standards obtained from DHI, Water and Environment, Denmark. Peak identities were further confirmed by online recording of absorbance spectra (400–700 nm) as described by Wright and Jeffrey (1997). Pigments were expressed as ratios to Chl *a* (by weight). In addition, fluorometrical analyses of Chl *a* concentrations were carried out in 2003. Seawater (500 mL) was filtered onto GF/C glass fibre filters and extracted in 10 mL 90% acetone (*v/v*) for 2 h at room temperature in darkness. Chl *a* concentrations were then determined using a Turner field fluorometer (Turner 10-AU-005-CE; Turner Designs Inc., Sunnyvale, California). Pigments were further divided into major taxonomic marker pigments (Table 2; Jeffrey and Vesk 1997) and photoprotective pigments, e.g., diadinoxanthin (Dd), diatoxanthin (Dt) (Olaizola and Yamamoto 1994), zeaxanthin, and lutein (Schlüter et al. 2000).

Nutrients and stoichiometry

Concentrations of total nitrate, silicate, and phosphate (the latter only in 2004) were analysed from unfiltered water samples. Samples from 0, 5, and 8 m and from 15, 25, and 35 m, respectively, were pooled. Phosphate samples were preserved with 1% (*v/v*) 4 $mol \cdot L^{-1}$ sulfuric acid and stored in the dark at 4 °C until analysed. Nitrate and silicate samples were stored cold (4 °C) and in the dark, without preservation, until analysis. Total P (TP) and total N (TN) were analysed on a auto-analyser (San Plus; Skalar Analytical Instruments, Breda, the Netherlands) with a photometric detector (Matrix SA 6250-02; Skalar) after persulfate digestion of nonfiltered samples. TP was determined with the molybdate-blue method at 880 nm (Norsk Standard NS 4725) and TN was determined as nitrate at 540 nm after reduction with cadmium (Norsk Standard NS 4745). Silicon was analysed according to the method described by Koroleff (1985).

Samples for analysis of particulate C, N, and P were taken on three occasions in 2003 (immediately before and immediately after the peak of the spring bloom and on the very last sampling day) and once in the postbloom period in 2004. Samples from 0 to 8 m and from 15 to 35 m were pooled. Volumes of 500 mL were filtered onto precombusted (3 h, 500 °C) GF/C filters. For particulate phosphate analysis, the filters were prewashed with HCl. All samples were stored at –20 °C until analysis. Particulate C and N were analysed on a elemental analyser (FlashEA 1112; Thermo Finnigan, Milano, Italy). Particulate P analyses consisted of placing the filters in 15 mL distilled water that was acidified (150 µL, 4.0 $mol \cdot L^{-1}$ H_2SO_4), adding peroxodisulfate (0.15 g $K_2S_2O_8$), and autoclaving (121 °C, 1 h). The particulate fraction of P was then analysed spectrophotometrically by the standard ammonium–molybdate method (Hessen et al. 2002).

Fig. 2. Development of temperature, salinity, and in situ fluorescence during the spring bloom in 2003 and after the spring bloom (2004) at sampling station K3.

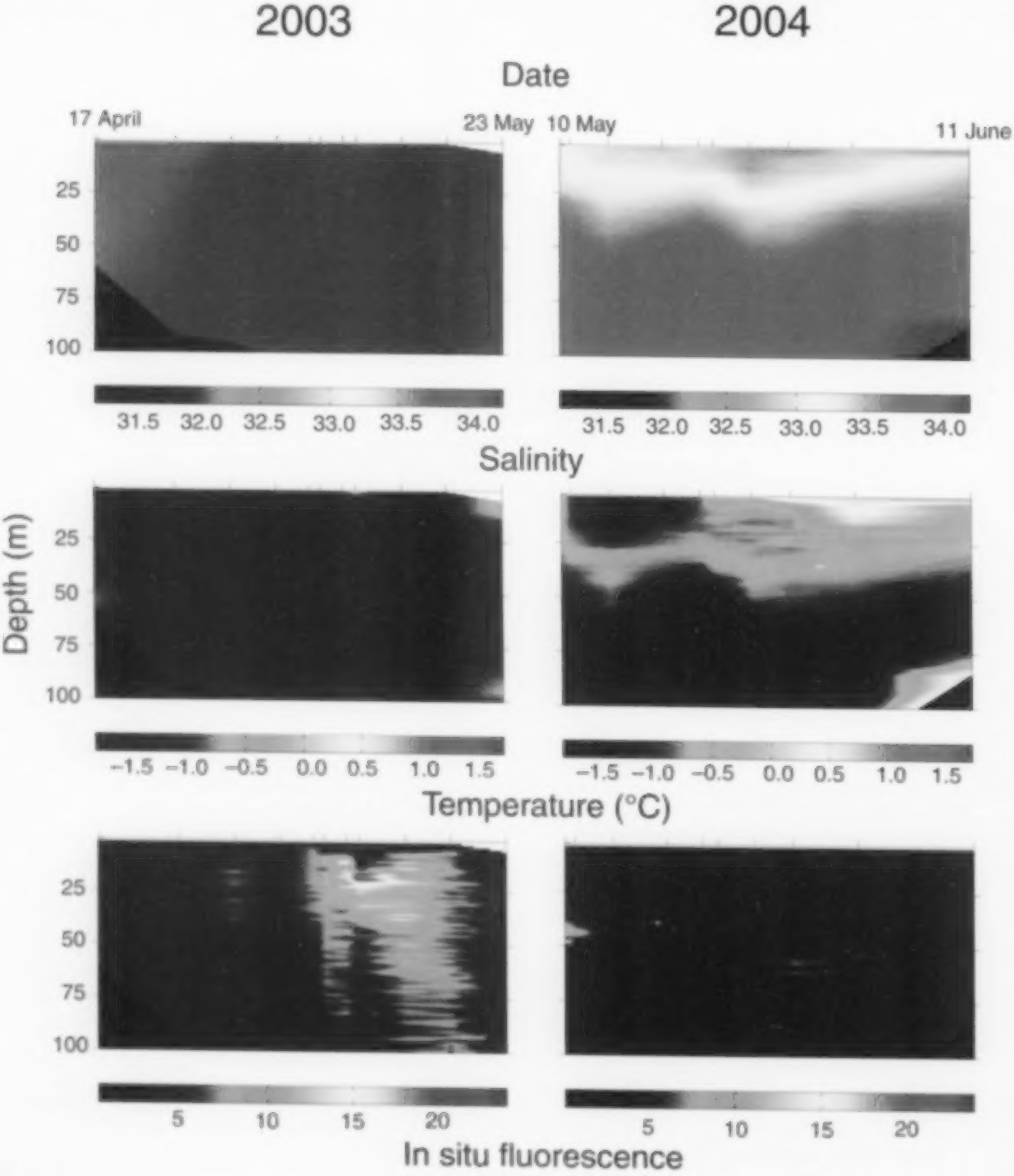

Fig. 3. Chlorophyll *a* (Chl *a*) concentrations ($\mu g \cdot L^{-1}$) obtained by high-performance liquid chromatography (HPLC) analysis (*a*) during spring bloom and (*b*) after spring bloom (0–8 m, ○; 15–35 m, ●).

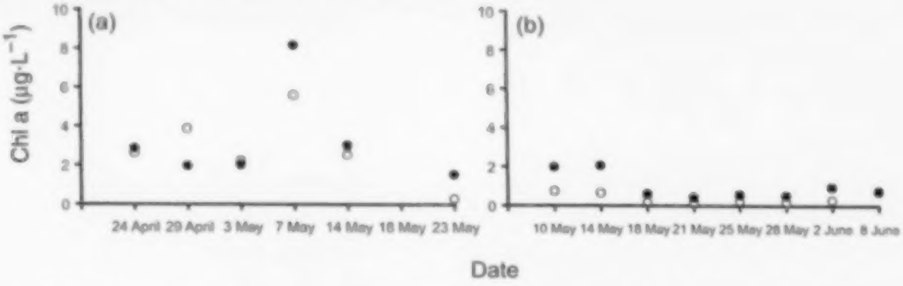

Fig. 4. Daily doses of ultraviolet (UV) radiation (erythemally (CIE) weighted) and stratospheric ozone values (Dobson units (DU)), measured on the roof of the Sverdrup Research Station in 2003 and 2004 (▲, ozone 2003; □, ozone 2004; solid bars, daily UV dose 2003; open bars, daily UV dose 2004).

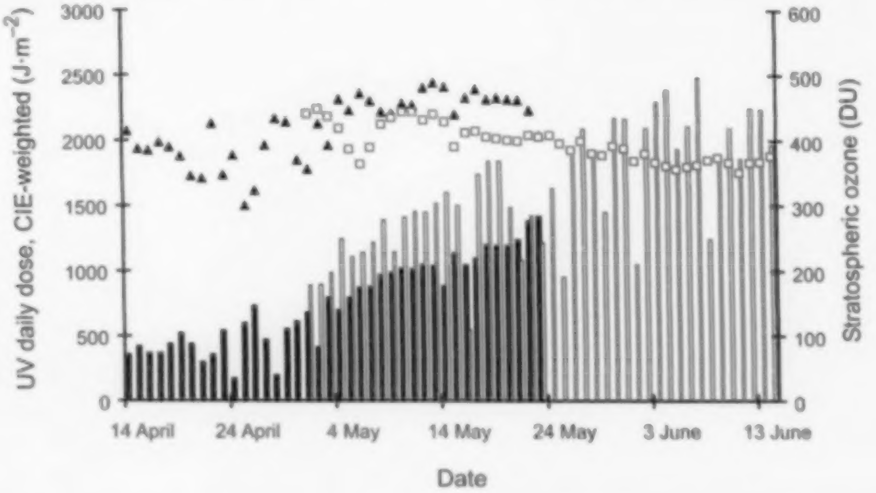

Statistical analyses

To estimate the proportion of variance in the fatty acid composition (%) of POM that can be explained by a linear combination of predictor variables (called environmental variables in CANOCO), a multivariate direct gradient analysis (redundancy analysis, RDA) was performed, using the CANOCO software 4.5 for Windows (ter Braak and Smilauer 2002). A detailed description of this method can be found in Legendre and Legendre (1998). First, from a number of environmental factors potentially affecting the variability in the data set, a subset of predictor variables is chosen based on their explanatory power and the significance of their contribution (tested by Monte Carlo permutation). This model is then used for a multivariate gradient analysis in which the response variables are constrained to be a linear combination of these predictor variables. From this analysis, object scores are calculated and an ordination plot is derived. Fatty acids accounting for less than 1% in all samples were removed from the data set before analysis, without recalculating the percentages of the remaining fatty acids. Nontransformed percentage values were used in all analyses. In the RDA, the samples and fatty acids were assigned scores on ordination axes, the first two axes of which are shown in the ordination biplot. Environmental variables are represented by arrows, pointing in the direction of maximum variance accounted for by the respective variable. The Monte Carlo permutation test was run with 9999 permutations, restricted for split-plot design, with a whole plot consisting of the samples taken on the same day. Whole plots were chosen to be freely exchangeable in the permutation test, but no permutation was allowed on the split-plot level. First, the marginal effects for all environmental variables were tested, and then the significant factors ($p < 0.05$) were included in the model by stepwise selection. The overall significance of the model was tested in another Monte Carlo permutation test on all canonical axes with 9999 permutations, restricted for split-plot design as described above. Selected supplementary variables were included in the analysis as passive variables to display them in the results plot.

The significance of dissimilarity in fatty acid and pigment composition between the two depth layers during the post-bloom period was tested with an ANOSIM (analysis of similarities; Clarke 1993; Clarke and Green 1988), using PRIMER 5.9.2. This procedure uses a test statistics (R) based on the difference between the average of all rank dissimilarities between objects between and within groups.

Fig. 5. K_d values for different wavelengths (312/310, 320, 340, 380, 400 nm), calculated from underwater ultraviolet measurements in 2003 and 2004.

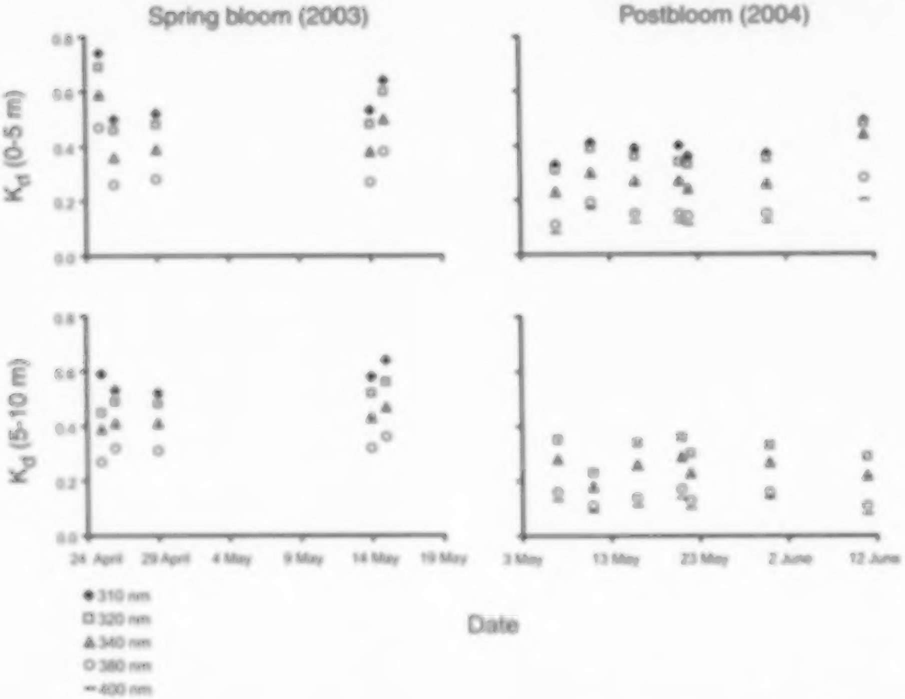

Fig. 6. Photosynthetically active radiation (PAR) measured on the roof of the Sverdrup Research station, Ny-Ålesund (hourly average values for May–June 2004).

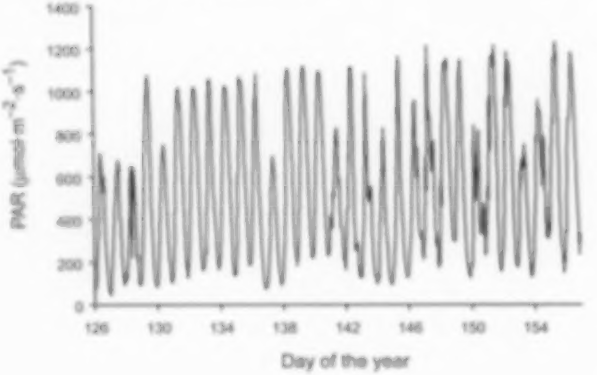

R values range in theory from –1 to 1, with *R* = 0 confirming the null hypothesis. Large (positive) *R* values indicate a clear separation of the groups, whereas small values indicate a within-group variability similar to the between-group variability. To elucidate the contribution of single fatty acids or pigment ratios to the average dissimilarity between groups, the SIMPER routine in PRIMER was used (Clarke 1993).

For testing differences in single variables between years or depths, *t* tests were applied, given that variances were homogenous (tested with Levene's test). If they were not homogenous, a nonparametric Mann–Whitney *U* test was used. For all tests, the threshold for significance was set at $p < 0.05$. All univariate analyses were carried out using STATISTICA 7.0 (StatSoft Inc. 2004).

Results

During the first sampling campaign in 2003, we followed a typical diatom-dominated spring bloom, whereas a postbloom situation was followed in 2004. The main focus of the study was to compare the fatty acid dynamics during both situations and identify the importance of the respective environmental factors, particularly light, for the observed changes.

Hydrography, UV radiation, and underwater light conditions

From mid-April until the end of May 2003, the uppermost 60 m of the water column was characterized by winter cold water (cf. Svendsen et al. 2002), with temperatures below –0.7 °C (Fig. 2). Salinity ranged from 34.1 to 34.4, with a homogenous vertical distribution. Vertical in situ fluorescence profiles showed the development of a spring bloom, with a peak in Chl *a* concentration on 10 May at about 20 m depth (>10 µg Chl $a \cdot L^{-1}$; Fig. 2). Other than on this day, Chl *a* was distributed evenly in the uppermost 50 m. Chl *a* values obtained by HPLC analyses ranged from <1 to 8 µg Chl $a \cdot L^{-1}$ (Fig. 3*a*). Stratospheric ozone values were high and stable (450 ± 31 Dobson units (DU), mean ± SD; Fig. 4). Daily doses of UVR (CIE-weighted) ranged from

Table 3. Underwater PAR intensities ($\mu mol \cdot m^{-2} \cdot s^{-1}$) measured during the postbloom period in Kongsfjorden (2004).

	16 May	21 May	22 May	31 May	11 June
PAR at different depths					
5 m	185	713	202	608	278
8 m	139	461	158	415	176
15 m	68	212	83	188	82
35 m	6	15	10	13	12
Weather	Overcast	Sunny	Overcast	Sunny	Overcast
Local time	1800	1400	1345	1615	1145

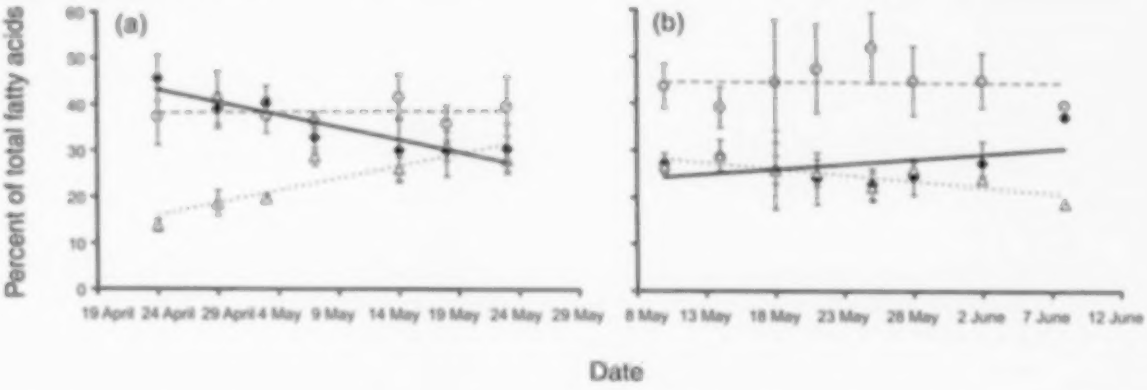

Fig. 7. Changes in the percentages of polyunsaturated (PUFA; solid diamonds), monounsaturated (MUFA; open triangles), and saturated fatty acids (SFA; shaded circles) (*a*) during spring bloom and (*b*) after spring bloom. Average values are shown for each sampling day calculated from the six (2003) or three (2004) different samples analysed per sampling day (PUFA, solid lines; MUFA, dotted lines; SFA, broken lines).

167 to 1414 $J \cdot m^{-2}$, increasing over the whole period because of an increase in solar angle (Fig. 4). K_d values for the four different wavelengths (312, 320, 340, and 380 nm) were constant throughout the sampling period (Fig. 5).

In 2004, water temperatures in the first half of May were homogenous (< –0.5 °C; see Fig. 2), with a lower salinity (33.0–33.6) in the upper 40–50 m (Fig. 2). There was a stable halocline at 50 m throughout the period from 8 May to 9 June. Because of local melting of drift ice, salinity close to the surface dropped below 33. In combination with the warming of the surface water starting in the middle of May, this led to stratification of the surface layer. The in situ fluorescence profiles indicated low phytoplankton concentrations during the entire sampling period, with a deep peak of varying intensity between 40 and 60 m (Fig. 2). This was confirmed by the HPLC analyses, showing less than 2 $\mu g \cdot L^{-1}$ in all samples (Fig. 3*b*). Throughout the period, stratospheric ozone was as high as in 2003, ranging from 350 to 450 DU (Fig. 4). CIE-weighted daily doses of UVR in air were between 890 and 2500 $J \cdot m^{-2}$ (Fig. 4), and 1% depths for UVA (320–400 nm) and UVB (280–320 nm) ranged from 20 to 29 m and from 12 to 14.5 m, respectively. All K_d values were lower than in the previous year (Fig. 5), owing to lower phytoplankton biomasses. PAR values measured at noon varied between 700 and 1200 $\mu mol \cdot m^{-2} \cdot s^{-1}$, depending on weather conditions; minimum values at night were 100–300 $\mu mol \cdot m^{-2} \cdot s^{-1}$ (Fig. 6). Underwater PAR intensities measured at the sampling depths are provided (Table 3). The 1% depth for PAR varied between 30 m and 40 m.

Fatty acid composition of POM

In 2003, two weeks before the Chl *a* maximum of the spring bloom (10 May), PUFAs made up 45% of the fatty acids in the POM, decreasing steadily to 28% by the end of May (Fig. 7). The major PUFAs were 20:5(*n*-3), three C18(*n*-3) PUFAs, and 16:4(*n*-1), followed by 22:6(*n*-3) (Table 4*a*). The decrease in PUFAs was mainly due to a decrease in 20:5(*n*-3) and 16:4(*n*-1). Over the same period, the relative amount of monounsaturated fatty acids (MUFAs) increased from 14% to 28%. Changes in MUFAs were attributed largely to 16:1(*n*-7), 18:1(*n*-9), and 18:1(*n*-7) (Table 4*a*). The percentage of saturated fatty acids (SFA) dominated by 14:0 and 16:0 ranged from 36% to 41% and did not change from mid-April to the end of May (Fig. 8). However, on an individual basis, 14:0 increased from an initial 4% to approximately 10% by mid-May.

A ranking of the environmental variables included in the RDA model is provided (Table 5). The multivariate analysis of the fatty acid composition of all POM samples from station K3 in 2003 showed a distribution of the samples along two main gradients (Fig. 8). The first gradient followed the decreasing nutrient availability (Si–N) and diatom dominance (indicated as a decreasing fucoxanthin – Chl *a* ratio). This gradient represented the temporal changes in fatty acid

Table 4a. Fatty acid composition (percent of total fatty acids) of particulate organic matter sampled at depths of 0–8 and 15–35 m

(*a*) During spring bloom 2003.

	KB 3							
	24 April		29 April		3 May		7 May	
	0–8 m	15–35 m	0–8 m	15–35m	0–8 m	15–35m	0–8 m	15–35m
Fatty acids								
14:0	3.9	3.8	7.0	5.1	4.5	5.1	9.6	8.6
15:0	0.8	1.1	0.6	1.1	0.9	0.8	0.6	0.5
16:0 pristanic	1.1	1.0	2.9	2.3	2.0	1.9	3.6	4.5
16:0	19.3	18.1	18.2	23.6	19.1	17.9	16.8	15.6
16:1(*n*-9)	0.3	0.4	0.1	0.4	0.2	0.1	0.2	0.2
16:1(*n*-7)	9.8	8.8	17.9	12.2	15.2	16.6	21.7	20.8
16:1(*n*-5)	0.8	1.1	1.0	1.8	0.6	0.2	1.7	1.6
16:2(*n*-7)	1.9	2.3	1.9	1.5	1.9	2.1	1.4	6.0
16:3(*n*-4)	0.8	1.2	1.9	1.5	1.5	1.7	0.9	1.3
16:4(*n*-1)	7.2	6.9	6.4	5.7	4.7	5.3	2.3	2.7
17:0 phytanic	0.2	0.2	0.2	0.3	1.1	2.4	1.0	1.2
17:0	3.5	4.4	3.2	3.8	4.0	3.7	2.3	2.6
18:0	9.9	5.2	3.8	8.0	5.3	4.9	2.5	2.3
18:1(*n*-9)	0.6	1.1	0.9	1.0	2.3	0.7	3.9	3.0
18:1(*n*-7)	0.8	0.7	0.4	0.6	0.7	0.5	0.8	0.7
18:2(*n*-6)	2.3	1.7	2.4	1.5	3.1	2.3	4.0	2.4
18:3(*n*-3)	1.5	1.6	1.1	0.9	1.6	1.4	1.2	0.9
18:4(*n*-3)	4.6	5.4	6.4	5.0	6.0	6.3	5.2	5.0
18:5(*n*-3)	4.6	4.8	3.5	4.1	5.4	4.9	4.0	2.8
20:0	0.5	0.6	0.3	0.5	0.4	0.4	0.2	0.2
20:3(*n*-3)	1.1	0.3	0.3	1.1	1.0	0.9	0.1	0.4
20:5(*n*-3)	14.6	15.7	14.1	11.9	10.7	12.1	9.3	9.4
22:0	0.1	0.3	0.1	0.1	0.0	0.0	0.2	0.0
22:6(*n*-3)	5.1	6.9	3.2	3.7	3.7	4.0	3.1	2.7
24:0	0.5	0.4	0.1	0.5	0.4	0.4	0.2	0.2
Sum SFAs	39.6	35.1	36.5	45.4	37.7	37.5	37.1	35.8
Sum MUFAs	13.5	13.9	20.8	16.5	20.3	19.1	29.1	28.2
Sum PUFAs	43.9	47.3	41.1	37.0	39.8	40.9	31.9	33.7
Sum (*n*-3) PUFAs	32.3	35.8	30.4	28.2	29.9	31.2	23.9	22.6
Sum (*n*-6) PUFAs	4.4	4.6	4.3	3.0	5.2	4.4	5.7	8.5
Ratio 16:1(*n*-7) to 16:0	0.5	0.5	1.0	0.5	0.8	0.9	1.3	1.3

(*b*) During the postbloom period in 2004.

	KB 3										
	10 May		14 May			18 May		21 May		25 May	
	0–8 m	15–35 m	0–8 m	15–35 m	50 m	0–8 m	15–35 m	0–8 m	15–35 m	0–8 m	15–35 m
Fatty acids											
14:0	8.4	8.7	9.1	9.2	8.0	7.9	8.2	6.7	7.8	6.4	9.1
14:1	1.4	1.0	1.2	1.2	0.9	1.2	0.9	1.4	1.0	1.3	1.5
15:0	1.2	1.2	1.2	0.8	1.3	1.3	0.8	1.4	0.9	1.5	1.4
16:0 pristanic	0.6	0.7	0.6	0.9	0.6	0.3	0.4	0.2	0.4	0.3	0.3
16:0	25.8	21.8	23.3	19.7	28.7	27.9	20.0	30.3	23.8	31.9	26.0
16:1(*n*-9)	1.3	2.4	1.2	0.6	1.6	1.3	0.6	1.7	1.1	1.8	1.2
16:1(*n*-7)	14.8	14.3	19.0	20.8	14.7	13.9	18.7	10.7	17.3	9.1	13.8
16:4(*n*-1)	1.1	2.4	1.5	1.8	2.0	1.1	2.4	1.1	2.3	1.2	1.1
17:0	1.0	0.8	0.9	0.9	1.0	1.0	0.6	1.0	0.7	0.9	0.8
18:0	8.2	6.0	5.5	3.8	7.1	12.8	4.5	11.5	5.5	13.0	7.0
18:1(*n*-9)	6.3	8.0	5.4	4.2	5.5	5.2	4.5	6.6	4.9	5.6	5.0
18:1(*n*-7)	1.7	1.8	1.9	2.0	1.9	1.9	3.0	2.4	2.8	2.3	2.4
18:2(*n*-6)	4.4	4.5	3.6	3.5	2.9	2.9	2.7	2.9	2.8	3.0	2.7
18:3(*n*-3)	1.6	1.4	1.2	1.1	0.9	0.9	0.8	1.1	0.9	1.0	1.0

during (*a*) the spring bloom in 2003 and (*b*) the postbloom period in 2004 at stations KB1, KB2, and KB3.

						KB 1		KB 2	
14 May		18 May		23 May		23 May		23 May	
0–8 m	15–35m	0–8 m	15–35m	0–8 m	15–35m	0–8 m	15–35m	0–8 m	15–35m
9.1	11.9	7.0	6.5	8.8	7.3	8.7	7.2	7.6	7.9
0.6	0.7	2.2	0.6	0.7	0.5	0.8	0.7	0.8	0.7
3.4	3.6	2.9	2.8	0.3	1.7	0.5	1.2	0.4	1.7
18.1	22.0	19.0	20.0	21.9	21.2	24.9	27.5	27.1	22.7
0.2	0.2	0.2	0.2	0.9	0.9	1.1	1.1	1.2	0.8
16.5	19.0	21.1	22.6	14.9	11.9	12.4	12.1	12.8	14.1
1.4	1.1	1.5	1.8	2.0	0.6	2.1	1.0	1.7	1.0
1.1	0.6	1.4	1.4	1.0	0.9	0.8	0.9	0.8	1.0
0.6	0.6	1.1	1.1	0.6	0.6	0.5	0.5	0.5	0.7
1.6	1.5	2.5	2.7	1.4	1.7	0.9	1.4	1.1	2.0
0.2	0.6	0.9	0.5	0.7	0.6	0.4	0.5	0.7	0.4
2.7	2.3	1.1	1.1	1.2	1.2	1.3	1.5	1.6	1.1
3.5	3.5	2.9	3.6	4.8	5.6	6.6	8.9	8.3	5.2
3.8	3.8	3.5	3.3	5.0	9.7	3.4	3.9	3.8	4.5
1.7	1.7	1.8	2.3	3.5	3.5	2.9	2.7	2.9	3.0
5.3	3.5	2.3	1.9	3.8	3.3	4.7	3.6	3.2	3.7
1.6	1.0	0.7	0.6	0.7	0.6	0.9	0.6	0.7	0.6
6.1	4.1	3.9	3.7	0.1	0.2	0.0	0.2	0.1	1.5
6.2	3.4	2.2	2.0	3.5	4.8	5.9	4.0	3.2	5.0
0.3	0.3	0.2	0.2	0.5	0.2	0.5	0.2	0.3	0.3
0.5	0.5	0.5	0.4	0.4	1.3	0.2	0.5	0.2	1.0
7.8	7.0	11.7	12.0	9.4	9.6	8.1	8.0	7.4	10.2
0.0	0.0	0.1	0.0	1.9	1.1	0.6	0.7	2.2	0.5
4.0	3.0	4.4	3.6	6.4	5.5	7.3	5.2	6.3	5.5
0.3	0.2	0.2	0.2	0.7	0.7	0.2	0.4	0.4	0.8
38.2	45.1	36.4	35.5	41.6	40.2	32.9	37.3	35.5	32.3
24.9	27.4	29.9	32.2	28.6	28.6	38.1	36.1	37.5	34.8
35.0	25.3	30.8	29.5	27.5	28.6	18.1	17.0	16.8	23.1
26.8	19.5	24.5	23.3	21.1	22.5	16.2	14.9	14.7	20.4
6.6	4.3	3.8	3.5	4.9	4.4	1.5	1.6	1.4	2.3
0.9	0.9	1.1	1.1	0.7	0.6	0.5	0.4	0.5	0.6

							KB 1			KB 2	
28 May			2 June			8 June	8 June			8 June	
0–8 m	15–35 m	60 m	0–8 m	15–35 m	60 m	0–8 m	0–8 m	15–35 m	30m	0–8 m	15–35 m
11.1	7.8	9.0	7.5	6.3	7.6	6.9	7.0	8.7	8.5	7.2	8.6
1.5	1.1	1.1	1.5	0.8	0.9	0.8	1.2	1.1	0.8	0.9	0.8
1.5	1.1	1.5	1.4	1.0	1.6	1.1	2.4	1.3	1.7	1.2	1.3
0.2	0.3	1.7	0.3	0.5	1.3	0.4	0.2	0.7	1.1	0.3	0.7
27.4	21.7	24.2	26.9	22.9	33.0	20.5	26.9	19.3	26.8	19.4	20.1
1.4	1.7	3.4	1.9	1.3	2.3	1.8	4.6	1.9	3.7	1.8	2.5
13.7	13.1	6.8	10.7	11.9	3.7	7.0	3.6	11.8	5.8	9.0	5.2
1.2	2.9	1.9	0.9	1.7	1.1	1.4	2.6	2.1	2.4	1.5	1.4
0.9	0.8	1.0	1.0	0.8	1.3	0.9	1.3	1.0	1.2	0.8	1.1
6.6	6.2	6.5	9.2	7.5	12.0	7.9	10.9	4.9	8.0	5.5	6.8
5.2	5.8	10.4	6.6	6.7	6.7	6.9	7.0	4.2	8.5	6.4	6.7
2.7	2.3	1.7	2.5	3.2	1.1	1.9	1.6	1.7	1.5	2.2	1.6
2.4	3.0	5.3	3.6	2.8	3.4	3.4	3.8	2.4	3.8	3.6	4.8
0.9	1.2	1.6	1.5	1.1	1.1	1.6	1.3	1.0	2.4	1.6	1.8

Table 4 (*concluded*).

(*b*) During the postbloom period in 2004.

	KB 3										
	10 May		14 May			18 May		21 May		25 May	
	0–8 m	15–35 m	0–8 m	15–35 m	50 m	0–8 m	15–35 m	0–8 m	15–35 m	0–8 m	15–35 m
18:4(*n*-3)	4.3	4.8	4.0	5.6	3.3	2.3	5.4	2.6	4.4	2.9	2.3
18:5(*n*-3)	4.4	3.8	3.9	4.8	2.2	2.4	3.3	2.1	2.9	3.1	2.4
20:0	0.5	0.4	0.5	0.3	0.7	0.8	0.3	0.8	0.5	0.8	0.6
20:1(*n*-9)	0.2	0.2	0.2	0.2	0.7	0.3	0.3	0.4	0.2	n.d.	0.5
20:5(*n*-3)	4.9	7.2	5.9	8.8	6.7	4.9	11.3	5.5	9.4	4.5	5.3
22:0	0.8	0.4	0.8	0.4	1.3	1.3	0.4	1.4	0.8	1.6	1.1
22:6(*n*-3)	4.9	4.6	6.3	5.7	3.7	5.5	5.9	4.9	5.2	4.7	10.5
24:0	0.5	0.4	0.5	0.2	0.7	0.7	0.2	0.7	0.4	0.9	0.5
Sum SFAs	49.6	42.5	44.3	38.4	50.8	55.6	37.1	55.7	42.5	59.5	48.3
Sum MUFAs	32.0	36.6	36.6	40.0	33.6	29.7	41.4	29.7	38.5	26.2	30.9
Sum PUFAs	18.4	20.8	19.1	21.5	15.6	14.7	21.4	14.6	19.0	14.3	20.9
Sum (*n*-3) PUFAs	38.9	38.0	38.6	42.2	35.2	36.6	43.2	37.0	40.2	39.3	43.1
Sum (*n*-6) PUFAs	9.0	8.6	6.4	6.6	6.7	6.9	5.5	7.5	6.0	8.2	6.3
Ratio 16:1(*n*-7) to 16:0	0.6	0.7	0.8	1.1	0.5	0.5	0.9	0.4	0.7	0.3	0.5

Note: SFA, saturated fatty acids; MUFA, monounsaturated fatty acids; PUFA, polyunsaturated fatty acids.

composition from early to late samples, with the highest percentages of PUFAs and diatom markers found in the early samples. Nutrients and the relative diatom biomass accounted for 27% and 5% of the variability in the data set, respectively (partial effects; Table 5). Perpendicular to this first gradient, POM fatty acid composition varied in correlation with the Chl *a* concentrations. Samples with highest Chl *a* content also contained the highest relative values of 16:1(*n*-7) and 16:0 pristanic, whereas 18:0 was found to be high in the samples with lowest Chl *a*. In general, samples taken on the same day clustered together, whereas no consistent pattern according to sampling depth was seen. Neither depth nor radiation proved to be significantly correlated with fatty acid composition (Monte Carlo permutation, $p > 0.05$, data not shown). Together, the three chosen environmental variables accounted for 49.3% of the total variability in the data set. The significance of all canonical axes was high (*F* ratio = 10.37, $p = 0.00013$).

In 2004, SFAs were the largest fraction of fatty acids throughout the entire sampling period, accounting for 39%–52% of total fatty acids (Fig. 7). No time trend was seen, but samples from the surface layer (0–8 m) contained significantly higher percentages of SFA (*t* test, $t = 3.7$, $n = 9$, $p = 0.002$) and had a lower content of PUFAs (*t* test, $t = -2.3$, $n = 9$, $p = 0.03$) than samples from 15–35 m (Table 4*b*). PUFAs and MUFAs were equally represented, ranging from 20% to 30%. Samples taken from the Chl *a* maximum (50–60 m) contained PUFA percentages as low as those from surface samples. The latter had high shares of 18:0 (around 10%), differing significantly from samples taken at 15–35 m (5%–7%; Mann–Whitney *U* test, $Z = 2.34$, $n = 9$, $p = 0.02$). Among the MUFAs, 16:1(*n*-7) was the most abundant fatty acid, with values between 10% and 20%, followed by 18:1(*n*-9) (4%–10%) and 18:1(*n*-7) (1%–3%). PUFAs were represented by several fatty acids occurring in similar abundances, with 20:5(*n*-3) and 22:6(*n*-3) usually reaching the highest values (5%–10%), followed by C18 PUFAs and finally 16:4(*n*-1) (1%–2.5%) (Table 4*b*).

An RDA of POM fatty acid composition separated the samples into two groups according to their sampling depth

Fig. 8. Results of the redundancy analysis (RDA) of the fatty acid composition of particulate organic matter (POM) sampled at station K3 during spring bloom (2003). Six samples for each sampling day are shown. The red arrows point in the direction of maximum variability explained by the respective environmental variable. Broken arrows indicate supplementary variables (which were inactive in the analysis).

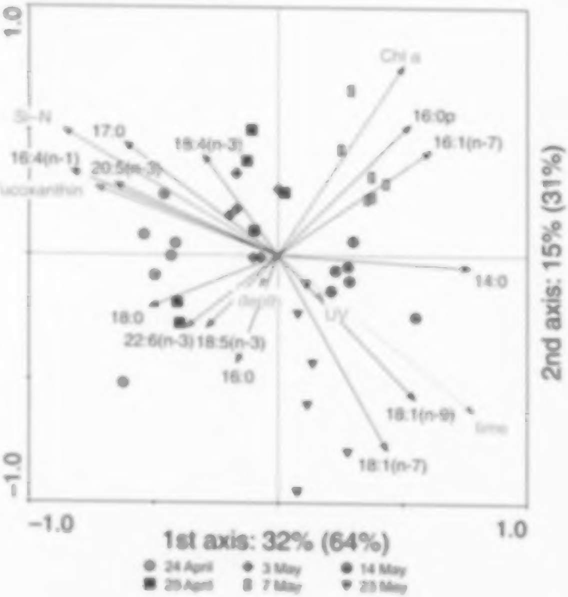

							KB 1			KB 2	
28 May			2 June			8 June	8 June			8 June	
0–8 m	15–35 m	60 m	0–8 m	15–35 m	60 m	0–8 m	0–8 m	15–35 m	30m	0–8 m	15–35 m
2.1	4.4	3.6	3.3	3.9	2.9	5.6	3.0	5.4	3.1	5.6	4.7
1.9	2.8	3.6	3.4	3.2	2.9	4.1	3.7	3.4	4.4	3.9	7.7
0.7	0.5	0.8	0.8	0.6	1.2	0.6	0.9	0.5	0.8	0.5	0.6
0.4	3.3	0.6	0.2	0.4	0.3	0.5	0.4	2.6	0.5	1.3	0.6
4.6	8.3	4.8	4.6	10.9	4.6	11.7	6.1	10.2	5.3	11.7	8.6
1.1	0.8	1.5	1.4	0.9	2.3	0.8	1.1	0.6	1.5	0.5	0.7
8.5	4.5	4.9	7.0	7.0	5.5	9.4	6.2	7.9	5.5	9.9	10.0
0.6	0.5	0.9	0.7	0.6	1.2	0.5	1.0	0.5	0.9	0.5	0.6
51.5	41.4	49.3	51.4	42.7	63.9	41.8	54.1	39.1	52.9	37.7	44.2
30.6	37.5	30.3	29.4	37.5	20.3	32.8	26.3	36.1	27.7	35.7	28.9
17.9	21.2	20.4	19.1	19.8	15.8	25.3	19.7	24.8	19.4	26.7	27.0
38.7	39.9	36.9	41.1	46.0	45.6	56.3	44.6	49.5	43.8	54.0	57.5
6.1	6.2	11.6	8.6	6.2	10.9	7.4	9.8	5.5	7.7	7.2	9.2
0.5	0.6	0.3	0.4	0.5	0.1	0.3	0.1	0.6	0.2	0.5	0.3

(Fig. 9). Of the three environmental factors that were chosen for the RDA model based on significance testing (Table 5), PAR and the relative amount of haptophytes represented the gradients along which the two sample groups differed most. PAR, however, had the strongest (negative) correlation with most of the major PUFAs (20:5(n-3), 16:4(n-1), 18:5(n-3), and to some extent also 18:4(n-3)), whereas 22:6(n-3) and 18:3(n-3) showed weak or no correlation with PAR, but rather were correlated with the relative biomass of flagellates found in the samples (Fig. 9). Surface (0–8 m) and deeper (15–35 m) POM samples were divided along the PAR gradient, with the deeper samples characterized by higher amounts of PUFAs, and the surface samples characterized by high 16:0 and 18:0 values. The zeaxanthin–Chl *a* ratio was strongly correlated with PAR (shown as a passive variable in the plot). Together, the three environmental variables accounted for 58% of the variability in the data set (Table 5), and the canonical axes were highly significant (F ratio = 6.5, p = 0.001). The haptophyte gradient was positively correlated with 18:4(n-3) (usually considered as one of the marker fatty acids for haptophytes; Table 1) and 16:1(n-7). The flagellate-dominated samples, taken on the last day, formed a group and were characterized by high 22:6(n-3) values. Differences in fatty acid composition between the two depth layers were tested with an ANOSIM test. Global differences were moderate but significant (Global R = 0.28, $p < 0.01$). Four fatty acids contributed more than 10% each to the average dissimilarity between the two depth layers: 16:1(n-7), 16:0, 20:5(n-3), and 18:0 (data not shown).

When comparing spring bloom and postbloom periods, we found that the fatty acid composition of POM at station K3 during the spring bloom contained, on average, a significantly larger percentage of PUFAs than during the postbloom period in 2004 (Table 6). C16 fatty acids and the C16 PUFA to C18 PUFA and 16:1(n-7) to 16:0 ratios were also significantly higher during the spring bloom than during the postbloom period. Both the relative amounts of SFA and MUFA were, on average, significantly higher in the samples from the postbloom period (Table 6).

Phytoplankton community composition

Throughout the bloom in 2003, the phytoplankton biomass based on cell counts (5–150 μg C·L^{-1}) was dominated by diatoms (72%–87%; Fig. 10). The dominance of diatoms decreased over time, also reflected in the ratio of fucoxanthin to Chl *a* (Fig. 11). Ice-associated diatoms such as *Nitzschia* spp., *Fragilariopsis cylindrus*, and *F. oceanica*, together with *Thalassiosira antarctica/gravida*, were most abundant in the early phase, whereas *T. nordenskioeldii*, *Chaetoceros socialis*, *C. furcellatus*, and *F. oceanica* were most abundant later. The colonial stage of the haptophyte *Phaeocystis pouchetii* was found in highest cell numbers, but because of its small cell size, it did not contribute more than 15% to the total biomass. This was also shown in low ratios of the haptophyte marker pigment 19′-butanoyloxyfucoxanthin (19′-but) to Chl *a* (data not shown). Unidentified flagellates (autotrophic and heterotrophic) were recorded in high abundances during the peak bloom. Dinoflagellates were less abundant but increased in abundances during the second half of the period. However, none of these two groups contributed substantially to the total biomass. The sum of chlorophyll breakdown products to Chl *a* varied between 5% and 25% and was generally lower at a depth of 0–8 m by the end of the sampling period (data not shown). This suggested that the bloom material was degrading and sinking out of this layer.

In 2004, total biomasses were much lower during the postbloom period than during spring bloom (5–30 μg C·L^{-1}), and Chl *a* concentrations never exceeded 1 μg·L^{-1} in the surface layer (0–8 m). A biomass peak was found at a depth of 50–60 m and was dominated by haptophytes, almost exclusively represented by *P. pouchetii*. Its colonial stage accounted for 50%–98% of the cell numbers in all samples until 21 May,

Table 5. Ranking of environmental variables that significantly (Monte Carlo permutation test in RDA, $p < 0.05$) influenced fatty acid composition of particulate organic matter (POM) (*a*) during and (*b*) after spring bloom in Kongsfjorden.

Environmental variable	*p* value	*F*	Explained inertia[a] Total (%)	Explained inertia[a] Species–environment (%)	Correlation Axis 1	Correlation Axis 2
(*a*) During spring bloom						
Si–N	0.05	12.8	27.4	55.6	–0.773	0.407
Chl *a*	0.01	10.0	16.9	34.3	0.454	0.620
Fucoxanthin:Chl *a*	0.05	3.13	5.0	10.1	–0.657	0.222
Total			49.3			
(*b*) After spring bloom						
Haptophytes	0.004	6.25	28.1	48.1	0.726	–0.093
PAR	0.015	5.53	19.4	33.2	–0.486	–0.658
Flagellates	0.017	3.67	10.9	18.7	–0.206	0.798
Total			58.4			

Note: The variables are ranked according to their explanatory power. For both models, the test of significance of all canonical axes was significant: (*a*) during spring bloom ($F = 10.37$, $p = 0.0001$), and (*b*) after spring bloom ($F = 6.5$, $p = 0.001$). PAR, photosynthetically active radiation.

[a] The total explained inertia refers to the percentage of variability in the whole data set, explained by the respective variable; species–environment refers to the relative amount of correlation between species and environmental variables explained in the chosen model (with three constrained axes).

Fig. 9. Results of the redundancy analysis (RDA) of the fatty acid composition of particulate organic matter (POM) sampled during the postbloom period (2004). Results from the pooled samples, i.e., two samples per day, are shown. The number close to the sample symbol depicts the sampling date; the colour coding indicates sampling depth. The red arrows point in the direction of maximum variability explained by the respective environmental variable. The broken arrow indicates a supplementary variable (inactive in the analysis) (shaded circles, 0–8 m; solid circles, 15–35 m).

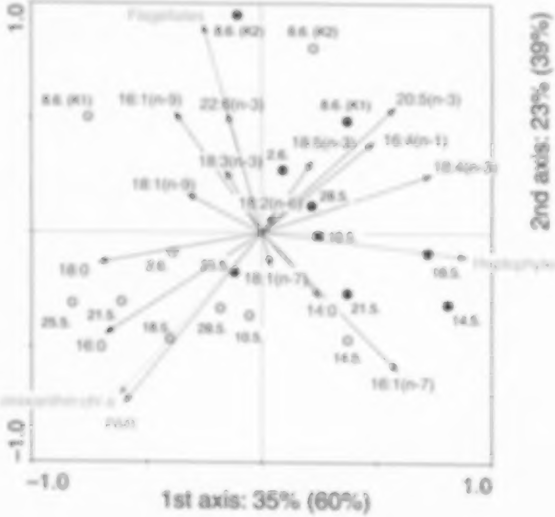

The 19′-but to Chl *a* ratios were usually at least 30%–50% higher in the deeper samples than at the surface (Fig. 12*a*). None of the other taxonomic marker pigments differed similarly consistently between the two depth layers (Fig. 12*a*). Contrary to the diatom-dominated spring bloom, the species composition was more variable (Fig. 10). For most species, many cells were in poor condition, judged from high numbers of spores, encysting cells, and empty frustules. In early May, diatoms were still dominating the biomass in the upper 30 m, as reflected in fucoxanthin – Chl *a* ratios of 0.6 (Fig. 12*a*). In the beginning, *T. nordenskioeldii* was most abundant but was progressively replaced by a variety of *Chaetoceros* species. Starting on 25 May, unidentified flagellates were found in substantial numbers, becoming increasingly abundant at all depths. Cryptophytes reached a peak during the second half of May, which was also visible in the development of the alloxanthin – Chl *a* ratio (Fig. 12*a*). The contribution of heterotrophs was high. Among the dinoflagellates, several *Gymnodinium* species were most abundant, reaching their highest biomass in the last 10 days of May. Peridinin, a pigment occurring exclusively in dinoflagellates, changed accordingly (Fig. 12*a*). Furthermore, heterotrophic ciliates were found in high numbers (up to 8000 cells·L^{-1}). Despite chlorophyte marker pigments being present in all samples (Chl *b*, neoxanthin, and prasinoxanthin), no species of this group was found in the cell counts. An ANOSIM of taxonomic pigment ratios yielded no difference between the two depth layers (Global $R = -0.036$, $p > 0.5$).

During spring bloom, slightly higher Dd to Chl *a* ratios were found in the surface samples, but the difference was not consistent (Fig. 11*b*). Under the stratified conditions during the postbloom period, however, several photoprotective pigments (zeaxanthin, lutein, Dd) were found in higher ratios to Chl *a* close to the surface compared with the deeper samples (Fig. 12*b*). With respect to the ratios of photoprotective pigments to Chl *a*, the two depth layers differed moderately (ANOSIM, Global $R = 0.189$, $p < 0.05$). The zeaxanthin to Chl *a* ratio accounted for 50% of the dissimilarity.

Nutrients and stoichiometry of POM

In spring 2003, nutrient concentrations (N and Si) were high until the beginning of May and dropped rapidly after the peak of the bloom (Table 7). No differences were found between the two depth layers. In 2004, both N and Si values

Table 6. Comparison (t tests) of fatty acids (%) identified in the particulate organic matter sampled at station K3 during spring bloom (2003) and after spring bloom (2004).

	Spring bloom (mean ± SD)	After spring bloom (mean ± SD)	p level
16:1(n-7)	16.4±4.5	13.0±4.5	0.0441
16:4(n-1)	3.8±2.2	1.6±0.6	0.0010
18:0	4.7±2.1	7.8±2.8	0.0010
20:5(n-3)	11.0±2.6	6.9±2.5	0.0007
Sum SFA	38.7±3.3	48.1±7.4	0.0001
Sum MUFA	23.8±6.3	33.0±5.3	0.0001
Sum PUFA	35.2±6.7	18.9±3.0	<0.0001
Ratio of 16:1(n-7) to 16:0	0.9±0.3	0.5±0.2	0.0049
C16	46.4±4.6	42.1±3.7	0.0167
C18	21.5±3.6	27.5±3.4	0.0001
Ratio of C16 PUFA to C18 PUFA	0.6±0.2	0.1±0.1	0.0001

Note: 2003, n = 14; 2004, n = 18. SD, standard deviation; SFA, saturated fatty acids; MUFA, monounsaturated fatty acids; PUFA, polyunsaturated fatty acids.

were already depleted at the start of our sampling (mainly below 1 µmol·L^{-1}; Table 7). Phosphate concentrations, measured only in 2004, were low (0.3 to 0.5 µmol·L^{-1}; Table 7). In 2003, both particulate C–N and C–P ratios (molar) were low and ranged from 4 to 6 and 60 to 80, respectively, with no temporal or spatial differences. In 2004, both C–N and C–P ratios were consistently higher (8–12 and 99–109, respectively), suggesting more nutrient-depleted cells in the postbloom situation.

Discussion

PUFAs during the spring bloom and postbloom periods

The observed differences in fatty acid composition and species succession between a diatom-dominated spring bloom and the postbloom period were, in general, well in accordance with those of previous studies (Mayzaud et al. 1989; Skerratt et al. 1995; Reuss and Poulsen 2002). The highest relative amount of PUFAs was found early in the bloom, well before its biomass peak, i.e., during the period of exponential growth when carbon is allocated predominantly to polar lipids, which constitute the membranes of the fast-growing microalgae (Parrish et al. 2005). The most dominant PUFAs during this early phase were the diatom markers 20:5(n-3) and 16:4(n-1) (also found by Mayzaud et al. 1989). The latter fatty acid has also been suggested as a biomarker for ice algae (Falk-Petersen et al. 1998). The postbloom period was characterized by lower relative amounts of PUFAs (15%–20% of total fatty acids), resembling previously reported profiles of non-diatom blooms from the Barents Sea (Henderson et al. 1991; Falk-Petersen et al. 1998; Scott et al. 2002). High fractions of 18:0 (up to 10%; Henderson et al. 1991; Falk-Petersen et al. 1998) were reported in these studies. This corresponds to the near 10% of 18:0 in POM that we found during postbloom conditions. In low-productivity waters in Antarctica, Fahl and Kattner (1993) found as much as 25% of 18:0 and attributed this to the poor quality of the POM, which consisted mainly of detritus and degrading material. Interestingly, the deep Chl *a* maximum in 2004 in our study showed similar characteristics, with SFAs as high as 64% and 16:1(n-7) to 16:0 ratios between 0.1 and 0.5. This, together with exceptionally high amounts of Chl *a* breakdown products in these samples, clearly points to senescent phytoplankton in poor physiological condition and demonstrates the strong dynamics and rapid qualitative and quantitative shifts from the spring bloom to the postbloom period.

Light and POM fatty acid composition

The potential impact of PAR and UVR on phytoplankton is inevitably determined by the average exposure time of cells to high irradiances. Hence, stratification of the water masses (or the lack of it) and mixing depths play a crucial role for the response of phytoplankton to high irradiances (Neale et al. 2003). The spring bloom in Kongsfjorden in 2003 developed in homogenous water masses without any physical barrier against sinking or vertical mixing of the cells, as has earlier been described as typical for high-latitude fjord ecosystems by Eilertsen (1993). Therefore, phytoplankton cells did not remain in the highly irradiated surface layers long enough to suffer from photodamage by PAR or UVR. This was supported by our data, yielding no significant explanatory contribution of radiation during the blooming period. During postbloom, however, when stratification counteracted vertical mixing, pronounced differences in fatty acid profiles between surface layers and deeper water were found. These differences occurred mainly along the light gradient, as shown in the RDA plot, and divided the samples according to their relative abundances of PUFAs versus 16:0 and 18:0. Interestingly, of the four fatty acids that contributed more than 10% each to the average dissimilarity between POM fatty acid compositions from the two depth layers, three that reacted strongest towards an increase in ambient irradiance in an outdoor experiment were the same. This study with a unialgal diatom culture was performed in Ny-Ålesund simultaneously with the postbloom sampling campaign (Leu et al. 2006*b*). We found a 50% reduction of the relative amount of all PUFAs upon exposure to PAR irradiances, corresponding to in situ values measured at a 8 m depth in Kongsfjorden (180–460 µmol·m^{-2}·s^{-1}). At the same time, SFAs and, mainly, 18:0 increased strongly. No effect of ambient or enhanced UVR on the relative amount of

Fig. 10. Total phytoplankton biomasses (µg C·L^{-1}) and percentage contribution of the main taxonomic groups during spring bloom (2003) and postbloom (2004) periods. Plotted values are calculated from cell counts from six or seven different depths per sampling day.

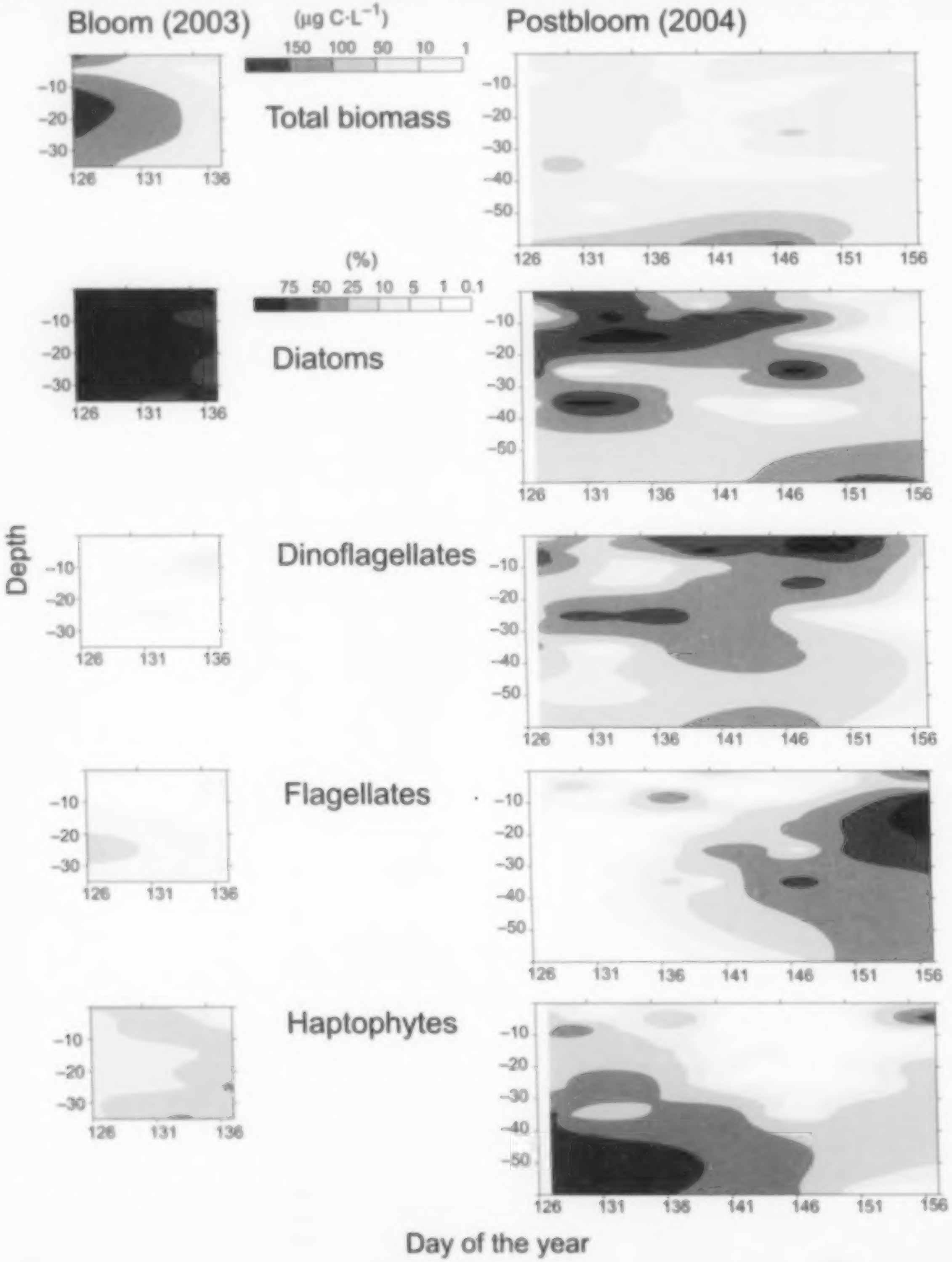

Fig. 11. Ratios of (*a*) fucoxanthin to Chl *a* and (*b*) diadinoxanthin to Chl *a* in the two depth layers during spring bloom (2003) (0–8 m, ○; 15–35 m, ●).

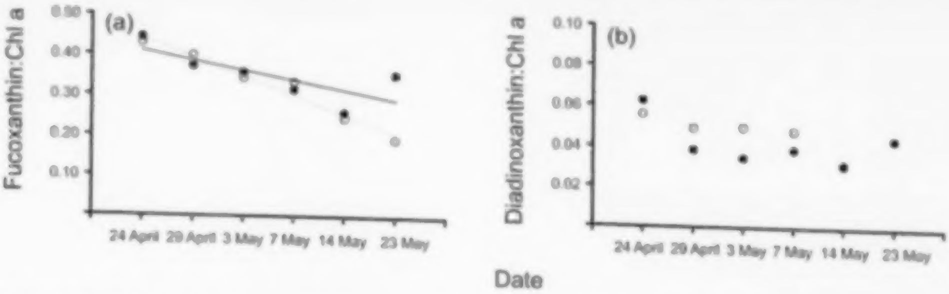

PUFAs was detected in that study, although the experimental UV intensities were higher than the values measured at the 8 m depth. It is difficult to disentangle the potential impact of two or more closely correlated environmental factors (as PAR and UVR) in a field study by means of statistical analysis only. However, additional laboratory studies addressing specifically the effect of UVR on fatty acid composition in three Arctic diatom species and one freshwater chlorophyte confirmed that UVR did not cause a decrease in the relative amount of PUFAs in any of the species investigated (Leu et al. 2006*a*, 2007). These results suggest that PAR might be more detrimental to PUFAs than UVR under natural conditions.

In addition to fatty acid composition, the ratios of all photoprotective pigments (zeaxanthin, lutein, Dd) to Chl *a* also differed consistently between the two depth layers, indicating further biochemical responses of phytoplankton to high irradiances in the uppermost 8 m. Zeaxanthin is formed by violaxanthin de-epoxidase that is activated when a plant cell is exposed to excess excitation energy (light) (Demmig-Adams 1990). Prolonged high-light stress might lead to a temporal accumulation of photoprotective pigments from the violaxanthin cycle, even in microalgae that are considered to possess the Dd cycle only (Lohr and Wilhelm 1999). An increase of cellular levels of lutein in response to increasing irradiance was found by Henriksen et al. (2002). At the same time, none of the taxonomic pigments showed a similar vertical pattern, apart from 19′-but. Thus, differences in species composition do not seem to be a likely explanation for the depth-dependent differences in fatty acid composition. Elemental ratios from both layers indicated nutrient depletion. The temporal resolution of these data was, however, not sufficient to include them in the RDA.

The role of species composition and nutrient availability

Apart from the effect of light under stratified conditions, changes in species composition and nutrient availability proved to be the major drivers of changes in POM fatty acid composition, as described by various authors before (see references in Introduction). During spring bloom, changes in species composition were well in accordance with changes in the respective fatty acid trophic markers. The decreasing dominance of diatoms was reflected in a linear decrease of their marker PUFAs, 20:5(*n*-3) and 16:4(*n*-1). Similarly, the increasing amounts of haptophytes were indicated by an increase in 14:0 and 18:1(*n*-9) and, to some extent, 18:1(*n*-7). Both tendencies (i.e., the increase in *Phaeocystis* and decrease in diatoms) were confirmed by corresponding changes in the marker pigment ratios to Chl *a*, fucoxanthin to Chl *a* and 19′-but to Chl *a*. The marginal effect of the former explained significantly nearly 20% of the total variability in the data set. However, because of its strong correlation with the nutrient availability, it accounted for only 5% in the chosen RDA model.

Temporal trends in the postbloom fatty acid profiles were less clear, owing to a continuously changing and more diverse phytoplankton community. Still, a significant correlation between fatty acid profiles and changes in species composition was found, represented by two of the three environmental factors on the RDA model, the relative biomass contributions of haptophytes and flagellates. Together, they accounted for 38% of the variability in the data set. Because flagellates are not a taxonomic group, a direct correlation to either marker pigments or fatty acid trophic markers is impossible. Respective samples were, however, characterized by the highest values of 22:6(*n*-3) and C18 PUFAs, both considered as trophic markers for dinoflagellates but also found in other flagellates. In general, taxonomic changes were not as clearly visible in the fatty acid profiles during the postbloom period as during spring bloom, which might be due to the larger contribution of detritus and nonphytoplankton constituents to POM.

Changes in species composition were important but still did not account for more than 20%–30% of the variability in POM fatty acid composition during the spring bloom and postbloom periods. Even though diatoms dominated strongly through all stages of the spring bloom in 2003 (72%–87% according to cell counts), we found a 40% reduction of PUFAs during one month, together with other major shifts in the fatty acid composition. We therefore suggest that changes in the algal physiological state also affected fatty acid composition. Nutrients were rapidly depleted during the spring bloom. In fact, nutrient depletion was probably the ultimate reason for its termination. Grazing pressure can most likely be excluded, as only very few large herbivorous copepods were observed feeding in the fjord (E. Leu, W. Walkusz, and S. Kwasniewski, unpublished data). Available concentrations of silicate and nitrate were confirmed (by the Monte Carlo permutation test) to be significantly correlated with the observed changes in fatty acid composition.

In experimental studies, nutrient limitation (mainly by phosphorus but also by nitrogen) has been shown to cause a decrease the PUFA content in microalgae (Reitan et al. 1994; Klein Breteler et al. 2005). Similar observations have

Fig. 12. Ratios of (*a*) taxonomic and (*b*) photoprotective pigments to Chl *a* in the two depth layers during the postbloom period (2004) (0–8 m, ○; 15–35 m, ●). 19′-But, 19′-butanoyloxyfucoxanthin; Dd, diadinoxanthin; Dt, diatoxanthin.

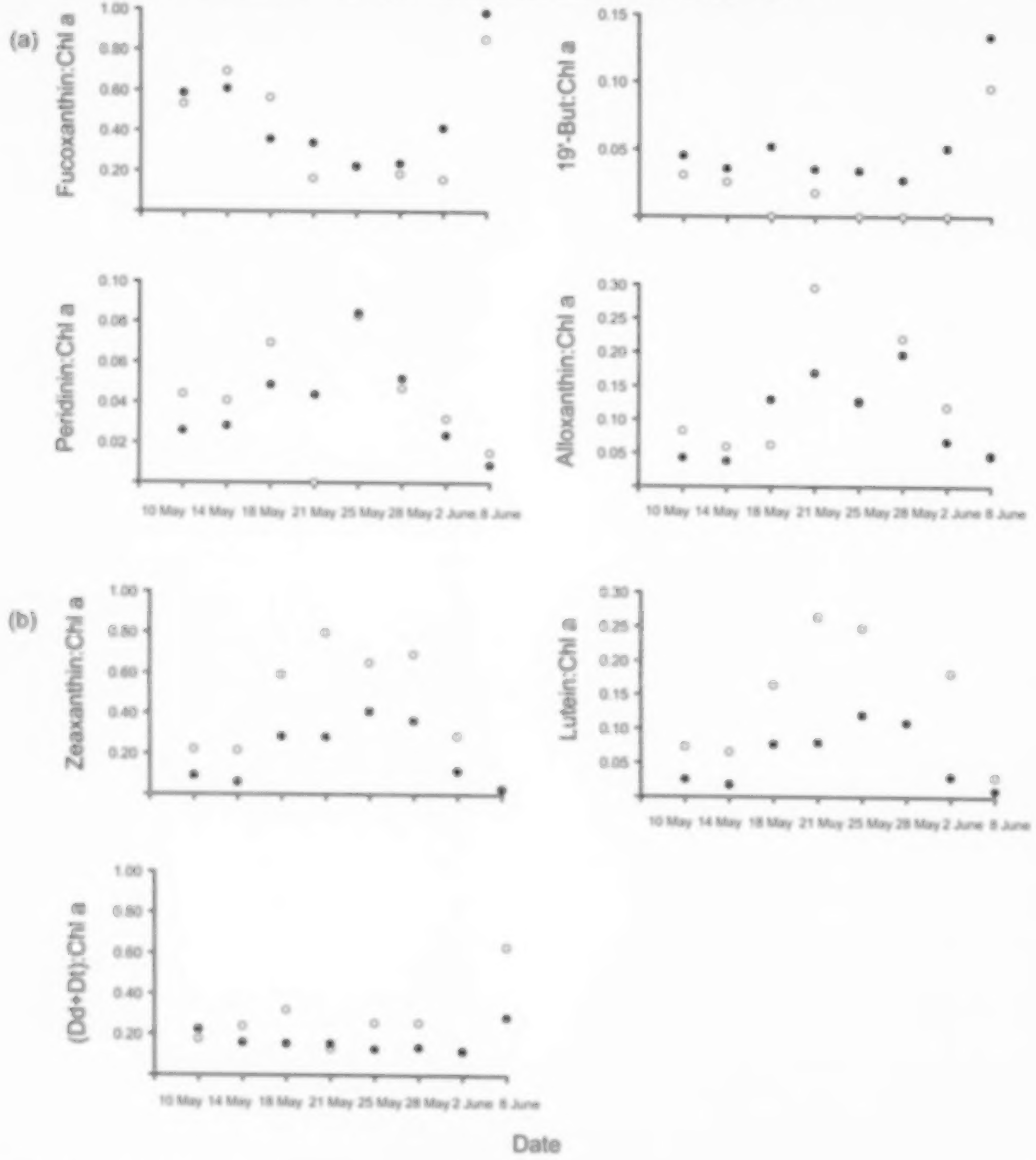

been made in the field during late stages of blooms (Parrish et al. 2005). When nutrients become increasingly depleted, the physiological state of the algae deteriorates, and their metabolism switches from growth and polar lipid synthesis to production of storage (neutral) lipids (Hayakawa et al. 1996). In phytoplankton, these are mainly triacyglycerols containing relatively high amounts of SFAs. In contrast to the fatty acids, the elemental composition of POM did not react as fast to nutrient depletion. No temporal changes in the C–N or C–P ratios were observed during the bloom. However, an immediate effect of nutrient depletion on the C–N–P ratios can be expected particularly if N or P are the limiting factors. If silicate was the main limiting factor affecting phytoplankton physiology, no change in the C–N–P

Table 7. Total nutrient concentrations (μmol·L⁻¹) in unfiltered seawater samples from station K3 sampled during the spring bloom (2003) and postbloom (2004) periods.

	Spring bloom (2003)						Postbloom (2004)				
	24 April	27 April	3 May	14 May	18 May	23 May	8 May	10 May	25 May	2 June	8 June
Si											
0–8 m		3.62	3.62	0.90	1.23	0.72	0.15	0.23	0.30	0.15	0.30
15–35 m		4.13	3.75	0.90	0.90	0.92	0.47	0.27		0.15	1.48
N											
0–8 m	12.50	13.21	12.50	7.07	9.64	5.79	0.36	0.36	0.14	0.36	0.57
15–35 m	13.93	13.21	13.93	7.93	8.79	7.07	0.36		0.36	0.36	2.21
P[a]											
0–8 m							0.35	0.29	0.32	0.32	0.58
15–35 m							0.52	0.48	0.32	0.42	0.58

[a] P was measured in 2004 only.

ratios should be expected. Both C–P and C–N ratios during the postbloom period in June (in 2004) were clearly higher than during spring bloom (in 2003), indicating some limitation.

Ecological considerations and food web implications

The results from the present study demonstrate a pronounced change in POM fatty acid composition over a brief period in April–May, spanning the peak bloom and early postbloom periods. Although these shifts may be accredited largely to phytoplankton community changes and the physiological state of the cells, our study strongly indicates that light also has the potential to affect phytoplankton fatty acid composition, especially during periods of stratification. If a spring bloom develops in nonstratified waters (as observed in our study), the detrimental impact of light is reduced by vertical mixing and thus only brief periods of exposure to high light intensities. In contrast, blooms in the marginal ice zone (MIZ) usually occur in strongly stratified water layers, with a distinct biomass peak close to the surface. We therefore suggest that our findings are relevant for primary production in polar oceans. If the ice cover in the Arctic retreats as predicted over the decades to come (Stroeve et al. 2005), the MIZ will increase its extension northwards and propagate close to the North Pole each year. This might cause not only a potential mismatch between light, nutrients, and autotrophs, but also a potential mismatch between phytoplankton and their consumers, notably copepod grazers (Hansen et al. 2003). The herbivorous copepods of *Calanus* spp. comprise up to 70%–80% of the zooplankton biomass in Arctic seas (Conover 1988; Hirche and Mumm 1992) and constitute the key link between primary production and higher trophic levels (Falk-Petersen et al. 1990, 2006). PUFAs play a crucial role in their reproduction. Eggs of *Calanus glacialis* contain >30% PUFAs, with 20:5(*n*-3) and 22:6(*n*-3) dominating (Hirche and Kattner 1993). *Calanus* spp. have to acquire these essential fatty acids from their phytoplankton diet. Gonad and egg production in all *Calanus* species occurring in the Arctic starts during winter, but two of them rely on spring phytoplankton for successful spawning (Hirche and Kattner 1993; Hirche et al. 1997; Niehoff et al. 2002). Because high-quality food is available to them only during a very brief period, a temporal mismatch or decrease in its quality may impair their recruitment. A decrease in the abundances of the large herbivorous copepods would have a severe impact on the transfer of biomass to higher trophic levels (Falk-Petersen et al. 1990, 2006).

We conclude that light, in addition to the well-known factors species composition and nutrient availability, has the potential to affect the POM fatty acid composition in situ. The described effects are likely to occur under stratified conditions, the typical situation for most phytoplankton blooms in ice-covered oceans. A correlation was found between exposure to high irradiances and reduced relative contents of PUFAs in POM. Because of its higher intensity and less rapid absorption in the water, PAR seems to be more detrimental than UVR to POM fatty acid composition. Seasonal ozone depletion, followed by higher UVB intensities, might increase these negative effects somehow but is not expected to have a severe impact on POM nutritional quality on a large scale. The ongoing reduction in sea ice concentration, however, might change timing, quantity, and quality of the available food source for pelagic herbivores. When trying to predict the future development of the Arctic pelagic ecosystem in an era of climate change, the detrimental potential of light, as well as its crucial role for the timing of autotrophic production, has to be considered.

Acknowledgements

The authors thank Wojtek Moskal, Anette Wold, and Wojciech Walkusz for their great assistance in collecting and processing all the samples. The taxonomic analysis of the phytoplankton samples by Dr. Jozef Wiktor was highly appreciated. The authors also thank Carl-Petter Nielsen (Norwegian Polar Institute) for providing the PAR data for Ny-Ålesund and Janne Søreide and Daniel Baumgärtner for assistance with some of the statistical analyses. The manuscript profited from the constructive comments of two anonymous reviewers. This study was financed by the Norwegian Research Council, project no. 150 331/720.

References

Anderson, T.R., and Pond, D.W. 2000. Stoichiometric theory extended to micronutrients: comparison of the roles of essential fatty acids, carbon, and nitrogen in the nutrition of marine copepods. Limnol. Oceanogr. **45**(5): 1162–1167.

Arendt, K.E., Jonasdottir, S.H., Hansen, P.J., and Gartner, S. 2005. Effects of dietary fatty acids on the reproductive success of the calanoid copepod *Temora longicornis*. Mar. Biol. **146**(3): 513–530.

Christie, W.W. 1982. Lipid analysis. Pergamon Press, New York.

Clarke, K.R. 1993. Non-parametric multivariate analyses of changes in community structure. Austr. J. Ecol. **18**: 117–143.

Clarke, K.R., and Green, R.H. 1988. Statistical design and analysis for a "biological effects" study. Mar. Ecol. Prog. Ser. **46**: 213–226.

Conover, R.J. 1988. Comparative life histories in the genera *Calanus* and *Neocalanus* in high latitudes of the northern hemisphere. Hydrobiologia, **167**: 127–142.

Cullen, J.J., and Neale, P.J. 1994. Ultraviolet radiation, ozone depletion, and marine photosynthesis. Photosynth. Res. **39**(3): 303–320.

Dahlback, A. 2002. Recent changes in surface ultraviolet solar radiation and stratospheric ozone at a High Arctic site. *In* UV Radiation and Arctic ecosystems. *Edited by* D.O. Hessen. Springer-Verlag, Berlin. pp. 1–22.

Dalsgaard, J., St. John, M., Kattner, G., Muller-Navarra, D., and Hagen, W. 2003. Fatty acid trophic markers in the pelagic marine environment. Adv. Mar. Biol. **46**: 225–340.

Demmig-Adams, B. 1990. Carotenoids and photoprotection in plants: a role for the xanthophyll cycle. Biochim. Biophys. Acta, **1020**: 1–24.

Eilertsen, H.C. 1993. Spring blooms and stratification. Nature (London), **363**: 24.

Engelsen, O., Hegseth, E.N., Hop, H., Hansen, E., and Falk-Petersen, S. 2002. Spatial variability of chlorophyll-*a* in the Marginal Ice Zone of the Barents Sea, with relations to sea ice and oceanographic conditions. J. Mar. Syst. **35**(1–2): 79–97.

Engelsen, O., Hop, H., Hegseth, E.N., Hansen, E., and Falk-Petersen, S. 2004. Deriving phytoplankton biomass in the Marginal Ice Zone from satellite observable parameters. Int. J. Remote Sens. **25**(7–8): 1453–1457.

Fahl, K., and Kattner, G. 1993. Lipid content and fatty acid composition of algal communities in sea ice and water from the Weddell Sea (Antarctica). Polar Biol. **13**(6): 405–409.

Falk-Petersen, S., Hopkins, C.C.E., and Sargent, J.R. 1990. Trophic relationships in the pelagic, arctic food web. *In* 24th European Marine Biology Symposium. *Edited by* M. Barnes and R.N. Gibson. Aberdeen University Press, Aberdeen, Scotland. pp. 315–333.

Falk-Petersen, S., Sargent, J.R., Henderson, J., Hegseth, E.N., Hop, H., and Okolodkov, Y.B. 1998. Lipids and fatty acids in ice algae and phytoplankton from the Marginal Ice Zone in the Barents Sea. Polar Biol. **20**(1): 41–47.

Falk-Petersen, S., Hagen, W., Kattner, G., Clarke, A., and Sargent, J. 2000. Lipids, trophic relationships, and biodiversity in Arctic and Antarctic krill. Can. J. Fish. Aquat. Sci. **57**: 178–191.

Falk-Petersen, S., Timofeev, S., Pavlov, V., and Sargent, J.R. 2006. Climate variability and possible effects on arctic food chains. The role of *Calanus*. *In* Environmental challenges in arctic–alpine regions. Arctic–alpine ecosystems and people in a changing environment. *Edited by* J.B. Ørbæk, I. Tombre, R. Kallenborn, E. Hegseth, S. Falk-Petersen, and A.H. Hoel. Springer Verlag, Berlin.

Folch, J., Lees, M., and Sloane Stanley, G. H. 1957. A simple method for isolation and purification of total lipids from animal tissue. J. Biol. Chem. (Baltimore), **226**: 497–509.

Foss, P., Guillard, R.R.L., and Liaaen-Jensen, S. 1984. Prasinoxanthin — a chemosystematic marker for algae. Phytochemistry, **23**: 142–144.

Goes, J.I., Handa, N., Taguchi, S., and Hama, T. 1994. Effect of UV-B radiation on the fatty acid composition of the marine phytoplankter *Tetraselmis* sp.: relationship to cellular pigments. Mar. Ecol. Prog. Ser. **114**(3): 259–274.

Gulati, R.D., and DeMott, W.R. 1997. The role of food quality for zooplankton: remarks on the state-of-the-art perspectives and priorities. Freshw. Biol. **38**(3): 753–768.

Hagen, W., and Auel, H. 2001. Seasonal adaptations and the role of lipids in oceanic zooplankton. Zool. Anal. Complex Syst. **104**(3–4): 313–326.

Hall, J.M., Parrish, C.C., and Thompson, R.J. 2002. Eicosapentaenoic acid regulates scallop (*Placopecten magellanicus*) membrane fluidity in response to cold. Biol. Bull. **202**(3): 201–203.

Hanelt, D. 1996. Photoinhibition of photosynthesis in marine macroalgae. Sci. Mar. **60**: 243–248.

Hansen, A.S., Nielsen, T.G., Levinsen, H., Madsen, S.D., Thingstad, T.F., and Hansen, B.W. 2003. Impact of changing ice cover on pelagic productivity and food web structure in Disko Bay, West Greenland: a dynamic model approach. Deep-Sea Res. **50**(1): 171–187.

Hayakawa, K., Handa, N., Kawanobe, K., and Wong, C.S. 1996. Factors controlling the temporal variation of fatty acids in particulate matter during a phytoplankton bloom in a marine mesocosm. Mar. Chem. **52**(3–4): 233–244.

Henderson, R.J., Olsen, R.E., and Eilertsen, H.C. 1991. Lipid composition of phytoplankton from the Barents Sea and environmental influences on the distribution pattern of carbon among photosynthetic end products. Polar Res. **10**(1): 229–237.

Henriksen, P., Riemann, B., Kaas, H., Sørensen, H.M., and Sørensen, H.L. 2002. Effects of nutrient-limitation and irradiance on marine phytoplankton pigments. J. Plankton Res. **24**(9): 835–858.

Hessen, D.O., Faerøvig, P.J., and Andersen, T. 2002. Light, nutrients, and P:C ratios in algae: grazer performance related to food quality and quantity. Ecology, **83**(7): 1886–1898.

Hirche, H.J., and Kattner, G. 1993. Egg production and lipid content of *Calanus glacialis* in spring — indication of a food-dependent and food-independent reproductive mode. Mar. Biol. **117**(4): 615–622.

Hirche, H.J., and Mumm, N. 1992. Distribution of dominant copepods in the Nansen Basin, Arctic Ocean, in summer. Deep-Sea Res. **39**(2A): S485–S505.

Hirche, H.J., Meyer, U., and Niehoff, B. 1997. Egg production of *Calanus finmarchicus*: effect of temperature, food and season. Mar. Biol. **127**(4): 609–620.

Jeffrey, S.W., and Vesk, M. 1997. Introduction to marine phytoplankton and their pigment signatures. *In* Phytoplankton pigments in oceanography. *Edited by* S.W. Jeffrey, R.F.C. Mantoura, and S.W. Wright. UNESCO, Paris. pp. 37–84.

Jeffrey, S.W., and Wright, S. 1994. Photosynthetic pigments in the haptophyta. *In* The haptophyte algae. *Edited by* J. Green and B. Leadbeater. Clarendon Press, Oxford. pp. 111–132.

Jeffrey, S.W., Sielicki, M., and Haxo, F.T. 1975. Chloroplast pigment patterns in dinoflagellates. J. Phycol. **11**: 374–385.

Kirk, J.T.O. 1994. Light and photosynthesis in aquatic ecosystems. 2nd ed. Cambridge University Press, Cambridge, UK.

Klein Breteler, W.C.M., Schogt, N., and Rampen, S. 2005. Effect of diatom nutrient limitation on copepod development: role of essential lipids. Mar. Ecol. Prog. Ser. **291**: 125–133.

Koroleff, F. 1985. Determination of silicon. *In* Methods of seawater analysis. *Edited by* K. Grasshoff, M. Erhardt, and K. Kremling. Verlag Chemie, Weinheim, Germany. pp. 174–185.

Legendre, P., and Legendre, L. 1998. Numerical ecology. 2nd ed. Elsevier Science, Amsterdam, the Netherlands.

Leu, E., Færøvig, P.J., and Hessen, D.O. 2006*a*. UV effects on the nutritional quality of *Selenastrum capricornutum* and their consequences for *Daphnia magna*. Freshw. Biol. **51**: 2296–2308.

Leu, E., Wängberg, S.-A., Wulff, A., Ørbæk, J.B., Falk-Petersen, S., and Hessen, D.O. 2006*b*. Effects of changes in ambient PAR and UV radiation on the nutritional quality of an Arctic diatom (*Thalassiosira antarctica* var. *borealis*). J. Exp. Mar. Biol. Ecol. **337**: 65–81.

Leu, E., Falk-Petersen, S., and Hessen, D.O. 2007. Ultraviolet radiation negatively affects growth but not food quality of Arctic diatoms. Limnol. Oceanogr. In press.

Lohr, M., and Wilhelm, C. 1999. Algae displaying the diadinoxanthin cycle also possess the violaxanthin cycle. Proc. Natl. Acad. Sci. U.S.A. **96**: 8784–8789.

Mayzaud, P., Chanut, J.P., and Ackman, R.G. 1989. Seasonal changes of the biochemical composition of marine particulate matter with special reference to fatty acids and sterols. Mar. Ecol. Prog. Ser. **56**(1–2): 189–204.

Mayzaud, P., Claustre, H., and Augier, P. 1990. Effect of variable nutrient supply on fatty acid composition of phytoplankton grown in an enclosed experimental ecosystem. Mar. Ecol. Prog. Ser. **60**(1–2): 123–140.

Neale, P.J., Helbling, E.W., and Zagarese, H.E. 2003. Modulation of UVR exposure and effects by vertical mixing and advection. *In* UV effects in aquatic organisms and ecosystems. *Edited by* E.W. Helbling and H.E. Zagarese. Royal Society of Chemistry, Cambridge, UK. pp. 107–134.

Niehoff, B., Madsen, S.D., Hansen, B.W., and Nielsen, T.G. 2002. Reproductive cycles of three dominant *Calanus* species in Disko Bay, West Greenland. Mar. Biol. **140**(3): 567–576.

Nishida, I., and Murata, N. 1996. Chilling sensitivity in plants and cyanobacteria: the crucial contribution of membrane lipids. Annu. Rev. Plant Physiol. Plant Mol. Biol. **47**: 541–568.

Olaizola, M., and Yamamoto, H.Y. 1994. Short-term response of the diadinoxanthin cycle and fluorescence yield to high irradiance in *Chaetoceros muelleri* (Bacillariophyceae). J. Phycol. **30**(4): 606–612.

Parrish, C.C., Thompson, R.J., and Deibel, D. 2005. Lipid classes and fatty acids in plankton and settling matter during the spring bloom in a cold ocean coastal environment. Mar. Ecol. Prog. Ser. **286**: 57–68.

Pennington, F.C., Haxo, F.T., Borch, G., and Liaaen-Jensen, S. 1985. Carotenoids of cryptophyceae. Biochem. Syst. Ecol. **13**: 215–219.

Reitan, K.I., Rainuzzo, J.R., and Olsen, Y. 1994. Effect of nutrient limitation on fatty acid and lipid content of marine microalgae. J. Phycol. **30**: 972–979.

Reuss, N., and Poulsen, L.K. 2002. Evaluation of fatty acids as biomarkers for a natural plankton community. A field study of a spring bloom and a post bloom period off West Greenland. Mar. Biol. **141**(3): 423–434.

Sakshaug, E. 2004. Primary and secondary production in the Arctic seas. *In* The organic carbon cycle in the Arctic Ocean. *Edited by* R. Stein and R.W. Macdonald. Springer-Verlag, Berlin. pp. 57–82.

Sakshaug, E., and Slagstad, D. 1991. Light and productivity of phytoplankton in polar marine ecosystems — a physiological view. Polar Res. **10**(1): 69–85.

Sargent, J.R., Bell, J.G., Bell, M.V., Henderson, R.J., and Tocher, D.R. 1995. Dietary origins and functions of long-chain (*n*-3) polyunsaturated fatty acids in marine fish. J. Mar. Biotechnol. **3**: 26–28.

Schlüter, L., Mohlenberg, F., Havskum, H., and Larsen, S. 2000. The use of phytoplankton pigments for identifying and quantifying phytoplankton groups in coastal areas: testing the influence of light and nutrients on pigment/chlorophyll *a* ratios. Mar. Ecol. Prog. Ser. **192**: 49–63.

Scott, C.L., Kwasniewski, S., Falk-Petersen, S., and Sargent, J.R. 2002. Lipids and fatty acids in the copepod *Jaschnovia brevis* (Jaschnov) and in particulates from Arctic waters. Polar Biol. **25**(1): 65–71.

Skerratt, J.H., Nichols, P.D., McMeekin, T.A., and Burton, H. 1995. Seasonal and inter-annual changes in planktonic biomass and community structure in eastern Antarctica using signature lipids. Mar. Chem. **51**(2): 93–113.

Skerratt, J.H., Davidson, A.D., Nichols, P.D., and McMeekin, T.A. 1998. Effect of UV-B on lipid content of three Antarctic marine phytoplankton. Phytochemistry, **49**(4): 999–1007.

Smetacek, V., and Nicol, S. 2005. Polar ocean ecosystems in a changing world. Nature (London), **437**: 362–368.

StatSoft Inc. 2004. STATISTICA 7.0. StatSoft Inc., Tulsa, Oklahoma.

Stauber, J.L., and Jeffrey, S.W. 1988. Photosynthetic pigments in fifty-one species of marine diatoms. J. Phycol. **24**: 158–172.

Stroeve, J.C., Serreze, M.C., Fetterer, F., Arbetter, T., Meier, W., Maslanik, J., and Knowles, K. 2005. Tracking the Arctic's shrinking ice cover: another extreme September minimum in 2004. Geophys. Res. Lett. **32**(4): L04501.

Svendsen, H., Beszczynska-Moeller, A., Hagen, J.O., Lefauconnier, B., Tverberg, V., Gerland, S., Oerbaek, J.B., Bischof, K., Papucci, C., Zajaczkowski, M., Azzolini, R., Bruland, O., Wiencke, C., Winther, J.G., and Dallmann, W. 2002. The physical environment of Kongsfjorden–Krossfjorden, an Arctic fjord system in Svalbard. Polar Res. **21**(1): 133–166.

ter Braak, C.F.J., and Smilauer, P. 2002. CANOCO reference manual and CanoDraw for Windows user's guide: software for canonical community ordination. Version 4.5. Microcomputer Power, Ithaca, NY.

Thompson, P.A., Guo, M., and Harrison, P.J. 1993. The influence of irradiance on the biochemical composition of 3 phytoplankton species and their nutritional value for larvae of the pacific oyster (*Crassostrea gigas*). Mar. Biol. **117**(2): 259–268.

Urabe, J., and Sterner, R.W. 1996. Regulation of herbivore growth by the balance of light and nutrients. Proc. Natl. Acad. Sci. U.S.A. **93**(16): 8465–8469.

Utermöhl, H. 1958. Zur Vervollkommnung der quantitativen Phytoplankton Methodik. Mitt. Int. Ver. Limnol. **9**: 1–38.

Vernet, M. 2000. Effects of UV radiation on the physiology and ecology of marine phytoplankton. *In* The effects of UV radiation in the marine environment. *Edited by* S. de Mora, S. Demers, and M. Vernet. Cambridge University Press, Cambridge, UK. pp. 237–278.

Wiktor, J. 1999. Early spring microplankton development under fast ice covered fjords of Svalbard, Arctic. Oceanologia, **41**(1): 51–72.

Wright, S., and Jeffrey, S. 1997. High-resolution HPLC system for chlorophylls and carotenoids of marine phytoplankton. *In* Phytoplankton pigments in oceanography. *Edited by* S. Jeffrey, R. Mantoura, and S. Wright. UNESCO, Paris, France. pp. 327–341.

Spatial and environmental correlates of fish community structure in Canadian Shield lakes[1]

Andrea Bertolo and Pierre Magnan

Abstract: We used data on fish species biomass from 38 lakes of the Canadian Shield (Québec) to determine the contribution of environmental (lake and watershed morphometry) and spatial (e.g., hydrographic connectivity and geographic coordinates) variables on fish community structure. By using a combination of multivariate analyses, we show that nearly half of the variation in the fish community structure is explained by the independent contributions of spatial and environmental factors. Walleye (*Sander vitreus*) and lake whitefish (*Coregonus clupeaformis*) were significantly associated with the absence of beaver (*Castor canadensis*) dams, whereas northern pike (*Esox lucius*) was positively correlated with beaver dam presence. Altitude and longitude, but not current patterns in lake connectivity, were the main explanatory spatial variables accounting for the observed pattern in fish community structure. Large piscivorous fish were associated with a reduced richness and biomass of small prey, suggesting that predation is a structuring factor in these lakes. By showing that geographic coordinates and altitude are better descriptors of fish community structure than hydrographic connections, our study suggests that past colonization routes are relatively more important than current ones in structuring fish communities at the landscape level. This interpretation is supported by recently published genetic data.

Résumé : Nous avons utilisé des données de biomasse des espèces de poissons dans 38 lacs du bouclier canadien (Québec) pour déterminer la contribution des variables environnementales (morphométrie du lac et du bassin versant) et spatiales (p. ex. connectivité hydrographique et coordonnées géographiques) sur la structure des communautés de poissons. En utilisant différentes analyses multivariables, nous avons montré que presque la moitié de la variation dans la structure des communautés de poissons est expliquée par une contribution indépendante de facteurs spatiaux et environnementaux. Le doré jaune (*Sander vitreus*) et le grand corégone (*Coregonus clupeaformis*) étaient significativement associés à l'absence de barrages de castor (*Castor canadensis*), alors que le grand brochet (*Esox lucius*) était corrélé directement avec la présence de barrages de castor. L'altitude et la longitude, mais pas les patrons actuels de connectivité entre les lacs, étaient les principales variables qui expliquaient les patrons observés dans la structure des communautés de poissons. Les grands piscivores étaient associés à une richesse spécifique et une biomasse réduites des petits poissons proies, suggérant que la prédation est un facteur structurant dans ces lacs. En montrant que les coordonnées géographiques et l'altitude sont de meilleurs descripteurs de la structure des communautés de poissons que les connexions hydrographiques, notre étude suggère que les anciennes voies de colonisation sont relativement plus importantes que les voies actuelles dans la structuration des communautés des poissons au niveau du paysage. Des données génétiques publiées récemment supportent cette hypothèse.

Introduction

Limnetic fish communities show patterns that can be explained in terms of biogeographic factors and physical–chemical gradients (Tonn and Magnuson 1982; Rahel 1984; Jackson et al. 2001). Although the fish communities of both small, physically unstable lakes (e.g., with strong seasonal variations in dissolved oxygen) (Tonn and Magnuson 1982; Tonn et al. 1992) and larger, more stable lake systems (Jackson and Harvey 1989; Paszkowski and Tonn 2000; Olden et al. 2001) have been the object of quantitative surveys, comparatively few studies have explicitly considered the role of spatial factors such as hydrographic patterns in lake connectivity (e.g., Olden et al. 2001), and only rarely have studies assessed it at large scales (e.g., Legendre and Legendre 1984). Yet, spatial patterns can be important in explaining the possible colonization routes and (or) the variation in both biotic and abiotic factors among lakes and thus may determine fish community structure by multiple pathways (Jackson et al. 2001).

Here, we examine relationships between attributes of lake fish communities and both environmental and spatial factors

Received 6 February 2006. Accepted 29 September 2006. Published on the NRC Research Press Web site at http://cjfas.nrc.ca on 16 December 2006.
J19151

A. Bertolo[2] and P. Magnan. Groupe de Recherche sur les Écosystèmes Aquatiques, Département de Chimie-Biologie, Université du Québec à Trois-Rivières, C.P. 500, Trois-Rivières, QC G9A 5H7, Canada.

[1] Contribution of the Groupe de recherche interuniversitaire en limnologie et en environnement aquatique (GRIL).

[2] Corresponding author (e-mail: andrea.bertolo@uqtr.ca).

Can. J. Fish. Aquat. Sci. **63**: 2780–2792 (2006)

doi:10.1139/F06-161

in an area larger by one order of magnitude than that studied by Olden et al. (2001). We used data from a survey of fish communities in 38 Canadian Shield lakes to determine (*i*) which environmental and spatial variables best account for patterns in fish community structure and (*ii*) the relative contribution (and statistical significance) of each of these components to the explained variation.

Even though fish species richness and community structure are predictable along large gradients of lake area and mean depth (Marshall and Ryan 1987; Matthews 1998), we do not expect that these factors will be important in structuring fish communities in this study because the study lakes are relatively homogeneous in morphology. In contrast, because the study lakes are distributed over an area of 30 000 km^2, it is likely that other environmental and geographic factors will influence fish communities. For example, we expect that spatial factors such as patterns of lake connectivity will be important structuring factors (Olden et al. 2001). Other potential structuring factors could be the presence of beaver (*Castor canadensis*) dams (Collen and Gibson 2001) and piscivorous fish (Chapleau et al. 1997), both of which varied among the study lakes. It has been shown that beaver dams can affect the community structure of freshwater fish (Collen and Gibson 2001) by their effects on the aquatic habitat and by the creation of barriers to fish migration, whereas predation by piscivores might be responsible for the extinction of prey species in lakes (Chapleau et al. 1997). The statistical approach we used should help to identify the relationships between these factors and fish community structure.

Materials and methods

Study lakes and fish sampling

Thirty-eight thermally stratified headwater lakes were selected on the basis of comparable size (fetch greater than 1 km), basin morphometry (maximum depth exceeding 5 m), and catchment properties (<6% of catchment occupied by wetlands) (Table 1; for more details, see Carignan et al. 2000). The lakes were accessible only by plane and are located within a 30 000 km^2 area surrounding the Gouin Reservoir, Québec, Canada (48°50′N, 75°00′W; Fig. 1). The landscape is typical of the Canadian Shield, with low relief and numerous lakes and wetlands. Our study lakes are larger than those studied in Wisconsin and Alberta by Tonn and Magnuson (1982), Rahel (1984), and Robinson and Tonn (1989) but are similar in size to those studied in Ontario and Alberta by Hinch et al. (1991) and Paszkowski and Tonn (2000). These Québec lakes are part of three major watersheds (the Outaouais, Saguenay, and Saint-Maurice rivers) that ultimately drain into the St. Lawrence River (Fig. 1).

Lake catchments experienced only limited disturbance until 1995, when nine of them experienced forest fires and nine others were logged by forestry companies. The effects of the forest fires and logging were studied on these lakes for the 3 years following the perturbation (between 1996 and 1998). Carignan et al. (2000) showed that fire and logging increased the concentrations of nutrients and major ions in these lakes through increased runoff from the watershed. Planas et al. (2000) found significant effects of the perturbations on the biomass of both benthic and pelagic algae, which increased in logged and burned lakes between 1996 and 1998. Furthermore, Patoine et al. (2000) found that the biomass of small-sized zooplankton (mostly rotifers) increased in burned-watershed lakes, whereas larger zooplankton (mostly calanoids) decreased in logged-watershed lakes. Between 1996 and 1997, St-Onge and Magnan (2000) found some negative effects of these perturbations on the abundance of the smallest size classes of both yellow perch (*Perca flavescens*) and white sucker (*Catostomus commersoni*), but they did not observe any effect at the population level. Therefore, because of the short-term nature of these perturbations and the fact that they did not have any detectable effects at the population level (St-Onge and Magnan 2000), it is unlikely that these perturbations biased our analyses. To verify this assumption and control for the potential undetected effects of these perturbations on community structure, we included the percent area of watershed logged or burned as an independent variable in our statistical analyses. To avoid collinearity problems, physicochemical and plankton variables, which were clearly affected by the watershed perturbations, were not included in our analysis.

For logistic reasons, 21 lakes were sampled in 1996 and 17 in 1997. This might have introduced some noise in the data owing to interannual differences in fish community structure, but it is unlikely that it biased our results because the choice of sampling a lake in a given year was made randomly. Each lake was sampled once between June and August. Fish were captured with experimental monofilament gill nets (102.3 m long × 2.7 m high) and had stretched mesh panels of 20, 24, 33, 36, 50, 60, 76, 90, and 100 mm (filament diameter of 0.17, 0.20, 0.20, 0.20, 0.20, 0.32, 0.32, 0.32, and 0.32 mm, respectively). Gill nets were set perpendicular to the shore, with small and large meshes alternating from the shore among gill nets. The nets were set at regular intervals around the lake, with the first net location being randomly located on aerial photographs. The fishing effort was six nets per night for <50 ha lakes, eight nets per night for 50–100 ha lakes, 10 nets per night for 100–150 ha lakes, and 12 nets per night for >150 ha lakes. The nets fished on average for 18 h 26 min ± 00 h 32 min (minimum–maximum: 17 h 13 min – 19 h 30 min), covering the period between 1600 and 1030. For all fish captured, total length (±1 mm) and mass (±0.1 g) were noted.

A total of 23 taxa were found in the study lakes (Table 2). Species determination was difficult in the field for cyprinids, and given the remoteness of our study area, it was not possible to bring specimens to the lab for more accurate identification. Unidentified cyprinids, if any, were used only as members of the "prey group" (see next section) and not used separately in the analyses.

Dependent variables

Fish species abundance has been shown to be a more sensitive response variable for studying community patterns than presence–absence data, even though the latter are in general less noisy (Rahel 1990). To select the most sensitive matrix of dependent variables in our analyses, we explicitly compared the sensitivity of relative abundance vs presence–absence data as descriptor variables of community structure. We first built matrices of relative abundance (biomass per unit of effort, BPUE) and presence–absence data to compare

Table 1. General characteristics of the study lakes.

Variable	Mean ± SD	Range
Lake area (km^2)	0.46±0.36	0.15–2.31
Altitude (m)	450±40	391–558
Maximum depth (m)	13.8±6.1	5.0–34.0
Mean depth (m)	4.8±1.8	2.1–10.0
Watershed area (km^2)	3.7±3.8	0.61–21.7
Residence time (years)	1.6±1.1	0.3–5.6
Lake slope (%)	7.6±3.5	3.0–18.3
Lake volume (m^3 × 10^6)	2.2±1.7	0.4–8.5
Epilimnion depth (m)	2.8±0.9	1.3–4.7
Epilimnion–hypolimnon ratio (volume)	1.4±1.5	0.29–8.3
Littoral area (%)^a	29.4±10.6	11.6–54.9
Chlorophyll *a* (μg·L^{-1})^b	1.9±0.5	0.9–3.2
Total phosphorus (μg·L^{-1})^b	7.0±1.9	4.9–11.8
Total nitrogen (μg·L^{-1})^b	233.1±41.1	158.3–332.1
Dissolved organic carbon (mg·L^{-1})^b	5.1±1.3	2.8–9.2
Secchi depth (m)^b	4.0±1.0	2.2–6.0
Fish species richness	4.6±1.8	1–9

[a] Defined as the area between the 0 m and 2 m isobaths.

[b] Only physicochemical data relative to unperturbed lakes are presented.

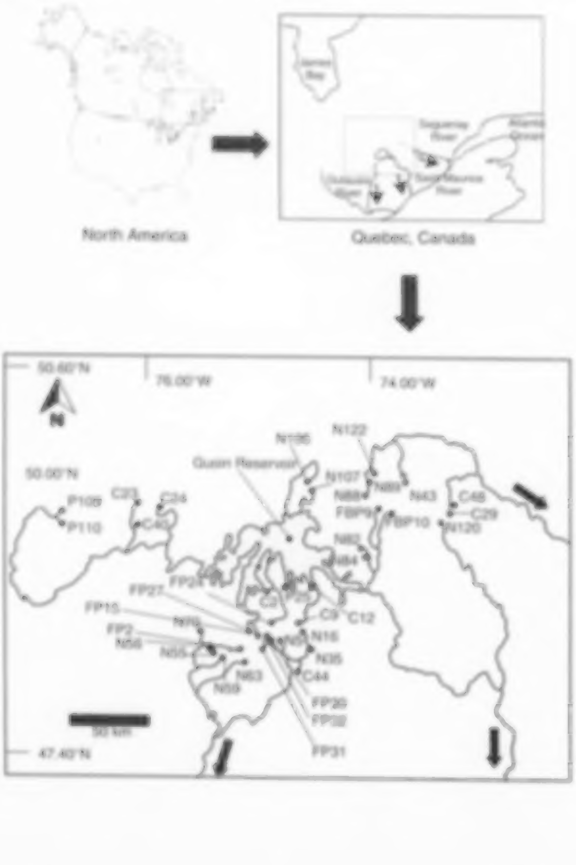

Fig. 1. Location of the study lakes. The close-up represents the location of the sampling sites within the three major watersheds draining into the St. Lawrence River: the Saguenay, Saint Maurice, and Outaouais rivers. Arrows indicate the direction of water flow.

the sensitivity of these variables as descriptors of community structure. Moreover, because it has been shown that gillnets underestimate the abundance of small-bodied fish (e.g., Olin and Malinen (2003) and references therein), we expect data on small-bodied species to be more affected by noise than data on larger ones. To verify this assumption, we ran the analyses both by including all species and by pooling small-bodied ones into a single "prey fish" group (see Table 2). We expect the prey fish group (composed mostly of cyprinids and gastrosteids) to be more sensitive to environmental factors (e.g., biotic ones) than individual small-bodied species and thus help in identifying patterns in fish community structure. Thus, we considered four matrices of dependent variables: presence–absence and BPUE fish data with all the individual species (hereafter "all species" matrix) or with small-bodied species pooled into the "prey fish" category (hereafter "main species" matrix). We then compared the amount of variation in each of these four matrices of dependent variables that was explained by the independent variables (see below) to estimate the performance of these fish community descriptors. The descriptor with the best performance was used in all subsequent analyses.

Species diversity × lake matrices were also built as dependent variables describing our fish communities. Because different measures of diversity–evenness can differ in their ability to discriminate among sites (Magurran 1988), we compared three different diversity indices: species richness (S), Shannon diversity (H), and evenness (Pielou's J) (Magurran 1988).

Independent variables

The matrix of environmental variables included variables that we expected might affect fish community structure and species diversity, such as shoreline development, percent of littoral area, epilimnion to hypolimnion ratio (Matthews 1998), the presence of a beaver dam at the lake outlet (Collen and Gibson 2001), and the percent area of the water-

Table 2. Occurrence of the fish species (and their code names) in the study lakes.

Common name	Scientific name	Code	Occurrence	
			No. of lakes	Percentage of lakes
White sucker	*Catostomus commersonii*	caco	31	81.6
Northern pike	*Esox lucius*	eslu	27	71.1
Yellow perch	*Perca flavescens*	pefl	25	65.8
Lake whitefish	*Coregonus clupeaformis*	copl	11	28.9
Fallfish	*Semotilus corporalis*	seco	10	26.3
Walleye	*Sander vitreus*	savi	9	23.7
Pearl dace[a]	*Margariscus margarita*	mama	7	18.4
Brook trout	*Salvelinus fontinalis*	safo	7	18.4
Burbot	*Lota lota*	lolo	7	18.4
Golden shiner[a]	*Notemigonus crysoleucas*	nocr	5	13.2
Lake chub[a]	*Couesius plumbeus*	copl	5	13.2
Finescale dace[a]	*Phoxinus neogaeus*	phne	5	13.2
Lake trout	*Salvelinus namaycush*	sana	2	5.3
Northern redbelly dace[a]	*Phoxinus eos*	pheo	2	5.3
Atlantic rainbow smelt[a]	*Osmerus mordax mordax*	osmo	2	5.3
Spottail shiner[a]	*Notropis hudsonius*	nohu	2	5.3
Ninespine stickleback[a]	*Pungitius pungitius*	pupu	1	2.6
Trout-perch[a]	*Percopsis omiscomaycus*	peom	1	2.6
Logperch[a]	*Percina caprodes*	peca	1	2.6
Blacknose shiner[a]	*Notropis heterolepis*	nohe	1	2.6
Common shiner[a]	*Luxilus cornutus*	luco	1	2.6
Brook stickleback[a]	*Culaea inconstans*	cuin	1	2.6
Cyprinid spp.[a,b]		cysp	8	21.1

[a] Species included in the "prey fish" group.

[b] Species not included in the analyses based on all species.

shed that was burned or logged. Lake morphometry and catchment properties (including the presence of a beaver dam at the lake outlet) were determined from 15–25 echosounder transects and aerial photographs (see methodological details in Carignan et al. 2000). Although we tried to reduce the variation in both lake area and maximum depth by selecting morphologically similar lakes, some variation for these variables was still present in our data set (Table 1). To control for this residual variation, lake area and maximum depth, which are considered key factors in determining fish species richness and composition at larger scales (Matthews 1998; Dodson et al. 2000; Amarasinghe and Welcomme 2002), were included in the analysis. A total of seven environmental variables were thus considered in the analyses.

To estimate the influence of hydrographic spatial structure on species assemblages, six different matrices were constructed. We compared their ability to extract patterns from the fish data in order to select the most effective one in subsequent analyses. The hydrographic network mapping the connections among lakes was first built using both paper and digital maps with scales from 1:20 000 to 1:250 000 (Fig. 1). Each branching point represents a node and a number was assigned to each node (Magnan et al. 1994). Then, a lake-by-node matrix (NODE) was constructed by assigning, for each lake, a value of one to all nodes connecting it to the origin or "root" and a value of zero to all other nodes. This procedure results in a hydrographic tree in which each lake is classified by a row vector of binary values (0 or 1) (for examples, see Magnan et al. 1994; Angers et al. 1999). Hydrographic trees estimate the isolation between any two lakes by determining the number of streams that a fish encounters when dispersing from one lake to another, but they do not measure distances between lakes.

Two additional matrices were built by measuring the watercourse distance (in kilometres) between each pair of lakes (WC1) and between each lake and each node (WC2). These two alternative measures of lake isolation should give better measures than the first approach (NODE) regarding the distances that a fish might have to travel from one lake to another. The watercourse distances were obtained by processing the information contained in digital maps with MapInfo software.

The last two isolation measures were obtained by integrating both watercourse distances (i.e., WC1) and differences in altitude between lakes. The matrix of differences in altitude between lakes (D_ALT) was built by calculating the average differences in altitude between the lakes and the closest hydrographic node connecting them. This measure reflects the altitude difference experienced by fish when moving from one lake to another via the hydrographic network. We then used WC1 and D_ALT to produce two orthogonal isolation measures (D_ELEV1 and D_ELEV2) following the method proposed by Olden et al. (2001). This approach starts by unfolding both of these 38 × 38 distance matrices (i.e., WC1 and D_ALT) from a triangular form into a continuous vector (for an example, see Legendre and Legendre 1998, p. 560). A matrix of 741 × 2 (i.e., the (38 ×

37)/2 + 38 rows and two columns) was created by combining the two vectors side by side. The two columns of this matrix were then used as variables in a principal component analysis (PCA) to construct D_ELEV1 and D_ELEV2, which are obtained from the first two axes of the PCA. The first PCA axis summarized the relationship between interlake watercourse distance and elevation difference. This set of 741 observations was then converted back into a triangular matrix of interlake distances (D_ELEV1), which corresponds to an integrated measure of the overall distance, both by water and elevation, between any two lakes. The second PCA axis is a stream gradient measure as it represents the relative change in elevation compared with distance by water (Olden et al. 2001). In a similar way, the 741 observations from axis II were converted back into a triangular distance matrix (D-ELEV2) (Olden et al. 2001).

Finally, as suggested by Legendre and Legendre (1998), we built a sixth matrix by including all terms of a cubic trend surface polynomial (TREND) based on geographic coordinates (including altitude). Even though this approach does not estimate the among-lake distances that fish experience moving from one lake to another, trend surface analysis is appropriate for describing broad-scale spatial trends in data (Legendre and Legendre 1998). Thus, given the relatively large spatial scale of our study area, we considered that it was informative to compare this approach with the other five presented above. This procedure allows one to estimate parameters of a trend surface regression equation of the form:

$$\begin{aligned}\mathrm{SR} = b_1X + b_2Y + b_3XY + b_4X^2 + b_5Y^2 + b_6X^2Y \\ + b_7XY^2 + b_8X^3 + b_9Y^3\end{aligned}$$

where X is the longitude and Y is the latitude in Cartesian coordinates. Because all of the lakes are headwater, we considered altitude as an indirect measure of lake isolation. Thus, we added the terms $b_{10}Z$ and $b_{11}Z^2$ to the equation, where Z is the altitude in metres above sea level. This equation represents a geographic surface that can be used to describe how a summary measure of the fish community structure (the SR variable, which in this study takes the form of the ordination axis score) varies over the matrix of X–Y–Z coordinates. The corresponding TREND matrix was composed of 38 rows (i.e., lakes) and 11 columns (i.e., the terms of the polynomial). The inclusion of quadratic, cubic, and interaction terms in the equation allowed the modelling of not only simple linear gradient patterns, but also more complex features such as patches or gaps (Borcard et al. 1992).

The selection of spatial variables to be used in subsequent analyses was based on their ability in extracting patterns from fish data. We first ranked the six sets of spatial predictors (i.e., NODE, WC1, WC2, D_ELEV1, D_ELEV2, and TREND) by comparing the amount of variation in fish data explained by each of them separately in canonical correspondence analysis (CCA) (see below). If possible, we partitioned the variation among them (see below) to see if the spatial predictors explained different portions of the variation on the fish data. We retained for further analyses the set of spatial variables explaining the largest part of the variation independently of the others. When they explained similar proportions of the variation and their effect was confounded, we considered them as equivalent. In this case, we selected the simplest set of spatial variables. The six sets were ranked on the basis of increasing construction complexity (i.e., amount of information needed to build them) as follows: TREND, NODE, WC1 and WC2, and D_ELEV1 and D_ELEV2.

Statistical analyses

We used CCA first to relate the matrix of the dependent variables (i.e., fish presence–absence and BPUE) to the six sets of spatial variables. This allowed us to select the matrix of spatial variables to be used in subsequent analyses. CCA was then used to relate the matrix of the dependent variables to two sets of predictor variables separately: environmental (lake and catchment characteristics) and spatial (i.e., the selected matrix). Used in combination with permutation tests, this procedure allowed us to evaluate the magnitude and statistical significance of effects associated with each component (Legendre and Legendre 1998). Explanatory variables were selected using a forward selection procedure, with a cutoff point of $p = 0.10$ (i.e., alpha-to-enter, as in multiple regression analysis), based on 9999 Monte Carlo permutations. The statistical significance of both selected variables and ordination axes ($\alpha = 0.05$) were assessed by means of a Monte Carlo permutation test ($n = 9999$). The collinearity between selected explanatory variables was controlled by eliminating those variables with a variance inflation factor (VIF) greater than 10 (ter Braak and Smilauer 1998). As environmental variables show spatial heterogeneity, the variation explained by environmental and spatial variables may be redundant. To explain this potential redundancy, variations in fish species assemblage were analyzed against the spatial and environmental variables combined, using the method of variation partitioning proposed by Borcard et al. (1992).

The method of variance partitioning uses CCA and partial CCA (i.e., a CCA with covariables) to partition the variation in species assemblage explained by independent variables into different components (see Borcard et al. (1992) for details of computations). In the analysis, the amount of fish community variance explained by independent variables was partitioned into "pure" environmental and "pure" spatial components using CCA and partial CCA. This procedure also allowed us to determine the portion of unexplained variation (Borcard et al. 1992). With this procedure, a part of the pure component explained by the spatial variables could in fact be related to environmental factors that are spatially structured and could thus contain unmeasured environmental gradients.

The significance of the relationship between single explanatory variables and fish taxa ($\alpha = 0.05$) was determined by using Van Dobben circles (ter Braak and Looman 1994). These ordination diagrams are built using the t values of canonical coefficients of the CCA and can be used to easily visualize the relationships between single dependent and independent variables in the analysis.

A correspondence analysis (CA) was used to summarize the fish community structure in a reduced space. For both CA and CCA, BPUEs were $\log(x + 1)$-transformed to reduce the effect of outliers on the ordination. Furthermore, rare species were downweighted by the standard downweighting function of CANOCO to reduce their unduly large influence in the analyses (ter Braak and Smilauer 1998). Finally, both CA and CCA assume a unimodal relationship between the dependent and independent variables. Detrended correspondence analysis (DCA) was used to verify this assumption. The range of the ordination scores obtained by DCA was greater than the threshold of three standard deviations, indicating that the use of unimodal methods was appropriate in this study (Jongman et al. 1995). Geographic coordinates were centred to a zero mean before computing the higher terms of the polynomial to reduce nonessential collinearity when fitting the polynomial. Here, the backward-selection procedure was used to reduce the number of terms in the CCA. This was preferred to the forward-selection procedure because if any of the higher terms had been retained by the forward-selection procedure, all terms of lower order (significant or not) must also have been retained to avoid any deformation of the model (Draper and Smith 1998). Ordinations (CCA, DCA, and Van Dobben circles) were done with the CANOCO program (version 4.02; ter Braak and Smilauer 1998).

We used stepwise multiple regression to determine (*i*) if fish species diversity was related to the above-mentioned environmental variables and the pooled BPUE of main piscivores and (*ii*) if total fish biomass was related to the environmental variables and fish species diversity. Fish species diversity indexes (S, H, and J) were used here as independent variables because it has been suggested that the total biomass in a community can be affected by species diversity (e.g., Loreau 1998). This procedure was applied to both the whole fish community and to "prey fish" only, considered a priori as more sensitive to piscivorous fish predation. Residual scatter plots, normal probability plots, and partial residual plots were used to determine if regression assumptions were satisfied. When these conditions were not fulfilled, the data were log- or square-root-transformed. Collinearity between the independent variables was evaluated by examination of the variance inflation factor (see above). To control for the potential relationships with sampling date and fishing time, these two variables were used as covariates in the analyses and discarded if not significant.

Results

Selection of the spatial variables

The trend surface analysis explained 33.6% ± 2.6% (mean ± standard deviation, SD) (range 33.4%–36.1%) of the variation in the fish data. This represented the largest proportions of variation explained by spatial descriptors, regardless of the dependent matrix used (i.e., presence–absence and BPUE of both the all species and main species matrices). Nine terms of the polynomial trends surface were selected for both analyses conducted on the all species data (presence–absence and BPUE), whereas seven terms were selected for the analyses conducted on the main species data (for details, see Environmental and spatial correlates of fish community structure).

The analyses conducted on the D_ELEV1 and D_ELEV2 matrices explained 13.2% ± 4.5% (range 10.2%–19.9%) and 11.8% ± 3.0% (range 7.4%–13.8%) of the variation, respectively. Two variables (distances from lakes N106 and P109) were retained by the forward-selection procedure in the D_ELEV1 matrix in both analyses based on all species (both presence–absence and BPUE). Distances from lakes FP24 and P109 were selected from the D_ELEV1 matrix in the analysis on the presence–absence of main species. Distances from lakes N43, N63, and N82 were selected from the D_ELEV1 matrix in the analysis of the BPUE of main species. The same two variables (stream gradient from lakes FP24 and N106) were selected in the D_ELEV2 matrix in all four analyses.

Twenty-five nodes were determined in the hydrographic tree of interlake connections (Fig. 1). No node was retained in the analysis based on the BPUE of main species or the NODE matrix, and only two nodes were retained by the forward-selection procedure in the other three analyses. The hydrographic node matrix explained a relatively small fraction of the variation in the fish data (6.5% ± 4.5%; range 0%–10.3%), whereas neither matrix of watercourse distances (WC1 and WC2) was significantly related to any of the four fish descriptors. A partial CCA analysis was thus possible only with the first four spatial descriptors. However, most of the partial CCAs, which included all the spatial covariables, were not significant (Table 3). Therefore, it was not possible to partition the variation among the different sets of spatial variables. Only the partial CCA based on the BPUE of main species (dependent variable) and TREND (independent variable) was significant: it explained 21.5% of the variation in the fish data after inclusion of the other spatial descriptors as covariables (i.e., NODE, D_ELEV1, and D_ELEV2) (Table 3). Moreover, partial CCAs using TREND as independent variables and the other spatial descriptors used separately as covariables were significant in most cases and explained a larger proportion of the variation than the CCAs based on the other three spatial descriptors. Therefore, we selected the trend surface polynomial as the simplest and most robust model explaining the largest proportion of the variation in fish data.

Descriptors of fish community structure

The CCA results showed that the amount of variation explained by environmental variables alone was fairly similar among the four matrices of dependent variables (i.e., presence–absence and BPUE of both the all species and main species matrices), ranging from 10.4% to 14.9% (Table 4). Similarly, the comparison of the four sets of models showed that the total amount of variation explained by the spatial descriptors (i.e., TREND) was fairly similar among the four matrices of dependent variables. Variance partitioning was not possible for the presence–absence matrix of all species. In the other cases, it showed that the environment explained on average 11% of the variation, whereas TREND explained on average 31.2%. The total amount of variation explained was in general greater when small-bodied species were grouped in the analysis, but slightly greater when using BPUEs rather than presence–absence data. Therefore, this matrix was considered as the most sensitive and was selected for all our analyses.

Fish community structure

Of 23 fish taxa (Table 2; Appendix A), six species had population biomasses (BPUE) exceeding 1% of the total BPUE averaged over lakes: northern pike (*Esox lucius*),

Table 3. Summary statistics of significant partial CCAs (α = 0.05) based on four spatial descriptors explaining the variation in fish data: lake interconnections in the hydrographic tree (NODE), a combined measure of watercourse and elevation distance between lakes (D_ELEV1), stream gradient (D_ELEV2), and trend surface polynomial (TREND).

	NODE (*N*)				D_ELEV1 (*D1*)				D_ELEV2 (*D2*)				TREND (*T*)			
	T[a]	*D1*	*D2*	All	*T*	*N*	*D2*	All	*T*	*N*	*D1*	All	*N*	*D1*	*D2*	All
(*a*) Presence or absence																
All species	ns	9.2	ns	ns	ns	12.2	9.8	ns	8.6	10.3	12.6	ns	28.0	27.6	31.3	ns
Main species	ns	ns	ns	ns	ns	14.6	11.2	ns	ns	12.4	12.9	ns	34.9	28.4	32.0	ns
(*b*) Relative biomass (BPUE)																
All species	ns	9.4	ns	ns	ns	12.2	9.1	ns	8.9	10.6	9.0	ns	30.3	30.5	29.9	ns
Main species	—	—	—	—	ns	—	14.4	ns	ns	—	ns	ns	—	ns	28.8	21.5

Note: The four matrices of spatial descriptors were also used as covariables (individually or jointly) in the different partial CCAs. None of the CCAs based on interlake watercourse (WC1) or lake-node (WC2) distances was significant. Four matrices were used as dependent variables; fish data were expressed as (*a*) presence or absence or (*b*) relative biomass (BPUE) for all fish species or main species only. For each fish data matrix, results are expressed as percent variation explained by the independent matrices after inclusion of the covariables. —, not analyzed because the correspondent CCA was not significant; ns, not significant after inclusion of the covariables.

[a] Covariables.

Table 4. Summary statistics of significant CCAs (α = 0.05) explaining the variations in fish data.

	Explained variation (%)		
	ENV	TREND	Total
(*a*) Presence or absence			
All species	10.4	34.2*	34.2
Main species	14.5* (11.8)	32.5* (29.8)	44.3
(*b*) Relative biomass (BPUE)			
All species	11.4* (9.2)	35.5* (33.3)	40.3
Main species	14.9* (12.1)	33.4* (30.6)	45.5

Note: Four matrices were used as dependent variables: fish data were expressed as (*a*) presence or absence or (*b*) relative biomass (BPUE) for all fish species or main species only. For each fish data matrix, results are expressed as the percent variation explained by the two independent matrices: environment (ENV) and trend surface polynomial (TREND). An asterisk (*) indicates those CCAs that remained significant (α = 0.05) after the inclusion of the covariables (i.e., partial CCAs). The pure contribution of each independent matrix is shown within parentheses only for significant pairs of partial CCAs. The total variation explained by significant partial CCAs is also shown (right column).

white sucker (*Catostomus commersoni*), lake whitefish (*Coregonus clupeaformis*), walleye (*Sander vitreus*), yellow perch (*Perca flavescens*), and brook trout (*Salvelinus fontinalis*) represented (mean ± SD) 38.7% ± 37.8%, 32.4% ± 33.8%, 8.3% ± 15.6%, 8.0% ± 15.7%, 3.8% ± 13.5%, and 3.6% ± 6.0% of the total BPUE, respectively. These species, along with fallfish (*Semotilus corporalis*) and burbot (*Lota lota*), which had average biomasses lower than 1%, occurred in at least 18% of the lakes. Only one small-bodied species included in the prey group (pearl dace, *Margariscus margarita*) also occurred in 18% of the lakes (Table 2). Among potential piscivores, pike and walleye showed the largest occurrence and biomass (Table 2; Appendix A).

The first two axes of the CA explained 53.7% of the variation in the BPUE of the main fish species. The first axis explained 36.9% of the variation in the data and separated lakes with northern pike (with or without walleye) from lakes with *Salvelinus* spp. (*S. fontinalis* and (or) *S. namaycush*) (Fig. 2*a*). The second axis explained 16.8% of the variation in the data and separated most lakes with northern pike only from lakes in which northern pike co-occurred with walleye (Fig. 2*b*). Walleye and lake whitefish had a very similar distribution and always occurred with northern pike (Appendix A). Yellow perch co-occurred frequently with northern pike, walleye, and lake whitefish but co-occurred with *Salvelinus* spp. in only two lakes (Appendix A). Fallfish showed a pattern similar to yellow perch but were scarcer. White sucker was present in most of the lakes, and its biomass tended to be associated positively with the first axis (Fig. 2*a*). Burbot was also mostly associated with the positive part of the first axis (Fig. 2*a*). Prey fish were associated with the positive parts of both axes I and II, and their biomass was inversely related to the biomass of large piscivores (Fig. 2). The biomass of prey fish was particularly low when northern pike and walleye co-occurred.

Environmental and spatial correlates of fish community structure

Of the seven environmental variables included in the CCA forward-selection procedure, only lake area and the presence of a beaver dam at the lake outlet were retained (Fig. 3*a*). The CCA model was significant ($P = 0.0029$) and the two first axes together explained 14.9% of the variability in fish community structure (9.9% and 5.0%, respectively) (Fig. 3*a*).

Brook trout, lake trout, and white sucker were significantly associated with lake area, whereas yellow perch and northern pike were only marginally associated (negatively) to this variable. However, the analysis was particularly influenced by lake C48, which had the largest surface area (2.3 km^2) in the sample. When lake C48 was excluded, the effect of lake area disappeared. Walleye and lake whitefish were both significantly associated with the absence of beaver dams, whereas northern pike was positively associated with the presence of a beaver dam. No watershed perturbation variables were retained by the forward-selection procedure.

The best model relating fish community structure to the trend surface polynomial explained 33.4% of the total varia-

Fig. 2. (*a*) Correspondence analysis (CA) ordination diagram of the relative biomass of the main fish species (BPUE). Species codes (Table 2) indicate the approximate locations of species centroids. Eigenvalues: axis 1 = 0.53; axis 2 = 0.27; sum of all unconstrained eigenvalues = 2.12. (*b*) Same as (*a*) but without species centroids and with circles indicating the lakes. Patterns related to the occurrence of selected species are shown, i.e., lakes with *Salvelinus* spp. are indicated by open circles; lakes with northern pike (*Esox lucius*), shaded circles; lakes with both northern pike and walleye (*Sander vitreus*), solid circles. Note that the random jitter option was used to avoid overlapping of data points. Asterisk (*) indicates that brook trout (*Salvelinus fontinalis*) was found in lake P109 in a subsequent sampling.

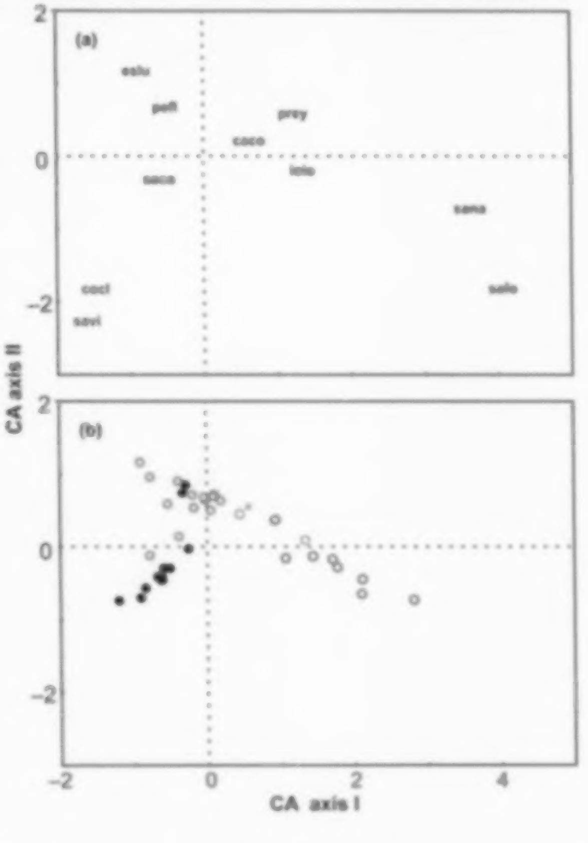

Fig. 3. Canonical correspondence ordination of the biomass of the main fish species (BPUE) and (*a*) environmental variables or (*b*) spatial variables (i.e., TREND) versus the relative biomass of main fish species (BPUE). The species abbreviations (Table 2) indicate the approximate locations of species centroids. Arrows represent the vectors of the selected environmental or spatial variables. In (*a*), the axes scaling is 1 for environmental variables and 0.38 for species. In (*b*), the axes scaling is 1 for spatial variables and 0.66 for species. For clarity, only those terms significantly associated with at least one of the fish taxa are shown. In both (*a*) and (*b*), bold lettering indicates those species significantly related to one of the independent variables, as revealed by *t* plot analysis.

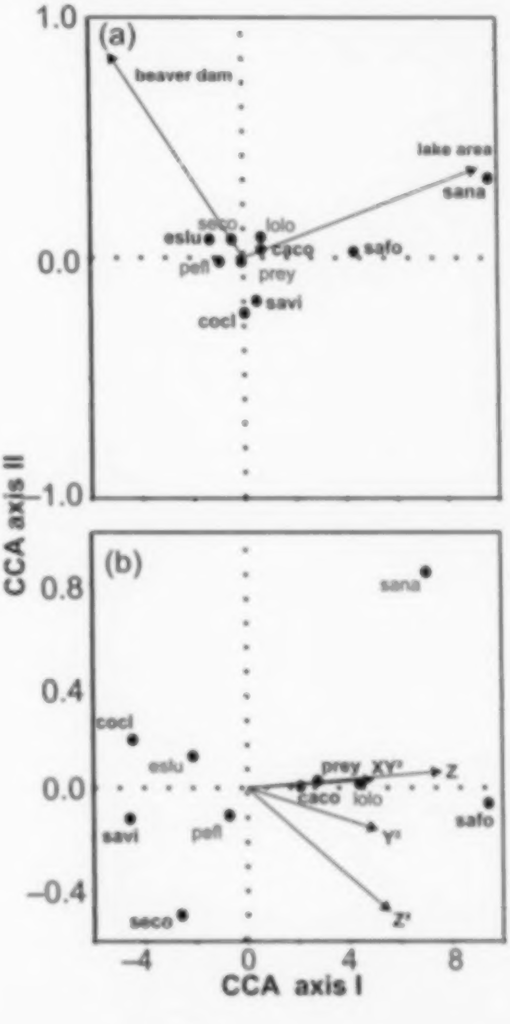

tion and included seven terms after the backward-selection procedure:

$$SR = b_1X + b_2Y + b_3XY + b_5Y^2 + b_7XY^2 + b_{10}Z + b_{11}Z^2$$

The first and second axes explained 21.9% and 4.8% of the variance, respectively, in the fish community structure and were mainly associated with altitude and the quadratic term for longitude (Fig. 3*b*, axis 1) and the quadratic altitude term (Fig. 3*b*, axis 2).

Altitude was significantly (positively) associated with brook trout, white sucker, and prey fish and negatively associated with lake trout, creek chub, and lake whitefish. Creek chub was also the only species correlated (negatively) with Z^2 and XY^2. A significant positive correlation was found between Y^2 and lake whitefish. No other terms were correlated with fish taxa. Altitude and longitude were correlated (Pearson's $r = 0.66$, $P < 0.0001$), with elevation increasing

Table 5. Regression models predicting fish species (*a*) richness (S), diversity (Shannon H), and evenness (Pielou J), and (*b*) total fish biomass (BPUE).

Dependent variable	Independent variable	Standardized regression coefficient	Partial R^2	Model R^2_{adj}	Model P
(*a*) All species					
S	—	—	—	—	>0.05
H	Beaver dam	–0.37 **	0.11		
	BPUE piscivores	0.51 ***	0.26	0.34	0.0003
J	Beaver dam	–0.39 **	0.15		
	Maximum depth	–0.28 *	0.14		
	BPUE piscivores	0.42 **	0.16	0.39	0.0003
(*b*) All species					
log(BPUE)	H	0.54 ***	0.29	0.27	0.0006
(*c*) Prey fish only					
log(S)	BPUE piscivores	–0.39 *	0.15	0.14	0.0120
H	—	—	—	—	>0.05
J	—	—	—	—	>0.05
(*d*) Prey fish only					
SQRT(BPUE)	BPUE piscivores	–0.29 **	0.31		
	S prey	0.47 **	0.36		
	H prey	0.27 *	0.04	0.68	<0.0001

Note: In (*a*), the biomass of piscivores (pooled BPUE of walleye and northern pike) was included on the list of independent variables. In (*b*), S, H, and J were included in the list of independent variables. (*c*) and (*d*) are the same as (*a*) and (*b*), respectively, but for the prey fish category only. In (*d*), the biomass of piscivores was included in the set of independent variables. Significance: *, $P < 0.05$; **, $P < 0.01$; ***, $P < 0.001$.

eastward, suggesting that their effects were partly confounded (Fig. 3*b*).

About 45.5% of the total variation in the fish community was explained jointly by environmental and spatial variables. The pure environmental and pure spatial variables accounted for 12.1% and 30.6%, respectively, of the total variation in the BPUEs of the main fish species, with the remaining variation (2.8%) explained by the component shared between the two.

Patterns in fish species diversity and total fish biomass

Fish species richness ranged from one to nine species. None of the explanatory variables was retained by the stepwise procedure to explain the variation in fish species richness (Table 5*a*). In contrast, the stepwise multiple regression revealed that the Shannon diversity index was negatively related to beaver dam presence and positively related to the biomass of large piscivores (Table 5). A similar result was obtained for fish species evenness (Pielou J index), but in this case, maximum depth was also included in the model (Table 5). The Shannon diversity index was the only variable retained to explain the variation in total fish biomass (Table 5*b*).

Prey fish species richness ranged from zero to six species. Stepwise multiple regression indicated that prey fish richness was negatively related to the biomass of large piscivores (Table 5*c*), which accounted for 14% of the variation. None of the explanatory variables was retained for either prey fish diversity or evenness (Table 5*c*). The biomass of large piscivores was inversely related to prey fish biomass, whereas prey fish richness and diversity were both directly related to prey fish biomass (Table 5*d*).

Discussion

Although the failure to integrate spatial variables into empirical ecological models can lead to the misinterpretation of spatially structured data (Legendre and Legendre 1998), studies explicitly addressing this issue for aquatic communities are still rare (cf. Jackson et al. 2001). We show here that nearly half of the variation in the fish community structure in a sample of boreal lakes is explained by the independent contribution of spatial and environmental factors. Unlike several previous studies (e.g., Olden et al. 2001), fish community structure was not clearly associated with the hydrographic network. Altitude, longitude, and the presence of beaver dams were the main explanatory variables. More specifically, our results suggest a potential link between the presence of beaver dams at the lake outlet and the absence of species such as walleye and lake whitefish. Beaver dams can be a barrier to fish movement and can dramatically alter stream habitats (Collen and Gibson 2001) such as the lake outlets. Outlets might be key spawning habitats for some species in these headwater lakes, which lack large inlets. Thus, beaver dams might have affected lacustrine fish communities by reducing the access to spawning areas for some species (i.e., neighbouring streams or lakes) (Rasmussen et al. 2002) or by altering the quality of the spawning areas situated in the outlet (Collen and Gibson 2001).

Surprisingly, both measures of watercourse distances used (WC1 and WC2) were unrelated to fish community structure; the hydrographic tree explained only a small portion of the variation in fish data. Only those spatial descriptors including altitude (TREND, D_ELEV1, and D_ELEV2) were successful in explaining a relatively large proportion of the variation in fish data. Moreover, the surface trend polynomial, despite the fact that it did not take into account watercourse distances, had a greater predictive power than both D_ELEV1 and D_ELEV2. This suggests that the predictive power of D_ELEV1 and D_ELEV2 might be due more to the inclusion of altitude differences rather than watercourse distances. Replacing watercourse distances by straight-line distances in the calculation of these two latter descriptors did not change their predictive power (results not shown), corroborating the view that the actual hydrographic network has little power to predict fish community structure in our lakes. These results contrast with those of Olden at al. (2001), who found a good concordance between patterns in interlake connectivity and fish occurrence patterns at a smaller scale.

The trend surface polynomial built from the lake geographical coordinates accounted by far for the highest proportion of the variation in fish BPUE explained by spatial descriptors. This suggests that a broad-scale spatial phenomenon shaped fish communities in these lakes. A possible mechanism could be linked to the postglaciation dispersion patterns, which were largely linked, at least at the beginning of the dispersal process, to lakes created by ice melt. Present drainage patterns do not necessarily reflect past drainage patterns in such dynamic landscapes, as suggested by large-scale biogeographic studies on the Québec fish fauna (Legendre and Legendre 1984). The genetic study by Gagnon and Angers (2006) supports this interpretation by showing that the genetic differences in four fish species in a subset of our study lakes were consistent with longitude but not with the current drainage system. These authors showed, for example, that northern pike and yellow perch populations situated 100 km apart latitudinally and in distinct watersheds were genetically more similar than populations situated in the same drainage and less than 30 km apart on a longitudinal axis (Gagnon and Angers 2006).

The strong relationship between altitude and fish community structure might be explained by the isostatic rebound that followed the glacier retreat. Isostatic rebound contributed to eliminating immigration routes from lowland into highland areas, and some fishes, particularly species with warm-water preferences (e.g., northern pike and walleye), may have been unable to recolonize highland areas. This could explain why *Salvelinus* spp. occur mostly in lakes with elevations higher than ca. 470 m, whereas the reverse was found for species like northern pike and walleye. According to the differences in the physiological capacities and the ecological preferences of each species, these species are in fact expected to have colonized this area at different times. Thus, despite its reduced range of variation, altitude seemed to be an important spatial factor structuring fish communities of this part the Canadian Shield. Hinch et al. (1991), having found that elevation (200–400 m) was important in explaining fish community composition in their Ontario lakes, came to a similar conclusion.

The negative relationship between the BPUE of large piscivores and both prey fish richness and prey BPUE adds to the growing evidence that the presence of top predators is associated with a reduction in small-bodied fish diversity and (or) abundance in temperate lakes (Chapleau et al. 1997; Findlay et al. 2000). The BPUE of large piscivores was also associated with greater Shannon diversity and Pielou evenness in the fish community, suggesting that piscivory, despite its negative relationship with small-bodied species richness, could contribute to maintaining a relatively high diversity in the fish communities by reducing the biomass of dominant species. *Salvelinus* spp. never co-occurred with large predators, also suggesting an effect of piscivory.

A relatively large part of the variation in the total fish biomass in our study lakes was explained by the Shannon diversity index. Similarly, both prey species richness and diversity were significantly related to prey fish BPUE. It is possible that fish species diversity was related to resource use complementarity, thus leading to higher biomass levels (Loreau 1998; Cardinale et al. 2002). At the level of the top predators, this complementarity could be due to differences in habitat use (in space and time) by walleye and northern pike (i.e., pelagic vs littoral predator with different light regimes), thus leading to an increase in the system's production (Ryder and Kerr 1978). In the case of benthivorous species, the co-occurrence of lake whitefish in lakes containing white sucker could have allowed a better exploitation of deep benthic prey.

The patterns in fish community structure observed in our study lakes are in accordance with the qualitative results of different authors who described the fish communities in lakes of the Canadian Shield (Johnson et al. 1977; Ryder and Kerr 1978; Marshall and Ryan 1987). These authors showed, for example, that northern pike is often the only top predator in these communities, whereas walleye, if present, co-occurs in most cases with northern pike. Our results help in understanding the factors behind these patterns. However, about 50% of the variability in the fish community structure was not accounted for by our analysis. This amount of unexplained variation means that other important factors not considered in our analysis (e.g., water chemistry or lake productivity) are likely to influence fish community structure. Moreover, a more accurate estimation of factors such as beaver dam impact might also have raised the proportion of the explained variation. However, our results show that considering only current connectivity when analyzing the patterns in lake fish communities is a shortcoming. Despite the relative simplicity of this approach, integrating geographic coordinates and elevation as proxies of past dispersion patterns at the landscape level can be highly informative. Olden et al. (2001) criticized such straight-line distance approaches, suggesting that we should consider spatial factors from an "as the fish swims" rather than an "as the crow flies" perspective. However, our results show that spatial factors related to "as the fish swam" are also of primary importance in multivariate approaches aimed at determining the current patterns of distribution of fish.

Acknowledgements

We thank the members of the Groupe de Recherche Interuniversitaire en Limnologie (GRIL) who were involved in this research program and, more specifically, Richard Carignan, Bernadette Pinel-Alloul, and Dolors Planas. We also thank Marco Rodriguez for his help with multivariate analyses and Raphaël Proulx for helpful discussions. Melanie Desrosier, Edenise Garcia, Stéphane Masson, Serge Paquet, Alain Patoine, and Isabelle St-Onge were particularly helpful with laboratory assistance and Mélanie Odion with the GIS data. We are also grateful to the many summer assistants who participated in the fieldwork. Lennart Persson, Bernadette Pinel-Alloul, and William T. Tonn gave valuable comments on previous versions of this paper. We thank Bernard Angers for providing Fig. 1. A. Bertolo was supported by a postdoctoral fellowship from the Groupe de Recherche Interuniversitaire en Limnologie (GRIL) and the Canada Research Chair in Freshwater Ecology. This project was supported by grants from the Sustainable Forest Management Network Center of Excellence and the Natural Sciences and Engineering Research Council of Canada to P. Magnan.

References

Amarasinghe, U.S., and Welcomme, R.L. 2002. An analysis of fish species richness in natural lakes. Environ. Biol. Fishes, **65**: 327–339.

Angers, B., Magnan, P., Plante, M., and Bernatchez, L. 1999. Canonical correspondence analysis for estimating spatial and environmental effects on microsatellite gene diversity in brook charr (*Salvelinus fontinalis*). Mol. Ecol. **8**: 1043–1053.

Borcard, D., Legendre, P., and Drapeau, P. 1992. Partialling out the spatial component of ecological variation. Ecology, **73**: 1045–1055.

Cardinale, B.J., Palmer, M.A., and Collins, S.L. 2002. Species diversity enhances ecosystem functioning through interspecific facilitation. Nature (London), **415**: 426–429.

Carignan, R., D'Arcy, P., and Lamontagne, S. 2000. Comparative impacts of fire and forest harvesting on water quality in Boreal Shield lakes. Can. J. Fish. Aquat. Sci. **57**: 105–117.

Chapleau, F., Findlay, C.S., and Szenasy, E. 1997. Impact of piscivorous fish introductions on fish species richness of small lakes in Gatineau Park, Quebec. Ecoscience, **4**: 259–268.

Collen, P., and Gibson, R.J. 2001. The general ecology of beavers (*Castor* spp.), as related to their influence on stream ecosystems and riparian habitats, and the subsequent effects on fish — a review. Rev. Fish Biol. Fish. **10**: 439–461.

Dodson, S.I., Arnott, S.E., and Cottingham, K.L. 2000. The relationship in lake communities between primary productivity and species richness. Ecology, **81**: 2662–2679.

Draper, N.R., and Smith, H. 1998. Applied regression analysis. 3rd ed. Wiley Series in Probability and Statistics, Wiley-Interscience, New York.

Findlay, C.S., Bert, D.G., and Zheng, L. 2000. Effect of introduced piscivores on native minnow communities in Adirondack lakes. Can. J. Fish. Aquat. Sci. **57**: 570–580.

Gagnon, M.-C., and Angers, B. 2006. The determinant role of post-glacial environment on the genetic structure of species: a comparative study. Mol. Ecol. **15**: 1051–1065.

Hinch, S.G., Collins, N.C., and Harvey, H.H. 1991. Relative abundance of littoral zone fishes: biotic interactions, abiotic factors, and postglacial colonization. Ecology, **72**: 1314–1324.

Jackson, D.A., and Harvey, H.H. 1989. Biogeographic associations in fish assemblages: local vs. regional processes. Ecology, **70**: 1472–1484.

Jackson, D.A., Peres-Neto, P.R., and Olden, J.D. 2001. What controls who is where in freshwater fish communities — the roles of biotic, abiotic, and spatial factors. Can. J. Fish. Aquat. Sci. **58**: 157–170.

Johnson, M.G., Leach, J.H., Minns, C.K., and Olver, C.H. 1977. Limnological characteristics of Ontario Lakes in relation to associations of walleye (*Stizostedion vitreum vitreum*), northern pike (*Esox lucius*), lake trout (*Salvelinus namaycush*), and smallmouth bass (*Micropterus dolomieui*). J. Fish. Res. Board Can. **34**: 1592–1601.

Jongman, R.H., ter Braak, C.J.F., and van Tongeren, O.F.R. 1995. Data analysis in community and landscape ecology. Cambridge University Press, New York.

Legendre, P., and Legendre, V. 1984. Postglacial dispersal of freshwater fishes in the Québec peninsula. Can. J. Fish. Aquat. Sci. **41**: 1781–1802.

Legendre, P., and Legendre, L. 1998. Numerical ecology. 2nd ed. Elsevier, Amsterdam.

Loreau, M. 1998. Biodiversity and ecosystem functioning: a mechanistic model. Proc. Natl. Acad. Sci. U.S.A. **95**: 5632–5636.

Magnan, P., Rodriguez, M.A., Legendre, P., and Lacasse, S. 1994. Dietary variation in a freshwater fish species: relative contributions of biotic interactions, abiotic factors, and spatial structure. Can. J. Fish. Aquat. Sci. **51**: 2856–2865.

Magurran, A.E. 1988. Ecological diversity and its measurement. Princeton University Press, Princeton, New Jersey.

Marshall, T.R., and Ryan, P.A. 1987. Abundance patterns and community attributes of fishes relative to environmental gradients. Can. J. Fish. Aquat. Sci. **44**: 198–215.

Matthews, W.J. 1998. Patterns in freshwater fish ecology. Chapman & Hall, New York.

Olden, J.D., Jackson, D.A., and Peres-Neto, P.R. 2001. Spatial isolation and fish communities in drainage lakes. Oecologia, **127**: 572–585.

Olin, M., and Malinen, T. 2003. Comparison of gillnet and trawl in diurnal fish community sampling. Hydrobiologia, **506–509**: 443–449.

Paszkowski, C.A., and Tonn, W.M. 2000. Community concordance between the fish and aquatic birds of lakes in northern Alberta, Canada: the relative importance of environmental and biotic factors. Freshw. Biol. **43**: 421–437.

Patoine, A., Pinel-Alloul, B., Prepas, E., and Carignan, R. 2000. Do logging and forest fires influence zooplankton biomass in Canadian Boreal Shield lakes? Can. J. Fish. Aquat. Sci. **57**: 155–164.

Planas, D., Desrosiers, M., Groulx, S.R., Paquet, S., and Carignan, R. 2000. Pelagic and benthic algal responses in eastern Canadian Boreal Shield lakes following harvesting and wildfires. Can. J. Fish. Aquat. Sci. **57**: 136–145.

Rahel, F.J. 1984. Factors structuring fish assemblages along a bog lake successional gradient. Ecology, **65**: 1276–1289.

Rahel, F.J. 1990. The hierarchical nature of community persistence: a problem of scale. Am. Nat. **136**: 328–344.

Rasmussen, P.W., Heisey, D.M., Gilbert, S.J., King, R.M., and Hewett, S.W. 2002. Estimating postspawning movement of walleyes among interconnected lakes of northern Wisconsin. Trans. Am. Fish. Soc. **131**: 1020–1032.

Robinson, C.L.K., and Tonn, W.M. 1989. Influence of environmental factors and piscivory in structuring fish assemblages of small Alberta lakes. Can. J. Fish. Aquat. Sci. **46**: 81–89.

Ryder, R.A., and Kerr, S.R. 1978. The adult walleye in the percid community — a niche definition based on feeding behaviour and food specificity. Am. Fish. Soc. Spec. Publ. **11**: 39–51.

St-Onge, I., and Magnan, P. 2000. Impact of logging and natural fires on fish communities of Laurentian Shield lakes. Can. J. Fish. Aquat. Sci. **57**: 165–174.

ter Braak, C.J.F., and Looman, C.W.N. 1994. Biplots in reduced-rank regression. Biom. J. **36**: 983–1003.

ter Braak, C.J.F., and Smilauer, P. 1998. CANOCO reference manual and user's guide to CANOCO for Windows: software for canonical community ordination (Version 4). Centre for Biometry, Wageningen, the Netherlands.

Tonn, W.M., and Magnuson, J.J. 1982. Patterns in the species composition and richness of fish assemblages in Northern Wisconsin Lakes. Ecology, **63**: 1149–1166.

Tonn, W.M., Paszkowski, C.I., and Holopainen, I.J. 1992. Piscivory and recruitment: mechanisms structuring prey populations in small lakes. Ecology, **73**: 951–958.

Appendix A

Table A1 appears on the next page (p. 2792).

Table A1. Occurrence of fish species in the study lakes.

Lake	caco	eslu	pefl	cocl	seco	savi	mama	safo	lolo	nocr	copl	phne	sana	pheo	osmo	nobu	pupu	peom	peca	nohe	luco	cuin	cysp
C12	×	×	×	×	×	×																	×
C2	×	×	×		×																		
C23		×	×	×		×																	
C24		×	×		×				×	×													
C29	×							×	×		×												
C40		×	×							×													
C44	×	×	×	×	×					×										×			
C48	×							×	×		×	×	×										
C9	×	×	×																				
FBP10	×	×	×				×																
FBP9	×	×			×																		
FP15	×	×	×	×	×	×																	×
FP2	×	×	×	×						×													
FP24		×	×																				
FP27	×								×				×						×				×
FP30	×	×	×	×		×																	×
FP31							×	×															
FP32	×	×	×	×		×	×																
N106	×						×	×			×												
N107	×	×	×																		×		
N120	×		×		×			×	×			×											
N122		×																					
N16	×							×															
N35	×	×	×				×																
N43	×	×	×	×					×														
N5	×										×												×
N55	×	×	×		×					×						×							
N56	×	×									×												
N59		×	×													×							
N63	×	×										×											
N70	×	×	×	×	×	×			×														
N82	×													×									×
N84	×	×	×		×	×																	×
N88	×	×					×																
N89	×	×	×	×		×						×											
P109	×		×				×					×			×								
P110	×		×					×						×	×		×	×				×	×
P25	×	×	×	×		×																	

Note: caco, *Catostomus commersonii*; eslu, *Esox lucius*; pefl, *Perca flavescens*; cocl, *Coregonus clupeaformis*; seco, *Semotilus corporalis*; savi, *Sander vitreus*; mama, *Margariscus margarita*; safo, *Salvelinus fontinalis*; lolo, *Lota lota*; nocr, *Notemigonus crysoleucas*; copl, *Couesius plumbeus*; phne, *Phoxinus neogaeus*; sana, *Salvelinus namaycush*; pheo, *Phoxinus eos*; osmo, *Osmerus mordax mordax*; nobu, *Notropis hudsonius*; pupu, *Pungitius pungitius*; peom, *Percopsis omiscomaycus*; peca, *Percina caprodes*; nohe, *Notropis heterolepis*; luco, *Luxilus cornutus*; cuin, *Culaea inconstans*; cysp, Cyprinid sp.

Genetic effects of ELISA-based segregation for control of bacterial kidney disease in Chinook salmon (*Oncorhynchus tshawytscha*)

Jeffrey J. Hard, Diane G. Elliott, Ronald J. Pascho, Dorothy M. Chase, Linda K. Park, James R. Winton, and Donald E. Campton

Abstract: We evaluated genetic variation in ability of Chinook salmon (*Oncorhynchus tshawytscha*) to resist two bacterial pathogens: *Renibacterium salmoninarum*, the agent of bacterial kidney disease (BKD), and *Listonella anguillarum*, an agent of vibriosis. After measuring *R. salmoninarum* antigen in 499 adults by enzyme-linked immunosorbent assay (ELISA), we mated each of 12 males with high or low antigen levels to two females with low to moderate levels and exposed subsets of their progeny to each pathogen separately. We found no correlation between *R. salmoninarum* antigen level in parents and survival of their progeny following pathogen exposure. We estimated high heritability for resistance to *R. salmoninarum* (survival $h^2 = 0.890 \pm 0.256$ (mean ± standard error)) independent of parental antigen level, but low heritability for resistance to *L. anguillarum* ($h^2 = 0.128 \pm 0.078$). The genetic correlation between these survivals ($r_A = -0.204 \pm 0.309$) was near zero. The genetic and phenotypic correlations between survival and antigen levels among surviving progeny exposed to *R. salmoninarum* were both negative ($r_A = -0.716 \pm 0.140$; $r_P = -0.378 \pm 0.041$), indicating that variation in antigen level is linked to survival. These results suggest that selective culling of female broodstock with high antigen titers, which is effective in controlling BKD in salmon hatcheries, will not affect resistance of their progeny.

Résumé : Nous évaluons la variation génétique de la capacité de saumons chinook (*Oncorhynchus tshwawytscha*) à résister à deux pathogènes bactériens, *Renibacterium salmoninarum*, l'agent de la maladie bactérienne du rein (BKD), et *Listonella anguillarum*, un agent de la vibriose. Après avoir mesuré l'antigène *R. salmoninarum* chez 499 adultes par dosage immuno-enzymatique ELISA, nous avons accouplé chacun de 12 mâles possédant des niveaux haut ou bas d'antigène avec deux femelles ayant des niveaux bas à modéré; nous avons ensuite exposé des sous-ensembles de leurs rejetons à chaque pathogène séparément. Il n'y a pas de corrélation entre le niveau d'antigène *R. salmoninarum* des parents et la survie des rejetons après une exposition aux pathogènes. L'héritabilité de la résistance à *R. salmoninarum* (survie $h^2 = 0{,}890 \pm 0{,}256$ (moyenne ± erreur type)) est élevée, quel que soit le niveau d'antigène des parents, mais celle de la résistance à *L. anguillarum* ($h^2 = 0{,}128 \pm 0{,}078$) est faible. La corrélation génétique entre ces survies ($r_A = -0{,}204 \pm 0{,}309$) est presque nulle. Les corrélations génétique et phénotypique entre la survie et les niveaux d'antigène chez les rejetons qui survivent à l'exposition à *R. salmoninarum* sont toutes deux négatives ($r_A = -0{,}716 \pm 0{,}140$; $r_P = -0{,}378 \pm 0{,}041$), ce qui indique que la variation du niveau d'antigène est relié à la survie. Ces résultats laissent croire que la sélection de stocks reproducteurs femelles ayant un fort titre d'antigène, une mesure efficace pour contrôler BKD dans les élevages de saumons, n'affectera pas la résistance à la maladie chez leurs rejetons.

[Traduit par la Rédaction]

Introduction

Over the past century, fish pathologists and fish culturists have improved hatchery practices considerably to reduce the likelihood and severity of disease outbreaks in cultured fish populations (Winton 2001). Nevertheless, the factors that lead to disease-induced mortality still pose prominent management and scientific problems, and research to control fish diseases has focused primarily on prevention and treatment. For some diseases, the processes of infection and progression of disease are now better understood at the cellular and molecular levels (e.g., Røed et al. 2002; Jansson et al. 2003;

Received 12 April 2006. Accepted 29 September 2006. Published on the NRC Research Press Web site at http://cjfas.nrc.ca on 16 December 2006.
J19271

J.J. Hard[1] and L.K. Park. National Marine Fisheries Service, Northwest Fisheries Science Center, Conservation Biology Division, 2725 Montlake Boulevard East, Seattle, WA 98112, USA.
D.G. Elliott, R.J. Pascho, D.M. Chase, and J.R. Winton. US Geological Survey, Biological Resources Division, Western Fisheries Research Center, 6505 NE 65th Street, Seattle, WA 98115, USA.
D.E. Campton. US Fish and Wildlife Service, Abernathy Fish Technology Center, 1440 Abernathy Creek Road, Longview, WA 98632, USA.

[1] Corresponding author (e-mail: jeff.hard@noaa.gov).

doi:10.1139/F06-163

Jhingan et al. 2003). Less well understood are the biological factors and mechanisms that determine host resistance to disease, including genetic variability (Price 1985; Arkush et al. 2002) and immunological competence (Toranzo and Barja 1993; Ellis 1999; Balfry et al. 2001).

One bacterial disease that can cause substantial mortality in cultured populations of anadromous salmonid fishes is bacterial kidney disease (BKD), a chronic condition caused by infection from *Renibacterium salmoninarum* (Fryer and Lannan 1993). The bacterium is transmitted horizontally between cohabiting individuals (Mitchum and Sherman 1981; Bell et al. 1984; Murray et al. 1992) and vertically from mothers to their progeny via infected oocytes (Evelyn et al. 1984*a*, 1984*b*; Lee and Evelyn 1989). *Renibacterium salmoninarum* evidently is not transmitted vertically from male parents to their progeny (Evelyn et al. 1986*a*, 1986*b*).

BKD is typically more severe in Chinook salmon (*Oncorhynchus tshawytscha*) than in most other salmonids (Bullock and Wolf 1986) and is particularly widespread among Chinook salmon reared at hatcheries in the Pacific Northwest (Raymond 1988). In general, BKD is difficult to control because effective vaccines have not yet been developed and antibiotic therapy is only partially effective (Elliott et al. 1989; Evenden et al. 1993). Oral chemotherapy of salmonids with erythromycin (i.e., via feeds) can reduce mortality but does not eliminate infection in all treated fish (Wolf and Dunbar 1959; Fryer and Sanders 1981; Austin 1985). Moreover, juvenile anadromous salmonids infected with *R. salmoninarum* while in fresh water may subsequently die of BKD upon entry into seawater (Banner et al. 1986; Elliott et al. 1995).

Many salmon hatcheries in the Pacific Northwest, particularly those propagating stream-type (spring or summer run) Chinook salmon, take precautions to limit epizootics of BKD (Maule et al. 1996; VanderKooi and Maule 1999). These precautions include the incubation of fertilized eggs from each female parent in isolated containers until all female parents can be tested for the prevalence of *R. salmoninarum* (Pascho et al. 1991; Elliott et al. 1997). Testing typically involves assaying kidney tissue of female parents for *R. salmoninarum* at the time of spawning by means of an enzyme-linked immunosorbent assay (ELISA) for specific antigens produced by this bacterium. Fertilized eggs from a female parent are culled, or segregated from the general hatchery population, if that female has a high ELISA absorbance or optical density (OD) value (e.g., OD > 1.0) indicative of a recent or present infection by *R. salmoninarum*. Broodstock culling or segregation significantly reduces the risk of BKD outbreaks in hatcheries because ELISA ODs are positively correlated with the severity of *R. salmoninarum* infection, and high ELISA ODs in adult females are associated with a higher risk of vertical transmission of the bacterium to progeny (Pascho et al. 1991; Elliott et al. 1997). These ELISA-based culling or segregation procedures have also been shown to improve survival of progeny following release from the hatchery (Pascho et al. 1993; Elliott et al. 1995).

However, such broodstock culling represents a form of selective breeding, and the long-term genetic consequences of this are unknown. For example, broodstock culling on the basis of ELISA OD could reduce BKD resistance in future generations if resistance is heritable and correlated positively with high ELISA titers at the time of spawning. In particular, selectively culling the progeny of female parents with high ELISA ODs could reduce resistance to *R. salmoninarum* in descendants if ELISA ODs at the time of reproduction are positively correlated with genetically based resistance to infection. Conversely, if genetic resistance to *R. salmoninarum* and ELISA ODs are uncorrelated or negatively correlated, then the genetic consequences of excluding female parents with high ELISA ODs should be benign or even beneficial. In this situation, genetic correlations with other diseases and traits related to resistance may be more important considerations in broodstock management.

Vibriosis is another bacterial disease of anadromous salmonid fishes that can cause high mortality in cultured fishes. Vibriosis is an acute systemic disease caused by several species of marine bacteria of the genera *Vibrio* and *Listonella*. These bacteria are usually contracted by salmonids in marine or brackish waters. Infection by *Listonella* and *Vibrio* spp. can cause high mortality in a number of fish species during residence or culture in salt water and, more rarely, in fresh water (Egidius 1987). Although vibriosis is often difficult to control, vaccination can be effective in preventing or ameliorating the intensity of this disease in salmonid culture (Austin and Austin 1987; Hjeltnes and Roberts 1993).

In this paper, we estimate genetic parameters associated with resistance to *R. salmoninarum* and *L. anguillarum* in a hatchery population of Chinook salmon. We are particularly interested in phenotypic and genetic correlations between (*i*) the primary phenotypic indicator of *R. salmoninarum* infection (ELISA OD titers) among adults at the time of spawning and (*ii*) resistance of their progeny to both pathogens. Specifically, we ask: Do adult Chinook salmon with high levels of *R. salmoninarum* antigen, as measured by ELISA OD level, yield progeny with a higher or lower genetic resistance to bacterial infection by either *R. salmoninarum* or *L. anguillarum* than progeny of adults with low levels of *R. salmoninarum* antigen? To address this question, we conducted a single-generation divergent selection experiment on male parents based on their ELISA ODs and then evaluated the mean disease resistance of their progeny as a potential response to selection (e.g., Hill 1972). We selected male parents on the basis of their ELISA ODs, rather than female parents, because females can transfer *R. salmoninarum* vertically to their progeny, resulting in a positive correlation between *R. salmoninarum* levels in the female parents and their progeny that would confound our ability to assess the genetic component of resistance. In contrast, males transmit only their genes to their progeny (Evelyn et al. 1986*a*, 1986*b*).

Although our principal interest relates to resistance to BKD, we included challenges involving *L. anguillarum* in our study so that we could test for a more general response to bacterial pathogens and assess potential genetic correlations between resistances to the two pathogens. Resistance to infection by *L. anguillarum* and *R. salmoninarum* appears to involve different aspects of the salmonid immune system, with humoral immunity more important for protection of fish against vibriosis (Ellis 1999, 2001) and cellular immunity likely more important for protection of fish against

BKD (Ellis 1999; Pascho et al. 2002). If ELISA ODs of parents are correlated with heritable differences among their progeny in resistance to infection by either pathogen, then selective culling of broodstock based on ELISA ODs of *R. salmoninarum* antigen may result in correlated responses to disease resistance in subsequent generations. Such responses would be cumulative over multiple generations and thus could have long-term genetic consequences for controlling disease in hatchery populations. Potential impacts on natural populations that spawn in association with hatchery-origin fish would also be a concern.

Materials and methods

Selection and breeding of parents

We sampled gametes and tissues from adult stream-type Chinook salmon returning to the Carson National Fish Hatchery (CNFH) in August 2001. The CNFH is located on the Wind River, a tributary to the Columbia River near Carson, Washington, USA. CNFH staff spawned a total of approximately 900 adult Chinook salmon at the facility on 15 and 22 August. During those spawning operations, we collected aliquots of milt from 415 males and approximately 600 eggs from each of 84 females, all selected at random. We stored gamete samples from each fish separately in plastic bags at 4 °C for approximately 8–12 h before fertilizing eggs in our experimental crosses (see below). We also collected fin clips and kidney samples for subsequent DNA extraction and ELISA assays, respectively, from all adults from which we sampled gametes. The DNA samples were for a corollary study dealing with gene mapping and not collected specifically for the breeding study described here.

We screened kidney samples from each of the 415 males and 84 females for the presence of *R. salmoninarum* within 4–12 h of gamete collection. At the time of spawning, we removed equal portions of tissue from anterior, middle, and posterior areas of the kidneys of each male and female. We homogenized and diluted the total kidney sample from each fish at 1:4 (*w/v*) in 0.01 $\text{mol}\cdot\text{L}^{-1}$ phosphate-buffered saline (PBS) (pH 7.4) containing 0.05% Tween 20 (PBS–T20), then heated the product at 100 °C for 15 min and centrifuged it at 8800*g* for 5 min at 22 °C. We tested the samples for presence of *R. salmoninarum* antigen by the ELISA II procedure of Pascho et al. (1991). We included controls and determined positive–negative threshold ODs as described by Pascho et al. (1987). We considered kidney samples with ODs $\leq$ 0.100 to be ELISA-negative (i.e., below detection limits for *R. salmoninarum* antigen). We assigned each fish that tested positive by the ELISA to a low, medium, or high *R. salmoninarum* antigen level according to the infection level criteria of Pascho et al. (1991). We considered fish with ELISA ODs between the detection limit (0.101) and 0.199 to have low antigen levels, those with ODs $\geq$ 0.200–0.999 to have medium antigen levels, and those with ODs $\geq$ 1.000 to have high antigen levels. ELISA ODs, which are expressed on a logarithmic scale, ranged from 0.073 to 3.232 for the tested males and from 0.080 to 3.231 for the tested females.

We used milt aliquots from males with the 13 lowest ELISA ODs (0.073–0.087) to fertilize the eggs from each of three random females (female ELISA OD was unrecorded at the time of spawning) in a paternal half-sib (HS) nested breeding design (1 male : 3 females), with the goal of retaining two full-sib (FS) families per sire and the proviso that only progeny (fertilized eggs) from females with lower ELISA ODs (~<0.3) would be retained to minimize the risk of vertical transmission of *R. salmoninarum* from mother to progeny. Such vertical transmission would confound the genetic analysis and needed to be minimized. We accounted for variation in dam ELISA OD statistically by treating it as an independent covariate in our evaluations of progeny disease resistance (see Data analysis below). Our approach reflected a trade-off between balancing the experimental design statistically — where all female parents truly represented a "random effect" — and confounding the results of the experiment itself by including progeny of females with high antigen titers. For example, for one HS family sired by a "low ELISA" male, we included only one FS family (i.e., progeny of one female parent) because, by chance, the other two female parents had ODs > 1.0. For another HS family, we included three FS families where all female parents had ELISA ODs < 0.1.

Similarly, we used milt aliquots from males with the 15 highest ELISA ODs (1.321–3.232) to fertilize eggs from each of three additional, randomly selected females (1 male : 3 females).

Overall, these crosses resulted in a total of 84 FS families: 39 families representing the progeny of the 13 males with the lowest ODs, and 45 FS families representing the progeny of the 15 males with the highest ODs. ELISA ODs for the 84 randomly selected female parents ranged from 0.080 to 3.231, but families in which the female parent had ELISA ODs greater than 0.30 were excluded from the challenge experiments (see below).

Throughout this paper, we refer to "high" and "low" families (sire groups) as representing the progeny of male parents (sires) with high (>1.3) and low (<0.09) ELISA ODs, respectively. We ultimately retained, for the bacterial challenge experiments, two FS families from each of 12 male parents within each sire group, with the exception noted above for the low families (see below).

Culture of progeny

Fertilized eggs from each of the original 84 FS family crosses were incubated in 84 separate buckets, each supplied separately with upwelling pathogen-free well water, at the CNFH. On 4 October 2001, at the eyed-egg embryo stage, we transferred embryos representing 36 FS families produced on the first spawning day from the CNFH to the US Fish and Wildlife Service (USFWS) Abernathy Fish Technology Center (AFTC) near Longview, Washington. We transferred eyed-egg embryos representing 34 FS families produced on the second spawning day to the AFTC on 11 October. We placed the eyed-egg embryos representing each family in a separate Heath incubator tray at the AFTC. The combined transfers of eyed-egg embryos between facilities involved a total of 70 FS families (both spawning days); we did not transfer embryos from 14 families either because of poor fertilization (or survival) success or because the female parent had a high ELISA OD (>0.7) indicating a medium to high likelihood that the eggs were infected with *R. salmoninarum*. On 28 November, we transferred "swim-up" fry representing 24 FS families from the first spawn take (10 low and 14 high ELISA OD sire families) from incubator trays to separate 1.2 m diameter circular fiberglass tanks (1 FS family per tank) at the AFTC. On 5 December, we transferred swim-up fry representing 24 additional FS families from the second spawn take (14 low and 10 high OD sire families) to 24 additional tanks. Pathogen-free well water at 13.5 °C supplied all tanks. Because of the limited number of tanks and the need to minimize potential vertical transmission of *R. salmoninarum*, these transfers involved culling 22 FS families with the goal that each male parent ($n = 24$) was represented by two FS families and no female parent had an ELISA OD > 0.30, as described previously. Overall, 24 of the retained 48 FS families represented 12 paternal HS families of 12 males with high ELISA ODs (mean = 2.636, range = 1.321–3.232); the other 24 FS families represented 12 HS families of 12 males with low ELISA ODs (mean = 0.083, range = 0.073–0.087). Thus, the breeding design resulted in two sire or treatment groups based on high or low ELISA ODs.

The ELISA ODs of the female parents of the 48 families retained for the bacterial challenges ranged from 0.080 to 0.274. Of these 48 females, 45 had ELISA ODs below the detection limit for *R. salmoninarum* (≤0.100). We considered two of the ELISA-positive fish to have low antigen levels (ODs = 0.109 and 0.171) and considered the third ELISA-positive fish to have a medium antigen level (OD = 0.274). A corollary analysis revealed no difference (Fisher exact test, $P \geq 0.3$) in survival of *R. salmoninarum*-challenged progeny of the females with the two highest kidney ELISA ODs (0.171 and 0.274) and the survival of *R. salmoninarum*-challenged progeny of the ELISA-negative females (OD = 0.084 and 0.095, respectively) that had been mated to the same male parents (ELISA OD for both males was 0.084). Hence, we detected no evidence that the ELISA-positive female parents contributed to vertical transmission of the bacterium or immunotolerance of their progeny.

Selection of male parents resulted in an unweighted divergent selection differential of 3.59 phenotypic standard deviations (SD) between the mean values for the high and low selected males relative to the population of 415 males screened before selection. The mean of selected males with high ODs was 0.53 SD higher than that of all males with ODs > 1.0, and the mean of selected males with low ODs was 0.78 SD lower than that of all males with ODs < 1.0.

Divergent selection of parents maximizes the efficiency and statistical power of the experimental design for detecting additive genetic variation among parents in parent–offspring comparisons (Hill and Thompson 1977). However, this selection, combined with the exclusion of female parents with high ELISA titers, can introduce bias in genetic parameter estimates based on a sib analysis (Falconer and Mackay 1996; Lynch and Walsh 1998). The degree of bias is unknown, but it would affect primarily ELISA OD and traits highly correlated genetically with that trait. That said, the primary goal of our study was not to obtain unbiased genetic parameter estimates but rather to maximize the power of determining whether ELISA ODs of parents are correlated genetically with their breeding values for disease resistance as measured by the mean resistance of their progeny. The core of our experimental design therefore consisted of two divergently selected treatment groups based on the highest and lowest ELISA ODs of the male parents, overlaid onto a North Carolina design 1 (Falconer and Mackay 1996) breeding scheme.

On 8–11 January 2002, we culled each FS family randomly to 200 fish to equalize rearing densities among families and optimize individual growth rates within each tank. On 8–11 April, we selected 165–168 fish randomly from within each FS family and injected them intraperitoneally with passive integrated transponder (PIT) tags. We removed nontagged fish within each family from the experiment.

Bacterial challenges

For bacterial challenges, we transported fish to the Western Fisheries Research Center (WFRC) in Seattle, Washington, and held them in circular tanks supplied with sand-filtered, UV-treated Lake Washington water at temperatures and densities described below for each challenge.

Listonella anguillarum challenges

We randomly netted and hand-counted 80 PIT-tagged fish from each FS family at the AFTC and transported them to the WFRC for a *L. anguillarum* challenge (2 May 2002). However, as expected, some minor counting errors did occur such that at least one family was represented by only 70 fish at the time of transport to the WFRC. For the challenge, we cultured *L. anguillarum* strain 775 (ATCC strain 68554) as described by Murray et al. (2003). On the basis of preliminary test challenges, we determined that a *L. anguillarum* concentration of 7.2×10^3 bacteria·mL^{-1} caused 50% mortality in 14 days at 17 °C. We therefore used this concentration in a *L. anguillarum* 775 waterborne challenge with 35 PIT-tagged fish from each FS family.

We performed the waterborne challenge on 9 July 2002, approximately 2 months after transport of fish (mean weight, 5.2 g) to the WFRC, in static, aerated water supplemented with 0.85% sodium chloride at a challenge density of 60 g·L^{-1}. We held 35 treatment fish from each FS family collectively in the bacterial suspension for 15 min. We also exposed 35 control fish from each FS family to uninoculated bacterial growth medium for 15 min in static, aerated water supplemented with 0.85% sodium chloride at a challenge density of 60 g·L^{-1}. After the 15-min exposure, we removed all fish from the challenge and control tanks and placed them into separate holding tanks at a density of 4.8 g·L^{-1}, maintaining them at 17 °C for 14 days after the challenge. We fed fish ad libitum with a commercial salmon diet (Bio-Oregon, Warrenton, Oregon) and removed dead fish from the control and challenge tanks daily and recorded the PIT tag numbers for each dead fish.

To confirm the presence of *L. anguillarum* in dead fish, we cultured kidney tissue from a sample of 10 mortalities collected in the first week of the *L. anguillarum* challenge group on agar plates and identified bacteria by the procedure of Murray et al. (2003); all fish in each sample tested positive for *L. anguillarum* infection. At the end of the challenge, we euthanized the surviving fish with tricaine methanesulfonate anesthetic (MS-222; Argent Chemical Laboratories, Redmond, Washington) and recorded their PIT tag numbers.

We tested for the presence of *L. anguillarum* in a sample of surviving fish from the control group (n = 30) and the challenge group (n = 20) by bacterial culture; all 50 surviving fish tested negative for *L. anguillarum* infection.

Renibacterium salmoninarum challenges

We transported the remaining PIT-tagged fish from each FS family (n = 74–98 fish per family) at the AFTC to the WFRC for the *R. salmoninarum* challenge (22 August 2002). The fish (mean weight, 30.2 g) in each family were divided equally between control and challenge tanks at the WFRC. We prepared, harvested, and quantified experimental cultures of *R. salmoninarum* (strain ATCC 33209; American Type Culture Collection, Manassas, Virginia) during September according to the procedures of O'Farrell et al. (2000). On 3 September 2002, we initiated the waterborne challenge in static, aerated 12 °C water at a challenge density of 51 $g\cdot L^{-1}$. We held the fish in the bacterial suspension of 1×10^7 $bacteria\cdot mL^{-1}$ for 24 h as described by O'Farrell et al. (2000). We exposed control fish to PBS–peptone for 24 h in static, aerated 12 °C water at a challenge density of 51 $g\cdot L^{-1}$. After challenge, we restored water levels in the tanks to provide a holding density of 18 $g\cdot L^{-1}$ and maintained fish at 12 °C on a commercial salmon diet (Bio-Oregon), fed at 2.1% body weight per day, for 14 weeks. We collected dead fish from control and challenge tanks daily and recorded the PIT tag number for each dead fish. At the end of the challenge, we euthanized all surviving fish with MS-222 and recorded their PIT tag numbers. We measured *R. salmoninarum* antigen levels in a sample of surviving fish from each FS family from the challenge group and from the control group (≤20 fish per family, depending on the number of survivors per family) by ELISA. We processed fish tissues and performed the ELISA according to the methods described previously, except that we sampled the entire kidney and spleen, and we diluted the tissue samples 1:8 (*w/v*) with PBS–T20.

Data analysis

We analyzed genetic and phenotypic variation in five traits among the progeny: (*i*) survival in the *R. salmoninarum* challenge (RS); (*ii*) days to death for mortalities in the *R. salmoninarum* challenge (RD); (*iii*) survival in the *L. anguillarum* challenge (LS); (*iv*) days to death for mortalities in the *L. anguillarum* challenge (LD); and (*v*) ELISA ODs of survivors of the *R. salmoninarum* challenge (OD). We coded individual survival (RS and LS) as binary traits (0 or 1) in each challenge and adjusted the data for the few mortalities observed in the control groups. (Only 25 control fish died in the *R. salmoninarum* experiment, 22 of which died after 154 days; seven control fish died in the *L. anguillarum* experiment, all on the first day. All control mortalities were uninfected.) Although days to death are expected to follow a Poisson distribution, we did not transform those data because logarithmic transformation of the right-skewed distributions did not significantly improve normality based on chi-square goodness-of-fit tests.

For each challenge, we calculated the FS family mean for each trait in the control group and subtracted that mean from the observed phenotype of each fish from the same family in the treatment group:

$$(1) \qquad y^{*}_{ijk} = y_{ijk} - \bar{x}_{ij}$$

where y^{*}_{ijk} is the adjusted phenotype of the trait for the kth progeny within the jth FS family for the ith sire in the treatment group, y_{ijk} is the observed phenotype of the trait (0 or 1 for binary traits) for the same individual, and $\bar{x}_{ij}$ is the mean phenotype of the trait for the ith–jth FS family in the control group.

For each trait, we estimated the partial regression coefficients of offspring phenotypes on their parental ELISA ODs by least squares. The regression model was

$$(2) \qquad y^{*}_{ijk} = b_0 + b_1 x_{1i} + b_2 x_{2ij} + e_{ijk}$$

where y^{*}_{ijk} is the corrected phenotype of the trait (eq. 1) for the kth progeny of the jth dam (FS family) and ith sire (HS family), x_{1i} is the ELISA OD of the ith sire, x_{2ij} is the ELISA OD of the jth dam mated to the ith sire, b_1 and b_2 are the partial regression coefficients on ELISA ODs, b_0 is the y intercept, and e_{ijk} is the residual error deviation from the regression. These regressions measure single-generation responses to selection among progeny when one group of parents (sires) is selected on the basis of their ELISA ODs, but the ELISA OD of the other group of parent (dams) may be correlated environmentally with progeny phenotypes and is thus treated as a covariate. The mean phenotypic value for the progeny of each male parent is an estimate of one-half of that male parent's breeding value for that trait (Falconer and Mackay 1996). The phenotypic covariance between ELISA ODs of male parents and disease-resistance traits of their progeny, as measured by the partial regression coefficient b_1 for each trait, is assumed to reflect a genetic correlation between those traits because the environmental correlation between them, measured separately on male parents and their offspring in two different environments, is expected to equal zero. This expectation is not true for female parents due to maternal environmental effects, including the potential transmission of *R. salmoninarum* vertically to their progeny. In this context, the partial regression of each progeny trait on dam ELISA OD removes the dam as a source of variation independent of sire effects.

We estimated variance components for each trait among progeny with a multivariate animal model (Kruuk 2004), calculating genetic and environmental components of covariance and their derivatives (heritability (h^2) and genetic correlation (r_A)) for each of the traits with restricted maximum likelihood (REML) (Patterson and Thompson 1971; Harville 1977; Shaw 1987). The mixed model for variance component estimation was of the form

$$(3) \qquad \boldsymbol{y} = \mathbf{X}\boldsymbol{b} + \mathbf{Z}\boldsymbol{s} + \mathbf{W}\boldsymbol{d} + \mathbf{I}\boldsymbol{e}$$

where $\boldsymbol{y}$ is the vector of trait phenotypes, $\mathbf{X}$ is the incidence (design) matrix for the fixed effect of the grand mean, $\mathbf{Z}$ is the incidence matrix for the random effect of sire, $\mathbf{W}$ is the incidence matrix for the random effect of dam, $\mathbf{I}$ is the error matrix, and $\boldsymbol{b}$, $\boldsymbol{s}$, $\boldsymbol{d}$, and $\boldsymbol{e}$ are vectors containing the effects of these fixed and random factors on the individual phenotype. The elements of the incidence matrices are 0 and 1 (1

Table 1. Summary statistics for five traits of juvenile Chinook salmon (*Oncorhynchus tshawytscha*) following bacterial challenges.

Trait	Sire group	*n*	Mean ± SE	V_P ± SE	CV (%)
RS	High	989	0.751±0.014	0.194±0.007	58.6
	Low	973	0.790±0.013	0.167±0.010	51.7
RD	High	246	102.1±2.0	707.3±58.1	26.0
	Low	204	105.5±2.0	604.1±61.3	23.3
OD	High	465	0.381±0.015	0.107±0.007	85.9
	Low	477	0.410±0.015	0.115±0.010	82.7
LS	High	706	0.184±0.015	0.151±0.008	211.2
	Low	724	0.215±0.015	0.168±0.009	190.6
LD	High	576	3.37±0.03	0.593±0.034	22.9
	Low	568	3.30±0.10	0.599±0.036	23.4

Note: RS, survival proportion of fish (progeny) in the *Renibacterium salmoninarum* challenge; RD, days to death for fish that died in the *R. salmoninarum* challenge; OD, corrected ELISA ODs (antigen titers) for fish that survived the *R. salmoninarum* challenge; LS, survival proportion of fish in the *Listonella* (*Vibrio*) *anguillarum* challenge; LD, days to death for fish that died in the *L. anguillarum* challenge; *n*, number of fish; V_P, phenotypic variance; CV, phenotypic coefficient of variation; SE, standard error. Estimates for RS and LS are expressed on the outward binary scale. Sire group refers to male Chinook salmon parents that were selectively bred on the basis of their high (1.321–3.232) or low (0.073–0.087) ELISA ODs.

if the *k*th individual is the progeny of the *i*th sire or *j*th dam, 0 otherwise). This model is easily reformulated in terms of the causal genetic and environmental components of variance and covariance that incorporate the vectors of breeding values (additive genetic effects), dominance deviations, and environmental deviations (Shaw 1987).

We used the program ASReml (Gilmour et al. 2002), which implements analysis of mixed linear models with REML, to estimate variance components and their derivatives for each trait, with maternal ELISA OD as a covariate. We employed REML estimation because estimates derived by least squares (e.g., multivariate analysis of variance) can be biased when family structure is unbalanced and the resulting trait covariance matrices are sparse (Henderson 1953; Searle et al. 1992). REML produces unbiased parameter estimates even in this case; in balanced designs, estimates from REML and least squares are equivalent (Searle et al. 1992; Knott et al. 1995). Clark (1990) showed empirically that estimates computed by the two methods can correspond well under a fairly typical experimental design. We did not constrain the parameter estimates. For the binary survival traits RS and LS, we transformed the heritability estimates to an underlying continuous scale of liability using the methods of Robertson and Lerner (1949) and Dempster and Lerner (1950). We computed the standard errors of these estimates according to Falconer and Mackay (1996) and Roff (1997). In an independent effort to relate observed variance components to those on the underlying scale for survival, we also estimated these components with a sire model using a probit link function (cumulative normal distribution function) with the residual variance set to 1. Where standard errors of genetic correlations could not be estimated by maximum likelihood, we computed these standard errors from the estimates of the genetic correlation, heritabilities, and their standard errors according to the methods of Reeve (1955), Robertson (1959), and Gilmour et al. (2002). We estimated the environmental correlation between each trait pair from the relationship between their phenotypic and genetic correlations according to Falconer and Mackay (1996).

Results

Survival following *Renibacterium* exposure

Mean survivals (RS) following challenge with *R. salmoninarum* were similar for progeny of sires with high and low ELISA ODs (0.751 ± 0.014 and 0.790 ± 0.013, respectively; Table 1). Survival within each FS family ranged from 0.395 to 0.952 for progeny of low ELISA sires and from 0.263 to 0.952 for progeny of high ELISA sires (Fig. 1). Over both sire groups, mean FS family size declined from 40.9 to 31.5 fish, whereas mean HS family size declined from 81.7 to 63.0 fish.

For fish that died following exposure to *R. salmoninarum*, mean days to death (RD) was similar for progeny of high and low ELISA sires (102.1 ± 2.0 days and 105.5 ± 2.0 days, respectively; Table 1). The distributions of RD were slightly skewed to the right with modes of approximately 80 and 90 days for the two sire groups, respectively (Fig. 2).

For fish that survived the *R. salmoninarum* challenge, mean ELISA OD (OD) was also similar for progeny of high and low ELISA sires (0.381 ± 0.015 and 0.410 ± 0.015, respectively; Table 1). OD among surviving fish ranged from approximately 0.1 to 1.9 with the distributions strongly skewed to the right (Fig. 3).

Survival following *Listonella* exposure

Mean survivals (LS) following challenge with *L. anguillarum* were similar for progeny of high and low ELISA sires (0.184 ± 0.015 and 0.215 ± 0.015, respectively; Table 1). Survival within each FS family ranged from 0.057 to 0.485 and from 0.071 to 0.310 for families of low and high ELISA sires, respectively (Fig. 1). Over both sire groups, mean FS family size declined from 29.8 to 6.0 fish, whereas mean HS family size declined from 59.6 to 11.9 fish.

For fish that died following exposure to *L. anguillarum*, death was rapid (1–7 days), with mean days to death (LD) similar for progeny of high and low ELISA sires (3.37 ± 0.03 days and 3.30 ± 0.10 days, respectively; Table 1). The

Fig. 1. Distributions of survivors among (*a* and *b*) 48 full-sib and (*c* and *d*) 24 half-sib families of juvenile Chinook salmon (*Oncorhynchus tshawytscha*) exposed to (*a* and *c*) *Renibacterium salmoninarum* (trait RS) and (*b* and *d*) *Listonella* (*Vibrio*) *anguillarum* (trait LS): progeny of fathers with low ELISA ODs, shaded bars; progeny of fathers with high ELISA ODs, solid bars.

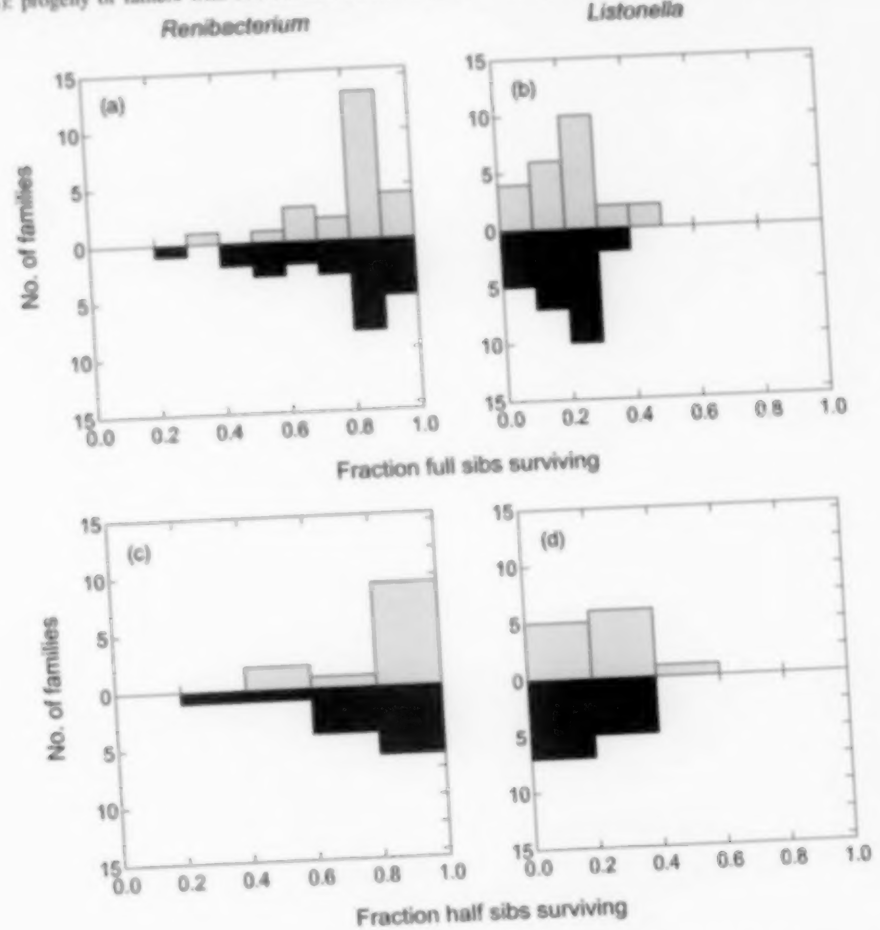

distributions of LD for the two sire groups were nearly identical, each with a mode of 3 days (Fig. 2).

Regressions of progeny traits on parental ELISA OD: *Renibacterium* trial

We observed no relationship between parental ELISA OD and mean survival (RS) of their progeny following exposure to *R. salmoninarum*. Mean survivals of progeny within FS and HS families were each uncorrelated with sire ELISA OD (Fig. 4). Similarly, mean survivals of progeny within each FS family were uncorrelated with dam ELISA OD within each sire group, but the range of dam ELISA ODs was low (Fig. 5) because female parents with values > 0.3 were excluded from the experiment, as described previously. Multiple regression of RS on parental ELISA OD, with the effect of dam OD treated as a covariate to adjust for potential maternal effects, further revealed no significant relationship between survival of progeny and ELISA OD of their male parents (FS families, $F_{[2,45]} = 0.296$, $P = 0.75$; HS families, $F_{[2,21]} = 0.230$, $P = 0.80$).

Among fish that died following the *R. salmoninarum* challenge, days to death (RD) of progeny was uncorrelated with dam ELISA OD for progeny in the low sire group ($F_{[1,202]}$ = 1.966, $P = 0.16$) but was significantly correlated with dam ELISA OD for progeny in the high sire group ($F_{[1,244]}$ = 11.500, $P < 0.01$; Fig. 6). RD was uncorrelated with sire ELISA OD ($t_{459} = 0.634$, $P = 0.53$; Fig. 6). Multiple regression of RD on parental ELISA ODs indicated a weak positive correlation between days to death of progeny and ELISA ODs of their male parents after adjusting for dam OD ($F_{[2,447]} = 2.836$, $P = 0.06$).

Among fish that survived the *R. salmoninarum* challenge, ELISA OD (OD) was uncorrelated with dam ELISA OD in either sire group (high sires, $F_{[1,463]} = 0.531$, $P = 0.47$; low sires, $F_{[1,475]} = 1.337$, $P = 0.25$). Similarly, sire ELISA OD had no detectable relation with ODs among surviving progeny ($t_{941} = 0.971$, $P = 0.33$; Fig. 7). Multiple regression of progeny OD on parental ELISA OD indicated no effect of sire OD when dam OD was used as a covariate ($F_{[2,939]}$ = 1.136, $P = 0.32$).

Fig. 2. Distributions (families combined) of days to death for juvenile Chinook salmon (*Oncorhynchus tshawytscha*) following exposure to (*a*) *Renibacterium salmoninarum* (trait RD) and (*b*) *Listonella* (*Vibrio*) *anguillarum* (trait LD): progeny of fathers with low ELISA ODs, shaded bars; progeny of fathers with high ELISA ODs, solid bars.

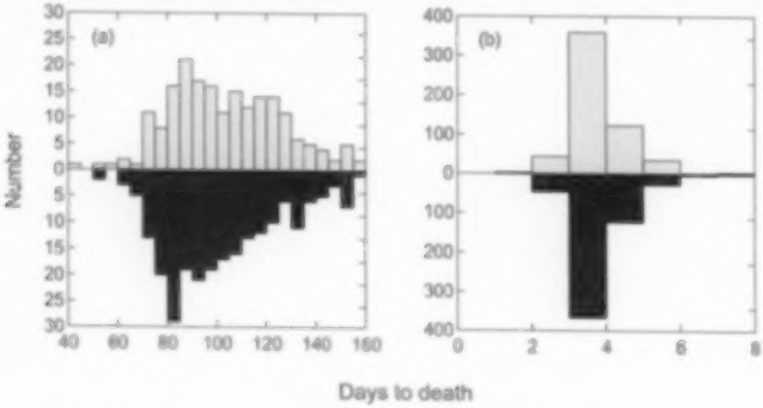

Fig. 3. Distributions of corrected ELISA ODs for juvenile Chinook salmon (*Oncorhynchus tshawytscha*) surviving exposure to *Renibacterium salmoninarum* (trait OD): progeny of fathers with low ELISA ODs, shaded bars; progeny of fathers with high ELISA ODs, solid bars.

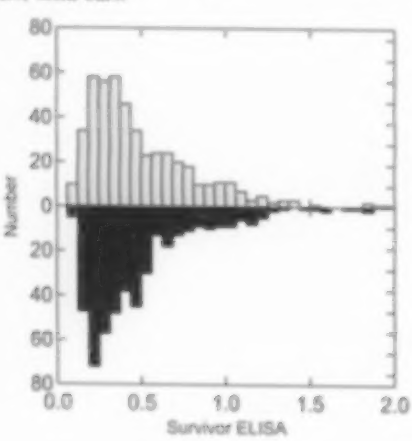

Regressions of progeny traits on parental ELISA OD: *Listonella* trial

We observed no relationship between parental ELISA OD and mean survival (LS) of their progeny following exposure to *L. anguillarum*. Mean survivals of progeny within FS and HS families were uncorrelated with sire ELISA ODs in the *L. anguillarum* challenge (Fig. 4). Mean survivals of progeny within FS families were similarly uncorrelated with dam ELISA OD within each sire group (Fig. 5). Multiple regression of LS on parental ELISA ODs, with the effects of dam OD treated as a covariate to adjust for potential maternal effects, revealed no relationship between survival of progeny and ELISA OD of their male parents (FS families, $F_{[2,45]} = 2.104$, $P = 0.13$; HS families, $F_{[2,21]} = 1.202$, $P = 0.32$).

Among fish that died following the *L. anguillarum* challenge, days to death (LD) of progeny was uncorrelated with dam ELISA OD for progeny in both the low sire group ($F_{[1,566]} = 1.773$, $P = 0.18$) and the high sire group ($F_{[1,574]} = 0.037$, $P = 0.85$; Fig. 6). LD was also uncorrelated with sire ELISA OD ($t_{1143} = 0.373$, $P = 0.71$; Fig. 6). Multiple regression of LD on parental ELISA ODs indicated no significant correlation between LD and sire OD with dam OD treated as a covariate to adjust for potential maternal effects ($F_{[2,1141]} = 1.063$, $P = 0.34$).

Heritabilities of traits measured on progeny

Heritability estimates (h^2) derived from REML estimates of sire and dam variance components for the three traits associated with the *R. salmoninarum* challenge were statistically significant; those for the two traits associated with the *L. anguillarum* challenge were not (Table 2). The h^2 (±SE) of RS (based on the sire component of variance under a threshold-liability model) with maternal ELISA OD as a covariate was 0.890 ± 0.256, indicating that nearly 90% of the observed phenotypic variation in survival among progeny was due to additive genetic variation among their male parents. An independent estimate for h^2 of RS using a probit link function was 0.336 ± 0.081. However, as noted previously, this heritable variation in survival among progeny was uncorrelated with ELISA OD of their male parents. By contrast, the threshold h^2 of LS was 0.128 ± 0.078, indicating that about 13% of the variation in progeny survival following exposure to *L. anguillarum* was due to additive genetic variation among male parents. An estimate for h^2 of LS using a probit link function was 0.061 ± 0.029. Heritability estimates for RD and LD were 0.350 ± 0.162 and 0.071 ± 0.047, respectively, indicating low to modest h^2 associated with days to death for progeny that died following exposure to each pathogen.

The h^2 of ELISA OD (OD) among survivors of the *R. salmoninarum* challenge was 0.271 ± 0.101, indicating significant genetic variation among survivors within HS families in bacterial antigen load (analysis of variance (ANOVA), $F_{[22,918]} = 3.089$, $P < 0.001$). However, as noted previously, this variation in OD among progeny was uncorrelated with ELISA OD of their male parents, thus indicating significant additive genetic variation among male

Fig. 4. Proportions of Chinook salmon (*Oncorhynchus tshawytscha*) progeny within each of (*a*) 48 full-sib families and (*b*) 24 half-sib families surviving exposure to *Renibacterium salmoninarum* (● and broken lines) and *Listonella* (*Vibrio*) *anguillarum* (△ and solid lines), as functions of sire ELISA ODs. Families of low (ELISA OD ≤ 0.1) and high (ELISA OD > 0.1) sire groups are shown in each plot. All regressions are not significant ($P > 0.05$).

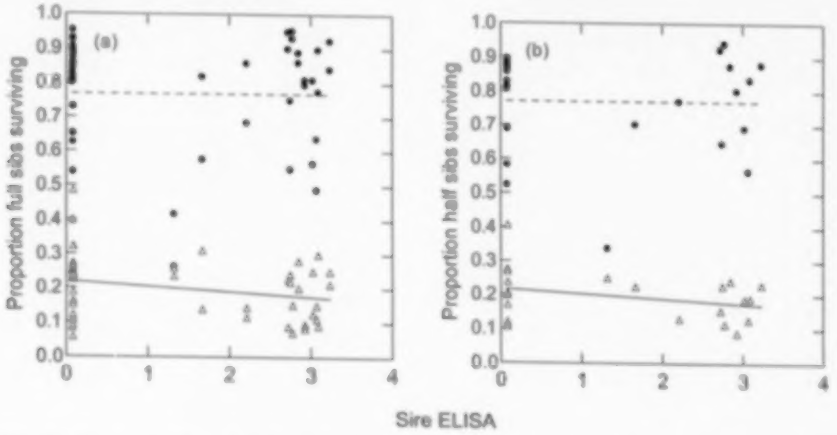

Fig. 5. Proportions of Chinook salmon (*Oncorhynchus tshawytscha*) progeny within each of 48 full-sib families surviving exposure to (*a*) *Renibacterium salmoninarum* (RS) and (*b*) *Listonella* (*Vibrio*) *anguillarum* (LS), as a function of dam ELISA ODs. Low sire group, fathers with low ELISA ODs (●); high sire group, fathers with high ELISA ODs (△). The regressions, not shown, are not significant ($P > 0.05$).

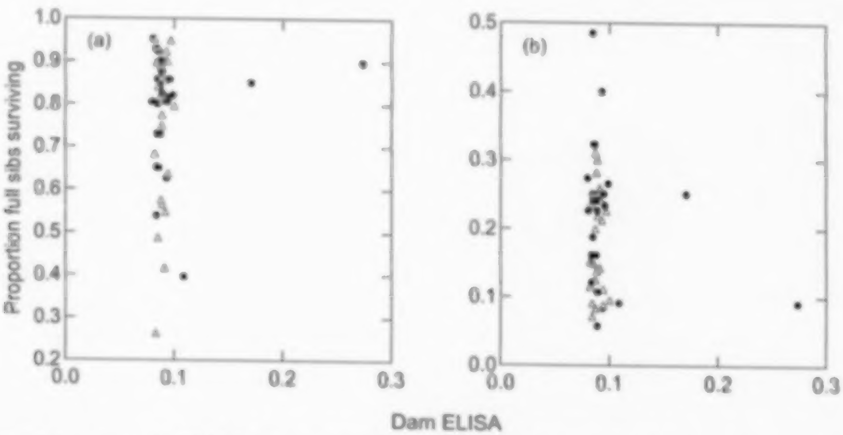

parents independent of that parent's ELISA OD. For example, the sire component of variance accounted for 6.9% of the total phenotypic variance in ODs among surviving progeny, but the sire's measured OD accounted for virtually none (<0.001%) of this variation in progeny OD.

Genetic and phenotypic correlations among traits

Genetic and phenotypic correlations for each pair of traits were similar in direction for most traits, but the magnitude of the estimated genetic correlations always exceeded those of corresponding phenotypic correlations (Table 2). RS and RD were uncorrelated phenotypically but highly positively correlated genetically ($r_P = -0.008 \pm 0.070$ and $r_A = 0.870 \pm 0.164$, respectively). LD and LS were weakly negatively correlated phenotypically ($r_P = -0.095 \pm 0.042$) but highly positively correlated genetically ($r_A = 1.193 \pm 0.467$). This positive correlation indicates that HS families with higher than average survivals following exposure to *L. anguillarum* tended to have progeny that survived longer on average among those that died. OD was negatively correlated both phenotypically ($r_P = -0.378 \pm 0.041$) and genetically ($r_A = -0.716 \pm 0.140$) with RS; OD was uncorrelated both phenotypically and genetically with the other traits. Phenotypic and genetic correlations between RS and LS were not significantly different from zero. Overall, 3 of the 10 genetic correlation estimates differed significantly from zero (between RS and RD, RS and OD, and LS and LD); all estimates were large, and those involving survival and longevity were positive.

Discussion

Previous investigations have provided insight into the genetic factors associated with phenotypic variation in disease resistance in fishes, including infectious bacterial diseases (Chevassus and Dorson 1990; Fjalestad et al. 1993; Jansson et al. 2003). The general conclusion is that genetic variation

Fig. 6. Days to death for Chinook salmon (*Oncorhynchus tshawytscha*) progeny that died following exposure to (*a* and *c*) *Renibacterium salmoninarum* (RS) and (*b* and *d*) *Listonella* (*Vibrio*) *anguillarum* (LS), as functions of (*a* and *b*) dam and (*c* and *d*) sire ELISA OD. Low sire group, fathers with low ELISA ODs (● and broken lines); high sire group, fathers with high ELISA ODs (△ and solid lines). The regressions of days to death on dam ELISA OD for progeny of the low sire group or on sire ELISA OD for progeny of either sire group are not significant ($P > 0.05$) in trials involving either pathogen. The regression of days to death on dam ELISA OD in the *Renibacterium* trial for progeny of the high sire group (*a*) is highly significant ($P < 0.01$).

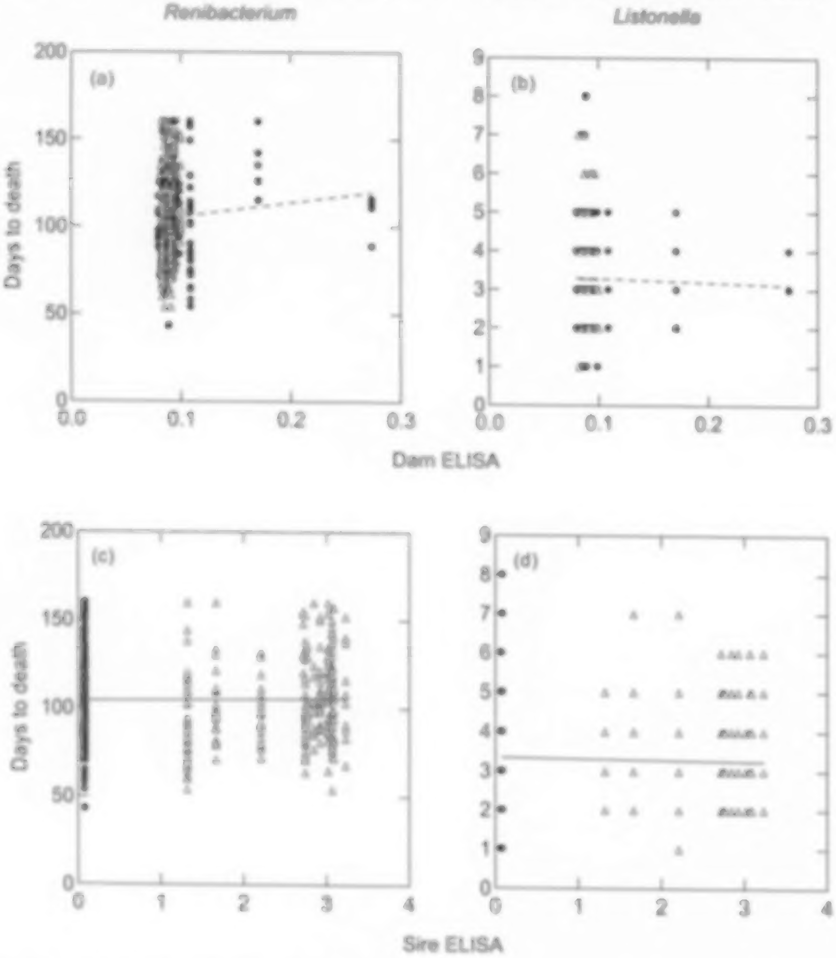

for resistance to disease is pathogen-specific and, for a particular pathogen, can vary considerably among salmonid species and among conspecific populations.

Genetic resistance to BKD

Although several studies have measured genetic variation for resistance to BKD in Atlantic and Pacific salmon, heritability estimates have ranged widely in magnitude among populations for many salmonid species. For example, Withler and Evelyn (1990) reported heritabilities of 0.90 ± 0.26 (0.53 ± 0.16 on the outward binary scale) and 0.26 ± 0.10 for survival and time to death, respectively, for coho salmon (*O. kisutch*) following intraperitoneal injection of *R. salmoninarum*. Similarly, Beacham and Evelyn (1992*a*) reported BKD survival heritabilities (threshold h^2) of 0.42 (0.26) and 0.66 (0.38) in two populations, respectively, of Chinook salmon, although the small number of families yielded large standard errors of those estimates (0.53 and 0.43, respectively). A third population exhibited a substantially lower survival heritability due to BKD relative to the first two populations (6.9% vs 42.1% and 29.4%, respectively), but no genetic variation for survival ($h^2 = 0.03 \pm 0.07$) and heritability estimates near zero for time to death (Beacham and Evelyn 1992*a*). Gjedrem and Gjøen (1995) estimated the heritability of mortality from BKD in an Atlantic salmon population as 0.38 (0.23 ± 0.010 on the binary scale). Other studies have yielded similar results (e.g., Suzumoto et al. 1977; Winter et al. 1980; Olivier et al. 1992).

Our heritability estimates for survival ($h^2 = 0.89 \pm 0.26$) and days to death ($h^2 = 0.35 \pm 0.16$) following challenges to *R. salmoninarum* are similar to or exceed those reported previously and reflect sufficient additive genetic variation to potentially result in significant selection responses to pathogen

Fig. 7. ELISA ODs for juvenile Chinook salmon (*Oncorhynchus tshawytscha*) surviving exposure to *Renibacterium salmoninarum* (trait OD) as functions of (*a*) dam and (*b*) sire ELISA OD. Low sire group, fathers with low ELISA ODs (● and broken lines); high sire group, fathers with high ELISA ODs (△ and solid lines). The regressions of survivor ELISA OD on dam ELISA OD for progeny of either sire group or on sire ELISA OD are not significant ($P > 0.05$).

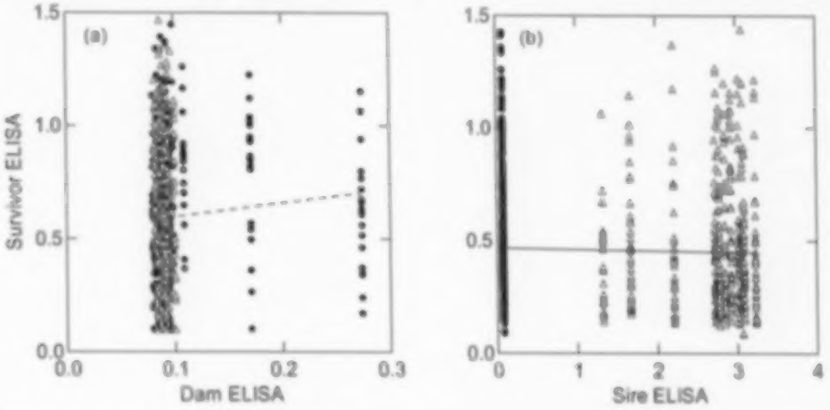

Table 2. Heritabilities and genetic and phenotypic correlations (± standard error) estimated for traits RS, RD, OD, LS, and LD (see Table 1 for trait descriptions).

Trait	RS	RD	OD	LS	LD
RS	**0.890±0.256**	−0.008±0.070	**−0.378±0.041**	−0.009±0.013	0.001±0.015
RD	**0.870±0.164**	**0.350±0.162**	−0.016±0.023	−0.015±0.015	−0.014±0.017
OD	**−0.716±0.140**	−0.223±0.308	**0.271±0.101**	−0.001±0.011	−0.011±0.012
LS	−0.204±0.309	−0.407±0.366	−0.013±0.374	0.128±0.078	**−0.095±0.042**
LD	0.023±0.325	−0.358±0.392	−0.355±0.363	**1.193±0.467**	0.071±0.047

Note: Parameters were estimated across sire groups with a multivariate animal model using restricted maximum likelihood (REML) with maternal ELISA titer (OD) as a covariate. On the diagonal, heritabilities; above the diagonal, phenotypic correlations; below the diagonal, genetic correlations. Heritabilities and correlations in bold differ significantly from zero. Heritabilities for RS and LS were transformed to an underlying, normally distributed scale of liability.

exposure. The significant heritability (0.27 ± 0.10) for ELISA OD among juvenile survivors reflects genetic variation for this trait as well, indicating a possible response toward reduced bacterial loads among hatchery-reared progeny that do survive BKD. However, including fish with ODs below the threshold detection limit may have inflated those heritability estimates, although artificially setting the ODs of these fish to the detection limit (0.1) did not yield estimates significantly different from those computed with the original ODs (analysis not shown). We conclude that spring Chinook salmon propagated at CNFH possess significant genetic variation for resistance to BKD, and this variation can potentially respond quickly to artificial or natural selection for increased or decreased resistance.

Genetic resistance to vibriosis

Like BKD, resistance to vibriosis is also population-specific (Balfry et al. 2001; Røed et al. 2002). However, variation in mean survival among populations of anadromous Atlantic and Pacific salmon has tended to be relatively low compared with survival after exposure to *R. salmoninarum* (see Refstie (1982) for an analysis in rainbow trout). For example, Gjedrem and Aulstad (1974) reported a heritability of 0.12 ± 0.05 for threshold survival (i.e., on the outward binary scale) for Atlantic salmon (*S. salar*) during an outbreak of vibriosis. Similarly, Standal and Gjerde (1987) estimated heritabilities of survival in Atlantic salmon exposed to *Vibrio* on the underlying scale ranging from 0.05 to 0.27 (approximately 0.03 ± 0.08 on the outward binary scale). Beacham and Evelyn (1992*a*, 1992*b*) reported heritabilities of 0.00–0.13 (±0.08–0.22) for mortality caused by *L. anguillarum* in each of three populations of Chinook salmon from British Columbia. Heritability estimates were similar for coho salmon and chum salmon (*Oncorhynchus keta*), but the corresponding estimates were somewhat higher for all three species when challenged with *V. ordalii*. However, in these latter studies, heritability estimates for time to death from vibriosis were not significantly different from zero. Gjedrem and Gjøen (1995) estimated the heritability of survival from vibriosis in an Atlantic salmon population to be 0.26 (0.13 ± 0.08 on the outward binary scale).

In our study, overall survival following exposure to *L. anguillarum* (~20%) was substantially less than overall survival following exposure to *R. salmoninarum* (~77%). Consistent with previous studies, we obtained a heritability for survival to vibriosis ($h^2 = 0.13 \pm 0.08$) that was substantially lower than the corresponding estimate for survival to BKD. Approximately 80% of all juveniles challenged with *L. anguillarum* died of vibriosis, and those mortalities were distributed similarly among HS families, thus resulting in a small heritability estimate. The much higher mortality rate and lower heritability for survival to *L. anguillarum* vs *R. salmoninarum* indicates that phenotypic variation for survival following exposure to the former bacterium is determined primarily by nongenetic factors, at least at the bacterial loads encountered during our challenge trial.

Genetic correlations among disease resistance traits

Although few in number, studies designed to estimate genetic correlations between resistances to more than one pathogen have led to different conclusions. Beacham and Evelyn (1992*a*) found for Chinook salmon that genetic correlations between pairwise survivals following separate challenges with *R. salmoninarum*, *L. anguillarum*, and *Aeromonas salmonicida* varied from weakly positive to weakly negative among three populations, but none was significantly different from zero. In one population of Atlantic salmon, Gjedrem and Gjøen (1995) found positive genetic correlations among survivals from BKD, vibriosis, and furunculosis, but the correlation between BKD and vibriosis survivals was not significant. Gjøen et al. (1997) reported a positive correlation between resistance to *A. salmonicida* and two species of *Vibrio* (*Listonella*), but they obtained negative correlations between resistance to any of the bacterial pathogens and resistance to infectious salmon anemia virus. A weak correlation between resistances to bacterial and viral pathogens would not be surprising as they involve different aspects of the fish's immune system (Van Muiswinkel et al. 1999). More recently, Henryon et al. (2005) tested the resistance of 63 FS families of rainbow trout to two bacterial diseases, enteric redmouth (caused by *Yersinia ruckeri*) and rainbow trout fry syndrome (caused by *Flavobacterium psychrophilum* and also known as bacterial coldwater disease), and to viral hemorrhagic septicemia. Although significant heritability for each disease was detected, there was only a weak correlation among the traits.

The pattern of genetic covariation among the five traits evaluated in our study is consistent with the hypothesis that resistances of CNFH Chinook salmon to *R. salmoninarum* and to *L. anguillarum* are not closely biologically linked. We did not detect significant genetic correlations between survivals (r_A = –0.20 ± 0.31) or between days to death (r_A = –0.36 ± 0.39) expressed in the two pathogen trials. We would therefore predict that natural or artificial selection to increase resistance to *R. salmoninarum* could produce a rapid positive response in increased resistance to BKD but no short-term correlated response in resistance to *L. anguillarum*.

The lack of a significant genetic correlation between resistance to BKD and resistance to vibriosis is arguably not surprising as *R. salmoninarum* is primarily a freshwater pathogen, whereas *L. anguillarum* is primarily a marine pathogen; these bacteria typically challenge salmonid hosts at distinct fish life history stages. Chinook salmon may first be exposed to *R. salmoninarum* during their juvenile freshwater life history phase and subsequently to *L. anguillarum* during their smolt outmigration phase in marine waters. The comparatively low, nonsignificant heritability estimate for resistance to *L. anguillarum* further precludes a significant genetic correlation between resistances to the two pathogens.

The genetic and phenotypic correlations between the traits, including survival and days to death, were often substantially different in magnitude, if not direction, for fish exposed to either *R. salmoninarum* or *L. anguillarum*. This pattern implies that the primary opportunities for short-term evolution of resistance of Chinook salmon to both *R. salmoninarum* and *L. anguillarum* would be underestimated by the observed variation in resistance. The environmental correlations between survival and days to death were similar for the two pathogens, indicating that environmental correlations in both challenges tended to mask the positive genetic relationships between survival and days to death for fish in both trials. In general, phenotypic correlations between traits were not reliable proxies for the underlying genetic correlations; where both differed significantly from zero, the estimates often differed substantially.

Genetic correlations between disease resistance and phenotypic indicators of infection

Several recent studies have focused on the inheritance of disease indicators such as tissue levels of a pathogen or the cellular or subcellular responses by the host following challenge (e.g., Balfry et al. 2001; Røed et al. 2002; Johnson et al. 2003). Røed et al. (2002) found a correlation between lysozyme levels and vibriosis-related mortality in rainbow trout selected for lysozyme activity, suggesting a connection between this activity and innate immunity. Johnson et al. (2003) found genetic variation for lysozyme activity in a population of Chinook salmon, but they found no clear relationship between lysozyme activity and survival when fish were challenged with *L. anguillarum* or *R. salmoninarum*. We are unaware of another study that has investigated the genetic correlation between resistance to BKD and the primary phenotypic indicator of BKD infection, ELISA OD.

We detected negative genetic and phenotypic correlations between disease resistance of juvenile Chinook salmon and ELISA OD, as measured in the surviving progeny. The presence of a genetic or phenotypic correlation between juvenile survival from BKD and *R. salmoninarum* bacterial antigen load, as measured by progeny ELISA ODs among survivors, suggests two levels of resistance that are biologically correlated. However, we found no correlation or relationship between ELISA OD of male parents and the mean phenotypic resistance of their progeny to either *R. salmoninarum* or *L. anguillarum*. This pattern indicates that antigen load and level of infection, particularly when measured by ELISA OD among sexually mature adult fish at the time of spawning, largely reflect environmental and not genetic sources of variation. The pattern is particularly interesting because the relatively high heritability for resistance to BKD that we estimated among HS families was uncorrelated with ELISA ODs of the male parents that produced those families.

We did detect a small but significant relationship between mean days to death of progeny in the *Renibacterium* challenge and ELISA ODs of their maternal parents, but only among those families sired by high ELISA OD males. These results suggest some potential genotype or environmental interactive effects among parental contributions. However, components of variance among FS progeny and the covariance between dam ODs and progeny phenotypes include maternal environmental effects and nonadditive genetic effects that are not heritable. As noted previously, *R. salmoninarum* can be transmitted vertically from female parent to their oocytes, and this transmission represents a maternal environmental effect that can significantly affect the disease phenotypes of progeny irrespective of any genetic mechanism for resistance. Indeed, the difference in the values of the dam and sire components of phenotypic variance can be used to estimate the sum of the maternal environmental effects and nonadditive (i.e., nonheritable) genetic effects (Falconer and Mackay 1996).

Genetic consequences of broodstock culling

Our results imply that selective culling of parents on the basis of their ELISA ODs, as currently practiced in salmon hatcheries in the Pacific Northwest to control BKD, does not adversely affect the mean resistance to BKD of their juvenile progeny. This conclusion assumes that the genetic mechanisms of resistance to BKD are the same in male and female Chinook salmon. We purposefully selected high and low male parents on the basis of their ELISA ODs because, unlike females, males do not transmit the bacterium vertically to their progeny. Our results would have confounded genetic and environmental effects if we had, instead, divergently selected female parents on the basis of their ELISA ODs or included female parents with high ODs in our breeding design.

Of course, our conclusions are likely to be specific to the population we tested (stream-type Chinook salmon at CNFH). However, we are unaware of any scientific literature to suggest that physiological mechanisms of resistance to *R. salmoninarum* differ among conspecific populations of stream-type (spring or summer run) Chinook salmon. Nevertheless, even if levels of genetic variation for resistance to BKD vary considerably among populations, that variation should have little or no effect regarding the absence of a phenotypic correlation between OD of the parents and the BKD or vibriosis resistance of their progeny. Consequently, we believe that our results and conclusions are likely to be applicable to other stocks of stream-type Chinook salmon in the Columbia River Basin, although this latter hypothesis needs to be tested.

Our conclusions implicitly assume also that the absence of a phenotypic correlation between ELISA ODs of male parents and mean resistance to BKD of their progeny accurately reflects the absence of a genetic correlation between those two traits. In other words, selective breeding on the basis of parental OD should not result in a correlated response in mean disease resistance of their progeny based on the results described here. As noted previously, however, environmental correlations can mask genetic correlations, thus making phenotypic correlations inaccurate indicators of genetic correlations. Nevertheless, given our experimental design, it is difficult to conceive of a single factor that could result in an environmental covariance between sire ODs at the time of spawning at the CNFH (Columbia River) and disease resistance of their juvenile offspring as measured under controlled experimental conditions at a different facility in a different geographic region (Puget Sound). This presumed absence of an environmental covariance between ODs of male parents and disease resistance of their progeny is reaffirmed by the inability of males to transmit *R. salmoninarum* vertically to their offspring and the general lack of paternal environmental effects among progeny for most vertebrate taxa that have been studied via breeding experiments. We therefore conclude that the genetic correlation between ELISA ODs of parents at the time of reproduction and their genetic breeding values for resistance to BKD, as measured by the mean survival or resistance of their progeny following direct challenge to *R. salmoninarum*, is not significantly different from zero. Although resistance to *R. salmoninarum* and BKD appears to be highly heritable in the specific stock we tested, this genetic resistance is not detectably correlated with the primary indicator of infection, ELISA OD, when measured on adult Chinook salmon at the time of reproduction. Selective exclusion or culling of potential parents from a hatchery broodstock based on high ELISA ODs is therefore not expected over a few generations to result in a correlated response to selection for increased or decreased resistance to BKD among the progeny.

We are unaware of any published or unpublished evidence that the prevalence of infection among adult Chinook salmon trapped at Columbia River hatcheries has increased since the initiation of the culling and (or) segregation of fertilized eggs from high ELISA OD females. In contrast, evidence from an unpublished study of Chinook salmon in Idaho suggests that culling of high ELISA OD females in some Chinook salmon populations may contribute to reduction of BKD outbreaks in subsequent generations (Munson and Johnson 2005). Unfortunately, most of the data from such studies have not been thoroughly analyzed, and confounding factors (e.g., antibiotic chemotherapy, changes in other fish hatchery practices or environmental conditions) may have affected some results. Nevertheless, the question of possible negative genetic consequences of broodstock culling to control BKD in salmon hatcheries has been raised repeatedly and clearly motivated the study described here. Our results are thus consistent with the general observation that the prevalence of BKD among adult Chinook salmon has not increased since the initiation of these broodstock culling protocols in the early 1990s.

Future challenges and needs

The rapidly expanding conservation role of salmon hatcheries in North America will continue to impose increasing demands on managers and technical personnel to control disease outbreaks and maintain populations without reducing the genetic fitness of those populations that must respond to future environmental challenges (Flagg et al. 2004). Because broodstock segregation and selection have proven to be effective management tools for controlling BKD in salmon hatcheries, the long-term genetic consequences of those activities must be understood to minimize genetic risks to both natural and cultured populations, particularly where those two groups may interbreed. Unfortunately, these potential genetic consequences are often overlooked because of the priority to keep fish alive when challenged with disease and nutritional problems. Enhanced scientific understanding of potential long-term genetic consequences through carefully designed quantitative genetic and immunological research could increase substantially the defensibility of management practices to control disease and other risks associated with artificial propagation. Improved characterization of the mechanisms controlling host resistance (i.e., a more direct measure of disease susceptibility) would aid in developing more reliable methods for screening individual fish based on phenotypic indicators of infection and conserving genetic resources associated with disease resistance. Carefully designed genetic studies, such as maintenance of pedigreed populations to evaluate genetic covariances over multiple generations (e.g., via DNA markers), could also provide information about the relative contributions of salmonid fishes with known infection levels to the persistence of diseases like BKD via transmission from parent to progeny. Finally, longitudinal studies that better characterize the temporal dynamics of infection and host response are important to better elucidate the mechanisms underlying host responses to bacterial pathogens.

Acknowledgements

We thank Kathy Clemens, Director of the USFWS Idaho Fish Health Center (Orofino, Idaho), for suggesting this research. We are grateful to LynnMarie "Chip" Applegate, Connie McKibben, Tony Murray, Maureen Purcell, and Stewart Alcorn of the USGS Western Fisheries Research Center; Jeff Poole, John Holmes, Richard Glenn, and the hatchery staff of the USFWS Abernathy Fish Technology Center; and manager Bill Thorson (retired) and personnel of the USFWS Carson National Fish Hatchery for their assistance with this study. We also thank Skip Walch, David Wills, Travis Collier, and David Hand of the USFWS Fisheries Program Office in Vancouver, Washington, for PIT tagging all the progeny and generating the resulting electronic data files. Jim Myers and Mike Ford of the NMFS Northwest Fisheries Science Center and two anonymous referees provided helpful reviews of the manuscript; Owen Hamel, Northwest Fisheries Science Center, directed us to some key papers. This study was funded in part by the Bonneville Power Administration, Portland, Oregon (Project 2000-072-0). The findings and conclusions in this report are those of the authors and do not necessarily represent the views of the US Fish and Wildlife Service, the National Marine Fisheries Service, or the US Geological Survey.

References

Arkush, K.D., Giese, A.R., Mendonca, H.L., McBride, A.M., Marty, G.D., and Hedrick, P.W. 2002. Resistance to three pathogens in the endangered winter-run chinook salmon (*Oncorhynchus tshawytscha*): effects of inbreeding and major histocompatibility complex genotypes. Can. J. Fish. Aquat. Sci. **59**: 966–975.

Austin, B. 1985. Evaluation of antimicrobial compounds for the control of bacterial kidney disease in rainbow trout, *Salmo gairdneri* Richardson. J. Fish Dis. **8**: 209–220.

Austin, B., and Austin, D.A. 1987. Bacterial fish pathogens. Halsted Press, New York.

Balfry, S.K., Maule, A.G., and Iwama, G.K. 2001. Coho salmon *Oncorhynchus kisutch* strain differences in disease resistance and non-specific immunity, following immersion challenges with *Vibrio anguillarum*. Dis. Aquat. Org. **47**: 39–48.

Banner, C.R., Long, J.J., Fryer, J.L., and Rohovec, J.S. 1986. Occurrence of salmonid fish infected with *Renibacterium salmoninarum* in the Pacific Ocean. J. Fish Dis. **9**: 273–275.

Beacham, T.D., and Evelyn, T.P.T. 1992*a*. Population and genetic variation in resistance of chinook salmon to vibriosis, furunculosis, and bacterial kidney disease. J. Aquat. Anim. Health, **4**: 153–167.

Beacham, T.D., and Evelyn, T.P.T. 1992*b*. Genetic variation in disease resistance and growth to chinook, coho, and chum salmon with respect to vibriosis, furunculosis and bacterial kidney disease. Trans. Am. Fish. Soc. **121**: 456–485.

Bell, G.R., Higgs, D.A., and Traxler, G.S. 1984. The effect of dietary ascorbate, zinc, and manganese on the development of experimentally induced bacterial kidney disease in sockeye salmon (*Oncorhynchus nerka*). Aquaculture, **36**: 293–311.

Bullock, G.L., and Wolf, K. 1986. Infectious diseases of cultured fishes: current perspectives. US Fish Wildl. Serv. Fish Wildl. Leaf. No. 5.

Chevassus, B., and Dorson, M. 1990. Genetics of resistance to disease in fishes. Aquaculture, **85**: 83–107.

Clark, A.G. 1990. Genetic components of variation in energy storage in *Drosophila melanogaster*. Evolution, **44**: 637–650.

Dempster, E.R., and Lerner, I.M. 1950. Heritability of threshold characters (with an Appendix by Alan Robertson). Genetics, **35**: 212–236.

Egidius, E. 1987. Vibriosis: pathogenicity and pathology. A review. Aquaculture, **67**: 15–28.

Elliott, D.G., Pascho, R.J., and Bullock, G.L. 1989. Developments in the control of bacterial kidney disease of salmonid fishes. Dis. Aquat. Org. **6**: 201–215.

Elliott, D.G., Pascho, R.J., and Palmisano, A. 1995. Brood stock segregation for the control of bacterial kidney disease can affect the mortality of progeny chinook salmon *Oncorhynchus tshawytscha* in seawater. Aquaculture, **132**: 133–144.

Elliott, D.G., Pascho, R.J., Jackson, L.M., Matthews, G.M., and Harmon, J.R. 1997. *Renibacterium salmoninarum* in spring–summer chinook salmon smolts at dams on the Columbia and Snake rivers. J. Aquat. Anim. Health, **9**: 114–126.

Ellis, A.E. 1999. Immunity to bacteria in fish. Fish Shellf. Immunol. **9**: 291–308.

Ellis, A.E. 2001. Innate host defense mechanisms of fish against viruses and bacteria. Dev. Comp. Immunol. **25**: 827–839.

Evelyn, T.P.T., Ketcheson, J.E., and Prosperi-Porta, L. 1984*a*. Further evidence for the presence of the kidney disease bacterium (*Renibacterium salmoninarum*) and the failure of iodine, in the form of povidone-iodine, to reduce the intra-ovum infection rate in water-hardened eggs. J. Fish Dis. **7**: 173–182.

Evelyn, T.P.T., Prosperi-Porta, L., and Ketcheson, J.E. 1984*b*. The salmonid egg as a vector of the kidney disease bacterium. *In* Fish diseases. 4th COPROQ Session. *Edited by* ACIUGRUP. Editora ATP, Madrid, Spain. pp. 111–117.

Evelyn, T.P.T., Prosperi-Porta, L., and Ketcheson, J.E. 1986*a*. Persistence of the kidney disease bacterium, *Renibacterium salmoninarum*, in coho salmon *Oncorhynchus kisutch* (Walbaum) eggs treated during and after water-hardening with povidone-iodine. J. Fish Dis. **9**: 461–464.

Evelyn, T.P.T., Prosperi-Porta, L., and Ketcheson, J.E. 1986*b*. Experimental intra-ovum infection of salmonid eggs with *Renibacterium salmoninarum* and vertical transmission of the pathogen with such eggs despite their treatment with erythromycin. Dis. Aquat. Org. **1**: 197–202.

Evenden, A.J., Grayson, T.H., Gilpin, M.L., and Munn, C.B. 1993. *Renibacterium salmoninarum* and bacterial kidney disease — the unfinished jigsaw. Annu. Rev. Fish Dis. **3**: 87–104.

Falconer, D.S., and Mackay, T.F.C. 1996. Introduction to quantitative genetics. 4th ed. Prentice-Hall, San Francisco, Calif.

Fjalestad, K.T., Gjedrem, T., and Gjerde, B. 1993. Genetic improvement of disease resistance in fish — an overview. Aquaculture, **111**: 65–74.

Flagg, T.A., Iwamoto, R.N., and Mahnken, C.V.W. 2004. Conservation hatchery protocols for Pacific salmon. Am. Fish. Soc. Symp. **44**: 603–619.

Fryer, J.L., and Lannan, C.N. 1993. The history and current status of *Renibacterium salmoninarum*, the causative agent of bacterial kidney disease in Pacific salmon. Fish. Res. **17**: 15–33.

Fryer, J.L., and Sanders, J.E. 1981. Bacterial kidney disease of salmonid fish. Annu. Rev. Microbiol. **35**: 273–298.

Gilmour, A.R., Gogel, B.J., Cullis, B.R., Welham, S.J., and Thompson, R. 2002. ASReml user guide. Release 1.0. VSN International Ltd., Hemel Hempstead, HP1 1ES, UK.

Gjedrem, T., and Aulstad, D. 1974. Differences in resistance to vibrio disease of salmon parr. Aquaculture, **3**: 51–59.

Gjedrem, T., and Gjøen, H.M. 1995. Genetic variation in susceptibility of Atlantic salmon, *Salmo salar* L., to furunculosis, BKD and cold water vibriosis. Aquacult. Res. **26**: 129–134.

Gjøen, H.M., Refstie, T., Ulla, O., and Gjerde, B. 1997. Genetic correlations between survival of Atlantic salmon in challenge and field tests. Aquaculture, **158**: 277–288.

Harville, D.A. 1977. Maximum likelihood approaches to variance component estimation and to related problems. J. Am. Stat. Assoc. **72**: 320–338.

Henderson, C.R. 1953. Estimation of variance and covariance components. Biometrics, **9**: 226–252.

Henryon, M., Berg, P., Olesen, N.J., Kjaer, T.E., Slierendrecht, W.J., Jokumsen, A., and Lund, I. 2005. Selective breeding provides an approach to increase resistance of rainbow trout (*Oncorhynchus mykiss*) to the diseases, enteric redmouth, rainbow trout fry syndrome, and viral haemorrhagic septicaemia. Aquaculture, **250**: 621–636.

Hill, W.G. 1972. Estimation of realised heritabilities from selection experiments. I. Divergent selection. Biometrics, **28**: 747–765.

Hill, W.G., and Thompson, R. 1977. Design of experiments to estimate offspring–parent regression using selected parents. Anim. Prod. **24**: 163–168.

Hjeltnes, B., and Roberts, R.J. 1993. Vibriosis. *In* Bacterial diseases of fish. *Edited by* V. Inglis, R.J. Roberts, and N.R. Bromage. Halsted Press, New York. pp. 109–121.

Jansson, E., Hongslo, T., Johannisson, A., Pilström, L., Timmusk, S., and Norrgren, L. 2003. Bacterial kidney disease as a model for studies of cell mediated immunity in rainbow trout (*Oncorhynchus mykiss*). Fish Shellf. Immunol. **14**: 347–362.

Jhingan, E., Devlin, R.H., and Iwama, G.K. 2003. Disease resistance, stress response and effects of triploidy in growth hormone transgenic coho salmon. J. Fish Biol. **63**: 806–823.

Johnson, R.M., Bryden, C.D., and Heath, D.D. 2003. Utility of genetically based health indicators for selection purposes in captive-reared chinook salmon, *Oncorhynchus tshawytscha*, Walbaum. Aquacult. Res. **34**: 1029–1036.

Knott, S.A., Sibly, R.M., Smith, R.H., and Møller, H. 1995. Maximum likelihood estimation of genetic parameters in life-history studies using the "animal model". Funct. Ecol. **9**: 22–26.

Kruuk, L.E.B. 2004. Estimating genetic parameters in natural populations using the "animal model". Philos. Trans. R. Soc. Lond. B Biol. Sci. **359**: 873–890.

Lee, E.G.H., and Evelyn, T.P.T. 1989. Effect of *Renibacterium salmoninarum* levels in the ovarian fluid of spawning chinook salmon on the prevalence of the pathogen in their eggs and progeny. Dis. Aquat. Org. **7**: 179–184.

Lynch, M., and Walsh, J.B. 1998. Evolutionary quantitative genetics. Sinauer Associates, Sunderland, Mass.

Maule, A.G., Rondorf, D.W., Beeman, J.W., and Haner, P.V. 1996. Incidence of *Renibacterium salmoninarum* in juvenile hatchery spring chinook salmon in the Columbia and Snake Rivers. J. Aquat. Anim. Health, **8**: 37–46.

Mitchum, D.L., and Sherman, L.E. 1981. Transmission of bacterial kidney disease from wild to stocked hatchery trout. Can. J. Fish. Aquat. Sci. **38**: 547–551.

Munson, A.D., and Johnson, K.A. 2005. Integrated management of BKD using ELISA-based culling. *In* Bacterial Kidney Disease — Challenges for the 21st century, 15–17 November 2005, Northwest Fisheries Science Center, Seattle, Washington. p. 25.

Murray, A.L., Pascho, R.J., Alcorn, S.W., Fairgrieve, W.T., Shearer, K.D., and Roley, D. 2003. Effects of various feed supplements containing fish protein hydrolysate or fish processing by-products on the innate immune functions of juvenile coho salmon (*Oncorhynchus kisutch*). Aquaculture, **220**: 643–653.

Murray, C.B., Evelyn, T.P.T., Beacham, T.D., Barner, L.W., Ketcheson, J.E., and Prosperi-Porta, L. 1992. Experimental induction of bacterial kidney disease in chinook salmon by immersion and cohabitation challenges. Dis. Aquat. Org. **12**: 91–96.

O'Farrell, C.L., Elliott, D.G., and Landolt, M.L. 2000. Mortality and kidney histopathology of chinook salmon *Oncorhynchus tshawytscha* exposed to virulent and attenuated *Renibacterium salmoninarum* strains. Dis. Aquat. Org. **43**: 199–209.

Olivier, G., Griffiths, S.G., Fildes, J., and Lynch, W.H. 1992. The use of Western blot and electroimmunotransfer blot assays to monitor bacterial kidney disease in experimentally challenged Atlantic salmon, *Salmo salar* L. J. Fish Dis. **15**: 229–241.

Pascho, R.J., Elliott, D.G., Mallett, R.W., and Mulcahy, D. 1987. Comparison of five techniques for the detection of *Renibacterium salmoninarum* in adult coho salmon. Trans. Am. Fish. Soc. **116**: 882–890.

Pascho, R.J., Elliott, D.G., and Streufert, J.M. 1991. Brood stock segregation of spring chinook salmon *Oncorhynchus tshawytscha* by use of the enzyme-linked immunosorbent assay (ELISA) and the fluorescent antibody technique (FAT) affects the prevalence and levels of *Renibacterium salmoninarum* infection in progeny. Dis. Aquat. Org. **12**: 25–40.

Pascho, R.J., Elliott, D.G., and Achord, S. 1993. Monitoring of the in-river migration of smolts from two groups of spring chinook salmon (*Oncorhynchus tshawytscha*) with different profiles of *Renibacterium salmoninarum* infection. Aquacult. Fish. Manag. **24**: 163–169.

Pascho, R.J., Elliott, D.G., and Chase, D.M. 2002. Comparison of traditional and molecular methods for detection of *Renibacterium salmoninarum*. *In* Molecular diagnosis of salmonid diseases. *Edited by* C.O. Cunningham. Kluwer Academic Publishers, Dordrecht, the Netherlands. pp. 157–209.

Patterson, H.D., and Thompson, R. 1971. Recovery of inter-block information when block sizes are unequal. Biometrika, **58**: 545–554.

Price, D.J. 1985. Genetics of susceptibility and resistance to disease in fishes. J. Fish Biol. **26**: 509–519.

Raymond, H.L. 1988. Effects of hydroelectric development and fisheries enhancement on spring and summer chinook salmon and steelhead in the Columbia River basin. N. Am. J. Fish. Manag. **8**: 1–24.

Reeve, E.C.R. 1955. The variance of the genetic correlation coefficient. Biometrics, **12**: 357–374.

Refstie, T. 1982. Preliminary results: differences between rainbow trout families in resistance against vibriosis and stress. Dev. Comp. Immunol. **1982**(Suppl. 2): 205–209.

Robertson, A. 1959. The sampling variance of the genetic correlation coefficient. Biometrics, **15**: 469–485.

Robertson, A., and Lerner, I.M. 1949. The heritability of all-or-none traits: viability of poultry. Genetics, **34**: 395–411.

Røed, K.H., Fevolden, S.-E., and Fjalestad, K.T. 2002. Disease resistance and immune characteristics in rainbow trout (*Oncorhynchus mykiss*) selected for lysozyme activity. Aquaculture, **209**: 91–101.

Roff, D.A. 1997. Evolutionary quantitative genetics. Chapman & Hall, New York.

Searle, S.R., Casella, G., and McCulloch, C.E. 1992. Variance components. Wiley, New York.

Shaw, R.G. 1987. Maximum-likelihood approaches applied to quantitative genetics of natural populations. Evolution, **41**: 812–826.

Standal, M., and Gjerde, B. 1987. Genetic variation in survival of Atlantic salmon during the sea-rearing period. Aquaculture, **66**: 197–207.

Suzumoto, B.K., Schreck, C.B., and McIntyre, J.D. 1977. Relative resistances of three transferrin genotypes of coho salmon (*Oncorhynchus kisutch*) and their hematological responses to bacterial kidney disease. J. Fish. Res. Board Can. **34**: 1–8.

Toranzo, A.E., and Barja, J.L. 1993. Virulence factors of bacteria pathogenic for coldwater fish. Ann. Rev. Fish Dis. **3**: 5–36.

VanderKooi, S.P., and Maule, A.G. 1999. Prevalence of *Renibacterium salmoninarum* in juvenile spring chinook salmon at Columbia and Snake river hatcheries, 1993–1996. J. Aquat. Anim. Health, **11**: 162–169.

Van Muiswinkel, W.B., Wiegertjes, G.F., and Stet, R.J.M. 1999. The influence of environmental and genetic factors on the disease resistance of fish. Aquaculture, **172**: 103–110.

Winter, G.W., Schreck, C.B., and McIntyre, J.D. 1980. Resistance of different stocks and transferrin genotypes of coho salmon, *Oncorhynchus kisutch*, and steelhead trout, *Salmo gairdneri*, to bacterial kidney disease and vibriosis. Fish. Bull. **77**: 795–802.

Winton, J.R. 2001. Fish health management. Chapter 9. *In* Fish hatchery management. 2nd ed. *Edited by* G. Wedemeyer. American Fisheries Society, Bethesda, Maryland. pp. 559–640.

Withler, R.E., and Evelyn, T.P.T. 1990. Genetic variation in resistance to bacterial kidney disease within and between two strains of coho salmon from British Columbia. Trans. Am. Fish. Soc. **119**: 1003–1009.

Wolf, K., and Dunbar, C.E. 1959. Test of 34 therapeutic agents for control of kidney disease in trout. Trans. Am. Fish. Soc. **88**: 117–124.

Physiological effects of simultaneous, abrupt seawater entry and sea lice (*Lepeophtheirus salmonis*) infestation of wild, sea-run brown trout (*Salmo trutta*) smolts

Alan Wells, Christal E. Grierson, Monique MacKenzie, Iain J. Russon, Helena Reinardy, Claire Middlemiss, Pål A. Bjørn, Bengt Finstad, Sjoerd E. Wendelaar Bonga, Christopher D. Todd, and Neil Hazon

Abstract: For wild, sea-run brown trout (*Salmo trutta*) smolts, the physiological consequences of abrupt transfer to seawater and simultaneous challenge with copepodid larvae of the sea louse, *Lepeophtheirus salmonis* (Krøyer, 1837), were investigated in the laboratory. Analysis of osmoregulatory, metabolic, and stress markers allowed the derivation of a sublethal threshold burden of *L. salmonis*, above which the host suffers major physiological stress. Noticeable lice effects, consistent across all measured markers, were not observed until *L. salmonis* developed to the mobile preadult and adult stages. Preadult *L. salmonis* caused significant increases in plasma chloride, osmolality, glucose, lactate, and cortisol and a significant reduction in haematocrit. Piecewise linear statistical approaches allowed the determination of abrupt changes in these physiological markers, attributable to the intensity of *L. salmonis* infestation on individual fish, and identification of overall threshold lice burdens. Thirteen mobile lice·fish^{-1} (weight range 19–70 g) was a consistent breakpoint across several physiological measures. This information will provide a valuable, objectively derived tool to aid in the formulation of effective wild fisheries management policy concerning *S. trutta* conservation.

Résumé : Nous avons étudié en laboratoire chez des saumoneaux sauvages de la truite brune (*Salmo trutta*) anadrome les conséquences physiologiques d'un transfert abrupt en eau de mer accompagné d'une confrontation simultanée avec des larves copépodites du pou de mer, *Lepeophtheirus salmonis* (Krøyer, 1837). L'analyse des indicateurs d'osmorégulation, de métabolisme et de stress permet de déterminer une charge seuil sublétale de *L. salmonis* au-dessus de laquelle l'hôte souffre d'un stress physiologique important. Les effets manifestes des poux, signalés de façon cohérente par tous les indicateurs, n'apparaissent que lorsque *L. salmonis* atteint les stades mobiles préadultes et adultes. Les *L. salmonis* préadultes causent des augmentations significatives du chlorure, de l'osmolalité, du glucose, du lactate et du cortisol du plasma, ainsi qu'une réduction significative de l'hématocrite. Des méthodes statistiques linéaires pas à pas permettent de déterminer les changements abrupts de ces indicateurs physiologiques causés par l'intensité de l'infestation des *L. salmonis* chez des poissons individuels et d'identifier les charges seuils globales de poux. Une charge de 13 mobiles poux·poisson^{-1} (étendue des masses 19–70 g) représente un point seuil commun à plusieurs mesures physiologiques. Ces données pourront servir d'outil utile et objectif pour la formulation d'une politique de gestion efficace des pêches de populations sauvages de *S. trutta* dans un objectif de conservation.

[Traduit par la Rédaction]

Introduction

Sea-run brown trout (hereafter referred to as sea trout, *Salmo trutta*) have an anadromous life history pattern and are exposed to a variety of environmental and biological challenges, including parasitic infection. Sea trout numbers in northwest Europe have fallen since the 1950s (Anonymous 2004), but during the late 1980s and early 1990s, the

---

Received 25 January 2006. Accepted 8 November 2006. Published on the NRC Research Press Web site at http://cjfas.nrc.ca on 15 December 2006.
J19131

A. Wells,[1] C.E. Grierson, H. Reinardy, C. Middlemiss, C.D. Todd, and N. Hazon. Gatty Marine Laboratory, University of St Andrews, St Andrews, Fife, KY16 8LB, United Kingdom.
M. MacKenzie. Centre for Research in Ecological and Environmental Modelling (CREEM), University of St Andrews, St Andrews, Fife, KY16 9LZ, United Kingdom.
I.J. Russon and S.E. Wendelaar Bonga. Department of Animal Ecology and Ecophysiology, Radboud University Nijmegen, Toernooiveld 1, 6525 ED, Nijmegen, the Netherlands.
P.A. Bjørn. Norwegian Institute of Fisheries and Aquaculture Research, Breivika, N-9291 Tromsø, Norway.
B. Finstad. Norwegian Institute for Nature Research (NINA), Tungasletta 2, N-7485 Trondheim, Norway.

[1] Corresponding author (e-mail: aw23@st-andrews.ac.uk).

Can. J. Fish. Aquat. Sci. 63: 2809–2821 (2006) doi:10.1139/F06-160

first reports of collapses in certain wild sea trout stocks, and the possible association of these collapses with sea lice (*Lepeophtheirus salmonis* (Krøyer, 1837)), arose in Ireland (Tully et al. 1993), Scotland (Northcott and Walker 1996), and Norway (Birkeland 1996). Unlike salmon, which undertake extensive oceanic migrations (Hansen and Jacobsen 2000), sea trout remain in nearshore waters throughout their marine residence (Klemetsen et al. 2003), and stock declines appear to be attributable primarily to increased marine mortality (Anonymous 1993, 1995; Northcott and Walker 1996). Caligid sea lice infestations can debilitate or kill the host fish (Pike and Wadsworth 2000), and there is very strong circumstantial evidence that sea lice derived from aquaculture pens have the potential to impact wild salmonids (Butler 2002; McKibben and Hay 2004; Penston et al. 2004).

Copepod sea lice, *L. salmonis* and *Caligus elongatus* Nordmann, 1832, are the primary marine ectoparasites of farmed and wild salmonids in the North Atlantic (Kabata 1979). Sea lice infestation of the host fish is characterized by stress and osmoregulatory imbalance, which occur once the parasites moult to the mobile preadult and adult stages (Bjørn and Finstad 1997; Dawson et al. 1998; Finstad et al. 2000). Feeding activity by preadult–adult sea lice can result in increased skin damage (Bjørn and Finstad 1998; Nolan et al. 1999; Pike and Wadsworth 2000), which can be fatal to hatchery-reared sea trout and salmon (Grimnes and Jakobsen 1996; Bjørn and Finstad 1997; Dawson et al. 1998). Infestation of sea trout smolts with large numbers of the sessile chalimus larval stages leads to increased plasma levels of the stress hormone cortisol (Bjørn and Finstad 1997). Cortisol causes a range of effects, including hydromineral imbalance, changes in intermediary metabolism, reduction in the immune response, and reduced capacity to tolerate subsequent or additional stressors (Barton and Iwama 1991; Wendelaar Bonga 1997). In addition, substances such as prostaglandin E_2 are produced by *L. salmonis* and have been reported to modulate the host immune response at the site of attachment (Fast et al. 2004).

Experimental studies on Atlantic salmon (*Salmo salar*) and Arctic char (*Salvelinus alpinus*) juveniles indicate that 30–50 attached chalimus larvae may cause the death of a 40 g postsmolt (Grimnes et al. 1996). In the case of sea trout, experimental data indicate that ~50 preadult and adult lice may cause the death of a 60 g postsmolt (Bjørn and Finstad 1997). However, from the perspective of conservation and management of wild and farmed salmonid stocks, the objective establishment of a threshold infestation intensity, above which there are significant but sublethal physiological effects on the host, is more important than the determination of lethal lice levels. Here, we report a threshold infestation intensity for wild sea trout infested by *L. salmonis*, which is derived from appropriate statistical models and which is consistent across a range of physiological measures.

Previous experimental reports of the physiological effects of *L. salmonis* infestation on sea trout are restricted to seawater (SW)-acclimated, hatchery-reared fish. These fish are much larger than wild sea trout smolts, and the fins of hatchery-reared fish (primary sites for first attachment of the infective copepodid stage of *L. salmonis* (Finstad et al. 1994)) often are stunted (Collins 1993), raising questions about the validity of extrapolating experimental outcomes to wild fish. In addition, acclimation to SW alone is a stressful process, and simultaneous challenge from ectoparasitic infestation during this early period of migration will constitute an important additional stressor. Here, in laboratory experiments designed to mimic environmentally realistic circumstances, we investigated the time course of physiological responses and identify sublethal threshold ectoparasite intensities for wild smolts transferred abruptly to SW and simultaneously challenged with *L. salmonis*.

Materials and methods

Wild sea trout smolts (mean weight 37.3 g; range 19.3–69.9 g) were trapped and netted from the River North Esk, east Scotland, from 18 to 24 May 2004 and transported (90 min) to the Gatty Marine Laboratory in a smolt tank containing constantly oxygenated fresh water. On arrival, smolts were dipnetted in an ad hoc fashion and distributed evenly across duplicated experimental tanks. To prevent desmoltification, fish were held in brackish water (468 ± 9 mosmol·kg^{-1}; 15‰) in eight, 300 L aquarium tanks under natural photoperiod (18 h light: 6 h dark). The initial stocking density was 42 fish per tank (total = 336; mean weight range from 36.3 ± 1.3 to 38.9 ± 1.4 g). Smolts were maintained in this manner for 7–13 days prior to experimentation. All fish were fed on chopped squid (Ammodytes Company Ltd., St Ives, Cornwall, UK) at a ration of ~2% body weight·day^{-1}. The sea trout smolts adapted to tank conditions in a relatively short period of time following an intensive period of hand-feeding, particularly at the start of the experiment, to the extent that fish in all experimental tanks were feeding well within 1 week of capture. Squid was fed throughout the experiment because commercial pellet was refused even when mixed with squid. Eighteen hours prior to the *L. salmonis* infestation, the flow of fresh water was stopped and the SW flow was increased accordingly. The salinity of the tanks reached full SW (972 ± 3 mosmol·kg^{-1}; 32‰) within 3 h, and the mean aquarium temperature was 14 ± 0.1 °C.

Ovigerous female *L. salmonis* were collected from Atlantic salmon at a commercial west Scotland fish farm and transported to the Gatty Marine Laboratory in cooled SW. Egg strings were removed from the lice and evenly distributed among six, 2 L conical flasks of filtered SW (10 °C). Flasks were continuously aerated to ensure that egg strings remained in constant motion. Nauplii began hatching within 24 h and were collected on a 40 µm filter and transferred to a 20 L plastic aquarium containing filtered, UV-sterilized, through-flowing SW. Larvae developed through the two naupliar moults to the infective copepodid stage. Small numbers of larvae were sampled daily and microscopically examined to monitor the rate of larval development. On the day of infestation, 2- to 4-day-old copepodid larvae were concentrated in 1 L of SW by filtering through a 40 µm filter. The total number of live copepodids was estimated from five replicate subsample counts (mean 22 lice·mL^{-1}; range 16–24).

At infestation, the volume of water in the experimental tanks was drained to one-third (100 L), and the water supply was turned off. The water was continuously aerated during the infestation to maintain a circulating current in the tanks. Copepodids were added in appropriate numbers (three times desired infestation intensity per fish) to achieve three duplicated infestation levels: ~10 lice·fish^{-1} (~1260 copepodids·tank^{-1}), ~30 lice·fish^{-1} (~3780 copepodids·tank^{-1}), and ~50 lice·fish^{-1} (~6300 copepodids·tank^{-1}). The duplicate control tanks (zero lice) were treated in an identical manner, but no copepodid larvae were added. Infestation progressed for 2 h in total darkness (Johnson and Albright 1991*a*), following which the experimental tanks were refilled and the 18 h light: 6 h dark photoperiod regime was reinstated.

Infested and control fish were sampled at 3, 7, 14, 21, and 28 days postinfestation (dpi). Fish were individually netted from the experimental tanks, taking care to minimize disturbance to the remaining fish, and killed by overdose of 2-phenoxyethanol (2.5 mL·L^{-1}) using separate containers for individual fish. On removal from the anesthetic, the spinal cord of each individual fish was severed using a scalpel blade. The anaesthetic was subsequently passed through a 40 µm filter to collect any dislodged *L. salmonis*. Five fish from each duplicate tank (10 fish for each lice intensity) were removed at each sampling date (except where mortalities made this impossible), and tissues were collected within 15 min. Blood samples (0.5 mL) were taken from the caudal blood sinus within 1 min of sacrifice, added to 50 µL 15% ammonium ethylenediaminetetraacetic acid (EDTA), and processed immediately (see below). The fish was then opened along the midventral line, and the liver was removed and freeze-clamped in liquid nitrogen to prevent glycogenolysis. The frozen liver was placed in a preweighed vial and stored at –80 °C until analysis. Fish carcasses were placed in individual plastic bags and stored at 4 or –20 °C for subsequent microscopic determination of *L. salmonis* numbers. All dissection was performed on a piece of paper towelling, and this also was bagged and subsequently examined for dislodged *L. salmonis*. The fork length and weight of all fish were recorded and expressed as the composite condition factor, Fulton's *K* (100 × weight in g × (length in cm)$^{-3}$). Ratio condition factors are sensitive to isometric variation and departures from the cube relationship, but the size range of experimental fish was narrow, and Fulton's *K* has been shown to have a high correlation with whole fish lipid content (Sutton et al. 2000; Neff and Cargnelli 2004).

Blood haematocrit was determined on fresh blood using a Compur microspin microhaematocrit centrifuge (Hawksley, Sussex, UK). Plasma was separated by centrifugation at 13 000 r/min (1 r = 2πrad; 13 225*g*) for 1 min and frozen at –80 °C until analysis. Plasma chloride was measured by colorimetric titration (chloride analyser model 925, Corning, Schiplo-Rijk, the Netherlands). Plasma osmolality was measured by freezing point depression (Roebling osmometer, Camlab, Cambridge, UK). Plasma glucose concentration was determined in duplicate using a commercially available kit (GL 2623, Randox Laboratories Ltd., Crumlin, Co. Antrim, UK), and absorbance was read at 490 nm. Plasma lactate concentration was determined in duplicate using commercially available lactate reagent (LC 2389, Randox Laboratories Ltd.) and read at 540 nm. Both of the latter assays were modified for use in 96 well plates, and absorbance was read on a plate reader (BioTek Instruments Inc., Winooski, Vermont, USA). Liver glycogen was assessed following hydrolysation by amyloglucosidase using the method of Keppler and Decker (1974). Plasma cortisol was measured by radioimmunoassay, as described by van Anholt et al. (2003).

Fig. 1. The 11 zones on the body of the infected sea-run brown trout (*Salmo trutta*) smolts examined for the presence of *Lepeophtheirus salmonis* (after Bjørn and Finstad 1998): A, head and operculum; B, anterior dorsal area of the body above the lateral line from the head to the posterior end of the dorsal fin; C, posterior dorsal area of the body above the lateral line from the posterior end of the dorsal fin to the caudal fin, including adipose fin; D, anterior ventral area of the body below the lateral line from the head to the posterior end of the dorsal fin; E, posterior ventral area of the body below the lateral line from the posterior end of the dorsal fin to the caudal fin; F, dorsal fin; G, pectoral fin; H, ventral fin; I, anal fin; J, caudal fin; K, gills. The anaesthetic solutions, plastic storage bags, and paper towelling on which dissection took place were also examined and are shown as zone L.

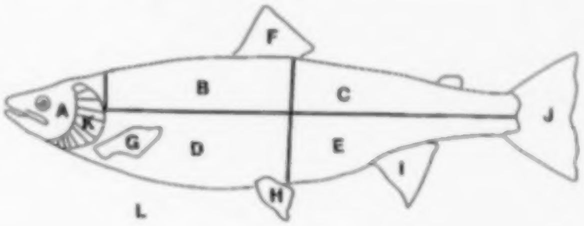

The body surface, fins, and gills were separated analytically into a total of 11 zones as previously described (Bjørn and Finstad 1998) (Fig. 1). These zones on all infected fish were examined for *L. salmonis*, and the frequencies of each developmental stage were recorded. *Lepeophtheirus salmonis* at the sessile first–second chalimus stages and third–fourth chalimus stages were pooled into two groups, termed C1 and C3, respectively. All *L. salmonis* stages were categorized and their sex determined according to Johnson and Albright (1991*b*) and Schram (1993).

Data analysis

The number of lice, fish length, fish weight, the condition factor of each fish, and dpi were considered as candidate variables in each statistical model. Further, each of these candidate variables was treated as a continuous variable. Length and weight were too highly correlated to allow both to be considered for model selection; their variance inflation factors (Fox and Monette 1992) were 26.57 and 25.38, respectively. Consequently, only length was considered for selection, since overall this variable returned slightly better fit results. Eight fish, sampled at 7 dpi from the high lice intensity group, had lice values above 100 (maximum 232), which resulted in a large gap in the range of the lice covariate. As a consequence, analyses at 7 dpi were carried out both with and without these heavily infected fish to ensure these very high values did not dominate model results. The reported analyses excluded these fish.

Table 1. Percent frequency and first appearance of the major developmental stages of *Lepeophtheirus salmonis*.

dpi	Frequency (%) Cop	C1	C3	PAM1	PAM2	PAF1	PAF2	AM	AF	GF
3	73	27								
7		33	67							
14			1	6	44	49	<1			
21							25	48	27	
28								38		62
First appearance (dpi)	—	2	7	10	12	10	14	15	20	28

Note: Infested fish ($n = 30$ at days 3, 7, and 14; $n = 20$ at day 21; and $n = 10$ at day 28) were sampled at 3, 7, 14, 21, and 28 days postinfestation (dpi). Stages are designated as follows: Cop, copepodid; C1, first and second chalimus stages combined; C3, third and fourth chalimus stages combined; PAM1, first preadult male; PAF1, first preadult female; PAM2, second preadult male; PAF2, second preadult female; AM, adult male; AF, adult female; GF, gravid female.

To incorporate the effects of lice, length, condition factor, and time, we fitted the potentially nonlinear relationships among each variable and the physiological measure of interest using generalized additive models (GAMs). GAMs were considered more appropriate than generalized linear models (GLMs) for this analysis, since GLMs do not naturally accommodate nonlinearities (on the link scale), and we had no a priori reason to assume that model relationships for these data were linear. GAMs were fitted to the data pooled across time to allow the detection of any significant ($p < 0.05$) effects due to lice, fish length, condition, and time. To detect any significant tank or duplicate tank effects, tank and tank duplicate variables were also included in each model. The tank loading (i.e., the lice loading targeted for the various tanks) was also considered for selection in each model with a significant lice relationship to ensure that tank loading was no longer significant once the number of lice per fish was included. No tank or tank duplicate effects were found to be significant, and so all data were pooled across tank loadings to obtain data across the lice range. GAM analysis was also carried out for each response at each time point to allow assessment of the way in which lice numbers and the other covariates change with time. This approach was considered appropriate because *L. salmonis* developed through their entire life cycle as the experiment progressed, and distinct life cycle stages of *L. salmonis* were observed at each experimental time point (Table 1). This decision to model each stress indicator at each time point was supported also by the data; significant lice–time interactions were detected for all stress measures when the data were pooled across time.

To determine abrupt changes (putative thresholds) in the lice relationship for each physiological measure, a piecewise linear approach was used. This approach assumes linearity between breakpoints and is commonly used to identify changes in functional form and (or) threshold values (Bernatchez and Wilson 1998; Molinari et al. 2001; Shea and Vecchione 2002), but this is the first application of the method to physiological studies of stress.

Observed lice values were used as candidate breakpoints in each model, and the number and location of the breakpoints for the piecewise linear models were objectively identified using Akaike's information criterion (AIC) (Akaike 1973). After the first breakpoint was identified and fixed in the model, the remaining set of unique lice values was considered for the second breakpoint. This forward selection procedure was repeated until the AIC score no longer improved. The model was constrained so that breakpoints were separated by at least three unique lice values to ensure each linear component fitted between breakpoints was supported by data, in keeping with the recommendations in Wold (1974). Owing to the relatively small sample sizes available at each time point (i.e., $n < 30$), the AIC_c score (Bedrick and Tsai 1994) was also used to establish if breakpoints were deemed necessary in each model. While the penalty term for the standard AIC score is fixed at 2 per parameter, the penalty term for the AIC_c score considers the sample size in the penalty term. This generally gives rise to a harsher penalty term than the standard AIC, and thus more simplistic models compared with the standard AIC score.

This breakpoint selection process also was carried out while including fish length and condition factor in each model. In practice, GAM analysis at each time point revealed that nonlinear relationships were justified only for the lice covariate, and so condition factor and length were included as linear terms in each model.

To ensure the complexity of a piecewise linear approach was suitable, the fit of each model (as judged by the AIC and AIC_c) was compared with more and less flexible alternatives. Specifically, each piecewise linear model was compared with the more restrictive standard linear term for lice and two more flexible models, which allow more flexible curves between the chosen breakpoints. B-splines were used to fit these models in R (R Development Core Team 2004), using a specified number of (internal) breakpoints. The AIC and AIC_c statistics formed the basis for these comparisons, and all models were fitted assuming a normal error distribution. Normality, independence, and constant error variance were checked using Shapiro–Wilk, Durbin–Watson, and Breusch–Pagan tests on the residuals (Breusch and Pagan 1979; Royston 1982; Fox 1997), and models found to exhibit nonconstant error variance were fitted inside a generalized least squares framework. This framework naturally

Table 2. Mean *Lepeophtheirus salmonis* abundance per tank on sampled sea-run brown trout (*Salmo trutta*).

	Low lice intensity		Medium lice intensity		High lice intensity	
dpi	Tank 1	Tank 2	Tank 1	Tank 2	Tank 1	Tank 2
3	10.6 (2.1, 1.8)	9.3 (3.3, 2.5)	19.9 (5.9, 4.6)	34.7 (11.8, 8.9)	53.2 (18.5, 13.8)	61.1 (6.7, 6.0)
7	22.8 (7.6, 5.8)	9.8 (1.9, 1.6)	31.6 (2.7, 2.5)	34.4 (5.0, 4.4)	88.6 (19.0, 15.7)	98.7 (34.3, 25.2)
14	12.8 (1.2, 1.1)	13.1 (4.0, 3.1)	32.4 (2.5, 2.4)	41.7 (3.3, 3.1)	77.5 (12.3, 10.6)	76.6 (11.8, 10.2)
21	7.9 (1.9, 1.6)	9.0 (4.4, 3.0)	28.5 (5.4, 4.5)	9.8 (1.1, 1.0)	—	—
28	2.7 (0.8, 0.7)	0.9 (0.6, 0.5)	—	—	—	—

Note: dpi, days postinfestation. Upper and lower standard errors, respectively, are shown in parentheses. $n = 5$ on each sampling occasion.

Table 3. Frequency distribution (%) of *Lepeophtheirus salmonis* on each body zone of sampled fish.

	Body surface					Fins					Gills	Anaesthetic
dpi	A	B	C	D	E	F	G	H	I	J	K	L
3	0.3	0.1	0.7	1.0	0.7	6.7	5.2	3.2	3.4	3.3	1.1	74.3
7	2.8	1.2	4.4	1.2	2.4	34.3	19.9	9.7	7.7	13.6	1.4	1.4
14	15.9	15.7	18.8	9.5	3.4	0.6	0.3	0.2	0.1	0.7	0.1	34.7
21	22.7	19.9	20.5	5.9	1.7	0	0	0	0	0	0	29.3
28	0	0	42.9	0	23.8	0	0	0	0	0	0	33.3

Note: dpi, days postinfestation. See Fig. 1 for the different body zones. The developmental stages of lice at each sampling point are shown in Table 1.

accommodates an increasing mean–variance relationship, which is often encountered with biological data.

Results

Development of *L. salmonis*

Lepeophtheirus salmonis numbers and developmental stage (Table 1) were assessed on sampled fish at each experimental time point (3, 7, 14, 21, and 28 dpi). However, as lice on mortalities also were counted, developmental data on intervening days was observed, allowing more accurate determination of the first appearance of the various *L. salmonis* stages on the fish (Table 1). Mobile, preadult *L. salmonis* were observed on fish from 10 dpi onwards. Only copepodids and early chalimus stages (C1) were found at 3 dpi. By 7 dpi, 67% of the *L. salmonis* had developed to the late chalimus stages (C3). One week later, the majority of male *L. salmonis* were at the second preadult stage, whereas the majority of female *L. salmonis* had reached only the first preadult stage. At day 21, most male *L. salmonis* had reached the adult stage, whereas females were either at the second preadult stage or the adult stage. By day 28, all *L. salmonis* were adults, 62% of which were gravid females.

Lepeophtheirus salmonis abundance in each experimental tank is presented (Table 2). Prevalence was 100% for all lice intensity groups on all sampling days, with the exception of the low lice intensity group at 28 dpi. In that latter sample (prevalence 80%), two fish from one of the duplicate tanks had no *L. salmonis*, but these were presumed to have been infested earlier in the experiment.

The frequency distribution of *L. salmonis* on the body surface of sampled fish is shown (Table 3). At 3 dpi, when 73% of the *L. salmonis* were at the copepodid stage (see Table 1), the majority (74%) of *L. salmonis* were found detached in the anesthetic solution (zone L). At 7 dpi, the majority of the *L. salmonis* were observed attached to the fins, with 34% on the dorsal fin (zone F). Only 1% of the *L. salmonis* were detached from the host and hence collected from the anesthetic solution. Once *L. salmonis* attained the mobile stage (14–21 dpi), the majority were recorded on the body surface, but a substantial percentage was also found dislodged in the anesthetic solution (14 dpi 34.7% and 21 dpi 29.3%). At 28 dpi, adult *L. salmonis* were observed only on the posterior zones C and E.

Mortalities

There was a single fish mortality in each of the control groups and the low lice infestation group. There were 37 mortalities in the high lice intensity group, which occurred between 10 and 14 dpi, and 17 mortalities in the medium lice intensity group between 15 and 20 dpi. For reasons of animal welfare, any remaining fish in the high and medium lice intensity tanks were sacrificed at 14 and 21 dpi, respectively. It was noticed that from 10 dpi onwards, infected fish in both the medium and high lice intensity groups showed a marked decrease in feeding, and this continued for the remainder of the experiment.

Size and condition factor

The exponent of the log length – log weight relationship was 2.90 (standard error = 0.002), which was a significant departure ($p < 0.05$) from an exponent of 3. Fulton's condition factor (K) assumes a cubic relationship between length and weight, but K here showed no significant length dependence ($K = 0.939 - 0.00058 \cdot \text{length}$; $r = 0.127$, $p = 0.099$), because of the restricted size range of the experimental fish (124–198 mm; 19.3–69.9 g). K was therefore deemed an appropriate measure of fish condition.

Generalized additive models

Predicted mean values with 95% confidence intervals based on the GAMs fitted at each time point are shown (Figs. 2–4). Specifically, predictions and associated intervals were gener-

Fig. 2. Predicted mean values with 95% confidence intervals for (*a*) haematocrit, (*b*) plasma chloride, and (*c*) plasma osmolality at four fixed lice (*Lepeophtheirus salmonis*) loadings: control (no lice), solid line and open circles; 10 lice·fish^{-1}, broken line and closed circles; 30 lice·fish^{-1}, broken line and open triangles; 50 lice·fish^{-1}, dotted line and closed triangles. The number of lice per fish was modelled as a continuous variable, and predictions for a range of lice values were obtained by fixing other covariates (length and condition factor) at their means for each time point. These predictions are based on separate models for each time point, and data are slightly offset for clarity.

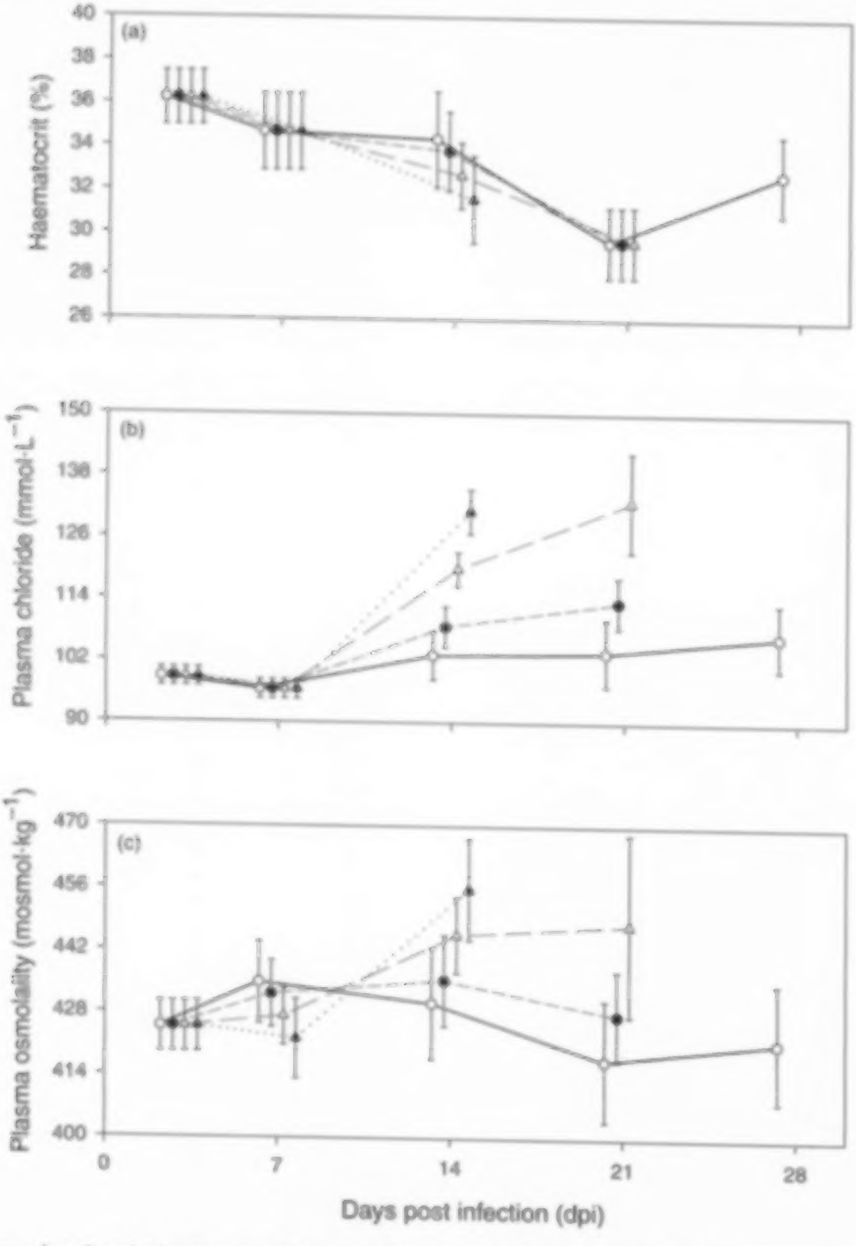

ated for fish of average length and of average condition at each time point using the fitted GAMs and lice levels of 0, 10, 30, and 50 lice·fish^{-1}. Predictions for 50 lice·fish^{-1} at 21 dpi and 10, 30, and 50 lice·fish^{-1} at 28 dpi were excluded from Figs. 2–4 to avoid extrapolation. The maximum levels at 21 and 28 dpi were 44 and 5 lice·fish^{-1}, respectively. Thus, to make predictions for higher lice levels at these time points would be ill advised.

No significant lice effects were observed at 3 or 7 dpi either for haematocrit or plasma chloride (Fig. 2), and whereas

Fig. 3. Predicted mean values with 95% confidence intervals for (*a*) plasma glucose, (*b*) plasma lactate, and (*c*) liver glycogen at four fixed lice (*Lepeophtheirus salmonis*) loadings: control (no lice), solid line and open circles; 10 lice·fish^{-1}, broken line and closed circles; 30 lice·fish^{-1}, broken line and open triangles; 50 lice·fish^{-1}, dotted line and closed triangles. The number of lice per fish was modelled as a continuous variable, and predictions for a range of lice values were obtained by fixing other covariates (length and condition factor) at their means for each time point. These predictions are based on separate models for each time point, and data are slightly offset for clarity.

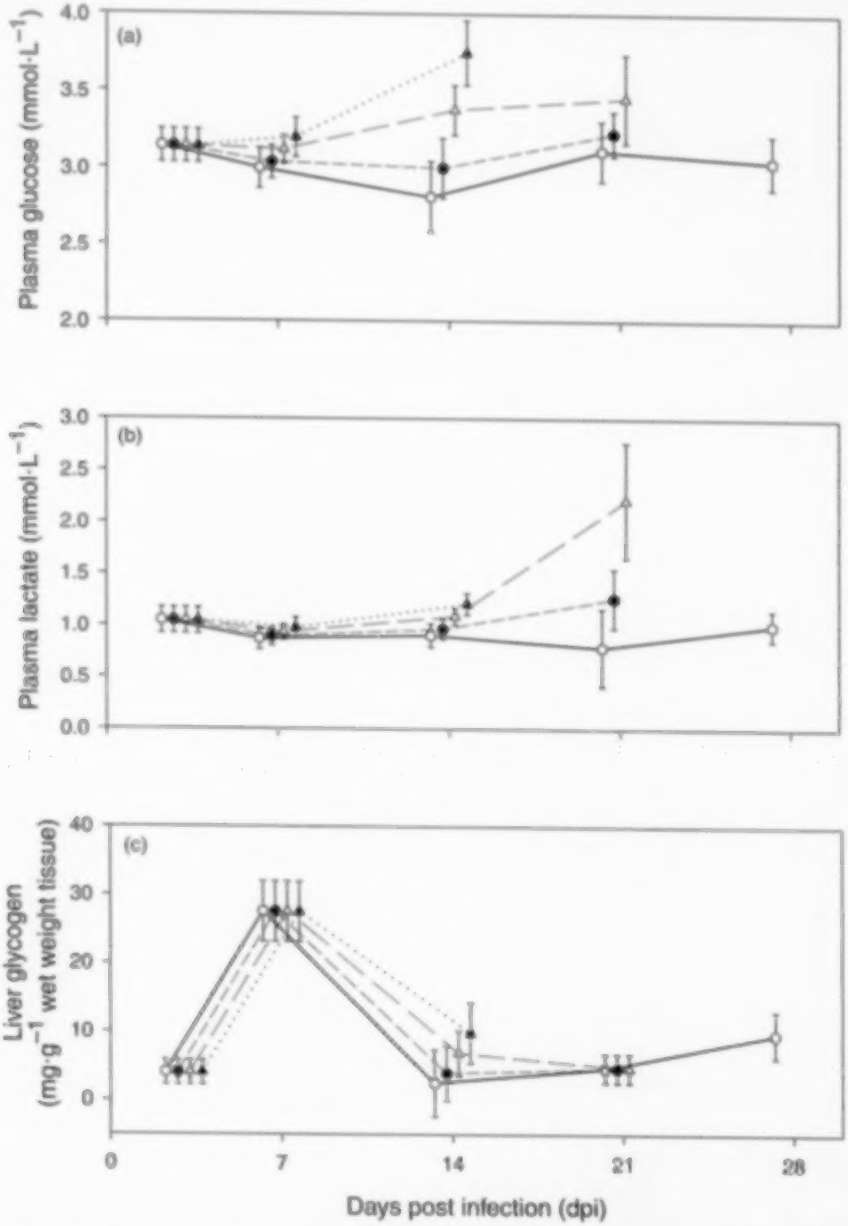

the lice relationship was not statistically significant at the 5% level for plasma osmolality at 3 dpi, there was some evidence of a lice effect at 7 dpi ($p = 0.06$; Fig. 2). A significant lice effect was apparent at 14 and 21 dpi for both plasma chloride and plasma osmolality. Despite there being no significant lice effects at 21 dpi for haematocrit, there was weak evidence ($p = 0.08$) of a lice effect at 14 dpi.

There was no evidence of a lice effect at either 3 or 28 dpi for plasma glucose, plasma lactate, or liver glycogen (Fig. 3); however, a lice effect was significant at 14 dpi for

Fig. 4. Predicted mean values with 95% confidence intervals for plasma cortisol at four fixed lice (*Lepeophtheirus salmonis*) loadings: control (no lice), solid line and open circles; 10 lice·fish^{-1}, broken line and closed circles; 30 lice·fish^{-1}, broken line and open triangles; 50 lice·fish^{-1}, dotted line and closed triangles. The number of lice per fish was modelled as a continuous variable, and predictions for a range of lice values were obtained by fixing other covariates (length and condition factor) at their means for each time point. These predictions are based on separate models for each time point, and data are slightly offset for clarity.

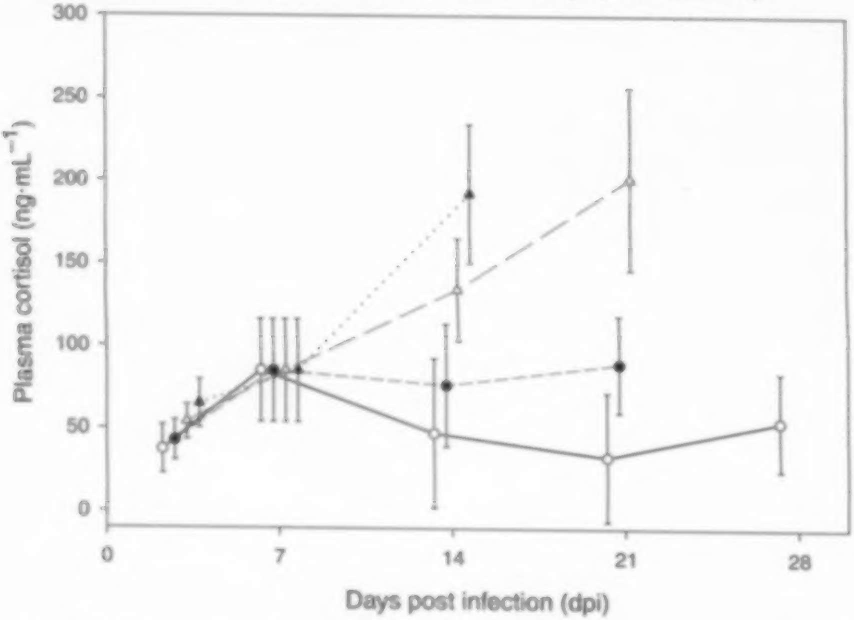

these three measures. While there were no lice effects at 7 dpi for liver glycogen, there was a significant elevation in liver glycogen concentration across all experimental groups at this time point. A significant lice effect was exhibited for plasma glucose at 7 dpi and plasma lactate at 21 dpi, whereas only weak evidence ($p = 0.08$) of a lice effect was evident at 21 dpi for plasma glucose. Plasma cortisol (Fig. 4) exhibited a significant lice effect at 3, 14, and 21 dpi, but lice effects were not statistically significant at the 5% level at 7 or 28 dpi. There was no evidence of a tank loading (i.e., initial infestation) effect at any time point.

Piecewise linear modeling

A single breakpoint at 11 lice·fish^{-1} was identified at just 3 dpi for plasma cortisol. Plasma cortisol was the only physiological measure with compelling evidence ($p = 0.01564$) for a lice effect at this early stage. At 7 dpi, plasma glucose and plasma osmolality were the only measures with evidence for a lice relationship (p values of 0.0393 and 0.067, respectively), and standard linear lice terms were preferred for these measures; these breakpoint results were unaffected by the exclusion of the eight heavily infected fish (see Materials and methods, Data analysis). Standard linear terms were preferred for lice for the plasma osmolality and haematocrit responses at 14 dpi, whereas a breakpoint at as few as 13 lice·fish^{-1} was identified for plasma cortisol at this time point (Fig. 5). The breakpoints identified were notably higher for plasma lactate (34, 43, 67 lice·fish^{-1}) and glucose (68 lice·fish^{-1}) at 14 dpi (Fig. 6); however, breakpoints for plasma glucose (6, 13 lice·fish^{-1}) and plasma lactate (13, 24 lice·fish^{-1}) were substantially reduced at 21 dpi (Fig. 6; Table 4). These breakpoint results were identical under the AIC and AIC$_c$ scores, except for plasma glucose at 21 dpi. In this case, the AIC$_c$ score deemed any breakpoints unnecessary, which suggests weaker evidence of a nonlinear relationship for this measure at 21 dpi.

The AIC and AIC$_c$ scores indicated that a standard linear lice term was preferable for the plasma chloride and plasma cortisol models at 21 dpi; increasing *L. salmonis* levels therefore resulted in a constant increase in these physiological measures. While this suggests the extra parameters required to fit piecewise linear terms for plasma chloride and plasma cortisol were not justified at 21 dpi, plasma chloride also identified a breakpoint at 13 lice·fish^{-1} when piecewise linear terms for lice were fitted (Table 4).

Discussion

The setting of an objectively derived minimum target sea lice burden known to have negligible physiological effects on the host is central to any strategy for monitoring *L. salmonis* impacts on wild and farmed fish. This is the first investigation of the physiological effects of *L. salmonis* infestation on wild sea trout smolts. Previous physiological studies of the impact of *L. salmonis* infection of Atlantic salmon smolts have concerned parasitic challenge of fully SW-acclimated juvenile host fish, some days or weeks after their experimental transfer to SW. Such data are of limited value in ascertaining the overall impact of ectoparasitic infection of wild fish, because *L. salmonis* infestation of the host fish can commence immediately on entry to SW. Pre-

Fig. 5. Results from the piecewise linear models with 95% confidence intervals (broken lines); where a standard linear term for lice was preferred (under Akaike's information criterion), a linear term is shown (e.g., *a* and *d*): (*a*) plasma osmolality at 14 days postinfestation (dpi), (*b*) plasma osmolality at 21 dpi, (*c*) plasma cortisol at 14 dpi, (*d*) plasma cortisol at 21 dpi. Breakpoint values are shown in Table 4.

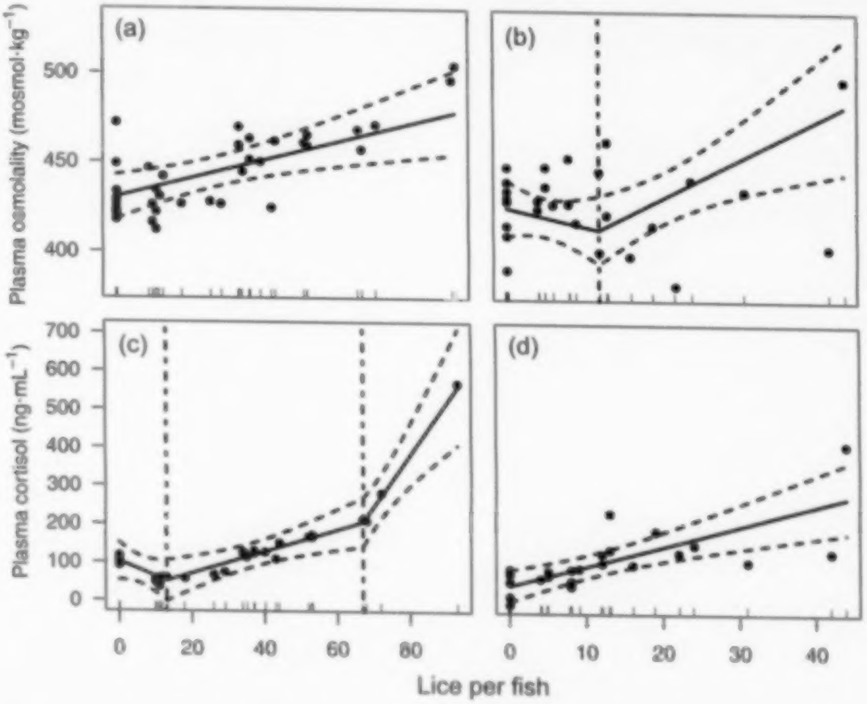

dominance of chalimus stages has been recorded for wild sea trout post smolts in areas adjacent to salmon farms (e.g., Tully et al. 1993), implying that fish are being rapidly infested by a pulse of copepodids soon after entering SW. Nonetheless, there also is the possibility that the mobile stages of *L. salmonis* can detach in response to the reduced salinity of estuarine conditions and prior to capture of the fish. The present study is the first attempt to model a single pulse of copepodid infestation and to determine a sublethal threshold number of lice per fish, above which significant physiological stress occurs.

Previous studies have demonstrated that the developmental time course of *L. salmonis* on sea trout (Bjørn and Finstad 1998) corresponds to that for Atlantic salmon (Grimnes and Jakobsen 1996; Johnson and Albright 1991*a*). Male *L. salmonis* on salmon develop faster than females, taking approximately 29–40 vs. 38–52 days, respectively, to reach the adult stage at 10 °C. In the present study, *L. salmonis* development was somewhat quicker than that described for hatchery-reared sea trout (Bjørn and Finstad 1998), reflecting the higher ambient water temperature in our aquarium (14 °C). The spatial distribution of *L. salmonis* over the body surface was similar to that previously described (Bjørn and Finstad 1998). However, only small percentages of copepodid and chalimus larvae (1.1%–1.4%) were here found on the gills, in contrast with the 16% reported by Bjørn and Finstad (1998) and 53% by Johnson and Albright (1991*a*). No adult or preadult *L. salmonis* were observed on the gills. A large proportion of the total number of copepodids and mobile *L. salmonis* also was recovered from the anesthetic solutions, emphasizing the importance of collection of detached and dislodged sea lice in this type of study.

Plasma chloride and osmolality

Mean plasma chloride levels remained relatively stable throughout the experimental period in the control group. No difference was observed between control and infested fish when the *L. salmonis* were at the late chalimus stage (7 dpi), in contrast with previous studies on hatchery-reared sea trout (Bjørn and Finstad 1997), but in agreement with experiments on Atlantic salmon (Grimnes and Jakobsen 1996; Grimnes et al. 1996). However, a significant parasite-induced increase in plasma chloride was apparent once *L. salmonis* reached the mobile preadult stages (14 and 21 dpi). This may be due in part to the increased feeding activity by mobile preadult *L. salmonis* and associated skin damage (Bjørn and Finstad 1998; Pike and Wadsworth 2000), leading to a reduction in osmoregulatory ability. In addition, disturbance both of water and ion homeostasis is a common result of stress in fish (Wendelaar Bonga 1997). The disturbance of hydromineral balance may arise from marked structural changes in the gills, such as necrosis of the branchial epithelial cells or epithelial lifting, which are mediated by cortisol (Wendelaar Bonga 1997). Epithelial lifting is defined as fluid infiltration in the intercellular spaces and sepa-

Fig. 6. Results from the piecewise linear models with 95% confidence intervals (broken lines): (*a*) plasma lactate at 14 days postinfestation (dpi), (*b*) plasma lactate at 21 dpi, (*c*) plasma glucose at 14 dpi, (*d*) plasma glucose at 21 dpi. Breakpoint values are shown in Table 4.

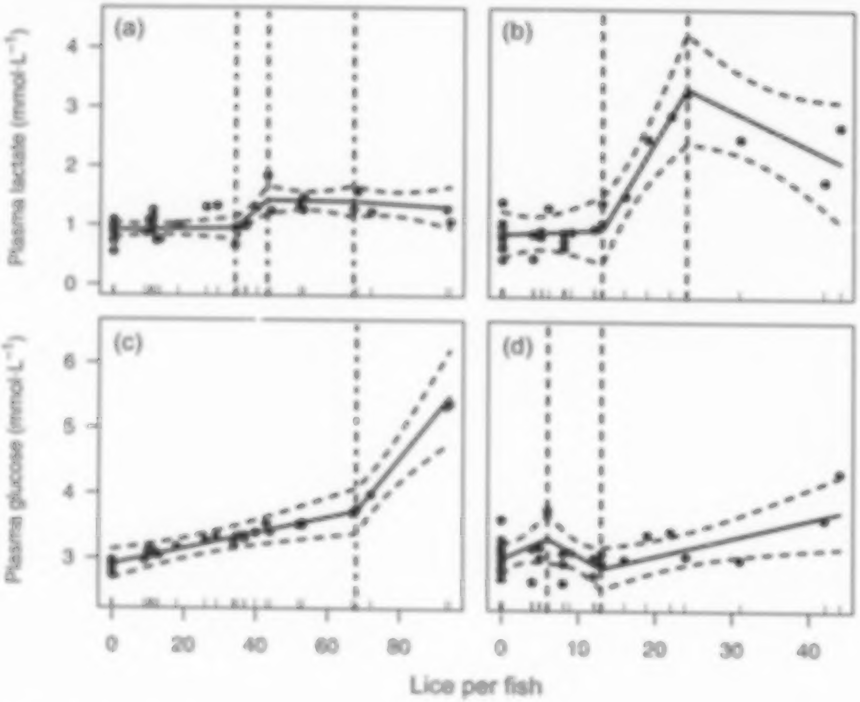

Table 4. Predicted breakpoints (lice loadings) at 21 days postinfestation (dpi) identified using piecewise linear models.

Physiological measure in plasma	Breakpoints
Glucose	6, 13
Lactate	13, 24
Osmolality	12
Chloride	Linear (6, 13, 24)
Cortisol	Linear (8, 24)

Note: In the interests of parsimony, Akaike's information criterion (AIC) statistic was used to discriminate between a standard linear term and a piecewise linear term for lice. Where a linear model was preferred (under the AIC), the breakpoints chosen using a piecewise approach are shown in parentheses.

ration of the epithelia from its basal membrane (Wendelaar Bonga and Balm 1999). However, physical changes in the gills could also arise from the grazing activity of larval *L. salmonis*. A parasite-induced increase for plasma osmolality was observed at 14 and 21 dpi, but there was also weak evidence for a lice effect at 7 dpi, when the parasites were still at the attached chalimus stage.

Plasma cortisol

An elevation in plasma cortisol is the most widely used indicator of stress in fish (Wendelaar Bonga 1997). Typically, plasma cortisol levels rise rapidly a few minutes after exposure to an acute stressor, and the return to normal levels may take one or more hours. When the stressor is chronic, cortisol levels may remain elevated, although well below peak levels reached during an acute stress event (Wendelaar Bonga 1997). Cortisol has a broad activity spectrum in fish, including the regulation of hydromineral balance, energy metabolism, and a reduction in the immune response. In the present study, an initial lice effect on cortisol was observed as early as 3 dpi, but by 7 dpi no lice effect was apparent. The lice effect at 3 dpi may indicate an initial acute stress arising from the process of copepodid attachment. During the first 2–3 dpi, fish in the medium and high lice intensity tanks often showed distinct "flashing" behavior (jumping clear of the water surface), as previously documented by Wootten et al. (1982). By 7 dpi, this behavior had effectively stopped and was not observed again until the *L. salmonis* developed to the mobile stages. The significant lice effect observed at 14 and 21 dpi may indicate chronic stress arising from increased feeding activity by mobile *L. salmonis*. These significantly elevated plasma cortisol concentrations are consistent with the well-characterized response to stress (Wendelaar Bonga 1997), and a similar response was observed in studies on hatchery-reared sea trout (Bjørn and Finstad 1997) and salmon (Fast et al. 2006).

Metabolic indicators

Both acute and chronic stress typically are associated with increased metabolic rate, because response to a stressor is energy-demanding (Mommsen et al. 1999). To satisfy the increased energy demand, fish mobilize substrates to fuel cellular processes. There have been many reports of an elevation of plasma glucose (hyperglycemia) and a decrease in liver glycogen (glycogenolysis) during stress (Wendelaar Bonga 1997); therefore, hyperglycemia is useful as a stress indicator in fish (Barton 2000). In addition to hyperglycemia, elevated plasma lactate levels have been reported following both acute and chronic stress (Farbridge and Leatherland 1992; Iversen et al. 1998). Anaerobic conditions caused by exhaustive exercise result in the breakdown of muscle glycogen to lactate, with some of this lactate being released into the bloodstream (Wood 1991). However, it is important to note that liver glycogen, plasma glucose, and plasma lactate all are influenced by the metabolic status and feeding history of the animal (Mommsen et al. 1999).

Plasma glucose, plasma lactate, and liver glycogen

There was a significant lice-induced elevation of both plasma glucose and plasma lactate concentrations at 14 and 21 dpi, perhaps reflecting an increased energy demand to the animal due to the stress of *L. salmonis* infestation. This increased energy demand may have resulted in anaerobic breakdown of muscle glycogen to lactate, perhaps connected to stress and the flashing behavior observed at this time. These extra energy demands may explain the significant lice effect observed for plasma glucose at 7 dpi.

The unavoidable short delay in freeze-clamping the liver samples (following prior removal of blood samples) may have resulted in a slight underestimation of liver glycogen content because of initiation of liver glycogen breakdown. However, liver sampling was completed within 3 min of sacrifice, in common with previous salmonid studies (Plisetskaya et al. 1994), and there was an equivalent delay in sampling for fish in all experimental groups. In general, there was an increase in liver glycogen (including the control group) at 7 dpi compared with all other time points. It is most likely that this increase was attributable to SW transfer, 1 week earlier. In the present study, liver glycogen concentration returned to levels approaching basal in all groups and remained low for the remainder of the experiment.

Identification of threshold parasite intensities

The piecewise linear approach permitted the objective identification of abrupt changes, or threshold intensities, which occurred as a result of the effects of increasing numbers of *L. salmonis* for each physiological measure. At 21 dpi, a strikingly consistent breakpoint of 12–13 lice·fish^{-1} was identified across the majority of physiological measures. Earlier studies of a restricted range of measures (plasma ions and cortisol) indicated that 50 mobile lice·fish^{-1} may cause the death of a small sea trout postsmolt (60 g; cf. our mean of 37 g) (Bjørn and Finstad 1997). Similarly, as few as 30 adult *L. salmonis* were found to cause significant osmoregulatory imbalance in plasma ion concentrations (Bjørn and Finstad 1997). This reported breakpoint–threshold of *L. salmonis* infestation intensity is markedly below those previously reported, because the present experimental approach is environmentally more relevant in reflecting the dual challenge of infestation of wild sea trout smolts and physiological acclimation to SW.

Identification of the 12–13 lice·fish^{-1} threshold is an essential prerequisite in formulating effective wild fisheries management and stock conservation policy, and these results should provide a sound basis for continued policy development (Heuch et al. 2005). For example, depending upon prevailing local circumstances, fishery managers may use a given proportion of returning fish above this threshold lice intensity as being indicative of a potentially threatening impact on local wild stocks. However, difficulties remain in translating physiological predictors into a useable tool in the management of both farmed and wild populations. For example, the age and size of first migrant juvenile sea trout are known to vary considerably throughout the species' geographic range (Klemetsen et al. 2003). However, in the absence of an objective means of scaling lice loadings on individual fish of differing size, we would recommend that the conservative and precautionary approach would be for wild fishery managers to adopt a critical level of 13 mobile *L. salmonis*·fish^{-1} for juvenile sea trout in their first sea year. This level would provide a clear indication of the proportion of sea trout within a population that are subject to physiological stress and potential death from sea lice infestation.

Acknowledgements

This study was carried out with the support of European Commission DG Fisheries contract No. Q5RS-2002-00730 "Sustainable Management of Interactions Between Aquaculture and Wild Salmonid Fish (SUMBAWS)". Fish were provided with the permission of the Esk District Salmon Fishery Board and were collected from the Kinnaber trap with the help of Fisheries Research Services personnel. We thank A.F. Walker for comments on the manuscript.

References

Akaike, H. 1973. Information theory and an extension of the maximum likelihood principle. *In* International Symposium on Information Theory, Tsahkadsor, Armenian SSR, 2–8 September 1971. *Edited by* B.N. Petrov and F. Csáki. Akademiai Kiado, Budapest, Hungary. pp. 267–281.

Anonymous. 1993. Report of the Sea Trout Working Group 1993. Department of the Marine, Abbotstown, Ireland.

Anonymous. 1995. Report of the Sea Trout Working Group 1994. Department of the Marine, Abbotstown, Ireland.

Anonymous. 2004. Statistical bulletin. Scottish salmon and sea trout catches, 2003. Fisheries Research Services, Aberdeen, UK. Rep. No. Fis/2004/1.

Barton, B.A. 2000. Salmonid fishes differ in their cortisol and glucose responses to handling and transport stress. N. Am. J. Aquacult. **62**: 12–18.

Barton, B.A., and Iwama, G.K. 1991. Physiological changes in fish from stress in aquaculture with emphasis on the response and effects of corticosteroids. Annu. Rev. Fish Dis. **1**: 3–26.

Bedrick, E.J., and Tsai, C.L. 1994. Model selection for multivariate regression in small samples. Biometrics, **50**: 226–231.

Bernatchez, L., and Wilson, C.C. 1998. Comparative phylogeography of Nearctic and Palearctic fishes. Mol. Ecol. **7**: 431–452.

Birkeland, K. 1996. Consequences of premature return by sea trout (*Salmo trutta*) infested with the salmon louse (*Lepeophtheirus salmonis* Kroyer): migration, growth, and mortality. Can. J. Fish. Aquat. Sci. **53**: 2808–2813.

Bjørn, P.A., and Finstad, B. 1997. The physiological effects of salmon lice infection on sea trout post smolts. Nord. J. Freshw. Res. **73**: 60–72.

Bjørn, P.A., and Finstad, B. 1998. The development of salmon lice (*Lepeophtheirus salmonis*) on artificially infected post smolts of sea trout (*Salmo trutta*). Can. J. Zool. **76**: 970–977.

Breusch, T.S., and Pagan, A.R. 1979. A simple test for heteroscedasticity and random coefficient variation. Econometrica, **47**: 1287–1294.

Butler, J.R.A. 2002. Wild salmonids and sea louse infestations on the west coast of Scotland: sources of infection and implications for the management of marine salmon farms. Pest Manag. Sci. **58**: 595–608.

Collins, R. 1993. Principles of disease diagnosis. *In* Aquaculture for veterinarians. *Edited by* L. Brown. Pergamon Press Ltd., Oxford, UK. pp. 69–89.

Dawson, L.H.J., Pike, A.W., Houlihan, D.F., and McVicar, A.H. 1998. Effects of salmon lice *Lepeophtheirus salmonis* on sea trout *Salmo trutta* at different times after seawater transfer. Dis. Aquat. Org. **33**: 179–186.

Farbridge, K.J., and Leatherland, J.F. 1992. Plasma growth hormone levels in fed and fasted rainbow trout (*Oncorhynchus mykiss*) are decreased following handling stress. Fish Physiol. Biochem. **10**: 67–73.

Fast, M.D., Ross, N.W., Craft, C.A., Locke, S.J., MacKinnon, S.L., and Johnson, S.C. 2004. *Lepeophtheirus salmonis*: characterization of prostaglandin E_2 in secretory products of the salmon louse by RP-HPLC and mass spectrometry. Exp. Parasitol. **107**: 5–13.

Fast, M.D., Muise, D.M., Easy, R.E., Ross, N.W., and Johnson, S.C. 2006. The effects of *Lepeophtheirus salmonis* infections on the stress response and immunological status of Atlantic salmon (*Salmo salar*). Fish Shellfish Immunol. **21**: 228–241.

Finstad, B., Johnsen, B.O., and Hvidsten, N.A. 1994. Prevalence and mean intensity of salmon lice, *Lepeophtheirus salmonis* Krøyer, infection on wild Atlantic salmon, *Salmo salar* L., postsmolts. Aquac. Fish. Manag. **25**: 761–764.

Finstad, B., Bjørn, P.A., Grimnes, A., and Hvidsten, N.A. 2000. Laboratory and field investigations of salmon lice *Lepeophtheirus salmonis* (Krøyer) infestation on Atlantic salmon (*Salmo salar* L.) post-smolts. Aquac. Res. **31**: 795–803.

Fox, J. 1997. Applied regression, linear models and related methods. Sage Publications, Thousand Oaks, Calif.

Fox, J., and Monette, G. 1992. Generalized collinearity diagnostics. J. Am. Stat. Assoc. **87**: 178–183.

Grimnes, A., and Jakobsen, P.J. 1996. The physiological effects of salmon lice infection on post-smolt of Atlantic salmon. J. Fish Biol. **48**: 1179–1194.

Grimnes, A., Finstad, B., and Bjørn, P.A. 1996. Økologiske og fysiologiske konsekvenser av lus på laksefisk i fjordsystem. NINA Oppdragsmelding, **381**: 1–38.

Hansen, L.P., and Jacobsen, J.J. 2000. Distribution and migration of Atlantic salmon, *Salmo salar* L., in the sea. *In* The ocean life of Atlantic salmon. Environmental and biological factors influencing survival. *Edited by* D. Mills. Fishing News Books, Oxford, UK. pp. 75–87.

Heuch, P.A., Bjørn, P.A., Finstad, B., Holst, J.C., Asplin, L., and Nilsen, F. 2005. A review of the Norwegian 'National Action Plan Against Salmon Lice on Salmonids': the effect on wild salmonids. Aquaculture, **246**: 79–92.

Iversen, M., Finstad, B., and Nilssen, K.J. 1998. Recovery from loading and transport stress in Atlantic salmon (*Salmo salar* L.) smolts. Aquaculture, **168**: 387–394.

Johnson, S.C., and Albright, L.J. 1991*a*. Development, growth, and survival of *Lepeophtheirus salmonis* (Copepoda, Caligidae) under laboratory conditions. J. Mar. Biol. Assoc. U.K. **71**: 425–436.

Johnson, S.C., and Albright, L.J. 1991*b*. The developmental stages of *Lepeophtheirus salmonis* (Krøyer, 1837) (Copepoda, Caligidae). Can. J. Zool. **69**: 929–950.

Kabata, Z. 1979. Parasitic Copepoda of British fishes. The Ray Society, London.

Keppler, D., and Decker, K. 1974. Glycogen: determination with amyloglucosidase. *In* Methods of enzymatic analysis. *Edited by* H.U. Bergmeyer. Academic Press, New York. pp. 1127–1131.

Klemetsen, A., Amundsen, P.A., Dempson, J.B., Jonsson, B., Jonsson, N., O'Connell, M.F., and Mortensen, E. 2003. Atlantic salmon *Salmo salar* L., brown trout *Salmo trutta* L., and Arctic charr *Salvelinus alpinus* (L.): a review of aspects of their life histories. Ecol. Freshw. Fish, **12**: 1–59.

McKibben, M.A., and Hay, D.W. 2004. Distributions of planktonic sea lice larvae *Lepeophtheirus salmonis* in the inter-tidal zone in Loch Torridon, Western Scotland in relation to salmon farm production cycles. Aquac. Res. **35**: 742–750.

Molinari, N., Daures, J.-P., and Durand, J.-F. 2001. Regression splines for threshold selection in survival data analysis. Stat. Med. **20**: 237–247.

Mommsen, T.P., Vijayan, M.M., and Moon, T.W. 1999. Cortisol in teleosts: dynamics, mechanisms of action, and metabolic regulation. Rev. Fish. Biol. Fish. **9**: 211–268.

Neff, B.D., and Cargnelli, L.M. 2004. Relationships between condition factors, parasite load and paternity in bluegill sunfish, *Lepomis macrochirus*. Environ. Biol. Fishes, **71**: 297–304.

Nolan, D.T., Reilly, P., and Wendelaar Bonga, S.E. 1999. Infection with low numbers of the sea louse *Lepeophtheirus salmonis* induces stress-related effects in postsmolt Atlantic salmon (*Salmo salar*). Can. J. Fish. Aquat. Sci. **56**: 947–959.

Northcott, S.J., and Walker, A.F. 1996. Farming salmon, saving sea trout; a cool look at a hot issue. *In* Aquaculture and sea lochs. *Edited by* K. Black. Scottish Association for Marine Science, Oban, UK. pp. 72–81.

Penston, M.J., McKibben, M.A., Hay, D.W., and Gillibrand, P.A. 2004. Observations on open-water densities of sea lice larvae in Loch Shieldaig, Western Scotland. Aquac. Res. **35**: 793–805.

Pike, A.W., and Wadsworth, S.L. 2000. Sealice on salmonids: their biology and control. Adv. Parasitol. **44**: 233–337.

Plisetskaya, E.M., Moon, T.W., Larsen, D.A., Foster, G.D., and Dickhoff, W.W. 1994. Liver glycogen, enzyme activities, and pancreatic hormones in juvenile Atlantic salmon (*Salmo salar*) during their first summer in seawater. Can. J. Fish. Aquat. Sci. **51**: 567–576.

R Development Core Team 2004. R: a language and environment for statistical computing. R Foundation for Statistical Computing, Vienna, Austria.

Royston, P. 1982. An extension of Shapiro and Wilk's *W* test for normality to large samples. Appl. Stat. **31**: 115–124.

Schram, T.A. 1993. Supplementary descriptions of the developmental stages of *Lepeophtheirus salmonis* (Krøyer, 1837) (Copepoda: Caligidae). *In* Pathogens of wild and farmed fish. Sea lice. *Edited by* G.A. Boxshall and D. Defaye. Ellis Horwood, Chichester, UK. pp. 30–47.

Shea, E.K., and Vecchione, M. 2002. Quantification of ontogenetic discontinuities in three species of oegopsid squids using model II piecewise linear regression. Mar. Biol. **140**: 971–979.

Sutton, S.G., Bult, T.P., and Haedrich, R.L. 2000. Relationships among fat weight, body weight, water weight, and condition factors in wild Atlantic salmon parr. Trans. Am. Fish. Soc. **129**: 527–538.

Tully, O., Poole, W.R., Whelan, K.F., and Merigoux, S. 1993. Parameters and possible causes of *Lepeophtheirus salmonis* (Krøyer) infesting sea trout (*Salmo trutta* L.) off the west coast of Ireland. *In* Pathogens of wild and farmed fish. Sea lice. *Edited by* G.A. Boxshall and D. Defaye. Ellis Horwood, Chichester, UK. pp. 202–213.

van Anholt, R.D., Spanings, T., Koven, W., and Wendelaar Bonga, S.E. 2003. Effects of acetylsalicylic acid treatment on thyroid hormones, prolactins, and the stress response of tilapia (*Oreochromis mossambicus*). Am. J. Physiol. **285**: R1098–R1106.

Wendelaar Bonga, S.E. 1997. The stress response in fish. Physiol. Rev. **77**: 591–625.

Wendelaar Bonga, S.E., and Balm, P.H.M. 1999. Histological and histopathological effects of stress. *In* Stress physiology in animals. *Edited by* P.H.M. Balm. Sheffield Academic Press, Sheffield, UK. pp. 178–204.

Wold, S. 1974. Spline functions in data analysis. Technometrics, **16**: 1–11.

Wood, C.M. 1991. Acid–base and ion balance, metabolism, and their interactions, after exhaustive exercise in fish. J. Exp. Biol. **160**: 285–308.

Wootten, R., Smith, J.W., and Needham, E.A. 1982. Aspects of the biology of the parasitic copepods *Lepeophtheirus salmonis* and *Caligus elongatus* on farmed salmonids, and their treatment. Proc. R. Soc. Edinb. Sect. B, **81**: 185–197.

Larval transport, vertical distribution, and localized recruitment in anadromous rainbow smelt (*Osmerus mordax*)

I.R. Bradbury, K. Gardiner, P.V.R. Snelgrove, S.E. Campana, P. Bentzen, and L. Guan

Abstract: We examined larval dispersal and behaviour in rainbow smelt (*Osmerus mordax*) from the Salmonier River estuary, Newfoundland, during 2003–2005. Riverine ichthyoplankton surveys indicate that larval transport into the estuary is restricted to a two-week period in late June. A passive drifter experiment and the spatial distribution of larvae and juveniles suggest limited dispersal and low export from the estuary. The estuary exhibited low inflow and stratification in summer and high inflow with a stable freshwater layer in fall. Summer and fall winds are primarily onshore. We hypothesised that larval vertical swimming behaviour limits dispersal and export. Larval vertical position and swimming ability were examined through lab-based experiments conducted 0–10 and 90 days after hatching. Measurements of swim speed indicate an order of magnitude ($p < 0.001$) improvement in swimming capacity between larvae and juveniles. One-week after hatching, larvae displayed consistent negative geotaxis, whereas juveniles were generally deeper and displayed negative geotaxis in light and positive geotaxis in the dark. The contrasting light-mediated geotactic behavior between development stages corresponds to ontogenetic shifts in swimming abilities and seasonal changes in estuarine circulation. We suggest that the interaction between behaviour, ontogeny, and hydrography results in limited transport and a tendency for estuarine-scale recruitment, despite an extensive pelagic period.

Résumé : Nous avons étudié la dispersion et le comportement des larves de l'éperlan arc-en-ciel (*Osmerus mordax*) dans l'estuaire de la rivière Salmonier, Terre-Neuve, en 2003–2005. Des inventaires de l'ichthyoplancton de la rivière indiquent que le transport des larves vers l'estuaire se fait seulement durant une période de deux semaines à la fin de juin. Une expérience avec un dériveur passif, d'une part, et la répartition spatiale des larves et des jeunes, d'autre part, laissent croire que la dispersion est limitée et l'exportation faible dans l'estuaire. Il y a une arrivée d'eau réduite et une stratification peu marquée dans l'estuaire en été; à l'automne, l'apport d'eau est important et il s'établit une couche stable d'eau douce. Les vents d'été et d'automne soufflent principalement vers le bord. Nous émettons l'hypothèse selon laquelle le comportement de nage verticale des larves limite la dispersion et l'exportation. Nous avons examiné la position verticale et la capacité de nage des larves dans des expériences de laboratoire faites 0–10 et 90 jours après l'éclosion. Les mesures de la vitesse de nage montrent une amélioration de l'ordre de 10 fois ($p < 0,001$) de la capacité de nage entre les stades de larve et de jeune. Une semaine après l'éclosion, les larves montrent une géotaxie négative soutenue, alors que les jeunes se retrouvent généralement en eau plus profonde et montrent une géotaxie négative durant l'éclairement et une géotaxie positive durant l'obscurité. Le changement contrasté de comportement géotaxique d'un stade à l'autre du développement sous l'influence de la lumière correspond à des modifications ontogéniques de la capacité de nage et à des changements saisonniers de la circulation de l'estuaire. Nous croyons que l'interaction entre le comportement, l'ontogénie et l'hydrographie a pour conséquence de limiter le transport; le recrutement a ainsi tendance à se faire à l'échelle de l'estuaire, malgré la longue période pélagique.

[Traduit par la Rédaction]

Introduction

Estuaries are highly productive regions that provide critical habitat for the early life stages of many marine fish and invertebrates (Bakun 1996). Dispersal, connectivity, and population structure within estuarine species may be regulated through life cycle closure associated with limited larval dispersal (Sinclair 1988). Measures of larval transport for

---

Received 23 May 2006. Accepted 29 September 2006. Published on the NRC Research Press Web site at http://cjfas.nrc.ca on 16 December 2006.
J19330

I.R. Bradbury[1] and P. Bentzen. Marine Gene Probe Laboratory, Biology Department, Life Sciences Centre, Dalhousie University, Halifax, NS B3H 4J1, Canada.
K. Gardiner, P.V.R. Snelgrove, and L. Guan. Ocean Sciences Centre and Biology Department, Memorial University of Newfoundland, NL A1C 5S7, Canada.
S.E. Campana. Population Ecology Division, Bedford Institute of Oceanography, P.O. Box 1006, Dartmouth, NS B2Y 4A2, Canada.

[1] Corresponding author (e-mail: ibradbur@dal.ca).

Can. J. Fish. Aquat. Sci. 63: 2822–2836 (2006) doi:10.1139/F06-164

fishes and invertebrate larvae are often elusive, complicated by interactions of hydrography (e.g., DiBacco et al. 2001), behaviour (Christy and Morgan 1998; Metaxas 2001; Cowen et al. 2006), and ontogeny (e.g., Hare et al. 2005), all of which are species-dependent. Nonetheless, understanding dispersal is critical to the conservation of many coastal populations, some of which are currently exhibiting dramatic declines in abundance (Sale et al. 2005).

In many instances, populations are structured in concert with estuarine dynamics (e.g., Bernatchez and Martin 1996; McLean et al. 1999). Indeed, the scale of dispersal in many estuarine species is inconsistent with predictions based on passive transport (e.g., Thorrold et al. 2001), a paradox that is often attributed to active behavioral modifications to drift trajectories (e.g., Cowen at al. 2000). However, for most invertebrate larvae and the early stages of many fish larvae, horizontal swimming ability may contribute little to horizontal displacement (Bradbury and Snelgrove 2001).

In areas of high current shear typical of many estuaries, active manipulation of vertical position may allow selective transport of larvae in response to tides or light conditions (e.g., Dauvin and Dodson 1990; Davis 2001). Active vertical migration has been demonstrated in multiple species of planktonic fish larvae, including walleye pollock (Theragra chalcogramma; Davis 2001) and bay anchovy (*Anchoa mitchilli*; Schultz et al. 2000). Regular vertical movements allow larvae to choose flow speed and direction, thereby influencing retention or transport to nursery grounds and sites favourable for survival (e.g., Davis 2001; de Graaf et al. 2004; Lee et al. 2005).

Rainbow smelt (*Osmerus mordax*) are small, schooling, pelagic fish that occur along the Atlantic coast of North America from Pennsylvania to Labrador (Scott and Scott 1998). Most populations are anadromous; adults migrate to inland rivers at night during the spring to spawn and then return to sea during the day (Scott and Scott 1988). Spawning migrations are usually restricted spatially and spawning usually occurs just above the head of tide (McKenzie 1964). Eggs are negatively buoyant and adhere to bottom substrate, with egg stage durations that range from 10 to 20 days. Larvae actively synchronize hatch timing to dusk (Ouellet and Dodson 1985*a*; Bradbury et al. 2004) and are approximately 5–6 mm after hatching and negatively buoyant in fresh and brackish water. Yolk sac absorption usually occurs at 7 days after hatching, and flexion occurs at approximately 31 days after hatching or at a standard length of 10–15 mm (Sirois et al. 1998; Bradbury et al. 2004). Upon hatch, larvae are transported to the estuary where they develop. Several studies suggest that larval smelt may use vertical migration to enhance estuarine retention (e.g., Ouellet and Dodson 1985*b*; Laprise and Dodson 1989), though there has been disagreement regarding the specific environmental cues involved (Rogers 1940; McKenzie 1964; Dauvin and Dodson 1990).

Our primary goal was to describe the dispersal of larval smelt and to evaluate active contributions (i.e., behavioral modification of vertical distribution) to dispersal trajectories. We address this goal through three interlinked approaches. First, we examine the spatial extent of horizontal dispersal during the pelagic larval stage within both the river and the estuary in order to estimate export from the estuary. Second, we examine the role that active alterations in depth play in horizontal displacement through hydrographic surveys, a passive drift experiment, and measurements of larval swim speed. Finally, we examine larval depth preference at 1–10 days and 90 days of age in response to various cues such as light and flow combinations. These experiments assume that cue responses observed in a lab setting are similar to responses in the field.

Materials and methods

Study location

Salmonier River estuary is located at the head of St. Mary's Bay on the south coast of the Avalon Peninsula (Fig. 1). The estuary is approximately 13 km long from the tidal head to where it empties into the bay, and widths range from 1.3 km at the mouth to 0.31–0.10 km at the head. Inflow into the estuary varies seasonally from high inflow periods in fall and spring ranging from 25 to 50 $m^3 \cdot s^{-1}$ to low inflow periods during summer characterized by flows of 1–3 $m^3 \cdot s^{-1}$. Oceanographic current patterns within St. Mary's Bay have not been studied. Modelling studies suggest currents are dominated by an inshore branch of the Labrador Current resulting in a counterclockwise flow that exits the bay on the western side (Sheng and Thompson 1996). Oceanography in neighbouring Placentia Bay is of similar shape and orientation and has been studied more extensively. Predominant currents and transport of pelagic eggs and larvae in Placentia Bay support the prediction of a counterclockwise flow with alongshore current speeds ranging from 0 to 5 $cm \cdot s^{-1}$ entering on the eastern side and exiting on along the western side with retention times of approximately 30 days (for details regarding flow and transport in Placentia Bay, see Bradbury et al. (2000, 2003)). It is likely that similar conditions exist in St. Mary's Bay, although retention times may be decreased given its smaller size in comparison with Placentia Bay.

Ichthyoplankton and oceanographic data collection

Dispersal from Salmonier River

Smelt spawning locations in Salmonier River were identified through interviews with local residents and subsequent snorkelling surveys during the spring of 2002. Larvae hatched uniformly at dusk and were sampled nightly at 2200, 10 m downstream of the spawning ground, during June 2003–2005 as they drifted from river spawning beds to the downstream estuary. Sampling is described in detail by Bradbury et al. (2004), but in brief, drift samples of eggs and larvae were sampled with a 30 cm ring net of 333 µm Nitex® mesh fitted with a flowmeter (General Oceanics Inc., Miami, Florida) approximately 10 m downstream from the Salmonier River spawning site. Water depth was <1 m and single 15-min samples were taken every night (at 2200) throughout the hatch period beginning in early June and continuing until all eggs in the river had hatched (early July) in order to describe seasonality in spawning and hatch patterns. River water temperature measurements were made with an ethanol thermometer at the time of sampling, and all plankton samples were preserved in 95% ethanol and identified to species level.

Fig. 1. (*a*) Map showing location of St. Mary's Bay in relation to Newfoundland, Canada. (*b*) Map of study sites indicating location of Salmonier River and Holyrood Pond. (*c*) Transects and oceanographic stations in Salmonier River estuary are indicated (●).

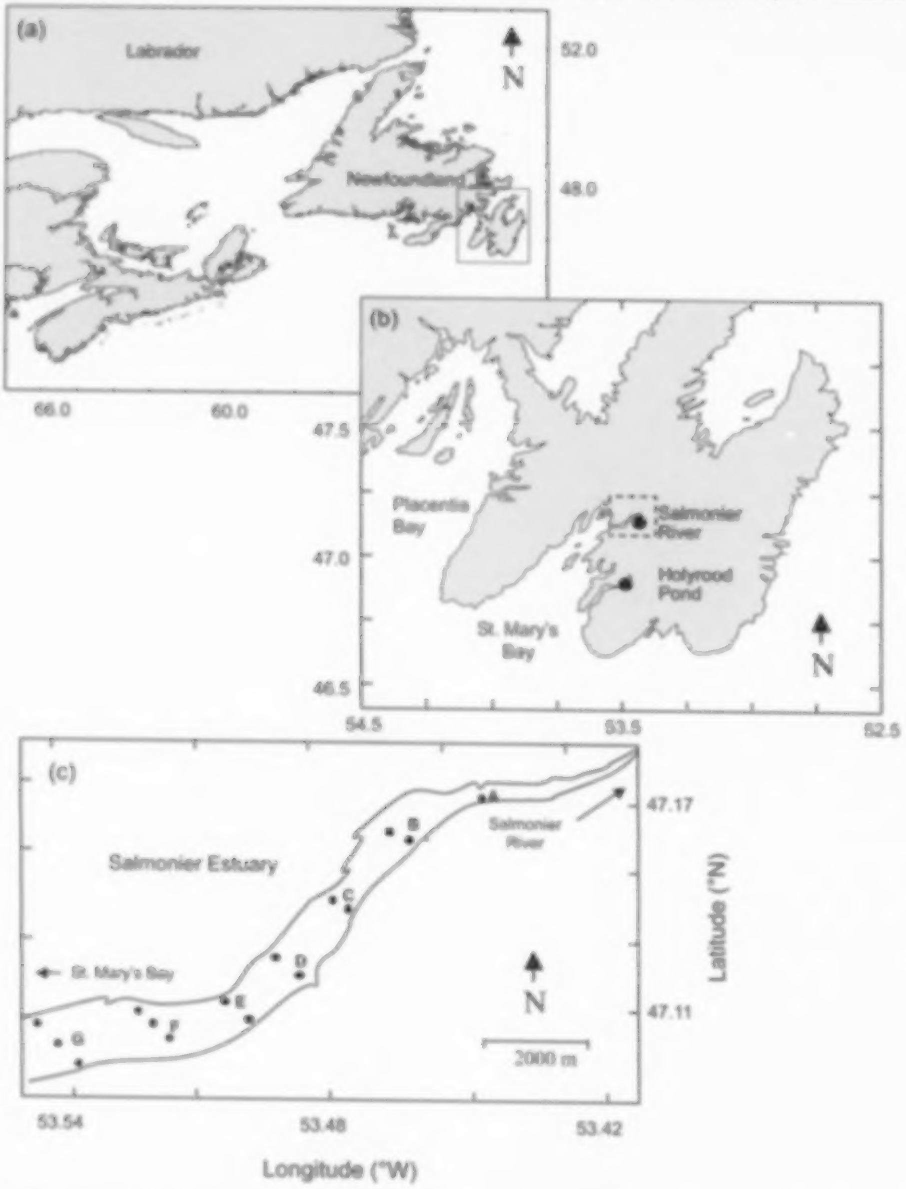
(a)
Labrador
N
52.0
Newfoundland
48.0
66.0
60.0
(b)
47.5
Placentia Bay
Salmonier River
47.0
Holyrood Pond
St. Mary's Bay
N
46.5
54.5
53.5
52.5
(c)
Salmonier Estuary
A
B
C
D
E
F
G
Salmonier River
St. Mary's Bay
N
2000 m
47.17
47.11
Latitude (°N)
53.54
53.48
53.42
Longitude (°W)

Dispersal within the estuary

Estuarine ichthyoplankton and hydrography were sampled across seven transects distributed throughout the estuary (Fig. 1, A–G) during 3–5 July 2005. Ichthyoplankton was sampled using a 1 m ring net towed obliquely across each transect through the water column for 10 min. Volumes filtered were estimated with a flowmeter (General Oceanics Inc.), and samples were processed as described above. Fifteen hydrographic stations (Fig. 1, ●) were sampled using a CTD (conductivity–temperature–depth) profiler (SBE 25 (15–18 November 2004) or SBE 19 (3–5 July 2005); Sea-Bird Electronics, Inc., Bellevue, Washington). Data was examined graphically to determine both vertical stratification and horizontal extension of surface penetration of freshwater into the estuary. Seasonal shifts in vertical stratification allowed examination of the magnitude of inflow and its penetration into the estuary, as well as potential export. Wind data were obtained from the Canadian Atmosphere and Environmental Service for Argentia, Placentia Bay (approximately 50 km away), for July to December of 2003, 2004, and 2005. Wind data were rotated 25° to align with the long axis of the estuary. Wind direction and speed were converted to wind stress (Large and Pond 1981) and filtered using an 8th-order Butterworth lowpass filter to allow interpretation of drag force per unit area transferred to water surface.

To examine predominant drift of surface water, a passive drifter release was conducted on 25 June 2005. Oranges were chosen as drifters because they are positively buoyant, visible at great distance, and biodegradable. Similar releases have been conducted and resulted in good approximations of predominant flow and transport of pelagic Atlantic cod eggs located in the upper mixed layer around coastal Newfoundland (e.g., Bradbury et al. 2000). A total of 1191 individually labelled oranges were released from the spawning location within the Salmonier River at 2200 to coincide with seasonal and daily peaks in hatch. Admittedly, given that they break the water surface, these oranges may be more responsive to wind stress and may therefore be more responsive to wind-driven flow than particles at depth. Nonetheless, the shallow depth of many parts of the river and negative geotaxis of larvae (see below) suggest that the drifter study is a reasonable approximation of passive drift. Oranges were recovered over the next 30 days based on visual surveys of beaches throughout St. Mary's Bay.

Early juvenile smelt were sampled within the Salmonier River estuary to provide the dual function of data on spatial and size-frequency distributions necessary to place the swim speed data within context of the larger population. Sampling took place during the fall (October to November) of 2003 and 2004 at each of 25 sites that spanned the estuary from river inflow to St. Mary's Bay. Sites were chosen based on distribution around the estuary, accessibility by small craft, and the presence of eelgrass (*Zostera* spp.) habitat. A 25 m demersal seine with 19 mm stretched mesh was deployed 50 m from shore. The seine samples 880 m^2 of habitat from the substrate to 2 m above the bottom and has a capture efficiency of 95% (Gotceitas et al. 1997).

Larval and juvenile swim speeds

Eggs were transported from the Salmonier River to the Ocean Sciences Centre of Memorial University and placed in aerated water from the river maintained at 10 °C. Eggs hatched within 15–20 days and yolk sac larvae could be maintained for approximately 10 days. Efforts to get the larvae to feed were unsuccessful, and larval data are therefore limited to individuals that were still feeding on yolk sac. On repeated trips to the Salmonier River estuary in the fall, juveniles were collected with the beach seine described above, but efforts to transport them to the lab were unsuccessful and resulted in high mortality. We therefore transported the swim tunnel (see below) to the river and conducted swim trials on freshly collected juveniles of unknown age. Nonfeeding preflexion larvae were held for a period during which no visible effects on survival were observed (<10 days). Postflexion juveniles captured in the field were acclimatized to the lab and held for a maximum of 12 h to minimize containment-associated behaviours.

To evaluate larval swimming abilities, larvae for a given developmental stage (reported as size) were selected haphazardly and carefully transferred to a small (60 mL total volume) Blazka swimming tunnel. A swimming tunnel is a tube through which flow is created via a small impellor connected to a variable-speed motor. Larval fish are placed in the tube and flow is altered via the impellor to test swimming ability by determining the flow speed at which a larva can no longer maintain its position in the tube (see Beamish 1978). Larvae were allowed to acclimate to the tunnel for 10–15 min in static flow. Swimming capacity was determined using a modified critical swimming velocity (U_{crit}) test (Brett 1964), where current velocity was increased gradually from static in 1 cm·s^{-1} increments every 2 min until the larvae could no longer maintain position for a full 2-min period. This measure of swim speed represents an upper end of swim potential, and sustained swim speeds are typically much smaller (L. Guan and P.V.R. Snelgrove, unpublished data). The equation used to calculate the U_{crit} of larvae followed Brett (1964):

$$U_{crit} = U + [(t/t_i)U_i]$$

where U represents penultimate speed, U_i represents velocity increment (1.0 cm·s^{-1}), t represents time swim in the final velocity increment, and t_i represents set time interval for each velocity increment (2 min).

The methodology for juveniles was similar to that used with larvae except that a larger swim tunnel (1.6 L volume) was required and the speed increments (U_i) for juvenile swim speed trials were 2.5 cm·s^{-1}. Ryland (1963) described the transverse velocity gradient in a tube 1.6 cm in diameter, which is similar in size to the tunnel used for the preflexion larvae examined in this study, and noted that velocity near the wall was lower than at the centre because of drag. All the reported swim speeds were for larvae near the centre of the tube to minimize the influence of the boundary layer on swim speed estimation. Nonetheless, we cannot completely rule out a minor boundary layer effect.

Vertical movement behavioural experiments

Fertilized smelt eggs were acquired from Holyrood Pond and the Salmonier River during spring spawning 2005 (Fig. 1). The Holyrood Pond population spawned first (May 2005), followed by the Salmonier River (June). To collect eggs, burlap pieces (1 m × 4 m) were placed over the substrate at locations where spawning had been observed the previous night (see Bradbury et al. (2004) for details on egg collection). Given the negative buoyancy and adhesive nature of the eggs, they quickly accumulated on the burlap, and we observed no effect of the burlap on spawning adults. Burlap pieces remained in the river until covered with fertilized eggs (typically several days), at which point the burlap was carefully transported to a nearby lab and the eggs were reared in 80 L aerated freshwater tanks maintained at 13 °C. Water quality was monitored until hatch with 50% water exchanges every second day. Because water exchanges in holding tanks were conducted on a 2-day cycle, the majority of larvae included in behavioural experiments were between 1 and 2 days old.

Initial experiments were performed on newly hatched preflexion larvae (0–10 days after hatching, noting that larvae feed primarily on yolk reserves during this period; Sirois et al. 1998) and experimental design followed Davis (2001). Larvae were added to clear plastic columns (182 cm tall, 15 cm diameter, 2 mm thick). Because larvae occur in both low salinity and brackish areas of the estuary, separate experiments were conducted with either fresh (0 psu) or brackish (15–20 psu) water obtained from the Salmonier River estuary. Larvae were added at a depth of 10–20 cm below the surface, taking care to minimize stress and damage. In the brackish water experiments, larvae were added well below the surface (~50–60 cm depth) to eliminate entrainment in the freshwater layer that might result from addition near the top of the column. In all treatments, larvae were negatively buoyant and, in the absence of vertical swimming, quickly descended to the bottom of columns.

Plastic columns were covered with multiple layers of black plastic to eliminate extraneous light contamination. Plastic shades were arranged in a series of 30 cm panels that could be opened in random order to allow enumeration and avoid systematic biases. Experiments were done at varying times throughout the day and night to eliminate potential innate responses (i.e., tidal or diel) that might be unrelated to experimental stimuli.

Five different treatments were tested in fresh and brackish water: (*i*) top light, no flow; (*ii*) bottom light, no flow; (*iii*) no light, no flow; (*iv*) top light with flow; and (*v*) no light with flow. In all cases, preflexion larvae were exposed to a given treatment for 1 h to allow them to respond to each treatment before visual inspection and counting. Because of their larger size and superior swimming ability, juveniles were exposed to treatments for only 15 min to allow them to respond to the cues before inspection. However, longer periods were initially tested (up to 1 h) to confirm that positions did not change substantially after 15 min. In all trials, counts were obtained at 10 cm depth increments, resulting in 18 depth interval counts per trial. Because of their small size and the potential for counting error, larvae were enumerated twice per trial and then averaged.

Fluorescent lights (13 watt) were used to simulate sunlight in all trials and were placed either above or below the tube depending on the trial (Fig 2*a*.). The light intensities varied from 50 μmol photons·m^{-2}·s^{-1} directly above or below the light source to 5.0 μmol photons·m^{-2}·s^{-1} at the point furthest from the source (Fig. 2*a*). Fluorescent lights minimized the effect of water heating on smelt behaviour. Although flow speeds in the Salmonier River estuary were not measured, flow speeds used in behavioural experiments approximated alongshore speeds common from coastal Newfoundland (Bradbury et al. (2000); see Discussion). Top and bottom flows were generated following Davis (2001). Bottom flows were created using a magnetic stirrer with a maximum flow speed of 5 cm·s^{-1} (Fig. 2*b*). Top flows were created by pumping compressed air through plastic tubing into the water to achieve flows of 5 cm·s^{-1} that were countercurrent to bottom flows. All flow experiments were done with simultaneous top and bottom flows to mimic actual estuarine shear conditions and create a wide range of flow and turbulence conditions within the column (Fig. 2*b*). Throughout all experiments, the room was kept dark and columns were maintained at 13 °C to match ambient water temperature of the rivers. Larvae did not show any adverse response to being held in the columns and survived and remained active for up to 10 days with no food addition (I.R. Bradbury, unpublished data). Air stones, though not present during the experiments because of the confounding effects they would have on flow, were added between trials in which limited availability necessitated reuse of larvae. The aeration ensured that oxygen gradients did not develop over time as fish selected specific depths.

Fig. 2. Experimental treatments of (*a*) light and (*b*) flow with depth in 2 m clear plastic columns (15 cm in diameter).

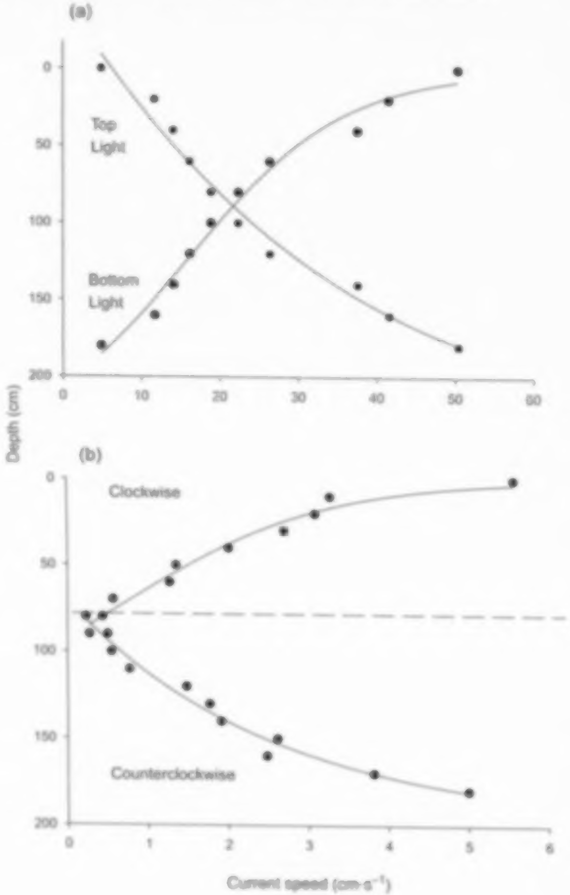

Preflexion larvae (average size = 6.2 mm, σ = 0.33 mm, maximum age ~2 days old) were added to each column by taking a 1 L sample from their rearing baths, which resulted in an average concentration of 1 larva per 100 cm^3. Concentrations varied, however, from 1 larva per 910 cm^3 to 1 larva per 16 cm^3 in some trials depending on availability. Comparisons among experiments with different concentrations of larvae indicated no concentration effect on outcomes.

Juveniles (average length = 43.9 mm, σ = 9.9 mm) were obtained in mid- to late October from the Salmonier River estuary by beach seining in eelgrass beds (Fig. 1). Because 4-month-old juveniles survived better in brackish water than freshwater, all experiments on juveniles were performed with water of salinity corresponding to the salinity where they were caught (approximately 20 psu). Juveniles were exposed to the same experimental treatments as the posthatch larvae with the exception of freshwater. Because of their larger size, juvenile numbers were maintained at lower concentrations than larvae, with an average of 1 juvenile per

467–695 cm^3. Concentration had no noticeable effect on behavioural responses.

Statistical analysis

Each treatment was replicated 10 times, alternating among treatments (i.e., top light, bottom light, no light) to ensure no systematic bias. Larvae and juveniles were changed as frequently as possible, but it was sometimes necessary to reuse individuals, particularly with juveniles. In light of problems associated with centre of mass descriptions for depth distributions (Hare et al. 2005), G tests were used to compare observed with expected (uniform) distributions of larval or juvenile rainbow smelt. For these comparisons, the expected distribution was that either larvae or juveniles would not respond to stimuli and would be haphazardly distributed among each 10 cm depth interval. Pooled G-statistic (G_{pooled}) values were initially determined using the pooled number of individuals per depth range per replicate for a given treatment (Sokal and Rohlf 1995). Heterogeneity between replicates was examined using a heterogeneity G test (G_{het}). However, power to detect heterogeneity may be impeded significantly by low numbers in the juvenile experiments where abundances of <5 individuals per depth range and, in some trials, <1 individual were common. Additional G tests compared pooled results from brackish water larval and juvenile experiments to determine whether the distributions of larval and juvenile stages differed.

Results

Larval inflow

Larval flux from the Salmonier River began on approximately day 160 (9 June) each year and peaked between days 170 (19 June) and 180 (29 June) (Fig. 3). In all three years, hatch was completed by day 190. Water temperatures within the river increased from 10 to 20 °C during the hatch period (Fig. 3, broken line). In all years, the majority of larval production was restricted to a four- to five-night period (Fig. 3) with peak hatch at water temperatures of ~16 °C.

Estuarine transport, hydrography, and swimming ability

Along-estuary wind measurements throughout the summer and fall of all three years indicate that the predominant wind stress is onshore (into the estuary; Fig. 4). Intermittent offshore wind events occurred, but were rare, inconsistent, and short in duration. CTD profiles suggest strong seasonal differences in river inflow. During the summer, the freshwater layer was virtually absent and surface salinities in the upper reaches of the estuary, ranged from 25 to 20 psu, and high surface salinities (30+ psu) were observed in two-thirds of the estuary. The fall was characterized by a stable freshwater layer (Fig. 5), and a greater horizontal extension of freshwater into the estuary, as exhibited by surface salinities that rarely exceeded 15 psu, even at the transition to the bay (Fig. 6*a*).

Fig. 3. Smelt (*Osmerus mordax*) larval abundance (● and solid lines) and water temperature (broken lines) in Salmonier River nightly at 2200 during spawning in June of (*a*) 2003, (*b*) 2004, and (*c*) 2005.

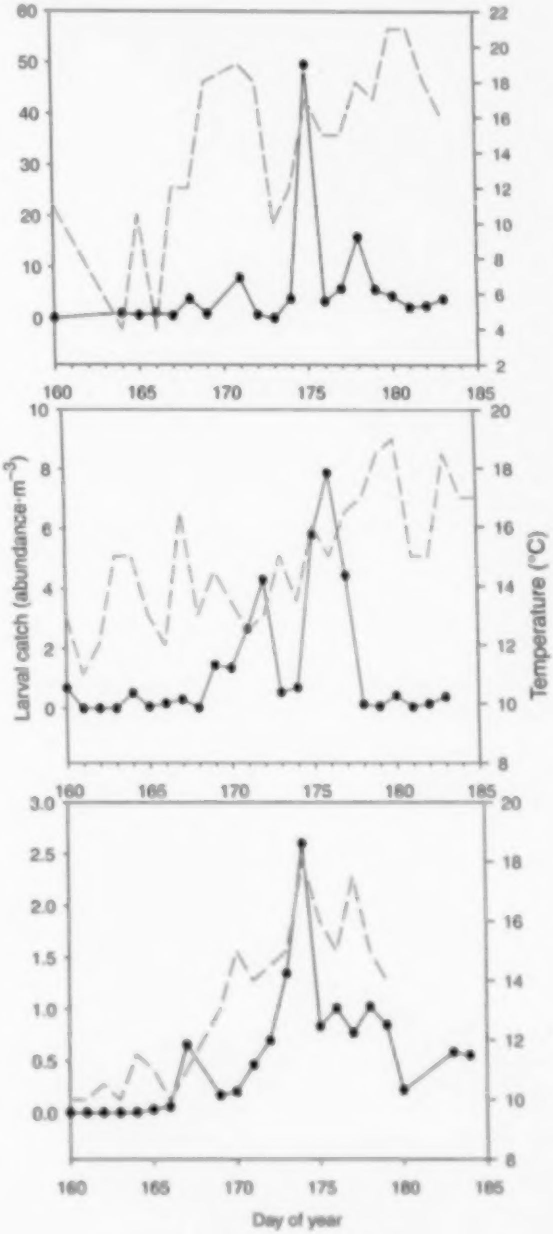

Horizontal dispersal was examined using passive drifters, as well as spatial patterns in larvae and juveniles during summer and fall, respectively. Passive drifters mirrored the extension of freshwater into the estuary in that most oranges were recovered within the upper one-third of the estuary (Fig. 6*b*). Similar declines with distance were observed in smelt larval abundance in July 2005, which varied from ~600 per tow in freshwater to near zero at the exit to the bay (Fig 6*b*). Similarly, juvenile catches were limited to the upper reaches of the estuary, with absence from mid- to outer

Fig. 4. Alongshore wind stress during summer and fall of (*a*) 2003, (*b*) 2004, and (*c*) 2005. All data were filtered with an 8th-order Butterworth filter and rotated to align with the Salmonier River estuary.

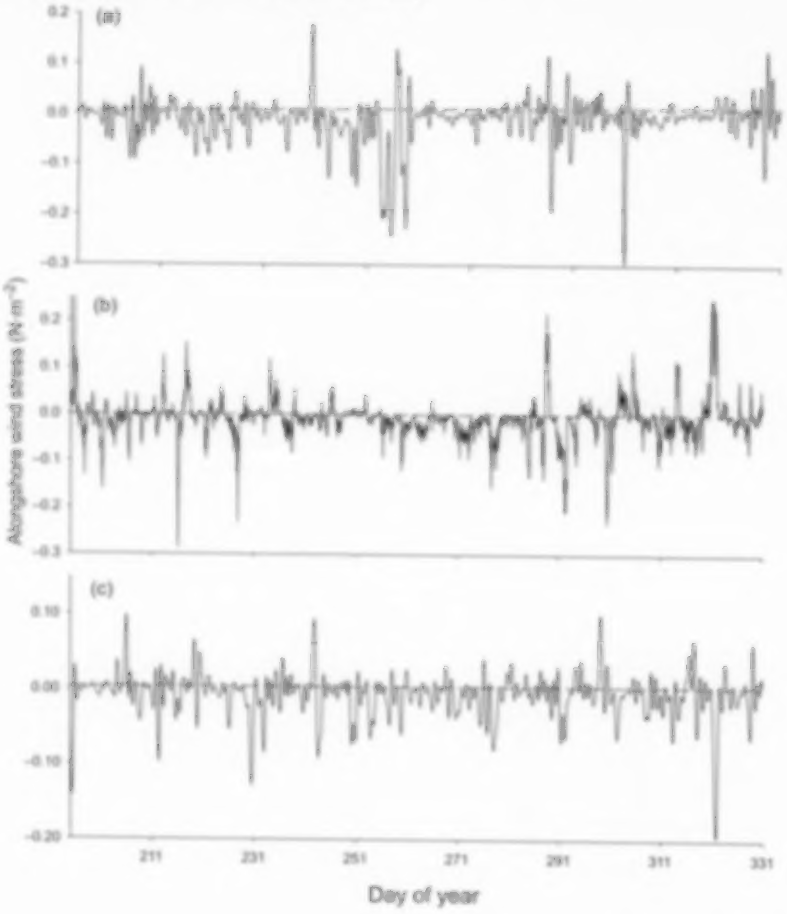

regions (Fig. 7), and significant catches (>10 individuals per tow) were limited to the same three locations in all three years (I.R. Bradbury, unpublished data).

Newly hatched preflexion larvae hatched out at sizes of 0.5 to 0.77 cm with corresponding critical swim speeds of ~2.7 to 3.8 cm·s^{-1} (Fig. 8). By contrast, swim speeds of postflexion juveniles were significantly faster ($p < 0.001$, df = 63); individuals ranging in size from 4.8 to 6.9 cm had corresponding swim speeds of ~11 to 50 cm·s^{-1}. These two size categories corresponded to the size frequency distributions of larvae and juveniles sampled in the Salmonier River and estuary, suggesting that the swim speeds were representative of natural populations.

Depth-preference experiments

Experiments with larvae in freshwater indicated that the majority of individuals were found at the surface (0–20 cm), irrespective of the presence of flow or whether lighting occurred from the top or bottom of the column (Figs. 9*a*–9*e*). For top lighting, the larval vertical distribution was significantly different from a uniform distribution ($G_{\text{pooled}} = 37.64$, $p = 0.002$; Fig. 9*a*), although there was significant heterogeneity among replicates ($G_{\text{het}} = 448.26$, $p < 0.001$). In the presence of bottom light (Fig. 9*b*), in addition to the major peak at the surface, a substantial number (~12%) of individuals were also found at a depth of 170–180 cm ($G_{\text{pooled}} = 31.10$, $p = 0.02$; $G_{\text{het}} = 417.57$, $p < 0.001$; Fig. 9*b*). In the absence of light, larvae were again distributed primarily near the surface (0–20 cm) of the columns ($G_{\text{pooled}} = 55.27$, $p < 0.001$; $G_{\text{het}} = 436.59$, $p < 0.001$; Fig. 9*c*). Larvae were distributed deeper in the column (0–50 cm) in the presence of flow than in the absence of flow (0–20 cm), but individuals were nonetheless primarily near the surface in both no-light trials ($G_{\text{pooled}} = 43.88$, $p < 0.001$; $G_{\text{het}} = 173.51$, $p < 0.001$; Fig. 9*d*) and top-light trials ($G_{\text{pooled}} = 34.18$, $p < 0.01$; $G_{\text{het}} = 217.24$, $p < 0.001$; Fig. 9*e*).

Larvae in brackish water without flow were also distributed primarily near the surface (0–20 cm), irrespective of light treatment, and they were more uniform among replicates. In the presence of top or bottom light, larvae remained in the upper 20 cm of the column (top light (Fig. 10*a*): $G_{\text{pooled}} = 86.43$, $p < 0.001$; $G_{\text{het}} = 72.73$, $p > 0.05$; bottom light (Fig. 10*b*): $G_{\text{pooled}} = 119.52$, $p < 0.001$; $G_{\text{het}} = 97.29$, $p > 0.05$). With no light stimulus, larvae were again found

Fig. 5. Salinity profiles at three locations within the Salmonier River estuary during (*a*–*c*) summer (3–5 July) 2005 and (*d*–*f*) fall (15–18 November) 2004. Locations coincide with transects G, D, and A, respectively (Fig. 1).

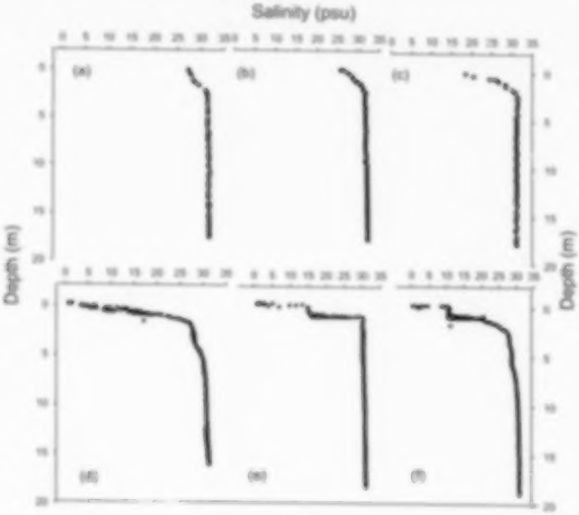

near the surface and most individuals were within the upper 20 cm (G_{pooled} = 112.32, $p < 0.001$; G_{het} = 53.4, $p > 0.05$; Fig. 10*c*). In the presence of countercurrent flows, larvae were again found at the surface (0–30 cm) (Figs. 10*d* and 10*e*) and at depths of 0–80 cm in the absence of light with flow (G_{pooled} = 124.00, $p < 0.001$; G_{het} = 146.57, $p > 0.05$; Fig. 10*d*). With light from above, the highest numbers of larvae were within the upper 20 cm of the column (G_{pooled} = 124.06, $p < 0.001$; G_{het} = 118.9, $p > 0.05$; Fig. 10*e*).

Unlike the posthatch larvae (Figs. 3–6), the juveniles showed varying responses to different treatments (Figs. 11, 12). Each of the juvenile treatments was significantly different from uniformity ($p < 0.001$). Juveniles congregated at 40–100 cm depth when light was from above (G_{pooled} = 33.59, $p = 0.009$; G_{het} = 181.11, $p > 0.05$; Fig. 11*a*) and in the upper half of the column (0–100 cm) with bottom light (G_{pooled} = 11.67, $p > 0.05$; G_{het} = 192.1, $p < 0.05$; Fig. 11*b*). When no light was present, juveniles were primarily within the bottom 10 cm of the column (G_{pooled} = 36.82, $p = 0.004$; G_{het} = 200.68, $p > 0.05$; Fig. 11*c*).

In flow, juveniles dispersed more evenly throughout the columns but, as with the larvae, were found closer to the surface when light was present (G_{pooled} = 23.22, $p = 0.14$; G_{het} = 90.85, $p > 0.05$; Fig. 12*a*) and deeper when light was removed (G_{pooled} = 27.58, $p = 0.8$; G_{het} = 215, $p < 0.05$). There was also a significant difference between the distribution of the larvae and the comparable juvenile distributions for each treatment (i.e., $p < 0.001$) with the juveniles consistently deeper than larvae.

Discussion

Estuaries have long been considered nursery grounds for a variety of marine and freshwater species (e.g., Able 2005). The role of estuaries as nursery grounds and their importance to the spatial ecology of marine organisms is directly tied to the ability of pelagic larvae to maintain themselves within these areas. We demonstrate restricted larval dispersal in rainbow smelt that was limited to the upper reaches of the Salmonier River estuary. Interestingly, ontogenetic shifts in larval behavior and vertical position coincide with seasonal increases in estuarine inflow that may contribute to retention and limit larval dispersal within the estuary. Our results suggest that horizontal displacement during the larval stage within the Salmonier River estuary was on the order of 5–10 km, as shown both in larval and juvenile spatial abundance data. These data indicate clear associations with the upper reaches of the estuary and little export into the bay. Similar spatial patterns in smelt larvae have been observed in other studies (e.g., Rogers 1940; Fortier and Leggett 1982).

Bradbury et al. (2006) demonstrated significant genetic differences ($F_{\text{ST}} \sim 0.10$) between smelt populations in coastal Newfoundland, indicative of restricted connectivity between these populations. The importance of restricted dispersal to population recruitment was stressed by Sirois and Dodson (2000), who suggested that dispersal from the estuarine turbidity maximum may result in suboptimal growth and low survival. Sirois and Dodson (2000) sug-

Fig. 6. (*a*) Changes in sea-surface salinity with distance from spawning in the Salmonier River estuary during the summer (○) and fall (●). Letters A–G refer to transects noted in Fig. 1. (*b*). Passive drifter (●) and smelt (*Osmerus mordax*) larval abundance (△) with distance from spawning ground, 3–5 July 2005. Broken line in (*b*) represents fit of exponential decay to larval abundance data, $f = Y_0 + 3.18 \times 10^4 e^{[illegible]}$, where X is distance from spawning location and f is larval abundance.

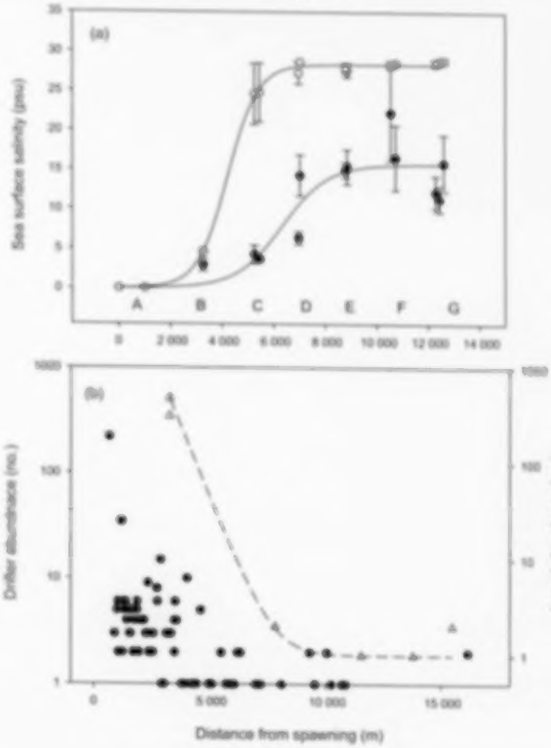

Fig. 7. Spatial distribution of juvenile young-of-the-year smelt (*Osmerus mordax*) sampled by beach seine in Salmonier River estuary in fall 2003 and 2004.

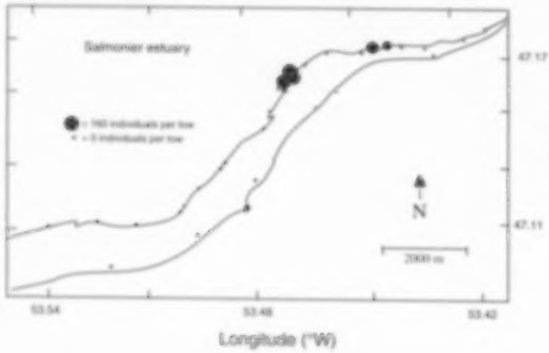

gested that retention within the productive upper reaches of the estuary was tightly linked to individual survival and was likely associated with high selection pressure. Similar linkages between survival, behaviour, and transport have been observed during late embryonic development, where hatch is synchronized to windows of low predation pressure (Bradbury et al. 2004). Nonetheless, no measures of larvae survival were made here, and we can only hypothesize that limited dispersal may lead to enhanced survival as observed elsewhere.

The hypothesis of limited larval dispersal is supported by the transport of surface drifters and the intrusion of freshwater during the summer months. The reduced export of surface waters during summer is consistent with limited transport of weakly swimming larvae located in these surface waters. This retention was somewhat surprising given that export of surface water is expected to be high in moderate to high inflow estuaries (e.g., DiBacco et al. 2001). However, the seasonal variation in river inflow on the southeastern coast of Newfoundland is extremely high, varying by an order of magnitude from relatively high inflow in spring (25–50 $m^3 \cdot s^{-1}$) and fall to low inflow during the summer (1–3 $m^3 \cdot s^{-1}$). The timing of larval entry into the estuary coincides with low seasonal freshwater inflow evident in vertical salinity profiles that is exacerbated by consistent onshore wind.

We observed clear, nonuniform patterns in the vertical distribution of smelt larvae. Recently hatched larvae displayed consistent negative geotaxis independent of light or flow. The observation of posthatch larvae aggregating at the surface is not unusual (e.g., Dame and Allen 1996; Davis 2001; Bennett et al. 2002), and in many cases, this is associated with positive buoyancy. Smelt larvae in our trials were consistently negatively buoyant, and the cessation of swimming always led to sinking of larvae. Interestingly, preflexion larvae seemed less able to maintain themselves at the surface in freshwater than in brackish water, but they nonetheless exhibited repetitive swimming and sinking behaviours. It is likely that increased buoyancy in brackish trials played some role in the decrease in individuals at depth, though it does not explain the accumulation of larvae at the surface.

The Salmonier River estuary is an example of a coastal plain estuary, and we observed a seasonal transition from a highly stratified estuary in fall to a very weakly stratified estuary in summer, when circulation is expected to result from the interaction of the turbulent forces of winds, tides, and baroclinic flow. Modelling studies in stratified estuaries suggest that freshwater inflow should result in a downstream movement and potential flushing of the estuary (e.g., Hellweger et al. 2004) balanced by inflow near the bottom (e.g., Pritchard 1967). Accordingly, it has been hypothesized that estuarine larvae at the surface are advected seaward (Dodson et al. 1989; Kimmerer et al. 1998). The increased intrusion of ocean water in the Salmonier River estuary in summer is consistent with reduced river flow and onshore wind stress. Unfortunately, we lack direct measures of flow within the Salmonier River estuary, though deYoung et al. (2000) found a residency time of 5–10 days for St. John's Harbour, which has similar freshwater inflow. Their study also noted mean seaward surface currents of ~ 4 $cm \cdot s^{-1}$ and 6 $cm \cdot s^{-1}$ at depth (10 m), with is consistent with the flow rates chosen for our vertical movement trials.

Fig. 8. (*a*) Larval length-frequency distributions and (*b*) critical larval velocity calculated for 0- to 10-day-old preflexion larvae (▲) and 90-day-old postflexion juvenile smelt (●; *Osmerus mordax*) from the Salmonier River estuary.

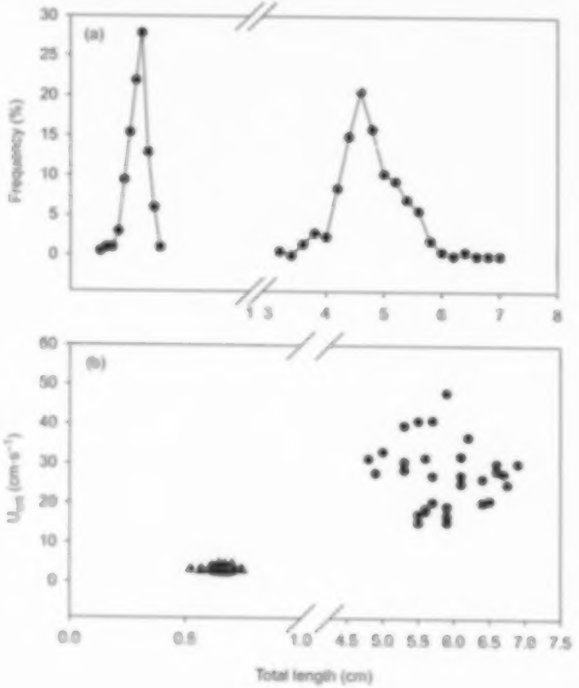

Along-estuary wind stress may play a significant role in dictating flow regimes (deYoung et al. 2000; Brown et al. 2004). Down-estuary wind stress may favour vertical stratification, whereas up-estuary wind stress may tend to break it down (i.e., wind straining, Scully et al. 2005). Moreover, modelling studies suggest that in the presence of onshore winds, surface propagules may be transported or retained near the shore in coastal estuaries, whereas they tend to be quickly dispersed in offshore winds (Blanton et al. 1999).

Fig. 9. Average abundance (± standard deviation) of smelt (*Osmerus mordax*) larvae (0–7 days) with depth under various experimental treatments based on 10 replicates of each: (*a*) top light, no flow; (*b*) bottom light, no flow; (*c*) no light, no flow; (*d*) no light with flow; and (*e*) top light with flow. All treatments in fresh (salinity 0 psu) water collected from spawning site.

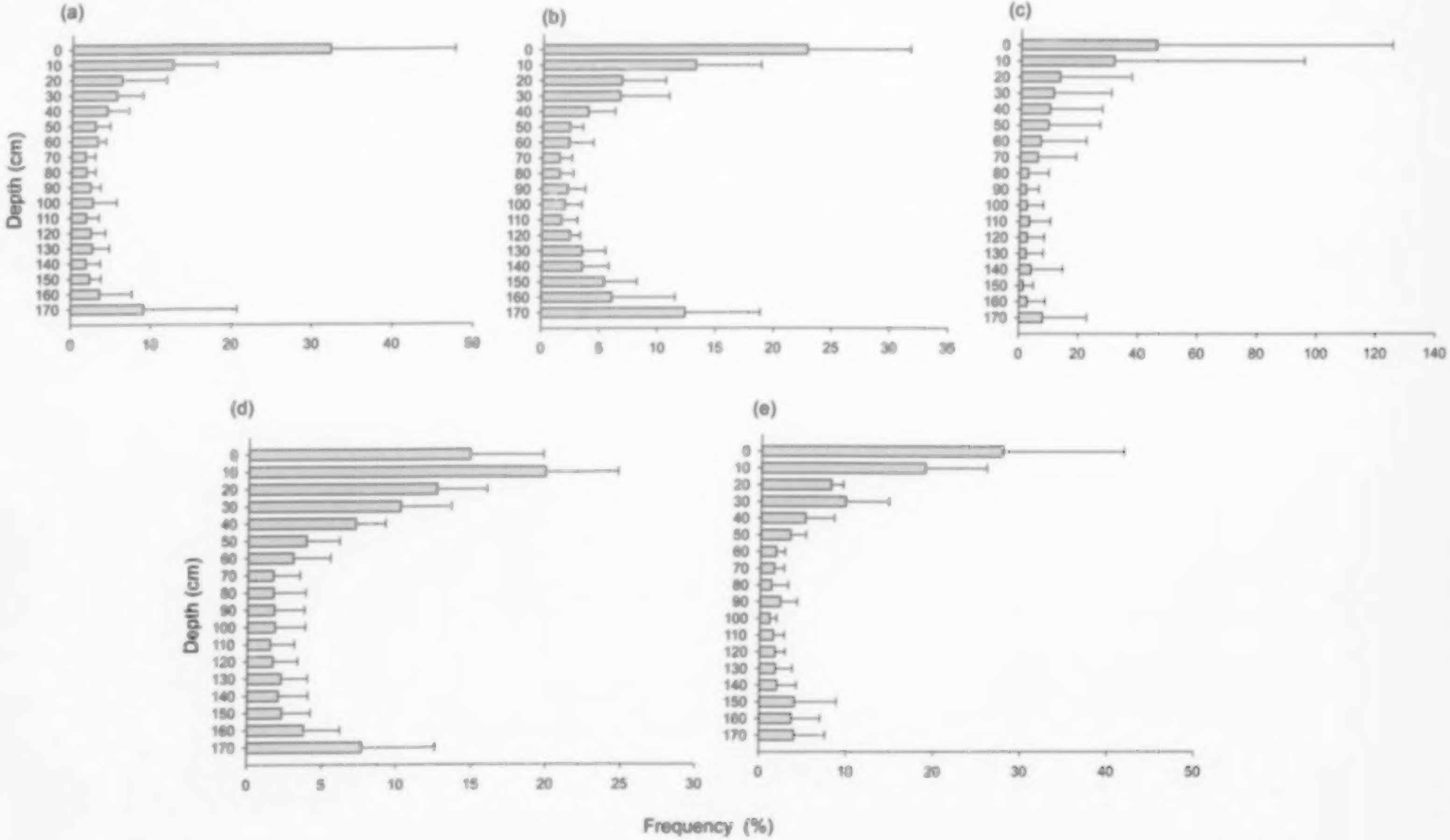

Fig. 10. Average abundance (± standard deviation) of smelt (*Osmerus mordax*) larvae (0–7 days) with depth under various experimental treatments based on 10 replicates of each: (*a*) top light, no flow; (*b*) bottom light, no flow, (*c*) no light, no flow; (*d*) no light with flow; and (*e*) top light with flow. All treatments in estuarine water (20 psu).

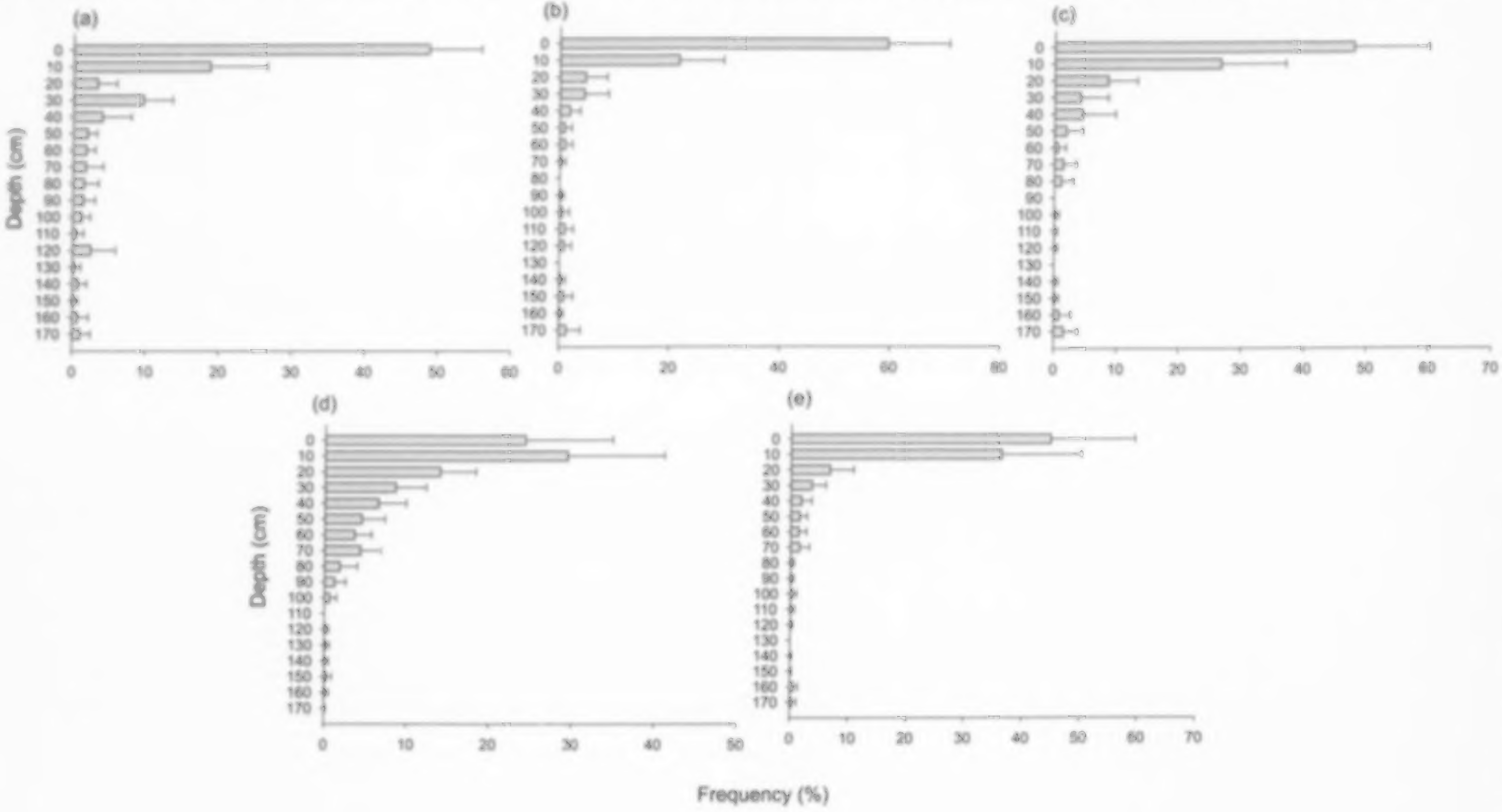

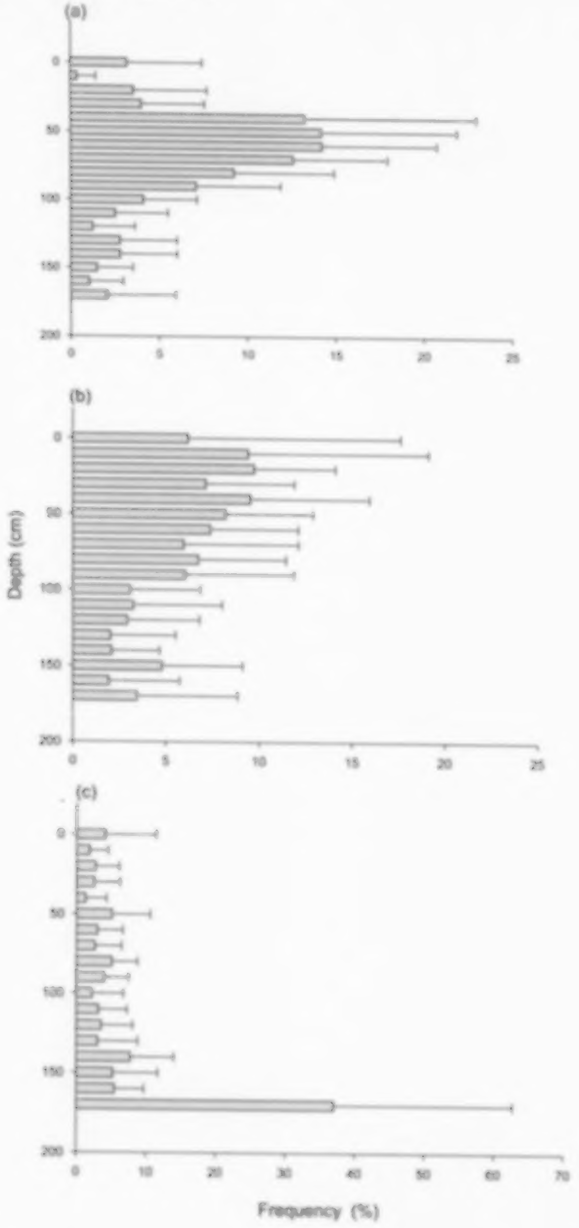

Fig. 11. Average abundance (± standard deviation) of smelt (*Osmerus mordax*) larvae (~90 days) with depth under various experimental treatments based on 10 replicates of each: (*a*) top light; (*b*) bottom light; and (*c*) no light. All treatments in estuarine water (20 psu).

This scenario is consistent with our drifter recoveries and our hypothesis that the dominant onshore wind stress in summer months may contribute to retention of preflexion larvae.

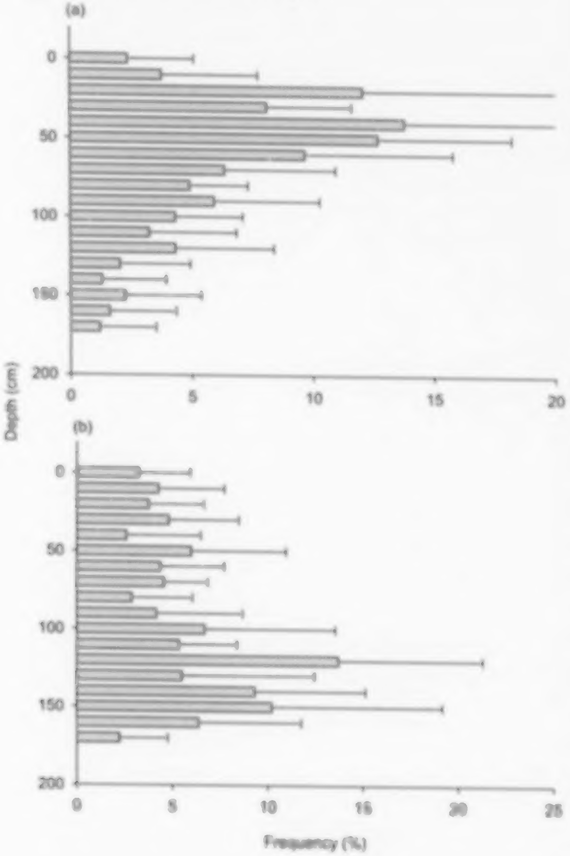

Fig. 12. Average abundance (± standard deviation) of smelt (*Osmerus mordax*) larvae (~90 days) with depth in response to light while exposed to countergradient current flow based on 10 replicates of each treatment: (*a*) top light and (*b*) no light. All treatments in estuarine water (20 psu).

In addition to onshore wind stress and reduced inflow, the convergent and restrictive nature of estuarine frontal formation may also influence larval transport (e.g., Largier 1993; Sarabun 1993). Surface flotsam and foam indicative of front formation are common in the upper reaches of the Salmonier River estuary in summer months and, in conjunction with spatial data on sea surface salinity, support the hypothesis of frontal formation well within the geographic boundaries of the estuary. Convergent flow at estuarine surface fronts has been noted to reach to tens of centimetres per second (Sarabun 1993) and can be intensified by onshore winds forcing denser water toward the front (Largier 1993). Moreover, given the role of topography in front formation, fronts may regularly recur at specific locations (O'Donnell 1993). Interestingly, the extension of freshwater beyond geographic boundaries in fall suggests that if a frontal plume exists, it may extend into St. Mary's Bay, likely reducing its close association with the upper reaches of the Salmonier River estuary.

There are several possible explanations for surface aggregation of posthatch larvae. Negative geotaxis may be linked to predator avoidance within natal rivers where high predation of smelt eggs and larvae by young salmonids has been noted (Bradbury et al. 2004). Within estuaries, however, larval predation is thought to be lower than in rivers (Sirois and Dodson 2000). Alternatively, aggregation at the surface of posthatch larvae may be a passive process resulting from positive buoyancy and limited swimming ability. Fortier and Leggett (1982) observed no vertical migration in larvae under 10 mm, suggesting that larvae smaller than this size may be unable to cross the pycnocline and maintain themselves either in surface (capelin) or bottom (herring) waters. Beyond this critical size, the amplitude of vertical migration increased with size in these species (Fortier and Leggett 1982), suggesting a size constraint on vertical migration behavior. Similarly, larvae of the congeneric *O. eperlanus* lack functional swim bladders and, along with their poorly developed fins, possess limited control over their location within the water column until they are between 12 and 15 mm in length (Urho 2002). For the larval stages examined here, which were all well below this size threshold, our observation of near-surface aggregation but weak critical swimming speed and little other obvious strong behavioural responses is generally consistent with these other studies.

In contrast to preflexion larvae, juveniles displayed consistent changes in vertical position, which appeared to represent positive and negative geotaxis cued by light. Juveniles also had substantially stronger swim capabilities than their larval counterparts, which would be expected to have a greater impact on their dispersal and active self-recruitment potential. Although flow had no large effect on vertical position, the response was blurred by flow and distributions were more diffuse, suggesting that juveniles may use active swim behaviour to avoid areas of high flow and to choose preferred weaker flow conditions. An ontogenetic increase in the potential for active behaviour to modify vertical position in larval fish is consistent with Bradbury et al. (2003), who predicted that the critical developmental stage for active behavioural influence on spatial pattern is approximately 10 mm.

Diel vertical migration (DVM) is a common behavior in estuarine fish and invertebrate larvae (e.g., Criales et al. 2005), where larvae surface at night and migrate to deeper water during daylight hours (Poulin et al. 2002). In contrast, we observed light-mediated vertical distribution responses that are consistent with a reverse diel vertical migration (RDVM; Ohman et al. 1983). Poulin et al. (2002) observed RDVM in gastropod larvae located in an advective, upwelling zone that enhanced coastal retention. Interestingly both behaviors (DVM and RDVM) have been reported for rainbow smelt depending on locality (Rogers 1940; Nellbring 1988; Laprise and Dodson 1989). The mechanisms responsible for contrasting behaviours are unknown but may be linked to local estuarine conditions or evolutionary divergence associated with glacial refugia (e.g., Bernatchez 1997). Interestingly, RDVM should increase risk of predation by visual predators (Pearre 2003). However the association of smelt larvae with areas of high turbidity (estuarine turbidity maximum, ETM) characteristic of many estuaries (e.g., Sirois and Dodson 2000; Lecomte and Dodson 2005) may reduce this risk. Moreover, in estuaries where larval predators undergo regular DVM, RDVM may act to counter predator behaviour (Ohman et al. 1983). Admittedly, our experiments were conducted over time periods with less than a 24-h cycle, and despite clear patterns associated with light and dark treatments, we can only hypothesize that observed patterns would hold over 24-h changes in light exposure.

The larval vertical movement documented here appears to be primarily geotactic and not phototactic, given that the majority of larvae remained at the surface even with bottom lighting. Similar behaviour has been noted for walleye pollock, which congregated on the surface irrespective of top or bottom lighting (Davis 2001). Contrary to Davis (2001), we did not observe any shifts from geotaxis to phototaxis in flow trials. There was an indication of positive phototaxis in freshwater larval trials, where secondary peaks of abundance were observed at the bottom in the presence of bottom light; however, the absence of this pattern in the brackish trials makes interpretation difficult.

Several field studies have documented vertical migration in smelt. McKenzie (1964) observed that smelt larvae usually occurred near the bottom, although low concentrations were observed at the surface at night. In the St. Lawrence River, Laprise and Dodson (1989) suggested that active retention in the maximum turbidity zone was achieved through tidally cued vertical migration; their reanalysis of data from Rogers (1940) suggested that such cues could explain the observed distributions. This finding is in stark contrast with our observations that suggest that flow plays only a secondary role in determining vertical position. Of course, movement related to foraging behaviour was not examined here and may be important in field situations, but Dauvin and Dodson (1990) suggested that vertical migration in smelt was not related to feeding. Admittedly, the developmental stages examined here do not directly overlap many previous studies in the St. Lawrence, which examined larvae 8–30 mm in size (e.g., Fortier and Leggett 1982). Nonetheless, our examination of pre- and post-flexion larvae highlights significant behavioural processes associated with each developmental stage.

The potential consequences for limited larval dispersal to the spatial ecology of coastal smelt populations are extensive. We suggest that restricted dispersal results in the formation of isolated demes associated with estuarine retention areas as predicted by the "member vagrant hypothesis" (Sinclair 1988). Similar observations based on genetic (Bernatchez and Martin 1996) and morphological (Frechet et al. 1983) data for the St. Lawrence River estuary suggest discrete populations associated with local retention areas. A similar comparison of genetic diversity and morphology for populations of smelt along Canada's eastern coast (Newfoundland, Nova Scotia, New Brunswick, Prince Edward Island) suggests that Newfoundland populations (based on 10 estuaries along the southeastern coast of Newfoundland) are subject to limited gene flow, resulting in isolated demes that respond independently to selection for morphology (Bradbury et al. 2006). Interestingly, populations in mainland Canada (i.e., Nova Scotia, Prince Edward Island, and New Brunswick) are not subject to consistent onshore winds and are characterized by significantly lower genetic structure and higher gene flow. One hypothesis for regional differences in gene flow between Newfoundland and mainland populations is that onshore winds and topography effectively retain weakly swimming, younger larvae until active behaviour can contribute significantly.

In conclusion, we observed short-distance larval dispersal in coastal smelt despite an extensive planktonic larval period. Retention appears to be the result of an ontogenetic shift in vertical behavior that coincides with seasonal changes in river inflow and predominant onshore winds. Such retention effectively restricts dispersal between estuaries, resulting in significant population structure. We suggest that larval dispersal in smelt is a complex interaction of seasonal changes in estuarine inflow and outflow, wind forcing, and ontogenetic shifts in swimming ability and behavior.

Acknowledgements

The authors thank all the summer students who assisted with this work. L. Barrett, B. Laurel, and D. Schneider advised on analysis and interpretation. The authors also thank M. Kelly, B. Oake, and the local residents of St. Mary's Bay who assisted in locating smelt runs. A.K. Gamperl kindly provided the swim tunnels. I. Fleming and D. Marshall provided constructive comments on an earlier draft of this manuscript. Funding was provided by National Sciences and Engineering Research Council of Canada, the Department of Fisheries and Oceans, The Killam Trust, and the Harris Centre of Memorial University.

References

Able, K.W. 2005. A reexamination of fish estuarine dependence: a reexamination of connectivity between estuarine and open habitats. Estuar. Coast. Shelf Sci. **64**: 5–17.

Bakun, A. 1996. Patterns in the ocean. Ocean processes and marine population dynamics. California Sea Grant College System, University of California, La Jolla.

Beamish, F.W.H. 1978. Swimming capability. *In* Fish physiology. Academic Press, New York. pp. 101–187.

Bennett, W.A., Kimmerer, W.J., and Burau, J.R. 2002. Plasticity in vertical migration by native and exotic estuarine fish in a fluctuating low salinity zone. Limnol. Oceanogr. **47**: 1496–1507.

Bernatchez, L. 1997. Mitochondrial DNA analysis confirms the existence of two glacial races of rainbow smelt *Osmerus mordax* and their reproductive isolation in the St. Lawrence River estuary (Quebec, Canada). Mol. Ecol. **6**: 73–83.

Bernatchez, L., and Martin, S. 1996. Mitochondrial DNA diversity in andromous rainbow smelt, *Osmerus mordax* Mitchill: a genetic assessment of the member–vagrant hypothesis. Can. J. Fish. Aquat. Sci. **53**: 424–433.

Blanton, J.O., Werner, F.E., Kapolnai, A., Blanton, B.O., Knott, D., and Wenner, E.L. 1999. Wind-generated transport of fictitious passive larvae into shallow tidal estuaries. Fish. Oceanogr. **8**(2): 210–223.

Bradbury, I.R., and Snelgrove, P.V.R. 2001. Contrasting larval transport in demersal fish and benthic invertebrates: the roles of behavior and advective processes in determining spatial pattern. Can. J. Fish. Aquat. Sci. **58**: 811–823.

Bradbury, I.R., Snelgrove, P.V.R., and Fraser, S. 2000. Transport and development of eggs and larvae of Atlantic cod, *Gadus morhua*, in relation to spawning time and location in coastal Newfoundland. Can. J. Fish. Aquat. Sci. **57**(9): 1761–1772.

Bradbury, I.R., Snelgrove, P.V.R., and Pepin, P. 2003. Passive and active behavioral contributions to patchiness and spatial pattern during the early life history of marine fishes. Mar. Ecol. Prog. Ser. **257**: 243–245.

Bradbury, I.R., Campana, S.E., Bentzen, P., and Snelgrove, P.V.R. 2004. Synchronized hatch and its ecological significance in rainbow smelt *Osmerus mordax* in St. Mary's Bay, Newfoundland. Limnol. Oceanogr. **49**: 2310–2315.

Bradbury, I.R., Coulson, M., Campana, S.E., and Bentzen, P. 2006. Morphological and genetic differentiation in anadromous rainbow smelt: disentangling the effects of geography and morphology on gene flow. J. Fish Biol. **69**(Suppl. C): 95–114.

Brett, J.R. 1964. The respiratory metabolism and swimming performance of young sockeye salmon. J. Fish. Res. Board Can. **21**: 1183–1226.

Brown, C.A., Holt, S.A., Jackson, G.A., Brooks, D.A., and Holt, G.J. 2004. Simulating larval supply to estuarine nursery areas: how important are physical processes to the supply of larvae to the Aransas Pass inlet. Fish. Oceanogr. **13**(3): 181–196.

Christy, J.H., and Morgan, S.G. 1998. Estuarine immigration by crab postlarvae: mechanisms, reliability and adaptive significance. Mar. Ecol. Prog. Ser. **174**: 51–65.

Cowen, R.K., Lwiza, K.M.M., Sponaugle, S., Paris, C.B., and Olson, D.B. 2000. Connectivity of marine populations: open or closed? Science (Washington, D.C.), **287**: 857–859.

Cowen, R.K., Paris, C.B., and Srinivasan, A. 2006. Scaling of connectivity in marine populations. Science (Washington, D.C.), **311**: 522–527.

Criales, M.M., Wang, J., Browder, J.A., and Robblee, M.B. 2005. Tidal and seasonal effects on transport of pink shrimp postlarvae. Mar. Ecol. Prog. Ser. **286**: 231–238.

Dame, R.F., and Allen, D.M. 1996. Between estuaries and the sea. J. Exp. Mar. Biol. Ecol. **200**: 169–185.

Dauvin, J.C., and Dodson, J.J. 1990. Relationship between feeding incidence and vertical and longitudinal distribution of rainbow smelt larvae (*Osmerus mordax*) in a turbid well-mixed estuary. Mar. Ecol. Prog. Ser. **60**: 1–12.

Davis, M.W. 2001. Behavioral responses of walleye pollock, *Theragra chalcogramma*, larvae to experimental gradients of sea water flow: implications for vertical distribution. Environ. Biol. Fishes, **61**: 253–260.

de Graaf, M., Jager, Z., Vreugdenhil, C.B., and Elorche, M. 2004. Numerical simulations of tidally cued vertical migrations of flatfish larvae in the North Sea. Estuar. Coast. Shelf Sci. **59**: 295–305.

deYoung, B. Schillinger, D., Zedel, L., and Foley, J. 2000. Circulation through the narrows of St. John's Harbour: summer and fall 1999. Physics and Physical Oceanography Technical Report 2000-1. Memorial University, St. John's, Newfoundland.

DiBacco, C., Sutton, D., and McConnico, L. 2001. Vertical migration behavior and horizontal distribution of brachyuran larvae in a low-inflow estuary: implications for bay–ocean exchange. Mar. Ecol. Prog. Ser. **217**: 191–206.

Dodson, J.J., Dauvin, J.C., Ingram, R.G., and d'Anglejan, B. 1989. Abundance of larval rainbow smelt (*Osmerus mordax*) in relation to the maximum turbidity zone and associated macroplanktonic fauna of the middle St. Lawrence Estuary. Estuaries, **12**: 66–81.

Fortier, L., and Leggett, W.C. 1982. Fickian transport and dispersal of fish larvae in estuaries. Can. J. Fish. Aquat. Sci. **39**: 1150–1163.

Frechet, A., Dodson, J.J., and Powles, H. 1983. Use of variation in biological characters for the classification of anadromous rainbow smelt (*Osmerus mordax*) groups. Can. J. Fish. Aquat. Sci. **40**: 718–727.

Gotceitas, V., Fraser, S., and Brown, J.A. 1997. The use of eelgrass beds (*Zostera marina*) by juvenile Atlantic cod (*Gadus morhua*). Can. J. Fish. Aquat. Sci. **54**: 1306–1319.

Hare, J.A., Thorrold, S.R., Walsh, H., Reiss, C., Valle-Levinson, A., and Jones, C.M. 2005. Biophysical mechanisms of larval ingress into Chesapeake Bay. Mar. Ecol. Prog. Ser. **302**: 295–310.

Hellweger, F.L., Blumberg, A.F., Schlosser, P., Ho, D.T., Caplow, T., Lall, U., and Honghai, L. 2004. Transport in the Hudson estuary: a modeling study of estuarine circulation and tidal trapping. Estuaries, **27**(3): 527–538.

Kimmerer, W.J., Burau, J.R., and Bennett, W.A. 1998. Tidally oriented vertical migration and position maintenance of zooplankton in a temperate estuary Limnol. Oceanogr. **43**: 1697–1709.

Laprise, R., and Dodson, J.J. 1989. Ontogeny and importance of tidal vertical migrations in the retention of larval smelt *Osmerus mordax* in a well-mixed estuary. Mar. Ecol. Prog. Ser. **55**: 101–111.

Large, W.G., and Pond, S. 1981. Open ocean momentum flux measurements in moderate to strong winds. J. Phys. Oceanogr. **11**: 324–336.

Largier, J.L. 1993. Estuarine front: how important are they? Estuaries, **16**(1): 1–11.

Lecomte, F., and Dodson, J.J. 2005. Distinguishing trophic and habitat partitioning among sympatric populations of the estuarine fish *Osmerus mordax* Mitchill. J. Fish Biol. **66**: 1601–1623.

Lee, J.T., Coleman, R.A., and Jones, M.B. 2005. Vertical migration during tidal transport of megalopae of *Necora puber* in coastal shallow waters during daytime. Estuar. Coast. Shelf Sci. **65**: 396–404.

Metaxas, A. 2001. Behavior in flow: perspectives on the distribution and dispersion of meroplanktonic larvae in the water column. Can. J. Fish. Aquat. Sci. **58**: 86–98.

McKenzie, R.A. 1964. Smelt life history and fishery in the Miramichi, New Brunswick. Bull. Fish. Res. Board Can. No. 144.

McLean, J.E., Hay, D.E., and Taylor, E.B. 1999. Marine population structure in an andromous fish: life history influences patterns of mitochondrial DNA variation in the eulachon, *Thaleichthys pacificus*. Mol. Ecol. **8**: S143–S158.

Nellbring, S. 1988. The ecology of smelts (genus *Osmerus*): a literature review. Nord. J. Freshw. Res. **65**: 116–145.

O'Donnell, J.O. 1993. Surface fronts in estuaries: a review. Estuaries, **16**(1): 12–39.

Ohman, M.D., Frost, B.W., and Cohen, E.B. 1983. Reverse diel vertical migration: an escape from invertebrate predators. Science (Washington, D.C.), **220**: 1404–1406.

Ouellet, P., and Dodson, J.J. 1985*a*. Tidal exchange of anadromous rainbow smelt (*Osmerus mordax*) larvae between a shallow spawning tributary and the St. Lawrence Estuary. Can. J. Fish. Aquat. Sci. **42**: 1352–1358.

Ouellet, P., and Dodson, J.J. 1985*b*. Dispersion and retention of anadromous rainbow smelt (*Osmerus mordax*) larvae in the middle estuary of the St. Lawrence River. Can. J. Fish. Aquat. Sci. **42**: 332–341.

Pearre, S. 2003. The hunger/satiation hypothesis in vertical migrati[illegible] history, evidence and consequences. Biol. Rev. Camb. Philos. Soc. **78**: 1–79.

Poulin, E., Palma, A.T., Leiva, G., Navarez, D., Pacheco, R., Navarrete, S.A., and Castilla, J.C. 2002. Avoiding offshore transport of competent larvae during upwelling events: the case of the gastropod *Concholepas concholepas* in Central Chile. Limnol. Oceanogr. **47**: 1248–1255.

Pritchard, D.W. 1967. What is an estuary: physical viewpoint. *In* Estuaries. *Edited by* G.H. Lauf. AAAS Press, Washington, D.C. pp. 3–5.

Rogers, H.M. 1940. Occurrence and retention of plankton with the estuary. J. Fish. Res. Board Can. **5**: 164–171.

Ryland, J.S. 1963. The swimming speeds of plaice larvae. J. Exp. Biol. **40**: 285–299.

Sale, P.F., Cowen, R.K., Danilowicz, B.S., Jones, G.P., Kritzer, J.P., Lindeman, K.C., Planes, S., Polunin, N.V., Russ, G.R., and Sadovy, Y.J. 2005. Critical science gaps impede use of no-take fishery reserves. Trends Ecol. Evol. **20**: 74–80.

Sarabun, C.C. 1993. Observations of a Chesapeake Bay tidal front. Estuaries, **16**: 68–73.

Schultz, E.T., Cowen, R.K., Lwiza, K.M.M., and Gospodarek, A.M. 2000. Explaining advection: do larval bay anchovy (*Anchoa mitchilli*) show selective tidal stream transport? ICES J. Mar. Sci. **57**: 360–371.

Scott, W.B., and Scott, M.G. 1988. Fishes of Atlantic Canada. Can. Bull. Fish. Aquat. Sci. No. 219.

Scully, M., Friedrichs, C., and Brubaker, J. 2005. Control of estuarine stratification and mixing by wind-induced straining of the estuarine density field. Estuaries, **28**(3): 321–326.

Sheng, J., and Thompson, K.R. 1996. Summer surface circulation on the Newfoundland and Grand Banks: the role of local density gradients and remote forcing. Atmosphere-Ocean, **34**: 257–284.

Sinclair, M. 1988. Marine populations. An essay on population regulation and speciation. Books in Recruitment Fishery Oceanography. University of Washington Press, Seattle, Wash.

Sirois, P., and Dodson, J.J. 2000. Critical periods and growth-dependent survival of larvae of an estuarine fish, the rainbow smelt *Osmerus mordax*. Mar. Ecol. Prog. Ser. **203**: 233–245.

Sirois, P., Lecomte, F., and Dodson, J.J. 1998. An otolith-based back-calculation method to account for time-varying growth rate in rainbow smelt, *Osmerus mordax*, larvae. Can. J. Fish. Aquat. Sci. **55**: 2662–2671.

Sokal, R.R., and Rohlf, F.J. 1995. Biometry. W.H. Freeman & Co., San Francisco, Calif.

Thorrold, S.R., Latkoczy, C., Swart, P.K., and Jones, C.M. 2001. Natal homing in a marine fish metapopulation. Science (Washington, D.C.), **291**: 297–299.

Urho, L. 2002. Characters of larvae — what are they? Folia. Zool. **51**: 161–186.

The index and/or table of contents has been removed and photographed separately within this volume year.

For roll film users, this information for the current volume year is at the beginning of the microfilm. For a prior year volume, this information is at the end of the microfilm.

For microfiche users, the index and/or contents is contained on a separate fiche.

30th Congress of the International Association of Theoretical and Applied Limnology

30ième Congrès de l'Association internationale de limnologie théorique et appliquée

Montréal, Canada

12 - 18

août | August

2007

Montréal sera l'hôte du 30è Congrès de l'Association internationale de limnologie théorique et appliquée du 12 au 18 août 2007.

Ce congrès sera l'un des plus importants rassemblements de limnologistes venant des quatre coins du monde. Il fournira une opportunité unique d'interagir et de partager des données provenant de différents champs d'étude, régions et cultures. Ce congrès scientifique reliera la recherche de pointe aux problèmes majeurs auxquels font face les eaux douces dans le monde entier.

SIL 2007 vous fournira également l'opportunité de découvrir Montréal, une ville entourée du majestueux Fleuve St-Laurent de toutes parts. Reconnue mondialement pour sa joie de vivre, sa vie culturelle et sa gastronomie, Montréal est une ville propre, stimulante, abordable et sécuritaire.

Visitez-nous au **www.sil2007.org** !

Montreal will host the 30th Congress of the International Association of Theoretical and Applied Limnology from the 12th to 18th of August 2007

This promises to be one of the largest gatherings of freshwater scientists from around the globe. It will provide a unique opportunity to share ideas and data from diverse studies, regions and cultures. This scientific congress will link cutting-edge research with the important applied problems the world's freshwaters currently face.

SIL 2007 will be an opportunity for you to discover Montréal, an island city surrounded by the majestic freshwaters of the St-Lawrence River. Renowned for its cultural life and gastronomy, Montréal is also stimulating, safe and affordable.

Visit us at **www.sil2007.org** !

Montréal

Contents (concluded) / Table des matières (suite et fin)

Nicholas R. Record and Brad de Young 2708–2721 Patterns of diel vertical migration of zooplankton in acoustic Doppler velocity and backscatter data on the Newfoundland Shelf

Carrie A. Holt and Randall M. Peterman 2722–2733 Missing the target: uncertainties in achieving management goals in fisheries on Fraser River, British Columbia, sockeye salmon (*Oncorhynchus nerka*)

Gideon Gal, Lars G. Rudstam, Edward L. Mills, Jana R. Lantry, Ora E. Johannsson, and Charles H. Greene 2734–2747 Mysid and fish zooplanktivory in Lake Ontario: quantification of direct and indirect effects

David Brickman 2748–2759 Risk assessment model for dispersion of ballast water organisms in shelf seas

Eva Leu, Stig Falk-Petersen, Slawomir Kwaśniewski, Angela Wulff, Kåre Edvardsen, and Dag O. Hessen 2760–2779 Fatty acid dynamics during the spring bloom in a High Arctic fjord: importance of abiotic factors versus community changes

Andrea Bertolo and Pierre Magnan 2780–2792 Spatial and environmental correlates of fish community structure in Canadian Shield lakes

Jeffrey J. Hard, Diane G. Elliott, Ronald J. Pascho, Dorothy M. Chase, Linda K. Park, James R. Winton, and Donald E. Campton 2793–2808 Genetic effects of ELISA-based segregation for control of bacterial kidney disease in Chinook salmon (*Oncorhynchus tshawytscha*)

Alan Wells, Christal E. Grierson, Monique MacKenzie, Iain J. Russon, Helena Reinardy, Claire Middlemiss, Pål A. Bjørn, Bengt Finstad, Sjoerd E. Wendelaar Bonga, Christopher D. Todd, and Neil Hazon 2809–2821 Physiological effects of simultaneous, abrupt seawater entry and sea lice (*Lepeophtheirus salmonis*) infestation of wild, sea-run brown trout (*Salmo trutta*) smolts

I.R. Bradbury, K. Gardiner, P.V.R. Snelgrove, S.E. Campana, P. Bentzen, and L. Guan 2822–2836 Larval transport, vertical distribution, and localized recruitment in anadromous rainbow smelt (*Osmerus mordax*)

Author Index for Volume 63 AI-1 Index des auteurs pour le volume 63 AI-1
Contents for Volume 63 C-1 Sommaire pour le volume 63 C-1

National Research Council Canada
Ottawa, Canada
K1A 0R6

Conseil national de recherches Canada
Ottawa, Canada
K1A 0R6

Postage paid at Ottawa
Publications mail
Registration No. 40062591

Port payé à Ottawa
Poste-publication
Enregistrement nº 40062591

USPS periodical postage paid at Plattsburgh, NY 12901, USA

Canadian Journal of Fisheries and Aquatic Sciences

Journal canadien des sciences halieutiques et aquatiques

Volume 63, Number 12, December 2006

Volume 63, numéro 12, décembre 2006

ANNOUNCEMENT / COMMUNIQUÉ

iii Call for nominations for the Timothy R. Parsons Medal in ocean sciences / Appel de candidatures pour la médaille Timothy R. Parsons (sciences de la mer)

RAPID COMMUNICATION / COMMUNICATION RAPIDE

Benjamin J. Laurel and Ian R. Bradbury 2603–2607 "Big" concerns with high latitude marine protected areas (MPAs): trends in connectivity and MPA size

ARTICLES / ARTICLES

M. Jake Vander Zanden, Sudeep Chandra, Sang-Kyu Park, Yvonne Vadeboncoeur, and Charles R. Goldman 2608–2620 Efficiencies of benthic and pelagic trophic pathways in a subalpine lake

Lilian B. Busse, Juliet C. Simpson, and Scott D. Cooper 2621–2638 Relationships among nutrients, algae, and land use in urbanized southern California streams

Akash R. Sastri and John F. Dower 2639–2647 Field validation of an instantaneous estimate of in situ development and growth for marine copepod communities

Vera N. Agostini, Robert C. Francis, Anne B. Hollowed, Stephen D. Pierce, Chris Wilson, and Albert N. Hendrix 2648–2659 The relationship between Pacific hake (*Merluccius productus*) distribution and poleward subsurface flow in the California Current System

Christophe Pampoulie, Daniel E. Ruzzante, Valérie Chosson, Thóra Dögg Jörundsdóttir, Lorna Taylor, Vilhjálmur Thorsteinsson, Anna Kristín Danielsdóttir, and Guðrún Marteinsdóttir 2660–2674 The genetic structure of Atlantic cod (*Gadus morhua*) around Iceland: insight from microsatellites, the *Pan* I locus, and tagging experiments

Ryan M. Utz and Kyle J. Hartman 2675–2686 Temporal and spatial variation in the energy intake of a brook trout (*Salvelinus fontinalis*) population in an Appalachian watershed

Allison E. Gamble, Russ Lloyd, John Aiken, Ora E. Johannsson, and Edward L. Mills 2687–2699 Using zooplankton biomass size spectra to assess ecological change in a well-studied freshwater lake ecosystem: Oneida Lake, New York

Katriina Tiira, Jorma Piironen, and Craig R. Primmer 2700–2707 Evidence for reduced genetic variation in severely deformed juvenile salmonids

Continued on inside back cover / Suite au verso

Canada

Printed in Canada by / Imprimé au Canada par
NRC Reprographic Services / Service de reprographie CNRC
Page production by / Mise en page par
NRC Research Press / Presses scientifiques du CNRC

0706-652X(200612)63:12;1-Q

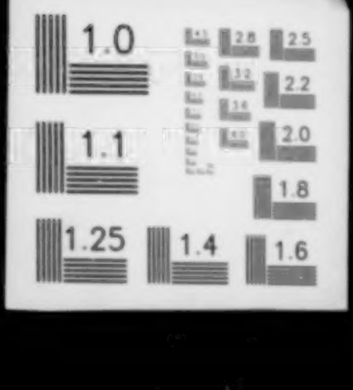
1.0
2.8
2.5
3.2
2.2
3.6
4.0
2.0
1.1
1.8
1.25
1.4
1.6